Hamidullah, . (1983) *Petrogenetic studies of the appinite suite of western Scotland*. PhD thesis.

http://theses.gla.ac.uk/5467/

PETROGENETIC STUDIES OF THE APPINITE SUITE OF WESTERN SCOTLAND

by

HAMIDULLAH

Thesis submitted in fulfilment of
the degree of Doctor of Philosophy
in the Faculty of Science, Department
of Geology, University of Glasgow

May 1983

CONTAINS

PULLOUTS

Dedicated to <u>my parents</u> and <u>my wife Ghazala</u>
for their love and devotion at all times
and to <u>our son Fahad</u> who missed us during
the years devoted to this research project

CONTENTS

Appendices

LIST OF FIGURES

Page

PART 1

Chapter 1 - Introduction

PART 2 BALLACHULISH APPINITE SUITE

Chapter 2 - Geological Setting and Petrography

Chapter 3 - Olivine

Chapter 4 - Clinopyroxene

Chapter 5 - Amphibole

Chapter 6 - Mica

Chapter 7 - Petrochemistry

Chapter 8 - Petrogenesis

PART 3 LOCH LOMOND APPINITE SUITE

Chapter 9 - Geological Setting and Petrography

Chapter 10 - Petrochemistry

PART 4

Chapter 12 - Comparative Studies

PART 5 TECTONIC SETTING, SOURCE OF MAGMA AND CONCLUSIONS

Chapter 13 - Tectonic Setting and Source of Magma

LIST OF TABLES

Acknowledgements

My primary and most sincere acknowledgement is certainly to my supervisor, Professor D. R. Bowes, not only for his great interest and guidance in the execution and writing up of this project, but also for providing much moral support whenever he felt that I needed it. Thanks are also due to the head of the department, Professor B. E. Leake, whose permission enabled this work to be carried out.

I acknowledge with thanks the receipt of samples, thin sections and analyses from Professor D. R. Bowes and Dr. A. E. Wright and also thank the Royal Society of Edinburgh for permission to reproduce map 1 of Bowes and Wright (1967). Special thanks are due to Mr. A. Herriot, Drs Gribble, Park and Halden and to B. Silva Filho of the Geology Department, University of Glasgow and to M. Idris Khan and Professor M. Q. Jan of Peshawar University, Pakistan, for critically reading parts of the manuscript. I am grateful to Dr. C. Farrow for his help in the probe work and computing and also to Drs Lutfullah and M. Giles for their assistance in computing.

The invaluable assistance of Mr. R. Morrison (technical), Mr. D. McLean (photography), Mrs. S. Hall (drafting) and Dr. Sheena and the departmental secretaries (typing) is also gratefully acknowledged.

I am also grateful to Ghazala's parents for having looked after our son Fahad in Peshawar while we were away during the time spent on this project. All members of my family, particularly my mother and brother, S. Waheedullah, also receive my gratitude for their moral support throughout the period of my study.

Finally, the financial support provided by the Ministry of Education, Government of Pakistan, under the Quaid-i-Azam Scholarship Scheme, is gratefully acknowledged.

Abstract

Mineral and rock chemistry together with petrography have been used in association with previously determined field relationships to elucidate magma genesis, conditions of crystallisation and geotectonic environment of the appinite suite of western Scotland and northwestern Ireland. The major part of the study has been related to the type area of this suite, that of the Ballachulish district in the parish of Appin. In addition, the major cluster of appinites in the Loch Lomond district has been studied together with appinites from Colonsay and Ardara, Dongal. Comparison has been made with the scyelite-pyroxenite-appinitic type rock association of Central Sutherland and with the lamprophyres of the Ballachulish district and lavas of Old Red Sandstone age (late Silurian) in western Scotland. These comparative studies have been used to establish which products of the late Caledonian igneous activity were comagmatic and to determine whether the appinite suite of the type area developed under unique conditions or whether comparable magma genesis, emplacement and crystallisation conditions were widespread in Caledonides.

The appinite suite of western Scotland and northwestern Ireland was developed from a volatile-rich basaltic magma. For the Ballachulish cluster the magma was of high-potassium calc-alkaline type and evolved towards a relatively continental environment. For the Ardara cluster it was transitional between calc-alkaline and tholeiitic and evolved towards an island arc environment while for the Loch Lomond cluster it was a normal calc-alkaline type evolved in environments intermediate between the other two.

In the Ballachulish appinite suite, olivine appeared on the liquidus at about 70-80 km depth. Subsequently emplacement into high crustal level occurred. With magma uprise being impeded by

structural traps of the folded Dalradian Supergroup, the rest of crystallisation occurred under decreasing temperature but highly variable P_{Gas} due to explosive activity in the subvolcanic pipes. Following olivine, the successive fractionation of clinopyroxene, amphibole, mica and plagioclase led to the progressive development of rocks from ultramafic to acidic compositions. In addition, accumulation of mafic phases occurred in the early stages of fractionation, under increasing P_{Gas} which led to explosive activity that disrupted the early formed cumulates followed by their upward movement as large "blocks", crystal mushes and individual crystals with variable proportions of the residual liquid. Thus, appinites, kentallenites and even diorites represent "mixed rocks" in which particular phenocrysts are not in a matrix representing the particular liquid with which they were in equilibrium. Explosive activity associated with the emplacement of the marginal ultramafic rocks, appinites and majority of the diorites occurred at higher P_{Gas} (4-5 kb) than that associated with the emplacement of kentallenites (1 kb). The late leucocratic diorites and granodiorites represent crystallisation from a residual liquid which probably also contained a small component of a hybrid secondary liquid produced by the solution of silica from quartzite, which formed structural traps, at high P-T. Gas-streaming continued after igneous emplacement of various rock types.

Corresponding petrogenetic processes were also responsible for the development of the Loch Lomond and Ardara clusters. However, due to the variable strengths of the structural traps, in the Loch Lomond cluster P_{Gas} reached before explosive breaching of the traps was generally not so high as at Ballachulish while in the Ardara cluster it was higher than both of the other two clusters.

The lamprophyres and lavas of the Old Red Sandstone age (late Silurian) are genetically related to the appinite suite.

The scyelite-pyroxenite-appinitic type rock association of Sutherland does not represent a cognate petrogenetic suite of rocks. Scyelite and SiO_2-poor appinitic type rocks are the products of crystallisation differentiation from a basaltic magma and are genetically related to the appinite suite. Pyroxenites and SiO_2-rich appinitic type rocks represent the hybrids of Ach'uain type.

The basaltic magma from which the various appinite clusters crystallised were mantle-derived, at depths of c. 200 km and associated with a northwestward dipping subduction zone in late Silurian time, i.e. in the latter stages of the Caledonian orogeny.

PART 1

CHAPTER 1 INTRODUCTION

Members of the appinite suite are intruded mostly into metasediments of the Dalradian Supergroup of the Caledonian orogenic belt in various parts of the Highlands and Islands of Scotland and Northwestern Ireland (Fig. 1.1; also see 1" = 10 mile Geol. Survey Sheet 1 for the distribution of the Dalradian metasediments). They make up a suite of rocks emplaced in subvolcanic pipes and are commonly associated with explosion-breccia. They occur in clusters some of which are spatially associated with Newer granites. A cluster in the Ballachulish district of Argyll formed the basis for the original definition of the term appinite (Bailey and Maufe 1916, p. 167-8) and for the demonstration of the subvolcanic characters and association with explosion-breccia (Bowes and Wright 1967). Another cluster occurs in the vicinity of Loch Lomond (see Fig. 9.1). Smaller clusters and isolated pipes also occur in other parts of Scotland. These include the masses intruded into Torridonian sediments of Colonsay and Ross of Mull in Argyll and those intruded into Moinian metasediments in the vicinity of Loch Shin, Sutherland (*cf.* Read 1961, plate 31). A major cluster also occurs in the Ardara district of County Donegal, Eire (see Pitcher and Berger 1972, fig. 7.3).

Appinite was defined by Bailey and Maufe (1916, p. 167-8) as the plutonic equivalent of vogesite and spessartite, *i.e.* of hornblende-rich lamprophyres; the name was taken from the local parish of Appin in the vicinity of Ballachulish. The original definition encompassed wide mineralogical variation including ultramafic as well as more common mafic types, with large crystals of hornblende a characteristic of many of the rocks. Subsequent work has shown that the suite of appinitic rocks present in pipe-like intrusions includes ultrabasic-ultramafic (peridotite, pyroxenite, hornblendite), basic to intermediate (kentallenite and many varieties of diorite) and acidic (granodiorite) types. In many of these amphibole and dark mica are present in significant proportions and in others olivine, pyroxene, amphibole and mica occur. With the existence of such variation some uses of the term "appinite" have been related to the overall rock association (appinite suite) and not to a particular member of the suite. However, when used in relation to a specific rock type, appinite has been used to designate a rock in which large idiomorphic amphibole dominates in a mafic rock of gabbroic to dioritic affinities. Many individual members of the suite were described around the turn of the century (Teall 1888; Dakyns and Teall 1892; Hill and Kynaston 1900; Clough 1905; Wyllie and Scott 1913) and the calcalkaline affinities indicated by Elders (1935).

The appinite suite has been referred to in the literature as of Old Red Sandstone age and is an expression of extensive igneous activity which characterised the latter stages of the Caledonian orogenic episode. This activity included the emplacement of lamprophyres, to which the appinites are related by definition, and the extrusion of the Lorne, Glen Coe and Ben Nevis lava piles. While generally referred to as being of early Devonian age, radiometric dating of Newer granites (such as the Ballachulish granite) at 410-400 m.y. (Brown 1972) indicates that the igneous activity took place in late Silurian times. Ages of 413 m.y. have been determined for appinites of Glen Creran and the lavas of Lorne and Glen Coe (Brown 1972) while an age of 415 m.y. for the Garabal Hill and Arrochar intrusions of the Loch Lomond cluster have been given by Briden (1970).

1.1 Theories of origin

The following is a summary of the theories proposed for the appinite suite in the Caledonides of Scotland and Ireland.

1. Hybridisation of solid ultramafic rocks or ultramafic magma with granitic magma (Deer 1935, 1950; Holgate 1950; Joplin 1959; Read 1961; Mercy 1965).
2. Limestone-granite reaction (Anderson 1937).

3. Crystallisation from a primary "basic" magma (Wyllie and Scott 1913) which Nockolds (1941) considered to be represented by pyroxene - mica diorite but which Money (1964) and Platten (1966) considered somewhat more basic. Nockolds (1941) further suggested that crystallisation differentiation resulted in the development, not only of the mafic - ultrabasic (appinite - diorite - pyroxenite - peridotite) association, but also of the much more voluminous granites. Earlier, Wyllie and Scott (1913) had interpreted the granitic rocks as having been developed from a separate magma. This is supported by recent studies (Hall 1966, 1972; Bell 1968; Pitcher and Berger 1972).
4. The development of mafic and ultramafic rocks by gravity differentiation followed by "appinitisation" of pyroxenic rocks and of metamorphic rocks of appropriate compositions. This involved their metamorphic recrystallisation to keep with physico-chemical conditions of the subsequent tenuous acid fluids (French 1966).
5. Crystallisation and magmatic differentiation in pipe-like intrusions of a gas-rich basaltic primary magma (Bowes *et al.* 1964; Ghaly 1964; Bowes and Wright 1967; Hall 1967; Groome and Hall 1974; Bowes and McArthur 1976; Wright and Bowes 1979).

Coarse-grained hornblendic rocks resulting from pegmatitic-type crystallisation associated with granitic rocks in the Channel Islands have also been referred to as being "appinites" (Wells and Bishop 1955). Such rocks appear to be quite different from the appinites originally defined by Bailey and Maufe (1916) and the mode of formation proposed by Wells and Bishop is not considered applicable in the case of the appinites of the Caledonides of Scotland and Ireland.

1.2 Scope of the present study

Following the mainly field-oriented studies in the Ballachulish and Loch Lomond districts reported by Bowes and Wright (1967), McArthur (1971) and Bowes and McArthur (1976), amongst others, there have been few laboratory-oriented studies to elucidate the petrogenesis of the appinite suite including the source of magma and crystallisation history. Wright and Bowes (1979) presented average major and trace element data for members of the suite but there are no known published data relating to mineral chemistry.

The present study represents a mainly geochemical approach to the petrogenesis of the appinite suite based largely on the field data and specimens collected in relation to the work referred to above.

Because of the variety of rock types present and of its significance as the type area, a considerable proportion of this study has been directed towards the appinite suite of the Ballachulish district. The large variety of rock types in a large number of the masses in the Loch Lomond district make the suite there ideal for study and for comparison with the Ballachulish rocks. Further comparison has been made using the information and material from Ardara, Colonsay and Sutherland in addition to the published information from there.

In view of the spatial and possible genetic relationships of the lamprophyre dykes, and the Lorne and Glen Coe lavas to the appinite suite of the Ballachulish and nearby districts, representative samples of these igneous masses have also been studied.

The major aims of this work were:

1. To determine magma genesis and relate it to a geotectonic environment.
2. To elucidate crystallisation conditions and histories of various members of the suite.

3. To establish which products of late Caledonian igneous activity (appinite, lamprophyre, lava *etc.*) were comagmatic.
4. To establish whether the appinite suite of S.W. Scotland developed under unique conditions or whether comparable magma genesis, emplacement and crystallisation conditions were widespread in the Caledonides.

1.3 Methods of study

Samples of representative suites of rocks from the Ballachulish and Loch Lomond districts, Colonsay, Sutherland and Donegal collected during previous work by Ghaly (1964), Bowes and Wright (1967) and McArthur (1971) were made available. These were supplemented by additional samples of the appinite suite in the Ballachulish district collected using the maps of Geological Survey (Sheet 53) and of Bowes and Wright (1967) and in Sutherland using the map of Geological Survey (Sheet 108). In addition suite representing the Glen Coe lavas were collected using the map of Geological Survey.

Petrographical observations were supplemented by modal analyses (estimated). Major and trace element data for 87 rock samples supplemented corresponding data for 120 rocks from the Ballachulish and Loch Lomond clusters supplied by D. R. Bowes and A. E. Wright. The new information has been obtained using spectrophotometric, flame photometric and atomic absorption methods (13 analyses - major elements) and X-ray fluorescence (67 analyses - major elements, 87 analyses -trace elements) - for analytical methods see Appendix A.1. Five hundred mineral analyses were carried out on the Cambridge 5 electron microprobe using EDS techniques, for 12 elements (see Appendix A.2 for methods). Of these selected analyses are given in the tables of Chapters 2-6, 9 and 12 and in Appendix B.1.

As an aid to the elucidation of petrogenesis, and in addition to the more commonly used plots of chemical data, modelling was carried out using the CMAS model (*cf.* Cox *et al.* 1979) in conjunction with the Data Reduction and Projection Scheme of O'Hara (1976), programmed by Giles (1980), and the ICL 2976 computer of the University of Glasgow; the background to this modelling is set out in Chapter 7.

XXXXX Modelling, using trace elements and major and trace elements was also carried out.

1.4 Plan of thesis

Following this introductory section (Part 1 - Chapter 1), the thesis is divided into four main parts. In Part 2 the Ballachulish appinite cluster is considered. Assessments of geological setting and petrography (Chapter 2) are followed by the mineral chemistry of olivine (Chapter 3), clinopyroxene (Chapter 4), amphibole (Chapter 5), mica (Chapter 6) and petrochemistry (Chapter 7). The final section of this part deals with the petrogenesis of the Ballachulish appinite suite (Chapter 8).

In Part 3 the Loch Lomond appinite cluster is considered in terms of its geological setting and petrography (Chapter 9) and rock chemistry (Chapter 10). In view of the general correspondence of petrographical and petrochemical characteristics of the appinites of this cluster with those of the Ballachulish cluster, the study made of mineral chemistry was in limited form and is included in the section of petrography. The final section of this part deals with the petrogenesis of the Loch Lomond appinite suite (Chapter 11).

Part 4 consists of comparative studies of appinites from Ardara (Donegal), Colonsay and Sutherland and of lavas (Chapter 12). Part 5 deals with tectonic setting and source of magma generation (Chapter 13) and conclusions (Chapter 14).

Appendices following the list of references, set out methods of rock analyses (Appendix A.1), mineral analyses (Appendix A.2), and data of mineral and rock analyses (Appendix B).

1.5 Major conclusions

While conclusions are set out in the relevant parts of the thesis, the following major conclusions are listed here to assist with the reading of the body of the thesis.

1. The appinite suites of the Ballachulish and Colonsay districts crystallised from a magma transitional between calcalkaline and alkaline (Chapter 7).
2. The appinite suite of the Loch Lomond district crystallised from a calcalkaline magma (Chapter 10).
3. The appinite suite of the Ardara district crystallised from a magma transitional between tholeiitic and calcalkaline (Chapter 12).
4. Olivine crystallised above 1600°C at a considerable depth before the magma entered into pipes (Chapter 3).
5. Clinopyroxene crystallised under conditions of increasing water pressure in the pipes (Chapter 4).
6. The large idiomorphic amphibole crystals in pipes of the Ballachulish cluster developed in a temperature range of 960°-770°C below 5 kb, and overgrowths on them in a temperature range of 790°-755°C at or above 5 kb P_{H_2O} (Chapter 5).
7. Phlogopite crystallised at a temperature of about 1000°C and P_{H_2O} of about 1 kb in the kentallenite of the Kentallen pipe while phlogopite and apatite appeared on the liquidus in a temperature range of 825°-770°C above 1 kb in the appinite of the Back Settlement pipe (Chapters 5 and 6).
8. The lamprophyres and lavas of the lower Old Red Sandstone magmatism (late Silurian) are genetically related to the appinite suite (Chapters 2, 7, 9, 12).
9. The scyelite - pyroxenite appinitic type rock association of Sutherland does not represent a cognate petrogenetic suite of rocks. Scyelites and SiO_2-poor appinitic type rocks are the products of

crystallisation differentiation from a basaltic magma and are genetically related to the appinite suite. Pyroxenites and SiO_2-rich appinitic type rocks represent the hybrids of Ach'uain type (Chapter 12).

10. The appinite suite of Western Scotland and northwestern Ireland represents magmatism associated with northwestward subduction. Variations in the magma compositions indicate that the Ballachulish and Colonsay masses developed towards relatively continental environments, the Ardara cluster towards an island arc environment and the Loch Lomond cluster in the environments intermediate between the other two (Chapter 13).

Figure 1.1 Distribution of the appinite suite, lavas and Newer granites of late Caledonian magmatism in Scotland and part of Ireland. (M.T. Moine thrust, G.G.F. Great Glen fault, H.B.F. Highland boundary fault, S.U.F Southern Uplands fault).

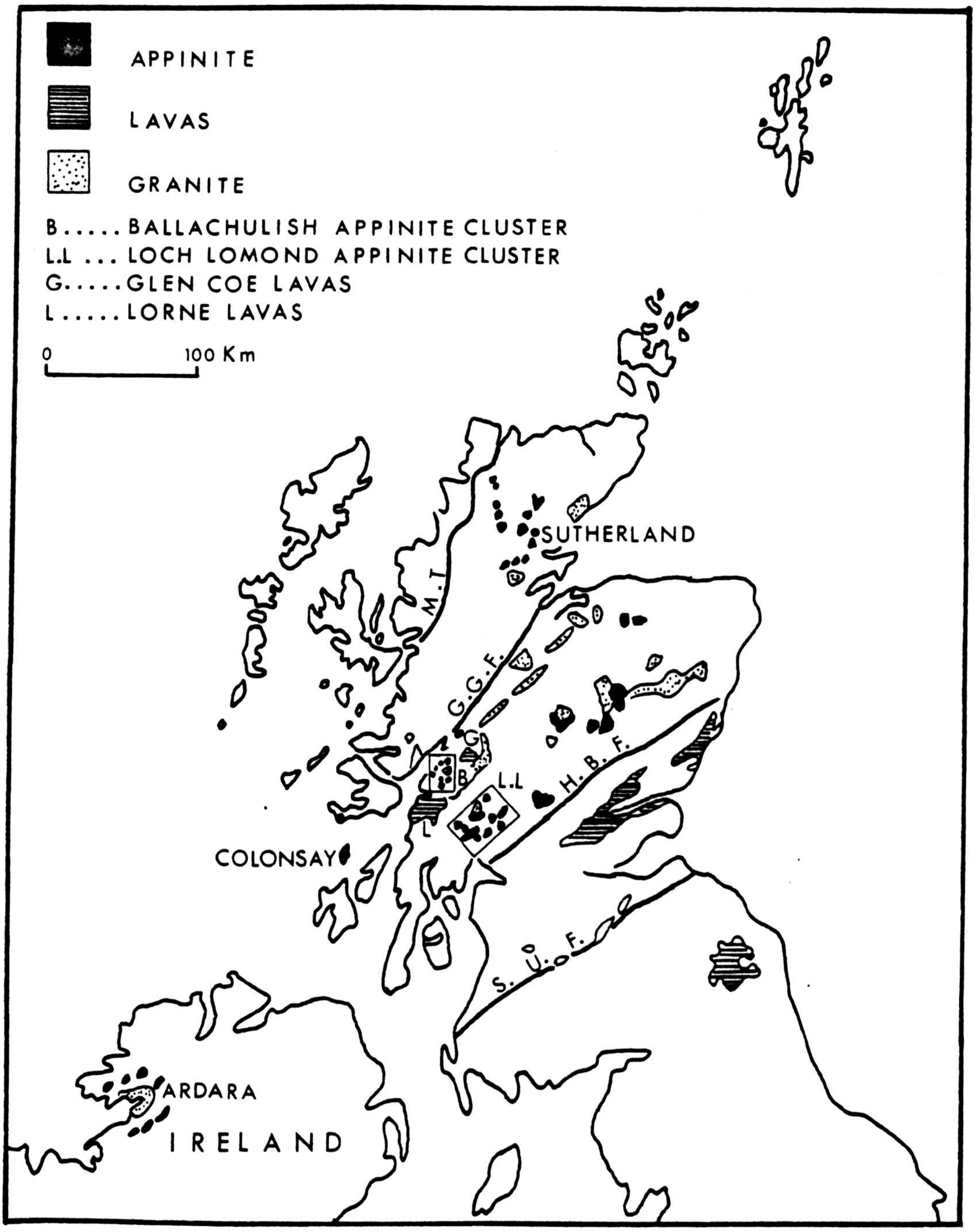
APPINITE
LAVAS
GRANITE
B.....BALLACHULISH APPINITE CLUSTER
L.L ...LOCH LOMOND APPINITE CLUSTER
G.....GLEN COE LAVAS
L.....LORNE LAVAS
0
100 Km
SUTHERLAND
M.T.
G.G.F.
G
B
L.L
L
H.B.F.
COLONSAY
S.U.F.
ARDARA
IRELAND

PART 2

BALLACHULISH APPINITE SUITE

CHAPTER 2 GEOLOGICAL SETTING AND PETROGRAPHY

2.1 Geological setting

Igneous-breccia masses of the Ballachulish appinite suite intrude into a variety of Dalradian metasediments in the district around the Ballachulish granite (Fig. 2.1). The field relations and structural control in pipes of the Kentallen-Ardsheal peninsula, north of the Ballachulish granite, have been dealt with by Bowes and Wright (1961, 1967) and Bowes (1962), in Gleann Chàrnan pipe by Bowes *et al.* (1963) and in pipes of the Glen Creran area by Bailey and Maufe (1960) and Platten (1966). Figure 2.2 sets out the distribution of igneous-breccia pipe masses in the Kentallen-Ardsheal peninsula district together with the main rock types present in various masses. Detailed maps and descriptions of the Back Settlement pipes are given by Bowes and Wright (1961, figs. 2, 3) while the description of other pipes on the Kentallen-Ardsheal peninsula are given by Bowes and Wright (1967, figs. 10, 12, 13, 14). Corresponding information for the Gleann Chàrnan masses are given by Bowes *et al.* (1963) and for the Glen Creran area masses by Bailey and Maufe (1960) and Platten (1966, fig. 3).

Major features relating to the location and emplacement of the Kentallen-Ardsheal peninsula pipes are:

1. The location of the pipes in the dome-shaped antiformal structural traps and along the regional cleavage and schistosity of the folded Dalradian rocks of the Cuil Bay Synform (Bowes and Wright 1967, map 1, fig. 15; also see Fig. 2.2).
2. The upward limit shown by the main pipe at Back Settlement indicating that it did not breach the surface (Bowes and Wright 1967, p. 121).

The main features in relation to the internal distribution of the Ballachulish appinite suite within the pipes are:

1. The association of variable amounts of breccia with igneous rocks in various pipes and the consistent breccia-igneous rock sequence of development.
2. The commonly observed sharp and vertical contacts as well as gradational contacts between country rocks, breccia and igneous rocks, *e.g.* the small pipe at Back Settlement and the large pipe at Rudha Mòr, respectively (Bowes Wright 1961, fig. 4, p. 297; Bowes and Wright 1967, p. 127 - 8).
3. The similar sequences of events shown by the Rudha Mòr, Ardsheal Hill - Lagnaha and Kentallen pipes, *i.e.* the formation of explosion - breccia, the emplacement of variable but generally volatile mafic - rich marginal types, the emplacement of diorite or kentallenite and, with the exception of the Kentallen pipe, the emplacement of leucocratic diorite.
4. The correspondence of events set out in 3 not only in the majority of the other pipes of the Kentallen - Ardsheal peninsula, but also in the Gleann Chàrnan pipe and in the Glen Creran pipes (Bowes and Wright 1967, p. 139; Bowes *et al.* 1963; Bailey and Maufe 1960; Platten 1966).
5. The development of lamprophyric margins of vogesitic mineralogy to the appinite of the large pipe at Back Settlement, the occurrence of lamprophyre as the major rock type and its gradational contact with the central appinite in the small pipe at Back Settlement (Bowes and Wright 1961, figs. 2,3; Bowes and McArthur 1976, fig. 2), the lamprophyric chilled marginal facies of spessartite composition

(Section 2.2A) in the Ardsheal Hill pipe (Walker 1927) and the chilled margins of kentallenite in the Kentallen pipe (Bowes and Wright 1967, fig. 14, p. 133).

6 . The presence of highly variable, gas-rich and usually ultramafic marginal rock types (*e.g.* Ardsheal Hill - Lagnaha, Rudha Mòr and Kentallen pipes, Fig. 2.2), the vertical banding in igneous rocks (*e.g.* in the pyroxene - mica diorite of the Rudha Mòr pipe and in the biotite hornblendite of the Ardsheal Hill pipe; Bowes and Wright 1967, p. 129, 130), the occurrence of highly carbonated and altered rocks in certain pipes (*e.g.* small pipes at Back Settlement and Rudha Mòr; Bowes and Wright 1961, p. 299; 1967, p. 129) and the presence of highly corroded blocks of breccia, mostly quartzite, in the pipes (*e.g.* Back Settlement, Rudha Mòr and Gleann Chàrnan pipes; Bowes and Wright 1961, 1967; Bowes *et al.* 1963) – all features indicative of considerable presence and movement of gas-rich phases.

7 . The close spatial and temporal relationship of the early lamprophyre dykes (vogesite and spessartite) with the igneous-breccia pipe masses (*e.g.* Kentallen and Rudha Mòr pipes) and their temporal separation from dykes of the other lamprophyric rocks (Bailey and Maufe 1960, p. 179, 195-202; Sheets 53, 62; Anderson 1935; Bowes 1962 , p. 119, fig. 1; Bowes and Wright 1967, fig. 10).

Specific features which are significant in the present study are:

1. The evidence for considerable gas-streaming and for crystallisation under high gas pressure in the pipes (Chapters 5, 6).
2. The evidence for variations of physical conditions in the pipes (Chapters 3, 4, 5, 6).
3. The generally corresponding crystallisation histories in the Ardsheal Hill - Lagnaha, Rudha Mòr and Kentallen pipes (and in many other pipes of the region) pointing to evolution from a common parent liquid (Chapter 7).

4. The chilled marginal facies associated with various rock types in the Kentallen, Ardsheal Hill and Back Settlement pipes, expected to be compositionally closer to the parent liquid (Chapters 3, 7).
5. The close spatial and temporal relationship of the early lamprophyre dykes with the igneous - breccia pipes of the appinite suite; these dykes are expected to indicate a genetic relationship with the appinite suite on the basis of chemical evidence (Chapter 7).

The overall model proposed for the emplacement and petrogenesis of the appinite suite (mainly after Bowes and Wright 1967 and Bowes and McArthur 1976) is summarised as follows:-

1. The uprise of gas-rich magma facilitated by regional structure including cleavage and schistocity.
2. Magma impeded by structural traps.
3. Explosive activity with shattering and brecciation of the country rock, mostly quartzite.
4. Emplacement of variable but generally mafic- and volatile-rich-types (including biotite·pyroxenite or hornblendite and appinite) under high gas pressure in the pipes.
5. Emplacement of kentallenite and pyroxene - mica diorite under low gas pressure in the pipes.
6. Emplacement of leucodiorite and granodiorite (or syenite, *i.e.* in Gleann Charnan pipe).

At the present level of erosion the majority of the pipes show mainly the products of events 4 and 5. The early lamprophyres are the hypabyssal equivalents of the various members of the appinite suite.

2.2 Petrography

The petrography of various rock types has also been described by several workers (Bailey and Maufe 1960; Bowes and Wright 1961; Bowes *et al.* 1963, 1964; Platten 1966; Bowes and McArthur 1976). Here only representative rock types (Table 2.1) are described from the selected pipes shown in Figure 2.1 with particular reference to features related to varying physical conditions in the pipes.

There is a very broad range of textural and mineralogical variation and in many cases determination of the precise limits of various rock types is very difficult. The following are some significant petrographic features of the appinite suite, particularly in the Ballachulish district.

1. There are both "hydrous" and "anhydrous" mineral assemblages, *e.g.* appinite and kentallenite, respectively (Figs. 2.3a, b).
2. Marked variation is shown in grain size, from large phenocrysts to small grains of olivine, clinopyroxene, amphibole and mica (*cf.* Figs. 2.3b, 2.4a).
3. Some minerals including olivine, clinopyroxene, amphibole and mica are highly zoned (Figs. 2.4a, b; also see Figs. 2.6a, 2.8c, 2.10c).
4. Rhythmic amphibole overgrowths occur on both stumpy and acicular idiomorphic hornblende crystals and there is the development of the "overgrowth-type" features on biotite. These features are seen in appinite and are particularly well shown in the Back Settlement pipe (Figs. 2.5a - c, 2.6a - b).
5. There are three habits of diopside in appinite, (i) as cores of the idiomorphic hornblende crystals, (ii) as grains in the groundmass and (iii) phenocrysts devoid of a rim of amphibole (Figs. 2.5b, 2.7a, b, c).
6. There are expressions of different reaction-relationships between various phenocrysts and liquids, represented by the highly resorbed nature of olivine, clinopyroxene and amphibole, the development of an orthopyroxene rim on olivine (in kentallenite) and the replacement of clinopyroxene by amphibole (in appinite and pyroxene - mica diorite) (Figs. 2.8a - c).

7. Plagioclase, as phenocryst, is almost exclusively only in the acidic types.
8. Granophyric and myrmekitic textures between feldspar and quartz occur in groundmass of hornblende diorite and leucocratic diorite.
9. Most of the minerals of the Bowen's reaction discontinuous series are present in some rocks with minerals high in the reaction series generally surrounded by minerals lower in the reaction series but with some instances of the reverse (*e.g.* phlogopite and biotite in clinopyroxene and amphibole; Figs. 2.4a, 2.5a, 2.7b).
10. There is a common association of particular accessory minerals with particular essential minerals, (i) primary magnetite and apatite with pargasite (Figs. 2.3a, 2.7a), (ii) primary sphene with actinolitic overgrowths (in appinite) and (iii) primary magnetite with clinopyroxene (Fig. 2.4a) (in both kentallenite and the lamprophyric marginal facies of the Ardsheal Hill pipe).
11. In many cases primary minerals show marked alterations, *e.g.* olivine altered to serpentine and magnetite, clinopyroxene to serpentine and uralite, amphibole to chlorite and magnetite (Fig. 2.9) and biotite to chlorite and epidote.
12. Both primary and secondary calcite occurs (in appinites and lamprophyres of the Back Settlement and Rudha Mòr pipes) (Fig. 2.5b).
13. Some biotite shows kink bands (in appinite from the small pipe at Back Settlement) (Fig. 2.6b).

2.2A General petrography of the rock types

Marginal ultramafic rocks

Mineralogically this group ranges from biotite - pyroxene - hornblende - feldspar rock (Rudha Mòr pipe, Table 2.1 – 1) through biotite pyroxenite/biotite hornblendite (Kentallen pipe, Table 2.1 – 2,3) to hornblendite (Ardsheal Hill pipe) which, in turn, grades to appinite with increasing feldspathic constituents.

The marginal ultramafic type of the Rudha Mòr pipe is made up of large platy amphibole, clinopyroxene, phlogopite, olivine and feldspar. Amphibole is pargasite which has thin actinolitic rims. It poikilitically encloses clinopyroxene and serpentinised olivine. Large and strongly zoned clinopyroxene crystals showing hourglass structure (Kerr 1959) also occur. Phlogopite surrounding amphibole and clinopyroxene shows kink bands and inclusions of apatite. Feldspar is mainly albite $(An_{<10})$ and is confined to interstices.

Appinite

The appinite (*cf*. Fig. 2.3a, Table 2.1 – 4) consists of acicular and stumpy idiomorphic pargasite, weakly to intensively zoned (*cf*. Fig. 2.4b) with rhythmic overgrowths varying from actinolite - ferro-actinolite to actinolitic - hornblende in composition (Chapter 5) set in a groundmass composed of clinopyroxene biotite, feldspar, quartz and primary calcite. The pargasite usually has a diopside core (Figs. 2.5a - b, 2.7a - b; Bowes *et al*. 1964, fig. 1). These features are characteristic of the appinite from the Back Settlement and some other pipes of the Kentallen - Ardsheal peninsula (*e.g*. Lagnaha pipe). However, overgrowths of actinolite developed on pargasite are also occasionally observed in appinite from the Gleann Chàrnan and Garbh Allt pipes and in cortlanditic appinite from the Màm na Stainge pipe (Fig. 2.5c). In the Garbh Allt pipe thin brownish-green and brown lines parallel to (110) and $(\overline{1}\overline{1}0)$ cleavages on pargasite, probably related to TiO_2 mobility due to Cruachan granite (*cf*. Fig. 2.1), are observed. Pseudomorphs of chlorite speckled with magnetite after amphibole are observed in appinite wherever the rock is carbonated (*cf*. Fig. 2.9).

The clinopyroxene both in the core of pargasite and in the groundmass is compositionally diopside (Figs. 2.5a - b, 2.7a - b; Chapter 4). It is corroded at its margins and is highly fractured particularly in the groundmass. Replacement of clinopyroxene by amphibole varies from a thin to a wide rim on the margins (*cf*. Figs. 2.8b, c). However, phenocrysts of clinopyroxene completely devoid of a rim of amphibole have also been noticed in appinite of the Back Settlement pipe (Fig. 2.7c). Common alteration of clinopyroxene to serpentine and uralite, and rarely to chlorite are observed.

Pale yellow to deep brown biotite surrounding amphibole, intergrown with it, and also occurring in its core occurs (Figs. 2.5a, 2.7b). It alters to chlorite and epidote. In the biotite-rich appinite (Back Settlement - small pipe) zoned and kink-banded biotite with an "overgrowth-type" feature is also observed (Fig. 2.6a, b).

The feldspars are orthoclase and albite (Table 2.2 – 1, 4, 6). Most is confined to the groundmass with interstitial quartz and primary calcite. Albite occasionally occurs in the green rim of pargasite (Fig. 2.7a).

Primary magnetite, sphene (Table 2.2 – 13, 14) and apatite are common accessories. Magnetite and apatite usually occur in the pargasite core (Figs. 2.3a, 2.7a) while sphene is partially surrounded by actinolitic overgrowths. Secondary calcite replacing feldspars and biotite also occurs in appinite of the small pipes at Back Settlement and Rudha Mòr.

Kentallenite

The kentallenite (*cf*. Fig. 2.3b, Table 2.1 – 6) named by Hill and Kynaston (1900) after the village of Kentallen, is composed of olivine, clinopyroxene and phlogopite phenocrysts set in a groundmass of phlogopite and feldspar.

Olivine (Fo_{83-77}) is compositionally zoned (*cf*. Fig. 3.1b). It is corroded at its margins, fractured, partially serpentinised and is surrounded by a reaction rim of orthopyroxene (Fig. 2.8a; Table 2.2 – 12). This reaction rim occurs in the kentallenite of both the Kentallen and the Barnamuc pipes.

Clinopyroxene (diopside, Chapter 4) is strongly zoned. Small grains of olivine, phlogopite, feldspar and primary magnetite occur in the clinopyroxene phenocrysts (Fig. 2.4a).

Zoned phlogopite (Chapter 6), usually associated with primary magnetite, surrounds olivine and clinopyroxene.

Anorthoclase (Table 2.2 – 5) is the dominant feldspar in the coarse-grained kentallenite. Where fresh, it occurs as large crystals with perfect (001) and less perfect (010) cleavages and shows polysynthetic twinning. Fine-grained and lamellar plagioclase (Table 2.2 –9) on the other hand, is the dominant feldspar of the microkentallenites.

Pyroxene - mica diorite

The pyroxene - mica diorite (Table 2.1 – 7) consists of large diopside phenocrysts (Chapter 4) which are strongly zoned, fractured and corroded at their margins. They are generally surrounded by biotite (Chapter 6) and chlorite after biotite, and occur in a groundmass made up of biotite, amphibole (pargasite with overgrowths of various compositions, Chapter 5), plagioclase and orthoclase (Table 2.2 – 2, 7, 10) . Diopside phenocrysts surrounded and replaced by amphibole, occasionally producing a pepper-mesh-like structure, have also been observed (Fig. 2.8c). Small grains of olivine present in some of the varieties are parallel to the zones in the cores of diopside phenocrysts (*cf.* Fig. 2.4a).

Pyroxene - hornblende - mica diorite

The pyroxene - hornblende - mica diorite has mineralogy between that of appinite and pyroxene - mica diorite (Table 2.1 –8). In the Ardsheal Hill pipe it is the dominant rock type. Amphibole-rich varieties have a high proportion of microcline which shows polysynthetic twinning and grid-iron structure.

Cortlandite

Cortlandite was originally defined as a rock mineralogically between dunite and hornblendite (Bailey and Maufe 1916) but used by

Bailey and Maufe (1960) to refer to a coarse-grained olivine - augite - hornblende rock. It is not a common rock in the Ballachulish district. The kentallenitic appinite of the Ardsheal Hill pipe (Table 2.1 – 5) approaches the original definition except that it contains a high proportion of feldspar. It is composed of platy amphibole crystals poikilitically enclosing olivine, clinopyroxene and phlogopite. Feldspar is mostly interstitial. In the cortlanditic appinite of the Màm na Stainge pipe are olivine and pleochroic hypersthene poikilitically enclosed in large hornblende crystals (Fig. 2.5c).

Leucocratic diorite and granodiorite

Leucocratic diorite and granodiorite (Table 2.1 – 9) has phenocrysts of plagioclase$_{(An_{20})}$ in a groundmass of orthoclase, quartz, biotite, primary sphene, apatite, magnetite, secondary calcite and chlorite and epidote after biotite. Plagioclase phenocrysts are zoned and twinned. Prismatic biotite grains, occasionally showing zoning and kink bands occur in the granodiorite of the Rudha Mòr pipe. Myrmekitic and graphic textures between quartz and feldspar are observed in the granodiorite of the Rudha Mòr and Ardsheal Hill pipes. The secondary calcite preferentially replaces plagioclase and biotite.

Hornblende syenite

The hornblende syenite (Gleann Chàrnan pipe) is mineralogically similar to appinite, except for a higher proportion of orthoclase.

Lamprophyres

The lamprophyre in the Back Settlement pipe is vogesitic in mineralogy (Table 2.1 – 10, Fig. 2.10a) (Streckeisen 1979). It shows a clear gradation to appinite (Fig. 2.10b) and is similar to it except for the grain size. Overgrowths of actinolite are observed on pargasite microphenocrysts. Clinopyroxene occurs in the cores of the pargasite crystals as well as in the groundmass. Pleochroic biotite with zones and kink bands, as in appinite (Figs. 2.6a, b), is also common in this rock.

The lamprophyric marginal facies of the Ardsheal Hill pipe is spessartitic (Streckeisen 1979). Both olivine-free and olivine-bearing spessartite occur. The olivine-free spessartite (Table 2.1 — 14) has zoned clinopyroxene as the only phenocryst (*cf*. Fig. 2.10c). Clinopyroxene also occurs in the fine-grained matrix with amphibole, biotite and feldspars (Table 2.2 — 3, 8, 11) and magnetite. Amphibole occurs as thin rims and off-shoots around the diopside phenocrysts producing bostonitic structure (Johanson 1931). With increasing feldspathic minerals this variety grades to andesitic lamprophyre (Table 2.1 — 15).

The olivine-bearing spessartite is similar to olivine-free spessartite except for the presence of phenocrysts of olivine (Chapter 3) in addition to those of clinopyroxene. Small grains of olivine and feldspar occur parallel to the zones in the core of clinopyroxene phenocrysts (Fig. 2.10c).

The early lamprophyric dykes and sheets, closely associated in time and space with pipes of the appinite suite (Kentallen and Rudha Mòr pipe, Table 2.1 — 13) are mineralogically very similar to olivine-free spessartite of the Ardsheal Hill lamprophyric marginal facies (Table 2.1 — 14). However, in some places, due to the predominance of amphibole over clinopyroxene, they compositionally approach vogesitic lamprophyre found at the margins of the appinite in the Back Settlement pipe (Table 2.1 — 10). The petrographic similarities of the early lamprophyres with appinites have been discussed by Bailey and Maufe 1960, p. 194, 227).

The later porphyrite and microdiorite dykes of the district are quite different from the early lamprophyres and appinites. They are considered to be too much feldspathic to be referred to as lamprophyres (Bailey and Maufe 1960, p. 227 - 30).

2.2B Discussion

Assessment of features of field relations and petrography observed by previous workers, and supplemented by new observations, permit many petrogenetic aspects of the appinite suite to be determined.

The very broad range of textural and mineralogical variation, the gradation from variety to variety, the existence of minerals commonly found in rocks of the basaltic suites (olivine clinopyroxene, plagioclase) and the high modal proportions of hydrous and volatile-bearing minerals (amphibole, biotite, apatite, calcite and opaque ores) indicate that the rocks of the appinite suite have been crystallised from a volatile-rich basaltic magma under varying conditions of crystallisation.

The petrography of the suite does not completely coincide with any particular type of basaltic rock association but has complex textural and mineralogical characters. The scarcity of olivine in the groundmass, the absence of titaniferous augite and of true alkali-minerals like nepheline and leucite in the rocks of the appinite suite discriminate it from a true alkali olivine basalt series (MacDonald and Katsura 1964). The presence of olivine phenocrysts, high modal percentage of amphibole and pleochroic hypersthene (Mâm na Stainge pipe) relate the suite to the calcalkaline rock series (Arculus and Curran 1972; Wyllie 1973; Ringwood 1974). However, the higher proportion of phlogopite, biotite and potassium feldspar discriminate the suite from rocks of the normal calcalkaline series.

The presence of a number of highly zoned minerals (Figs. 2.4a - b, 2.6a), the rhythmic amphibole overgrowths (Figs. 2.5a - c), the "overgrowth-type" features developed on biotite (Figs. 2.6a - b), the products of different reaction relationships between minerals and liquid (Figs. 2.8a - c) and both the normal and reverse order of appearance of minerals of the Bowen's discontinuous reaction series in rocks of the appinite suite, all indicate that crystallisation occurred under extremely varying physical conditions. These conditions have been deduced by comparison with the experimental studies of high water pressure crystallisation of basaltic magma (Bowes and Wright 1967, fig. 16). The development of the rhythmic amphibole overgrowths on hornblende crystals with pyroxene in the hornblende core and in the rock matrix in appinite has been explained by increasing gas pressure followed by rhythmic variations and subsequent sudden drop in the gas pressure (Bowes and Wright 1967; Bowes and McArthur 1976, fig. 10). The alternating green and colourless bands of actinolitic overgrowths on hornblende crystals (Figs. 2.5a - c; also see Fig. 5.2a) differ from actinolite and tremolite occurring in irregular fibrous shapes as a product of alteration of clinopyroxene and hornblende mostly produced due to later gas-streaming in the pipes. The later gas-streaming took place along with the development of chlorite pseudomorphs after amphibole in which the original areas occupied by pargasite and actinolitic overgrowths can still be distinguished (Fig. 2.9). These features support the interpretation of Bowes *et al.* (1964) that these overgrowths represent the products of igneous crystallisation.

The crystallisation of clinopyroxene phenocrysts devoid of a rim of amphibole has been attributed to reversion from amphibole to pyroxene due to a great decrease in the water content of the magma (Bowes *et al.* 1964, p. 972). However, these phenocrysts are extremely fractured (Fig. 2.7c) indicating that they were effected by the major events of build-up and release of gas pressure which developed overgrowths on hornblende crystals. This shows that these phenocrysts crystallised before amphibole. The lack of amphibole rim may be related to the later corrosion of amphibole from these phenocrysts.

The association of primary magnetite and apatite with hornblende (Figs. 2.3a, 2.7a) and sphene with amphibole overgrowths in appinite also indicates high gas pressure. The occurrence of some primary magnetite and phlogopite in the cores of zoned clinopyroxene phenocrysts (Fig. 2.4a) and a high modal proportion of phlogopite associated with primary magnetite surrounding clinopyroxene phenocrysts and occurring in the rock matrix in kentallenite (*cf.* Fig. 2.3b) indicate that the gas pressure increased after the crystallisation of clinopyroxene in kentallenite.

Although most of the calcite in appinite is of primary origin (*cf.* Fig. 2.5b), secondary calcite also occurs in appinite, lamprophyre and granodiorite, replacing feldspar and biotite particularly in the small pipes at Back Settlement and Rudha Mòr (see Section 2.2A). The secondary calcite has been developed as a result of post solidification gas-streaming (carbonation). Gas-streaming (hydration) was also responsible for the development of the high proportions of serpentine after olivine and clinopyroxene, uralite after clinopyroxene and amphibole, chlorite after amphibole and chlorite and epidote after biotite in rocks of the above pipes.

The petrographic similarities of the rocks of the appinite suite and of their chilled margins with the early lamprophyre dykes, which themselves represent a wide variation in mineralogy, such as shown by the earlier suite, indicate that the early lamprophyre dykes represent successive off-shoots by the various members of the appinite suite.

2.3 Conclusions

1. Structural control of the surrounding country rocks has played an important role in the evolution of the rock types in pipes of the Ballachulish appinite suite.
2. The generalised sequence of events in Rudha Mòr and Ardsheal Hill - Lagnaha pipes was (i) the formation of explosion - breccia, (ii) the emplacement of volatile and mafic-rich marginal types, (iii) the emplacement of kentallenite or diorite and (iv) the emplacement of leucocratic diorite or granodiorite. Other pipes show only some

of the corresponding events at the present level of erosion.

3. The early lamprophyres show close spatial and temporal relationships with the rocks of the appinite suite while the N-E - trending porphyrite dykes are of later age than the appinite suite and the early lamprophyres.
4. On the basis of petrography the Ballachulish appinite suite stands midway between alkaline and calcalkaline series.
5. The textural and mineralogical characters of the rocks indicate crystallisation under highly variable gas pressure. Rocks with higher proportions of hydrous minerals (marginal hornblendite and appinite) reflect higher gas pressure while rocks with higher proportions of anhydrous minerals (kentallenite and pyroxene - mica diorite) reflect lower gas pressure.
6. Minerals have generally crystallised according to the normal order of the Bowen's discontinuous reaction series. With some instances of the reverse order, this indicates variable gas pressure.
7. Rhythmic actinolitic overgrowths on pargasite crystals (in appinite) are the products of igneous crystallisation. Their rhythms represent fluctuation in gas pressure.
8. Two habits of diopside in appinite, as in cores of idiomorphic hornblende crystals and as grains in the groundmass, represent identical crystallisation conditions.
9. Diopside phenocrysts devoid of the amphibole rim in appinite of the Back Settlement pipe probably crystallised before amphibole.
10. The abundance of phlogopite and associated magnetite surrounding clinopyroxene phenocrysts in kentallenite, indicate increasing gas pressure.
11. Most of the calcite in appinite is of primary origin. Secondary calcite, serpentine, uralite, chlorite and epidote in certain rocks of the small pipes at Back Settlement and Rudha Mòr, reflect

post-crystallisation gas streaming in these pipes.

12. The early lamprophyre dykes are the hypabyssal equivalents of the rocks of the appinite suite. Vogesite corresponds with appinite, spessartite with kentallenite and pyroxene - mica diorite and probably some felsite dykes with leucocratic diorite and granodiorite.

Figure 2.1. Outline geological map of the Ballachulish district showing the distribution of the appinite suite; based on Sheet 53 (Ben Nevis and Glen Coe) of Geological Survey of Great Britain and Bowes and Wright (1967).

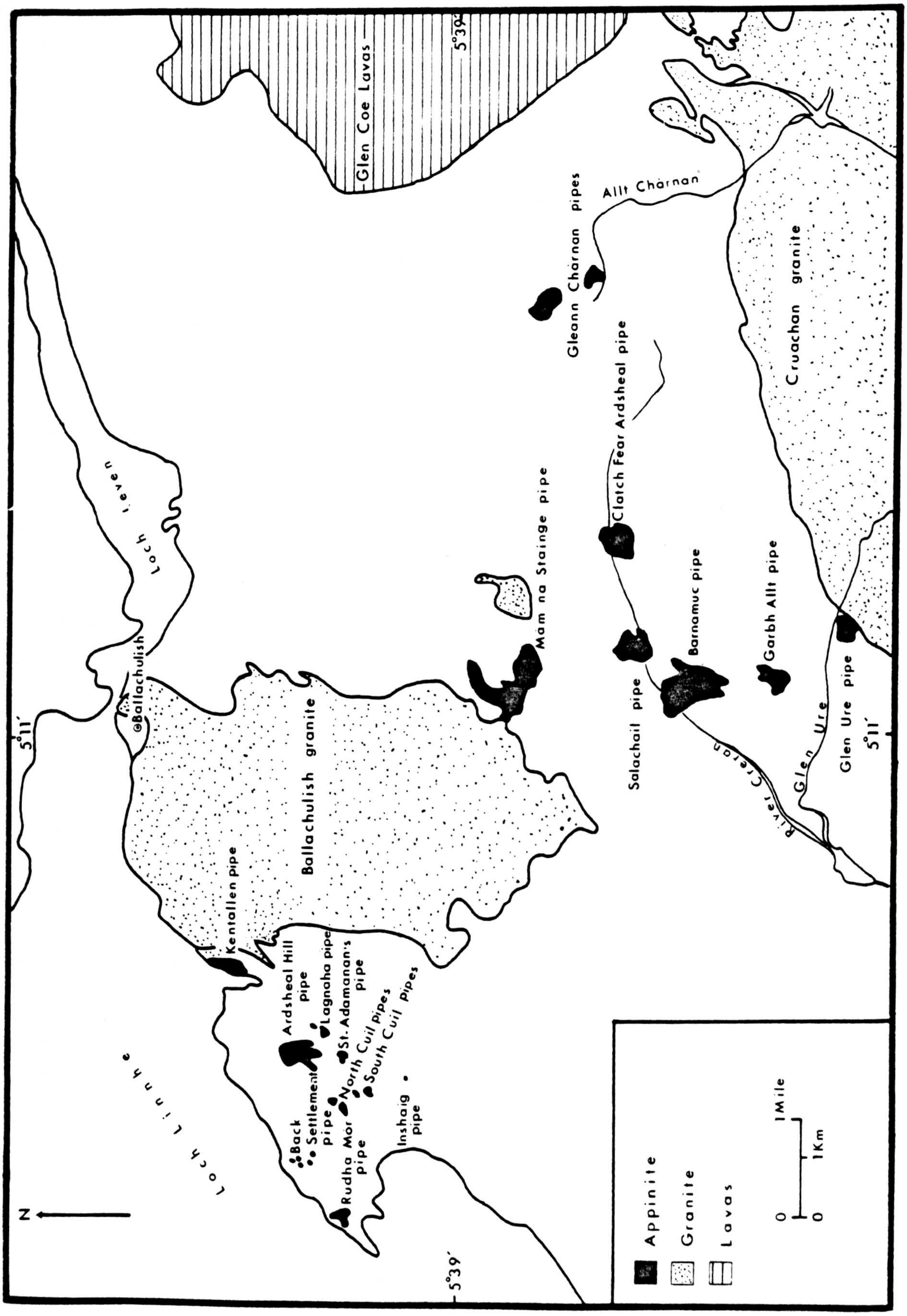
Glen Coe Lavas
5°39'
Allt Chàrnan
Gleann Chàrnan pipes
Cruachan granite
Clatch Fear Ardsheal pipe
Mam na Stainge pipe
Loch Leven
Ballachulish
5°11'
Ballachulish granite
Barnamuc pipe
Garbh Allt pipe
Salachail pipe
River Creran
Glen Ure
Glen Ure pipe
5°11'
Kentallen pipe
Ardsheal Hill pipe
Lagnaha pipe
St. Adamanan's pipe
North Cuil pipes
South Cuil pipes
Back Settlement pipe
Rudha Mòr pipe
Inshaig pipe
Loch Linnhe
N
5°39'
Appinite
Granite
Lavas
0 1 Mile
0 1 Km

Figure 2.2. The distribution of igneous-breccia pipe masses in the Kentallen-Ardsheal peninsula (reproduction of Bowes and Wright 1967, map 1).

D. R. Bowes, "The Explosion-breccia Pipes near Kentallen, Scotland, and their geological setting".

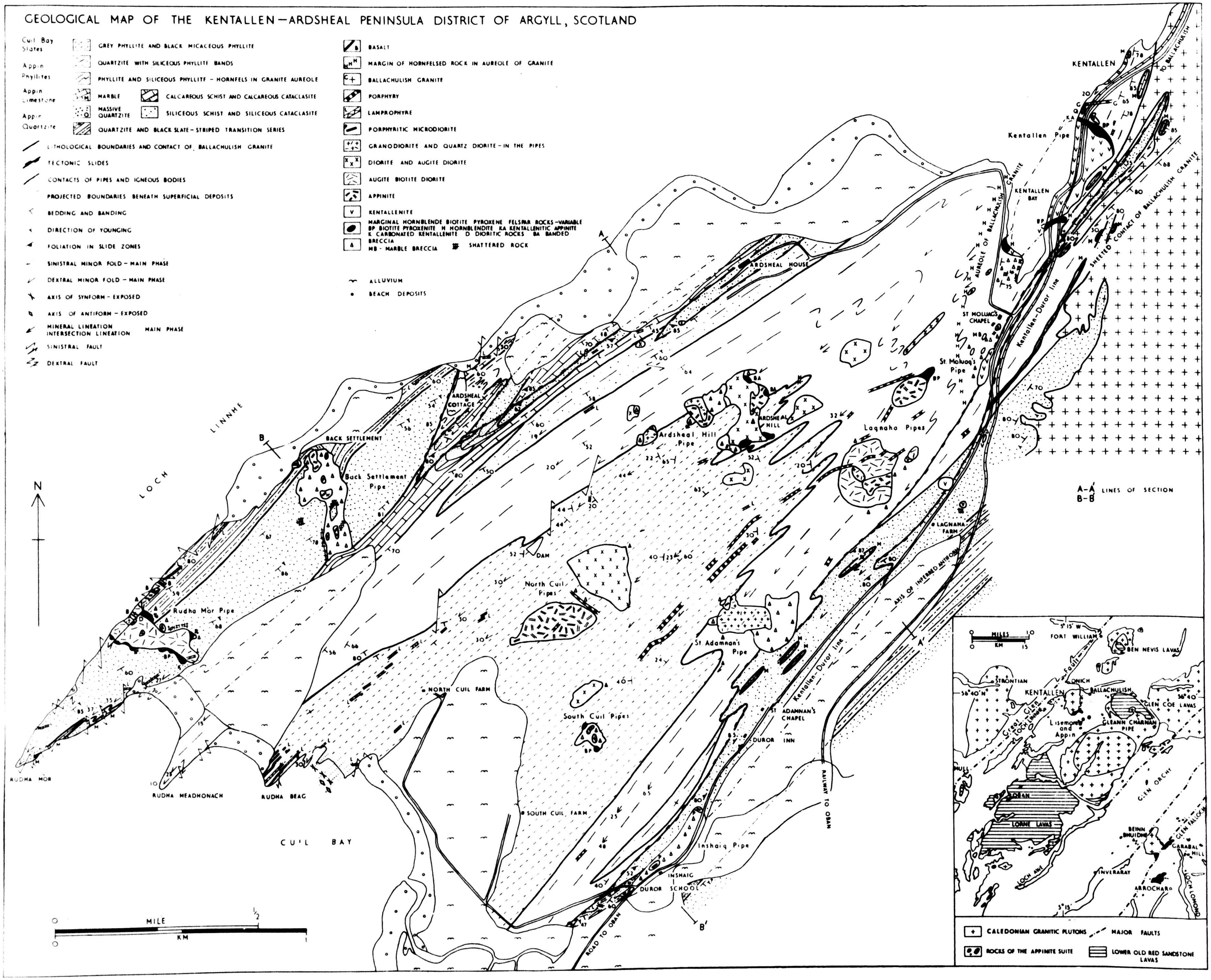

Figure 2.3.

(a) Appinite, showing idiomorphic pargasite crystals (P) in a groundmass of feldspar and quartz (clear). Minute grains of magnetite (very dark) associated with pargasite can also be seen; Back Settlement pipe. PPL x 10.

(b) Kentallenite showing phenocrysts of olivine (Ol), diopside (D) and phlogopite (Ph) in a groundmass of feldspar and phlogopite; Kentallen pipe. PPL x 10.

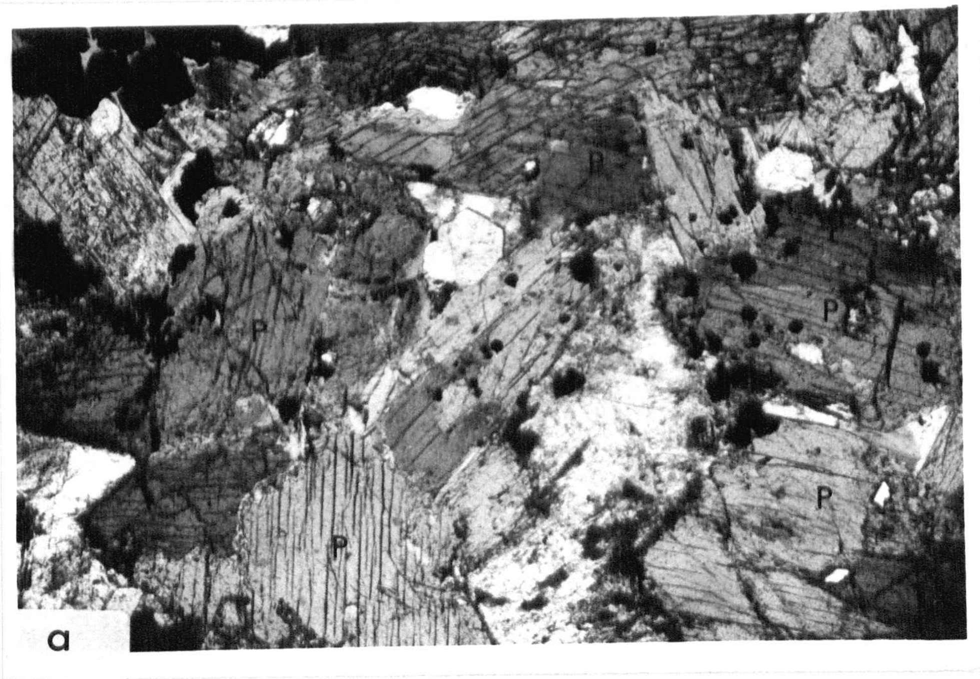
P
P
P
P
P
a


D
D
D
Ph
Ol
Ph
b

Figure 2.4.

(a) Zoned diopside with small crystals of olivine (fractured) and inclusions of phlogopite (grey), magnetite (very dark) and feldspar (clear) in a groundmass of phlogopite, feldspar and magnetite. Phenocrysts and highly corroded small crystals of olivine (fractured) can also be seen; kentallenite, Kentallen pipe. XN x 7.

(b) Zoned pargasite, biotite - appinite, Rudha Mòr. XN x 39.

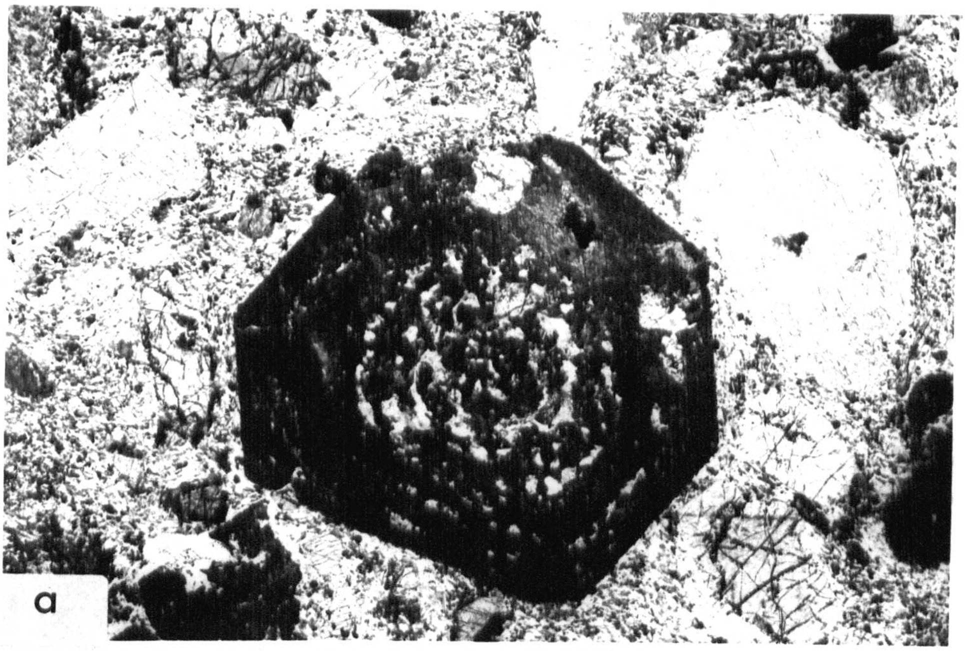
a

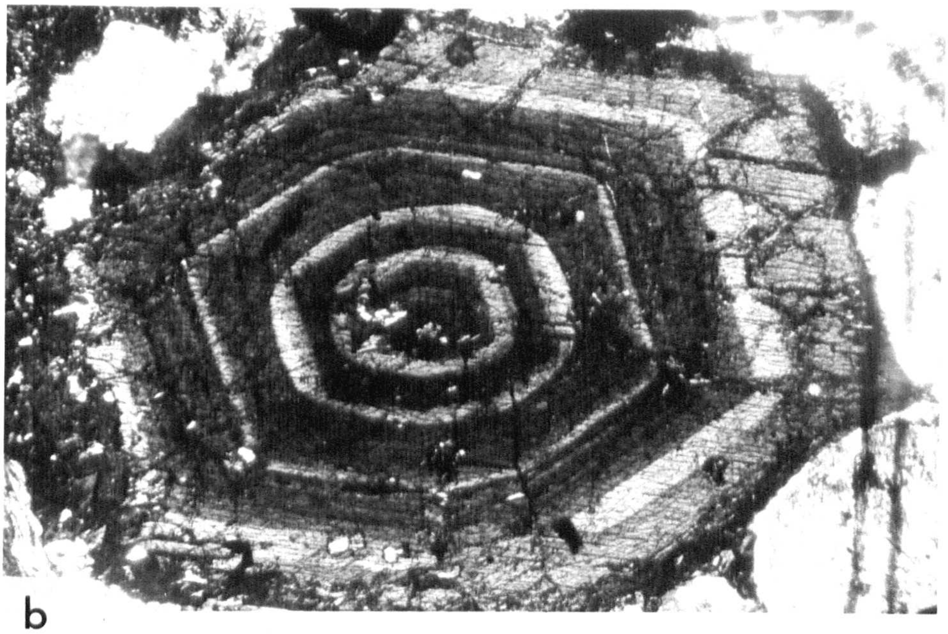
b

Figure 2.5.

(a) Rhythmic overgrowths of actinolite (A) on pargasite (P). Grains of biotite (B) and diopside (D) occurring as core to pargasite can also be seen; appinite, Back Settlement. PPL x 31.

(b) Two pargasite crystals (dark) with actinolitic overgrowths (A) and diopside cores (D). Pargasite on the left has a much larger overgrowth on terminal face. Pargasite on the right has a "sawtooth" shaped overgrowth (Bowes *et al.* 1964) with a thin discontinuous rim on prismatic face. Primary calcite (C) interstitial to all minerals in the groundmass is also seen; appinite, Back Settlement. PPL x 31.

(c) Part of a large pargasite phenocryst (P) with overgrowths of actinolite (A). Olivine (Ol), hypersthene (H) and feldspar can be seen in pargasite; cortlanditic appinite, Màm na Stainge. PPL x 10.

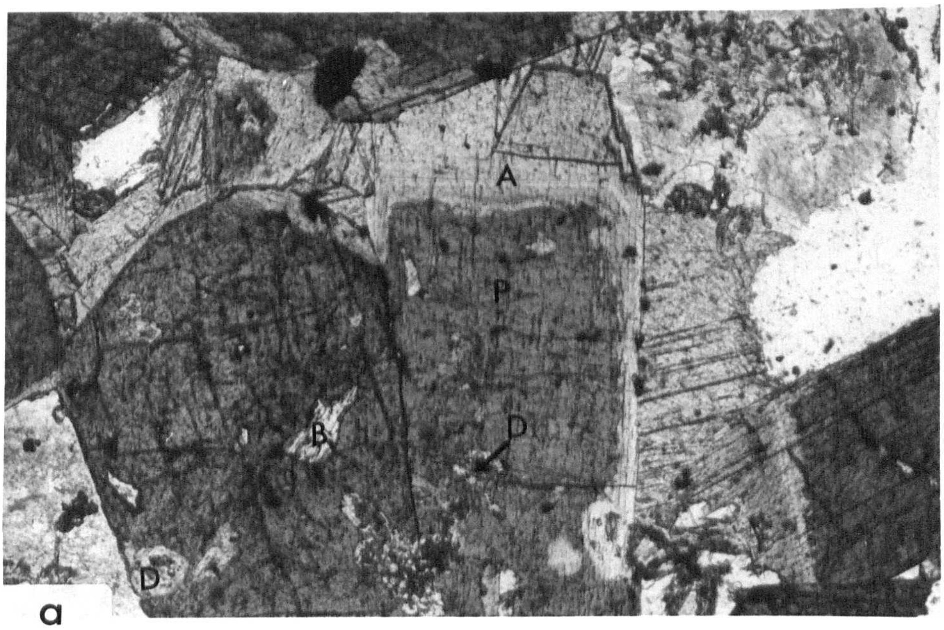

a

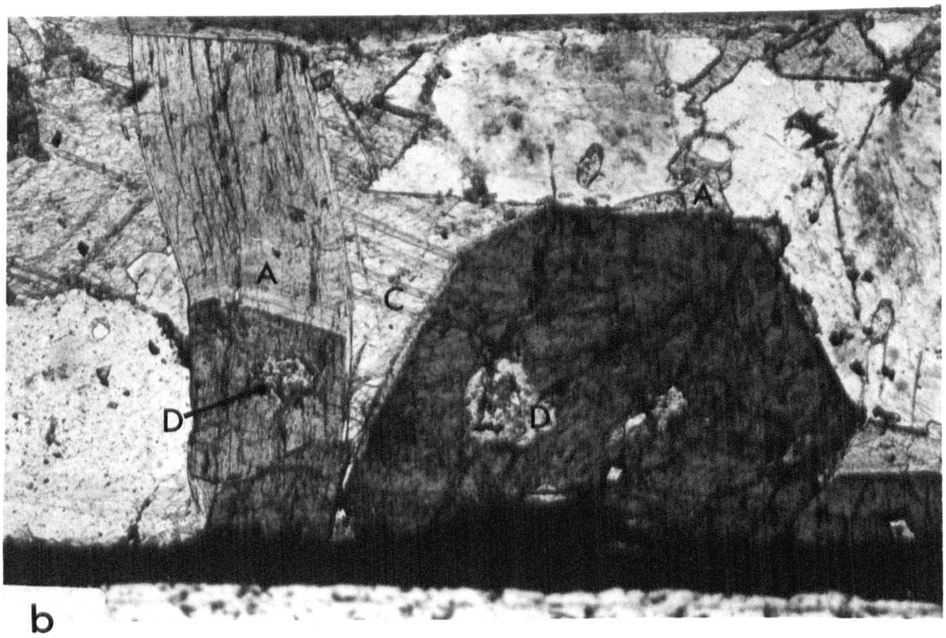

b

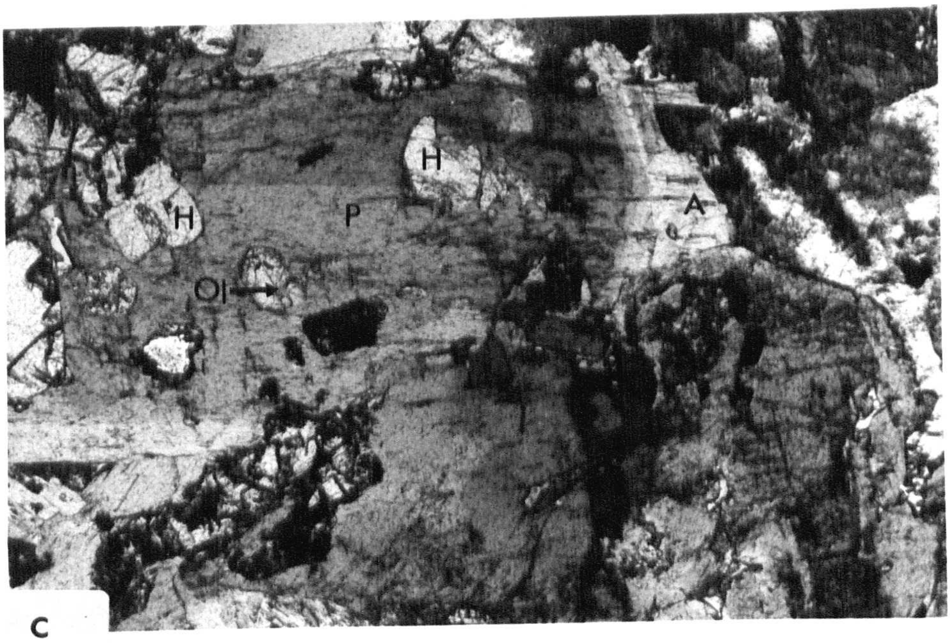

c

Figure 2.6.

(a) Zoned biotite (B) with an "overgrowth-type" feature (BO) developed on it; appinite, small pipe, Back Settlement. PPL x 50.

(b) Biotite, showing "overgrowth - type" feature (BO) and kink bands, from the same specimen as in Figure 2.6a. PPL x 63.

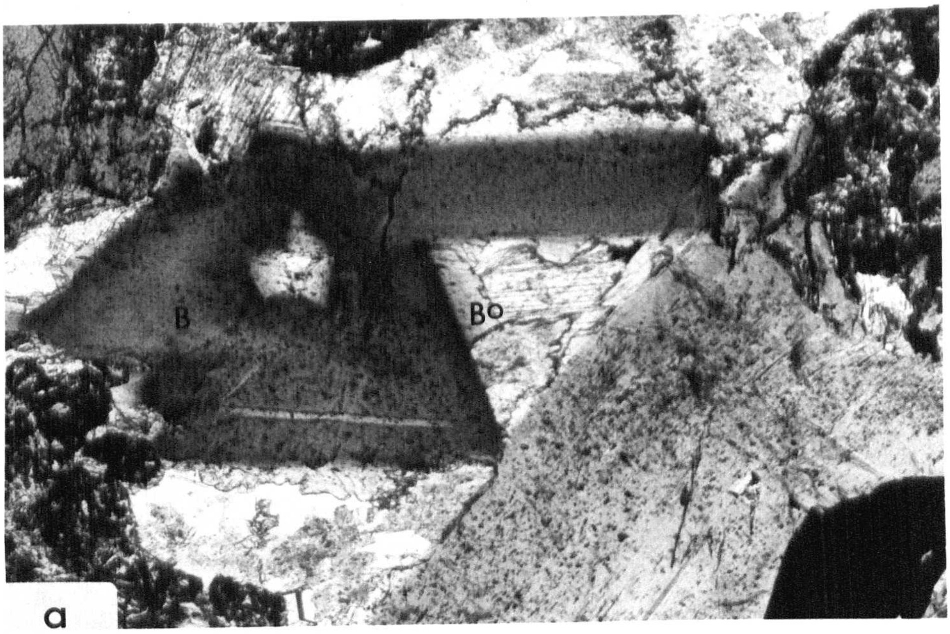
B
Bo
a

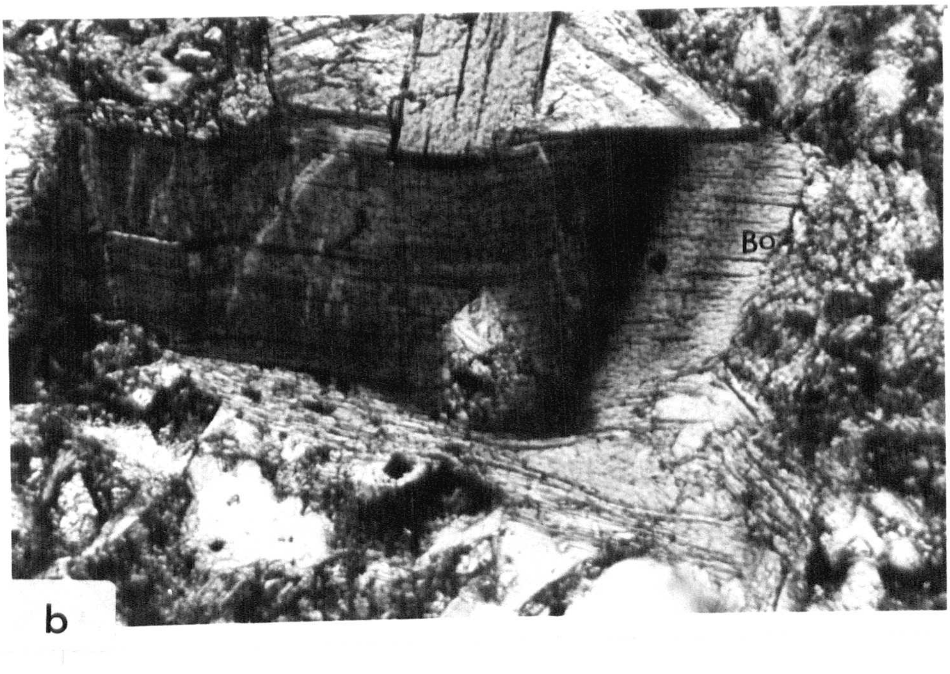
Bo
b

Figure 2.7.

(a) Diopside (D) and feldspar (albite) (F) occurring in the large pargasite crystal (P) as well as in the groundmass. Apatite grains (Ap) can be seen in the lower left pargasite crystal; appinite, Back Settlement. XN x 31.

(b) Pargasite (P) with diopside (D) and biotite (B) in core; appinite, Back Settlement. PPL x 31.

(c) Diopside phenocryst fractured and corroded at margins, appinite, Back Settlement. PPL x 31.


D
D
F
P
Ap
D
D
P
a

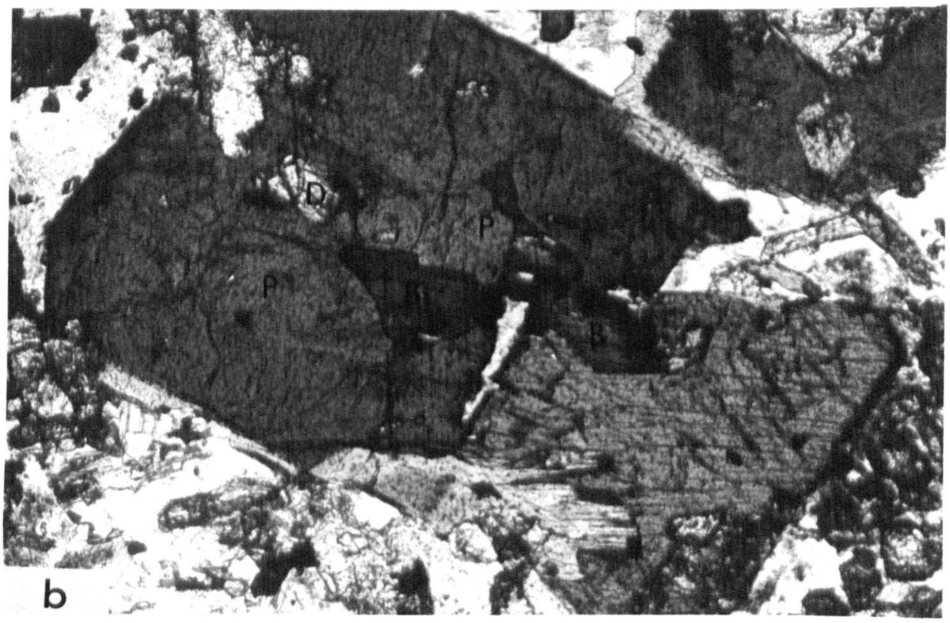
D
P
P
B
b


c

Figure 2.8.

(a) Olivine phenocryst partially altered to magnetite and serpentine and surrounded by a reaction rim of orthopyroxene; kentallenite, Kentallen. PPL x 10.

(b) Amphibole (dark) with diopside core (D); appinite, Rudha Mòr. PPL x 10.

(c) Zoned clinopyroxene phenocryst showing reaction relation with surrounding amphibole. Patches of biotite and chlorite are associated with amphibole producing a pepper-mesh-type structure; pyroxene-mica diorite, Rudha Mòr. PPL x 10.

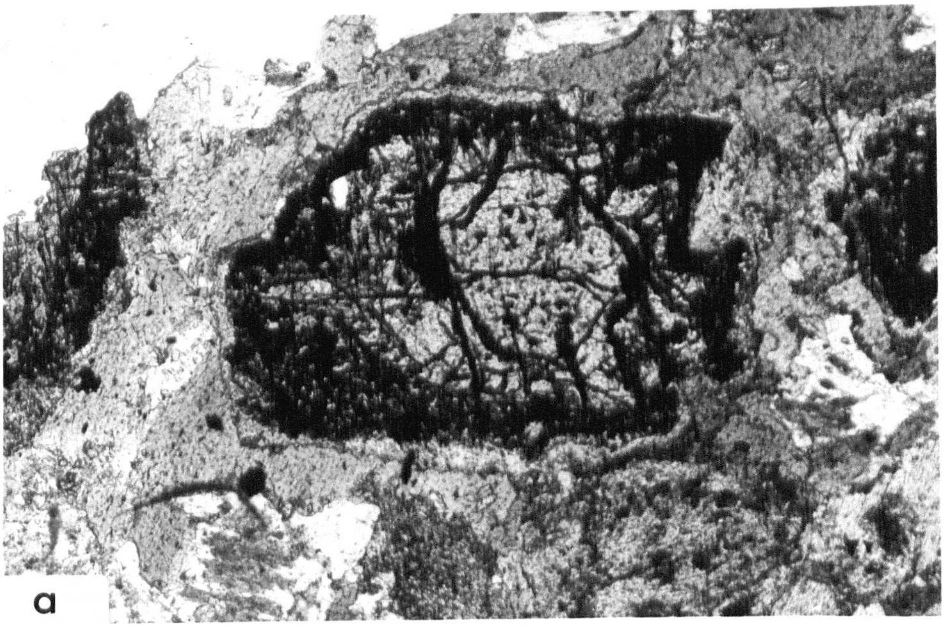
a

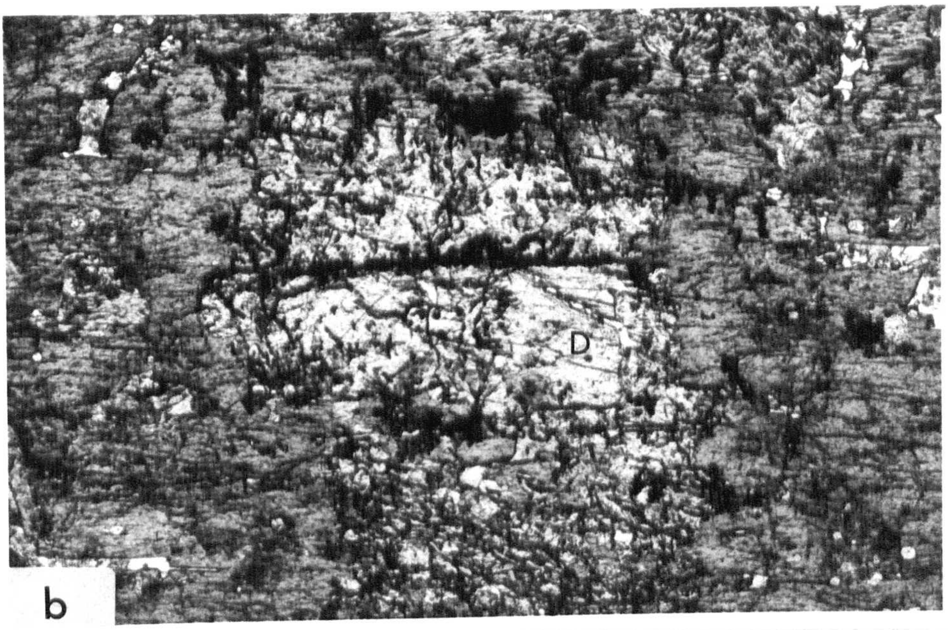
D
b

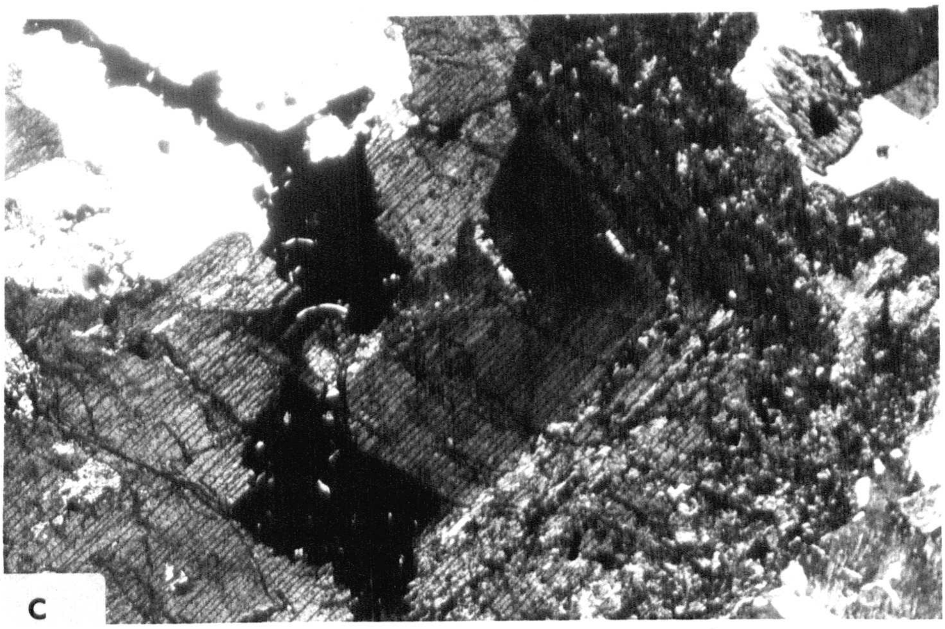
c

Figure 2.9. Chlorite pseudomorphs after amphibole. Original areas of "sawtooth" shape actinolitic overgrowths (A) on the pargasite main crystals can still be recognised. Specks of secondary magnetite are also seen on this pseudomorph; mesocratic lamprophyre small pipe, Back Settlement. PPL x 31.

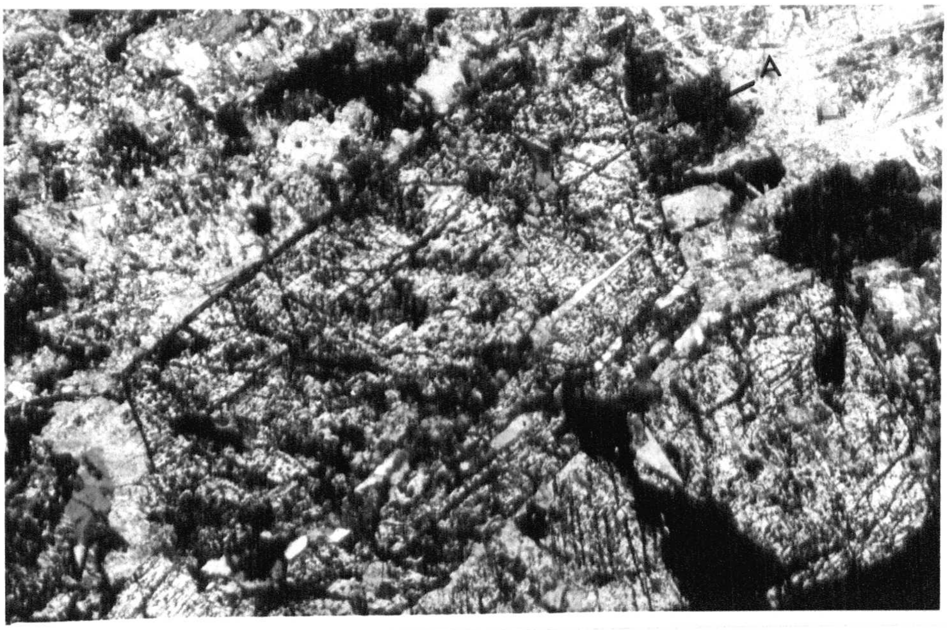
A

Figure 2.10.

(a) Vogesitic lamprophyre occurring as chilled marginal facies to appinite shown in Figure 2.3a, Back Settlement. PPL x 10.

(b) Gradation of appinite (on the left) and lamprophyre (on the right), shown in Figures 2.3a and 2.10a. PPL x 10.

(c) Zoned clinopyroxene phenocryst with small grains of olivine partially or totally altered to magnetite and patches of feldspar, aligned parallel to the zones; olivine-bearing spessartite, Ardsheal Hill. XN x 7.


a

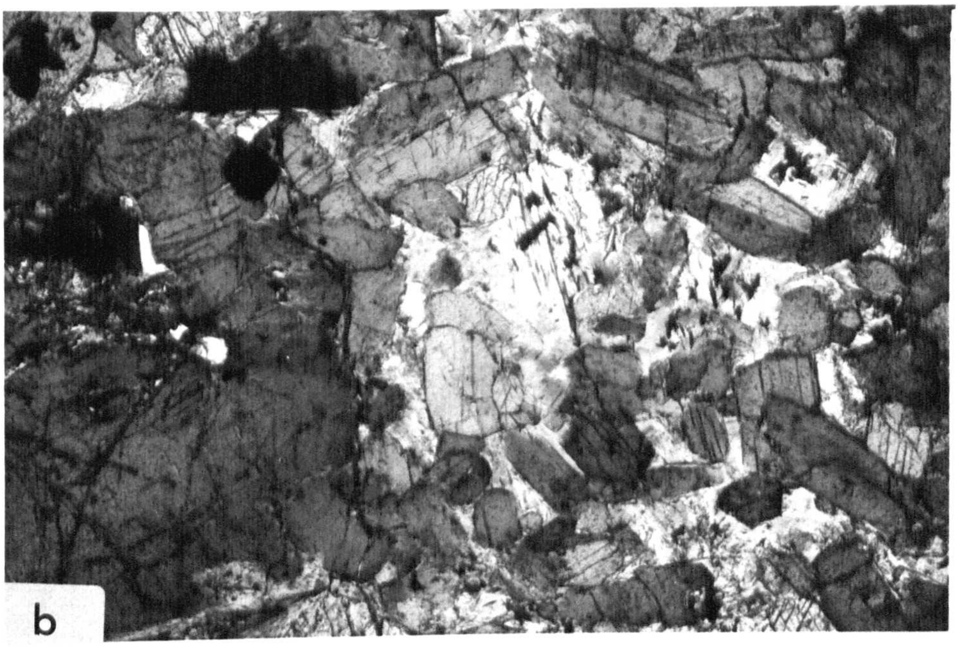
b

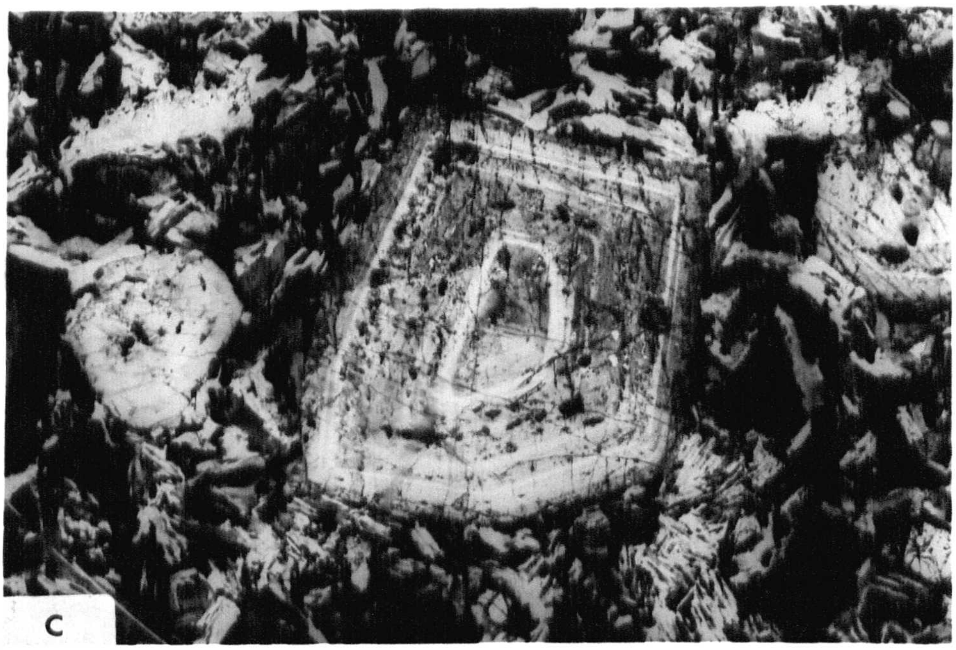
c

Table 2.1. Means and standard deviations of the major and trace element analyses and estimated modal compositions of the representative rock types from the Ballachulish appinite suite.

Coarse-grained facies

	1		2		3		4*	
	Mean (2 anals)	S.D.	Mean (2 anals)	S.D.	Mean (2 anals)	S.D.	Mean	S.D.
SiO_2	45.31	0.66	45.10	1.38	46.25	0.12	48.31	3.66
TiO_2	1.26	0.01	1.23	0.21	1.05	0.16	0.97	0.29
Al_2O_3	11.00	1.20	10.59	1.51	8.53	3.41	12.71	1.74
Fe_2O_3	2.57	0.77	3.09	1.66	3.07	0.50	2.60	0.98
FeO	6.40	0.16	6.78	0.35	6.95	0.00	6.63	1.18
MnO	0.10	0.01	0.14	0.03	0.11	0.02	0.13	0.3
MgO	14.19	2.54	17.35	0.53	19.90	5.09	11.60	2.46
CaO	8.85	0.35	8.65	0.04	8.04	1.61	8.40	1.79
Na_2O	1.53	0.68	1.67	0.44	1.38	0.86	2.44	0.70
K_2O	3.12	0.88	2.51	1.72	2.12	0.39	2.13	0.67
P_2O_5	0.11	0.04	0.06	0.05	0.04	0.01	0.25	0.13
H_2O+	3.38	0.90	2.17	0.26	1.94	1.00	2.65	0.86
CO_2	1.80	0.76	0.49	0.25	0.29	0.10	1.31	1.52
Total	99.62		99.83		99.67		100.13	
			Trace elements (p.p.m.)					
Cr	296	111	758	61	965	408	453	179
Co	74	1	70	5	69	12	43	12
Ni	148	1	357	82	459	244	160	90
Ba	1750	254	1025	784	1005	318	899	372
Ce	22	32	32	4	30	42	37	7
Cl	291	86	439	74	442	122	263	136
Cu	405	141	43	6	36	14	107	73
Ga	8	5	7.5	2	5	4	11	3
La	10	14	10	1	37	11	43	24
Li	6.5	5	11	8	9.5	0.7	10	5

Nb	*3*	*4*	*7.5*	*10*	*6*	*8*	*8*	*8*
Pb	9	1	8	4	6	8	15	6
Rb	90	1	58	51	55	18	44	18
S	1359	1578	638	403	574	372	868	1191
Sc	53	6	55	4	46	20	43	16
Sr	464	184	411	145	355	196	833	291
Th	2.5	0.7	3.5	2	1.5	0.7	5	2
V	255	30	301	70	283	98	223	63
Y	7	3	14	6	13	6	16	4
Zn	68	12	62	11	64	14	93	24
Zr	44	20	55	22	47	32	87	26

Modal analyses

Olivine	5.0	5.0	2.0	3.5	0.0	-	0.0	-
Clinopyroxene	40.0	3.5	60.0	10.0	5.0	5.0	20.0	21.0
Amphibole	5.0	4.5	10.0	3.5	70.0	2.5	45.0	17.5
Phlog.-biot.	27.0	7.5	20.0	0.0	10.0	3.5	5.0	3.5
Plagioclase	10.0	8.0	5.0	1.5	10.0	12.0	15.0	24.2
Anorthoclase	0.0	-	0.0	-	2.0	2.8	0.0	-
Orthoclase	0.0	-	0.0	-	0.0	-	3.0	1.6
Perthite	0.0	-	0.0	-	0.0	-	0.0	-
Quartz	3.0	3.0	0.0	-	0.0	-	4.0	1.5
Calcite (prim.)	2.0	1.5	0.0	-	0.0	-	4.0	3.0
Opaque ores	Tr	-	2.0	3.5	1.5	0.7	0.5	0.6
Apatite (prim.)	Tr	-	0.0	-	1.5	-	0.5	1.0
Sphene (prim.)	Tr	-	0.0	-	0.0	-	1.0	1.0
Chlorite (sec.)	Tr	-	0.0	-	0.0	-	1.0	0.3
Epidote (sec.)	0.0	-	0.0	-	0.0	-	1.0	-
Serpentine (sec.)	4.0	5.0	0.0	-	0.0	-	0.0	-
Uralite (sec.)	0.0	-	0.0	-	0.0	-	0.0	-
Sericite (sec.)	0.0	-	1.0	0.7	0.0	-	0.0	-
Fine-grained mixt.	4.0	6.0	0.0	-	0.0	-	0.0	-
Total	100		100		100		100	

Table 2.1. (Contd.)

Coarse-grained facies

	5		6*		7*		8	9*	
	Mean (2 anals)	S.D.	Mean	S.D.	Mean	S.D.		Mean	S.D.
SiO_2	50.16	0.37	48.89	1.58	57.76	1.92	50.82	66.08	2.08
TiO_2	0.77	0.10	0.63	0.21	0.63	0.12	0.77	0.30	0.09
Al_2O_3	15.81	0.06	12.53	1.16	16.65	1.90	14.10	16.01	0.64
Fe_2O_3	2.99	0.27	2.11	0.61	1.79	0.75	2.23	1.11	0.55
FeO	5.76	0.68	6.41	0.63	3.33	1.37	6.04	1.45	0.67
MnO	0.14	0.00	0.12	0.02	0.07	0.02	0.14	0.03	0.02
MgO	5.80	1.97	14.84	2.98	4.24	2.36	8.29	1.60	0.71
CaO	8.29	0.13	7.19	2.07	4.11	1.33	8.12	1.90	0.64
Na_2O	3.40	0.37	2.56	0.26	3.76	0.61	3.33	4.63	0.70
K_2O	2.39	0.15	2.20	0.95	4.31	1.56	2.58	3.69	1.13
P_2O_5	0.34	0.03	0.28	0.08	0.26	0.09	0.35	0.14	0.07
H_2O+	2.55	0.44	2.02	0.74	2.08	0.88	3.14	2.05	0.34
CO_2	0.29	0.13	0.43	0.52	0.91	1.26	0.56	1.19	0.71
Total	98.69		100.21		99.90		100.47	100.18	
			Trace elements (p.p.m.)						
Cr	214	8	759	220	83	73	367	50	70
Co	26	3	56	12	12	10	37	8	-
Ni	71	6	430	186	49	96	134	34	46
Ba	1140	226	770	181	1120	153	890	1403	730
Ce	47	4	46	16	87	218	40	30	26
Cl	232	9	422	154	319	182	167	143	45
Cu	81	0.01	83	20	82	48	110	66	49
Ga	82	96	8	2	14	2	16	14	1
La	45	35	41	20	61	33	95	62	15
Li	10	4	7	4	10	7	12	8	3

Nb	4	1	5	2	9	5	0	9	5
Pb	15	5	20	7	23	9	12	22	9
Rb	52	14	61	24	131	49	43	84	27
S	35	11	205	177	767	782	110	1502	1680
Sc	150	158	27	10	1055	433	27	6	8
Sr	1383	28	965	168	10	7	1075	795	200
Th	5	0	4	2	9	3	5	9	4
V	592	549	189	30	227	273	181	65	20
Y	15	1	14	1	13	4	13	7	2
Zn	100	1	73	23	66	21	92	25	15
Zr	92	8	86	20	227	96	10	176	38

Modal analyses

Olivine	5.0	5.3	15.0	9.0	0.0	-	0.0	0.0	-
Clinopyroxene	15.0	10.0	40.0	14.5	45.0	-	15.0	0.0	-
Amphibole	30.0	15.5	0.0	-	5.0	-	15.0	0.0	-
Phlog.-biot.	5.0	2.0	10.0	4.5	10.0	-	10.o	10.0	8.0
Plagioclase	30.0	1.5	20.0	13.5	35.0	-	45.0	60.0	22.5
Anorthoclase	5.0	2.5	10.0	15.0	0.0	-	0.0	0.0	-
Orthoclase	2.0	1.5	0.0	-	0.0	-	2.0	4.0	1.5
Perthite	0.0	-	0.0	-	0.0	-	0.0	1.0	1.0
Quartz	0.0	-	0.0	-	0.0	-	0.0	10.0	15.0
Calcite (prim.)	0.0	-	0.0	-	0.0	-	0.0	5.0**	1.5
Opaque ores	4.0	2.5	4.0	1.0	Tr	-	3.0	1.0	0.7
Apatite (prim.)	Tr	-	1.0	0.5	1.0	-	1.0	0.5	0.7
Sphene (prim.)	Tr	-	0.0	-	0.0	-	2.0	1.0	1.0
Chlorite (sec.)	0.0	-	0.0	-	2.0	-	2.0	5.5	2.5
Epidote (sec.)	0.0	-	0.0	-	0.0	-	1.0	0.0	-
Serpentine (sec.)	2.0	1.7	0.0	-	0.0	-	0.0	0.0	-
Uralite (sec.)	0.0	-	0.0	-	0.0	-	0.0	0.0	-
Sericite (sec.)	2.0	2.5	0.0	-	0.0	-	0.0	0.0	-
Fine-grained mixt.	0.0	-	0.0	-	0.0	-	3.0	2.0	3.5
Total	100		100		100		100	100	

Table 2.1. (Contd.)

Fine-grained facies

	10		11*		12		13		14		15
	Mean (2 anals)	S.D.	Mean	S.D.	Mean (3 anals)	S.D.	Mean (3 anals)	S.D.	Mean (2 anals)	S.D.	
SiO_2	47.43	0.18	49.00	3.07	50.66	0.66	51.40	0.94	55.49	4.49	60.94
TiO_2	0.91	0.13	0.76	0.14	0.70	0.02	1.06	0.60	0.75	0.06	0.66
Al_2O_3	14.05	1.19	13.82	1.03	13.98	0.81	13.44	1.79	16.06	1.15	16.99
Fe_2O_3	2.49	0.86	2.07	0.84	3.89	0.10	2.18	0.97	2.70	0.53	1.94
FeO	6.88	0.59	6.32	1.14	5.16	0.15	5.54	0.36	4.95	0.50	3.95
MnO	0.13	0.01	0.13	0.03	0.16	0.01	0.09	0.01	0.16	0.01	0.11
MgO	8.99	0.85	8.62	2.21	7.9	0.48	7.64	1.47	7.42	0.89	3.53
CaO	8.11	0.58	7.73	1.54	9.75	0.37	7.27	1.39	4.66	5.53	1.21
Na_2O	2.69	0.01	2.79	0.70	3.54	0.50	2.97	0.80	2.68	0.44	1.98
K_2O	2.57	0.53	2.14	0.46	2.54	0.12	2.24	0.48	3.12	2.01	4.10
P_2O_5	0.43	0.27	0.28	0.12	0.31	0.01	0.31	0.03	0.18	0.14	0.08
H_2O+	2.76	0.79	3.11	1.36	0.67	0.68	3.41	2.01	2.25	1.07	3.57
CO_2	2.79	1.97	3.29	3.08	0.14	0.21	2.87	1.38	0.44	0.22	0.87
Total	100.23		100.06		98.59		100.42		100.77		99.93
Trace elements (p.p.m.)											
Cr	260	39	316	153	205	18	230	162	200	80	101
Co	39	6	46	15	38	2	48	26	25	16	2
Ni	85	6	126	77	46	4	126	13	45	30	10
Ba	725	148	825	331	842	110	833	315	986	386	995
Ce	65	14	48	18	53	4	35	31	61	30	65
Cl	246	5	241	105	-	-	224	167	-	-	-
Cu	97	109	121	110	67	13	186	193	63	57	83
Ga	-	-	12	8	14	6	9	7	21	13	26
La	47	3	34	20	14	2	27	6	27	25	37
Li	10	3	14	10	-	-	10	4	-	-	-

Nb	7	1	5	3	7	0	2	4	10	14	18
Pb	15	12	24	10	11	2	21	6	19	4	10
Rb	57	16	57	17	54	6	36	33	115	69	127
S	2220	2757	1913	2408	-	-	1739	2439	-	-	-
Sc	36	1	34	14	-	-	38	17	-	-	-
Sr	817	73	942	356	1039	23	648	587	713	619	207
Th	6	0	6	2	4	2	6	152	9	1	17
V	220	17	222	74	-	-	185	156	-	-	-
Y	18	4	15	3	9	6	16	4	18	13	21
Zn	94	18	89	16	70	9	72	18	46	13	80
Zr	98	8	102	21	64	6	108	29	217	10	187

Modal analyses

Olivine	0.0	-	5.0	10	5.0	2.0			0.0	-	0.0
Clinopyroxene	10.0	10.1	17.0	15	33.0	3.5	34.0	1.0	30.0	-	0.0
Amphibole	40.0	7.0	18.0	14	5.0	5.5	6.0	6.0	12.0	3.5	20.0
Phlog.-biot.	15.0	7.5	5.0	3	5.0	5.0	10.0	14.0	5.0	5.0	10.0
Plagioclase	5.0	7.2	37.5	15.5	40.0	12.0	30.0	0.0	45.0	3.5	40.0
Anorthoclase	0.0	-	0.0	-	0.0	-	0.5	0.7	0.0	-	0.0
Orthoclase	5.0	4.3	1.0	2.0	Tr	-	0.5	0.7	Tr	-	10.0
Perthite	0.0	-	0.0	-	0.0	-	-	-	0.0	-	0.0
Quartz	10.0	4.3	5.0	6.0	0.0	-	5.0	7.0	4.0	6.0	20.0
Calcite (prim.)	7.0**	7.0	2.5**	5.0	0.0	-	5.0**	7.0	0.0	-	9.0
Opaque ores	1.0	0.5	5.5	5.2	5.0	1.5	4.0	1.5	4.0	4.0	Tr
Apatite (prim.)	0.5	0.5	Tr	-	0.5	0.1	Tr	-	0.0	-	0.0
Sphene (prim.)	0.5	1.1	1.0	1.5	0.5	-	Tr	-	0.0	-	0.0
Chlorite (sec.)	2.0	5.0	2.5	5.0	5.0	4.0	0.0	-	0.0	-	0.0
Epidote (sec.)	0.0	-	0.0	-	1.0	1.5	0.0	-	0.0	-	Tr
Serpentine (sec.)	0.0	-	0.0	-	0.0	-	0.0	-	0.0	-	Tr
Uralite (sec.)	0.0	-	0.0	-	0.0	-	0.0	-	0.0	-	0.0
Sericite (sec.)	0.0	-	0.0	-	0.0	-	0.0	-	0.0	-	0.0
Fine-grained mixt.	0.0	-	0.0	-	0.0	-	5.0	-	0.0	-	0.0
Total	100		100		100		100		100		100

Table 2.1. (Contd.)

1	Ultramafic rock, Rudha Mòr pipe.
2	Biotite pyroxenite, Kentallen pipe.
3	Biotite hornblendite, Kentallen pipe.
*4	Appinite, large pipe, Back Settlement.
5	Kentallenitic appinite, Ardsheal Hill pipe.
*6	Kentallenite, Kentallen pipe.
*7	Pyroxene - mica diorite, Rudha Mòr pipe.
8	Pyroxene - hornblende - mica diorite, Ardsheal Hill pipe.
*9	Leucocratic diorite and granodiorite.
10	Vogesitic lamprophyre, Back Settlement pipe.
*11	Average of lamprophyre dykes and marginal facies.
12	Olivine-bearing spessartite, Ardsheal Hill pipe.
13	Average of lamprophyre dykes.
14	Olivine-free spessartite, Ardsheal Hill pipe.
15	Andesitic lamprophyre, Ardsheal Hill pipe.
*	Major and trace element analyses from Wright and Bowes (1979).
**	Values including some secondary calcite.

Table 2.2. Mean chemical compositions of feldspar and other accessory minerals in the appinite suite of Ballachulish district.

	1		2	3	4	
	Mean (19 anals)	S.D.			Mean (4 anals)	S.D.
SiO_2	64.55	0.12	64.32	64.05	64.26	0.02
TiO_2	0.15	0.04	0.00	0.27	0.20	0.05
Al_2O_3	18.61	0.41	18.76	18.43	18.92	1.00
Fe*O	0.00	-	0.00	0.15	0.15	0.00
MnO	0.00	-	0.00	0.00	0.00	-
MgO	0.00	-	0.61	0.00	0.14	0.09
CaO	0.01	0.01	0.11	0.00	0.12	0.01
Na_2O	0.28	0.18	0.40	1.09	1.70	0.82
K_2O	16.24	0.05	16.32	15.83	15.59	0.04
Total	99.84		100.52	99.82	100.08	

	5		6	7		8	
	Mean (12 anals)	S.D.		Mean (2 anals)	S.D.	Mean (2 anals)	S.D.
SiO_2	64.32	0.02	67.32	67.92	0.65	67.56	0.60
TiO_2	0.23	0.09	0.06	0.00	-	0.00	-
Al_2O_3	20.28	0.07	20.36	19.91	0.55	20.65	0.50
Fe*O	0.27	0.09	0.00	0.00	-	0.00	-
MnO	0.00	-	0.00	0.00	-	0.00	-
MgO	0.00	-	0.00	0.00	-	0.00	-
CaO	1.18	0.22	0.61	0.16	0.1	0.18	0.2
Na_2O	5.50	0.88	11.68	11.41	0.29	11.91	0.30
K_2O	8.19	0.09	0.10	0.09	0.06	0.10	0.0
Total	99.97		99.83	99.49		100.40	

	9		10	
	Mean (3 anals)	S.D.	Mean (2 anals)	S.D.
SiO_2	63.50	0.35	64.12	0.18
TiO_2	0.00	-	0.00	-
Al_2O_3	22.52	0.36	21.95	0.31
Fe*O	0.00	-	0.00	-
MnO	0.00	-	0.00	-
MgO	0.00	-	0.47	0.12
CaO	3.92	0.05	2.02	0.11
Na_2O	8.74	0.18	11.11	0.50
K_2O	0.69	0.13	0.09	0.02
Total	99.37		99.26	

Table 2.2. (Contd.)

	11		12		13		14	
	Mean (2 anals)	S.D.	Mean (5 anals)	S.D.	Mean (3 anals)	S.D.	Mean (4 anals)	S.D.
SiO_2	62.80	0.56	56.46	0.46	0.74	0.16	30.43	1.71
TiO_2	0.24	0.04	0.00	-	1.35	0.45	36.92	0.65
Al_2O_3	22.79	0.55	0.10	0.07	1.68	0.22	1.99	0.7
Fe*O	0.44	0.04	13.47	0.5	88.06	2.52	1.20	0.20
MnO	0.00	-	0.00	-	0.00	-	0.00	-
MgO	0.00	-	29.25	1.00	0.00	-	0.00	-
CaO	3.99	0.08	0.7	0.25	0.38	0.26	29.23	0.54
Na_2O	7.82	0.12	0.00	-	0.00	-	0.00	-
K_2O	1.96	0.67	0.00	-	0.00	-	0.00	-
Cr_2O_3	0.00	-	0.00	-	0.16	0.09	0.24	0.10
NiO	0.00	-	0.00	-	0.13	0.09	0.00	-
CoO	0.00	-	0.00	-	0.96	0.87	0.72	0.10
Total	100.04		99.98		93.46		100.74	

1 Orthoclase, appinite, Back Settlement pipe (Table 7.1 – 9).

2 Orthoclase, pyroxene - mica diorite, Rudha Mòr pipe (Table 7.1 – 39).

3 Orthoclase, lamprophyric marginal facies, Ardsheal Hill pipe (Table 7.1-22).

4 Orthoclase, appinite, Garbh Allt pipe (Table 7.1 – 79).

5 Anorthoclase, kentallenite, Kentallen pipe (Table 7.1 – 52).

6 Albite, appinite, Back Settlement pipe (Table 7.1 – 9).

7 Albite, pyroxene - mica diorite, Rudha Mòr pipe (Table 7.1 – 39).

8 Albite, lamprophyric marginal facies, Ardsheal Hill pipe (Table 7.1–22).

9 Oligoclase, kentallenite, Kentallen pipe (Table 7.1 –52).

10 Oligoclase, pyroxene - mica diorite, Rudha Mòr pipe (Table 7.1 – 39).

11 Andesine, lamprophyric marginal facies, Ardsheal Hill pipe (Table 7.1 – 22).

12 Orthopyroxene, kentallenite, Kentallen pipe (Table 7.1 – 52).

13 Magnetite (primary), appinite, Back Settlement pipe (Table 7.1 – 9).

14 Sphene (primary), appinite, Back Settlement pipe (Table 7.1 – 9).

CHAPTER 3 OLIVINE

Olivine is not a common constituent in many rocks of the appinite suite. However, it is present as 5 - 30 and 3 - 5%, in the kentallenites and cortlandites, respectively. It is also present (5 - 20%) in the lamprophyric marginal facies of the Ardsheal Hill pipe. Variation in its composition in the different rock types reflects the physical conditions of crystallisation. It also forms a basis for assessing which of the various rock types were formed by olivine fractionation and whether the crystallisation was from a basaltic melt or from an olivine-depleted melt. Of particular value is its significance in determining whether the lamprophyric marginal facies of the Ardsheal Hill pipe represents the original ("primary") liquid from which the whole appinite suite was derived.

Both phenocrysts and small crystals (in the fabric of the "groundmass" of the rock; Figs. 2.3b; 2.4a) from the kentallenite of the Kentallen pipe (Table 7.1 — 52) and from the lamprophyric marginal facies of the Ardsheal Hill pipe (Table 7.1 — 21) have been analysed. Phenocrysts which are compositionally zoned (Fig. 3.1b; also see Fig. 2.8a) were selected because compositional variations from core to margins reflect varying melt compositions and physical conditions with the core composition representing the earliest stage of crystallisation in the particular rock. The small grains were analysed to determine whether they represent crystallisation after the formation of the phenocrysts was complete or whether they represent parts of highly fractured and corroded phenocrysts. Representative analytical data are given in Table 3.1.

A plot of Fe in unit cell *vs*. Fo contents indicates that the majority of the compositions occur in the chrysolite field (Fig. 3.1a). The two analyses that plot in the hyalosiderite field are from the outer parts of phenocrysts in the lamprophyric margins of the Ardsheal Hill pipe (Fig. 3.1b). While there is some overlap, the olivine in the kentallenite is more Fo-rich than that from the lamprophyric facies of the Ardsheal Hill pipe.

3.1 Chemistry of single grains

The two selected zoned olivine phenocrysts have compositions which vary from Fo_{83} to Fo_{77} and Fo_{74} to Fo_{69}, respectively (Fig. 3.1b). In both there is a strong negative correlation between Fe in unit cell and Fo (Fig. 3.1a). In zones with Fo $<$ 82 MnO (representing Mn) varies negatively and Ni varies positively with Fo. In zones with Fo $>$ 82 there is a large increase in MnO and decrease in Ni with a small decrease in Fo (Fig. 3.1c). This shows that Mn was independently substituted for Ni in the early stages of crystallisation but that the substitution of both elements became strongly dependent on Mg $\rightleftharpoons$ Fe substitution in the later stages.

3.2 Overall chemistry of olivine

The small olivine crystals in both intrusions follow the trend of the phenocrysts on Fe in unit cell *vs.* Fo and MnO *vs.* Fo variation diagrams (Figs. 3.1a, d). Those from the Kentallen pipe plot close to their corresponding phenocrysts while some of the small olivine crystals from the Ardsheal Hill pipe have even higher Fo than their corresponding phenocrysts. Ni varies with a constant Fo in these grains (Fig. 3.1e) while Co varies negatively with a steep slope for olivine from the Kentallen pipe and positively with a comparatively gentle slope for olivine from the Ardsheal Hill pipe (Fig. 3.1f). This shows that the decrease in Ni with decreasing Fo has been compensated for by Mn as well as by Co in olivine from the Kentallen pipe. The different partitioning of Ni and Co between the olivine from the Kentallen pipe and Ardsheal Hill pipe is associated with different partitioning of Si and CaO. Si varies while Fe remains nearly constant in olivine from the Kentallen pipe. In olivine from the Ardsheal Hill pipe Fe varies while Si remains nearly constant (Fig. 3.1g). Similarly CaO (representing Ca) against Fo varies in olivine from the Kentallen pipe while it is nearly constant in olivine from the Ardsheal Hill pipe (Fig. 3.1h).

3.3 Temperature estimation

On the basis of Fo contents at 1 kb pressure (ignoring the Mn substitution for Fe), crystallisation temperatures of 1850°-1810°C and 1825°-1770°C are indicated by the olivines from the Kentallen pipe and Ardsheal Hill pipe, respectively (Bowen and Schairer 1935). These estimates show general correspondence to estimates of 1870°-1827°C and 1841°-1687°C, respectively, obtained from the extrapolation of the data of French and Cameron (1981; see Fig. 3.2a). As Mg - Fe partitioning between olivine and melt is known to show little variation at constant temperature for a considerable range of pressure (Longhi *et al.* 1978), the determined temperatures are considered to be reasonable estimates. The absence of Ti is consistent with such high temperatures of crystallisation.

3.4 Pressure estimation

The absence of orthopyroxene as a phenocryst in the rocks of the pipes containing olivine indicates that these members of the appinite suite did not crystallise at pressures greater than 5 kb (Irvine and Findly 1972). However, the estimated temperatures for olivine crystallisation points to the beginning of crystallisation of olivine at a greater depth than that represented by this pressure. The presence of a reaction rim of orthopyroxene around olivine in the kentallenite of the Kentallen pipe (Fig. 2.8a) points to this part of crystallisation being below 2.3 kb while the absence of such a reaction rim in the lamprophyric marginal facies of the Ardsheal Hill pipe indicates that the pressure there did not drop below 2.3 kb following the crystallisation of olivine (Boyd *et al.* 1964; O'Hara and Stewart 1966). However, the suppression of such a reaction relationship between olivine and melt in the Ardsheal Hill pipe could be due to a drop in magma temperature to < 1500°C, related to emplacement into relatively cool country rocks (see Deer *et al.* 1966, p. 5).

3.5 Fractional and equilibrium crystallisation of olivine and determination of the parental magma

To determine the compositions of liquids which were in equilibrium with olivines, mole % MgO *vs.* FeO for various rocks from the Kentallen and Ardsheal Hill pipes are compared to the Fo contents of the olivine from these pipes (Fig. 3.2b). For both the kentallenites from the Kentallen pipe (Table 7.1 – 47-52) and the olivine-bearing spessartite from the chilled margins of the Ardsheal Hill pipe (Table 7.1 – 19-21) the Fo proportions calculated from the rock analyses are higher than those determined directly by microprobe analyses for the olivine crystals themselves. In contrast, for both the olivine-free spessartite from the lamprophyric margins and the leucocratic diorite from the Ardsheal Hill pipe (Table 7.1 – 22, 23, 24, 27) the calculated Fo composition from the rock analyses correspond with the determined composition of the olivine crystals in the kentallenite. This indicates that these rocks represent the results of olivine fractionation. Their equilibrium with olivine in the Kentallen pipe rather than with those in the Ardsheal Hill pipe may be the result of (1) Fe used in Fo determination of olivine crystals representing total Fe, (2) crystallisation of olivine at pressure higher than 1 kb, or (3) the Fe^{2+} content of the rocks not being a good guide to the Fe^{2+} contents of the original magma (Cox *et al.* 1979).

$K^{ol-Mag}_{Fe\ Mg}$ for olivine from the Kentallen pipe and olivine-free spessartite from the Ardsheal Hill pipe is 0.3. This is in close correspondence to the value between olivine and basaltic melt (Sato

1977) and supports the interpretation of these being in equilibrium. However, $K^{ol-Mag}_{Ni\ Mg}$ for the same pair is 357 which is very much higher than the values of 2, 2.3 and 2.6 for olivine and basaltic melt given by Sato (1977). In addition olivine from the Kentallen pipe occurs both in and above the field of equilibrium crystallisation. If the Ni content which is below the detection limit could have been determined for the olivine from the marginal facies of the Ardsheal Hill pipe, it is expected that the occurrence of this mineral in the field of fractional crystallisation of Sato (1977) would be demonstrated (*cf.* Fig. 3.2c).

The maximum Ni content in olivine from the Kentallen pipe (*c.* 3800 p.p.m.) is close to the *c.* 3400 p.p.m. in olivines which crystallise from magmas resulting from 25% melting of peridotite (Sato 1977). This is consistent with the other evidence indicating that olivine from the Kentallen pipe crystallised from a basaltic melt.

The lower Ni content of olivine from the lamprophyric marginal facies of the Ardsheal Hill pipe as compared to that from the kentallenite of the Kentallen pipe can be related to changes, either in physical conditions or melt composition (*cf.* Nicholls *et al.* 1971; French and Cameron 1981). The Fe *vs.* Si and Co and CaO *vs.* Fo variations show a major change in the Si-activity of the melt from which this olivine was crystallised (Figs. 3.1f - h; Takahashi 1978). Such changes in the Si-activity can be brought about both by changes in pressure and melt composition (Nicholls *et al.* 1971). The olivine-free spessartites and other feldspathic varieties from the lamprophyric marginal facies of the Ardsheal Hill pipe have 52-60% SiO_2 (Table 7.1 – 22-25) and are evolved from the olivine-bearing spessartite through olivine and clinopyroxene fractionation (Chapter 7). This shows that due to the fractional crystallisation of olivine the residual melt composition became progressively richer in SiO_2 in the lamprophyric margins of the Ardsheal Hill pipe. This also indicates that the entry of Ni into olivine in the olivine-bearing spessartite was affected by changes in the melt composition, particularly the stage of SiO_2-saturation.

If olivine from the Kentallen pipe was still in equilibrium with liquid from which it crystallised, then the kentallenite is likely to represent the original or the least fractionated basaltic melt in the appinite suite. The average CaO in olivines from the Kentallen pipe and Ardsheal Hill pipe is 0.20 and 0.14 wt. %, respectively (Table 3.1), while the average CaO proportions in the corresponding host rocks are 7.2 and 6.0 wt. % (Table 2.1). As the relationship between the CaO of olivine and of a melt has been shown by Watson (1979) to be wt. % CaO in olivine = 0.0275 wt. % CaO in liquid, then the CaO in an olivine can be used to determine the composition of the liquid from which the mineral crystallised. In the cases of olivines from the Kentallen and Ardsheal Hill pipes, the corresponding liquids should have 7.3 and 5.1 CaO (wt. %), respectively. For the Kentallen rocks the value is in close correspondence with the determined average CaO in the rocks while it is much lower than the determined average CaO for the Ardsheal Hill rocks. This evidence further supports the interpretation of olivine from the Kentallen pipe as having been in equilibrium with the liquid from which it crystallised and that the original melt for the suite was similar to the average kentallenite composition (Table 2.1). It also supports the interpretation that the lamprophyric marginal facies of the Ardsheal Hill pipe does not represent the "original" melt composition but that it represents a product of a high degree of olivine fractionation as well as some clinopyroxene accumulation. Tie lines between the average compositions of olivine and clinopyroxene from the kentallenite of the Kentallen pipe and from the lamprophyric marginal facies of the Ardsheal Hill pipe also support these interpretations (Fig. 3.2d).

3.6 Conclusions

1. Olivine in the kentallenite of the Kentallen pipe started crystallising close to 1800°C at a pressure greater than 5 kb.
2. Some of the kentallenite groundmass compositions represent the least fractionated melt and are in compositional equilibrium with their olivine phenocrysts.
3. Olivine in the fine-grained marginal (lamprophyric) facies of the Ardsheal Hill pipe started crystallising at a lower temperature and pressure, from an olivine-fractionated and comparatively more felsic liquid than the olivine in the Kentallen pipe, *i.e.* not from the "original" melt.

Figure 3.1

(a) Compositional fields for olivines from the Ballachulish appinite suite on the basis of Fo contents (after Deer *et al.* 1962).

(b) Schematic representation of concentrically zoned olivine phenocrysts; zone boundaries are arbitrary and numbers 1-13 and 15-20 represent analyses in Table 3.1.

(c) Variations of Ni and MnO against Fo in the phenocrysts of Figure 3.1b; detection limit for Ni is treated as being zero and numbers with symbols correspond to analyses in Table 3.1.

(d-h) Variations of MnO, Ni and Co *vs*. Fo, Fe *vs*. Si and CaO *vs*. Fo, respectively, in concentrically zoned phenocrysts and small olivine crystals from the kentallenite of the Kentallen pipe and the lamprophyric marginal facies of the Ardsheal Hill pipe; for detection limits of various elements see Appendix A.2; symbols as in Figure 3.1a.

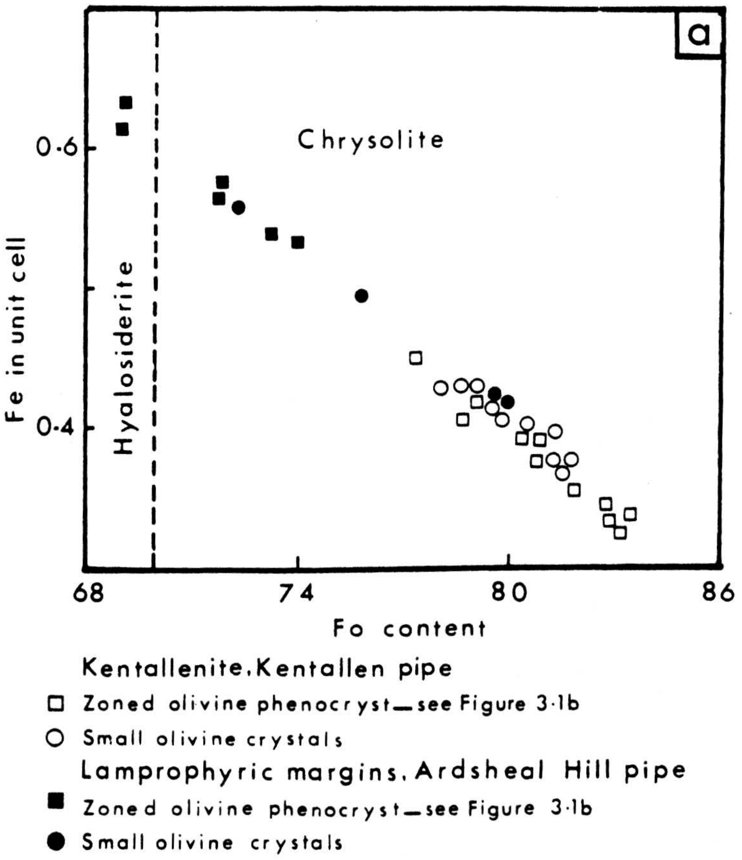

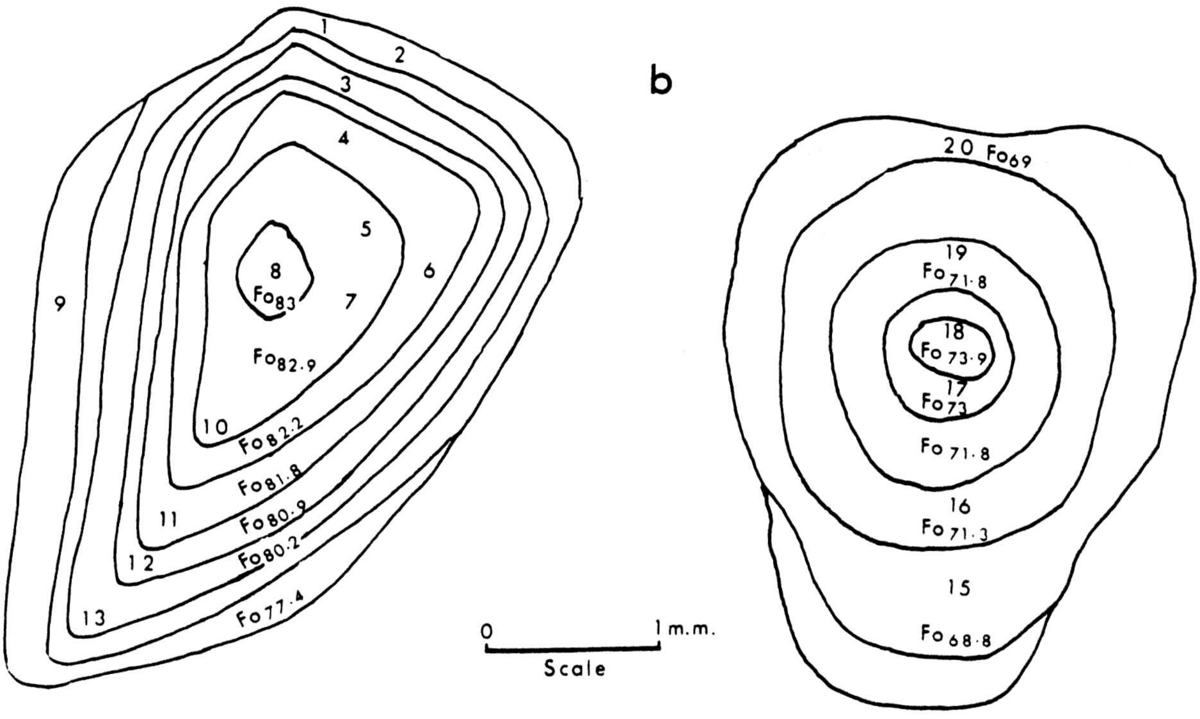

Kentallenite, Kentallen pipe

Lamprophyric marginal facies, Ardsheal Hill pipe

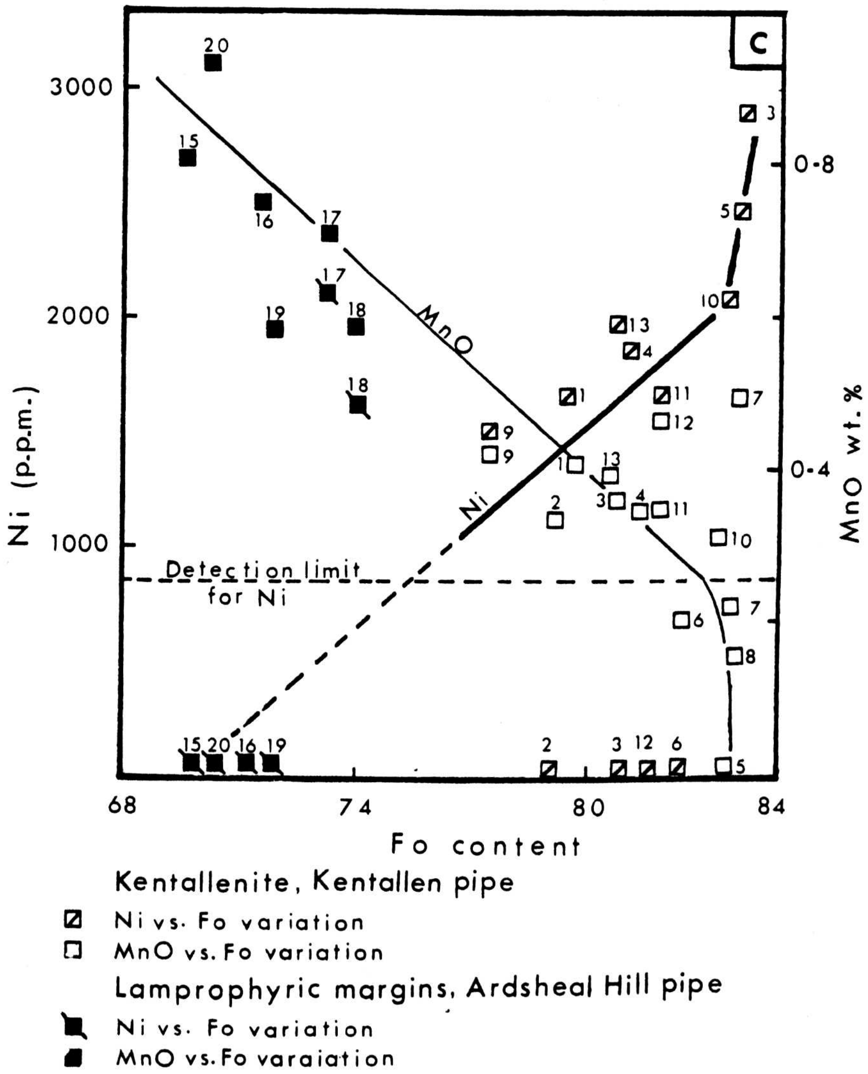
C
Ni (p.p.m.)
3000
2000
1000
MnO wt. %
0·8
0·4
68
74
80
84
Fo content
MnO
Ni
Detection limit for Ni
20
15
16
17
17
19
18
18
9
9
1
1
2
13
13
3
4
4
11
11
12
3
5
10
10
7
7
6
8
5
15 20 16 19
2
3 12 6
Kentallenite, Kentallen pipe
▨ Ni vs. Fo variation
☐ MnO vs. Fo variation
Lamprophyric margins, Ardsheal Hill pipe
■ Ni vs. Fo variation
■ MnO vs. Fo varaiation

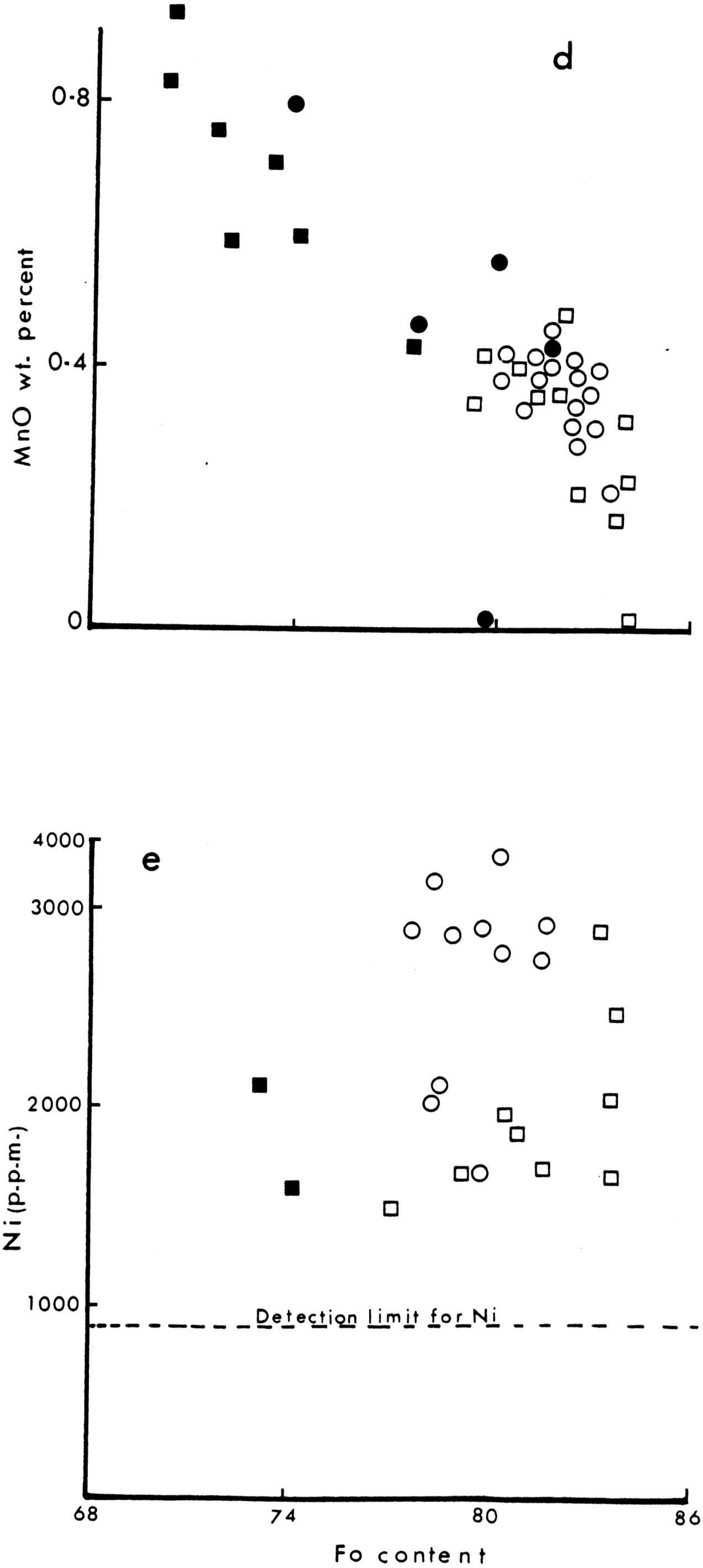
d
0·8
0·4
0
MnO wt. percent
e
4000
3000
2000
1000
Ni (p.p.m.)
Detection limit for Ni
68
74
80
86
Fo content

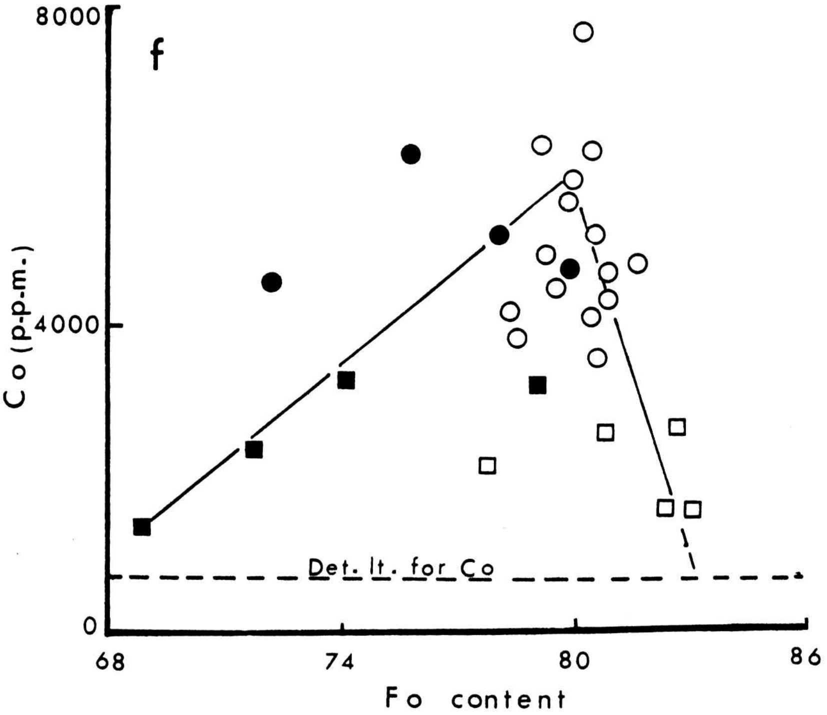
f
8000
4000
0
Co (p.p.m.)
Det. lt. for Co
68
74
80
86
Fo content

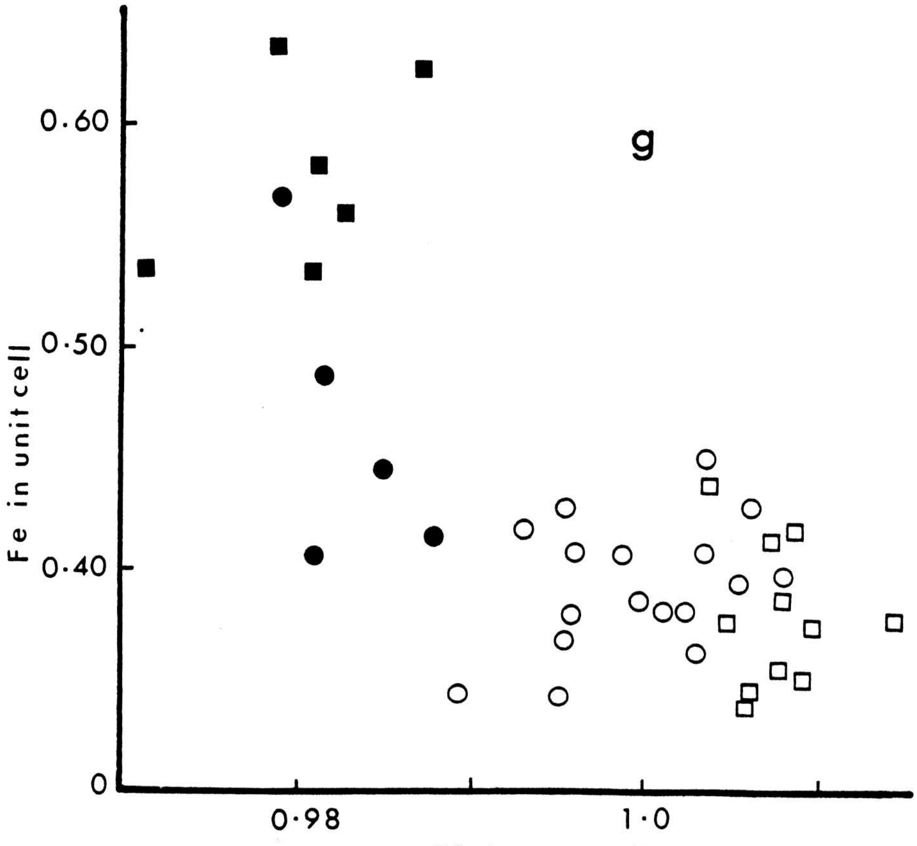
g
0.60
0.50
0.40
0
Fe in unit cell
0.98
1.0
Si in unit cell

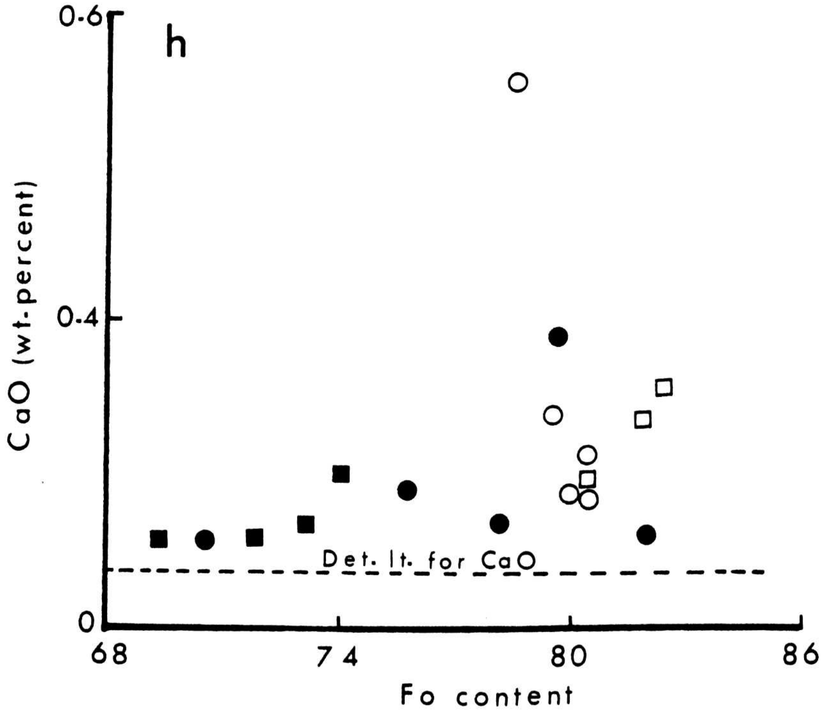
h
CaO (wt. percent)
0·6
0·4
0
Det. lt. for CaO
68
74
80
86
Fo content

Figure 3.2

(a) Temperature estimation for concentrically zoned olivine phenocrysts from the Kentallen and Ardsheal Hill pipes (Fig. 3.1b) on the basis of extrapolation of MgO contents (after French and Cameron 1981).

(b) Relationship between mole % of MgO and FeO in various rock types to compositions of olivine at 1 atm. pressure (after Roeder and Emsile 1970).

(c) Discrimination diagram suggesting equilibrium crystallisation for the Kentallen pipe olivine and fractional crystallisation for the Ardsheal Hill pipe olivine (after Sato 1977); symbols as in Fig. 3.1.

(d) Tie lines for the average olivine and clinopyroxene compositions from the kentallenite of the Kentallen pipe and the lamprophyric marginal facies of the Ardsheal Hill pipe.

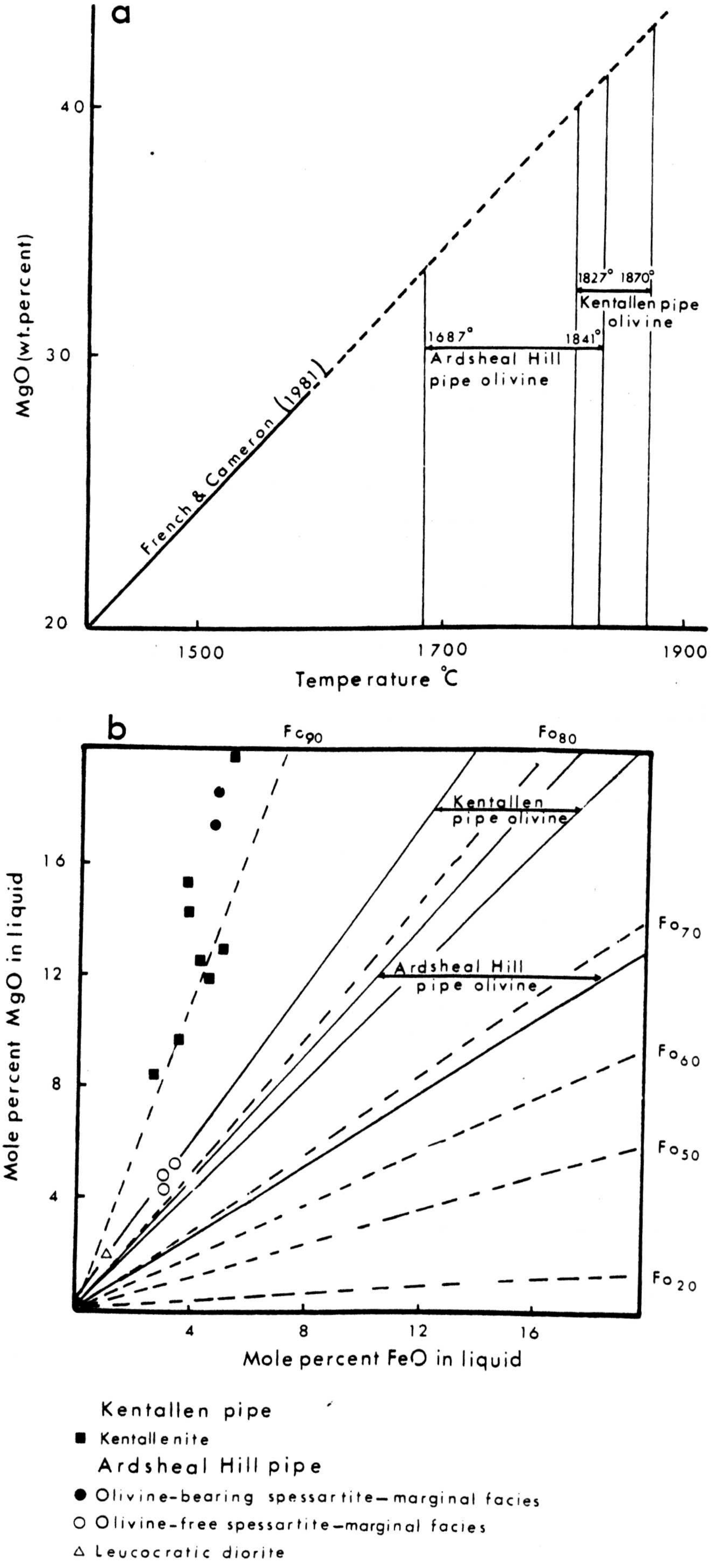
a
MgO (wt. percent)
20
30
40
Temperature °C
1500
1700
1900
French & Cameron (1981)
1687°
1841°
Ardsheal Hill pipe olivine
1827°
1870°
Kentallen pipe olivine
b
Mole percent MgO in liquid
4
8
12
16
Mole percent FeO in liquid
4
8
12
16
Fo90
Fo80
Fo70
Fo60
Fo50
Fo20
Kentallen pipe olivine
Ardsheal Hill pipe olivine
Kentallen pipe
■ Kentallenite
Ardsheal Hill pipe
● Olivine-bearing spessartite–marginal facies
○ Olivine-free spessartite–marginal facies
△ Leucocratic diorite

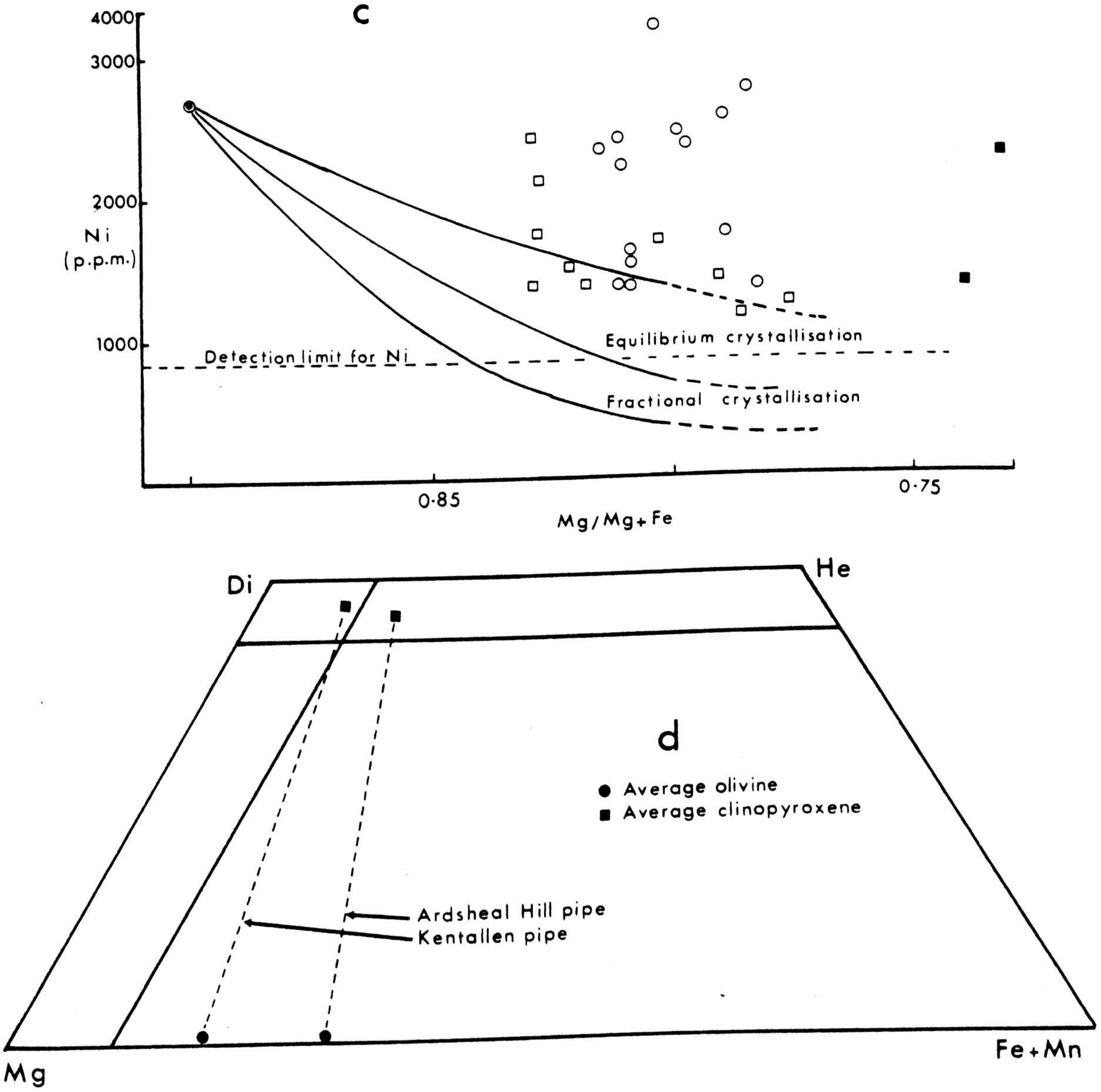
c
4000
3000
2000
1000
Ni (p.p.m.)
Detection limit for Ni
Equilibrium crystallisation
Fractional crystallisation
0·85
0·75
Mg/Mg+Fe
Di
He
d
● Average olivine
■ Average clinopyroxene
Ardsheal Hill pipe
Kentallen pipe
Mg
Fe+Mn

Table 3.1. Olivine compositions from the appinite suite of the Ballachulish district.

Olivine from kentallenite, Kentallen pipe (Table 7.1 – 52)

	Concentrically zoned olivine (Fig. 3.1b)													Small crystals	
	1	2	3	4	5	6	7	8	9	10	11	12	13	14 Mean (17 anals)	S.D.
SiO_2	39.12	38.66	39.46	39.69	39.80	39.88	39.70	39.27	39.07	39.20	39.31	39.00	38.77	39.00	0.40
Al_2O_3	0.24	0.00	0.00	0.00	0.00	0.00	0.00	0.00	0.00	0.00	0.00	0.00	0.00	0.03	0.08
FeO	18.92	19.42	17.85	16.64	16.24	16.55	15.94	16.12	20.83	16.30	16.95	17.86	18.11	18.25	0.84
MnO	0.41	0.33	0.36	0.35	0.00	0.21	0.23	0.16	0.43	0.36	0.35	0.45	0.39	0.37	0.06
MgO	41.02	41.53	42.30	42.83	43.67	42.93	43.58	44.10	40.15	43.82	42.55	42.04	40.96	41.23	0.70
CaO	b.d	b.d	0.13	0.11	b.d	0.32	b.d	b.d	b.d	b.d	0.27	b.d	0.18	0.18	0.06
Total	99.71	99.94	100.10	99.62	99.71	99.89	99.45	99.65	100.48	100.55	99.43	99.47	98.41	99.06	
	Trace elements (p.p.m.)														
Co	b.d.	b.d.	b.d.	1842	b.d.	b.d.	2629	b.d.	2179	1564	b.d.	2244	b.d.	4721	1664
Ni	1679	b.d.	b.d.	1827	2493	b.d.	1628	2873	1479	2016	1627	b.d.	1938	2185	1046
	Formulae on the basis of 4 oxygens														
Si	1.00	0.99	1.00	1.01	1.01	1.01	1.01	1.00	1.00	0.99	1.00	1.00	1.01	1.005	0.005
Al	0.01	0.00	0.00	0.00	0.00	0.00	0.00	0.00	0.00	0.00	0.00	0.00	0.00	0.001	0.003
Fe	0.41	0.42	0.38	0.35	0.34	0.35	0.34	0.34	0.45	0.45	0.36	0.38	0.39	0.396	0.020
Mn	0.01	0.01	0.01	0.01	0.00	0.00	0.00	0.00	0.01	0.01	0.01	0.01	0.01	0.010	0.000
Mg	1.57	1.59	1.60	1.62	1.64	1.62	1.65	1.67	1.54	1.65	1.62	1.61	1.58	1.490	0.280
Ca	0.00	0.00	0.00	0.00	0.00	0.01	0.00	0.00	0.00	0.00	0.01	0.00	0.00	0.000	0.000
Fo content	79.3	79.1	80.8	82.2	82.8	82.2	82.9	83.1	77.4	82.9	81.8	80.9	80.2	80.0	1.04

Table 3.1. (Contd.)

Olivine from lamprophyric marginal facies,
Ardsheal Hill pipe (Table 7.1-21)

	Concentrically zoned olivine (Fig. 3.1b)						Small crystals	
	15	16	17	18	19	20	21 Mean (5 anals)	S.D.
SiO_2	36.37	37.51	37.47	36.16	37.14	36.61	37.78	0.57
Al_2O_3	0.00	0.00	0.23	0.00	0.24	0.00	0.29	0.06
FeO	28.17	26.49	24.48	23.77	25.76	27.72	21.19	2.59
MnO	0.81	0.75	0.70	0.59	0.58	0.93	0.45	0.29
MgO	34.60	36.82	37.18	37.60	36.80	34.25	39.84	2.15
CaO	b.d	0.21	0.13	0.20	0.13	0.12	0.16	0.14
Total	99.95	101.78	100.19	98.32	100.65	99.63	99.26	
	Trace elements (p.p.m.)							
Co	1332	b.d.	b.d.	3415	2390	3273	4908	920
Ni	b.d.	b.d.	2301	1603	b.d.	b.d.	b.d.	-
	Formulae on the basis of 4 oxygens							
Si	0.98	0.98	0.98	0.97	0.98	0.99	0.98	0.006
Al	0.00	0.00	0.01	0.00	0.01	0.00	0.008	0.004
Fe	0.63	0.58	0.54	0.53	0.57	0.62	0.490	0.09
Mn	0.02	0.02	0.01	0.01	0.01	0.02	0.008	0.004
Mg	1.39	1.44	1.46	1.50	1.45	1.38	1.56	0.064
Ca	0.00	0.00	0.00	0.00	0.00	0.00	0.004	0.005
Fo content	68.8	71.3	73.0	73.9	71.8	69.0	77.0	3.17

FeO = total iron

b.d. below detection (for detection limits see Appendix A.2).

CHAPTER 4 CLINOPYROXENE

Phenocrysts of concentrically zoned clinopyroxene are an important constituent of the kentallenites, pyroxene - mica diorites and of lamprophyric marginal facies of the Ardsheal Hill pipe. In the appinites clinopyroxene occurs as corroded crystals in the cores of idiomorphic amphibole and as grains of the rock matrix (Table 7.1; see section 2.2).

A study of the composition of the clinopyroxene in these different habits was undertaken to (1) determine chemical substitutions related to zoning, (2) assess the petrogenetic significance of the two habits of the clinopyroxene in appinites and (3) use the clinopyroxene chemistry for recognition of the magmatic affinity of the appinite suite.

4.1 Chemistry

Concentrically zoned phenocrysts from the kentallenite of the Kentallen pipe (Fig. 2.3b, 2.4a), pyroxene - mica diorite of the Rudha Mòr pipe (Fig. 2.8c), lamprophyric marginal facies of the Ardsheal Hill pipe (Fig. 2.10c) and clinopyroxene from both the cores of idiomorphic amphiboles and the rock matrix of the appinite from the Back Settlement pipe (Figs. 2.5a, b; 2.7a, b) all have compositions close to the boundary between the diopside and salite fields (Fig. 4.1a; Table 4.1). A negative correlation is shown between Fe and Mg, Al_6 and Si and Na and Ca while a positive correlation is shown between Mg and Si, Ti and Al_6, Mn and Fe and Ti and Fe (Figs. 4.1b, c, e - j). Cr *vs*. Ti plots are highly scattered but there is also an overall negative correlation between them (Fig. 4.1d). There is no clear correlation between either Na or Ca against Mg or Si or Fe or Al.

Based on the observed variations the following substitution is proposed for M_1 and the tetrahedral site in the clinopyroxene of the appinite suite.

$Si + Mg + Cr^{3+} \rightleftharpoons Al + Fe(Mn) + Ti^{4+}$

This interpretation is supported by the linear negative trend of the plots given by the respective sums of these elements (Fig. 4.1k).

An independent Ca $\rightleftharpoons$ 2Na substitution is suggested for the M_2 site as no correlation is observed between the elements occupying the M_1 and M_2 sites.

In the unit cell Mg + Fe + Mn + Ti + Al_6 is usually >1 and Ca + Na is mostly <1 (Table 4.1). This shows that the M_1 site is completely occupied by Mg, Fe, Mn, Ti and Al_6 while Ca and Na occur in the M_2 site. The deficiency in the M_2 site can be compensated by elements exceeding 1 in the M_1 site.

Mg and Si generally decrease while Ti, Fe and Al increase from cores towards margins of the zoned phenocrysts (Table 4.1). However, the variations of these elements are not regular as indicated by the small breaks in several variation diagrams (Figs. 4.1f - k). This indicates that the zoning in the clinopyroxene of the appinite suite is related to the inverse relationship of Si and Mg with Ti, Al and Fe. This is similar to that shown for zoned clinopyroxene from camptonitic lamprophyres elsewhere (Deer *et al.* 1977; *cf.* Velde and Tourton 1970).

4.2 Comparison of clinopyroxene cores of amphibole and in the rock matrix

The clinopyroxene present in the cores of large idiomorphic amphibole crystals in some of the appinites has been interpreted as representing a different stage of crystallisation to that of the clinopyroxene in the rock matrix resulting from return to relatively lower gas pressure crystallisation conditions following explosive release of volatiles after overgrowth formation (Bowes and McArthur 1976; fig. 10). The essentially identical conditions of crystallisation operative at the respective times when the two habits developed is shown by their essentially similar compositions in the two samples of appinite from the Back Settlement (Table 4.1 – 35-38).

If the two habits of clinopyroxene represent two different stages of crystallisation, the clinopyroxene of the rock matrix must represent crystallisation from a residual melt poorer in Ca and Mg than the melt from which the clinopyroxene in the amphibole cores crystallised because of crystallisation of earlier-formed clinopyroxene and amphibole. The resultant compositions of the clinopyroxene would be expected to reflect such compositional differences of the melt even if the two habits were developed under identical physical conditions. As they do not, it is concluded that there was only one stage of clinopyroxene crystallisation and that was early in the crystallisation histories before the development of the idiomorphic amphibole crystals. Clinopyroxene in the rock matrix is interpreted as representing highly fractured early-formed phenocrysts (Fig. 2.7c) or grains on which either amphibole did not nucleate or from which it has been removed by corrosion.

4.3 Petrogenetic implications

As the characteristics of clinopyroxene are considered to be the best criteria for recognition of the magmatic affinity of the basaltic suites (Kushiro 1960; Le Bas 1962; Deer *et al.* 1963, 1977), the nature of this mineral group plays an important role in petrogenetic assessment of the appinitic suite. The lack of two pyroxenes in the suite, the more calcic and less variable composition of its clinopyroxene as compared to those from the non-alkaline suites and their general compositional variation parallel to the Di - He join (Fig. 4.2) suggest an alkaline nature for the magma (Deer *et al.* 1963, 1977). However, on the basis of SiO_2 *vs.* Al_2O_3 and Al_z *vs.* TiO_2 variations, the clinopyroxenes from the appinite suite plot in the non-alkaline (calcalkaline, high-alumina and tholeiitic) field (Fig. 4.3a, b). Taken as a whole, these criteria suggest a transitional nature between alkaline and non-alkaline for the appinite suite. However, the mutual inconsistencies between conclusions based on an individual criterion raise the question as to whether the trend in the pyroxene quadrilateral (Fig. 4.2) and the contents of SiO_2, TiO_2 and Al_2O_3 of the clinopyroxenes reflect the nature of the parental magma, or whether they reflect control by physical conditions and the order of appearance of various phases.

Assessment of the role of plagioclase crystallisation and its effect on variation in magma composition assists in finding an answer. No plagioclase crystallised as phenocrysts in the appinite suite before or along with clinopyroxenes (Chapters 2, 7). Its late appearance is consistent with the high and uniform contents of Ca in the clinopyroxenes, features not seen in clinopyroxene of the suites in which plagioclase crystallised earlier than clinopyroxene (Fig. 4.2). The clinopyroxene from the appinite suite closely corresponds to the synthetic clinopyroxenes crystallised under high water pressure (>7 kb), with olivine, clinopyroxene and phlogopite in the respective order of appearance from a melt of highly potassic rock (Edgar *et al.* 1976). In contrast, clinopyroxene from the transitional basaltic series of Sidlaw Hills in which the crystallisation order is olivine, plagioclase and clinopyroxene show a trend with sharply decreasing Ca contents (Gandy 1973, 1975). These data point to the high Ca in clinopyroxene of the appinite suite and the behaviour of their trend in the quadrilateral being due to the late appearance of plagioclase. This conclusion is comparable to that of Gibb (1973), who attributed the low Ca content in clinopyroxenes from the Shiant Isles sill to the early precipitation of plagioclase.

With the appinite suite showing characters transitional between alkaline and calcalkaline (Chapter 7), the clinopyroxene compositions would be expected to lie across the boundary of non-alkaline and normal alkaline fields of Kushiro (1960) and Le Bas (1962; see Fig. 4.3a, b). However, most of the clinopyroxene plots are in the non-alkaline field indicating higher SiO_2 and lower Al_2O_3 or Al_z and TiO_2 than expected on the basis of the composition of the rock suite. This can be attributed to the order of appearance of various phases with the entry of Ti into the clinopyroxenes being effected by the coeval precipitation of Ti-rich phlogopite and magnetite with the clinopyroxene phenocrysts in the kentallenite of the Kentallen pipe (see section 2.2; Fig. 2.4a). In addition, as there is a negative correlation between SiO_2 and Al_2O_3 and a positive correlation between Al_z and TiO_2 (Figs. 4.3a,b), it is likely that the entry of Al and Si into clinopyroxene was subject to the same controls as those proposed for Ti.

The increase of Al and Ti from cores towards margins in the zoned clinopyroxene phenocrysts of the appinite suite (Table 4.1) and the positive correlation between Al_z and TiO_2 indicate that both Al_z and TiO_2 increased in the clinopyroxenes with increasing fractionation (Fig. 4.3b). The variation trend of clinopyroxene from the appinites (A → B on Fig. 4.3b) diverges significantly from the general fractionation trend proposed by Le Bas (1962) for clinopyroxene of the non-alkaline rocks which is related to decreasing Al_z with increasing Ti. The trend of increasing Al_z with increasing Ti in the clinopyroxene of the appinite suite may be due to increasing P_{H_2O} in the pipes as crystallisation proceeded (*cf*. Deer *et al*. 1977, p. 258). Such an explanation is in line with proposals for increase in gas pressure in the pipes during the early stages of crystallisation (Bowes and Wright 1967; Bowes and McArthur 1976).

4.4 Conclusions

1. The major elements responsible for zoning in the clinopyroxene phenocrysts are Mg, Si, Ti and Al.
2. Clinopyroxene as cores of the idiomorphic amphibole crystals and the clinopyroxene in the rock matrix of appinite from the Back Settlement pipe represent a single stage of crystallisation that

took place before amphibole appeared on liquidus.

3. The chemical characteristics of clinopyroxene are related to crystallisation conditions rather than to the magmatic affinity of the appinite suite with increasing P_{H_2O} during crystallisation playing a role.

Figure 4.1 Clinopyroxene from the appinite suite, Ballachulish district.

(a) Compositional fields in the pyroxene quadrilateral (after Hess and Poldervaart 1951).

(b-j) Variations of Fe *vs*. Mg, Al_6 *vs*. Si, Cr *vs*. Ti, Na *vs*. Ca, Mg *vs*. Si, Ti *vs*. Al_6 and Mn and Ti *vs*. Fe.

(k) Combined substitutional variation between M_1 and tetrahedral sites.

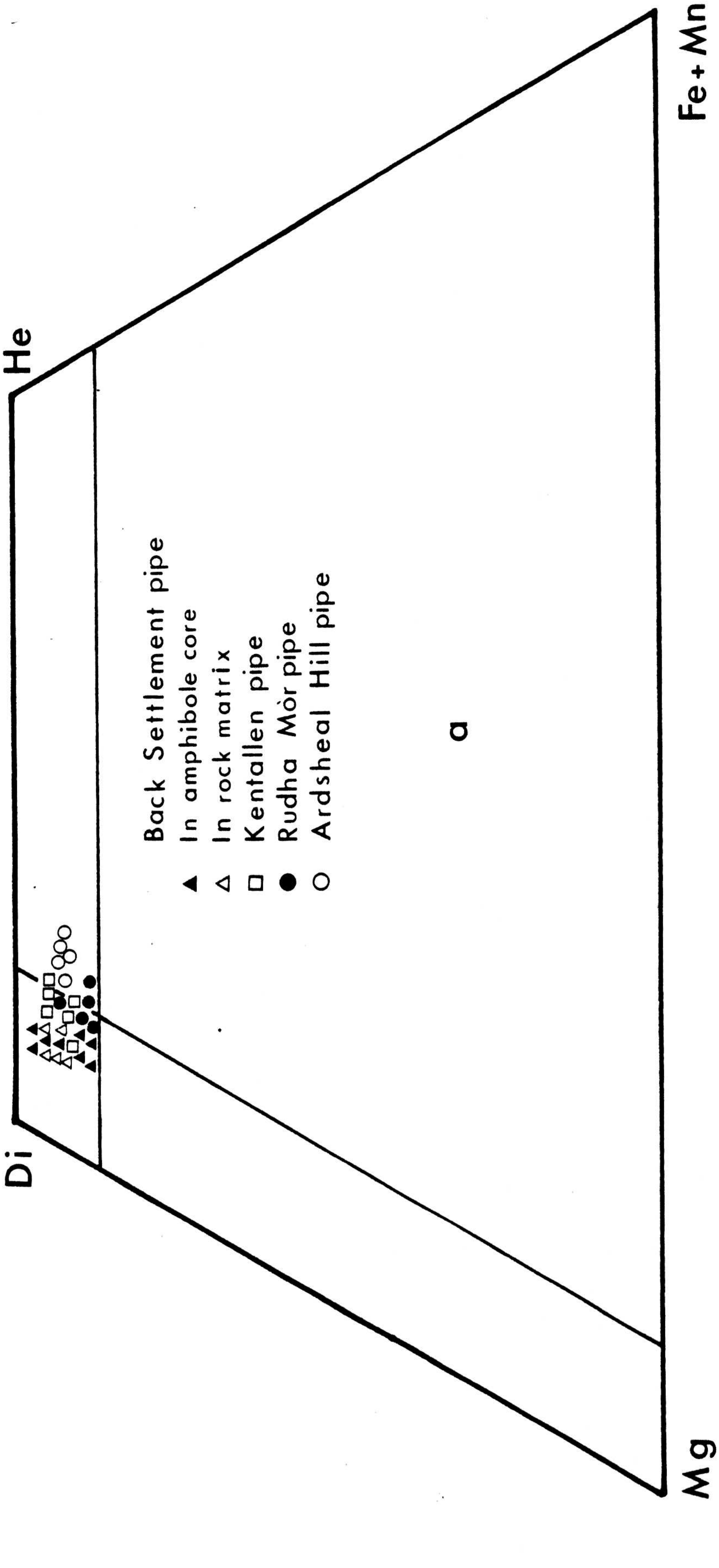
Di
He
Mg
Fe + Mn
▲ Back Settlement pipe In amphibole core
△ In rock matrix
□ Kentallen pipe
● Rudha Mòr pipe
○ Ardsheal Hill pipe
a

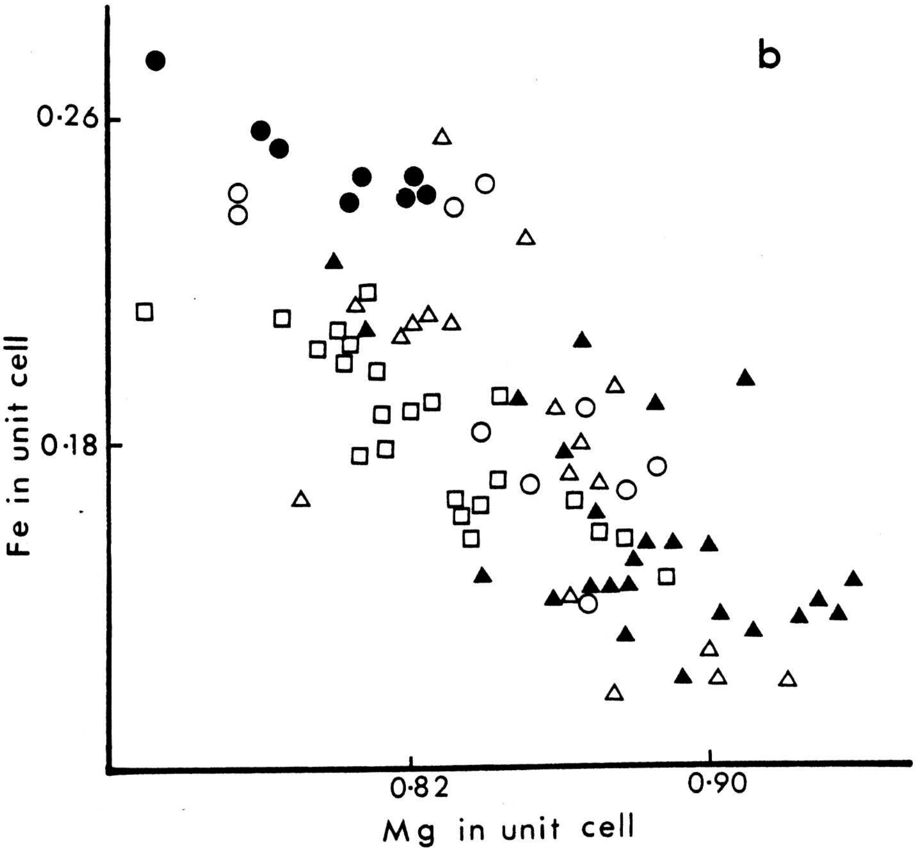
b
0·26
0·18
Fe in unit cell
0·82
0·90
Mg in unit cell

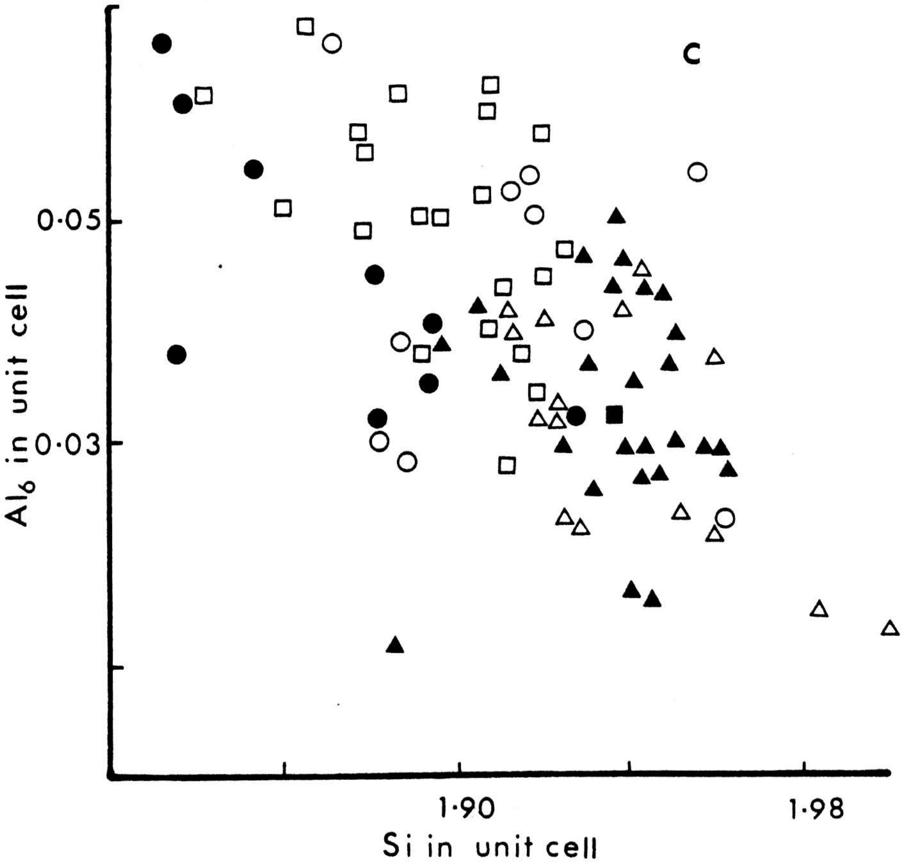
c
0·05
0·03
Al_6 in unit cell
1·90
1·98
Si in unit cell

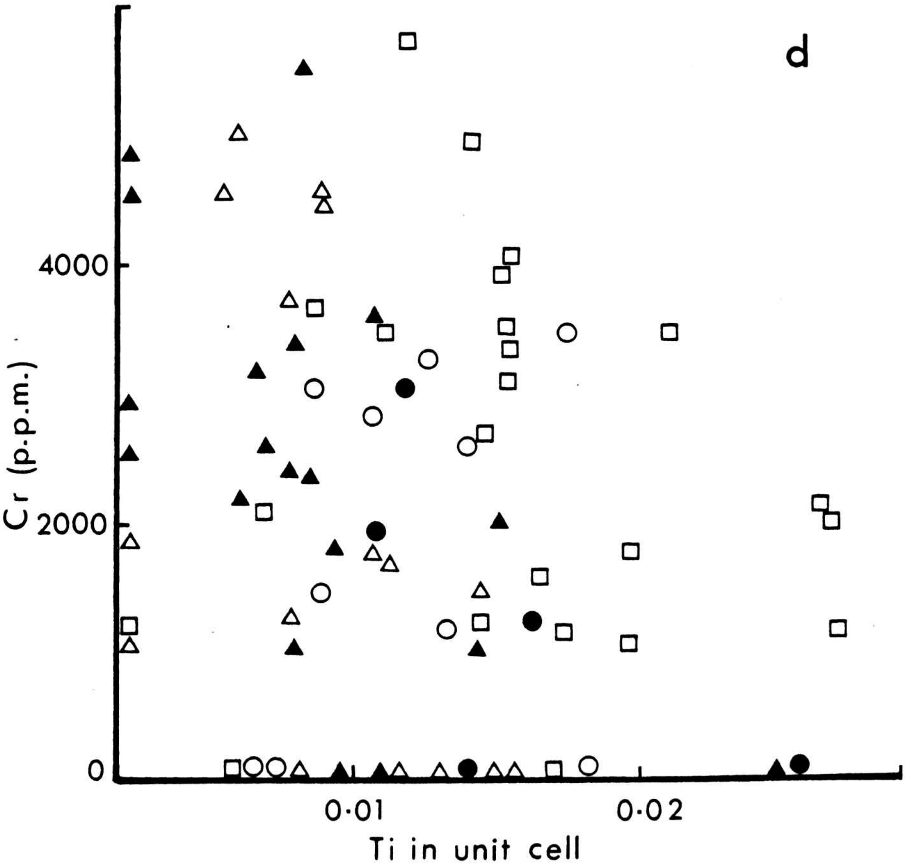
d
Cr (p.p.m.)
4000
2000
0
0·01
0·02
Ti in unit cell

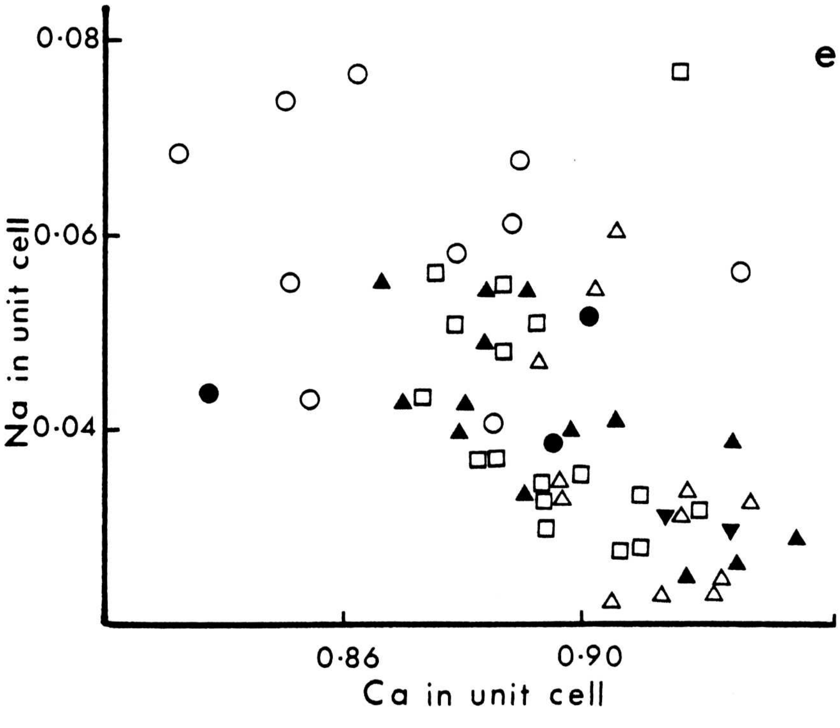
e
Na in unit cell
0·08
0·06
0·04
0·86
0·90
Ca in unit cell

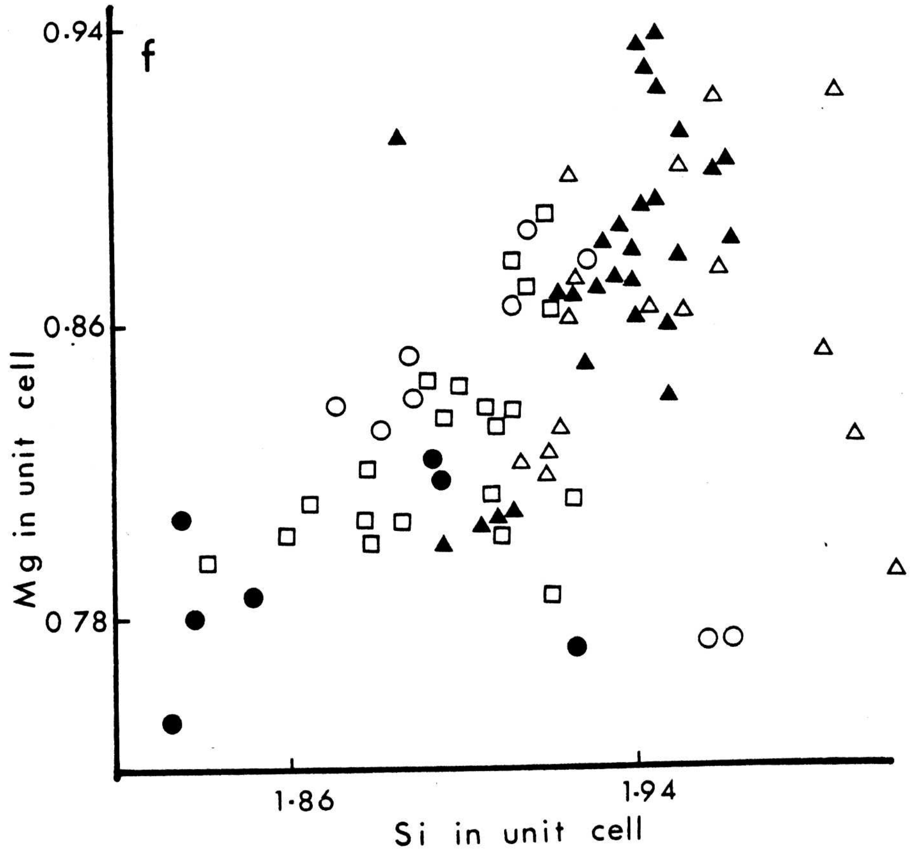
f
0·94
0·86
0 78
Mg in unit cell
1·86
1·94
Si in unit cell

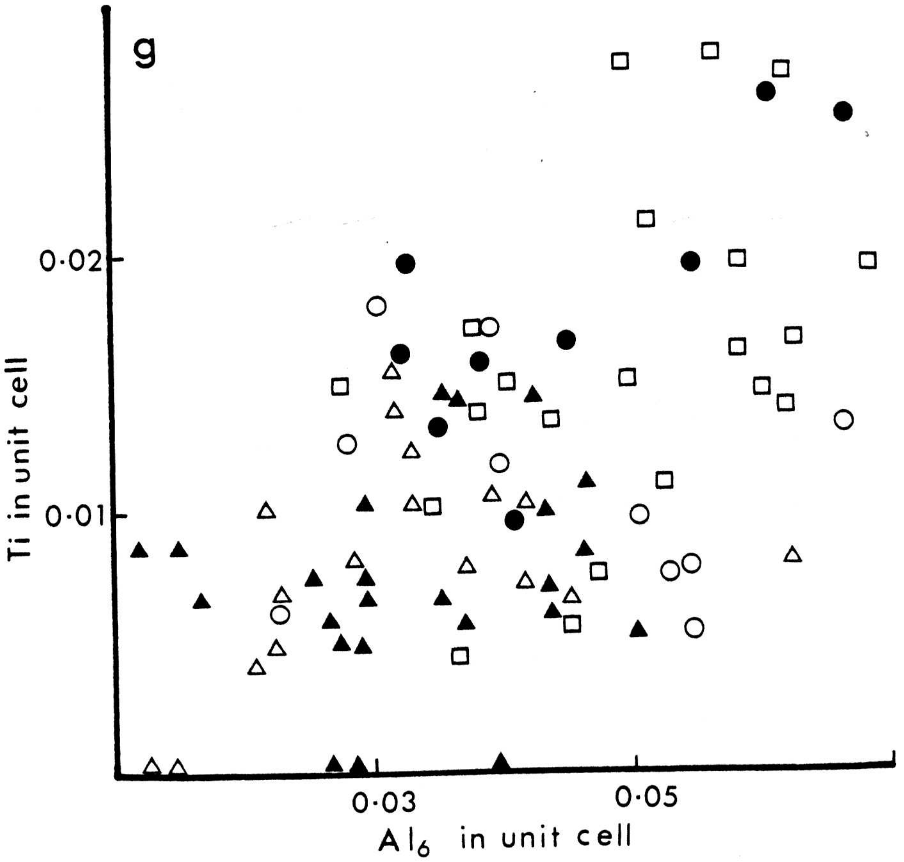
g
0·02
0·01
Ti in unit cell
0·03
0·05
Al₆ in unit cell

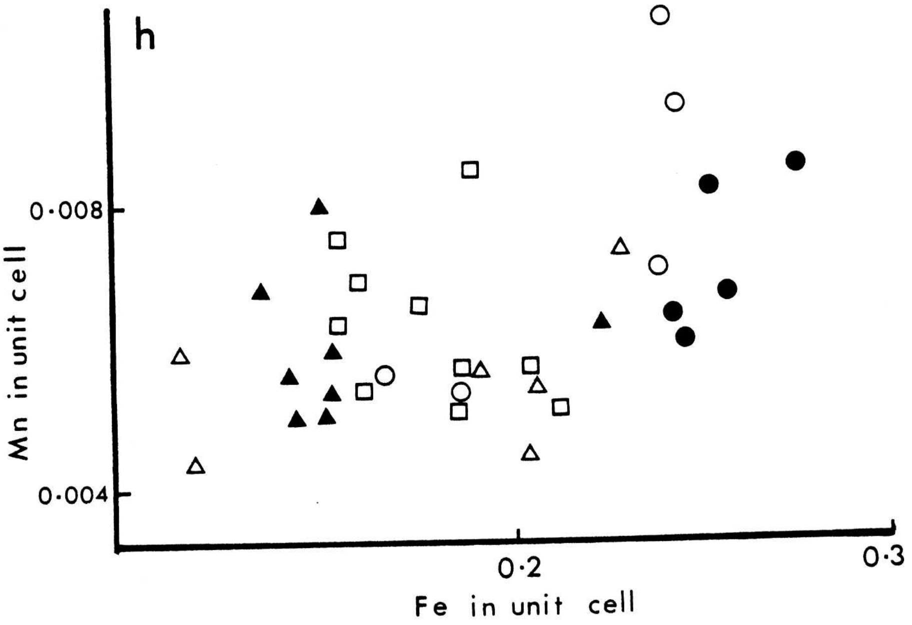
h
0·008
0·004
Mn in unit cell
0·2
0·3
Fe in unit cell

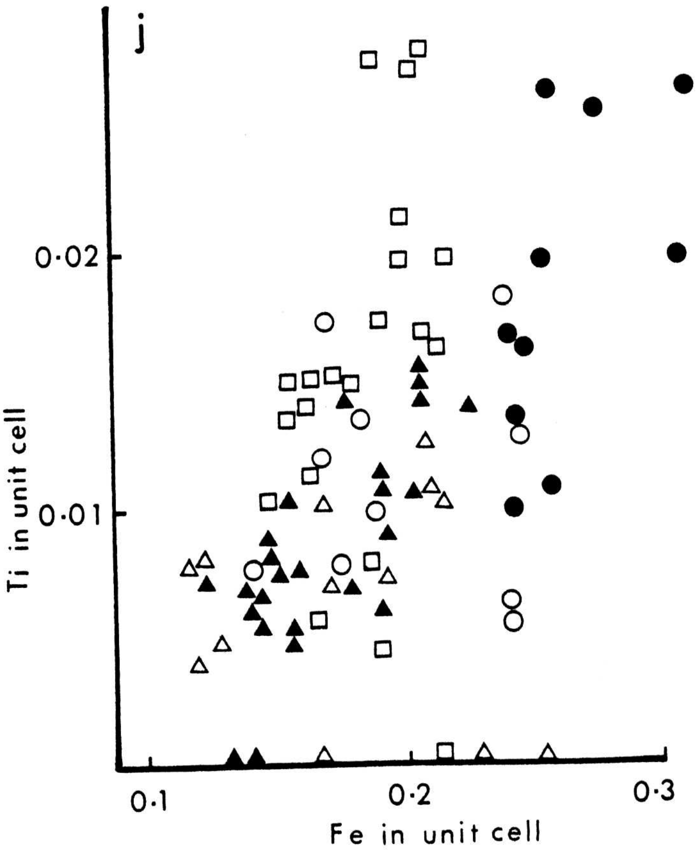
j
0·02
0·01
Ti in unit cell
0·1
0·2
0·3
Fe in unit cell

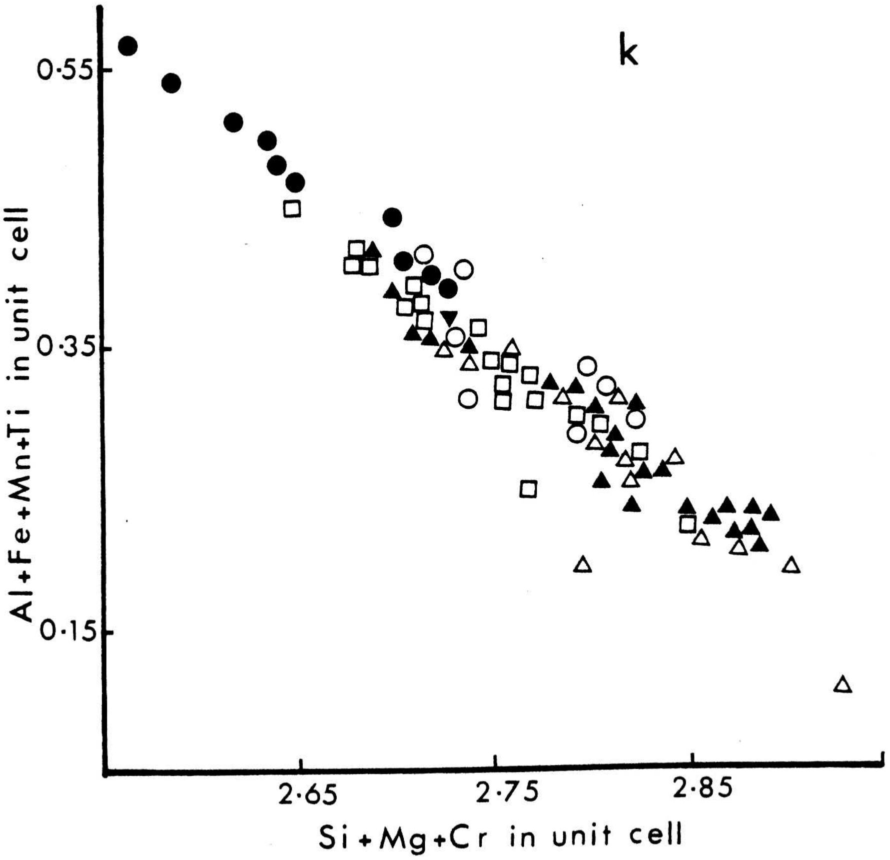
k
0·55
0·35
0·15
Al+Fe+Mn+Ti in unit cell
2·65
2·75
2·85
Si+Mg+Cr in unit cell

Figure 4.2 Comparison of clinopyroxene from the Ballachulish appinite suite with compositions of clinopyroxenes in basaltic rocks and related series. The tholeiitic and alkalic trends are reproduced from Barberi *et al.* (1971).

1. Alkalic basaltic trachyte series, Black Jack teschenite sill, New South Wales.
2. Alkalic basaltic trachyte series, Japan.
3. Alkalic series, Gough Island.
4. Skaergaard series, Greenland.

For tholeiitic series dotted lines are tie lines of two pyroxene assemblages; for localities of the tholeiitic, not numbered, see the above authors. Fields of the clinopyroxene from the Sidlaw Hills lavas (Gandy 1975) and from a highly potassic rock, East Africa (Edgar *et al.* 1976) are also shown.

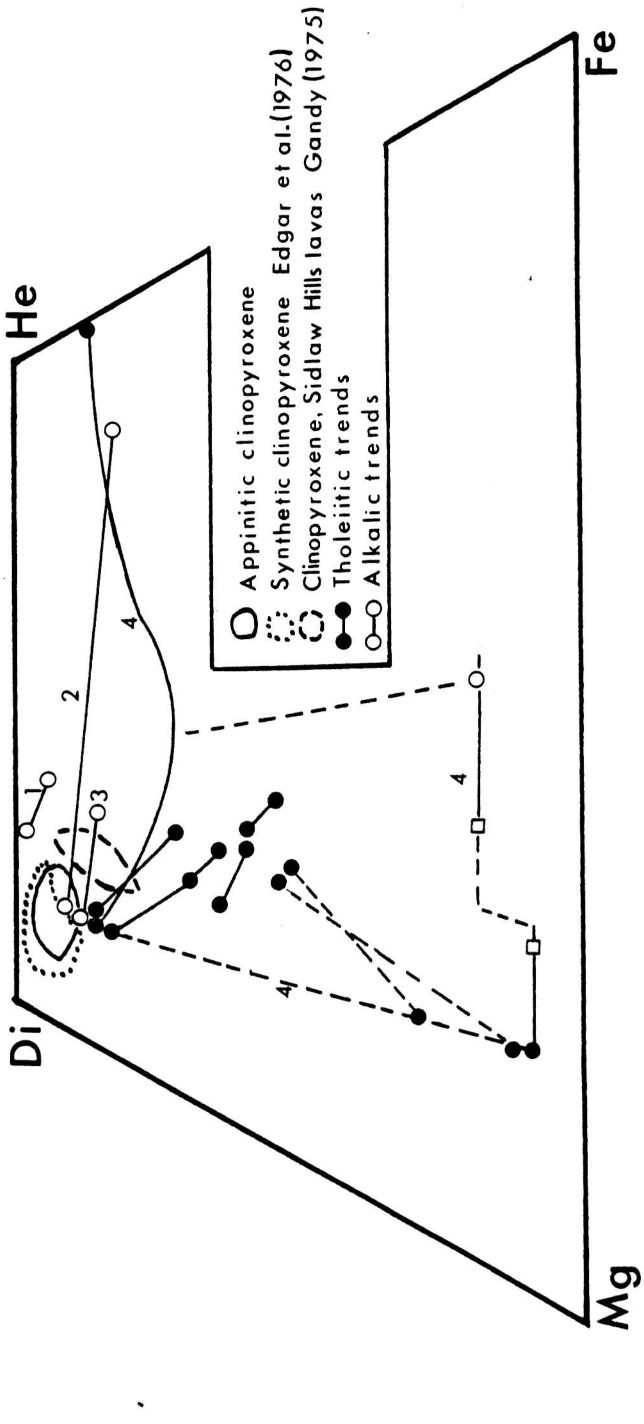
Di
He
Mg
Fe
Appinitic clinopyroxene
Synthetic clinopyroxene Edgar et al.(1976)
Clinopyroxene, Sidlaw Hills lavas Gandy (1975)
Tholeiitic trends
Alkalic trends
1
2
3
4
4
4

Figure 4.3 Discrimination diagrams on the basis of (a) SiO_2 *vs.* Al_2O_3 and (b) Al_z *vs.* TiO_2 for clinopyroxene from the appinite suite, Ballachulish district (after Kushiro 1960; Le Bas 1962).

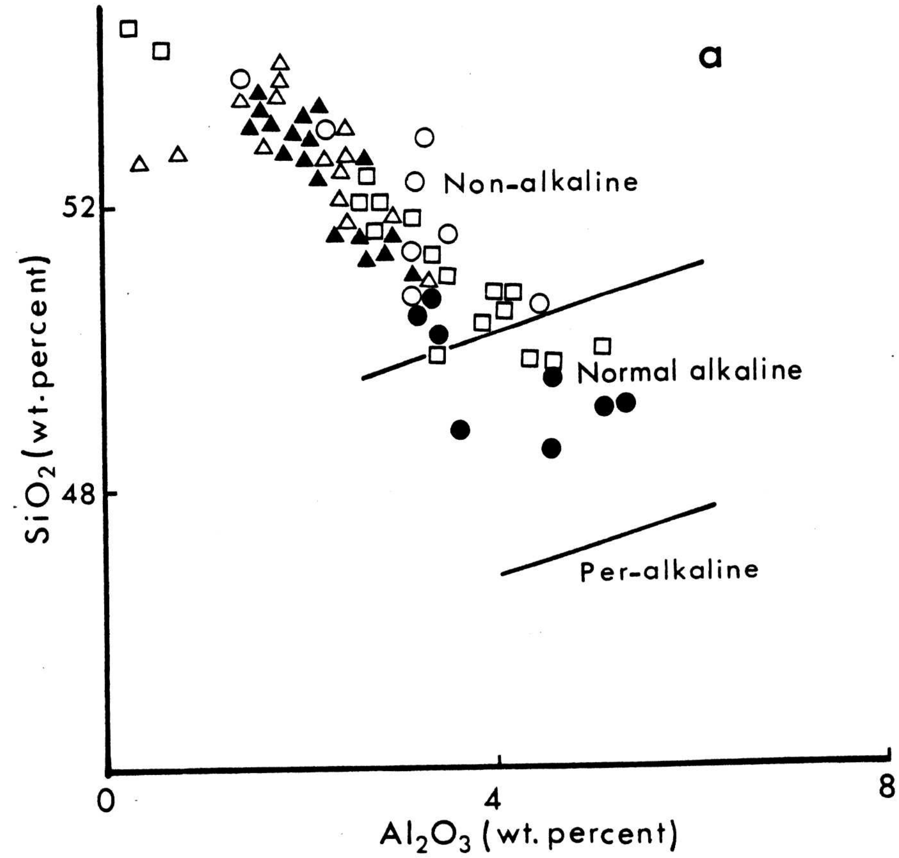
a
Non-alkaline
Normal alkaline
Per-alkaline
SiO_2 (wt. percent)
52
48
0
4
8
Al_2O_3 (wt. percent)

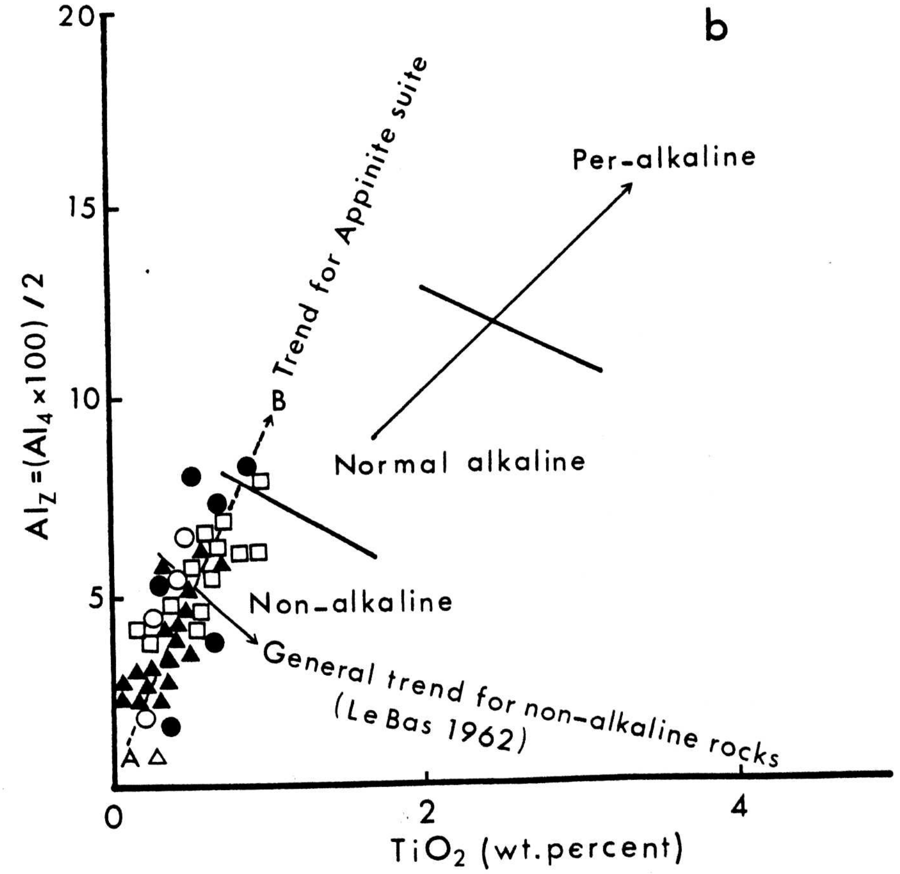
b
20
15
10
5
0
2
4
$Al_Z = (Al_4 \times 100) / 2$
TiO_2 (wt. percent)
Trend for Appinite suite
B
A
Per-alkaline
Normal alkaline
Non-alkaline
General trend for non-alkaline rocks
(Le Bas 1962)

Table 4.1. Clinopyroxene compositions from the appinite suite of the Ballachulish district.

	1	2	3	4	5	6	7	8	9	10
SiO_2	51.77	51.80	51.99	52.05	50.98	52.40	50.75	50.83	49.77	50.76
TiO_2	0.58	0.54	0.50	0.20	0.54	0.37	0.70	0.61	0.75	0.50
Al_2O_3	3.15	3.05	2.82	2.85	3.51	2.68	4.14	3.32	4.34	4.00
FeO	6.80	5.41	5.28	5.39	5.24	5.82	7.00	6.15	6.39	5.72
MnO	0.00	0.00	0.00	0.00	0.22	0.00	0.00	0.27	0.00	0.21
MgO	14.22	15.16	15.84	15.72	15.05	16.29	14.65	15.23	14.42	14.57
CaO	22.30	23.28	22.59	22.73	23.01	22.76	22.24	22.39	22.71	23.31
Na_2O	0.76	0.44	0.71	0.49	0.00	0.46	0.51	0.47	0.46	0.00
Total	99.58	99.68	99.73	99.43	98.55	99.78	99.99	99.27	99.84	99.07
					Trace elements (p.p.m.)					
Cr	1581	3532	1231	2109	4053	3462	1779	1144	3484	2700
					Formulae on the basis of 6 oxygens					
Si	1.92	1.91	1.91	1.92	1.90	1.91	1.88	1.89	1.86	1.89
Ti	0.02	0.01	0.01	0.00	0.01	0.01	0.02	0.02	0.02	0.01
Al	0.14	0.13	0.12	0.12	0.15	0.11	0.18	0.14	0.19	0.17
Fe	0.21	0.16	0.16	0.16	0.15	0.15	0.21	0.19	0.20	0.18
Mn	0.00	0.00	0.00	0.00	0.01	0.00	0.00	0.01	0.00	0.01
Mg	0.79	0.83	0.87	0.86	0.83	0.89	0.81	0.84	0.80	0.81
Ca	0.89	0.92	0.89	0.90	0.92	0.89	0.88	0.89	0.91	0.93
Na	0.05	0.03	0.05	0.03	0.00	0.03	0.04	0.03	0.03	0.00
Al_4	0.08	0.09	0.09	0.08	0.10	0.09	0.12	0.11	0.14	0.11
Al_6	0.06	0.04	0.03	0.04	0.05	0.02	0.06	0.03	0.05	0.06

Table 4.1. *(Contd.)*

	11	12	13	14	15	16	17	18	19	20 Mean (4 anals)	S.D.
SiO_2	50.66	50.98	50.81	49.90	51.00	49.76	51.77	52.07	50.29	51.46	0.24
TiO_2	0.99	0.54	0.51	0.97	0.59	0.69	0.49	0.54	0.97	0.40	0.09
Al_2O_3	4.04	3.42	3.38	5.04	3.28	4.57	3.04	2.67	3.86	3.05	0.4
FeO	6.71	5.53	5.61	6.61	6.61	6.32	5.10	5.11	6.04	5.65	0.52
MnO	0.00	0.00	0.20	0.00	0.18	0.00	0.20	0.24	0.18	0.16	0.01
MgO	14.50	15.26	15.27	14.47	14.40	14.52	15.19	16.03	14.74	14.87	0.35
CaO	22.02	22.38	22.12	22.90	22.07	22.06	23.26	22.55	21.93	22.71	0.06
Na_2O	0.78	0.41	0.20	0.38	0.51	0.66	0.00	0.68	0.70	0.19	0.27
Total	99.70	98.46	98.10	100.27	98.84	98.58	99.05	99.89	98.71	98.42	
					Trace elements (p.p.m.)						
Cr	1163	3344	3925	2153	b.d.	1043	4930	3086	2026	5713	3652
					Formulae on the basis of 6 oxygens						
Si	1.88	1.90	1.90	1.84	1.91	1.86	1.91	1.91	1.88	1.91	0.01
Ti	0.03	0.01	0.01	0.03	0.02	0.02	0.01	0.01	0.03	0.06	0.07
Al	0.18	0.15	0.15	0.22	0.15	0.20	0.13	0.14	0.17	0.13	0.17
Fe	0.21	0.17	0.18	0.20	0.21	0.20	0.16	0.16	0.19	0.17	0.21
Mn	0.00	0.00	0.01	0.00	0.01	0.00	0.01	0.01	0.01	0.01	0.00
Mg	0.80	0.84	0.81	0.80	0.81	0.81	0.83	0.88	0.82	0.82	0.02
Ca	0.87	0.89	0.91	0.91	0.88	0.88	0.92	0.89	0.88	0.90	0.01
Na	0.05	0.03	0.01	0.03	0.04	0.05	0.00	0.05	0.01	0.01	0.02
Al_4	0.12	0.10	0.10	0.16	0.09	0.14	0.09	0.09	0.12	0.09	0.01
Al_6	0.06	0.05	0.05	0.06	0.06	0.06	0.05	0.05	0.05	0.04	0.00

Table 4.1. (Contd.)

	21	22	23	24	25	26	27	28	29	30	31	32	33	34
SiO_2	51.90	52.36	51.55	52.45	52.92	51.28	50.50	50.10	49.49	48.49	49.09	49.15	50.63	50.49
TiO_2	0.35	0.28	0.62	0.43	0.28	0.46	0.48	0.57	0.69	0.56	0.92	0.90	0.35	0.47
Al_2O_3	3.03	3.18	3.51	2.56	3.29	3.21	4.46	3.40	4.58	4.54	5.06	5.29	3.31	3.21
FeO	6.10	5.69	5.57	5.49	4.66	7.90	5.90	7.82	8.05	7.75	8.19	8.78	7.70	7.72
MnO	0.17	0.00	0.00	0.18	0.00	0.30	0.00	0.00	0.26	0.19	0.21	0.27	0.00	0.20
MgO	15.75	16.26	15.62	16.02	16.09	15.31	15.19	14.66	14.10	14.31	13.99	13.54	14.69	14.73
CaO	21.02	21.78	22.64	21.61	22.97	21.56	21.72	22.22	22.60	22.21	22.33	22.49	22.43	22.45
Na_2O	0.95	0.61	0.86	0.77	0.96	1.03	1.06	1.06	0.53	0.00	0.70	0.00	0.00	0.00
Total	99.27	100.15	100.37	99.51	101.17	101.05	99.31	99.30	99.77	98.75	99.79	100.42	99.11	99.27
Trace elements (p.p.m.)														
Cr	2817	1466	3478	3258	3041	1166	2599	b.d.	b.d.	1232	b.d.	b.d.	1899	b.d.
Formulae on the basis of 6 oxygens														
Si	1.92	1.92	1.89	1.93	1.91	1.89	1.87	1.88	1.85	1.83	1.84	1.83	1.89	1.89
Ti	0.01	0.01	0.02	0.01	0.01	0.01	0.01	0.02	0.02	0.02	0.03	0.03	0.01	0.01
Al	0.13	0.14	0.15	0.11	0.14	0.14	0.19	0.15	0.20	0.20	0.22	0.23	0.15	0.14
Fe	0.18	0.17	0.17	0.17	0.14	0.24	0.18	0.24	0.25	0.24	0.26	0.27	0.24	0.24
Mn	0.01	0.00	0.00	0.01	0.00	0.01	0.00	0.00	0.01	0.01	0.01	0.01	0.00	0.01
Mg	0.87	0.87	0.85	0.88	0.87	0.84	0.84	0.82	0.79	0.81	0.78	0.75	0.82	0.82
Ca	0.83	0.85	0.89	0.85	0.89	0.85	0.86	0.89	0.90	0.90	0.89	0.90	0.90	0.90
Na	0.07	0.04	0.06	0.05	0.07	0.07	0.08	0.04	0.00	0.05	0.00	0.00	0.00	0.00
Al_4	0.08	0.08	0.11	0.07	0.09	0.11	0.13	0.12	0.15	0.17	0.16	0.17	0.11	0.11
Al_6	0.05	0.06	0.04	0.04	0.05	0.03	0.06	0.03	0.05	0.03	0.06	0.06	0.04	0.03

Table 4.1. (Contd.)

	35		36		37		38	
	Mean (12 anals)	S.D.	Mean (10 anals)	S.D.	Mean (12 anals)	S.D.	Mean (7 anals)	S.D.
SiO_2	52.66	0.68	52.72	0.85	52.36	0.77	52.29	0.32
TiO_2	0.28	0.17	0.34	0.12	0.23	0.13	0.32	0.14
Al_2O_3	2.21	0.55	2.23	0.53	2.27	0.39	2.39	0.11
FeO	5.22	0.95	5.68	1.28	5.23	0.87	5.56	0.95
MnO	0.07	0.10	0.11	0.19	0.02	0.06	0.04	0.09
MgO	15.79	0.75	15.60	0.78	16.30	0.67	15.92	0.39
CaO	23.18	0.42	23.23	0.19	22.43	0.33	22.60	0.32
Na_2O	0.21	0.24	0.30	0.21	0.51	0.28	0.44	0.34
Total	99.62		100.21		99.35		99.56	
Trace elements (p.p.m.)								
Cr	2125	1825	2051	2088	1466	1468	1677	2878
Formulae on the basis of 6 oxygens								
Si	1.93	0.02	1.93	0.02	1.93	0.02	1.92	0.01
Ti	0.01	0.00	0.01	0.00	0.01	0.00	0.01	0.00
Al	0.09	0.02	0.09	0.02	0.09	0.02	0.12	0.00
Fe	0.16	0.03	0.17	0.04	0.16	0.03	0.17	0.03
Mn	0.01	0.01	0.00	-	0.00	-	0.00	-
Mg	0.87	0.04	0.85	0.04	0.89	0.03	0.87	0.02
Ca	0.91	0.02	0.91	0.01	0.88	0.01	0.89	0.01
Na	0.02	0.02	0.02	0.01	0.04	0.02	0.03	0.03
Al_4	0.07	0.02	0.07	0.02	0.07	0.02	0.08	0.01
Al_6	0.02	0.01	0.02	0.01	0.02	0.01	0.01	0.01

1-19	Compositions of zones of concentrically zoned diopside phenocrysts, kentallenite, Kentallen pipe (Table 7.1 – 52; *cf*. Figs. 2.3b, 2.4a).
20	Average compositions of other diopside grains from the same rock as 1-19.
21-27	Compositions of zones of concentrically zoned diopside - salite phenocrysts, pyroxene-mica diorite, Rudha Mòr pipe (Table 7.1–39; *cf*. Fig. 2.8c).
28-34	Compositions of zones of a concentrically zoned salite phenocryst, lamprophyric marginal facies, Ardsheal Hill pipe (Table 7.1 – 21 ; *cf*. Fig. 2.10c).
35	Diopside cores in idiomorphic amphiboles in appinite, Back Settlement (Table 7.1 – 9; *cf*. Figs. 2.5a, b; 2.7a, b).
36	Diopside grains in matrix of the same rock as 35 (*cf*. Fig. 2.7a).
37	Diopside cores in idiomorphic amphiboles in appinite, Back Settlement; 4 m from 35.
38	Diopside grains in matrix of the same rock as 37.

FeO = total iron

Ni and Co are below detection limit (see Appendix A.2).

CHAPTER 5 AMPHIBOLE

The amphibole occurring as weak to intensely zoned, large iodiomorphic crystals with rhythmic overgrowths of actinolite in appinite (Figs. 2.4b, 2.5a-c) and hornblendite, and less frequently in pyroxene - mica diorite (Chapter 2), was studied to (a) determine the elements responsible for the zoning, (b) confirm what has been interpreted as actinolite resulting from igneous crystallisation is compositionally actinolite (Bowes *et al.* 1964), (c) find out various substitutions taking place, (d) determine the physical conditions of amphibole crystallisation, (e) establish whether the chemical peculiarities of the appinite suite are shown in the amphibole chemistry and (f) determine the Si contents related to particular Ca + Na + K contents in the actinolites.

5.1 Chemistry

Amphiboles from the appinite of Back Settlement, Ardsheal Hill and Garbh Allt and from both the marginal biotite - pyroxene - hornblende - feldspar rock and the pyroxene - mica diorite of the Rudha Mòr pipe (Table 7.1 – 9,12, 29, 39; Appendix B.2-20) have $(Ca + Na)_B \geq 1.34$ and $Na_B < 0.67$; accordingly they are calcic amphiboles (Table 5.1, Appendix B.1). The large idiomorphic crystals which are a characteristic feature of the appinites are all pargasite while the overgrowths vary from actinolite through actinolitic - hornblende to magnesio - hornblende (Fig. 5.1).

5.1A Single amphibole crystal

A large idiomorphic crystal of pargasite with prominent overgrowths from Back Settlement was selected for detailed investigation (Fig. 5.2a; Table 5.1). Both its brown core and a green rim are pargasitic while the alternating green and colourless overgrowths are actinolitic. There is a decrease in the Ti content from centre to margins with a break at the interface of brown core and green rim (Fig. 5.2b).

Corresponding breaks occur at the same position in the Fe:Mg and Ti:Mg ratios. These ratios also show breaks in the overgrowths, corresponding to boundaries of the bands of different colour (Figs. 5.2c, d). There is no variation in the proportion of Al_4 with varying Ti contents in the pargasite but it increases with Ti in the overgrowths (Fig. 5.2e). The brown to green variation in the colour is attributed to decrease in Ti (Lemeon 1980), such a variation being attributed to decreasing temperature and increasing oxygen fugacity by Helz (1973). The intensity of green colour in overgrowths corresponds to changes in the Fe^{3+} proportion which also increases with increasing oxygen fugacity (Miyashiro 1973).

As phlogopite - biotite, apatite and primary magnetite usually occur in the green rim of the pargasite (*cf.* Figs. 2.3a, 2.5a, 2.7a, b) and sphene in the overgrowths, the compositional breaks in pargasite and overgrowths, can be attributed to the simultaneous crystallisation of the above Ti-bearing minerals (M. Q. Jan and R. A. Howie personal commun.) and the precipitation of apatite which enriches the Mg and Ti contents of the melt relative to the crystallising phases (Ryerson and Hess 1979).

5.1B Overall chemistry

Taking the amphiboles from the various pipes, there are inverse correlations between Fe and Mg and between Na and Ca (Fig. 5.3a, b); these suggest simple $Mg \rightleftharpoons Fe(Mn)$ and $Ca \rightleftharpoons 2Na$ exchange reactions. K *vs.* Ca varies positively in the pargasite but negatively in the overgrowths except in magnesio - hornblendes (Fig. 5.3c). This may be due to $Ca \rightleftharpoons NaM_4$ and $K_A \rightleftharpoons Na_A$ substitutions in the pargasite and $Ca \rightleftharpoons NaM_4$ + A-site substitution in the overgrowths. As the plots for magnesio - hornblende show scatter on both Na *vs.* Ca and K *vs.* Ca variation diagrams, a combination of the above substitutions is proposed.

A negative correlation is observed between Al and Mg for all the amphiboles except the pargasites from the Rudha Mòr pipe (Fig. 5.3d). No relationship has been found between Fe and Al_4 and there is a clear relationship between Al_4 and Mg/Mg + Fe (*cf.* Figs. 5.1a, b). This can be attributed to a tschermakitic type substitution ($Si + Mg \rightleftharpoons 2Al$) except for the pargasite of the Rudha Mòr pipe for which a $3Si \rightleftharpoons 4Al$ substitution is proposed.

Al_4 varies positively with A-site occupancies in all amphiboles (Fig. 5.3e). In the case of both the pargasites and the magnesio - hornblendes, the overall trend is parallel to a 1:1 line but in the case of the overgrowths of actinolite and actinolitic - hornblende compositions, the shape of the line is considerably steeper and approximately parallel to that for amphiboles from the Finnmarka complex (Czmanske and Wones 1973). This indicates a higher edenitic substitution in the pargasites and magnesio - hornblendes than in the actinolites and actinolitic - hornblendes. As Al_4 varies negatively with NaM_4 in the pargasites and shows no strong correlation in the overgrowths (see Fig. 5.4), a $Si + NaM_4 \rightleftharpoons Al_4$ + A-site substitution is suggested for pargasites and $Si + \boxed{A} \rightleftharpoons Al_4$ + A-site substitution for the overgrowths.

Ti apparently varies positively with Al_4 in all amphiboles (Fig. 5.3f). However, there is a high-Ti group corresponding to the brown cores and low-Ti group to the green rims of pargasites in which Al_4 is actually constant with varying Ti in individual pargasite grains as shown by the compositions determined from the selected single amphibole crystal from the Back Settlement pipe (see Fig. 5.2e). Ti varies positively with Mg in both the brown core and the green rim and negatively in the overgrowths of the above crystals (Fig. 5.2d). Accordingly, $Mg + Ti^{4+} \rightleftharpoons 2Fe^{3+}$ or $Mg + Ti^{4+} \rightleftharpoons Fe^{3+} + Al_6$ substitutions are indicated in the pargasites and a $Si + Mg \rightleftharpoons 2Al + Ti^{4+}$ substitution in the overgrowths.

The lack of correlation between Al_6 and Si in the pargasites (Fig. 5.3g) may produce an extra positive charge in M_1 - M_3 sites. This can be compensated by $\boxed{M_1 - M_3} + Mn \rightleftharpoons Al_6$ type substitution in the brown cores for which Mn *vs.* Al_6 plots show a negative correlation (Fig. 5.3h). As Al_6 remains constant in the green rims, it probably compensates the marked decrease in Ti (*cf.* Fig. 5.2b).

5.2 Pressure estimation

The pargasites lie well below the 5 kb line of Raase (1974) while the overgrowths of actinolite and actinolitic - hornblende straddle this line; the magnesio - hornblendes occupy an intermediate position (Fig. 5.3g). This suggests a higher pressure for the growth of the overgrowths than for the pargasites. If the pressure estimate for metamorphism using the NaM_4 *vs.* Al_4 is relevant to the products of igneous crystallisation, then the overgrowths have crystallised below 3 kb (Fig. 5.4; Brown 1977). This estimate of pressure is considerably lower than that derived using the plot of Raase (1974), the difference being due to the lack of a strong correlation between NaM_4 contents and Al_4 in the overgrowths. If it is legitimate to extrapolate pressures towards the magnesio - hornblende and pargasite compositions in Figure 5.4, then pressures for these were 3 - 4 and 2 - 4 kb, respectively. These values correspond with those determined from the method of Raase.

Leake (1965, 1971) found that the higher the Al_6 in amphiboles, the higher the pressure of formation. However, both the maximum Al_6 limit of Leake and the 5 kb line of Raase are based on the associated Al_4 contents (Fig. 5.3g). Accordingly, the estimates of pressure on the basis of the Raase method seem to be the more acceptable.

5.3 Temperature estimatimation

Temperature of growth for the single amphibole crystal (Fig. 5.2a) on the basis of Ti contents using comparison with experimental data

(Fig. 5.5a) gives the following:

	Brown core	Green rim
Upper limit	845°-830°C	780°-745°C
Lower limit	825°-805°C	755°-700°C

Using an extrapolation on the basis of all the Ti going into amphibole rather than having other Ti-bearing phases and apatite crystallising together with the green rims of pargasite and sphene together with overgrowths (*i.e.* Ti variation followed the AB line in Fig. 5.2b), the Ti contents have been recast in the model of Helz (1973). From this the following temperatures were deduced for the green rim of the pargasite (Fig. 5.5b):

Upper limit	825°-805°C
Lower limit	805°-770°C

The occasional association of albite with the greenest part of the pargasite in the appinite of the Back Settlement pipe (Fig. 2.7a) supports the lower limit temperature estimates as albite crystallises in the Ab - An system at 770°C at pressures of 3 - 4 kb P_{H_2O} (Yoder *et al.* 1957; Deer *et al.* 1963).

Temperature ranges of 795°-760° and 790°-755°C are estimated for magnesio - hornblendes and other overgrowths, respectively.

Considering the maximum Ti obtained from amphiboles of the various pipes (Table 5.1, Appendix B.1) pargasite appeared on the liquidus at 960°C in Ardsheal Hill pipe, at 940°C in Rudha Mòr pipe, at 900°C in the Back Settlement and below 900°C in the Garbh Allt pipe.

5.4 Chemical peculiarities of the appinite suite reflected in the amphibole chemistry

On the basis of Al_4 *vs.* A-site variation pargasites from the appinite suite have certain chemical characteristics similar to those of synthetic amphiboles from melts varying from tholeiitic to alkali basaltic (Fig. 5.3e). However, there are marked differences indicated by their variation trend which does not correspond with any one of those of the basaltic suites of Helz (1973). These features suggest crystallisation of pargasite from a melt transitional between alkaline and non-alkaline. The general compositional correspondence of the actinolitic overgrowths with the trend of amphibole from granite rocks of the Finnmarka complex points to crystallisation from a residual liquid of high Si-activity. The production of such liquid could have resulted from the early crystallisation of clinopyroxene and pargasite in the pipes. This interpretation is supported by the positive correlation of the average Mg/Mg + Fe ratios in the pargasite against these ratios in their host rocks, *i.e.* the strong dependence of the amphibole composition on the composition of the melt from which it has been crystallised (Fig. 5.6). However, plots of the above ratios for the overgrowths are scattered. This indicates that other factors, like changing oxygen fugacity and gas pressure disturbed the relationship during the crystallisation of the overgrowths (see Binns 1965a, b).

5.5 Maximum Si limit with associated Ca + Na + K

The pargasites lie below while the majority of the overgrowths lie above the line in a Si *vs.* Ca + Na + K plot which Leake (1971) considers to represent the compositional limit of amphiboles of igneous derivations (Fig. 5.7). The maximum Si in a half unit cell for the amphiboles in overgrowths is 7.91. This is considerably in excess of the figure of 7.45 given by Leake (1971) and that of 7.64 reported by Czmanske and Wones (1973). Accordingly a revised limit is given in Figure 5.7.

5.6 Conclusions

1. The large idiomorphic amphibole crystals are compositionally pargasitic and their zoning is mainly due to Ti variation.
2. The majority of the overgrowths are compositionally actinolites and their rhythmic variations are due to varying Fe^{3+} contents.
3. The compositional breaks in pargasite and overgrowths are due to

the simultaneous crystallisation of Ti-bearing minerals and apatite.

4. Pargasite crystallised below 5 kb P_{H_2O} in a temperature range of 960°-770°C in most of the pipes while overgrowths were developed at about 5 kb P_{H_2O} in a temperature range of 800°-750°C.
5. Phlogopite, primary magnetite, apatite and albite appeared on liquidus below 5 kb P_{H_2O} in a temperature range of 825°-770°C in the Back Settlement pipe.
6. The pargasite composition is strongly dependent on its host rock composition and reflects the transitional nature of the appinite suite.
7. The overgrowths have developed from a more silicic liquid than that from which pargasite has crystallised.
8. The maximum Si limit in a half unit cell of overgrowths exceeds that proposed by Leake (1971) for igneous amphiboles; the maximum figure is 7.91.

Figure 5.1 Compositional fields for amphibole from the Ballachulish appinite suite (after Leake 1978).

CALCIC AMPHIBOLES; $(Ca+Na)_B \geq 1{\cdot}34$; $Na_B < 0{\cdot}67$

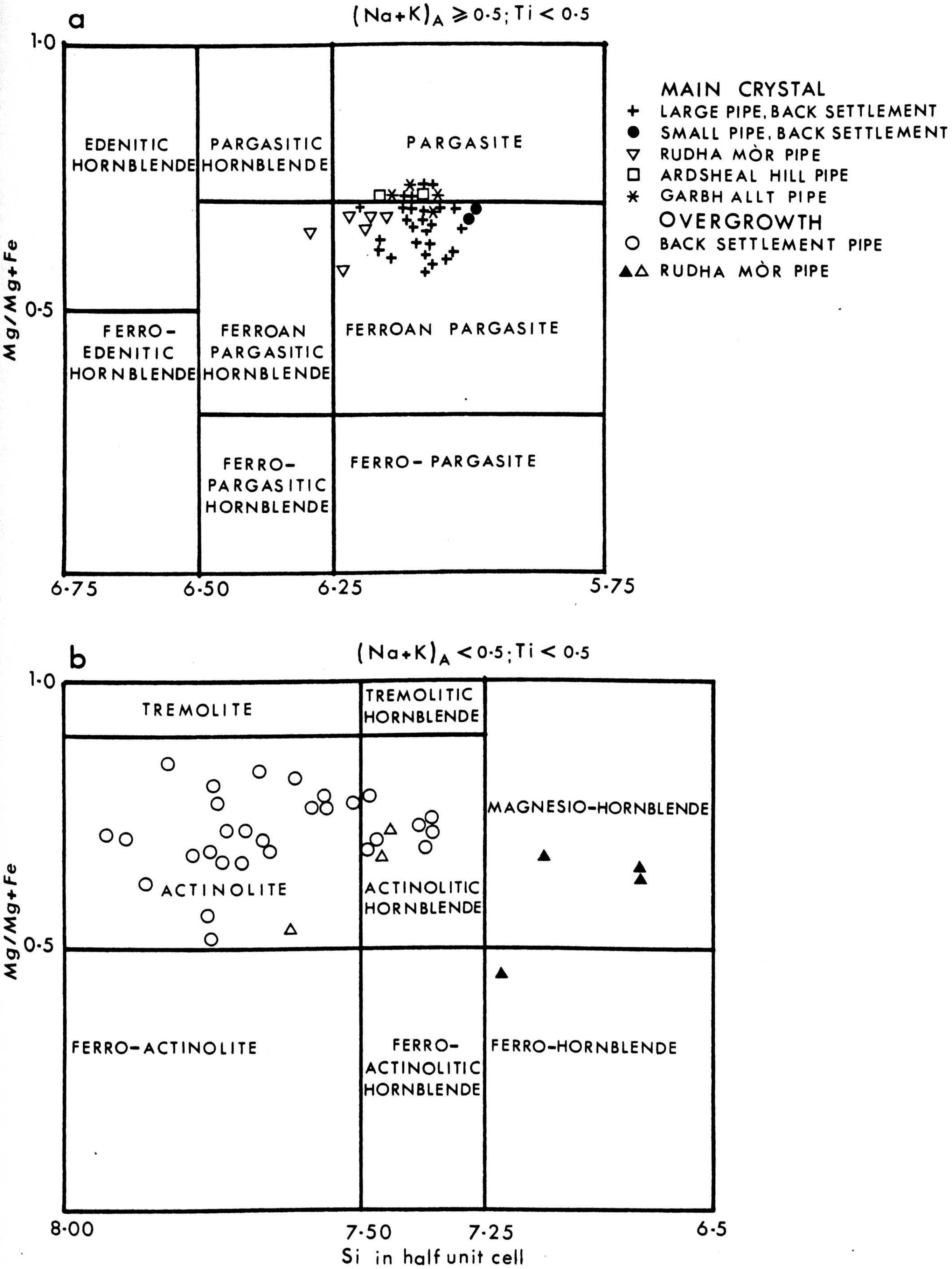

Figure 5.2

(a) Schematic representation of the selected amphibole crystal from the appinite of the Back Settlement pipe. Dotted lines represent arbitrary zones (A_1 - A_4, B_1 - B_3) based on equally decreasing Ti (in half unit cell) from centre towards margins. Numbers 1-17 represent analyses in Table 5.1.

(b) Half unit cell Ti in various zones of the selected amphibole crystal and maximum half unit cell Ti in actinolitic overgrowths and magnesio - hornblendes.

(c-e) Half unit cell variations of Fe and Ti against Mg and Ti against Al_4, respectively.

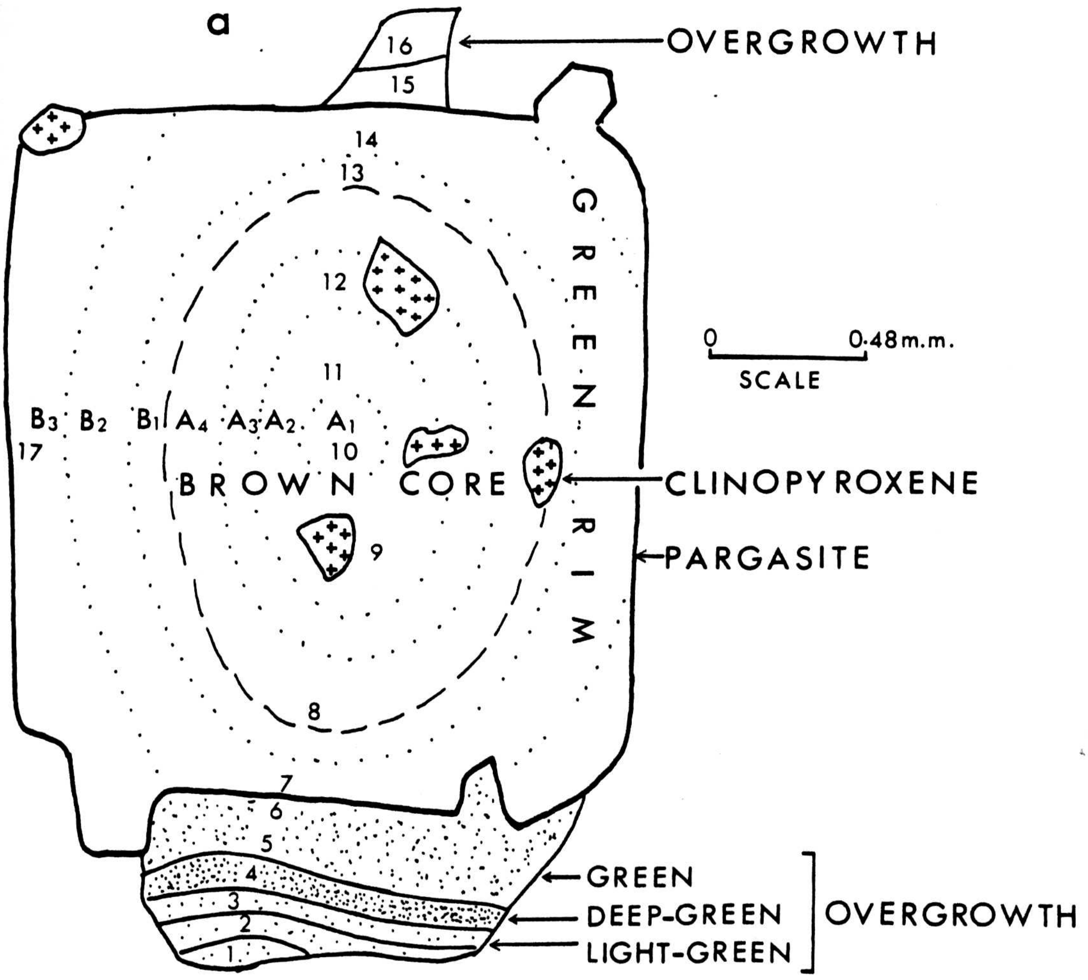
a
OVERGROWTH
16
15
14
13
12
11
10
9
8
7
6
5
4
3
2
1
GREEN RIM
0
0·48m.m.
SCALE
B3 B2 B1 A4 A3 A2 A1
17
BROWN CORE
CLINOPYROXENE
PARGASITE
GREEN
DEEP-GREEN
LIGHT-GREEN
OVERGROWTH

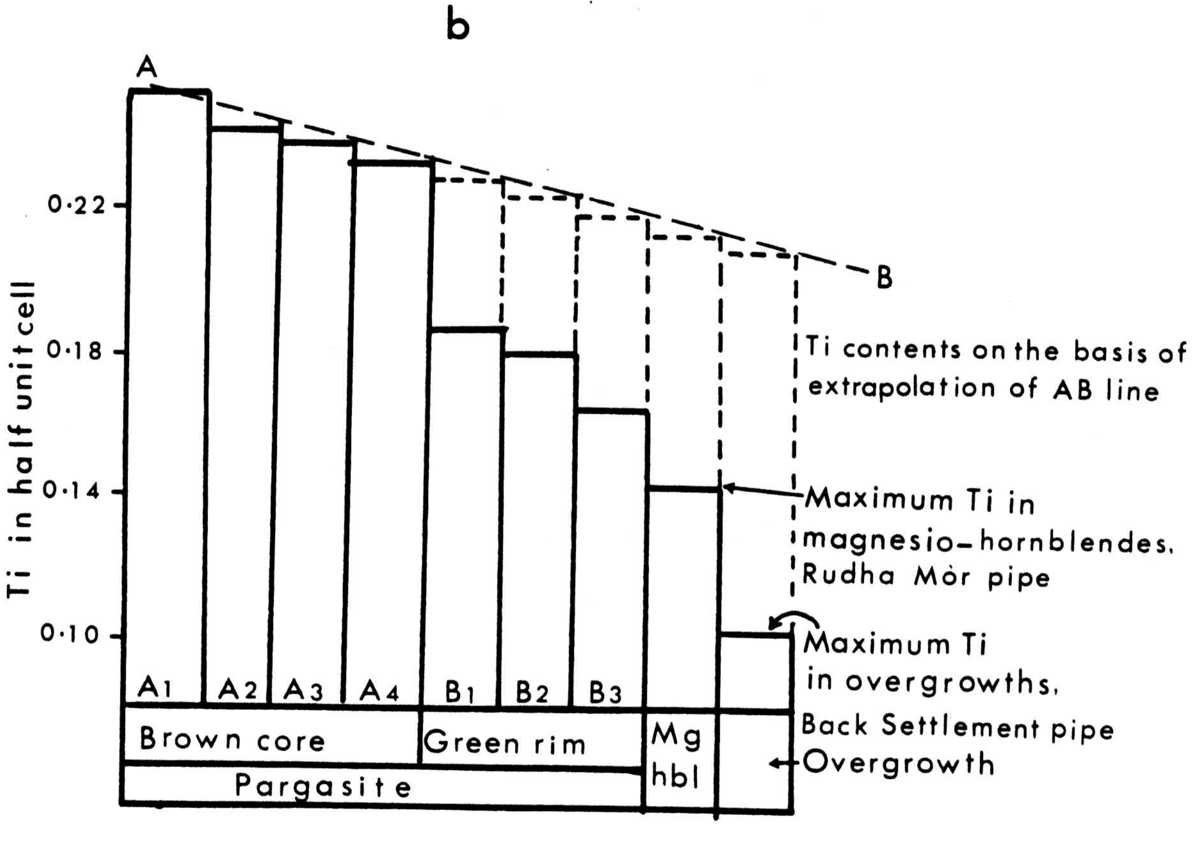
b
A
B
Ti in half unit cell
0·22
0·18
0·14
0·10
Ti contents on the basis of extrapolation of AB line
Maximum Ti in magnesio-hornblendes, Rudha Mòr pipe
Maximum Ti in overgrowths, Back Settlement pipe
Overgrowth
A1 A2 A3 A4 B1 B2 B3
Brown core
Green rim
Mg hbl
Pargasite

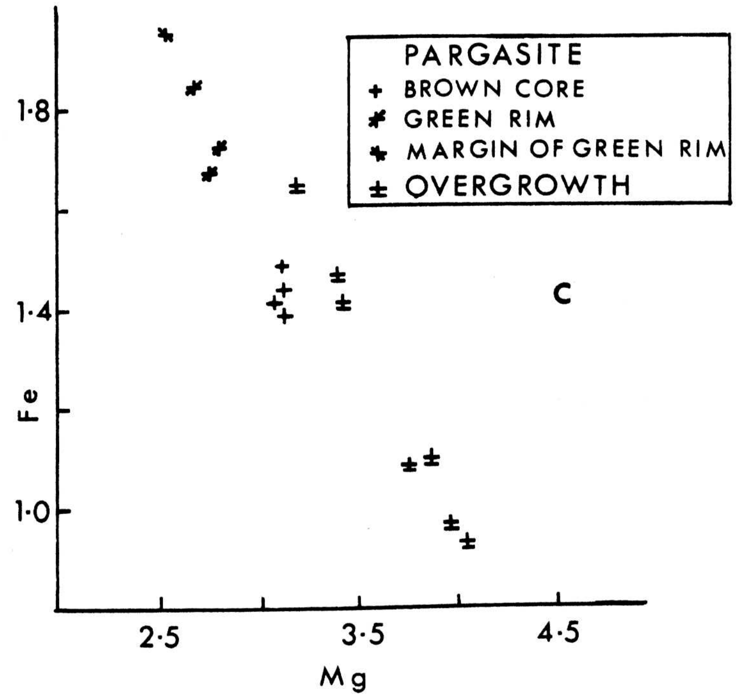
PARGASITE
+ BROWN CORE
✱ GREEN RIM
✱ MARGIN OF GREEN RIM
± OVERGROWTH
c
1·8
1·4
1·0
Fe
2·5
3·5
4·5
Mg

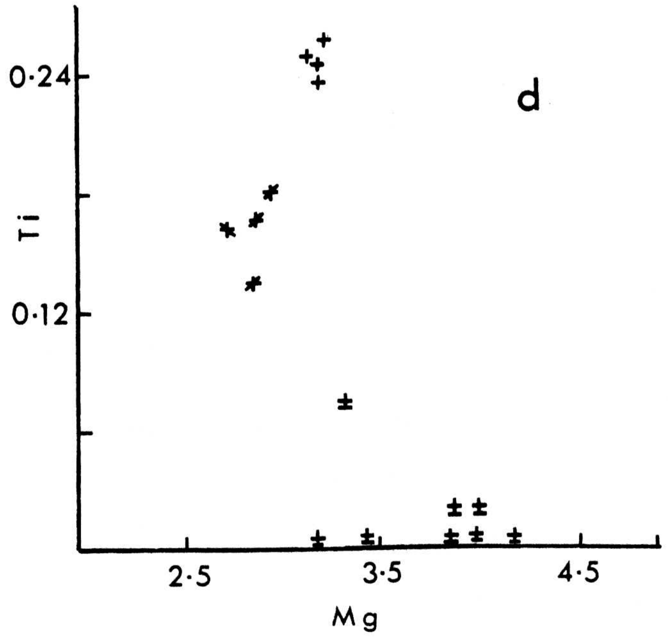
d
0·24
0·12
Ti
2·5
3·5
4·5
Mg

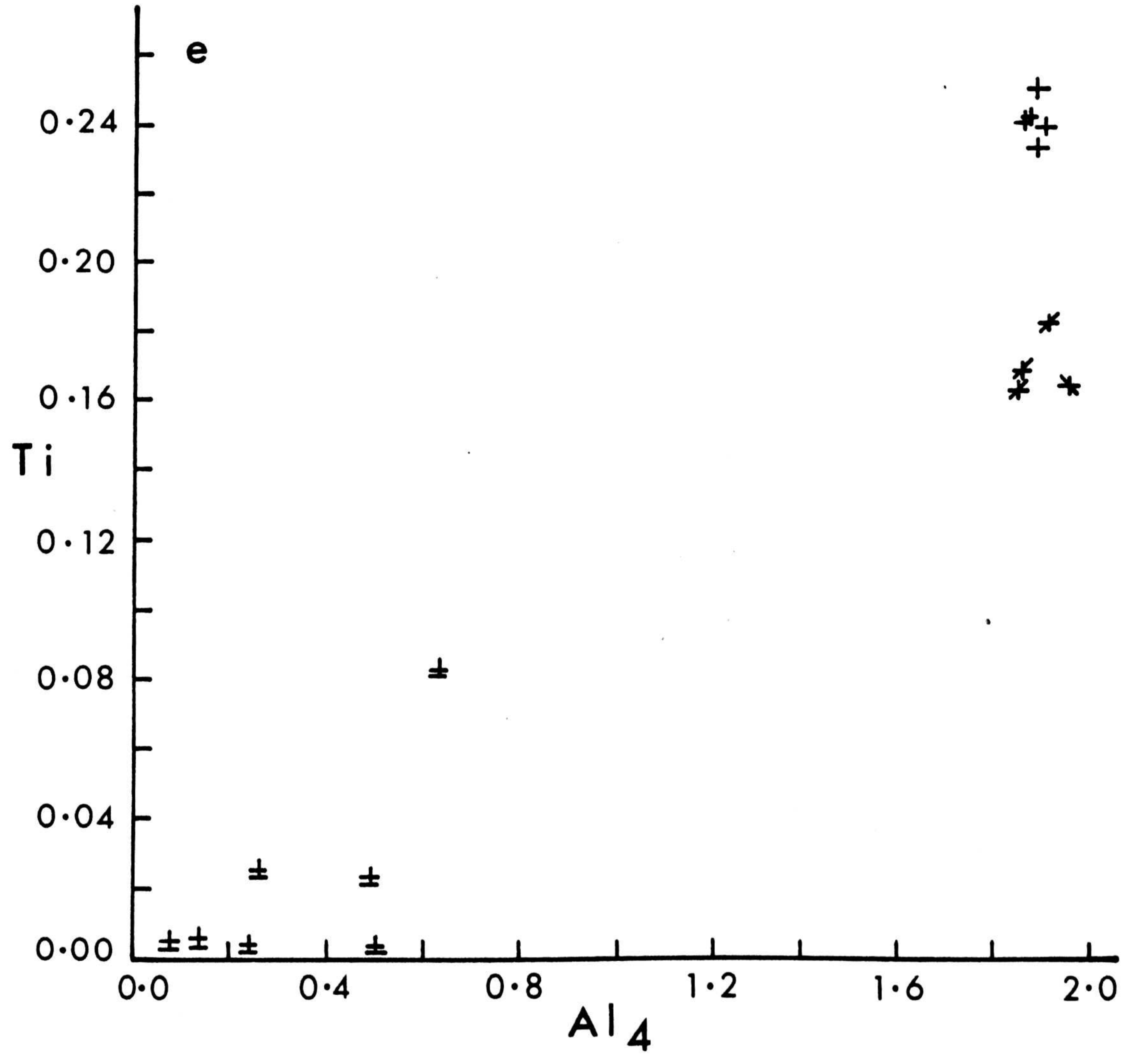
e
0·24
0·20
0·16
Ti
0·12
0·08
0·04
0·00
0·0
0·4
0·8
1·2
1·6
2·0
Al_4

Figure 5.3 (a-h) Half unit cell variations of Fe *vs.* Mg, Na and K *vs.* Ca, Al *vs.* Mg, Al_4 *vs.* A-site, Ti *vs.* Al_4, Al_6 *vs.* Si and Mn *vs.* Al_6, respectively, in amphiboles from the Ballachulish appinite suite (symbols as in Fig. 5.1), with comparisons.

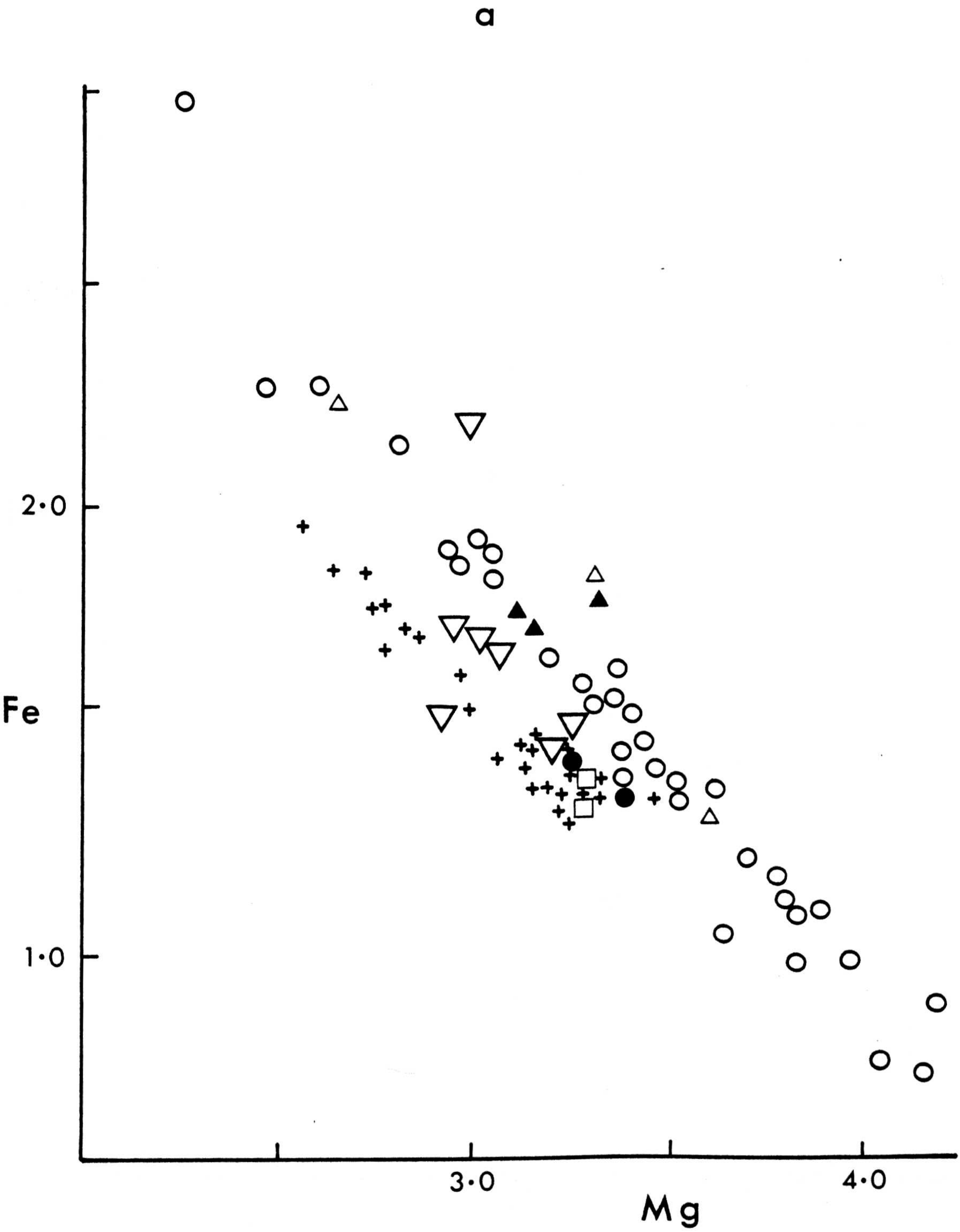
a
2·0
1·0
Fe
3·0
4·0
Mg

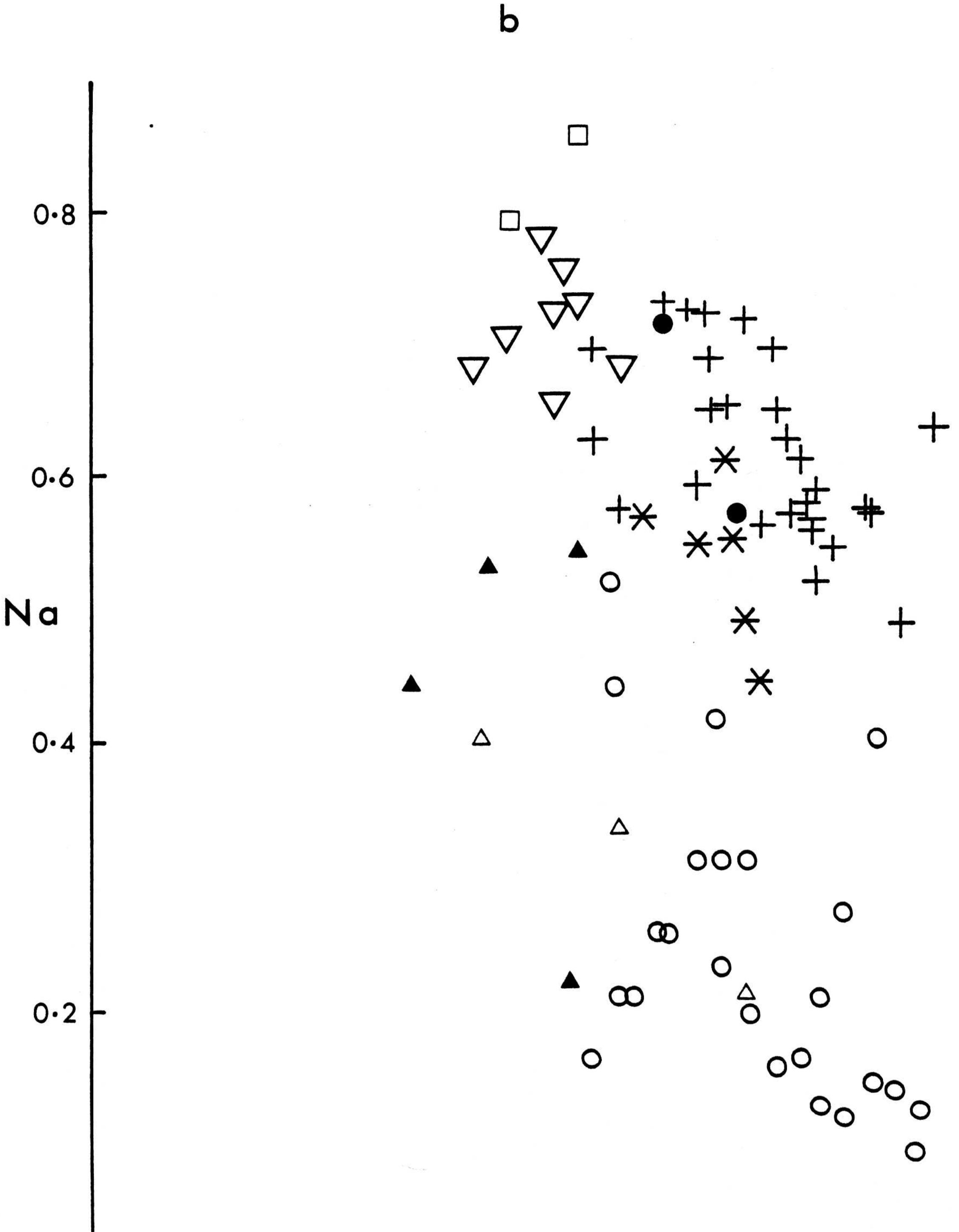
b
Na
0·8
0·6
0·4
0·2
0·0
1·60
1·70
1·80
1·90
2·00
Ca

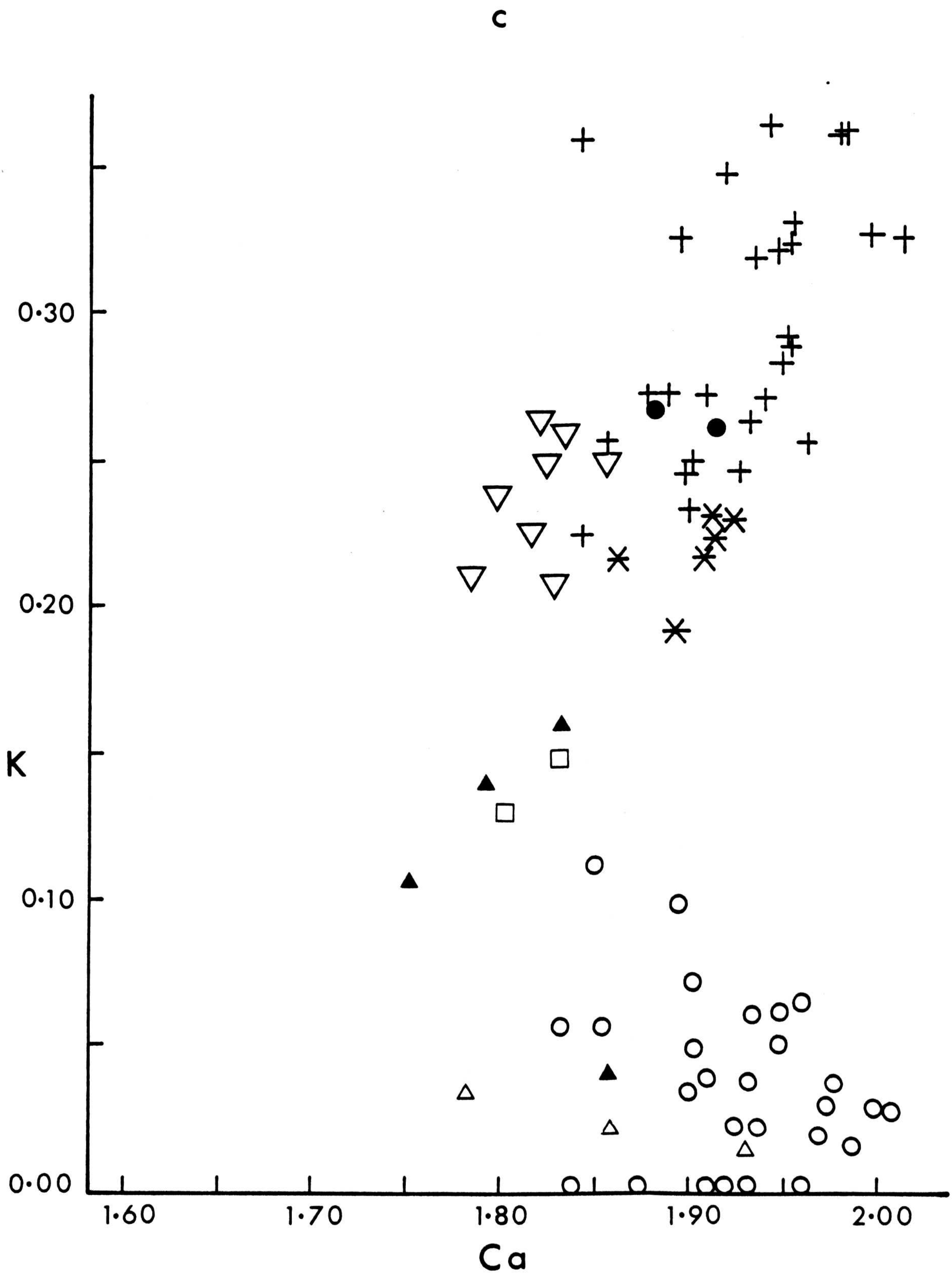
c
K
0·30
0·20
0·10
0·00
1·60
1·70
1·80
1·90
2·00
Ca

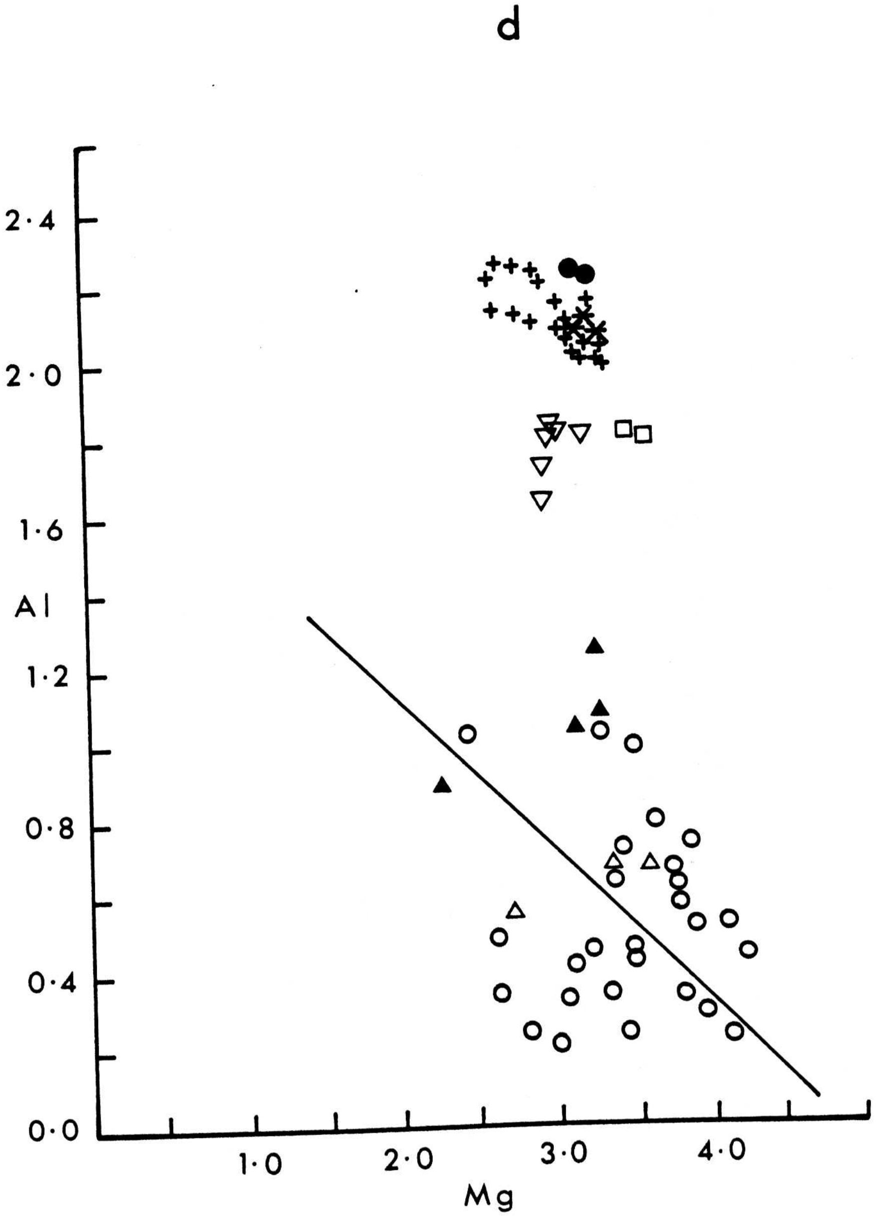
d
2·4
2·0
1·6
Al
1·2
0·8
0·4
0·0
1·0
2·0
3·0
4·0
Mg

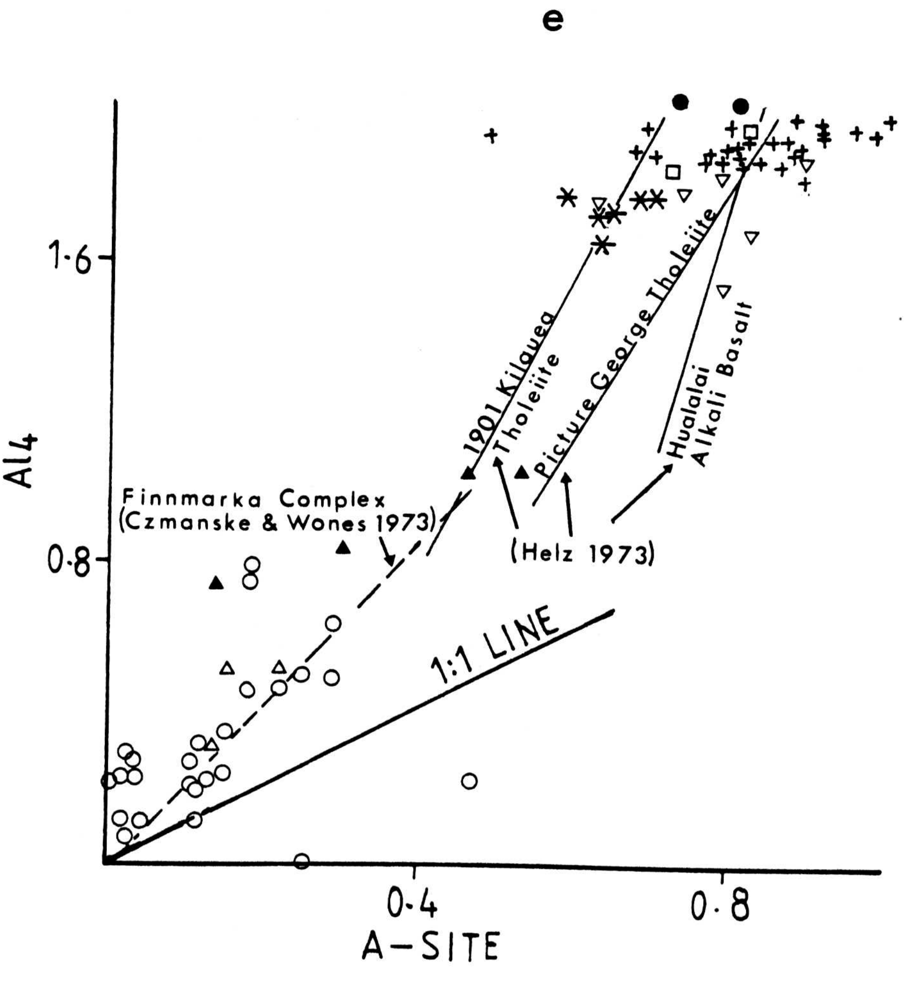
e
Al4
1·6
0·8
0·4
0·8
A–SITE
1:1 LINE
Finnmarka Complex
(Czmanske & Wones 1973)
1901 Kilauea Tholeiite
Picture George Tholeiite
Hualalai Alkali Basalt
(Helz 1973)

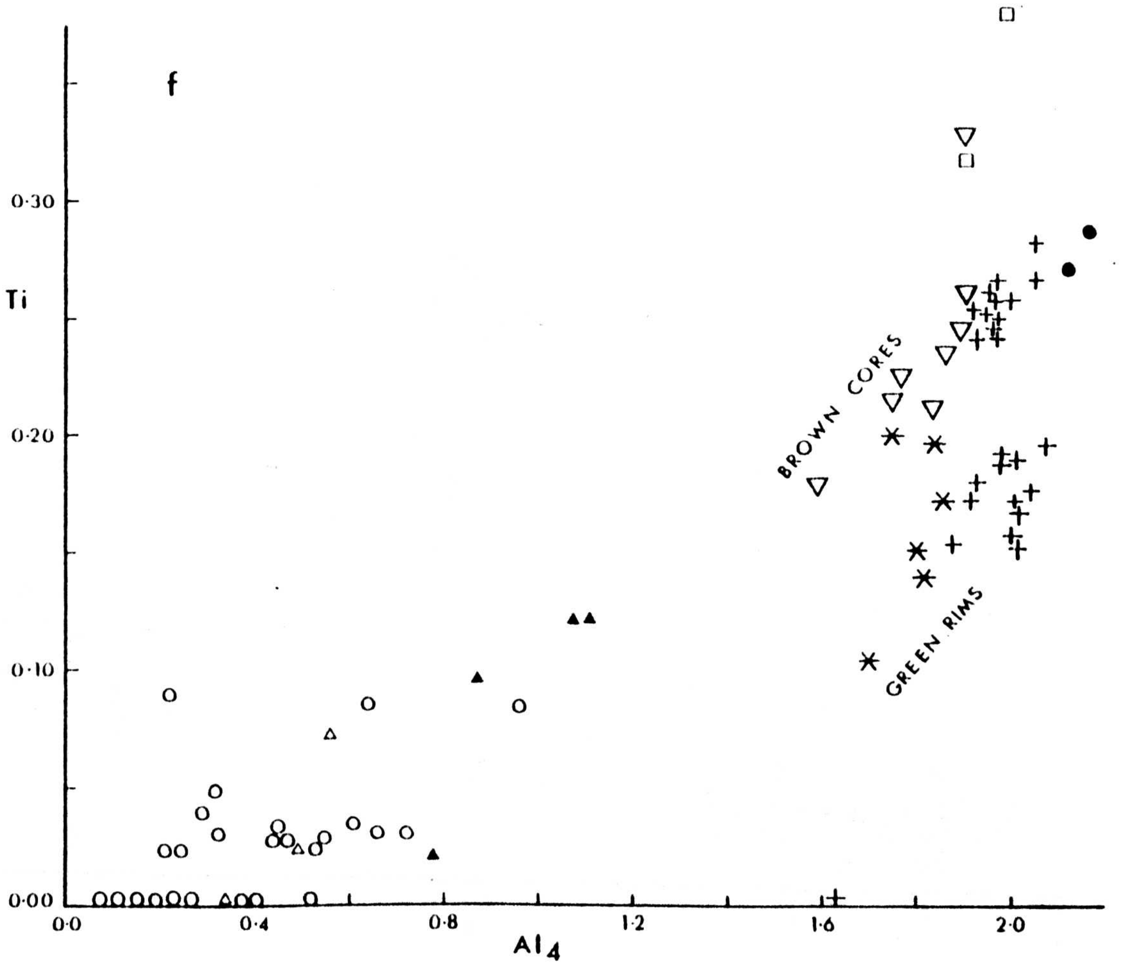
f
Ti
0·30
0·20
0·10
0·00
0·0
0·4
0·8
1·2
1·6
2·0
Al4
BROWN CORES
GREEN RIMS

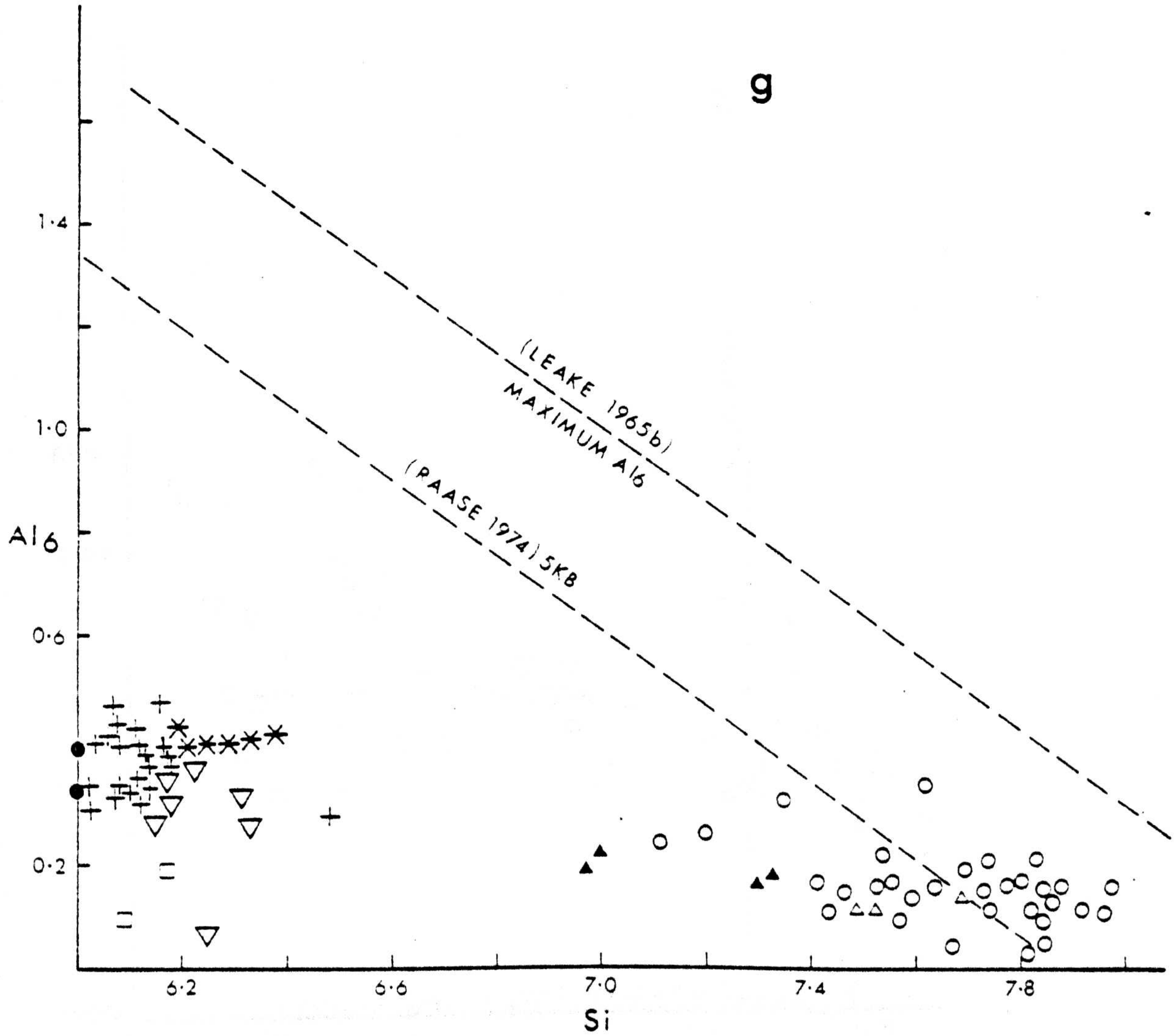
g
(LEAKE 1965b)
MAXIMUM Al6
(RAASE 1974) 5KB
Al6
1·4
1·0
0·6
0·2
Si
6·2
6·6
7·0
7·4
7·8

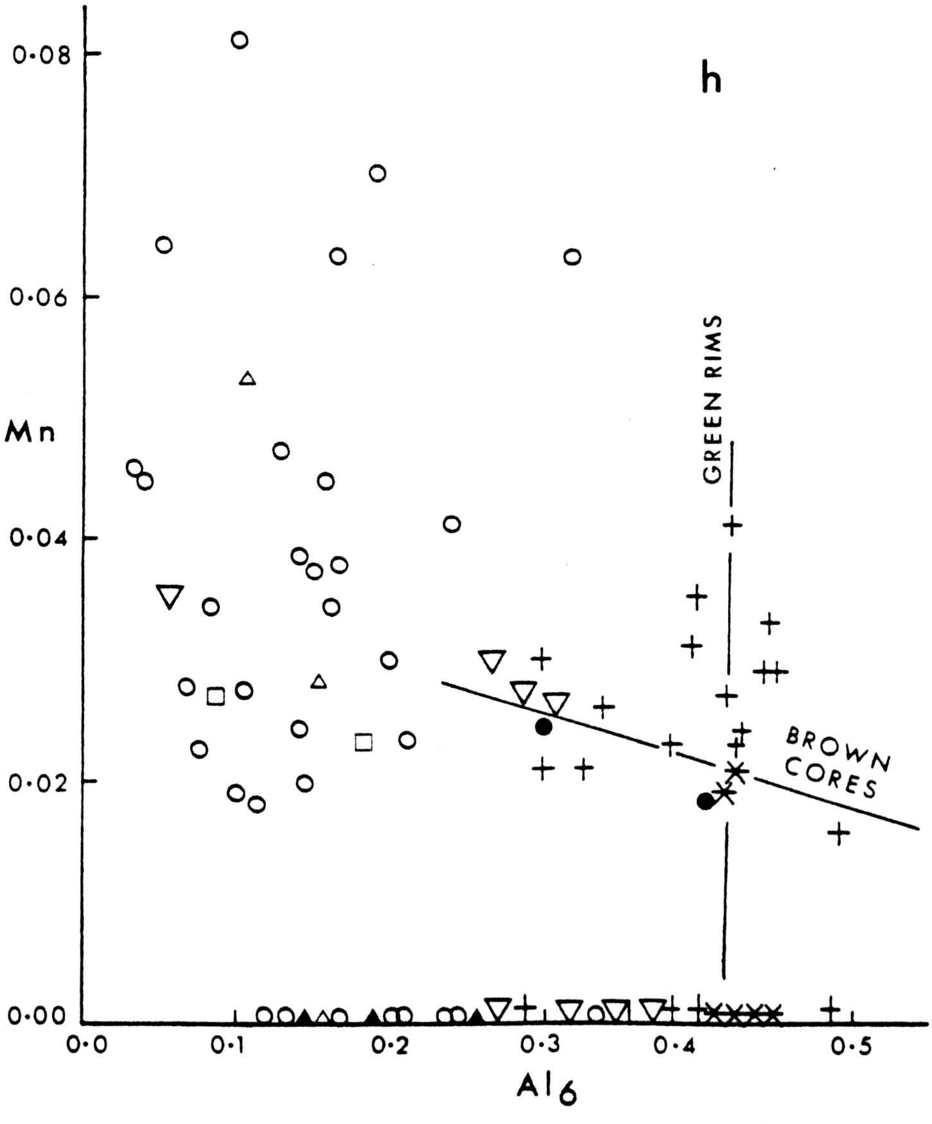
h
Mn
0·08
0·06
0·04
0·02
0·00
0·0
0·1
0·2
0·3
0·4
0·5
Al6
GREEN RIMS
BROWN CORES

Figure 5.4 Tentative estimates of the relationship between pressure and NaM_4 content; after Brown (1977); see text for explanation; symbols as in Figure 5.1.

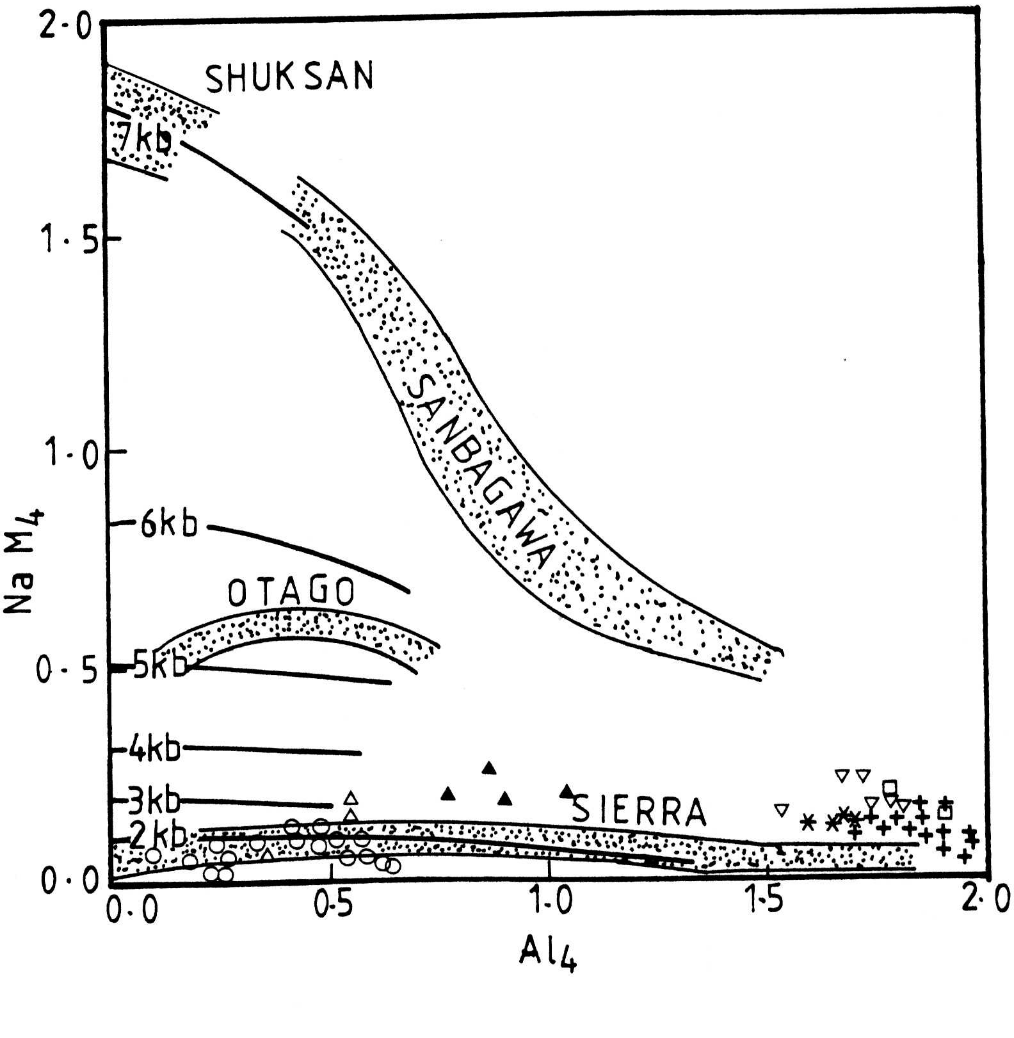
2·0
1·5
1·0
0·5
0·0
Na M$_4$
0·0
0·5
1·0
1·5
2·0
Al$_4$
SHUKSAN
7kb
SANBAGAWA
6kb
OTAGO
5kb
4kb
3kb
2kb
SIERRA

Figure 5.5 Temperature estimates for amphiboles of the Ballachulish appinite suite on the basis of Ti contents (Helz 1973).

(a) Estimates for the selected pargasite crystal (Fig. 5.2a) on the basis of actual Ti contents.

(b) Estimates for the green rim of pargasite and actinolite overgrowths from the Back Settlement pipe and for magnesio - hornblendes for the Rudha Mòr pipe on the basis of extrapolated Ti contents in Figure 5.2b.

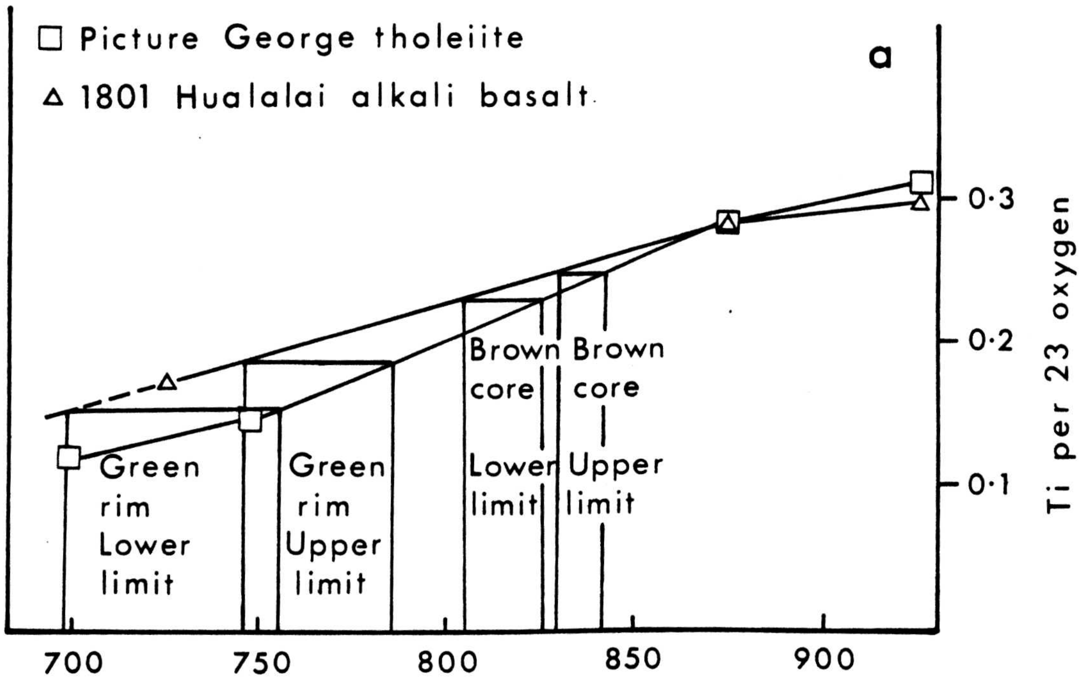
□ Picture George tholeiite
△ 1801 Hualalai alkali basalt
a
Green rim Lower limit
Green rim Upper limit
Brown core Lower limit
Brown core Upper limit
0·3
0·2
0·1
Ti per 23 oxygen
700
750
800
850
900

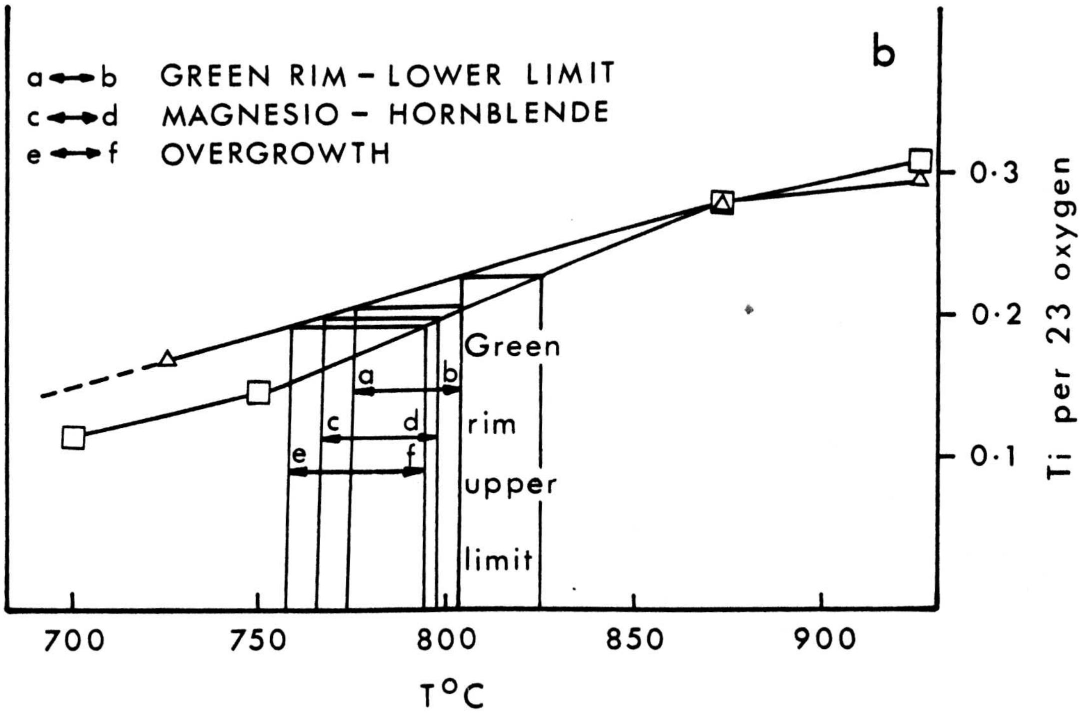
a ↔ b GREEN RIM – LOWER LIMIT
c ↔ d MAGNESIO – HORNBLENDE
e ↔ f OVERGROWTH
b
a
b
c
d
e
f
Green rim upper limit
0·3
0·2
0·1
Ti per 23 oxygen
700
750
800
850
900
T°C

Figure 5.6 Plots of the average Mg/Mg + Fe ratios in amphiboles from the Ballachulish appinite suite against this ratio in their host rocks.

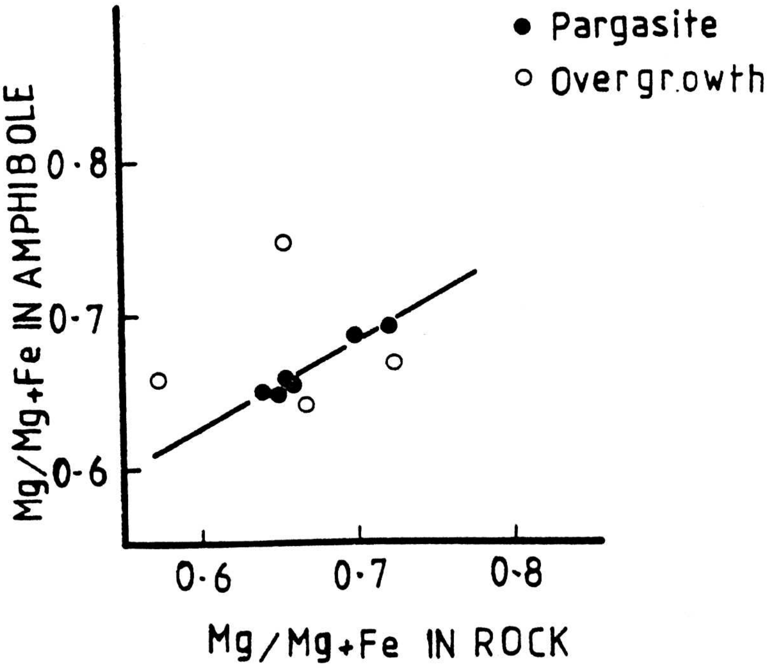
● Pargasite
○ Overgrowth
Mg/Mg+Fe IN AMPHIBOLE
0·8
0·7
0·6
0·6
0·7
0·8
Mg/Mg+Fe IN ROCK

Figure 5.7 Ca + Na + K *vs*. Si (half unit cell; symbols as in Fig. 5.1).

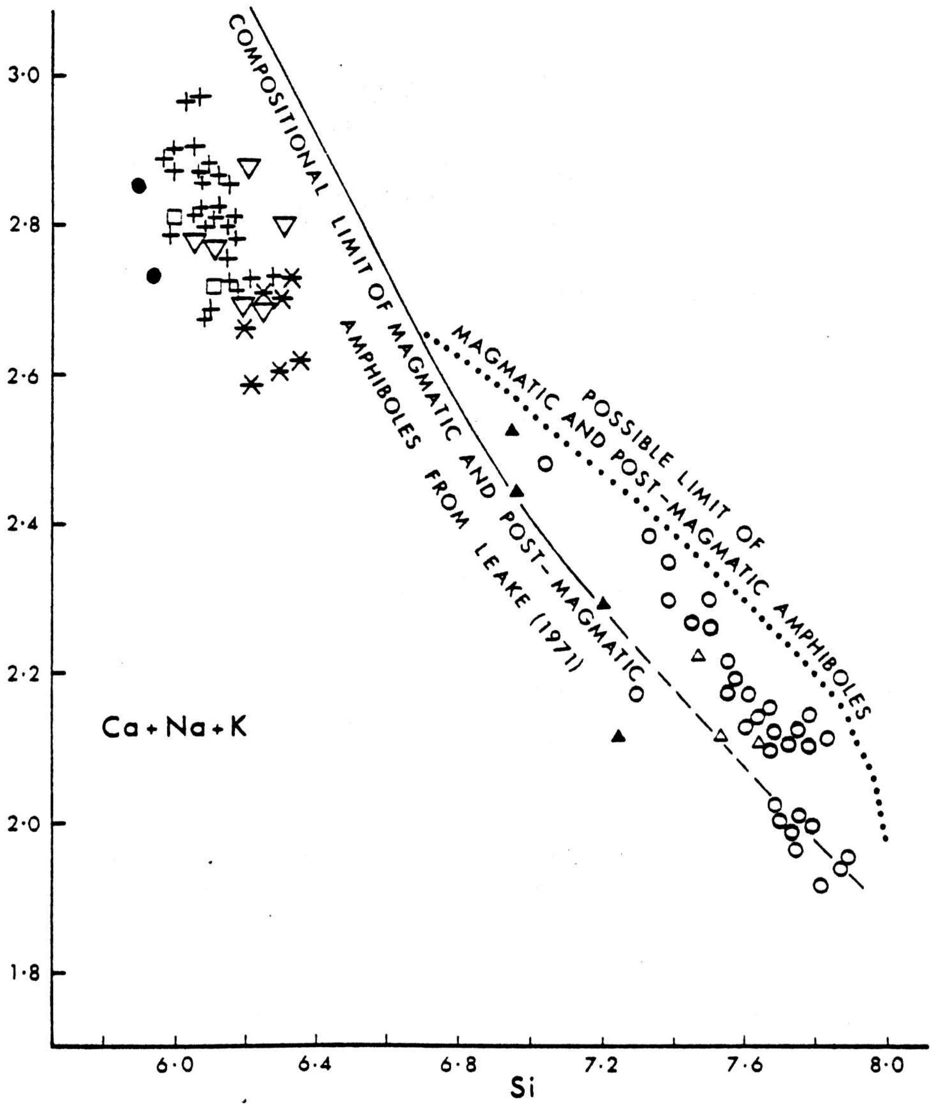
3·0
2·8
2·6
2·4
2·2
2·0
1·8
Ca + Na + K
6·0
6·4
6·8
7·2
7·6
8·0
Si
COMPOSITIONAL LIMIT OF MAGMATIC AND POST-MAGMATIC AMPHIBOLES FROM LEAKE (1971)
POSSIBLE LIMIT OF MAGMATIC AND POST-MAGMATIC AMPHIBOLES

Table 5.1. Analyses of the zoned pargasite crystal and its overgrowths shown in Figure 5.2a; appinite, large pipe, Back Settlement. (Table 7.1 – 9).

	1*	2*	3*	4*	5*	6*	7	8	9
SiO_2	54.26	55.52	56.93	55.95	55.10	53.47	41.24	41.73	41.77
TiO_2	0.00	0.00	0.00	0.22	0.00	0.21	1.48	2.11	2.18
Al_2O_3	2.59	1.45	1.59	1.95	2.15	3.49	13.34	12.65	12.76
FeO	13.87	11.87	6.31	8.40	9.24	9.37	13.45	12.15	11.58
MnO	0.25	0.31	0.16	0.24	0.00	0.19	0.13	0.24	0.00
MgO	14.83	16.16	20.05	18.99	17.97	18.37	12.34	14.33	14.20
CaO	12.77	12.60	13.32	13.00	12.90	12.81	12.21	12.14	12.43
Na_2O	0.00	0.00	0.41	0.55	0.44	0.98	2.03	2.29	1.91
K_2O	0.00	0.14	0.19	0.22	0.29	0.36	1.71	1.46	1.37
Total	98.57	98.04	98.95	99.51	98.09	99.25	97.92	99.09	98.19

Trace elements (p.p.m.)

Cr	b.d.	b.d.	b.d.	b.d.	b.d.	b.d.	b.d.	b.d.	b.d.
Co	b.d.	1761	b.d.	1349	b.d.	b.d.	1849	b.d.	b.d.

Formulae on the basis of 23 oxygens

Si	7.77	7.91	7.85	7.76	7.79	7.51	6.15	6.12	6.15
Ti	0.00	0.00	0.00	0.02	0.00	0.02	0.17	0.23	0.24
Al	0.44	0.24	0.26	0.32	0.36	0.58	2.35	2.19	2.21
Fe	1.66	1.41	0.73	0.97	1.10	1.10	1.68	1.49	1.42
Mn	0.03	0.04	0.02	0.03	0.00	0.02	0.02	0.03	0.00
Mg	3.16	3.43	4.12	3.92	3.78	3.85	2.74	3.13	3.11
Ca	1.96	1.92	1.97	1.93	1.95	1.93	1.95	1.91	1.96
Na	0.00	0.00	0.11	0.15	0.12	0.27	0.59	0.65	0.54
K	0.00	0.02	0.03	0.04	0.05	0.06	0.32	0.27	0.26
Al_4	0.23	0.09	0.15	0.24	0.21	0.49	1.85	1.88	1.85
Al_6	0.04	0.08	0.03	0.07	0.13	0.09	0.50	0.30	0.36

Table 5.1 (Contd.)

	10	11	12	13	14	15*	16*	17
SiO_2	41.72	41.58	41.59	40.13	40.85	51.55	53.06	40.51
TiO_2	2.27	2.18	2.17	1.61	1.52	0.76	0.00	1.44
Al_2O_3	12.64	12.68	12.96	13.08	12.71	4.28	3.97	13.53
FeO	11.38	11.44	11.47	13.57	14.71	12.26	9.19	15.63
MnO	0.17	0.21	0.00	0.00	0.24	0.23	0.31	0.23
MgO	14.44	14.16	14.36	12.38	12.02	15.91	17.85	11.38
CaO	12.34	12.31	12.27	12.25	12.10	12.35	12.95	12.34
Na_2O	2.00	2.02	2.44	1.66	1.78	1.11	0.98	1.97
K_2O	1.95	1.51	1.41	1.69	1.73	0.52	0.38	1.90
Total	98.91	98.09	98.66	96.37	97.66	98.96	98.68	98.39

Trace elements (p.p.m.)

Cr	b.d.	b.d.	b.d.	b.d.	963	b.d.	b.d.	b.d.
Co	b.d.	b.d.	2626	1788	3463	b.d.	2028	1422

Formulae on the basis of 23 oxygens

Si	6.12	6.14	6.10	6.10	6.15	7.38	7.50	6.06
Ti	0.25	0.24	0.24	0.18	0.17	0.08	0.00	0.17
Al	2.19	2.20	2.24	2.34	2.25	0.72	0.66	2.39
Fe	1.40	1.41	1.41	1.72	1.85	1.47	1.09	1.96
Mn	0.02	0.03	0.00	0.00	0.03	0.03	0.04	0.03
Mg	3.16	3.11	3.14	2.80	2.70	3.39	3.76	2.54
Ca	1.94	1.95	1.93	1.99	1.95	1.89	1.96	1.98
Na	0.57	0.58	0.69	0.49	0.52	0.30	0.27	0.57
K	0.36	0.28	0.26	0.33	0.33	0.09	0.07	0.36
Al_4	1.88	1.86	1.90	1.90	1.85	0.62	0.50	1.94
Al_6	0.31	0.34	0.34	0.44	0.40	0.10	0.16	0.45

FeO = total iron; numbers with asterisks indicate overgrowths; b.d. = below detection limit (see Appendix A.2); Ni is below the detection limit for all analyses.

CHAPTER 6 MICA

Mica commonly occurs as phenocrysts in kentallenite and as large crystals in pyroxene - mica diorite and many of the marginal ultramafic rocks. It is also present in variable proportions (<5 - 20%) in some appinites, hornblende diorites and lamprophyres (Table 7.1; also see Chapter 2). Zoned crystals of mica are very common (Figs. 2.6a, b), particularly in the kentallenite of the Kentallen pipe.

An analytical study of mica was carried out to determine (1) the elements responsible for zoning, (2) the various substitutions that take place and (3) the physical conditions of mica crystallisation in various pipes.

6.1 Chemistry

Analytical data for mica from the kentallenite of the Kentallen pipe (Table 7.1 – 52; Fig. 2.3b), appinite of the Back Settlement pipe (Table 7.1 – 9; *cf*. Figs. 2.5a, 2.6a-b, 2.7b) and pyroxene - mica diorite of the Rudha Mòr pipe (Table 7.1 – 39) are given in Table 6.1. A plot of 6Fe/Mg + Fe *vs*. Al shows that the compositions of most of the analysed micas of the Rudha Mòr pipe lie in the main biotite field while those from the other two pipes lie in the phlogopite field (Fig. 6.1).

6.1A Single phlogopite crystal

An extensively zoned phlogopite phenocryst from the kenallenite of the Kentallen pipe was selected for detailed investigation (Fig. 6.2a; Table 6.1 – 1-8). Both Ti and Fe show a negative correlation against Mg/Mg + Fe (Fig. 6.2b) with higher Ti and Fe proportions in the dark brown zone at the margin (anal. 8) and lower Ti and Fe proportions in the light brown zone close to the olivine - phlogopite interface (anal. 5). However, the dark brown zone for which analyses 1, 2 and 3 were made shows higher Ti:Fe ratios as compared to the dark brown zone at the margin (anal. 8). This indicates a greater correspondence between the intensity of the brown colour and the Ti content which in micas increases with increase in temperature and decrease in pressure (Robert 1976). The increasing Fe contents of mica can be attributed only to increasing crystallisation.

6.1B Overall chemistry

On the basis of 6Fe/Mg + Fe *vs*. Al plots (Fig. 6.1) a phlogopite - siderophyllite-type substitution is proposed. There is a negative correlation between Fe and Mg and between Ti and Mg but the micas of the three pipes show significant differences. For example in the Kentallen pipe a decrease in Mg is compensated for by a lower proportion of Fe and higher proportion of Ti in phlogopite than is the case for the other pipes (Figs. 6.3a, b).

Mg *vs*. Si and Ti *vs*. Al show positive correlations for the micas from all the pipes (Figs. 6.3c, d). The correspondence between Mg and Si is better, and the proportional dependence of Ti on Al_4 is higher, in phlogopite from the Kentallen pipe than in the micas from the other two pipes. On these bases the entry of Ti into phlogopite in the Kentallen pipe and into micas from the other pipes is consistent, respectively, with the following substitutions:

$2Si + Mg \rightleftharpoons 2Al_4 + Ti^{4+}$ (Robert 1976) and

$8Si + 8Mg \rightleftharpoons 12Al + 4Fe^{2+}(Mn) + Ti^{4+}$

There is a negative Ca *vs*. Mg correlation for Kentallen pipe phlogopite; plots for the micas from the other two pipes show scattering (Fig. 6.3e). K varies positively with Si in micas from all the pipes (Fig. 6.3f). Substitutions similar to those proposed by Olech (1979) would appear to have been operative in relation to the entry of Ca into phlogopite. The substitution

$K + Mg + 2Si \rightleftharpoons Ca + Al_6 + 2Al_4$

is applicable to phlogopite in the Kentallen pipe and the substitution

$K + Si \rightleftharpoons Ca + Al_4$

is applicable to micas from all the pipes.

6.2 Temperature and pressure estimation

Based on TiO_2 contents and using comparison with experimental data of Robert (1976) a crystallisation temperature close to 1000°C and P_{H_2O} close to 1 kb are indicated for the phlogopite of the Kentallen pipe but lower temperatures and higher pressures for micas from the Back Settlement and Rudha Mòr pipes (see Section 6.1A). This is in correspondence with temperature and pressure estimates made for mica from the appinite of the Back Settlement pipe (825° - 770°C), based on the association of phlogopite grains with the green rims of the pargasite crystals (Chapter 5).

6.3 Conclusions

1. The major element responsible for zoning in mica is Ti.
2. The phlogopite in the kentallenite of the Kentallen pipe crystallised at about 1000°C and 1 kb P_{H_2O}.
3. The phlogopite - biotite from the Back Settlement and Rudha Mòr pipes crystallised at comparatively lower temperatures and higher pressures than those deduced for the phlogopite of the Kentallen pipe.

Figure 6.1 Mica compositions from the Ballachulish appinite suite based on plots of 6Fe/Mg + Fe *vs*. Al (after Deer *et al*. 1966).

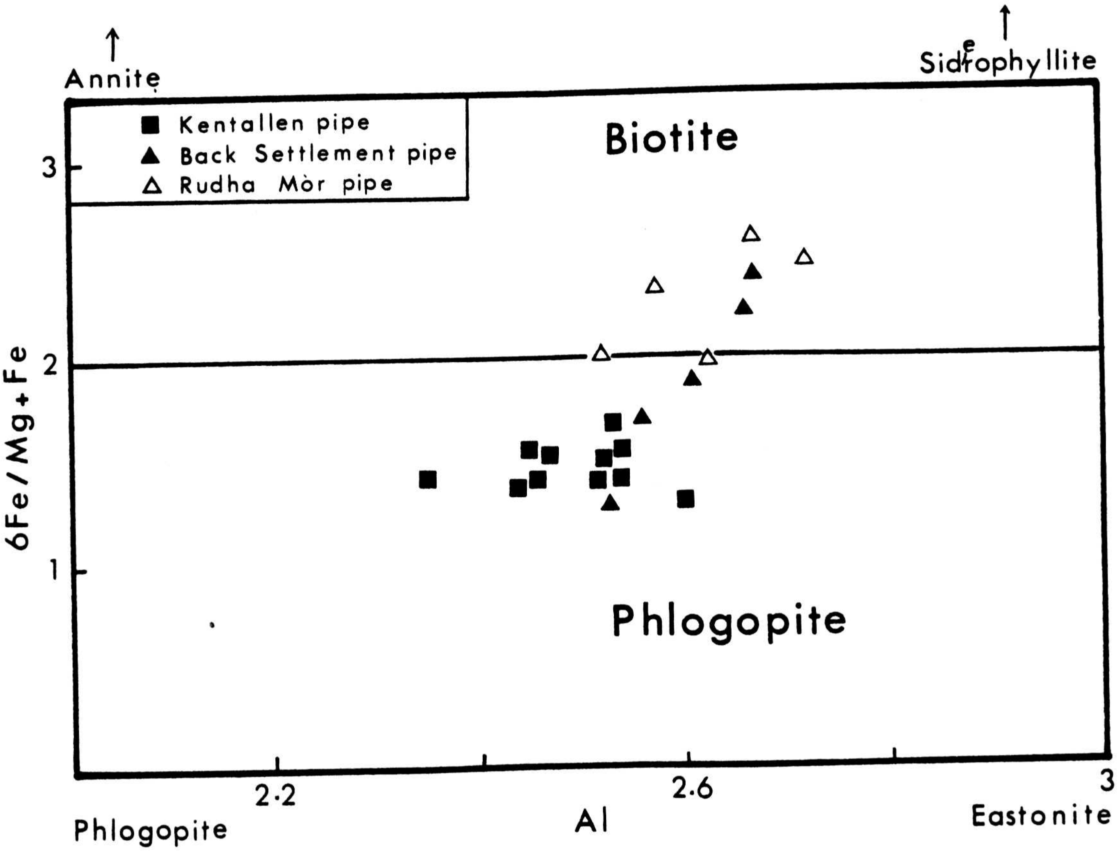
Annite
Sidrophyllite
■ Kentallen pipe
▲ Back Settlement pipe
△ Rudha Mòr pipe
Biotite
Phlogopite
6Fe/Mg+Fe
3
2
1
2·2
2·6
3
Phlogopite
Al
Eastonite

Figure 6.2

(a) Schematic representation of the zoned phlogopite crystal from the kentallenite of the Kentallen pipe; numbers 1-8 correspond to analyses in Table 6.1.

(b) Fe and Ti *vs*. Mg/Mg + Fe variations in the zoned phlogopite shown in Figure 6.2(a).

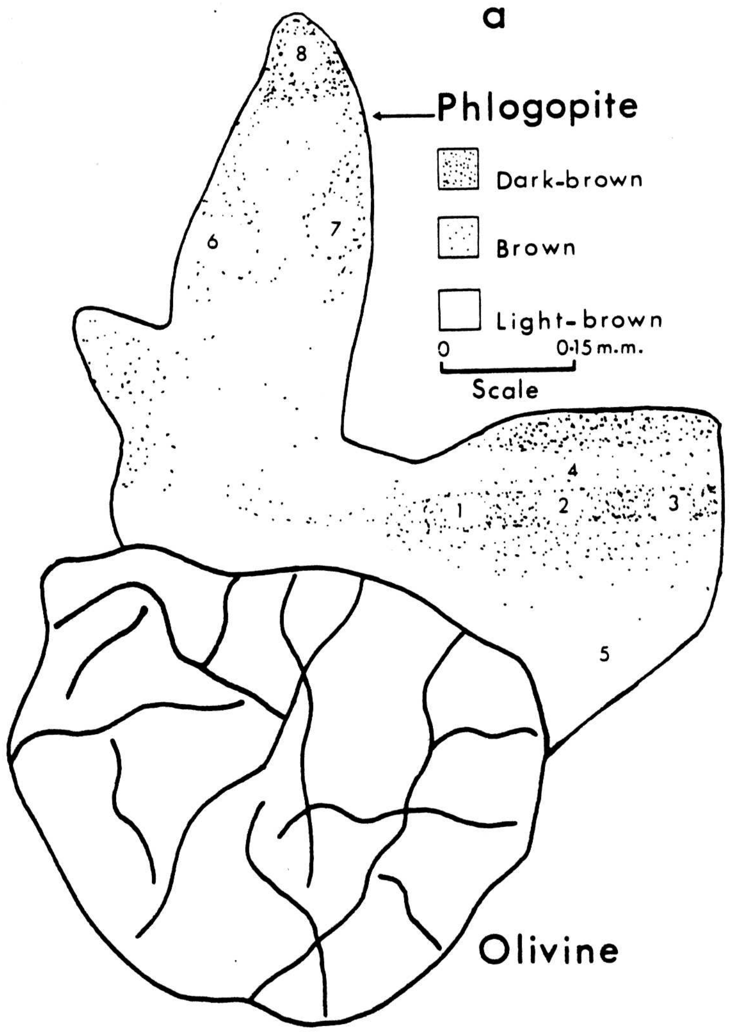
a
Phlogopite
Dark-brown
Brown
Light-brown
0 0·15 m.m.
Scale
8
6
7
4
1
2
3
5
Olivine

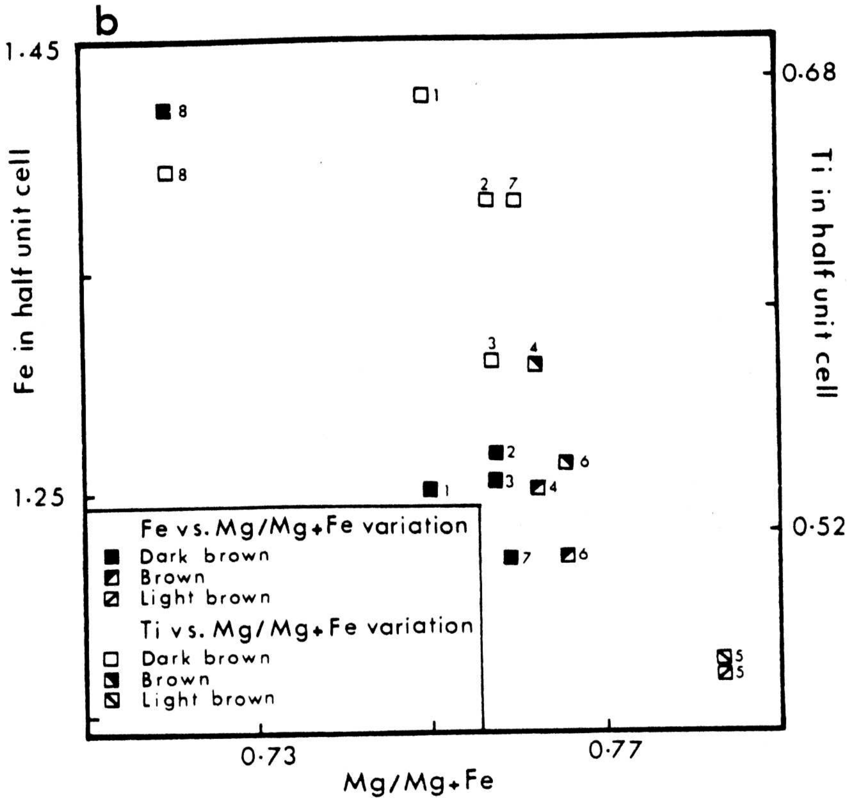
b
1·45
1·25
Fe in half unit cell
0·68
0·52
Ti in half unit cell
0·73
0·77
Mg/Mg+Fe
8
8
1
2
7
3
4
2
6
3
4
1
7
6
5
5
Fe vs. Mg/Mg+Fe variation
Dark brown
Brown
Light brown
Ti vs. Mg/Mg+Fe variation
Dark brown
Brown
Light brown

Figure 6.3 (a-f) Half unit cell variations of Fe and Ti *vs.* Mg, Mg *vs.* Si, Ti *vs.* Al_4, Ca *vs.* Mg and K *vs.* Si, in micas from the Ballachulish appinite suite (symbols as in Fig. 6.1; in Figs. 6.3c and d solid line = Kentallen pipe, broken line = other pipes).

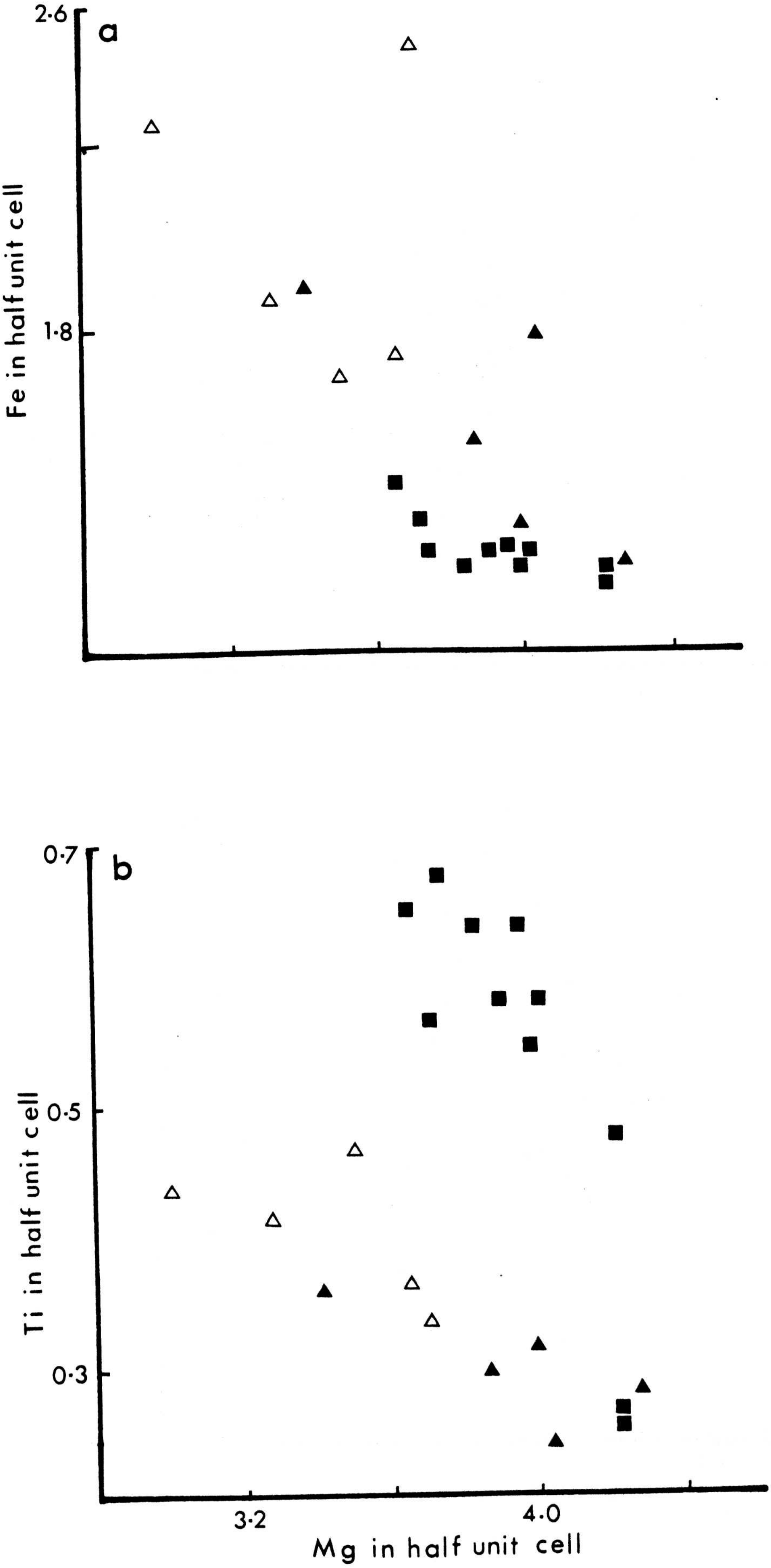
2·6
a
1·8
Fe in half unit cell
0·7
b
0·5
0·3
Ti in half unit cell
3·2
4·0
Mg in half unit cell

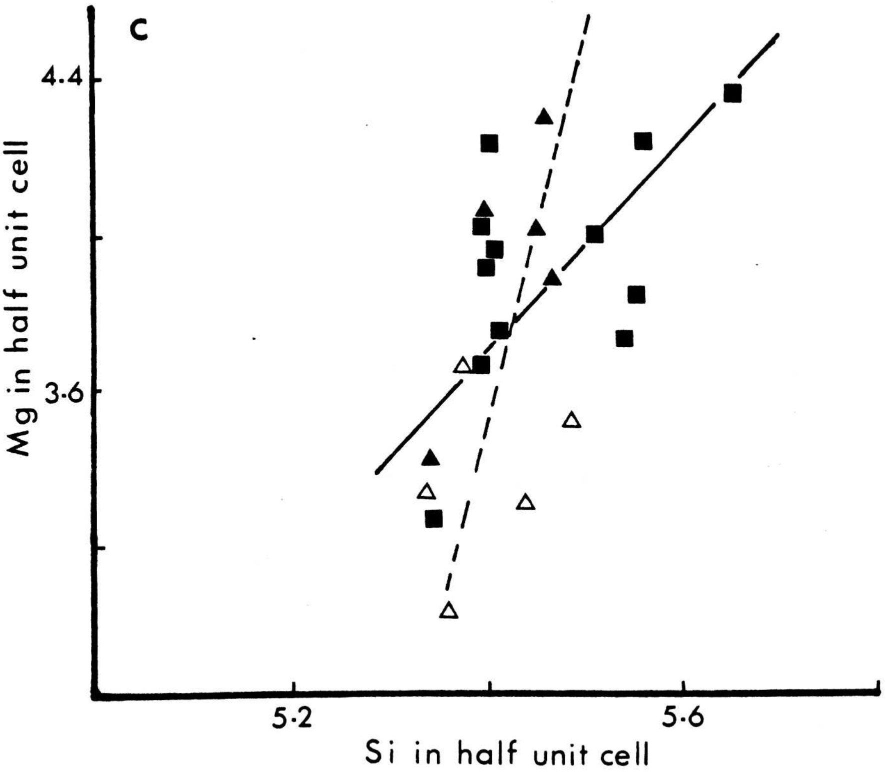
c
4·4
3·6
5·2
5·6
Mg in half unit cell
Si in half unit cell

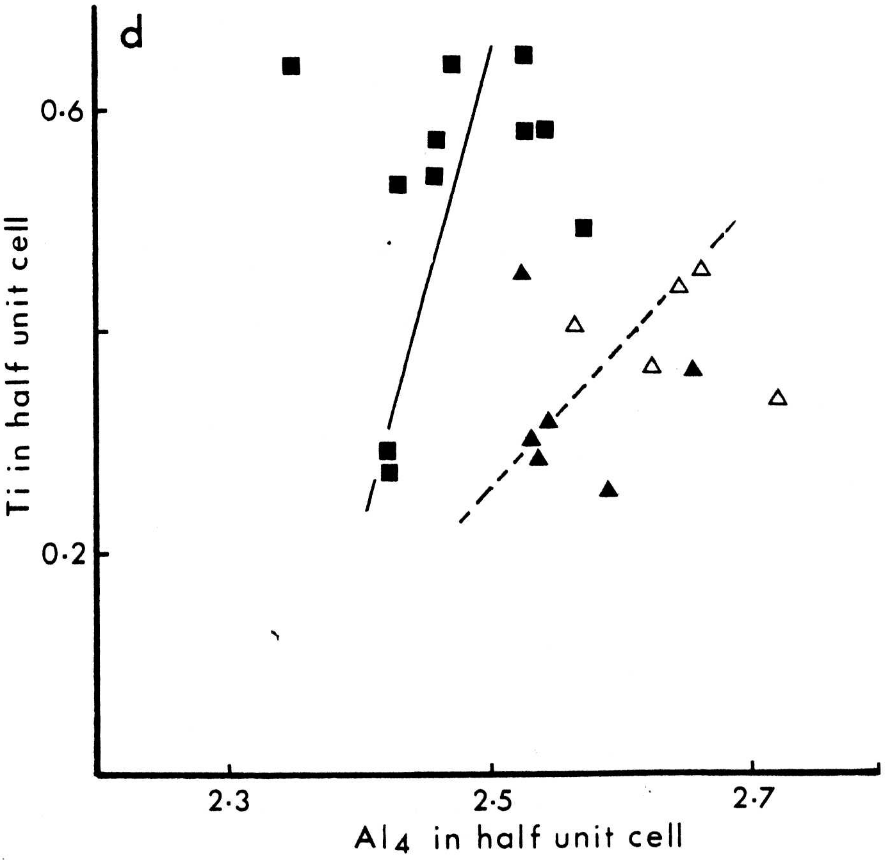
d
0·6
0·2
2·3
2·5
2·7
Ti in half unit cell
Al4 in half unit cell

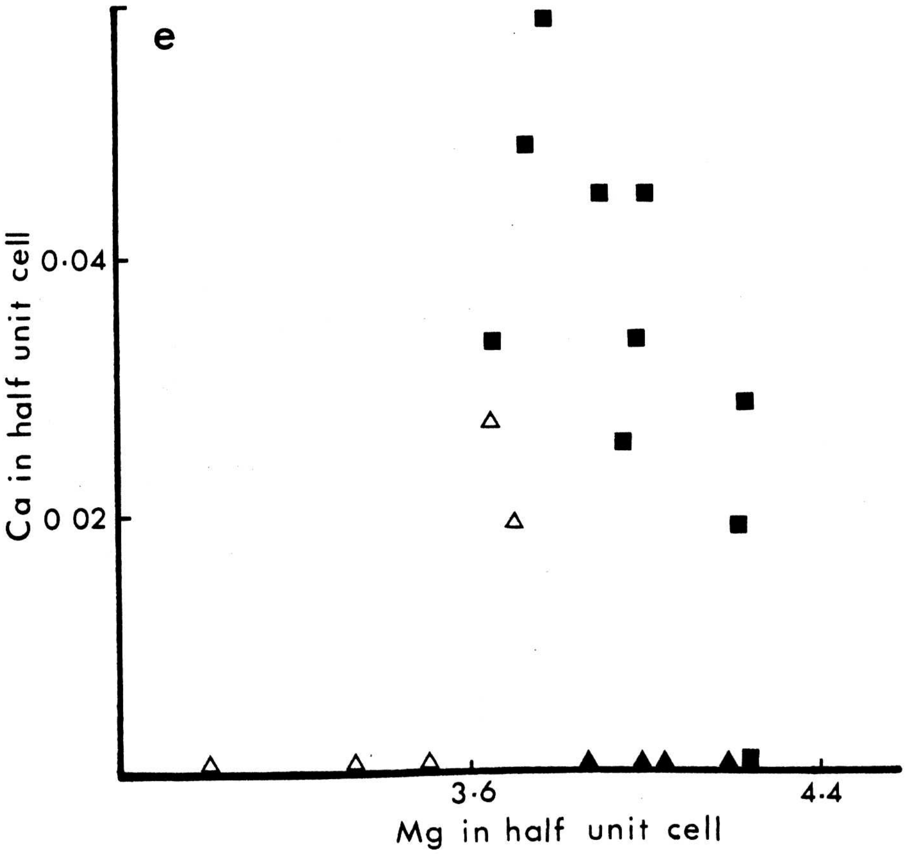
e
0·04
0 02
Ca in half unit cell
3·6
4·4
Mg in half unit cell

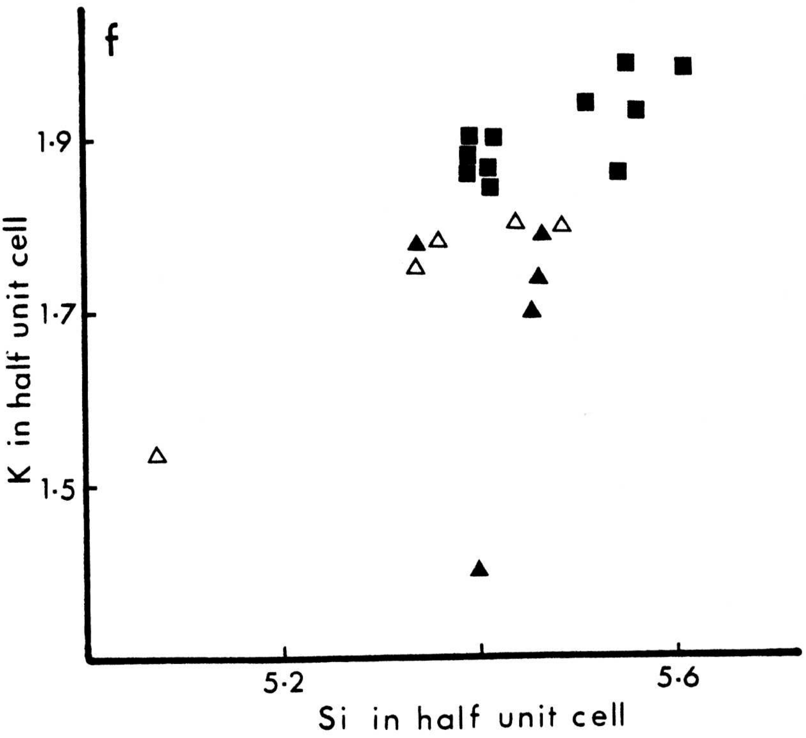
f
1·9
1·7
1·5
K in half unit cell
5·2
5·6
Si in half unit cell

Table 6.1. Phlogopite - biotite compositions from the Ballachulish appinite suite.

	1	2	3	4	5	6	7	8	9 Mean (4 anals)	S.D.	10 Mean (5 anals)	S.D.	11 Mean (5 anals)	S.D.
SiO_2	37.19	36.83	37.65	37.65	36.92	37.26	37.71	36.62	37.32	0.20	35.80	1.16	36.23	1.43
TiO_2	6.15	5.75	5.37	5.37	4.31	4.89	5.73	5.84	3.95	2.27	2.84	0.66	3.39	0.63
Al_2O_3	14.71	14.25	15.01	14.94	15.00	14.07	13.52	14.54	14.78	0.45	15.68	0.41	14.77	1.16
FeO	10.26	10.29	10.43	10.43	9.53	9.85	9.86	11.53	9.97	0.35	12.76	2.40	16.26	2.50
MnO	0.00	0.20	0.18	0.18	0.00	0.00	0.00	0.15	0.00	0.00	0.07	0.11	0.04	0.08
MgO	17.25	18.04	18.27	18.78	19.33	18.06	17.46	16.63	18.26	1.92	18.89	1.86	15.70	1.36
CaO	0.31	0.16	0.29	0.29	0.12	0.21	0.37	0.21	0.75	0.15	0.00	0.00	0.08	0.09
Na_2O	0.53	0.00	0.58	0.00	0.00	0.00	0.00	0.36	0.13	0.18	0.86	0.29	0.73	0.21
K_2O	9.91	9.95	10.14	10.14	10.18	10.27	10.56	10.10	10.11	0.30	8.77	0.82	8.88	0.75
Total	96.31	95.47	97.92	97.78	95.39	94.61	95.21	95.97	95.27		95.17		96.08	
							Trace elements (p.p.m.)							
Co	b.d.	b.d.	b.d.	b.d.	1902	b.d.	b.d.	b.d.	1137	494	2648	1173	984	1080
							Formulae on the basis of 22 oxygens							
Si	5.41	5.41	5.40	5.40	5.41	5.51	5.55	5.40	5.51	0.04	5.43	0.05	5.41	0.22
Ti	0.67	0.63	0.58	0.58	0.47	0.54	0.63	0.65	0.46	0.28	0.32	0.07	0.38	0.07
Al	2.52	2.47	2.54	2.52	2.59	2.45	2.35	2.52	2.57	0.07	2.79	0.06	2.60	0.20
Fe	1.25	1.26	1.25	1.25	1.17	1.22	1.21	1.42	1.27	0.08	1.62	0.31	2.02	0.31
Mn	0.00	0.03	0.02	0.02	0.00	0.00	0.00	0.02	0.00	0.00	0.01	0.01	0.00	0.00
Mg	3.74	3.95	3.90	4.01	4.22	3.98	3.83	3.65	4.01	0.40	3.80	0.39	3.49	0.30
Ca	0.05	0.02	0.04	0.04	0.02	0.03	0.06	0.03	0.01	0.01	0.00	0.00	0.01	0.01
Na	0.15	0.06	0.16	0.00	0.00	0.00	0.00	0.10	0.01	0.03	0.10	0.08	0.21	0.06
K	1.84	1.86	1.85	1.85	1.90	1.94	1.98	1.90	1.90	0.08	1.80	3.01	1.69	0.14
Al_4	2.52	2.47	2.54	2.52	2.59	2.45	2.35	2.52	2.49	0.04	2.59	0.06	0.05	0.05
Al_6	0.00	0.00	0.00	0.00	0.00	0.00	0.00	0.00	0.09	0.04	0.21	0.03	2.54	0.17

Table 6.1. (Contd.)

1 - 8 Zoned titan - phlogopite phenocryst, kentallenite, Kentallen pipe (Table 7.1 —52); see Fig. 6.2a; also see Fig. 2.3b).

9 Phlogopite phenocrysts in the same rock as 1 - 8.

10 Phlogopite - biotite crystals surrounding amphibole and occurring in its core; appinite, Back Settlement pipe (Table 7.1 — 9 ; *cf*. Figs. 2.5a-b, 2.6a-b, 2.7b).

11 Biotite (large crystals), pyroxene - mica diorite, Rudha Mòr (Table 7.1 — 39).

FeO = total iron;

b.d. = below detection limit (see Appendix A.2; Ni and Cr are below the detection limit in all the analyses).

CHAPTER 7 PETROCHEMISTRY

Using analyses of 82 representative specimens of the appinite suite from the Back Settlement pipe (11), the Ardsheal Hill - Lagnaha pipes (20), the Rudha Mòr pipe (15), the Kentallen pipe (13), other small pipes on the Kentallen - Ardsheal peninsula (5), the Gleann Chàrnan pipes (5) and pipes of the Glen Creran area (13), it can be shown that the overall variation from ultramafic to mafic and less frequently to feldspathic types ranges from 44 to 70 wt. % SiO_2 (Table 7.1, Appendix B.2). On an alkali *vs.* SiO_2 diagram most of the compositions lie in a field which defines a continuous differentiation trend along the boundary between alkaline and subalkaline fields. This indicates transitional characters between the mildly alkaline and the high alumina basalt series (Fig. 7.1). Some members with subalkaline characters variously plot in the fields of continental, island arc and oceanic alkali olivine basalt series.

The continuous differentiation trend is also shown on an AFM plot. However, this indicates affiliation to the calcalkaline series, particularly for the intermediate and acidic members (Fig. 7.2). The majority of the compositions lie below the field of the alkali olivine basalt series but for the ultramafic members the overall trend of the compositional field is generally parallel to that of the field of the alkaline rock series with evidence of some mild iron-enrichment in some appinites (Table 7.1 – 10-13; Appendix B.2 – 6,7).

The high total alkalis are due to the higher K_2O proportion than is normal in the calcalkaline series (*cf.* Wright and Bowes 1979). On the basis of this, and the above features, the appinite suite is considered to be part of a high-potassium calcalkaline series, other representatives of which have been reported from several parts of the world (*e.g.* Cape Nelson, Eastern Papua - Jakeš and Smith 1970;

Northwestern Nigeria - McCurry and Wright 1977).

7.1 Major element variations

The continuous variation in major element chemistry is well represented by plots of S.I. *vs.* various oxides. In the case of SiO_2 the change, at about S.I. of 35, from the flat pattern shown for the 65-35 range of S.I. is related to the production of SiO_2-rich liquids following the appearance and crystallisation differentiation of nepheline normative amphibole (Fig. 7.3a). The continuous curvilinear trends shown by the MgO and Al_2O_3 *vs.* S.I. plots reflect fractionation and the progressive development from ultramafic rocks and kentallenites through appinites (and lamprophyres) to feldspathic appinites and leucocratic diorites (Figs. 7.3b, c). The Na_2O *vs.* S.I. plot also displays the same pattern as the Al_2O_3 *vs.* S.I. plot. There is a somewhat similar trend shown by the K_2O *vs.* S.I. plot but with far too much spread to match it with confidence to other specific trends (Fig. 7.3d). This spread is due to the variable proportions of phlogopite and biotite which Wright and Bowes (1979) attributed to the introduction of K_2O associated with volatiles.

Although showing considerable variation above S.I. 30 because of the crystallisation of the opaque ores in some appinites, the FeO *vs.* S.I. plot also reflects the same fractionation process (Fig. 7.3e). The spread above S.I. values of 30 is also partly due to the replacement of the dominant olivine and clinopyroxene fractionation in kentallenites and some ultramafic rocks (lower FeO) by the dominant amphibole fractionation in appinites (higher FeO).

The considerable scatter shown on the Fe_2O_3 *vs.* S.I. plot reflects the variable proportion of magnetite (Fig. 7.3f). This is interpreted as an indication of highly varied oxygen fugacities during the course of fractional crystallisation. In addition, P_O was not always directly proportional to P_{H_2O}. This conclusion is based on the existence of spessartite samples from the Ardsheal Hill pipe (Table 7.1 – 18-24) which, as a result of crystallisation of opaque ores, contain lower proportions of hydrous minerals but show higher Fe_2O_3 than the appinites from the same pipe.

The scatter of MnO (Fig. 7.3g) is not as great as that for Fe_2O_3. This reflects Fe^{2+} - Mn^{2+} substitution and represents the combination of the more regular pattern of FeO association with the crystallisation of olivine, clinopyroxene and amphibole and the Fe_2O_3 scatter associated with magnetite crystallisation.

The progressive replacement of olivine and clinopyroxene by amphibole, phlogopite, biotite and opaque ores (titan - magnetite) in ultramafic and mafic rocks (S.I. > 30) is shown by an increase in TiO_2 (Fig. 7.3h). In addition, the decrease in the fractionation of these TiO_2-bearing phases in intermediate and feldspathic rocks (S.I. < 30) is shown by a decrease in TiO_2. These variations reflect the combination of all features shown by the previous plots.

The greater scatter of CaO above than below S.I. of 45, the more regular pattern at lesser values, and its overall decrease with decreasing S.I., is consistent with the fractionation of Ca-bearing phases like clinopyroxene and amphibole (Fig. 7.3j). However, as the residual liquids were enriched in Al_2O_3 (Fig. 7.3c), Ca-rich plagioclase could not have been an important factor in the fractionation process except in the leucodiorites and granodiorites (see Chapter 2; Table 7.1 – 40, 46). The higher CaO in certain appinites can be attributed to their higher proportions of apatite and calcite (Table 7.1 – 2, 3, 5-7, 10, 11). This conclusion is supported by the variation of P_2O_5 and CO_2 against S.I. (Figs. 7.3k, l). Generally P_2O_5 increases from ultramafic to mafic rocks and decreases from intermediate to feldspathic rocks, the change of slope being at about S.I. 35. This indicates the build up of P_2O_5 in the magma in the early stages of fractionation and the appearance and subsequent fractionation of apatite.

Variation in the CO_2 proportions is not considered to be representative of the fractional crystallisation. The general variability shown by the CO_2 *vs.* S.I. plots is related to the highly carbonated and altered nature of the rocks from the small pipes at Back Settlement and Rudha Mòr (Chapter 2).

The petrogenetic information obtained from the oxides *vs.* S.I. variations are consistent with the pattern of the development of various rocks shown by field relationships, for example in the Ardsheal Hill - Lagnaha, Rudha Mòr and Kentallen pipes in which there is a considerable variety of rock types (*cf.* Fig. 2.2). The generally regular patterns of variation shown by some constituents indicate that the various rock types of the appinite suite in the various pipes represent a cognate petrogenetic suite derived from a common parent magma. The less regular or highly scattered patterns can be explained on the basis of varying crystallisation conditions in different pipes (Chapters 2 - 6). However, no information can be obtained from these plots concerning the successive appearance of different phases on the liquidus under varying physical conditions during the various stages of fractional crystallisation in different pipes. This is obtained from the plots in the CMAS tetrahedron model of Cox *et al.* (1979).
Assessment of these plots permits the petrogenetic histories to be explained in relation to different environments (see Chapters 2 - 6; Bowes and Wright 1967; Bowes and McArthur 1976).

7.2 Fractional crystallisation on the basis of CMAS model

Back Settlement pipe

Plots of the compositions of rocks of the appinite suite in the CMAS model reveal that two fractionation trends were operative (see explanation of Fig. 7.4 for calculation of plotted parameters):

(i) A clinopyroxene - amphibole fractionation led to the formation of mica-poor appinites and lamprophyres (Table 7.1 — 6, 7, 10, 11). Rocks resulting from this fractionation trend are those which plot below the pargasite position and the plots define a gentle curve which is close to being parallel to the clinopyroxene - Ky join in a projection from Qtz into the En - Ky - Wol plane (Fig. 7.4a). Such plots are compatible with the early crystallisation of clinopyroxene and the replacement of clinopyroxene by amphibole (see Chapters 4, 5).

(ii) A clinopyroxene - amphibole - biotite fractionation led to the formation of relatively mica-rich appinites and lamprophyres (Table 7.1 — 1-5, 8, 9). Rocks resulting from this fractionation trend are those which plot in an elongate field which is generally parallel to the pargasite - feldspar join and much closer to the pargasite position than the products of the other fractionation trend. Such plots are compatible with biotite fractionation having played a role but one that was minor compared with that of clinopyroxene and amphibole.

The dominant role of clinopyroxene and amphibole fractionation in the petrogenesis of all the rock types from the Back Settlement pipes is supported by the rock compositions plotting between clinopyroxene (Diop) and pargasite both in the projection from Ky into the En - Plag - Qtz plane and also in the projection from Wol into the Ky - Diop - Qtz plane (Figs. 7.4b, c; Qtz apices are not shown in these Figures). Such plots are consistent with the evolutionary history deduced from petrography and mineral chemistry, *i.e.* of crystallisation under highly variable volatile pressure with clinopyroxene fractionation reflecting initial low pressure and amphibole and biotite fractionation reflecting higher pressures. In both of these projections the En - Plag and Ky - Diop join, respectively, can be regarded as traces of the planes of SiO_2-saturation and the absence of compositions that plot below these planes (towards Qtz) reflects the absence of acidic rock types in the Back Settlement pipes-(see Table 7.1).

Ardsheal Hill - Lagnaha pipes

Two major fractionation processes can be deduced.

(i) A clinopyroxene - amphibole - biotite fractionation was dominant in the majority of the coarse-grained rocks (Table 7.1 — 12-17). Both in the projections from Qtz into the En - Ky - Wol plane and the projections from Ky into the En - Plag - Qtz plane, plots of these rocks define a trend that is generally parallel to the En - Feldspar (Plag) join (Figs. 7.4d, e). In the former closer affiliation with compositional positions of pargasite and phlogopite are shown; in the latter the closer affiliation seen is with pargasite and clinopyroxene. The fractionation process that is deduced from these plots is similar to that deduced for the mica-rich appinites and lamprophyres from the Back Settlement pipe on the basis of their similar variations in the above projections (Fig. 7.4a, b).

The plots show that in the feldspathic appinites and leucocratic diorite (Table 7.1 — 17, 27, 31) clinopyroxene - amphibole - biotite fractionation was replaced by plagioclase fractionation. On these projections the progressively greater proximity of plots of these rock types to the position of feldspar (Plag) are shown. From interpretation of these Figures the appearance and progressive increase to dominance of plagioclase on the liquidus can be deduced from the bend and gap, respectively, as far as the coarse-grained facies are concerned.

(ii) An olivine - clinopyroxene fractionation process led to the development of the lamprophyric marginal facies which contains olivine and clinopyroxene as phenocrysts (Chapters 2, 3, 4). The early appearance of olivine on the liquidus is shown by the plots of the olivine-bearing lamprophyres (Table 7.1 — 18-21) being parallel to the En - feldspar join (below the pargasite position) in the projection from Qtz into the En - Ky - Wol plane (Fig. 7.4d). The disappearance of olivine and the dominance of clinopyroxene on the liquidus in the olivine-free lamprophyres (Table 7.1 — 22-24) are indicated by the divergence from the other trend into a trend parallel to the clinopyroxene - Ky join. Corresponding features are shown by the plots of the olivine-bearing and olivine-free lamprophyres in the projection from Ky into the En - Plag - Qtz plane (Fig. 7.4e). The lesser correspondence of the olivine-free lamprophyres with the position of plagioclase in these projections compared with the feldspathic appinites and leucocratic diorites indicates that plagioclase played a very minor role in the later stages of this particular fractionation process. This is consistent with the restriction of plagioclase to the groundmass in these rocks (Chapter 2).

Rudha Mòr pipe

A fractionation process similar to that described for the coarse-grained facies of the Ardsheal Hill - Lagnaha pipes is indicated by the disposition of plots on a trend parallel to the En - feldspar join in a projection from Qtz into the En - Ky - Wol plane (Fig. 7.4f). However, evidence that olivine fractionation was pronounced before the appearance of clinopyroxene on the liquidus is provided by the position of the plots of one of the ultramafic rocks being towards olivine (En apex). This is consistent with the presence of olivine in the ultramafic types of this pipe (Table 7.1 — 32-34).

The plots for lamprophyric dykes from the Rudha Mòr pipe (Table 7.1 — 38, 40, 42) also indicate the marked role of clinopyroxene-amphibole-biotite fractionation. These plots lie close to those of appinites and pyroxene-mica diorites from the same pipe in this and other projections. This provides further evidence of the genetic relationship of the lamprophyres and members of the appinite suite (see Chapter 2).

Kentallen pipe

Evidence concerning the fractionation history of the Kentallen pipe is provided by compositional plots in several projections in the CMAS model, with the projection from Qtz into the En - Ky - Wol plane being of particular value (Fig. 7.4g). In it plots of the marginal ultramafic rocks lie on a trend that is generally parallel to the En - pargasite join with some being close to the position of pargasite. This reflects the operation of olivine fractionation followed and subsequently replaced by clinopyroxene - amphibole - phlogopite fractionation. This fractionation trend corresponds with that deduced for the ultramafic rocks of the Rudha Mòr pipe (*cf*. Fig. 7.4f).

If the mean kentallenite composition (Table 2.1 – 6) represents the original "primary" magma (Chapter 3), then the position of the plots of the chilled margin of kentallenite just above the pargasite position on the side towards clinopyroxene indicates evolution from the parent liquid through a dominant fractionation of olivine and clinopyroxene, before phlogopite became a prominent crystallising phase. On the other hand, those kentallenites whose plots lie on the En - Ky join side of the position of pargasite and show greater affinity to phlogopite than to clinopyroxene represent crystallisation after phlogopite became a prominent fractionating phase. This interpretation is consistent with the scarcity of phlogopite in the chilled margin of the kentallenite mass (Table 7.1 – 51).

The kentallenites and the lamprophyre whose plots are below the mean kentallenite composition and the diorite and biotite - feldspar vein which plot closer to the feldspar position are interpreted as representing progressively developed residual products.

Small pipes on Kentallen - Ardsheal peninsula

Plots of the limited data available for these pipes are not presented here. However, for the rocks of the North Cuil and South Cuil pipes and the St Adamanan's pipe these data are consistent with the operation of fractionation processes similar to those described for the coarse-grained facies of the Ardsheal Hill pipe. On the basis of petrography of the rocks in the St Moluag's pipe the fractionating phases were similar to those in the non-cumulate kentallenites of the Kentallen pipe.

Gleann Chàrnan and Glen Creran pipes

On the basis of plots in the CMAS model the fractionation processes operative in the Gleann Chàrnan pipe and the Màm na Stainge, Salachail, Garbh Allt and Glen Ure pipes of the Glen Creran area were similar to that operative both in the Back Settlement pipes and in the development of the coarse-grained facies of the Ardsheal Hill - Lagnaha pipes. This is consistent with the petrographic similarities between the rock types from these pipes. In the case of the Burnamuc pipe in Glen Creran, the kentallenite has similar fractionating phases to the non-cumulate kentallenite of the Kentallen pipe (*cf.* Figs. 7.4h, j).

Discussion and conclusions based on CMAS model

The majority of the rock types from the Ballachulish appinite suite closely follow the variation trends of the Kentallen pipe shown in projection from Qtz into the En - Ky - Wol plane (Fig.7.4h; also see Fig 7.4j) This is consistent with the conclusion that a parent liquid similar in composition to the mean kentallenite was the starting point for fractionation in all the pipes of the region. That olivine fractionation took place in the early stages of crystallisation is shown not only by the affinities of the ultramafic rocks to olivine in these projections but also by the divergence of the general trend from very close to the olivine position in a projection from Fo into the En - Ky - Wol plane (Fig. 7.4k).

Following olivine there was successive fractionation of clinopyroxene, amphibole and phlogopite (or biotite) and of plagioclase in the later stages. This was associated with variation of P_{Gas} (Chapters 4 - 6) and resulted in the progressive development of ultramafic rocks, kentallenites, appinites (and lamprophyres) and leucocratic diorite or granodiorite (*cf.* Fig. 7.4h).

On the basis of this interpretation of the overall fractionation trend, the marginal ultramafic rocks, some kentallenites and appinites whose compositions plot towards the En apex with respect to that of the mean kentallenite in a projection from Qtz into the En - Ky - Wol plane (Fig. 7.4h) formed as cumulates. On the other hand, those rock types which have their plots towards the position of feldspar, with respect to the mean kentallenite are interpreted as representing liquid compositions.

A number of petrographic and field observations can be explained on the basis of such a crystallisation history. For example, in the one intrusion at Kentallen, the kentallenite in some parts shows a weak banding reminiscent of that seen in some layered igneous masses (Bowes and Wright 1967, p. 129, 133) while in other parts orthopyroxene is seen rimming olivine phenocrysts (Fig. 2.8a) and phlogopite seen rimming olivine and clinopyroxene phenocrysts (*cf.* Fig. 2.3b), pointing to the existence of liquids over a considerable range of decreasing temperature. This contrast of features *viz.* those of cumulates and those of liquid compositions, is shown in the suite as a whole. For example the kink banded biotite common in many of the marginal varities and in some of the kentallenites and appinites (*cf.* Fig, 2.6b) is indicative of emplacement of an almost solid mass of crystals while the presence of xenoliths showing evidence of reaction in the Gleann Chàrnan (Bowes *et al.* 1963, p. 26, 29, fig. 5) and other pipes indicates emplacement of liquids. In addition, banding with features consistent with undercooling related to rapid migration of water occurs in the Rudha Mòr diorite (Bowes and Wright 1967, p. 129). These diorites plot towards feldspar with respect to the mean kentallenite in a projection from Qtz into the En - Ky - Wol plane (Fig. 7.4h) indicating that they represent liquid compositions and not cumulates.

The major conclusions based on the compositional variation of the appinite suite in the CMAS model are:

1. A parent liquid similar in composition to the mean kentallenite was the starting point for fractionation in all the pipes.
2. Some rocks (*e.g.* marginal ultramafic types and some kentallenites and appinites) represent cumulates. These are the rocks that were emplaced as crystal mushes.
3. Most of the rocks of the suite represent liquid compositions. These are the rocks that show reaction relations consistent with magmatic reaction.
4. Some intrusions as the kentallenite of the Kentallen pipe are partly cumulates, or cumulates disrupted during emplacement as crystal mush, and partly represent liquid composition.
5. Olivine fractionation took place in the early stages.
6. Following olivine there was successive fractionation of clinopyroxene, amphibole and phlogopite (or biotite) and of plagioclase in the later stages. This resulted in the progressive development of the ultramafic rocks, kentallenites, appinites (and lamprophyre) and leucocratic diorite or granodiorite.

7.3 Trace element chemistry

Continuous variation trends reflecting differentiation and progressive development from ultramafic rocks and kentallenites, through appinites (and lamprophyre) to diorites and granodiorites are also shown by Ni, Cr and Co *vs.* MgO plots (Figs. 7.5a, b, c). The extremely high Ni and Cr contents of certain ultramafic rocks and kentallenites indicate a high degree of fractional crystallisation involving olivine in the early stages (see Chapter 3). The scatter in Co *vs.* MgO plots (Fig. 7.5c) is probably related to magnetite crystallisation, with up to 2.87 wt. % CoO present in magnetite from the appinite of the Back Settlement pipe (Table 2.2 – 13). The positive correlations between V *vs.* Co and V *vs.* Fe_2O_3 (Figs. 7.5d, e) are consistent with this interpretation.

The high V contents (> 800 p.p.m.) relative to Fe_2O_3 (*cf.* Fig. 7.5e) are related to the crystallisation of titan - magnetite in certain appinites from the Ardsheal Hill pipe, which are markedly rich in TiO_2 (Table 7.1 – 12).

The continuous variation trend with a positive slope shown by Rb *vs.* K_2O reflects the simultaneous concentration of both these elements into residual liquids during fractionation (Fig. 7.5f). The spread is due to the crystallisation of the variable proportions of amphibole, phlogopite and biotite in different rocks as amphibole is discriminant against Rb relative to K_2O while phlogopite and biotite have the reverse effect (Beswick 1976).

Due to the lack of the Ca-rich plagioclase fractionation in ultramafic to intermediate rocks (Chapter 2; section 7.2) Sr has also concentrated into residual liquids. This is shown by the positive correlation between Sr and Na_2O (Fig. 7.5g). The greater spread shown in the *c.* 4-6 wt. Na_2O range reflects the crystallisation of Na_2O-rich plagioclase in feldspathic appinites and leucocratic diorites.

On the basis of the average concentrations of La, Ce and Y (Wright and Bowes 1979; Table 2.1) together with their averages in the whole appinite suite it can be shown that with increase in fractionation the residual liquid became enriched in La (Fig. 7.6). This is shown by its higher concentration in the mean granodiorite of the appinite suite and lower concentration in the mean ultramafic rock as compared to the mean kentallenite and the average for the whole appinite suite. In the case of Ce and Y there is a considerable overlap and a regular pattern similar to that shown by La can not be deduced from their mean compositions. This results from these elements behaving both compatibly and incompatibly between different crystallising phases and their corresponding liquids (Pearce and Norry 1979).

The exceptionally high Ce content of the mean pyroxene - mica diorite is not consistent with the interpretation of Nockolds (1941) that it represents the parent liquid. Rather this rock unit must represent a high degree of clinopyroxene and probably some plagioclase fractionation. However, the Ce content of the mean kentallenite is closer to the average Ce content of the rest of the rock types as well as to the average Ce content of the whole appinite suite. This gives further support to the interpretation of the mean kentallenite as approximating to the composition of that of the original "primary" liquid.

The higher Ce as compared to La and Y is the distinctive feature of the Ballachulish appinite suite when compared to other high-potassium calcalkaline series (see Albini *et al.* 1980).

High S contents are shown by the rock types from the Back Settlement and Rudha Mòr pipes while high Cl contents are shown by the rock types from the Kentallen and Gleann Chàrnan pipes (Table 7.1; also see Wright and Bowes 1979). There is no correlation between these elements and their variations are not considered to be representative of fractional crystallisation. S has probably participated in the formation of pyrite in the later stages of crystallisation while Cl has entered into phlogopite, amphibole and apatite (Smith *et al.* 1981).

7.4 Magmatic affinity and tectonic implications

The following features are indicative of the Ballachulish appinite suite being derived from high-potassium calcalkaline magma in a continental environment.

1. The path followed by Ni *vs.* SiO_2 variation occurs in the field of calcalkaline rock series; it has the relatively steep slope shown by other calcalkaline rock series in contrast to the flat pattern shown by tholeiitic suites (Fig. 7.7a, b).
2. The increasing Sr in the residual liquids and the steep rare earth patterns (Figs. 7.5g, 7.6) are characteristics of a calcalkaline suite (Gill 1979).
3. The K % (1.82) in the mean kentallenite and the average K/Rb ratio (∿400) for the whole suite (*cf.* Fig. 7.7c) are between those determined for the island arc basalt sequence (K % = 0.5, maximum K/Rb ratio = 750) and continental ultrapotassic and shoshonitic rocks (K % = 2.5, K/Rb ratio = 250) - see Beswick (1976).
4. The Zr/Y *vs.* Zr plots are essentially in the "within plate basalt" field, indicating a continental tectonic environment (Fig. 7.7d).

7.5 Conclusions

1. The major and trace element chemistry of the Ballachulish appinite suite is consistent with crystallisation differentiation of a high-potassium calcalkaline magma (transitional between alkaline and calcalkaline) that evolved in a continental tectonic environment.
2. A parent liquid similar to the mean kentallenite composition was the starting point for fractionation in all the pipes.
3. Some rocks (*e.g.* marginal ultramafic types and some kentallenites and appinites) represent cumulates but most of the rocks of the suite represent liquid compositions.
4. Some intrusions as the kentallenite of the Kentallen pipe are partly cumulates, or cumulates disrupted during emplacement as crystal mush, and partly represent liquid compositions.
5. Olivine was the earliest mineral on the liquidus followed by successive fractionation of clinopyroxene, amphibole, phlogopite or biotite and plagioclase (in the later stages). This was associated with variable

gas pressure and resulted in the progressive development of ultramafic rocks, kentallenites, appinites (and lamprophyres) and leucocratic diorite or granodiorite.

6. Some magnetite and apatite fractionation also took place, particularly with amphibole fractionation (in appinites). However, magnetite and apatite never became prominent fractionating phases on the liquidus. It was amphibole fractionation rather than magnetite fractionation that resulted in a non-iron enrichment trend for most of the differentiation path as in many calcalkaline rock series.
7. The early lamprophyre dykes, which are associated in time and space with the appinite suite, are genetically related to it.

Figure 7.1. Alkali *vs*. SiO_2 diagram for the Ballachulish appinite suite with division into various fields after Schwarzer and Rogers (1974). Key to rock symbols is on fold out sheet following Figure 7.4k.

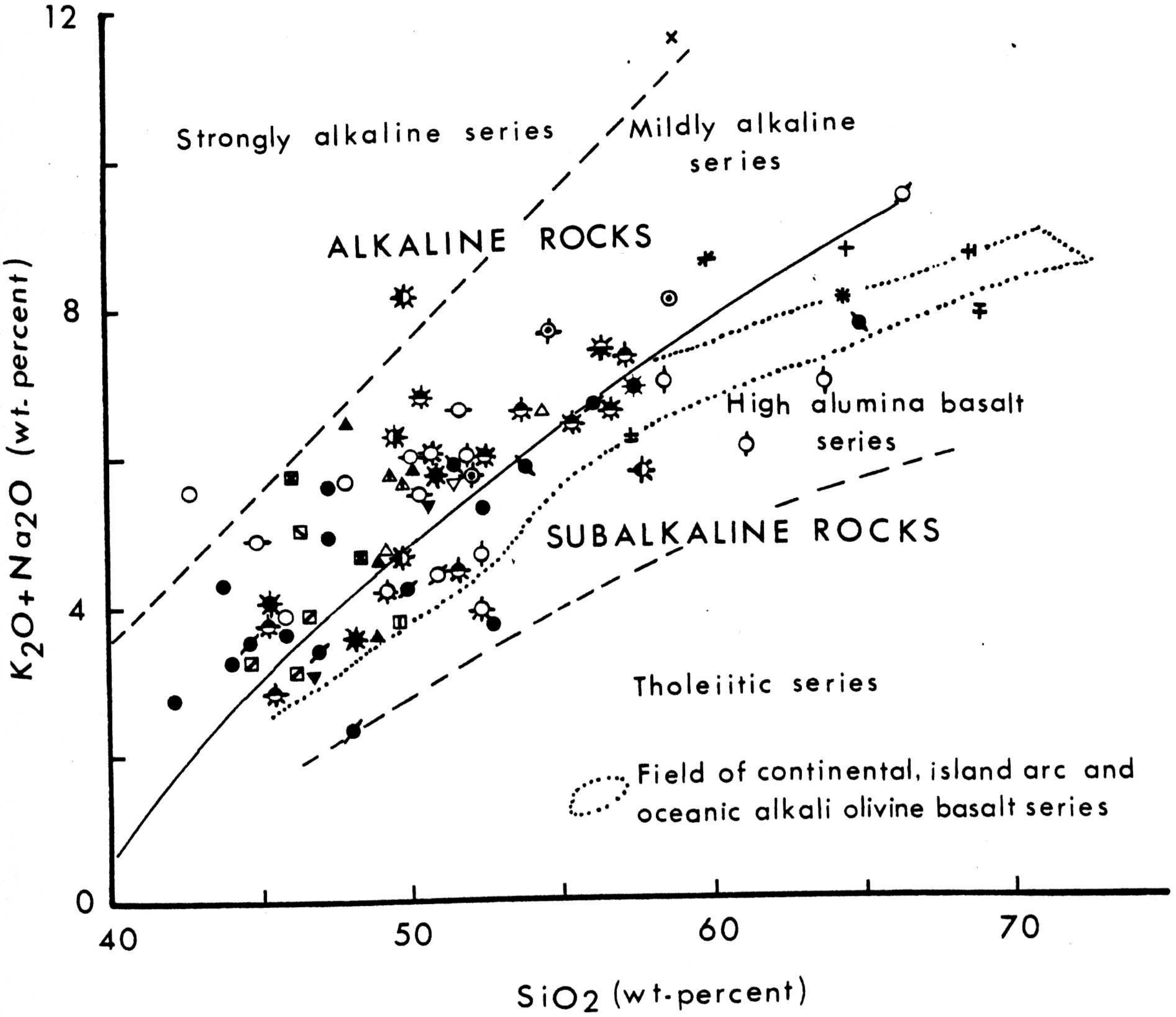
12
8
4
0
40
50
60
70
K_2O+Na_2O (wt. percent)
SiO_2 (wt-percent)
Strongly alkaline series
Mildly alkaline series
ALKALINE ROCKS
High alumina basalt series
SUBALKALINE ROCKS
Tholeiitic series
Field of continental, island arc and oceanic alkali olivine basalt series

Figure 7.2. AFM diagram for the Ballachulish appinite suite (key to symbols is on fold out sheet following Figure 7.4k; fields after Schwarzer and Rogers 1974).

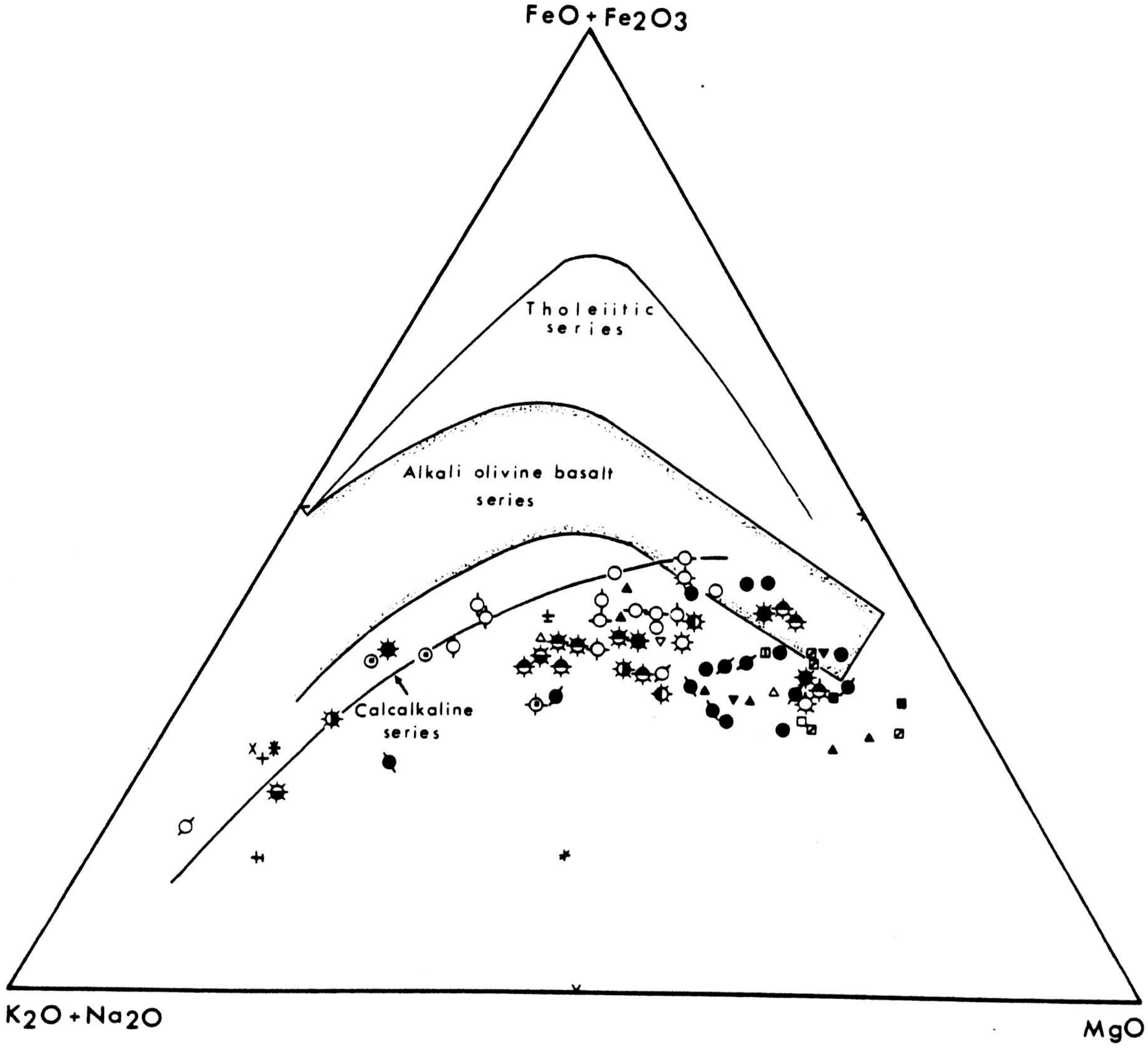
FeO + Fe2O3
Tholeiitic series
Alkali olivine basalt series
Calcalkaline series
K2O + Na2O
MgO

Figure 7.3 (a - l). Plots of SiO_2, MgO, Al_2O_3, K_2O, FeO, Fe_2O_3, MnO, TiO_2, CaO, P_2O_5 and CO_2 against S.I. respectively (key to symbols is on fold out sheet following Figure 7.4k).

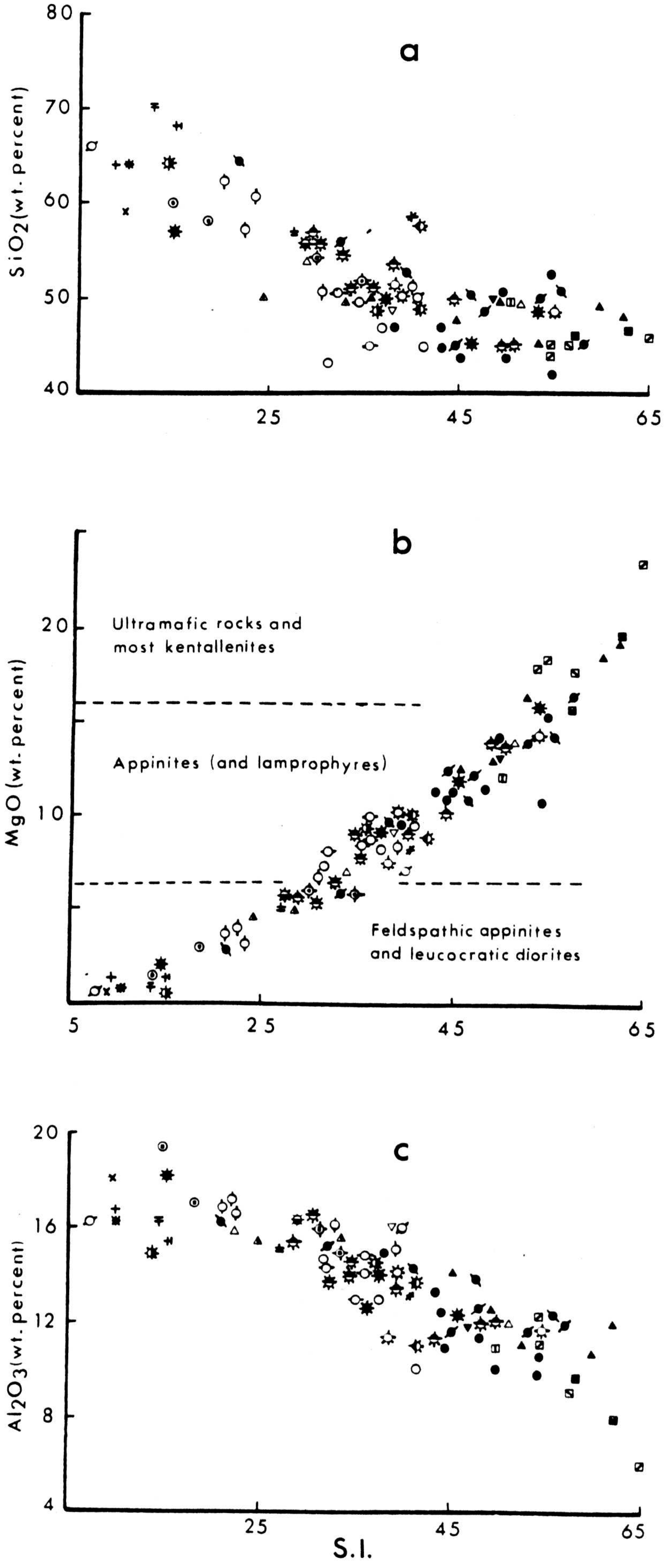
a
SiO2(wt. percent)
80
70
60
50
40
25
45
65
b
MgO (wt. percent)
Ultramafic rocks and
most kentallenites
Appinites (and lamprophyres)
Feldspathic appinites
and leucocratic diorites
20
10
5
25
45
65
c
Al2O3(wt. percent)
20
16
12
8
4
25
45
65
S.I.

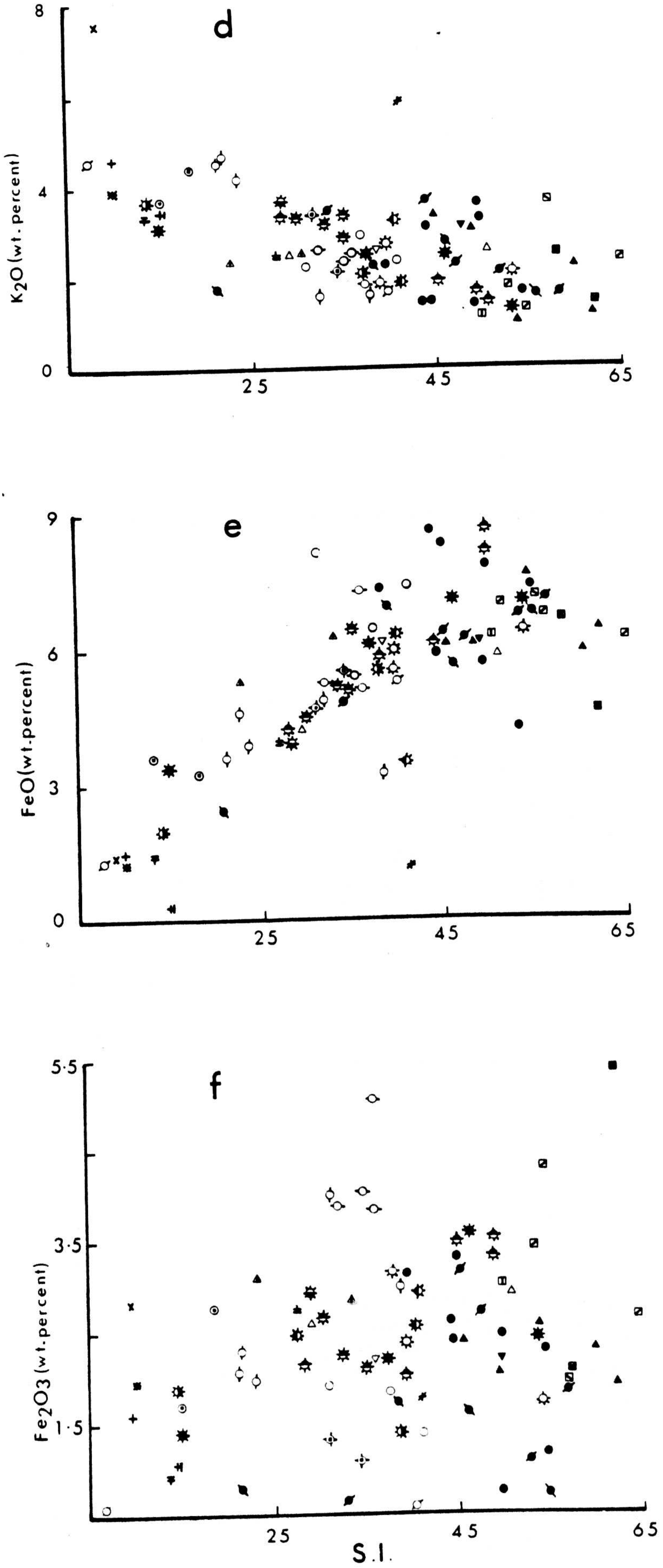
d
K2O (wt. percent)
8
4
0
25
45
65
e
FeO (wt. percent)
9
6
3
0
25
45
65
f
Fe2O3 (wt. percent)
5·5
3·5
1·5
25
45
65
S.I.

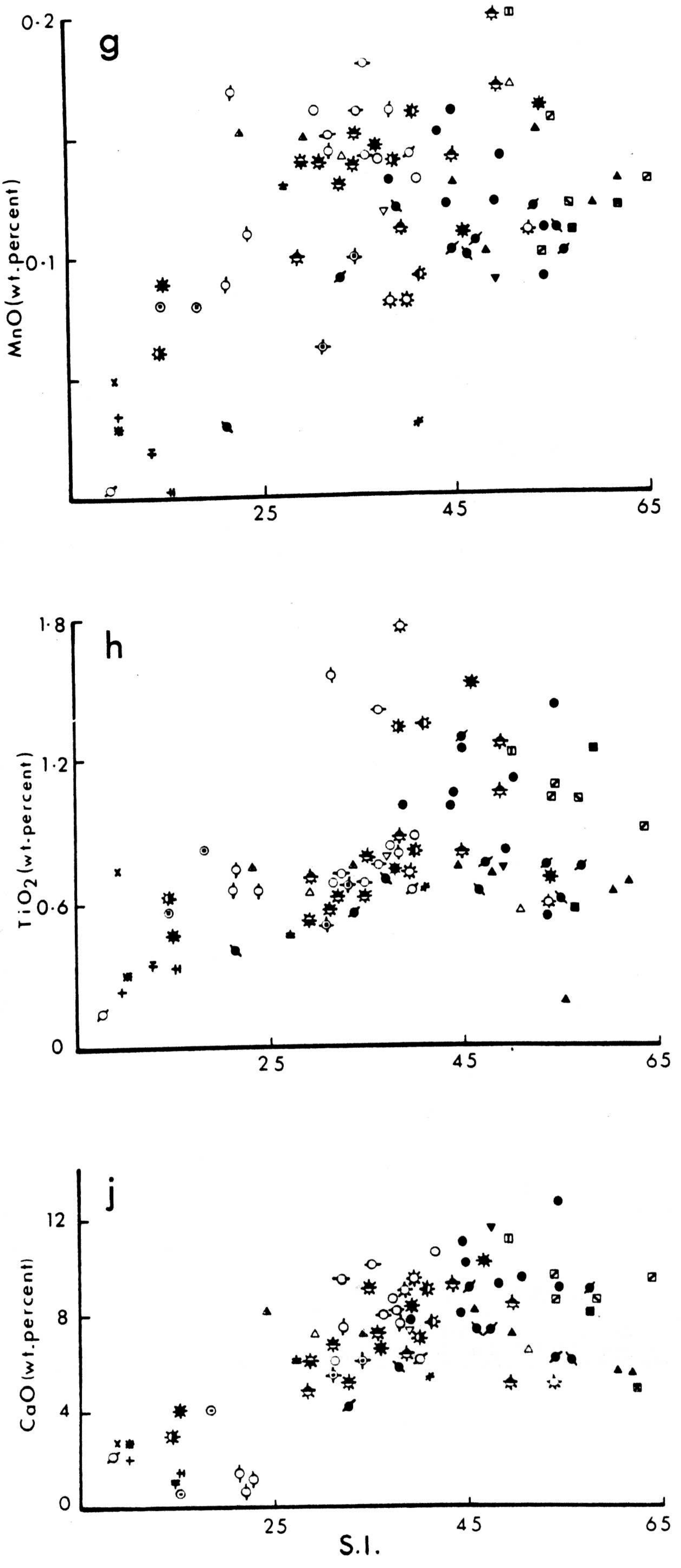
g
0·2
0·1
MnO(wt.percent)
25
45
65
h
1·8
1·2
0·6
0
TiO2(wt.percent)
25
45
65
j
12
8
4
0
CaO(wt.percent)
25
45
65
S.I.

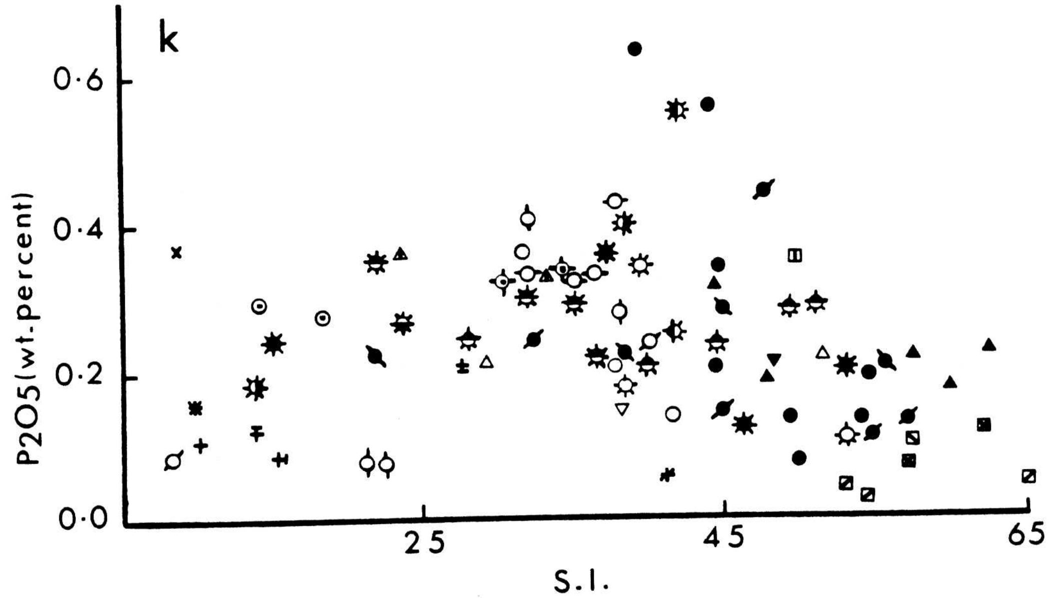
k
P2O5(wt.percent)
0·0
0·2
0·4
0·6
25
45
65
S.I.

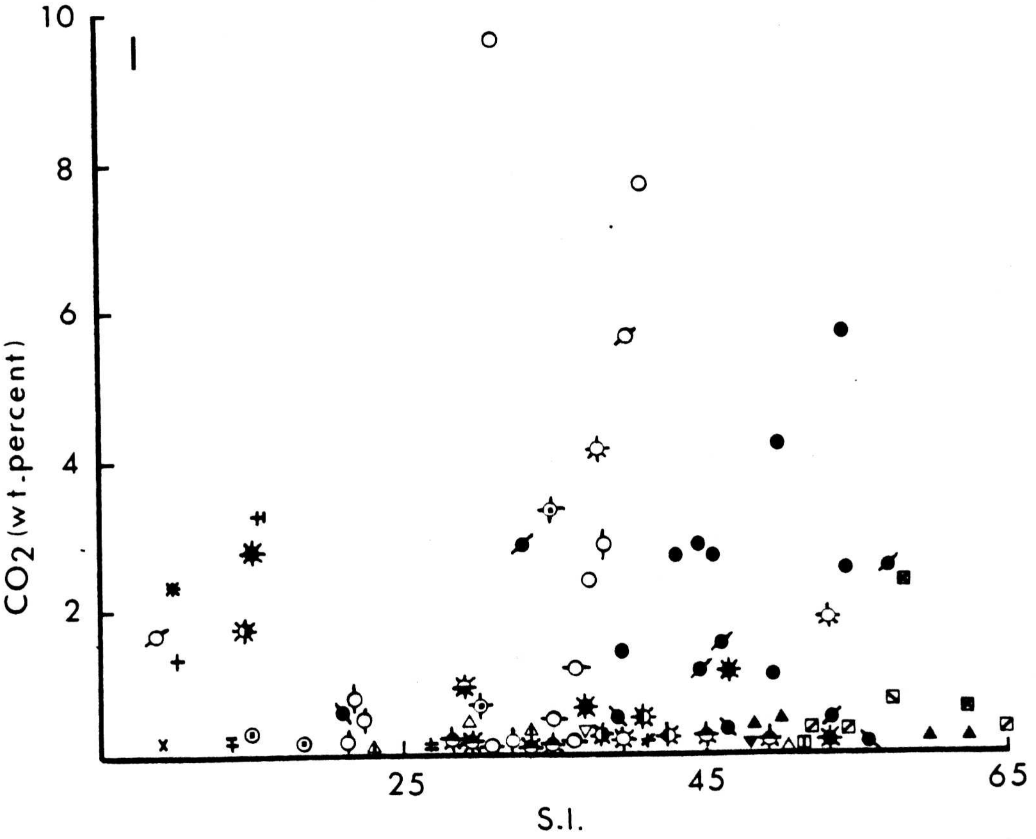
l
CO2(wt.percent)
2
4
6
8
10
25
45
65
S.I.

Figure 7.4 (a - k). Variation of the Ballachulish appinite suite in the CMAS fractionation model shown by projections into various planes from particular points. C-M-A-S end members are recalculated from oxide wt. % as:

$C = 100(CaO - 3.333P_2O_5 + 2Na_2O + 2K_2O) \times 56.08/Sum$

$M = 100(MgO + FeO + MnO + NiO - TiO_2) \times 40.32/Sum$

$A = 100(Al_2O_3 + Fe_2O_3 + Cr_2O_3 + TiO_2 + Na_2O + K_2O) \times 101.96/Sum$

$S = 100(SiO_2 - 2Na_2O - 2K_2O) \times 60.05/Sum$

where $Sum = (CaO - 3.333P_2O_5 + 2Na_2O + 2K_2O) \times 56.08 + (MgO + FeO + MnO + NiO - TiO_2) \times 40.32 + (Al_2O_3 + Fe_2O_3 + Cr_2O_3 + TiO_2 + Na_2O + K_2O) \times 101.96 + (SiO_2 - 2Na_2O - 2K_2O) \times 60.05$; (O'Hara 1976). Key to rock symbols for Figures 7.4 h - k is given on fold out sheet following Figure 7.4k.

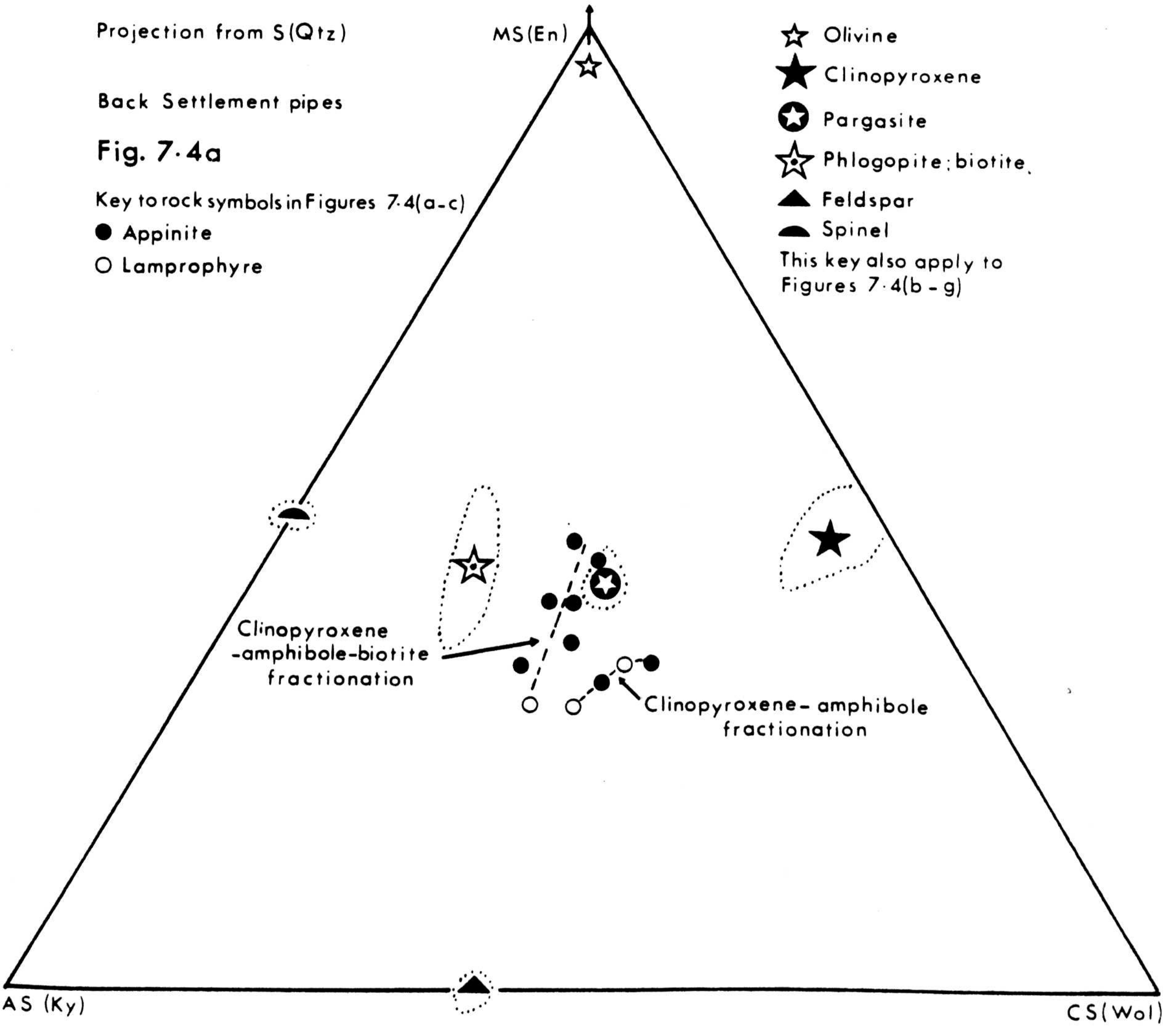

Fig. 7·4a

Projection from S(Qtz)
Back Settlement pipes
Key to rock symbols in Figures 7·4(a-c)
● Appinite
○ Lamprophyre
MS(En)
☆ Olivine
★ Clinopyroxene
Pargasite
Phlogopite; biotite
▲ Feldspar
Spinel
This key also apply to Figures 7·4(b-g)
Clinopyroxene -amphibole-biotite fractionation
Clinopyroxene- amphibole fractionation
AS (Ky)
CS(Wol)

Back Settlement pipes

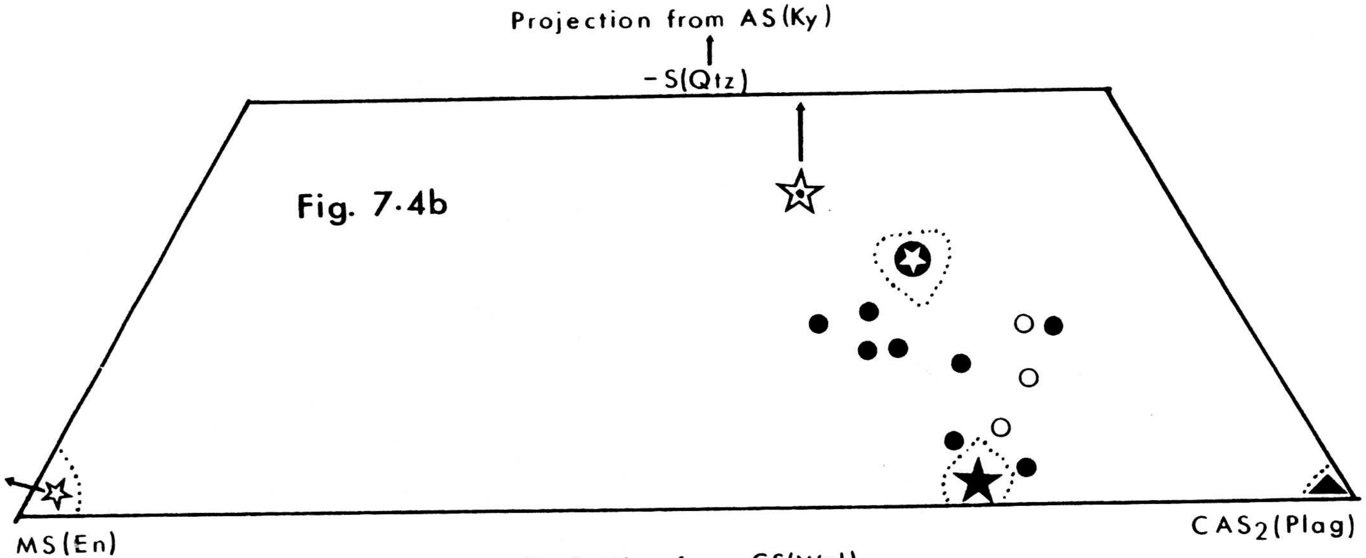

Fig. 7·4b

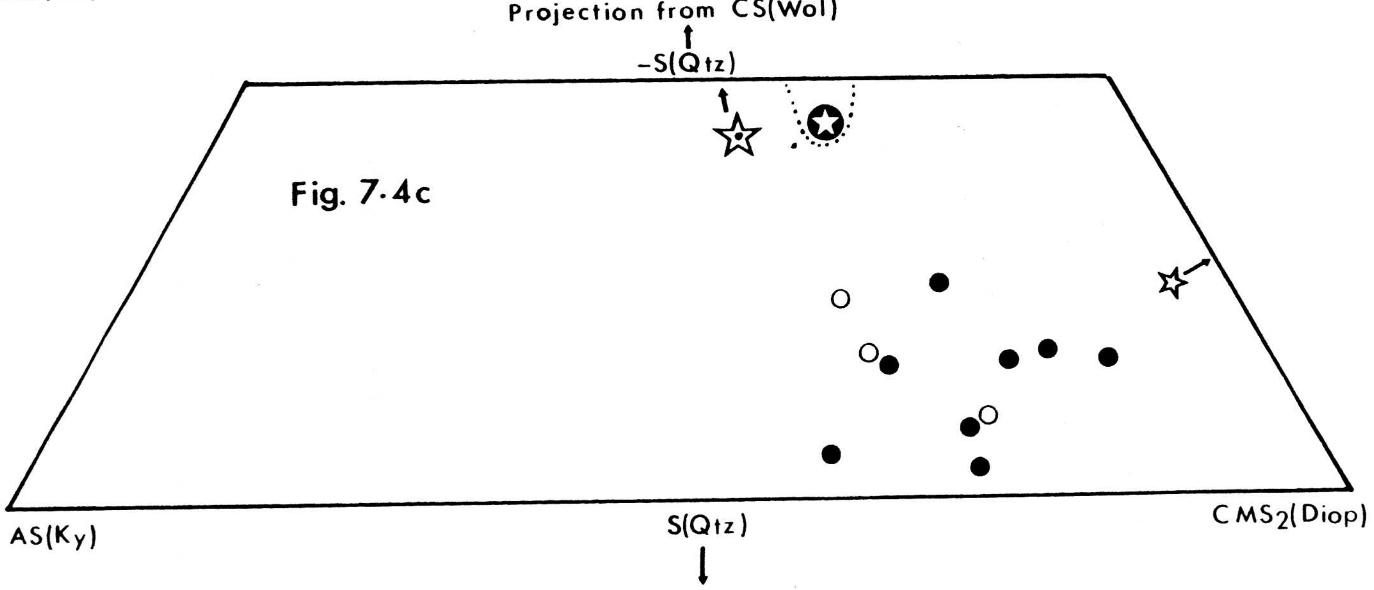

Fig. 7·4c

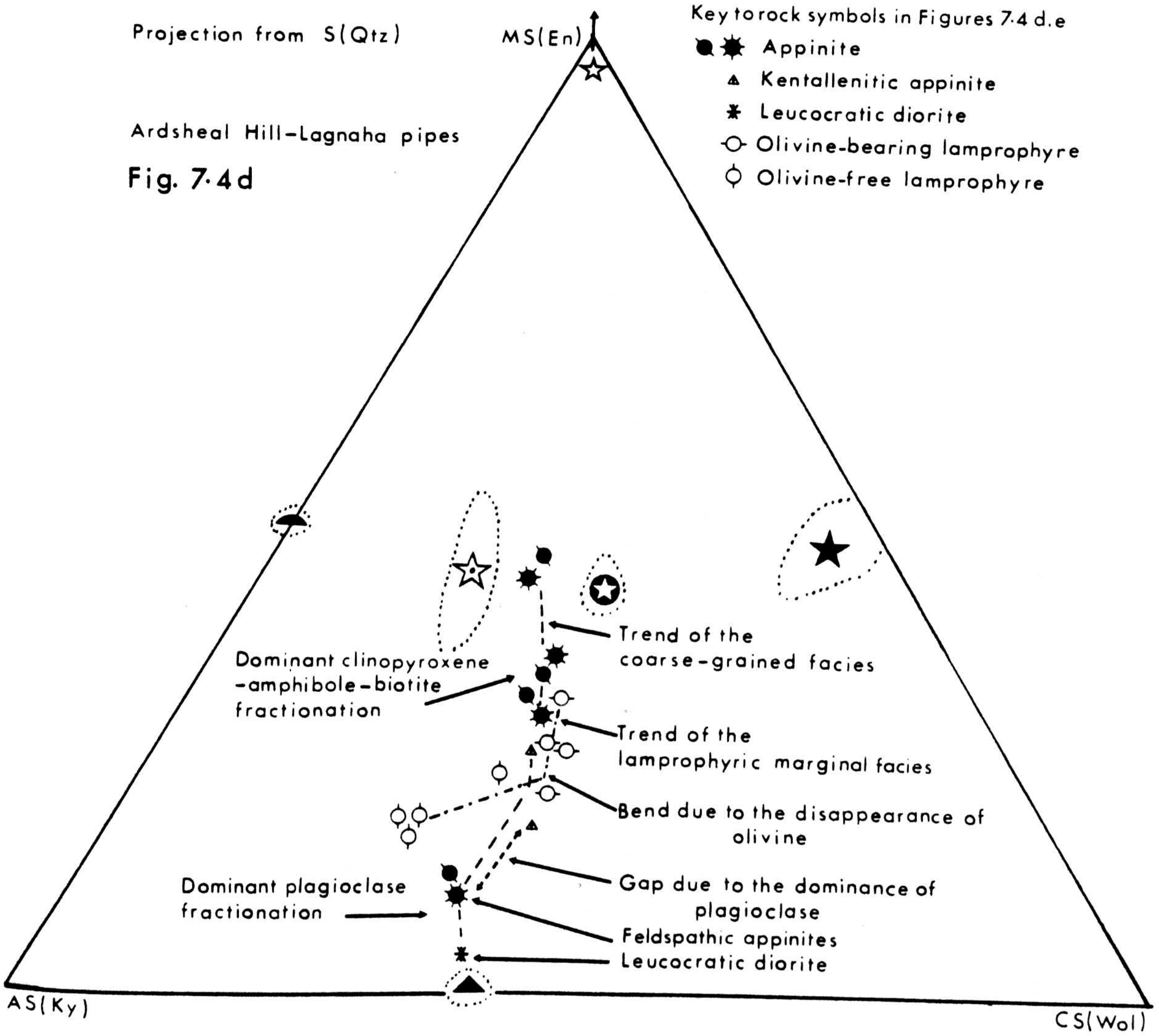
Projection from S(Qtz)
Ardsheal Hill–Lagnaha pipes
MS(En)
AS(Ky)
CS(Wol)
Key to rock symbols in Figures 7·4 d.e
Appinite
Kentallenitic appinite
Leucocratic diorite
Olivine-bearing lamprophyre
Olivine-free lamprophyre
Trend of the coarse-grained facies
Dominant clinopyroxene -amphibole-biotite fractionation
Trend of the lamprophyric marginal facies
Bend due to the disappearance of olivine
Gap due to the dominance of plagioclase
Dominant plagioclase fractionation
Feldspathic appinites
Leucocratic diorite

Fig. 7·4d

Ardsheal Hill–Lagnaha pipes

Projection from AS(Ky)

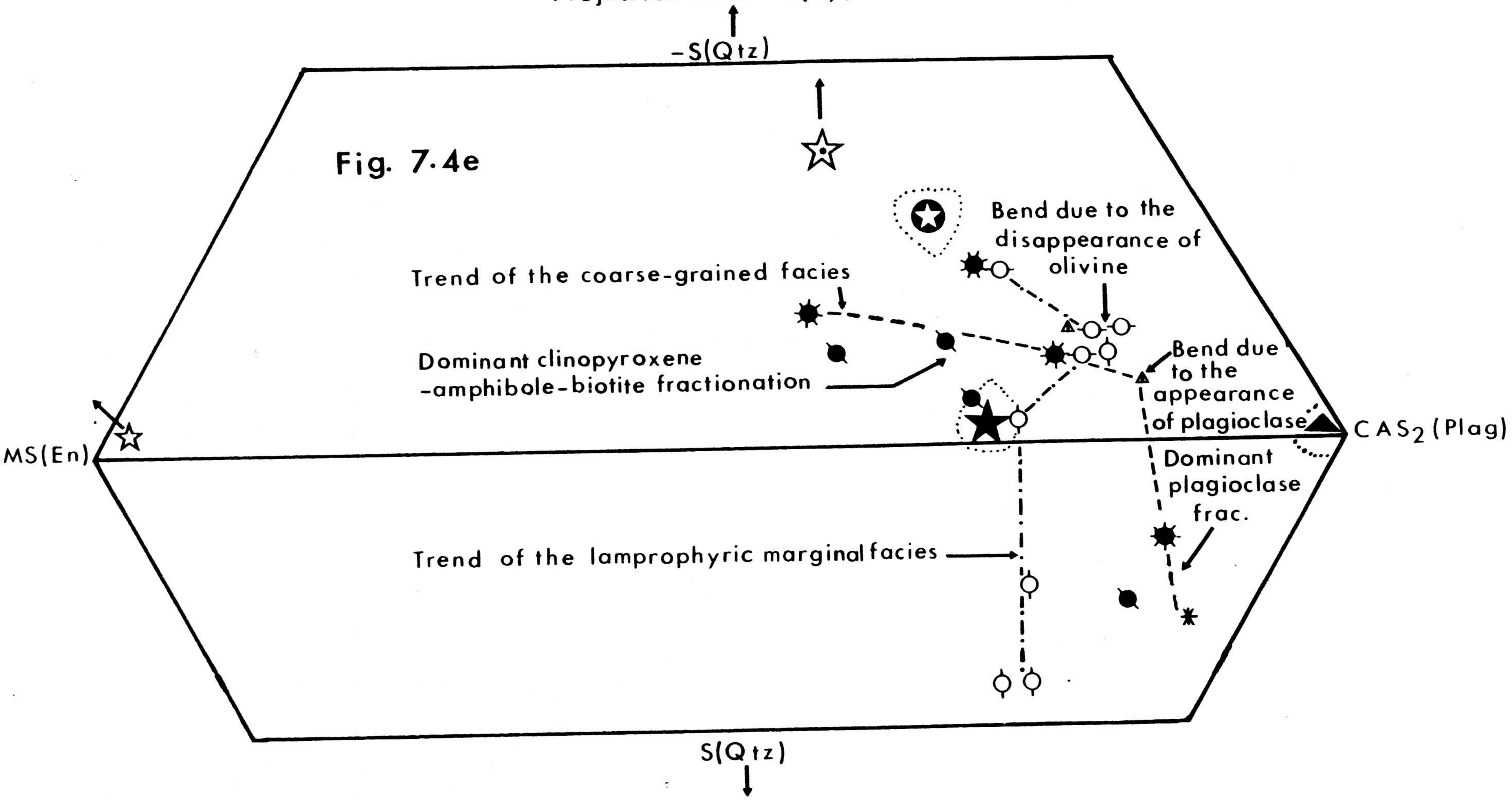
Fig. 7·4e

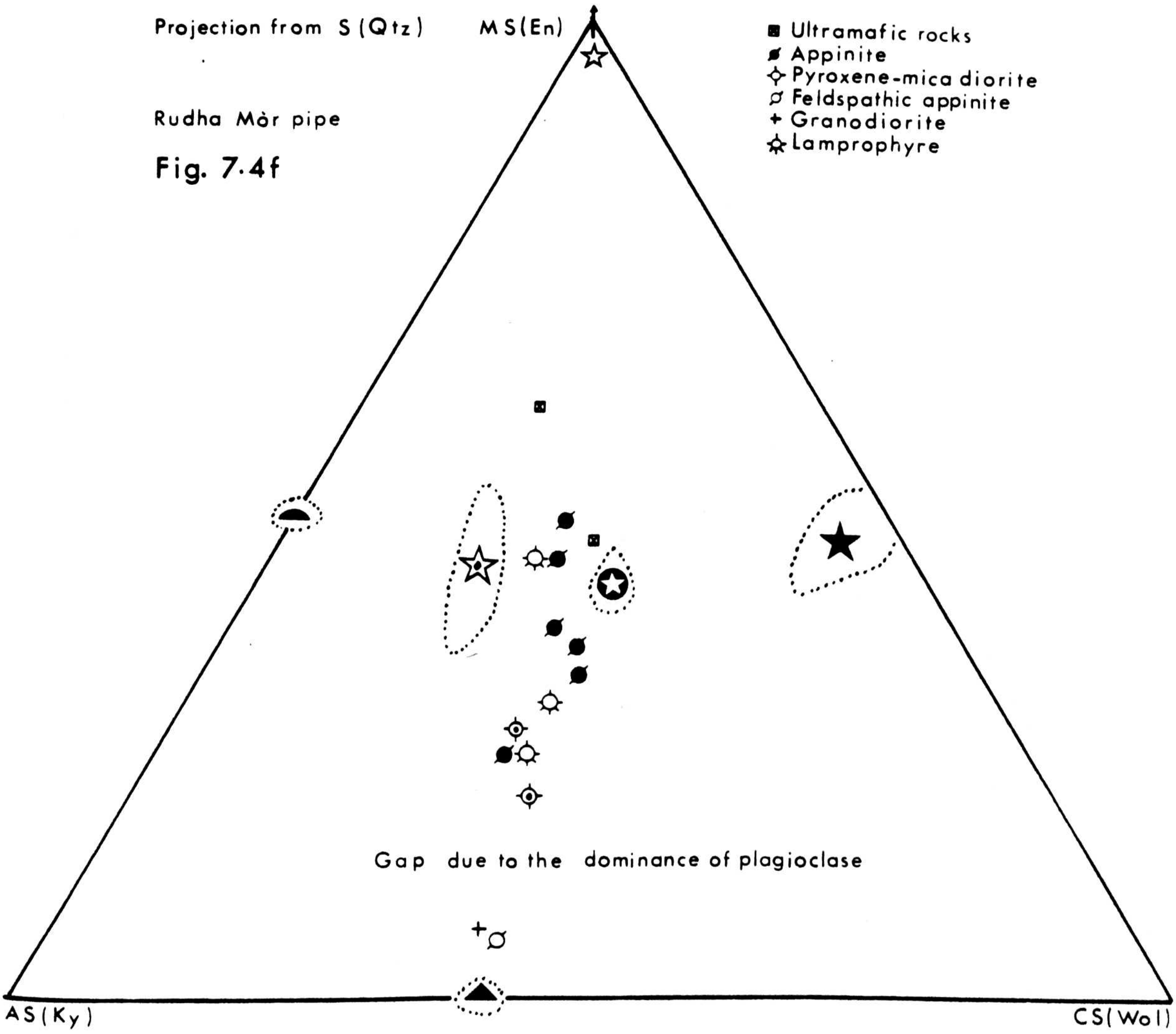
Projection from S (Qtz)
Rudha Mòr pipe
Fig. 7·4f
MS(En)
AS(Ky)
CS(Wol)
■ Ultramafic rocks
● Appinite
✧ Pyroxene-mica diorite
ø Feldspathic appinite
+ Granodiorite
✯ Lamprophyre
Gap due to the dominance of plagioclase

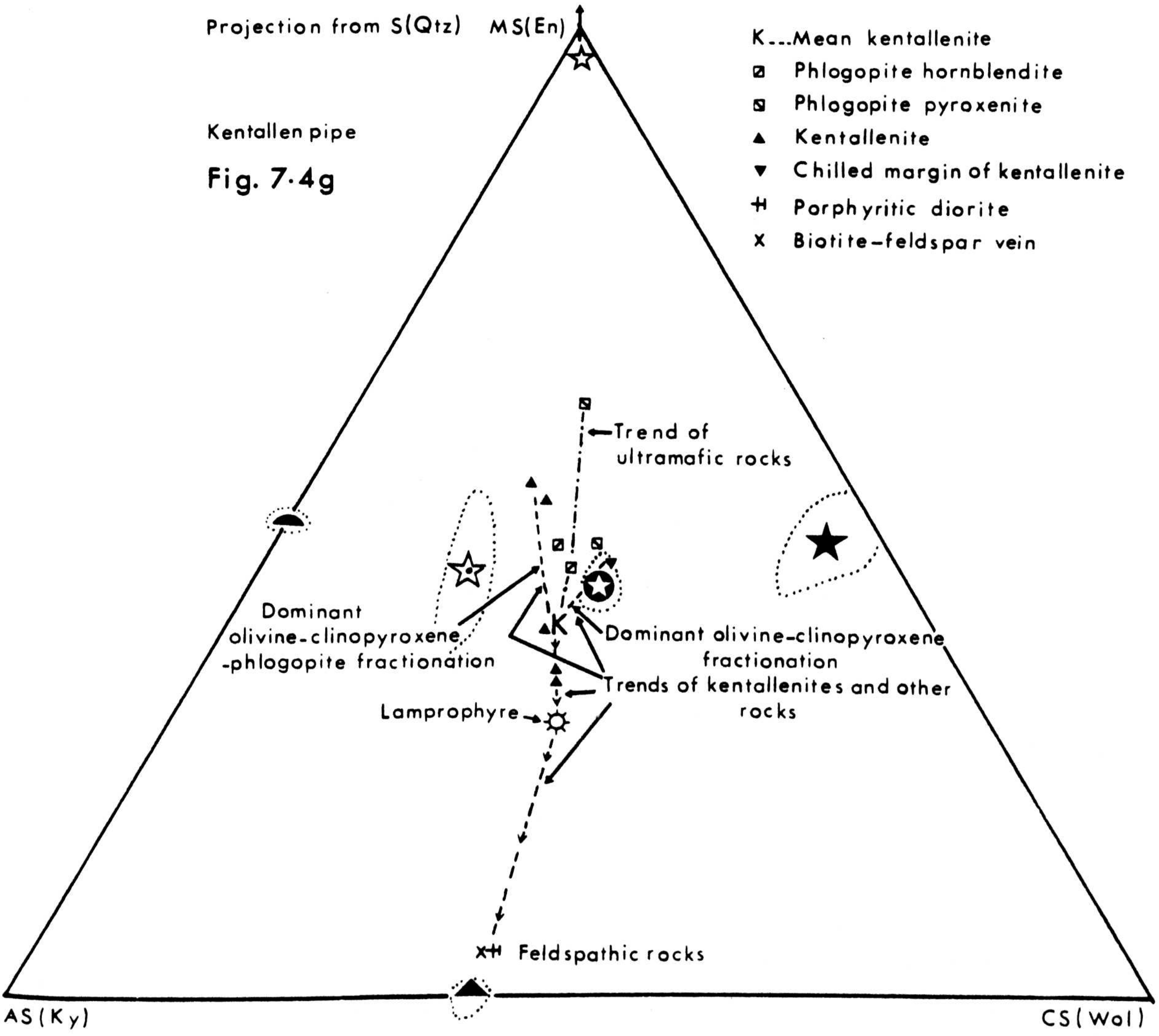
Projection from S(Qtz)
MS(En)
AS(Ky)
CS(Wol)
Kentallen pipe
Fig. 7·4g
K...Mean kentallenite
▨ Phlogopite hornblendite
▨ Phlogopite pyroxenite
▲ Kentallenite
▼ Chilled margin of kentallenite
+ Porphyritic diorite
X Biotite-feldspar vein
Trend of ultramafic rocks
Dominant olivine-clinopyroxene-phlogopite fractionation
Dominant olivine-clinopyroxene fractionation
Trends of kentallenites and other rocks
Lamprophyre
K
Feldspathic rocks

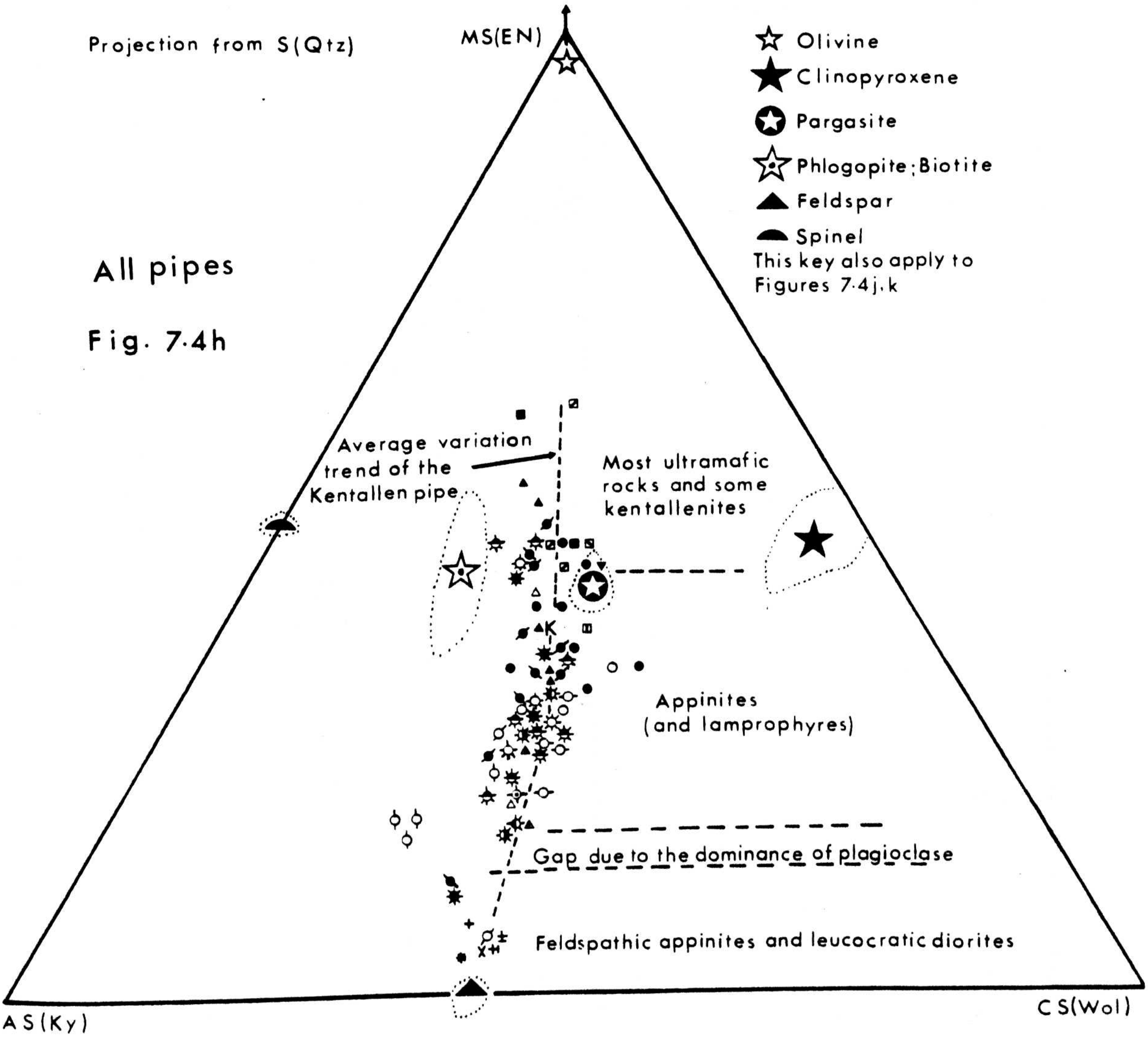
Projection from S(Qtz)
MS(EN)
☆ Olivine
★ Clinopyroxene
Pargasite
Phlogopite; Biotite
▲ Feldspar
Spinel
This key also apply to Figures 7·4j,k
All pipes
Fig. 7·4h
Average variation trend of the Kentallen pipe
Most ultramafic rocks and some kentallenites
K
Appinites (and lamprophyres)
Gap due to the dominance of plagioclase
Feldspathic appinites and leucocratic diorites
AS(Ky)
CS(Wol)

Fig. 7·4j

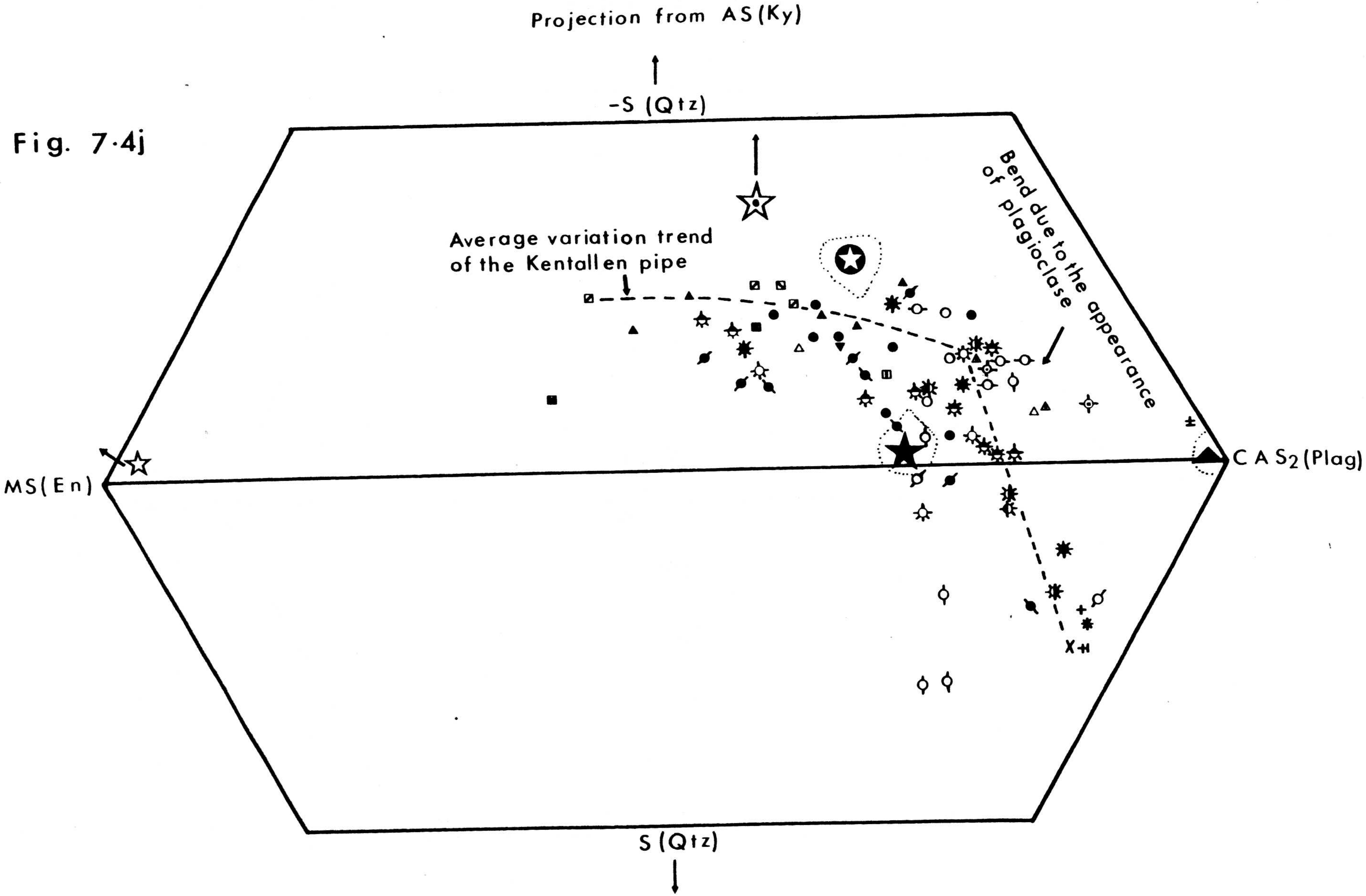
Projection from AS(Ky)
-S (Qtz)
Average variation trend of the Kentallen pipe
Bend due to the appearance of plagioclase
MS(En)
C A S_2(Plag)
S (Qtz)

Fig. 7.4k

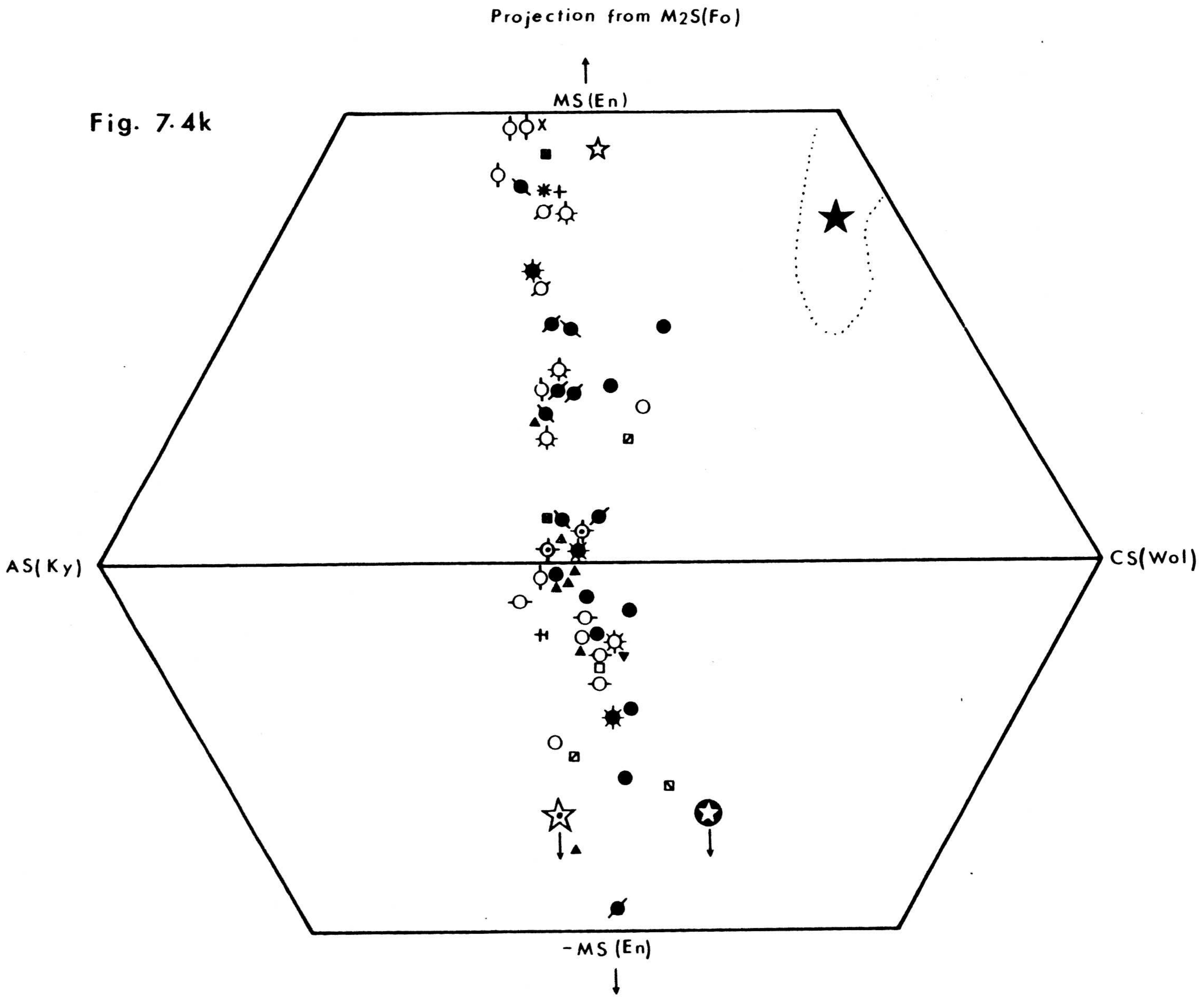

Fold out sheet

Back Settlement pipes
● Appinite
○ Lamprophyre
Ardsheal Hill pipe
✹ Appinite
◬ Kentallenitic appinite
✱ Leucocratic diorite
-o- Olivine-bearing lamprophyre
ϕ Olivine-free lamprophyre
Lagnaha pipe
● Appinite
Rudha Mòr pipes
⊠ Ultramafic type
● Appinite
⌖ Pyroxene-mica diorite
ø Feldspathic appinite & diorite
+ Granodiorite
✧ Lamprophyre
Kentallen pipe
◩ Phlogopite hornblendite
◪ Phlogopite pyroxenite
▼ Chilled margin of kentallenite
▲ Kentallenite
ᚐ Porphyritic diorite
☼ Lamprophyre
x Biotite-feldspar vein
North Cuil pipe
▽ Microkentallenite
∓ Leucocratic diorite
Above Duror Inn
⊙ Pyroxene-mica diorite
Inshaig pipe
✶ Felsite with chalcopyrite
Gleann Chàrnan pipe
✡ Appinite
Glen Creran:
Màm na Stainge pipe
◫ Corlanditic appinite
✢ Hornblende diorite
Clatch Fear Ardsheal pipe
✹ Appinite
Salachail pipe
✹ Appinite
Barnamuc pipe
△ Kentallenite
Garbh Allt pipe
✹ Appinite
Glen Ure pipe
✹ Appinite
± Leucocratic diorite

Figure 7.5 (a - g). Plots of Ni, Cr and Co *vs.* MgO, V *vs.* Co and Fe_2O_3, Rb *vs.* K_2O and Sr *vs.* Na_2O, respectively (key to rock symbols is on fold out sheet following Figure 7.4k).

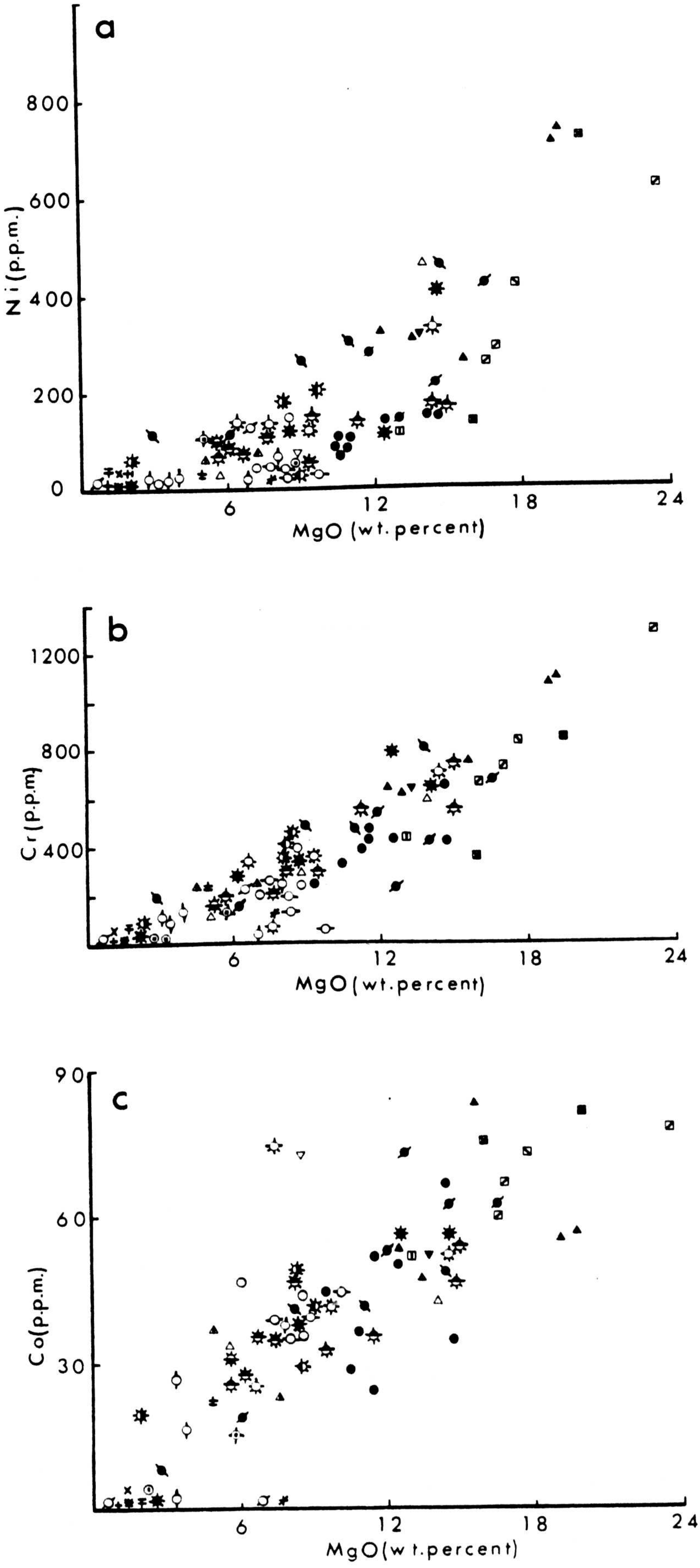
a
800
600
400
200
0
Ni (p.p.m.)
6
12
18
24
MgO (wt. percent)
b
1200
800
400
Cr (p.p.m)
6
12
18
24
MgO (wt.percent)
c
90
60
30
Co(p.p.m.)
6
12
18
24
MgO(wt.percent)

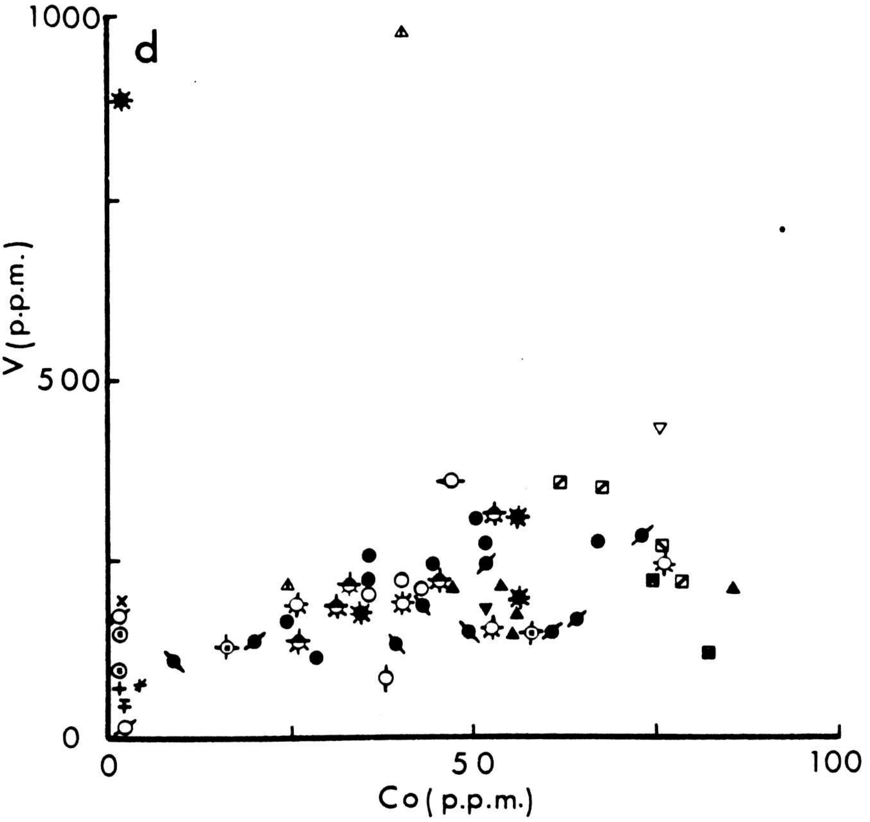
d
1000
500
0
V (p.p.m.)
0
50
100
Co (p.p.m.)

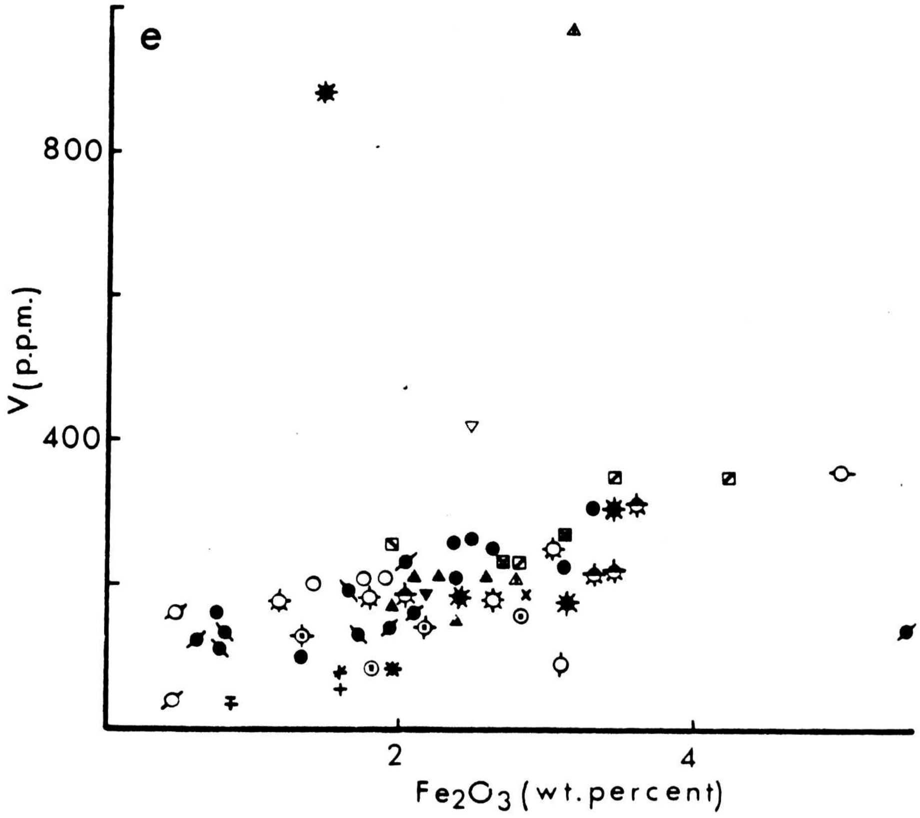
e
800
400
V (p.p.m.)
2
4
Fe2O3 (wt. percent)

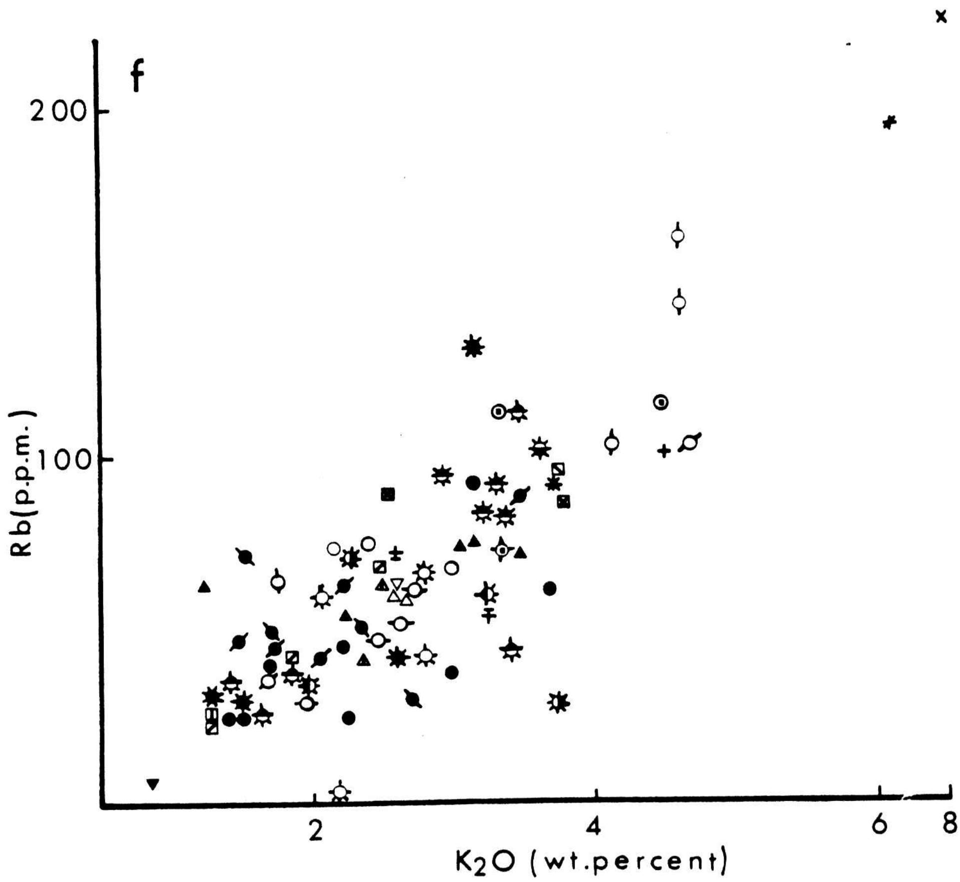
f
200
100
Rb(p.p.m.)
2
4
6
8
K2O (wt.percent)

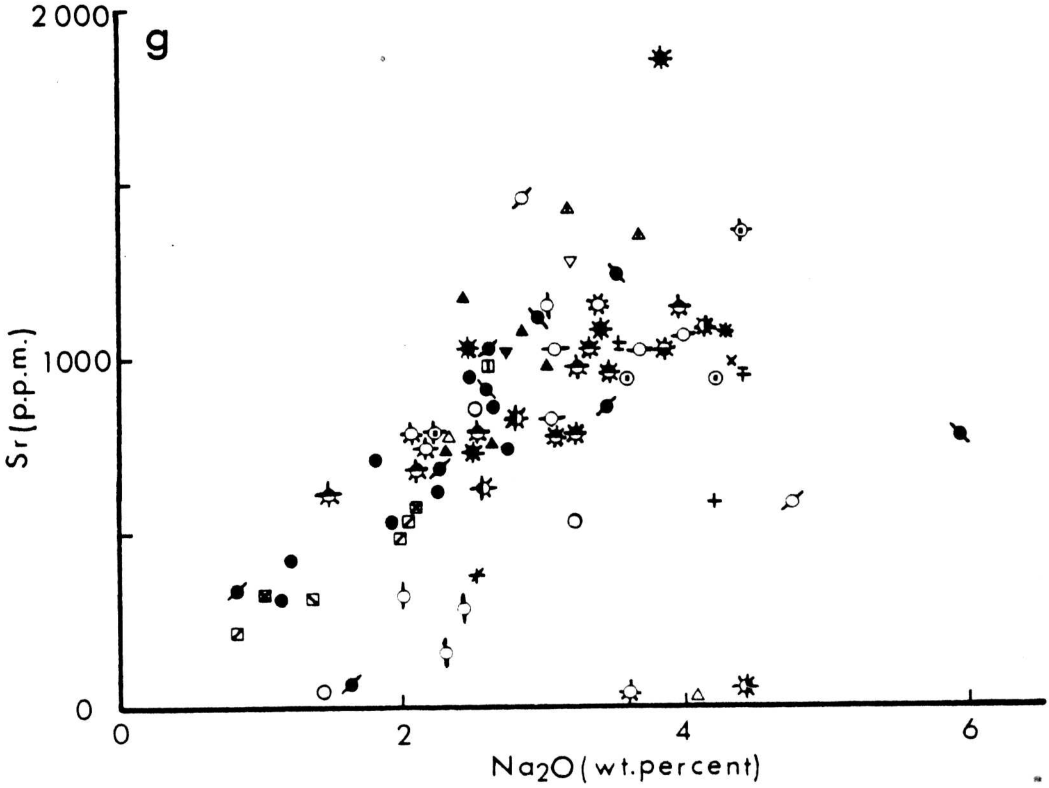
g
2000
1000
0
Sr(p.p.m.)
0
2
4
6
Na2O(wt.percent)

Figure 7.6. La, Ce and Y patterns of the representative mean compositions and of their average concentrations in the appinite suite.

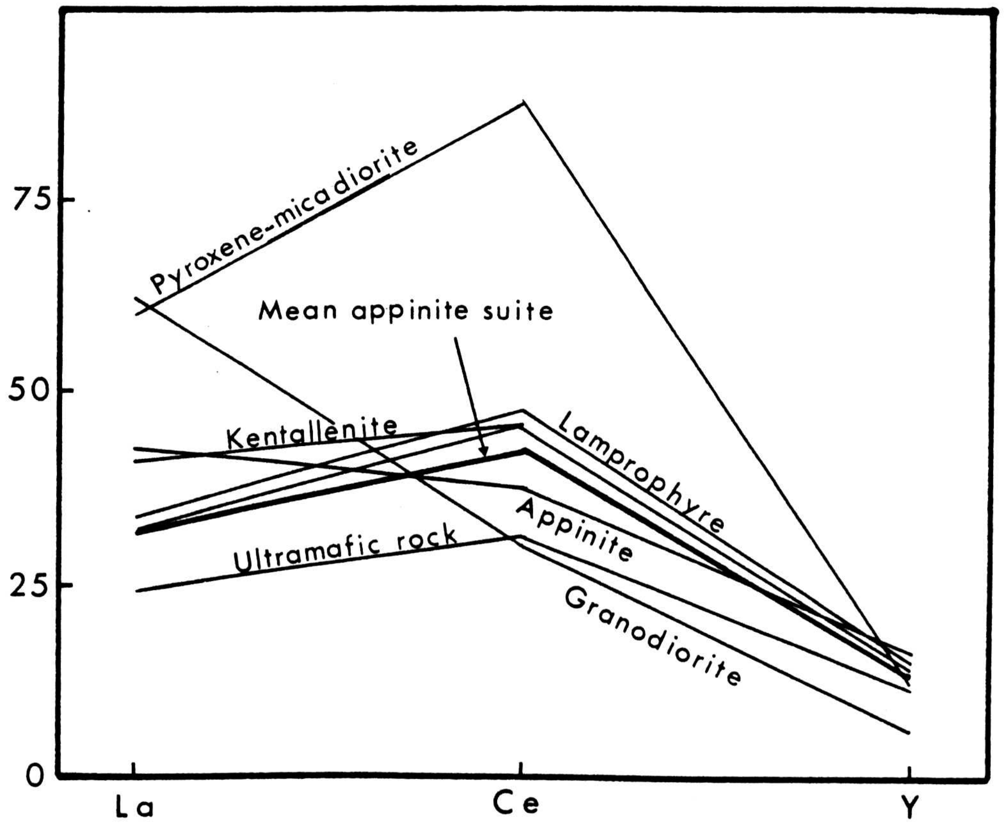
75
50
25
0
La
Ce
Y
Pyroxene-micadiorite
Mean appinite suite
Kentallenite
Lamprophyre
Appinite
Ultramafic rock
Granodiorite

Figure 7.7.

(a-b) Plots of Ni *vs.* SiO_2 and comparison with orogenic andesite suites (after Gill 1979).

(c) Plots of K/Rb *vs.* K_2O.

(d) Plots of Zr/Y *vs.* Zr and comparison with compositional fields of basalts in different geotectonic environments (after Pearce and Norry 1979).

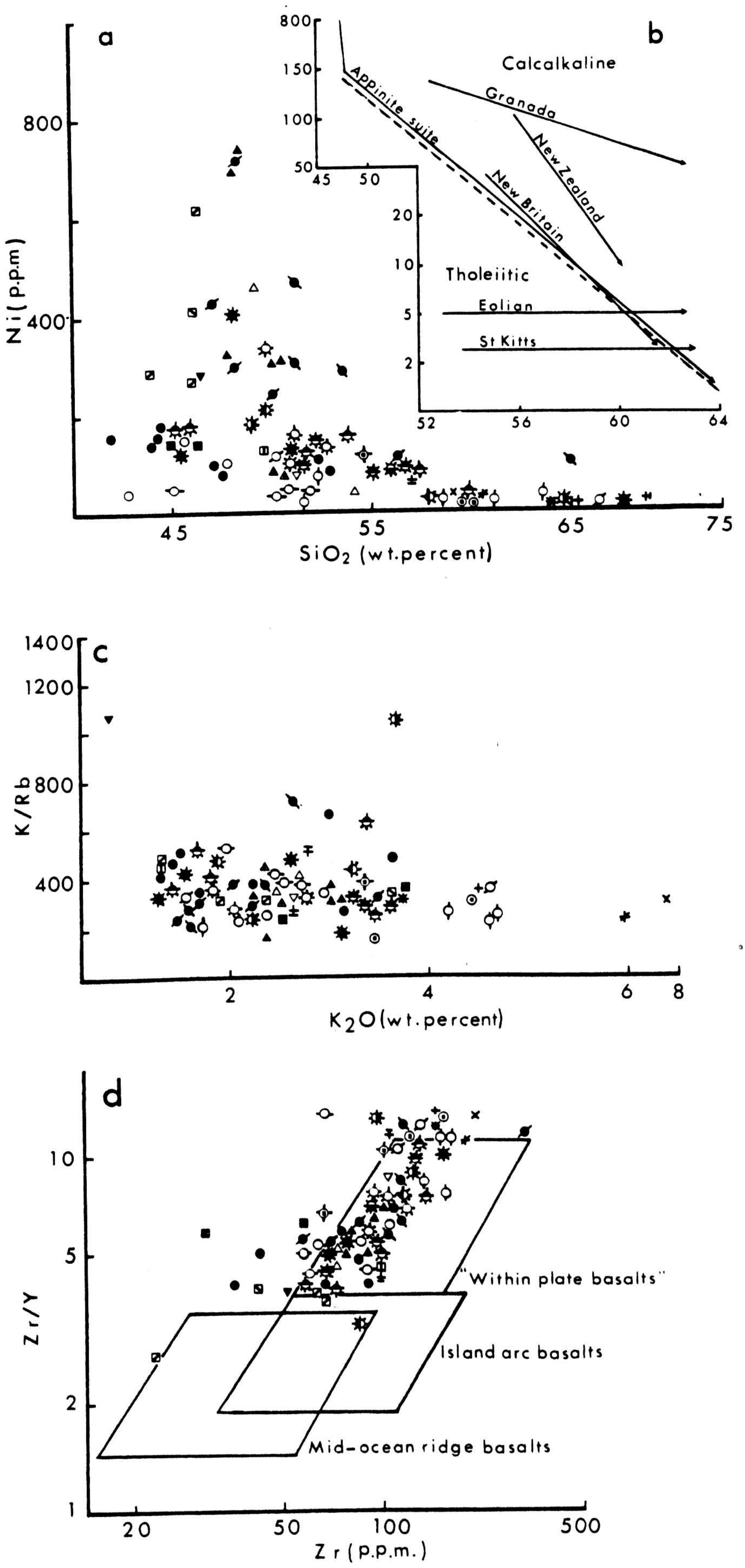
a
Ni (p.p.m)
800
400
45
55
65
75
SiO₂ (wt.percent)
b
800
150
100
50
45
50
Calcalkaline
Granada
Appinite suite
New Zealand
New Britain
20
10
5
2
Tholeiitic
Eolian
St Kitts
52
56
60
64
c
1400
1200
K/Rb
800
400
2
4
6
8
K₂O (wt.percent)
d
10
5
2
1
Zr/Y
"Within plate basalts"
Island arc basalts
Mid-ocean ridge basalts
20
50
100
500
Zr (p.p.m.)

Table 7.1. Major and trace element analyses and estimated modal compositions of rocks from pipes on Kentallen-Ardsheal peninsula, Ballachulish region.

	Small pipe, Back Settlement							Large pipe, Back Settlement			
	1	2	3	4	5	6	7	8	9	10	11
SiO_2	42.70	43.90	43.96	45.30	45.60	47.30	47.56	41.72	47.00	52.22	52.74
TiO_2	0.64	1.12	1.23	1.10	0.86	1.00	0.82	1.41	0.99	0.83	0.57
Al_2O_3	14.52	9.59	11.25	13.30	9.90	14.90	13.21	10.60	12.70	11.73	9.76
Fe_2O_3	1.76	2.45	3.31	2.40	1.41	3.10	1.88	2.33	2.60	0.73	1.28
FeO	8.00	7.80	8.29	8.70	7.29	7.30	6.46	7.33	5.80	5.66	4.12
MnO	0.16	0.14	0.16	0.15	0.13	0.13	0.14	0.09	0.12	0.12	0.11
MgO	6.91	14.51	12.22	11.40	8.61	9.60	8.39	14.77	10.80	11.13	10.54
CaO	6.49	9.54	10.12	8.30	10.73	7.70	8.52	8.95	11.00	8.74	12.78
Na_2O	3.42	1.19	1.88	2.30	1.41	2.70	2.69	1.20	2.60	1.75	2.43
K_2O	2.13	3.15	1.50	1.40	2.35	2.20	2.95	1.67	3.00	3.62	1.28
P_2O_5	0.36	0.08	0.33	0.55	0.14	0.63	0.24	0.19	0.20	0.14	0.14
H_2O	3.41	2.80	3.53	2.90	4.52	2.20	3.32	4.64	1.00	2.05	1.74
CO_2	9.51	4.08	2.69	2.70	7.61	1.40	4.18	5.46	2.70	1.07	2.55
Total	99.01	100.35	100.47	100.50	100.56	100.16	100.36	100.46	100.51	99.79	100.04
				Trace elements (p.p.m.)							
Cr	215	639	417	414	497	288	233	418	386	444	314
Co	40	67	50	51	43	44	35	35	38	24	28
Ni	46	153	150	170	150	81	90	153	100	109	84
Ba	400	970	390	250	780	620	830	880	730	1340	740
Ce	80	10	20	15	0	75	55	0	15	25	30
Cl	157	198	226	203	260	243	250	151	216	184	163
Cu	233	175	297	188	63	174	20	62	25	33	60
Ga	10	9	8	13	0	14	14	8	11	7	10
La	55	25	0	0	0	45	50	0	70	25	55
Li	27	21	4	15	41	12	8	10	2	8	8

Nb	7	36	14	7	0	8	6	4	6.	0	0
Pb	52	2	12	13	19	7	24	8	16	17	16
Rb	76	93	24	25	78	46	69	40	38	61	25
S	8013	1924	3414	2758	1036	4170	270	344	111	147	308
Sc	25	69	58	34	66	37	35	54	62	37	41
Sr	527	310	544	611	44	766	869	411	846	703	944
Th	5	7	6	4	2	6	6	2	8	4	5
V	222	264	304	269	200	232	208	221	252	166	118
Y	17	9	17	18	12	21	16	8	13	14	17
Zn	92	68	68	98	97	82	107	84	70	76	74
Zr	93	37	69	88	68	92	104	41	80	97	122

Modal analyses

Olivine	-	0	0	-	0	← 0 →		-	0	0	0
Clinopyroxene	-	20	0	-	0	← 15 →		-	25	50	50
Amphibole	-	35	50	-	60	← 30 →		-	45	5	10
Phlog.-biot.	-	20	3	-	20	← 3 →		-	5	0	0
Plagioclase	-	0	5	-	0	← 15 →		-	15	0	0
Anorthoclase	-	0	0	-	0	← 0 →		-	0	0	0
Orthoclase	-	5	10	-	5	← 4 →		-	4	30	25
Perthite	-	0	0	-	0	← 0 →		-	0	0	0
Quartz	-	8	15	-	10	← 10 →		-	3	0	0
Calcite (prim.)	-	7	10*	-	5	← 10* →		-	Tr	5	3
Opaque ores	-	0	1	-	Tr	← →		-	1	2	5
Apatite	-	0	1	-	0	← Tr →		-	0	0	0
Sphene (prim.)	-	0	0	-	0	← 3 →		-	1	5	5
Chlorite (sec.)	-	0	0	-	0	← 10 →		-	0	3	2
Epidote (sec.)	-	0	0	-	0	← 0 →		-	1	0	0
Serpentine (sec.)	-	0	0	-	0	← 0 →		-	0	0	0
Uralite (sec.)	-	0	0	-	0	← 0 →		-	0	0	0
Sericite (sec.)	-	5	0	-	0	← 0 →		-	0	0	0
Fine-grained mixt.	-	0	5	-	0	← 0 →		-	0	0	0
Total		100	100		100	← 100 →			100	100	100

Table 7.1. (Contd.)

	Ardsheal Hill pipe, coarse-grained facies						Ardsheal Hill pipe, lamprophyric marginal facies					
	12	13	14	15	16	17	18	19	20	21	22	23
SiO_2	45.19	48.15	49.90	50.43	50.82	57.40	44.80	50.13	50.46	51.41	51.62	52.23
TiO_2	1.52	0.70	0.78	0.76	0.77	0.47	1.40	0.72	0.68	0.71	1.58	0.80
Al_2O_3	12.82	12.96	15.86	15.77	14.10	18.18	14.60	14.32	13.05	14.57	15.97	15.24
Fe_2O_3	3.51	2.36	2.80	3.18	2.23	1.44	5.00	3.87	4.00	3.81	3.85	3.08
FeO	7.07	6.95	6.25	5.28	6.04	3.44	7.20	5.01	5.31	5.15	4.85	5.31
MnO	0.11	0.16	0.14	0.14	0.14	0.09	0.14	0.18	0.16	0.15	0.15	0.16
MgO	12.36	14.64	7.20	6.41	8.29	2.02	9.80	8.16	8.20	7.34	6.79	8.05
CaO	10.11	6.62	8.20	8.38	8.12	4.03	8.10	9.95	9.99	9.32	7.19	7.87
Na_2O	2.49	2.43	3.14	3.67	3.33	3.79	3.00	3.01	3.59	4.01	4.43	3.00
K_2O	1.50	1.25	2.50	2.28	2.58	3.10	1.90	2.53	2.43	2.67	1.62	1.70
P_2O_5	0.11	0.20	0.32	0.36	0.35	0.24	0.43	0.32	0.31	0.33	0.40	0.28
H_2O	1.95	4.00	2.86	2.24	3.14	2.50	1.90	1.36	0.64	0.00	1.33	1.50
CO_2	1.10	0.07	0.39	0.20	0.56	2.92	1.20	0.01	0.38	0.02	0.05	0.28
Total	99.84	100.49	100.34	99.10	100.47	99.63	99.47	99.57	99.20	99.49	99.83	99.49
					Trace elements (p.p.m.)							
Cr	796	657	220	208	367	10	50	192	199	226	-	257
Co	55	56	24	38	37	0	46	35	39	39	-	37
Ni	127	406	75	67	134	2	31	47	49	42	-	67
Ba	676	746	980	1300	890	1070	480	716	893	917	-	1260
Ce	0	30	50	45	40	135	60	56	54	48	-	40
Cl	159	211	239	226	167	133	166	-	-	-	-	307
Cu	37	61	82	81	110	50	103	57	62	81	-	104
Ga	13	10	14	150	16	17	18	20	8	15	-	12
La	30	30	20	70	95	80	40	14	15	12	-	10
Li	4	18	7	13	12	13	8	-	-	-	-	5
Nb	6	7	5	4	0	8	4	7	7	8	-	0

Pb	11	16	12	19	12	26	19	9	11	14	-	22
Rb	29	31	62	42	43	131	30	54	48	61	-	66
S	341	165	43	27	110	442	1062	-	-	-	-	55
Sc	72	23	39	262	27	4	60	-	-	-	-	31
Sr	744	1013	1403	1363	1075	1873	803	1030	1022	1066	-	1151
Th	3	3	5	5	5	12	4	4	2	6	-	8
V	306	196	204	970	181	894	360	-	-	-	-	86
Y	14	14	15	16	13	17	21	12	2	14	-	9
Zn	81	99	101	100	92	77	115	64	67	81	-	37
Zr	70	82	87	98	100	219	93	60	71	62	-	210

Modal analyses

Olivine	← 0	→	← 5	→	0	-	5	←	25	→	0	0
Clinopyroxene	← 5	→	← 30	→	10	-	25	←	10	→	30	30
Amphibole	← 30	→	← 10	→	10	-	10	←	10	→	10	15
Phlog.-biot.	← 10	→	← 0	→	5	-	0	←	0	→	5	5
Plagioclase	← 20	→	← 35	→	50	-	50	←	50	→	45	40
Anorthoclase	← 0	→	← 8	→	0	-	0	←	0	→	0	0
Orthoclase	← 0	→	← 0	→	10	-	0	←	Tr	→	Tr	Tr
Perthite	← 0	→	← 0	→	0	-	0	←	0	→	0	0
Quartz	← 0	→	← 0	→	4	-	0	←	0	→	8	0
Muscovite (prim.)	← 0	→	← 0	→	0	-	0	←	0	→	0	0
Calcite (prim.)	← 0	→	← 0	→	0	-	0	←	0	→	0	0
Opaque ore	← 3	→	← 7	→	0	-	10	←	5	→	2	10
Apatite (prim.)	← 0	→	← 0	→	0	-	0	←	0	→	0	0
Sphene (prim.)	← 0	→	← 0	→	0	-	0	←	0	→	0	0
Chlorite (sec.)	← 2	→	← 0	→	5	-	0	←	0	→	0	0
Epidote (sec.)	← 0	→	← 0	→	1	-	0	←	0	→	0	0
Serpentine (sec.)	← 0	→	← 5	→	0	-	0	←	0	→	0	0
Uralite (sec.)	← 0	→	← 0	→	0	-	0	←	0	→	0	0
Sericite (sec.)	← 0	→	← 0	→	0	-	0	←	0	→	0	0
Fine-grained mixt.	← 30	→	← 0	→	5	-	0	←	0	→	0	0
Total	100		100		100		100	←	100	→	100	100

Table 7.1. (Contd.)

	Ardsheal Hill pipe, lamprophyric marginal facies						Small pipe, Lagnaha			Rudha Mòr pipe		
	24	25	26	27	2	29	30	31	32	33	34	35
SiO_2	58.58	60.94	63.66	64.20	51.01	51.26	53.69	64.96	44.85	45.78	46.96	47.33
TiO_2	0.71	0.66	0.62	0.30	0.63	0.58	0.72	0.40	1.27	1.26	0.73	0.50
Al_2O_3	16.87	16.99	16.48	16.15	14.05	12.70	14.12	16.59	10.15	11.85	10.90	10.80
Fe_2O_3	2.33	1.94	2.06	1.95	1.61	0.73	1.70	0.73	2.02	3.12	1.92	2.12
FeO	4.60	3.95	3.60	1.23	5.52	6.72	6.96	2.47	6.52	6.39	6.98	6.88
MnO	0.17	0.11	0.09	0.03	0.10	0.11	0.12	0.03	0.11	0.10	0.10	0.14
MgO	3.85	3.53	3.28	1.28	11.06	14.19	9.04	2.90	15.99	12.40	16.27	19.30
CaO	1.45	1.21	0.96	2.90	6.92	6.18	5.66	1.51	8.60	9.10	7.00	7.07
Na_2O	2.37	1.98	2.37	4.27	3.07	2.59	3.52	6.00	1.05	2.02	1.62	2.15
K_2O	4.55	4.10	4.57	3.73	2.65	1.56	2.34	1.65	2.50	3.75	1.64	1.50
P_2O_5	0.08	0.08	0.08	0.17	0.29	0.22	0.25	0.26	0.08	0.14	0.13	0.25
H_2O	3.01	3.57	1.50	2.02	2.86	2.61	3.11	2.46	4.02	2.74	3.81	2.77
CO_2	0.60	0.87	0.12	2.22	0.43	0.10	0.30	0.61	2.34	1.26	2.53	0.10
Total	99.17	98.94	99.39	100.46	100.20	99.55	101.53	100.57	99.50	99.91	100.59	100.91
	Trace elements (p.p.m.)											
Cr	143	101	79	24	463	853	553	193	375	217	685	1093
Co	14	2	20	0	42	48	38	8	75	73	61	57
Ni	24	10	26	10	301	462	286	131	149	147	430	643
Ba	712	995	879	1140	1300	990	1160	390	1930	1570	780	560
Ce	83	65	74	65	40	35	35	10	45	0	10	5
Cl	-	-	-	118	285	219	253	203	230	352	238	489
Cu	23	83	146	46	93	86	173	150	305	50	96	106
Ga	30	26	26	13	9	8	11	16	5	12	6	7
La	45	37	35	80	0	30	65	50	20	0	50	30
Li	-	-	-	9	12	6	7	13	3	10	12	6
Nb	20	18	16	10	5	5	6	8	0	6	6	4

Pb	16	10	12	26	14	30	18	7	10	9	18	18
Rb	164	127	144	93	30	74	50	45	91	89	42	4
S	-	-	-	4524	349	488	37	930	243	2475	840	122
Sc	-	-	-	2	25	22	18	23	49	57	29	21
Sr	275	207	139	1051	1321	886	1243	706	334	595	70	767
Th	10	17	-	8	6	4	7	7	3	2	7	2
V	-	-	-	86	196	148	135	103	234	277	148	149
Y	28	21	22	9	15	14	16	5	5	9	13	10
Zn	55	80	71	37	81	77	86	18	60	77	85	90
Zr	224	187	232	210	102	112	115	134	30	59	78	70

Modal analyses

Olivine	-	0	0	0	0	Tr	0	0	← 5	→	10	0
Clinopyroxene	-	0	20	0	25	10	20	0	← 30	→	10	30
Amphibole	-	20	25	0	10	5	40	10	← 10	→	30	10
Phlog.-biot.	-	10	0	3	15	20	5	2	← 30	→	20	30
Plagioclase	-	40	50	40	30	20	25	65	← 15	→	20	20
Anorthoclase	-	0	0	0	0	0	0	0	← 0	→	0	0
Orthoclase	-	10	0	20	0	0	5	5	← 0	→	0	0
Perthite	-	0	0	0	0	0	0	1	← 0	→	0	0
Quartz	-	20	0	25	0	0	0	5	← 0	→	4	0
Muscovite (prim.)	-	0	0	10	0	0	0	0	← 0	→	0	0
Calcite (prim.)	-	0	0	1	0	0	0	0	← 1	→	0	0
Opaque ore	-	0	5	1	1	2	1	1	← Tr	→	Tr	0
Apatite (prim.)	-	0	0	0	1	0	Tr	Tr	← Tr	→	0	0
Sphene (prim.)	-	0	0	0	0	0	1	1	← Tr	→	Tr	0
Chlorite (sec.)	-	0	0	0	5	3	1	10	← 0	→	0	0
Epidote (sec.)	-	Tr	0	0	1	0	Tr	0	← 0	→	1	0
Serpentine (sec.)	-	0	0	0	1	5	0	0	← 1	→	5	0
Uralite (sec.)	-	0	0	0	1	30	Tr	0	← 2	→	0	0
Sericite (sec.)	-	0	0	0	10	5	2	0	← 0	→	0	0
Fine-grained mixt.	-	0	0	0	0	0	0	0	← 5	→	0	10
Total		100	100	100	100	100	100	100	100		100	100

Table 7.1. (Contd.)

	Rudha Mòr pipe										
	36	37	38	39	40	41	42	43	44	45	46
SiO_2	47.93	48.18	48.90	49.87	50.36	51.05	52.47	54.45	56.10	64.43	66.21
TiO_2	0.59	0.76	0.58	0.74	0.61	0.74	1.76	0.55	0.54	0.24	0.15
Al_2O_3	8.12	13.55	11.95	11.76	16.21	14.77	11.40	16.07	15.28	16.52	16.05
Fe_2O_3	5.38	2.65	1.73	2.03	0.45	1.14	3.06	1.27	0.63	1.53	0.47
FeO	4.63	6.09	6.47	6.72	5.21	5.40	5.27	4.53	4.96	1.50	1.56
MnO	0.12	0.11	0.11	0.12	0.14	0.10	0.08	0.06	0.09	0.03	0.00
MgO	20.19	11.86	14.15	14.60	6.79	6.28	7.45	5.94	6.01	1.25	0.84
CaO	4.87	7.22	5.15	6.21	6.00	6.18	8.09	5.86	3.81	2.21	2.08
Na_2O	0.80	2.53	2.12	2.24	2.79	3.52	2.05	4.34	3.40	4.14	4.72
K_2O	1.45	2.18	2.01	2.01	1.64	2.18	1.80	3.35	3.45	4.50	4.60
P_2O_5	0.12	0.44	0.17	0.17	0.27	0.32	0.18	0.32	0.23	0.10	0.09
H_2O+	5.43	3.23	4.48	3.20	3.68	5.36	3.54	2.60	2.76	2.44	1.86
CO_2	0.60	1.67	1.88	0.39	5.53	3.21	4.05	0.63	2.96	1.26	1.69
Total	100.23	100.47	99,70	100.06	99.68	100.25	100.20	99.98	100.22	100.15	100.32
	Trace elements (p.p.m.)										
Cr	841	502	644	409	246	318	42	146	164	13	12
Co	82	52	52	63	0	25	76	15	18	0	0
Ni	723	299	337	239	127	141	122	114	114	10	7
Ba	430	880	660	2000	880	1000	470	1100	930	1810	1080
Ce	0	45	0	35	55	0	45	40	95	15	5
Cl	256	399	159	190	207	64	211	313	308	130	191
Cu	53	99	110	88	23	120	404	92	67	31	93
Ga	3	11	8	7	10	0	13	15	12	14	14
La	55	15	0	15	30	20	30	20	30	80	55
Li	8	15	14	9	9	7	15	9	8	6	4
Nb	4	4	10	9	9	7	0	6	6	6	7

Pb	13	18	16	19	30	22	15	14	18	20	22
Rb	47	61	60	43	39	0	41	72	87	100	105
S	566	479	4087	2071	1388	521	4548	377	401	194	161
Sc	24	21	27	34	18	21	55	19	15	1	2
Sr	339	1032	731	671	1452	0	799	1368	845	599	593
Th	3	8	7	5	10	6	8	4	12	7	14
V	133	240	158	160	166	174	244	132	132	60	47
Y	11	13	12	14	16	20	13	10	15	5	7
Zn	113	96	91	86	106	84	51	74	75	48	11
Zr	63	79	94	89	140	140	102	129	380	205	181

Modal analyses

Olivine	5	5	-	0	0	← 0	→	0	-	-	0
Clinopyroxene	20	35	-	30	0	← 33	→	10	-	-	0
Amphibole	30	5	-	35	0	← 2	→	10	-	-	15
Phlog.-biot.	30	20	-	5	15	← 0	→	5	-	-	0
Plagioclase	15	10	-	25	60	← 30	→	45	-	-	70
Anorthoclase	0	0	-	0	0	← 1	→	0	-	-	0
Orthoclase	0	0	-	0	1	← 1	→	0	-	-	5
Perthite	0	0	-	0	0	← 0	→	0	-	-	5
Quartz	0	5	-	4	4	← 10	→	5	-	-	0
Calcite (prim.)	0	3	-	0	8*	← 10*	→	3	-	-	0
Opaque ore	0	1	-	0	2	← 3	→	1	-	-	1
Apatite (prim.)	0	1	-	1	0	← Tr	→	1	-	-	0
Sphene (prim.)	0	Tr	-	Tr	0	← Tr	→	1	-	-	0
Chlorite (sec.)	0	0	-	0	10	← 0	→	15	-	-	4
Epidote (sec.)	0	0	-	0	0	← 0	→	1	-	-	0
Serpentine (sec.)	0	0	-	0	0	← 0	→	3	-	-	0
Uralite (sec.)	0	0	-	0	0	← 0	→	0	-	-	0
Sericite (sec.)	0	0	-	0	0	← 0	→	0	-	-	0
Fine-grained mixt.	0	15	-	0	0	← 10	→	0	-	-	0
Total	100	100		100	100	100		100			100

Table 7.1. (Contd.)

Kentallen pipe

	47	48	49	50	51	52	53	54	55	56	57	58	59
SiO_2	44.13	46.08	46.16	46.34	46.38	47.72	48.33	48.81	50.08	50.32	50.69	58.72	68.29
TiO_2	1.38	1.08	0.94	1.17	0.15	0.74	0.63	0.67	0.72	0.79	0.70	0.74	0.32
Al_2O_3	11.66	9.52	6.12	10.94	11.34	13.98	10.80	11.49	13.45	12.85	14.15	18.09	14.83
Fe_2O_3	4.27	1.92	2.72	3.42	2.60	2.39	2.27	1.93	2.08	2.24	2.35	2.82	1.13
FeO	7.03	6.53	6.95	6.95	7.85	6.00	5.96	6.45	6.12	6.12	5.96	1.47	0.39
MnO	0.16	0.12	0.13	0.10	0.15	0.13	0.12	0.13	0.10	0.09	0.08	0.05	0.00
MgO	16.97	17.73	23.50	16.30	15.47	12.15	19.05	19.54	13.14	13.30	9.21	1.41	1.81
CaO	8.68	8.62	6.90	9.18	11.91	7.88	5.69	5.35	6.66	6.60	8.90	3.30	1.59
Na_2O	1.99	1.36	0.77	1.99	2.23	3.00	2.30	2.37	2.81	2.68	3.33	4.27	4.20
K_2O	1.30	3.73	2.40	1.84	0.80	3.40	2.22	1.25	3.08	3.10	2.75	7.42	4.41
P_2O_5	0.03	0.10	0.05	0.04	0.29	0.34	0.18	0.23	0.23	0.27	0.34	0.36	0.09
H_2O+	1.99	2.36	2.65	1.23	1.25	1.82	2.68	1.23	1.43	1.87	1.34	0.92	1.59
CO_2	0.32	0.67	0.37	0.22	0.26	0.48	0.20	0.15	0.38	0.16	0.21	0.16	0.12
Total	99.91	99.82	99.66	99.72	100.68	100.05	100.43	99.60	100.28	99.59	100.01	99.73	98.77
Trace elements (p.p.m.)													
Cr	715	801	1254	676	736	609	1061	1086	615	616	330	45	-
Co	67	74	78	61	85	54	55	57	46	51	42	2	-
Ni	299	415	632	286	286	319	700	736	318	323	116	34	-
Ba	470	1580	1230	780	550	780	630	550	1000	780	1030	1420	-
Ce	30	35	0	60	40	70	40	0	65	25	60	75	-
Cl	492	387	356	528	178	488	538	430	625	498	398	654	-
Cu	39	48	26	46	44	107	79	67	94	91	35	123	-
Ga	9	6	3	8	9	9	7	4	9	8	13	15	-
La	15	5	30	45	25	65	0	0	50	60	30	45	-
Li	6	17	9	10	3	5	5	6	9	6	8	5	-
Nb	15	0	12	0	0	7	4	5	10	5	0	11	-

Pb	11	6	12	1	9	19	18	18	30	17	26	41	-
Rb	22	94	68	42	6	74	55	64	77	78	66	215	-
S	924	354	311	837	76	134	142	48	181	92	148	182	-
Sc	58	53	32	60	45	33	17	17	29	33	37	8	-
Sr	514	309	217	494	1237	984	727	762	1082	1006	1145	881	-
Th	2	5	2	1	2	4	2	6	7	2	5	13	-
V	351	251	214	352	204	205	157	170	202	182	180	202	-
Y	19	10	9	18	13	14	12	13	14	15	14	9	-
Zn	55	70	74	54	84	17	83	75	78	77	81	37	-
Zr	71	40	24	70	51	81	75	83	107	101	83	296	-

Modal analyses

Olivine	5	0	← 0	→	15	15	-	30	35	5	0	-	-
Clinopyroxene	50	66	← 10	→	55	35	-	25	10	25	35	-	-
Amphibole	15	10	← 66	→	0	0	-	0	0	0	10	-	-
Phlog.-biot.	20	20	← 10	→	5	10	-	7	20	15	20	-	-
Plagioclase	4	4	← 3	→	20	35	-	0	30	25	30	-	-
Anorthoclase	0	0	← 5	→	0	0	-	33	0	25	0	-	-
Orthoclase	0	0	← 0	→	0	0	-	0	0	0	0	-	-
Perthite	0	0	← 0	→	0	0	-	0	0	0	0	-	-
Quartz	0	0	← 0	→	0	0	-	0	0	0	0	-	-
Calcite (prim.)	0	0	← 0	→	0	0	-	0	0	0	0	-	-
Opaque ore	5	0	← 1	→	5	2	-	3	5	5	5	-	-
Apatite (prim.)	0	0	← 2	→	0	1	-	2	0	Tr	0	-	-
Sphene (prim.)	0	0	← 0	→	0	0	-	0	0	0	0	-	-
Chlorite (sec.)	0	0	← 0	→	0	0	-	0	0	0	0	-	-
Epidote (sec.)	0	0	← 0	→	0	0	-	0	0	0	0	-	-
Serpentine (sec.)	0	0	← 0	→	0	0	-	0	0	0	0	-	-
Uralite (sec.)	0	0	← 3	→	0	0	-	0	0	0	0	-	-
Sericite (sec.)	1	0	← 0	→	0	0	-	0	0	0	0	-	-
Fine-grained mixt.	0	0	← 0	→	0	2	-	0	0	0	0	-	-
Total	100	100	← 100	→	100	100		100	100	100	100	-	-

Table 7.1. (Contd.)

Back Settlement pipe

1-4	Appinite.
5-7	Vogesitic lamprophyre.
8-11	Appinite.

Ardsheal Hill pipe

12-13	Banded appinite.
14-15	Kentallenitic appinite.
16-17	Feldspathic appinite.
18-21	Olivine-bearing spessartite.
22-24	Olivine-free spessartite.
25	Andesitic lamprophyre.
26	Felsite.
27	Fine-grained leucocratic diorite.

Lagnaha pipe

28-30	Appinite.
31	Feldspathic appinite.

Rudha Mòr pipe

32-33	Biotite - clinopyroxene - hornblende - feldspar rock (marginal ultramafic facies).
34-37	Biotite appinite.
38	Lamprophyre (dyke).
39	Appinite.
40	Feldspathic diorite (dyke).
41	Pyroxene - mica diorite.
42	Lamprophyre (dyke).
43	Pyroxene - mica diorite.
44	Appinite (marginal facies).
45	Feldspathic appinite.
46	Granodiorite.

Kentallen pipe

47-48	Biotite pyroxenite (marginal facies).
49-50	Biotite hornblendite (marginal facies).
51	Minor kentallenite (chilled margin).
52-56	Kentallenite.
57	Lamprophyre.
58	Biotite feldspar vein.
59	Porphyritic diorite (dyke).

* Values including secondary calcite.

CHAPTER 8 PETROGENESIS

On the basis of information about field relationships, petrography and mineral and rock chemistry, presented in Chapters 2-7, it is possible to evaluate an overall petrogenetic model for the appinite suite and to assess the genesis of the rock type called appinite together with that of the associated rocks of the appinite suite.

The generalised sequence of events deduced from the field relationship of breccia and various igneous rocks in some of the composite pipes of the Kentallen - Ardsheal peninsula district is:

1. Uprise of gas-rich basaltic magma.
2. Magma uprise impeded by structural traps.
3. Explosive activity.
4. Emplacement of variable but generally mafic-rich types.
5. Emplacement of kentallenite or pyroxene-mica diorite.
6. Emplacement of leucocratic and/or granodiorite.

The regular patterns of the major and trace element plots, the successive fractionation of olivine, clinopyroxene, amphibole, mica and plagioclase shown by CMAS plots and the coincidence or parallelism of the trends for different pipes indicate both the cognate nature of the suite and the dominant control of fractional crystallisation (Sections 7.1, 7.2, 7.3). The considerable petrographic variation seen can be accounted for on the basis of crystallisation differentiation from an original magma of a high-potassium calc-alkaline characters, under variable P_{Gas} (Sections 2.2; also see Chapter 7). With estimates of the crystallisation temperature for olivine in the kentallenite of the Kentallen pipe and for that in the lamprophyric marginal facies of the Ardsheal Hill pipe being c. 1800°C (Section 3.3) and the evidence of Kushiro (1965, fig. 2.3) and Wyllie (1971, fig. 8.14) that forsterite can be the first solely liquidus phase at 25 kb pressure and > 1600°C in basaltic magma produced by the melting of a peridotitic mantle, it can be deduced that olivine appeared on the liquidus at c. 70-80 km depth. However, the pressure estimates for crystallisation of much of the appinite suite, the occurrence of explosion-breccias and the type of deformation shown by the host rocks, all indicate emplacement at high crustal levels. The presence of olivine in some masses but not in other is accounted for the complete resorption of olivine in some instances. This interpretation is based on the evidence of olivine-liquid reaction relationships, shown by most of the olivine-bearing rocks (Section 2.2).

8.1 Crystallisation history in relation to emplacement and explosive activity

8.1A Kentallen pipe

The occurrence, in the marginal ultramafic rocks, of olivine in the cores of the clinopyroxene phenocrysts without a rim of orthopyroxene, like that seen in the kentallenite of the main intrusive mass, indicates a drop in the magma temperature to $< 1500^{\circ}$C (see Deer et al. 1966, p.5); this is related to emplacement into high level and relatively cool country rocks. The order of appearance of various phases is olivine, clinopyroxene, pargasite and phlogopite (Section 7.2). The pargasitic amphibole crystallised in a temperature range of 950° - 770°C and a P_{H_2O} of 2-4 kb (cf. Sections 5.2, 5.3), so the clinopyroxene must have appeared on the liquidus above 960°C and probably in a range of c. 1125° - 1050°C, under a P_{H_2O} of <1 kb (see Yoder & Tilley 1962, fig. 29). Its crystallisation led to the release of gas phase (Yoder 1965, p.88-9). Restriction of gas uprise led to clinopyroxene crystallisation under increasing P_{H_2O} and subsequently to its replacement by amphibole. In the pyroxenite, phlogopite developed before the appearance of amphibole, probably in a temperature range of c. 1050° - 950°C and under a P_{H_2O} of 1-2 kb. However, in the hornblendite, phlogopite developed at the latter stages of pargasite crystallisation as it did in the appinite of the Back Settlement pipe where a temperature range of 825° - 770°C and a P_{H_2O} of 2-4 kb have been determined (cf. Sections 5.1A, 5.2, 5.3, 6.2).

The pressure-temperature estimates for the marginal ultramafic rocks of the Kentallen pipe indicate crystallisation in a temperature range of 1125° - 770°C and in a P_{H_2O} range of $<$1-4 kb, with pyroxenites representing higher temperature and lower P_{H_2O} crystallisation than hornblendites. Increasing P_{H_2O} associated with crystallisation led to major explosive activity. P-T estimates for crystallisation suggest that this occurred at a P_{H_2O} of 4 kb and at a temperature of 770°C (Fig. 8.1a). The explosion-breccia seen in some marginal parts of the pipe (Bowes & Wright 1967, fig. 14) was developed at this stage.

All the pyroxenites and hornblendites show olivine, clinopyroxene, amphibole and phlogopite enrichment with respect to the mean kentallenite composition, which is considered as representing the original "primary" magma on the basis of CMAS plots. These rocks are interpreted as representing cumulates (Section 7.2) with the accumulation of mafic phases having occurred in a temperature range of 1125° - 770°C and under a P_{H_2O} of $<$1-4 kb (cf. Fig. 8.1a). However, the presence of the kink-banded mica in these rocks points to emplacement into their present position as a crystal mush. This emplacement is related to the major explosive activity and was presumably rapid. Any cumulate texture that may have developed before the major explosive activity would have been destroyed during emplacement. The banding seen in the margin ultramafic rocks of northwestern part of the pipe (Bowes & Wright 1967, fig. 14) is interpreted as a "crystal mush" flow phenomenon. The generally vertical or subvertical disposition of this banding, parallel to the contact with country rocks is consistent with such an interpretation.

Rocks with a composition consistent with having been a residual liquid associated with the accumulation of mafic phases are rare in the marginal parts of the pipe. However, the marginal kentallenitic appinite (called kentallenite by Bowes 1962) contains a much higher proportion of feldspar than the mafic phases and shows olivine-clinopyroxene-amphibole-mica reaction relationships. In addition, it is the host for partly digested inclusions and angular blocks of quartzite up to 1 m across (see Bowes & Wright 1967, fig. 14, p.133) that must have been brought upwards at least several hundreds of metres. These features indicate that the marginal kentallenitic appinite represents, at least in parts, a residual liquid for the marginal ultramafic rocks whose uprise must have been rapid and even violent. In addition, it would appear to represent a mixture of crystal mush representing explosively disrupted cumulates together with the products of crystallisation of residual magma. The smaller size of the mica flakes in this rock compared with those in most of the rocks at Kentallen (Bowes 1962, p.120) is related to their crystallisation from the residual liquid after the major explosive activity under decreased P_{H_2O} (< 1 kb) (cf. Fig. 8·1a) rather than crystallisation as a cumulate phase. Feldspar crystallisation followed.

The existence of rocks which in part seem to be representative of the liquid composition and the absence of extreme feldspathic differentiates in the marginal parts of the pipe, points to most of the residual liquid having been explosively "splattered" upwards through the crystal mush in varying proportions.

The existence of a chilled margin to the kentallenite mass which makes up the central and the major part of the pipe and the presence of olivine in it, indicate emplacement of magma from depth following the emplacement of the marginal types. The reaction rim of orthopyroxene surrounding olivine indicates a temperature of 1550° - 1500°C and a P_{H_2O} of < 2.3 kb (possibly <1 kb) for this stage of crystallisation (Fig. 8.1b; Section 3.4; also see Deer <u>et al</u>. 1966, p.5). This indicates the emplacement of high temperature magma high up into the crust with the retention of a temperature sufficiently elevated for orthopyroxene crystallisation and the medium to coarse grain size of the chilled facies, related to emplacement into hot rocks. With decreasing temperature the reaction between olivine and liquid stopped and clinopyroxene appeared on the liquidus at a temperature of 1125°C (cf. Fig. 8.1a). Crystallisation of clinopyroxene again led to the release of a gas phase and phlogopite phenocrysts developed under a P_{H_2O} of 1 kb at a temperature of 1000°C (Section 6.2).

With the CMAS plots indicating that the kentallenite body includes olivine-clinopyroxene-phlogopite rocks which have the composition of cumulates, the temperature range of c. 1500° - 1000°C, possibly 1125° - 1000°C under a P_{H_2O} of $\leqslant$1 kb must correspond to the period of crystal accumulation. The medium-grained groundmass which is present in varying proportions represents the composition of the residual liquid (cf. Section 2.2A). However, its crystallisation (at a temperature of $<$ 1000°C — Fig. 8.1b) was at a lower P_{H_2O} than that existing at the time of the development of the large phlogopite flakes. Explosive activity associated with this pressure decrease following the development of cumulates would account for many of the features of the fabric of kentallenite mass. For example, it explains the varying nature and disposition of banding. Near the southwestern contact this has the appearance of igneous cumulate layering in rocks representing cumulate composition, yet the banding dips variably at 10° and 40°, towards the contact: breaking of cumulates into very large blocks during explosive activity and independent movement of these disrupted blocks during subsequent uprise of crystal mush or residual liquid would account for this. The steeply dipping banding (70 SW — Bowes & Wright 1967, fig. 14) 100 - 200 m to the NE is also in rocks representing cumulate compositions but in which the mica flakes are kink banded:

upward flow of a mush of what was a semi-consolidated cumulate following explosive activity would account for these features. In the southeastern corner of the mass banded rocks representing liquid composition and without kink banded biotite dip at 45° away from the contact with the marginal facies which also dips in the same direction while 100 m northwards the marginal facies has vertical banding that parallels its outer and inner contacts: viscous flow of residual liquid carrying varying proportions of crystals of partly consolidated, then explosively disrupted cumulate would account for features in the coarse-grained kentallenite. Magmatic flow related to the rapid uprise of the primary magma would account for features in the marginal facies. Thus the main central part of the kentallenite body consists variously of (1) the products of crystallisation differentiation with associated crystal accumulation, (2) explosive disruption of these products into large masses, groups of crystals or individual crystals, a process possibly largely controlled by the relative proportions of cumulate crystals and interprecipitate liquid in the particular part of the intrusion, (3) movement of blocks, crystals and residual liquid present in varying proportions in different parts and (4) crystallisation of residual liquid.

Despite the main mass of kentallenite representing such a hetrogeneous assemblage, the mean composition of its various parts appears to approximate to that of the original "primary" magma (Section 3.4). It might have been expected that the composition of the chilled margin would more closely correspond to that of the "primary magma". However, the olivine composition indicates that the composition of the chilled margin near the northeastern corner of the pipe is incompatible with that required for the "primary" magma, while the CMAS plots indicate a higher degree of clinopyroxene enrichment there than in any other part of the main body of the kentallenite (Section 7.2). In addition, some olivine enrichment may also have occurred with clinopyroxene.

Following the emplacement of kentallenite, the successive emplacement of biotite-feldspar veins and lamprophyric dykes probably represents development from a residual liquid that was entrapped at relatively deeper levels during the second explosive activity. In addition, those biotite-feldspar veins which are rich in K_2O and P_2O_5 (Section 7.1) could contain a component of hybrid secondary liquid produced by the interaction of the residual liquid with quartzite, particularly where the liquid had penetrated along cracks and fissures in shattered or brecciated rocks (see Bowes & Wright 1967, p.139).

8.1B Back Settlement pipes

The occurrence of appinite with lamprophyric chilled margins in the main pipe and the evidence of an appinite-lamprophyre gradation in the small pipe (Section 2.2A; Bowes & Wright 1961) indicate the high level emplacement of liquids. The correspondence in composition of clinopyroxene in the cores of the large idiomorphic pargasite crystals and that occurring in the groundmass in some appinites from the main pipe is interpreted as indicating only one stage of clinopyroxene crystallisation and one that preceded the development of the idiomorphic hornblende crystals (Section 4.2). As the composition of the clinopyroxene of both habits corresponds to that in the kentallenite of the Kentallen pipe, corresponding P-T conditions (P_{H_2O} = c. <1 - 1.5, T^oC = c. 1125° - 1000°C) must have been operative (Figs 8.1b, 8.2a). The determined temperature (900° - 770°C) and P_{H_2O} (2 - 4 kb) conditions of the subsequently crystallised pargasite crystals (Sections 2.2A, 5.2, 5.3) not only indicates a temperature decrease but that the crystallisation of clinopyroxene was associated with a build up of gas pressure: this is related to restriction of upward gas movement by a structural trap.

Between clinopyroxene and pargasite crystallisation, i.e. in a temperature range of c. 1000° - 900°C and a P_{H_2O} of c. 1.5 - 2 kb, corrosion of clinopyroxene took place while the outer green rim of the pargasite and the co-evally crystallised micas developed in a temperature range of c. 825° - 770°C under a P_{H_2O} of 3-4 kb (Fig. 8.2d, Sections 5.1A, 5.6, 6.2). The successive development of the rhythmic overgrowths of magnesio-hornblende and actinolite composition was dominantly on idiomorphic pargasite crystals but in a few instances on corroded clinopyroxene. The temperature range of 800° - 750°C and a P_{H_2O} of 4-5 kb indicate a further decrease in temperature and increase in P_{H_2O}, the latter indicating the continued existence of a trap impeding the uprise of gas. The rhythms in overgrowths are interpreted as due to variation in oxygen fugacity (Fig. 8.2a; Sections 5.1A, 5.2, 5.3) associated with limited breaching of the trap followed by partial sealing up.

The occurrence of a groundmass composed dominantly of feldspars indicate a drop in P_{H_2O} from c. 5 kb probably to $<$1 kb, a drop that is related to the development of explosion-breccia and the development of a pipe-shaped diatreme which was the locus of explosive emplacement of igneous material (Bowes & Wright 1961; Bowes et al. 1964). This igneous material consisted of the residual liquid which crystallised at a temperature of $<$ 750°C together with the previously formed crystals. Many of the clinopyroxene grains in the groundmass have a fractured appearance and thus may represent the explosively disrupted products of (?cumulate) crystals.

The small pipe is interpreted as an off-shoot of the main pipe and seems likely to represent the locus of explosive release of gas (Bowes & Wright 1961, p.304). However, the evidence from the CMAS plots (Section 7.2) that some parts of it represent cumulates while other parts represent liquid compositions points to the emplacement of masses of already formed crystals as well as of residual liquid. The kink-banded nature of biotite flakes in the biotite-rich appinite point to movement of crystal mushes. The presence of lamprophyric rocks is indicative of the uprise of the residual liquid and the "gradation" between lamprophyre and appinite figured by Bowes and McArthur (1976) could represent a boundary between the residual magma and cumulates carried upwards during the explosive release of gas. What is clear is that only crystallisation of mafic phases had occurred before explosive activity.

The magmatic history established for the small pipe is also applicable to the main pipe. Some parts of it are dominantly composed of disrupted cumulates emplaced as mushes while in other parts early formed minerals are associated with the products of crystallisation of the residual liquid now seen as a lamprophyric matrix. There are all variants from rocks dominantly composed of cumulate amphibole to rocks dominantly composed of lamprophyric matrix.

The high proportion of biotite in the leucocratic lamprophyre and the biotite-rich appinite from the small pipe is interpreted by Bowes and Wright (1961) as due to potassium-enrichment during emplacement. In the case of the former type this interpretation is consistent with potassium enrichment into residual liquid during fractionation (Section 7.1). However, in the case of the latter type which represents a cumulate on the basis of CMAS plots and also shows higher K_2O contents as compared to biotite-poor appinite (Sections 7.1, 7.2), the high proportion of biotite can be related to disruption and upwards movement of that part of "cumulate" which was developed as a result of the coeval crystallisation and accumulation of biotite and amphibole, i.e. in a temperature range of <u>c</u>. 825° - 770°C under a P_{H_2O} of 3-4 kb (c.f. Fig. 8.2a).

The highly altered and carbonated nature of some of the appinite and some of the lamprophyres from the small pipe indicates that gas-streaming (hydration and carbonation) also continued after igneous emplacement of various rock types. The relatively high proportion of CO_2 in these rocks compared with those in other pipes (Section 7.1) suggests CO_2 release from the adjacent Appin Limestone.

There are no rock types in the Back Settlement pipe that correspond with those resulting from the second phase of explosive activity in the Kentallen pipe (c.f. Fig. 8.1b). In addition, on the basis of crystallisation conditions and mode of emplacement the appinite of Back Settlement show a general correspondence to the marginal ultramafic rocks (particularly hornblendite) of the Kentallen pipe (see Figs 8.1a, 8.2a; Section 8.1A). All this evidence indicates that the formation of the Back Settlement pipe resulted from one phase of explosive activity which corresponds to that responsible for the emplacement of the marginal ultramafic rocks in the Kentallen pipe (see Bowes & Wright 1967, p.139).

8.1C Rudha Mòr pipes

On the basis of CMAS plots the marginal ultramafic rocks from both the large and small pipes (Bowes & Wright 1967, fig. 10; c.f. Section 7.2), represent cumulates. Many contain kink-banded mica pointing to emplacement as crystal mushes with the banding in appinite from the small pipe probably related to such emplacement phenomenon. These features indicate a general correspondence with the marginal ultramafic rocks from the Kentallen pipe. However, the presence of actinolitic overgrowths on pargasite crystals in the marginal rocks from both the main and small pipes indicate that, as in the Back Settlement pipe, the explosive activity associated with the formation of explosion-breccias and the emplacement of marginal rocks followed the build up of P_{H_2O} to 5 kb.

The carbonated kentallenite occurring in close association with the ultramafic rocks along the southeastern margin of the large pipe probably represents, at least in part, the modified product of the residual liquid from which pyroxene, amphibole and biotite of the marginal ultramafic rocks crystallised. Thus it has affinities with the marginal kentallenitic appinite from the Kentallen pipe (see Section 8.1A).

Also on the basis of CMAS plots the pyroxene-mica diorite of both the large and small pipes represents a liquid composition. Its near-vertical banding in parts of the large pipe has been attributed to undercooling related to rapid migration of water (Bowes & Wright 1967, fig. 10, p.127-129). This is consistent with the emplacement of a liquid, as is the occurrence of reacted blocks of quartzite surrounded by lamprophyric material (c.f. Bowes & Wright 1965, figs 2-4). The mass of ultramafic material apparently within the diorite at the central-western part of the large pipe is best explained as a xenolithic block of the marginal material.

The emplacement of the diorite generally corresponds in sequential development with the emplacement of the main mass of kentallenite in the Kentallen pipe. However, respective mineral chemistries indicate somewhat different crystallisation conditions with the clinopyroxenes showing that temperature was lower and P_{H_2O} higher in the Rudha Mòr diorite (c.f. Sections 4.1, 4.3). In addition, the replacement of clinopyroxene by amphiboles of pargasite and magnesio-hornblende compositions and the association of biotite with amphiboles in the Rudha Mòr diorite, all indicate development in a temperature range of <u>c</u>. 940° - 770°C under a P_{H_2O} of <u>c</u>. 2 - 4.5 kb (Sections 2.2A, 5.2, 5.3, 6.2); these conditions differ from those of kentallenite crystallisation ($T = 1550° - 1000°C$, $P_{H_2O} = <1 - 1$ kb). As at Kentallen, the presence of feldspar in the groundmass indicates a drop in P_{H_2O} after the development of amphiboles and points to a second phase of explosive activity in the pipe. This was at a temperature of <u>c</u>. 770°C and a

P_{H_2O} of 4.5 kb (Fig. 8.2b) and followed by the upward movement of the residual liquid together with variable proportion of already crystallised mafic phases.

The lamprophyres which cross-cut both diorite and appinite, in both large and small pipes, are interpreted as the products of residual liquids of dioritic composition that were trapped at deeper level as was the case for corresponding rocks in the Kentallen pipe.

On the basis of chemical features both the granodiorite of the large pipe and the leucocratic diorite of the small pipe are consistent with being comparable and the feldspathic products complementary to the more mafic other rocks of the igneous complex (Sections 7.1, 7.2). However, the local evidence of a quartzite-diorite transition zone and the evidence for the transfer of silica from quartzite blocks into the magma (Bowes & Wright 1965, p.466-7, figs 2-4) presumably by solution in H_2O at high T, point to an extension of the range of differentiation into even more acidic type than would have otherwise occurred. However, this did not change the course of crystallisation (c.f. Yoder 1979, p.134). Crystallisation conditions for the main diorite of the Rudha Mòr were P_{H_2O} of <1 - 4.5 kb and a temperature of c. 1100° - 770°C, with 4.5 kb and 770°C the favoured conditions (Fig. 8.2b). Crystallisation conditions for last emplaced masses of granodiorite and leucocratic diorite are considered to have been P_{H_2O} of < 1 kb and a temperature of <770°C.

The highly altered and carbonated nature of some rocks, particularly in the small pipe, indicate post-crystallisation gas-streaming similar to that in the small pipe at Back Settlement (Section 8.1B).

8.1D Ardsheal Hill - Lagnaha pipes

The occurrence in the marginal parts of (1) the Ardsheal Hill pipe of biotite-pyroxene-hornblende-feldspar rock and appinite which in parts approaches kentallenitic appinite, (2) the northern of the two Lagnaha pipes of pyroxenite and (3) in both of the northern and southern Lagnaha pipes of appinite together with the evidence of CMAS plots which shows that the marginal rocks in these pipes variably represent cumulates and liquid compositions indicates the emplacement of crystal mushes and residual liquid in variable proportion from place to place (see Bowes & Wright 1967, fig. 12; Sections 2.2A, 7.2, 8.1A-D). Confirmatory evidence for this interpretation is produced by the existence of explosion-breccias together with the highly fractured and deformed nature of many of the hornblende crystals in biotite-pyroxene-hornblende-feldspar rock from the Ardsheal Hill pipe, features that are consistent with explosive disruption of cumulates; the banding in this rock (Bowes & Wright 1967, p.180) can be related to a mush flow phenomenon. In addition the presence of actinolitic overgrowths on pargasite crystals in appinite also indicates variable gas pressure associated with explosive activity with P_{H_2O} of c. 5 kb. These various features indicate a genesis that is generally comparable with that for the marginal ultramafic rocks of the Kentallen and Rudha Mòr pipes. The marginal kentallenite in a small pipe to the east of the main Lagnaha pipe is interpreted as representing the residual liquid and as corresponding with the marginal carbonated kentallenite of the large pipe at Rudha Mòr and the marginal kentallenitic appinite at Kentallen (c.f. Section 8.1A, 8.1C).

The existence of a chilled lamprophyric marginal facies of the diorite on the northwestern margin of the Ardsheal Hill mass and of rocks of the same complex which contain olivine without a reaction rim of orthopyroxene indicate the emplacement of liquid from depth with a simultaneous drop in temperature to $< 1500^{\circ}C$, following the emplacement of the marginal types (c.f. Sections 2.2A, 3.5, 8.1A). On the basis of CMAS plots the lamprophyric marginal facies and related diorites (feldspathic appinites) from both the Ardsheal Hill and Lagnaha pipes represent liquid compositions (Section 7.2). This is consistent with evidence of clinopyroxene-amphibole reaction relationship in diorites and with interpretation that the lamprophyric marginal facies represent an olivine-fractionated melt, i.e. not the "primary" magma (Section 3.6). The banding with a dip angle of 30° in diorite from the northeastern margin of the main Lagnaha pipe and with a dip angle of 50° in diorite from the small pipe, east of the main Lagnaha pipe can be related to viscous flow of the residual liquid carrying variable proportions of the early formed mafic phases. Thus it has affinities with that seen in the coarse-grained kentallenite representing liquid composition, from the Kentallen pipe. However, the near-vertical banding in diorite from the eastern margin of the main Lagnaha pipe can be attributed to undercooling related to rapid migration of water and thus it corresponds with that seen in diorite from the large pipe at Rudha Mòr (see Sections 8.1A, 8.1C; Bowes & Wright 1967, figs 10, 12, 14, p.129).

The emplacement of diorites corresponds in sequential development with the emplacement of the main mass of kentallenite at Kentallen and with that of the pyroxene-mica diorite at Rudha Mòr. However, the composition of clinopyroxene from the lamprophyric marginal facies indicates that somewhat higher P_{H_2O} and lower temperature than those suggested for the development of clinopyroxene in the kentallenite of the Kentallen pipe ($P_{H_2O} = < 1 - 1$ kb; T = c. 1125° - 1000°C - c.f. Fig. 8.1b) were operative (c.f. Sections 4.3, 8.1A). Also, in the diorites the replacement of clinopyroxene by amphibole and the association of biotite with amphibole, all indicate development in a temperature range of c. 900° - 770°C, under a P_{H_2O} of c. 2 - 4.5 kb. The presence of feldspar in the groundmass indicates a drop in P_{H_2O} after the development of amphibole. This evidence indicates that there was a second phase of explosive activity at a temperature of c. 770°C under a P_{H_2O} of 4.5 kb (c.f. Sections 2.2A, 8.1B, 8.1C). These P-T conditions closely correspond with those operative during the development of the pyroxene-mica diorite at Rudha Mòr (Fig. 8.2b) but differ markedly from the conditions of kentallenite crystallisation (Fig. 8.1b). Upwards movement of the residual, liquid carrying variable proportions of the early crystallised mafic phases, must have followed the second phase of explosive activity.

The lamprophyre dyke which cross-cuts the explosion-breccia at the southwestern margin of the main Ardsheal Hill pipe and another one about 100 m to the northwest (Bowes & Wright 1967, fig. 12), are interpreted as the products of the residual liquid of dioritic composition.

On the basis of chemical features the granodiorite and quartz diorite (leucocratic diorite) from the Ardsheal Hill and Lagnaha pipes are consistent with being feldspathic differentiates (Section 7.1, 7.2). However, in many places these rocks show petrographic similarities to the quartzite-diorite transition zone at Rudha Mòr and to the transfused feldspathic rims of the quartzite blocks at Gleann Chàrnan (c.f. Bowes et al. 1963, Bowes & Wright 1965, 1967). Therefore, the removal of silica from quartzite at depth may have also played some role in the formation of acidic rocks at Ardsheal Hill and Lagnaha as it did in the Rudha Mòr pipe (Section 8.1C); this interpretation is consistent with the presence of the quartzite fragments in the diorites (Bowes & Wright 1967, p.131). P-T conditions ($P_{H_2O} < 1$ kb, T = $< 770^{\circ}$C) suggested for the crystallisation of the acidic rocks at Rudha Mòr may also correspond to those in Ardsheal Hill and Lagnaha pipes.

8.1E Small pipes on Kentallen-Ardsheal peninsula, Gleann Chàrnan pipe and pipes of the Glen Creran area

Pressure-temperature estimates for igneous and explosive activity in these pipes are inferred from their comparison with the four major pipes described above (Section 8.1A-D) on the basis of field relationships, petrography and crystallisation history. These data are given in table 8.1. Thus the marginal biotite-pyroxenite of the southerly mass of South Cuil corresponds with the marginal pyroxenite from the Kentallen and Rudha Mòr pipes (crystallisation conditions of $P_{H_2O} = < 1 - 2$ kb, T = 1125° - 960°C). However, the replacement of clinopyroxene by amphibole in the pyroxenite of the South Cuil mass indicates that its emplacement to the present level as a crystal mush, due to an explosive activity, occurred at a higher P_{H_2O} (c. 4 - 4.5 kb) and lower temperature (c. 770°C). The appinite from the southerly mass of North Cuil and the marginal appinite from St. Adamanan's pipe correspond with appinite from the large pipe at Back Settlement (c.f. Fig. 8.2a). The diorites with microkentallenitic margins from the northerly masses of North Cuil and South Cuil and the granodiorite from the southerly mass of South Cuil and from St. Adamanan's pipe corresponds with respective rock types from the Rudha Mòr and Ardsheal Hill - Lagnaha pipes while the kentallenite from St. Moluag's pipe corresponds with the non-cumulative part of the main body of kentallenite at Kentallen (Sections 8.1A, C, D).

Although basic rocks are not exposed in the Inshaig pipe, the extensive development of explosion-breccia indicates that crystallisation from a basic magma under high P-T conditions may have occurred at relatively deeper level. Thus, the porphyritic microdiorite and felsite are interpreted as representing development from a residual liquid produced from fractional crystallisation in a basic magma. The higher SiO_2 and K_2O and lower FeO and MnO in felsite (Section 7.1) may account for the presence of a component of a hybrid secondary liquid produced from the interaction of the residual liquid with breccia blocks of both quartzite and phyllite, at deeper level (c.f. Section 8.1A). This interpretation is consistent with the existence of the intrusive-breccia in the northern part of the pipe, containing blocks surrounded by a thin light coloured zone (Bowes & Wright 1967, pl. 1F) which points to reaction with residual liquid. All these features indicate a general correspondence with the acidic rocks from the Rudha Mòr and Ardsheal Hill-Lagnaha pipes, therefore, comparable crystallisation conditions ($P_{H_2O} < 1$ kb, T = <770°C) are presumed to have been operative (c.f. Sections 8.1C-D).

The evidence of the CMAS plots that the appinite of the Gleann Chàrnan pipe in part represents cumulate and in part liquid composition (Section 7.2), points to the emplacement of masses of already crystallised mafic phases as well as of residual liquid. This is consistent with the presence of kink-banded mica in some parts indicating the emplacement of crystal mushes and with the presence of transfused quartzite blocks indicating the uprise of the residual liquid (see Bowes et al. 1963; Bowes & Wright 1965). The occurrence of idiomorphic hornblende crystals with overgrowths indicates crystallisation in a temperature range of c. 960° - 750°C under a P_{H_2O} of c. 2 - 5 kb. The existence of feldspar in the groundmass points to a subsequent drop in P_{H_2O}. This was related to major explosive activity at a P_{H_2O} of 5 kb and at a temperature of 750°C. All these features show a general correspondence with the appinite from the large pipe at Back Settlement (c.f. Section 8.1B). However, there is no corresponding development of clinopyroxene either as cores in the idiomorphic hornblende crystals or in the groundmass (c.f. Section 2.2A). Either the clinopyroxene did not appear or it was completely absorbed before the appearance of amphibole on the liquidus. This points to the development of high gas pressure at an earlier stage of crystallisation history and at a higher temperature in the Gleann Chàrnan pipe than in the Back Settlement pipe (c.f. Yoder & Tilley 1962), presumably because of the greater strength of structural trap. The development of syenite as the final intrusion rather than of granodiorite as in the Rudha Mòr and Ardsheal Hill -

Lagnaha pipes results from the evolution of P_{H_2O} at the relatively earlier stages of fractionation before biotite was a dominant fractionating phase on the liquidus. This means that the residual liquid which reacted with quartzite impeding its upward path was both richer in K_2O and at a high temperature than the corresponding liquid in the Rudha Mòr and Ardsheal Hill - Lagnaha pipes; syenite then was formed, not granodiorite (see Bowes & Wright 1965, p.469). The intrusion of syenite following the major explosive activity in the pipe and the presence of feldspar in it points to crystallisation under low P-T conditions ($P_{H_2O} < 1$ kb, $T < 750^{\circ}C$). This is consistent with the absence of the reaction rim around quartzite xenoliths present in syenite (Bowes et al. 1963, p.29; Bowes & Wright 1965, p.470).

The cortlandite in the Màm na Staing pipe of the Glen Creran area (Fig. 2.1; Bailey & Maufe 1960, p.211) is a cumulate while the associated cortlanditic appinite (and hornblende diorite) represent liquid compositions with variable proportion cumulate minerals (Section 7.2). The presence of hypersthene in the cores of large idiomorphic hornblende crystals in both the cortlandite and the cortlanditic appinite (Section 2.2A) indicates the retention of temperature in a range of c. 1500° - $1125^{\circ}C$ for a considerable time, before the appearance of clinopyroxene on the liquidus (at a temperature of c. $1125^{\circ}C$ — see Yoder & Tilley 1962). The development of actinolitic overgrowths on pargasite crystals and the presence of feldspar in the groundmass points to a major explosive activity in the pipe, at $750^{\circ}C$ and P_{H_2O} of 5 kb, followed by the upward movement of the explosively disrupted cumulates and residual liquid carrying variable proportion of the early formed crystals. This pattern of development is generally similar to that of the marginal rock types in the Kentallen, Rudha Mòr and Ardsheal Hill - Lagnaha pipes, with cortlandite corresponding to the marginal pyroxenite and hornblendite and the cortlanditic appinite to the marginal kentallenitic appinite and carbonated kentallenite of these pipes (Sections 8.1A-D).

The small mass of kentallenite occurring in the vicinity of the Màm na Stainge pipe and the kentallenite of the Barnamuc pipe (Bailey & Maufe 1960, p.32) corresponds with those parts of the main kentallenite mass of the Kentallen which represents liquid composition (c.f. Sections 7.2, 8.1A; Table 8.1). Thus these rocks represent a second phase of the emplacement of magma from depth in the Glen Creran area.

The central pyroxene-mica diorite of the Barnamuc pipe which is similar to the associated kentallenite except for the lower proportion of olivine (Bailey & Maufe 1960, p.213) probably represents development from a residual kentallenitic liquid that was trapped at relatively deeper level during the explosive activity which occurred at a P_{H_2O} of 1 kb and at a temperature of 1000°C with the emplacement of kentallenite. Crystallisation of pyroxene-mica diorite probably occurred at a temperature of <1000°C and at a P_{H_2O} of <1 kb. This differs from the crystallisation conditions of the diorites from Rudha Mòr and Ardsheal Hill - Lagnaha where P_{H_2O} was $<1 - 4.5$ kb and T was c. 1125° - <750°C.

On the basis of crystallisation history the appinite from Salachail, Clach Fear Ardsheal, Garbh Allt and Glen Ure pipes correspond with those parts of appinite from the Back Settlement pipe which represent liquid composition (c.f. Section 7.2; Fig. 8.2a; Table 8.1). However, the absence of actinolitic overgrowths on pargasite crystals in the appinites of Salachail, Clach Fear Ardsheal and Glen Ure pipes indicate that the major explosive activity in these pipes occurred at a P_{H_2O} of 4 kb and at a temperature of 770°C (see Table 8.1).

The emplacement of the central leucocratic diorite has followed the major explosive activity in the Garbh Allt and Glen Ure pipes (Table 8.1). The correspondence of these rocks with the granodiorite from the Rudha Mòr pipe on the basis of petrographic and chemical features (Section 7.1, 7.2) indicate that comparable processes of formation (Section 8.1C) and crystallisation conditions (P_{H_2O} of <1 kb, T $<770^{\circ}$C) were operative. This is consistent with the evidence of transfusion (and some partial melting) of the country rocks, particularly quartzite, by the intruding appinitic magma in several pipes of the Glen Creran area (Platten 1982).

8.2 Use of the terms appinite, kentallenite and cortlandite

Because the petrogenesis shows that the rocks referred by Bailey and Maufe (1916, p.167-8) as appinites represent the variable products of a number of cognate processes, they cannot be simply placed into a classification pigeon hole. Rather they must be considered in terms of the different processes they represent. These include crystallisation under variable P_{H_2O}, crystal accumulation, crystallisation from residual magma, and the explosive mixing of cumulates and residual liquid. When viewed in this light the original definition which was essentially descriptive can be seen to include the products of all these processes. The reference to (1) practically every member of the discontinuous reaction series, (2) amphibole as the most prominent mineral, (3) the variable nature of the feldspar in the matrix and (4) the many minerals associated with the presence of volatiles are explained in the petrogenetic scheme presented here as is the concept of appinites being the plutonic equivalents of hornblende-rich lamprophyres. What is now known is that in many instances the medium-grained more lamprophyric parts represent the composition of the residual liquid while the coarse "phenocrysts" represent cumulate material. Hence the term 'appinite suite' is very useful in terms of encompassing a wide compositional range of a cognate igneous rock derived from a basaltic melt. The term appinite is also useful to refer to those rocks composed dominantly of cumulate amphibole together with a matrix representing some residual liquid. However, particular "phenocrysts" in appinite may not be, and probably are not, in a matrix representing the particular liquid with which they were in equilibrium. While the presence of rhythmic overgrowths on the amphibole crystals is found in many appinites, and in the regions investigated are constantly in rocks that are termed 'appinite', there are appinites which do not show overgrowths.

Like the rock appinite, the rock kentallenite is also a mixture of the products of more than one process. The same applies to cortlandite and to many of the diorites. Probably only the granodiorites and leucocratic diorites represent the products of only one process, although the residual liquid from which they crystallised probably has a component of hybrid secondary liquid.

The terms appinite and appinite suite have essentially been applied in a Scottish context. However, it would be very surprising if comparable condition and processes were not operative in basic igneous rocks elsewhere, where the products have been given more conventional names.

Figure 8.1(a-b) Representation of pressure-temperature conditions for igneous and explosive activity in the Kentallen pipe.

Kentallen pipe

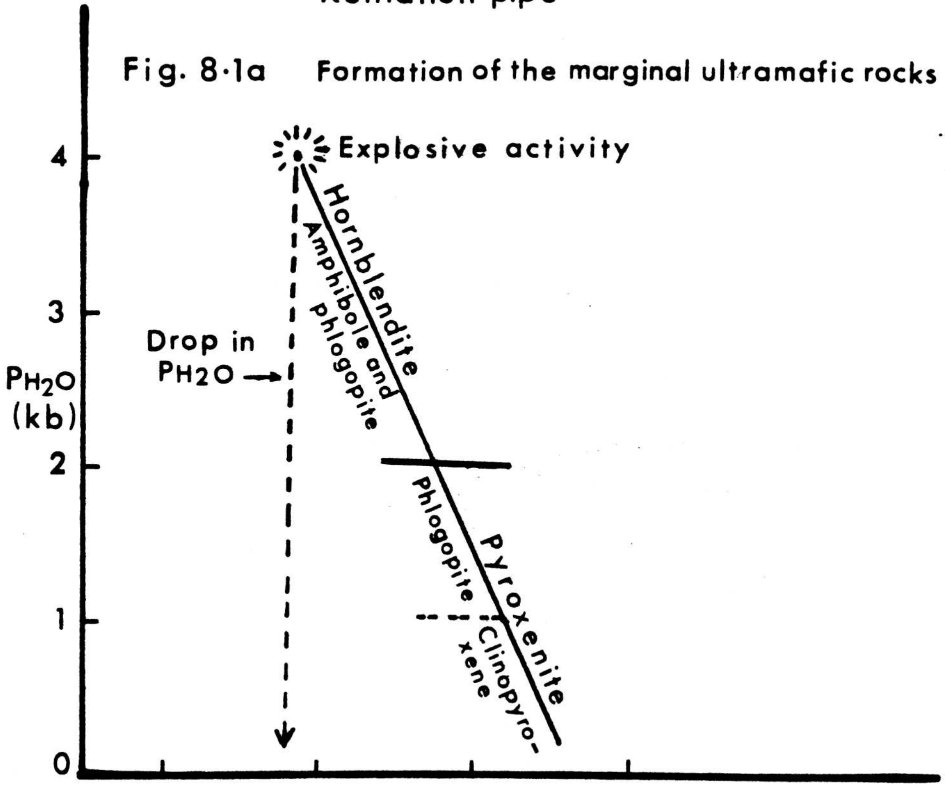

Fig. 8·1a Formation of the marginal ultramafic rocks

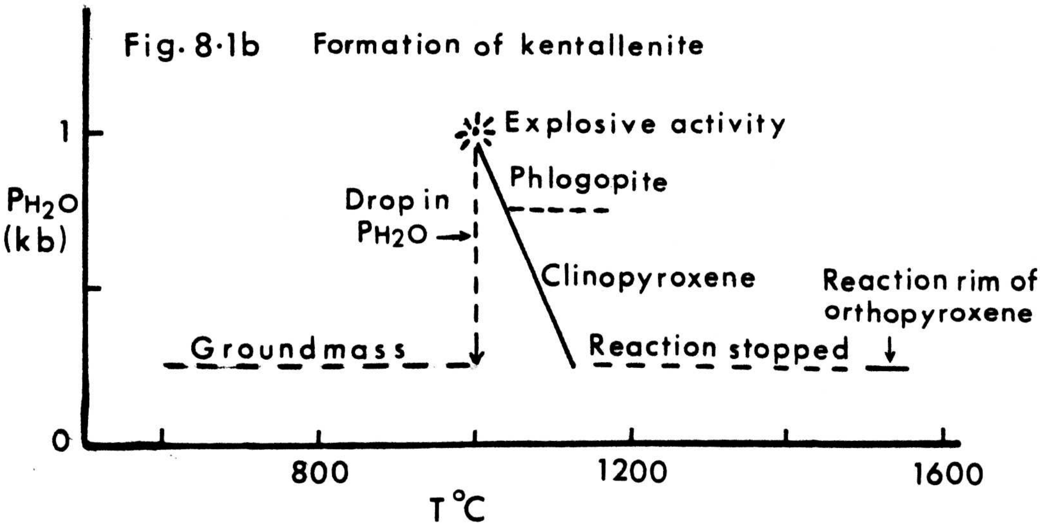

Fig. 8·1b Formation of kentallenite

Figure 8.2(a-b) Representation of pressure-temperature conditions for igneous and explosive activity in the large pipe at Back Settlement (a) and the pyroxene-mica diorite of the large pipe at Rudha Mòr (b).

Fig.8·2a Back Settlement pipe

Formation of appinite

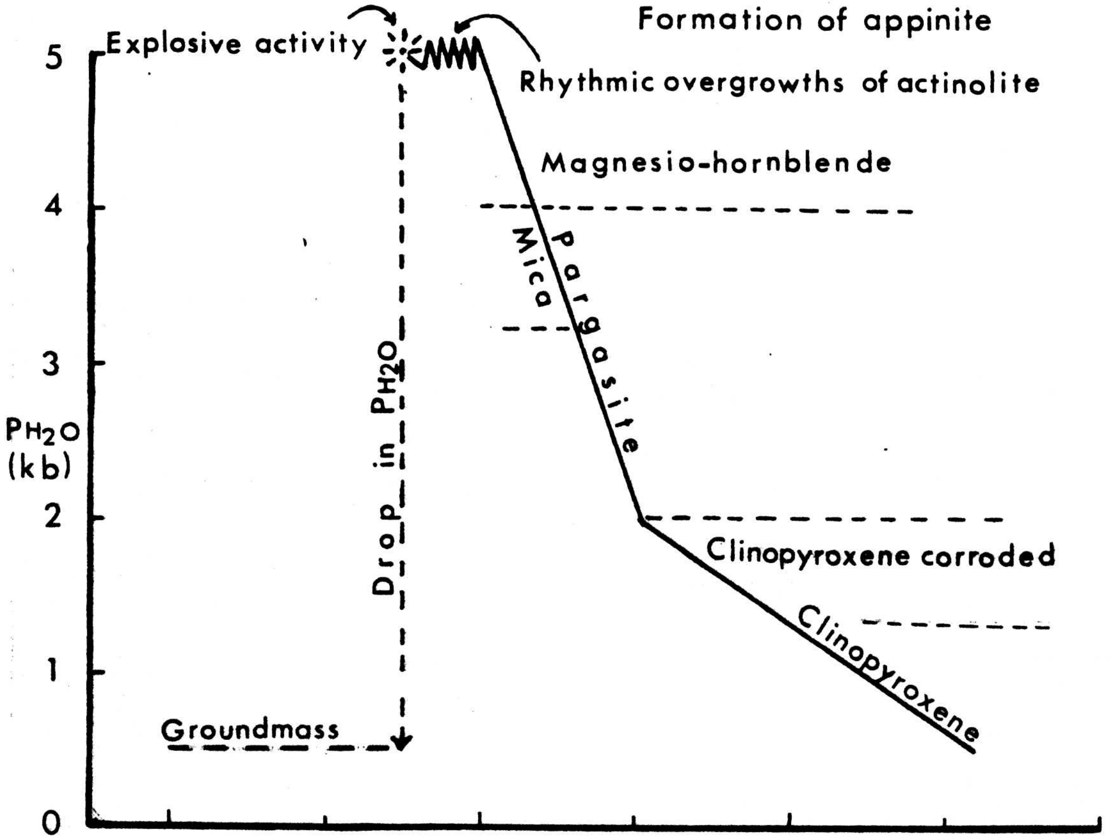

Fig. 8·2b Rudha Mòr pipe

Formation of pyroxene-mica diorite

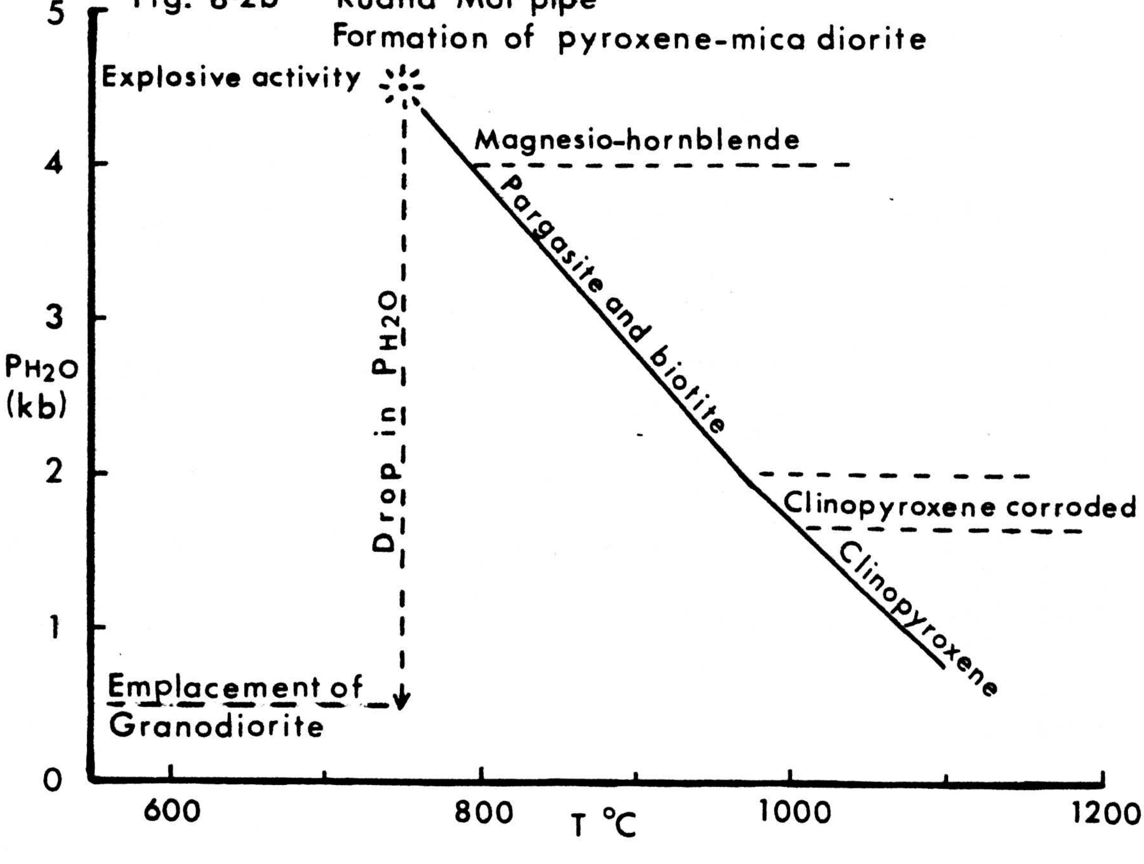

Table 8.1 Pressure-temperature estimates of igneous and explosive activity

	North Cuil pipes				South Cuil pipes						
	Northerly mass		Southerly mass		Northerly mass		Southerly mass				
Rock type/ Explosive activity	Diorite	Explosive activity	Appinite	Explosive activity	Diorite	Explosive activity	Biotite pyroxenite	Explosive activity	Diorite	Explosive activity	Granodiorite
$T^{\circ}C$	c.1100°-770°	770°	1125°-750°	750°	c.1100°-770°	770°	1125°-960°	c.770°	c.1100-770°	770°	<770°
P_{H_2O} in kb	<1-4.5	4.5	<1-5	5	<1-4.5	4.5	<1-2	c.4-4.5	<1-4.5	4.5	<1 kb

	St. Adamanan's pipe			St. Moluag's pipe		Inshaig pipe
Rock type/ Explosive activity	Appinite	Explosive activity	Granodiorite	Kentallenite	Explosive activity	Felsite/porphyritic microdiorite
$T^{\circ}C$	1125°-750°	750°	<750°	<1500°-1000°	1000°	<750°
P_{H_2O} in kb	<1-5	5	<1	<1-1	1	<1

	Gleann Chàrnan pipe			Màm na Stainge pipe				Salachail and Clach Fear Ardsheal pipes	
Rock type/ Explosive activity	Appinite	Explosive activity	Syenite	Cortlandite and cortlanditic-appinite	Explosive activity	Kentallenite	Explosive activity	Appinite	Explosive activity
$T^{\circ}C$	960°-750°	750°	<750°	c.1500°-750°	750°	c.1550°-1000°	1000°	1125°-770°	770°
P_{H_2O} in kb	2-5	5	<1	<1-5	5	<1-1	1	<1-4	4

	Barnamuc pipe			Garbh Allt pipe			Glen Ure pipe		
Rock type/ Explosive activity	Kentallenite	Explosive activity	Diorite	Appinite	Explosive activity	Leucocratic diorite	Appinite	Explosive activity	Leucocratic diorite
$T^{\circ}C$	1550°-1000°	1000°	<1000°	1125°-750°	750°	<750	1125°-770°	770°	<770°
P_{H_2O} in kb	<1-1	1	<1	<1-5	5	<1	<1-4	4	<1

PART 3

LOCH LOMOND APPINITE SUITE

CHAPTER 9 GEOLOGICAL SETTING AND PETROGRAPHY

9.1 Geological setting

Igneous - breccia masses of late Silurian - early Devonian age intruded into various Dalradian metasediments occur in the vicinity of Loch Lomond and to the north of the head of Loch Fyne, make up the appinite suite of the Loch Lomond district (Fig. 9.1; also see Geological Survey of Scotland 1" = 1 mile Sheets 37, 38, 45, 46). The main Arrochar intrusion with its surrounding smaller satellite masses to the west of Loch Lomond and the small intrusions of Inversnaid and Glen Gyle to the east of the loch have been described as "the Arrochar intrusive complex" by Anderson (1935). The intrusions of Ben Glas and Cruachan Cruinn have also been studied by Anderson (1937) as "intrusions of Glen Follach area". The Garabal Hill complex and the Glen Fyne Granite were described as "the Garabal Hill - Glen Fyne igneous complex" by Nockolds (1941). Further work on the appinite suite of the Loch Lomond district, including the intrusions of Glen Shira and other isolated masses in the area, was done by Money (1964) and McArthur (1971). Early lamprophyre dykes and sheets and later porphyrites (see Chapter 2) of the Loch Lomond region have also been investigated by all the above-mentioned workers.

The distribution of these masses is shown in Figure 9.1. Detailed map descriptions of the Arrochar complex, the intrusions of Ben Glas, Cruachan Cruinn, Glen Shira and other smaller isolated intrusions of the area are given by Anderson (1935, figs. 2,3; 1937 , fig. 1) and McArthur (1971, map 1 - 9; also see Hill and Kynaston 1900; Hill 1905). Corresponding information about the appinite suite masses of the Garabal Hill - Glen Fyne complex can be obtained from Nockolds (1941, plate 24).

The following are major features of the intrusions:

1. The various rock types were emplaced into pipe-like intrusions mostly with nearly vertical junctions between the country rocks, breccia and igneous units (*e.g.* Inversnaid, Glen Gyle, Ben Glas, Glen Shira and Cruachan Cruinn; Anderson 1935, p. 271-273; 1937 , p. 461; McArthur 1971, p. 25, 58, 59, 69).
2. Structural elements including folds, cleavage, joints and foliation in the Dalradian metasediments controlled the location and emplacement of various masses.
3. A variable amount of breccia is associated with igneous rocks and there is a consistent breccia - igneous rock sequence of development (Money 1964; McArthur 1971).
4. The breccias generally show a lack of exotic fragments and a composition mainly of angular fragments of local rock types (*e.g.* Inversnaid, Ben Glas and Cruinn intrusion; McArthur 1971, p. 25, 69, 76, 90), the limited transport being indicative of limited gas activity in the pipes compared with that in pipes of the Ballachulish region (Chapter 2).
5. Pyroxene - mica diorite is the dominant rock type in many masses, particularly in the larger ones (Arrochar and Garabal Hill, Fig. 9.1).
6. The following sequence of development is suggested by Anderson (1935, p. 267, 280, 281) for the rocks of the main Arrochar intrusion: pyroxene - mica diorite (fine- and medium-grained diorite and kentallenite), appinite (and coarse-grained diorite and ultramafic rocks), quartz diorite and granodiorite.
7. The following sequence of development is suggested by Nockolds (1941, p. 507) for the rocks of the Garabal Hill complex: ultramafic rock, gabbro, pyroxene - mica diorite, appinite (coarse appinitic diorite, appinite, medium appinitic diorite) and xenolithic diorite.
8. In smaller masses surrounding the main Arrochar intrusion and in

Inversnaid, Glen Gyle, Ben Glas, Cruachan Cruinn and Glen Shira masses (Fig. 9.1) the complete sequences recorded for the Arrochar and Garabal Hill masses do not occur but the order seen is not inconsistent with that set out in 6-7 (above) (see Anderson 1935, 1937 ; McArthur 1971).

9. Early lamprophyres are in close spatial and temporal relationship with rocks of the appinite suite (*e.g.* Glen Gyle and Ben Glas intrusions; McArthur 1971, p. 25, 51, 52, 69, 70; maps 3, 6, 8; also see Anderson 1935, p. 273; Nockolds 1941, p. 481).

A comparative study of the Loch Lomond appinite suite has been carried out to elucidate those features which make this suite different from the Ballachulish appinite suite. These features include the apparently lower gas activity and the dominant occurrence of pyroxene - mica diorite, particularly in the Garabal Hill - Glen Fyne complex. It also forms a basis for assessing the validity of conclusions deduced from the petrogenesis of the Ballachulish appinite suite.

9.2 Petrography and mineral chemistry

The petrography of the various rock types of the Loch Lomond appinite suite has been described by several workers (Hill and Kynaston 1900; Anderson 1935, 1937 ; Money 1964; McArthur 1971). Accordingly this account is limited to those features directly relevant to the mineral chemistry and crystallisation conditions in the pipes. Within the very broad range of textural and mineralogical variation seen, the following are of particular relevance.

1. There are both hydrous and anhydrous mineral assemblages present (in appinite and pyroxene - mica diorite, respectively).
2. There is marked variation in grain size from phenocrysts up to 9 mm (Figs. 9.2, 9.3, 9.4) to grains of olivine, clinopyroxene, amphibole, mica and plagioclase of < 0.3 mm.
3. Olivine, clinopyroxene, amphibole and plagioclase are highly zoned in parts (Figs. 9.2b, 9.4).

4. Amphibole is present as large hornblende crystals which poikilitically enclose olivine, clinopyroxene and plagioclase (in peridotite and cortlandite) (Fig. 9.2c), and as stumpy and acicular idiomorphic hornblende which occasionally have clinopyroxene cores and very occasionally have actinolitic overgrowths (in appinite) (Figs. 9.3a, b).
5. Expressions of different reaction relationships between various phenocrysts and liquids are shown by the highly resorbed nature of olivine, clinopyroxene and amphibole, the development of orthopyroxene rims on olivines (in kentallenite) and the replacement of clinopyroxene by amphibole (in appinite and pyroxene - mica diorite) (Figs. 9.2a, 9.3c).
6. Most of the minerals of the Bowen's discontinuous reaction series are present in some rocks with minerals high in the reaction series generally surrounded by minerals lower in the reaction series but with some instances of the reverse (*e.g.* biotite in clinopyroxene, Nockolds 1941, p. 457; biotite intergrown with hornblende in certain appinites).
7. Plagioclase phenocrysts occur in most of the basic to acidic rock types (*e.g.* gabbro, pyroxene - mica diorite, granodiorite) (Fig. 9.4).
8. Granophyric intergrowths between feldspar and quartz occur in the groundmass of hornblende diorite and acidic rocks.
9. Accessory minerals including primary magnetite, sphene and apatite occur with magnetite commonly associated with hornblende (in appinite) (Fig. 9.3a).
10. Olivine shows alteration to serpentine, clinopyroxene and hornblende to uralite, biotite to chlorite and epidote and plagioclase to sericite (in marginal rocks).
11. Primary calcite is present as a minor phase (in some appinites); secondary calcite also occurs (in most of the carbonated and altered rocks).

9.2A Pyroxenite

The pyroxenite (Table 9.1 – 1) of the main Arrochar intrusion is an equigranular coarse-grained rock with densely packed zoned clinopyroxene crystals which are clouded with specks of opaque ore and surrounded and replaced by amphibole at their margins. There are inclusions of olivine and some orthopyroxene grains and some interstitial biotite.

The composition of the clinopyroxene varies from diopside to salite and calcic-augite, close to the boundary between diopside - salite and endiopside - augite fields (Fig. 9.5, Table 9.2 – 1). Some of the zoned crystals have a core of diopside, a middle zone of salite and an outer rim of augite. Amphibole replacing clinopyroxene is of magnesio - hornblende composition (Fig. 9.6, Table 9.4 – 7).

9.2B Peridotite

The peridotite of the main Arrochar intrusion (Table 9.1 – 2) contains large platy and zoned hornblende crystals (with a brown core and green rim) poikilitically enclosing olivine, clinopyroxene (endiopside and calcic-augite; Fig. 9.5, Table 9.2 – 3) and plagioclase$_{(An_{66})}$ (Table 9.6 – 12) in the core (Fig. 9.2c). Plagioclase and phlogopite (Fig. 9.7, Table 9.5 – 4) occur interstitially.

9.2C Gabbro

The gabbros of the Garabal Hill - Glen Fyne complex (Table 9.1 – 3) generally contain clinopyroxene, orthopyroxene, plagioclase$_{(An_{58})}$ and biotite crystals with interstitial orthoclase and accessory amounts of magnetite and apatite (Nockolds 1941). In the hornblende-bearing gabbro large clinopyroxene crystals are surrounded and replaced by amphibole. Biotite, plagioclase and magnetite occur in the cores of clinopyroxene crystals.

9.2D Appinite

The appinites of the Loch Lomond region (Table 9.1 – 4) contain large idiomorphic amphibole crystals in a groundmass usually of plagioclase, quartz, orthoclase and some biotite.

The amphibole crystals are variously pargasite, ferroan-pargasite. ferroan-pargasitic-hornblende, tschermakite and tschermakitic hornblende (Fig. 9.6, Table 9.4 – 1-6). Where zoned, cores with compositions of tschermakite and pargasite and outer rims of magnesio-hornblende and actinolite have been observed (Fig. 9.6, Table 9.4 – 9, 10, 13, 14, 15). Such crystals are without rhythmic overgrowth of actinolite, such as found in appinites of the Ballachulish region (Chapters 2, 5). However, in certain instances the hornblende crystals show an overgrowth of actinolite on one of their terminal faces (Fig. 9.3b). Clinopyroxene with compositions of salite and calcic-augite (Fig. 9.5, Table 9.2 – 5) occur occasionally as cores to stumpy hornblende crystals in appinite from the main Arrochar mass (Fig. 9,3a).

Plagioclase$_{(An_{25-38})}$ occurs as zoned phenocrysts in the appinite of the main Arrochar and Glen Shira masses (Table 9.6 – 5,7) but when present in the groundmass the feldspar is albite (Table 9.6 – 4). Quartz and orthoclase may occur interstitially. Primary calcite, when present, is interstitial to both orthoclase and quartz while secondary calcite replaces plagioclase. Primary magnetite, apatite and sphene are common accessories. Chlorite and epidote after biotite also occur.

9.2E Kentallenite

The kentallenites of the Loch Lomond region (Table 9.1 – 5) have phenocrysts of olivine, clinopyroxene and biotite with rims of biotite surrounding some olivines and clinopyroxenes. The groundmass contains anorthoclase, plagioclase, biotite and primary magnetite.

Where zoned, olivine phenocrysts have forsteritic cores and chrysolitic rims (Table 8.3 – 1, 2). Reaction rims of orthopyroxene (bronzite; Table 9.2 – 7, Fig. 9.5) surrounding olivine are common (Fig. 9.2a). Pleochroic hypersthene has been reported from the kentallenite exposed in Allt an t-Sithain, Glen Shira (Anderson, 1935).

Biotite, pleochroic from light brown to deep brown, has a composition close to the boundary between the biotite and phlogopite fields (Fig. 9.7; Table 9.5 – 2). Anorthoclase is dominant feldspar in the equigranular coarse-grained kentallenite while plagioclase$_{(An_{54})}$ (Table 9.6 – 13) is practically the only feldspar of the porphyritic marginal kentallenite (Glen Shira masses). Opaque ores, apatite and sphene are rare accessories.

9.2F Pyroxene - mica diorite

The pyroxene - mica diorites of the Loch Lomond region (Table 9.1 – 6) are composed of phenocrysts of zoned augite (Figs. 9.2b, 9.5; Table 9.2 – 4) and plagioclase$_{(An_{\sim 50})}$ (Fig. 9.4) in a groundmass of plagioclase$_{(An_{39-52})}$ (Table 9.6 – 8, 11), biotite, quartz and orthoclase. Grains of highly corroded and partially altered olivine (Fo_{74}; Table 9.3 – 3) and of pleochroic hypersthene and inclusions of feldspar occasionally occur in the cores of clinopyroxene phenocrysts which usually have rims of amphibole of magnesio - hornblende composition (Figs. 9.3c, 9.6; Table 9.4 – 11) and biotite (Fig. 9.7; Table 9.5 – 1). Quartz and orthoclase interstitially occur to plagioclase. Primary magnetite, sphene, apatite and secondary chlorite and epidote after biotite are also noticed.

Pyroxene - mica diorite grades to pyroxene diorite (Table 9.1 – 7) with decrease in mica and to appinitic diorite (Appendix B.3 – 67) with increase in amphibole. Plagioclase phenocrysts$_{(An_{30})}$ (Table 9.6 – 9) have also been noticed in the latter variety at Garabal Hill.

9.2G Quartz diorite and granodiorite

The quartz diorite and granodiorite (Table 9.1 – 8) contain phenocrysts of zoned plagioclase$_{(An_{48})}$ (Table 9.6 – 10), biotite (Fig. 9.7;

Table 9.5 — 3) and amphibole in a groundmass of plagioclase, biotite, quartz and orthoclase. The amphibole phenocrysts are usually of magnesio-hornblende and actinolitic-hornblende compositions (Fig. 9.6; Table 9.4 — 12). Pargasite crystals with actinolitic rims also occur. Quartz and orthoclase occur in granophyric intergrowths. Primary magnetite, sphene, apatite and pyrite are accessories. These are commonly associated with biotite.

9.2H Lamprophyres

The majority of the lamprophyre dykes which cut the appinitic masses are vogesitic in mineralogy (Table 9.1 — 9). They contain microphenocrysts of prismatic hornblende in a groundmass of anorthoclase, orthoclase (Table 9.6 — 1,2) and plagioclase$_{(An_{<10})}$.

The lamprophyre dykes which precede the emplacement of the appinitic bodies are spessartites (Anderson 1935; Nockolds 1941; Money 1964; McArthur 1971). These dykes are mineralogically similar to the lamprophyric marginal facies described from the Ardsheal Hill pipe of the Ballachulish region (Chapter 2) with clinopyroxene and olivine occurring as phenocrysts.

With decrease in ferromagnesium minerals the lamprophyres grade to porphyritic microdiorites. The term felsite was used by Money (1964) for their highly altered varieties (Table 9.1 — 10).

9.3 Comparison with the Ballachulish appinite suite

The rock types of the Loch Lomond cluster show significant similarities to those from the Ballachulish cluster on the bases of texture, mineralogy and mineral chemistry (see Chapters 2-6). However, the following petrographic features discriminate the Loch Lomond cluster from the Ballachulish cluster:

1. In appinites, the proportions of clinopyroxene and biotite are lower, rhythmic overgrowths on hornblende crystals and clinopyroxene as cores to hornblende crystals are scarcer and plagioclase instead

of orthoclase is the common groundmass feldspar.

2. In kentallenites from the Arrochar and Glen Shira masses, reaction rims of amphibole surround clinopyroxene phenocrysts while in pyroxene - mica diorite these are less commonly developed.
3. In mafic and ultramafic rocks the proportions of pleochroic hypersthene are greater than in those of the Ballachulish cluster (Table 9.1; see also Table 2.1).
4. In many of the mafic and intermediate rocks there are Ca-rich plagioclase phenocrysts and in certain peridotites Ca-rich plagioclase occurs in cores of the large hornblende crystals (Fig. 9.2c).

The Loch Lomond cluster can also be discriminated from the Ballachulish cluster on the basis of the following features of mineral chemistry.

1. The Ca contents of the clinopyroxenes are lower and decrease with fractionation (Fig. 9.5; also see Fig. 4.1a).
2. A significant number of idiomorphic hornblende crystals have tschermakite and magnesio-hornblende compositions (Fig. 9.6; see also Fig. 5.1, Table 5.1).

9.4 Discussion

The more frequent occurrence of orthopyroxene, the lower proportions of potassium-bearing minerals (biotite, orthoclase) and the presence of the Ca-rich plagioclase in many of the mafic and intermediate rock types of the Loch Lomond appinite suite as compared to those from the Ballachulish appinite suite, place the former suite closer to the calcalkaline rock series. The differences between the magma compositions of the two clusters (Chapters 7, 10) are also expressed in their mineral chemistry, *e.g.* the lower alkali contents of many of the hornblende crystals (tschermakites and magnesio - hornblendes) and the lower Mg and K contents of mica in ultramafic and mafic rocks from the Loch Lomond cluster.

The lower Ca contents and their decrease with fractionation in clinopyroxenes (Fig. 9.5) may be partly related to the calcalkaline nature of the parent liquid (Chapter 10; also see Kushiro 1960; Le Bas 1962). However, it is mostly due to the appearance of Ca-rich plagioclase$_{(An_{50})}$ (occurring as phenocrysts as well as small crystals in the cores of platy hornblendes) in the early stages of crystallisation (see Chapter 4). This was responsible for the development of gabbros in the Garabal Hill - Glen Fyne complex.

The early appearance of Ca-rich plagioclase in ultramafic, mafic and intermediate rocks indicates a P_{H_2O} of < 1 kb at this particular stage of crystallisation (Barberi *et al.* 1971). The high modal percentages of volatile-bearing minerals (amphibole and biotite), the replacement of clinopyroxene by amphibole and the presence of many secondary minerals in most of the marginal rock types reflect an increase in gas pressure as the crystallisation proceeded. The presence of highly zoned phenocrysts and the expressions of various reaction relationships between crystallising phases and liquids indicate changes in crystallisation conditions, particularly in gas pressure (see Chapters 2-6). The scarcity of rhythmic overgrowths on hornblende crystals in appinite indicates that the gas pressure generally did not exceed 2-4 kb in pipes of the Loch Lomond region (see Chapter 5). This may be related to the strength of the structural traps encountered by the intruding appinitic magma in the Loch Lomond region not being as great as formed by quartzite in the Ballachulish region (*e.g.* Back Settlement pipe; Chapters 2, 5). This interpretation is supported by the scarcity of exotic rock types in the breccias and by the low degree of rounding in the breccias, the limited transport being indicative of lower gas pressures (see Chapter 2; Bowes and Wright 1961, 1967; Bowes *et al.* 1964; McArthur 1971; Bowes and McArthur 1976).

The petrography of the early lamprophyres of the Loch Lomond region is also consistent with the interpretation that these dyke rocks are the successive differentiates of the appinitic magma, as are the various plutonic rocks of the appinite suite. This conclusion corresponds with that drawn from the lamprophyre dykes of the Ballachulish region (Chapters 2, 7).

9.5 Conclusions

1. The field relationship of the Loch Lomond appinite suite indicates the emplacement of appinitic magma mostly into pipe-like intrusions.
2. Structural control of the surrounding country rocks has played an important role in the evolution of various rock types in different intrusions.
3. The lack of exotic and well rounded fragments of breccia indicates a limited transport of material due to lower gas activity in pipes of the Loch Lomond region as compared to those at Ballachulish. This is supported by petrography and mineral chemistry.
4. On the basis of petrography and mineral chemistry the Loch Lomond appinite suite is closer to the calcalkaline series than the Ballachulish appinite suite.
5. Various reaction relationships between phenocrysts and liquids indicate considerable changes in crystallisation conditions, while zoning in phenocrysts and the normal and reverse orders of appearance of the minerals of Bowen's discontinuous reaction series indicate fluctuation in gas pressure.
6. Appinite (and peridotite) generally crystallised under a maximum gas pressure of 2-4 kb. The other members of the suite crystallised below this pressure. Plagioclase phenocrysts indicate $P_{H_2O} < 1$ kb.
7. The lower Ca contents and their decrease with fractionation in clinopyroxenes from the Loch Lomond cluster compared with those from the Ballachulish cluster, are due to the early appearance of Ca-rich plagioclase in the latter cluster.

8. The early lamprophyres (and felsite) dykes, associated in time and space with pipes of the Loch Lomond cluster represent successive differentiates of the appinitic magma.
9. Alteration and carbonation of the marginal rocks in most of the intrusions are due to the escape of gases during and after crystallisation.

Figure 9.1. The distribution of igneous - breccia pipe masses in the Loch Lomond region (reproduction of McArthur 1971, map 2).

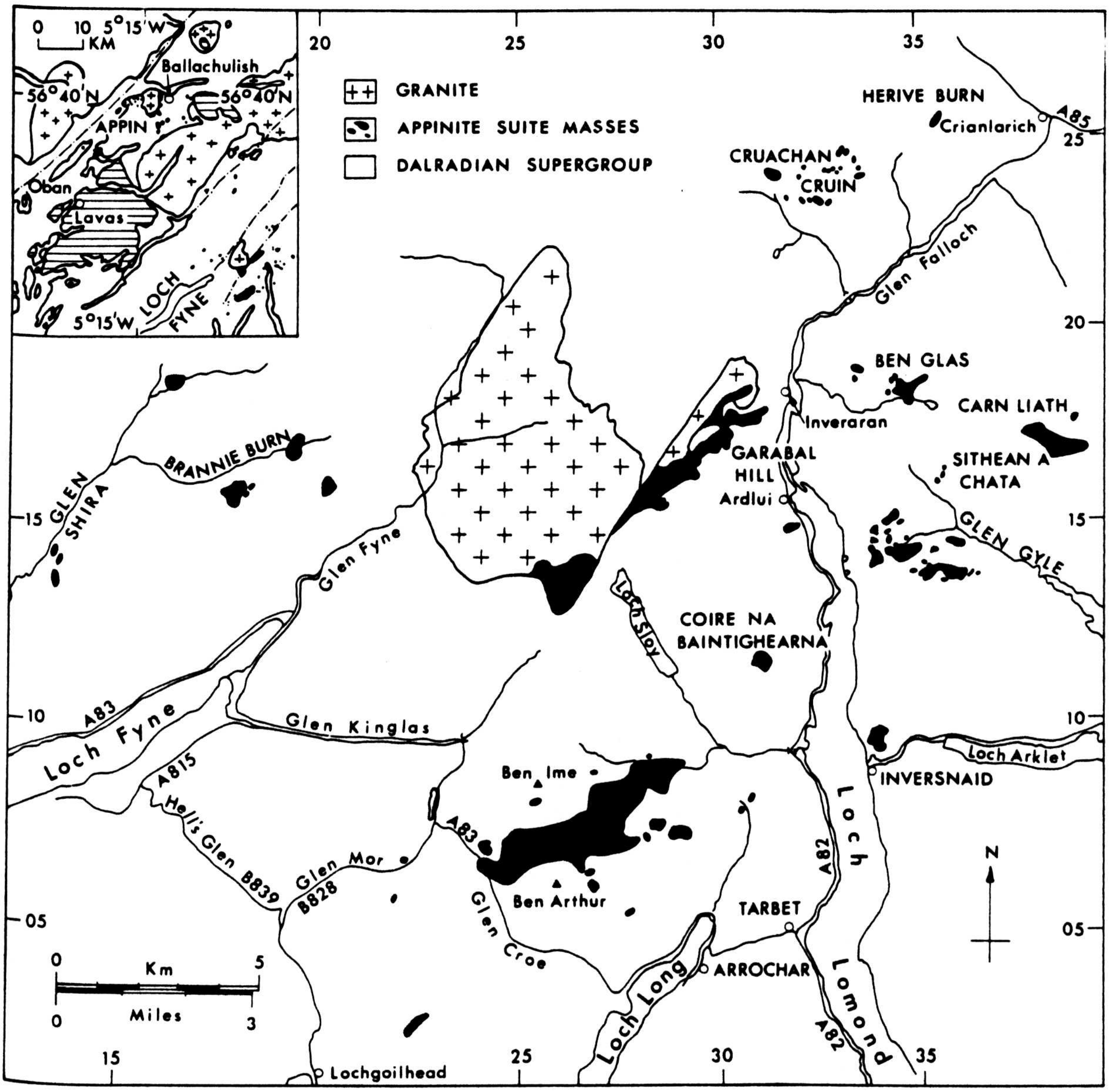
0 10 KM
5°15'W
Ballachulish
56°40'N
56°40'N
APPIN
Oban
Lavas
LOCH FYNE
5°15'W
GRANITE
APPINITE SUITE MASSES
DALRADIAN SUPERGROUP
20
25
30
35
HERIVE BURN
Crianlarich
A85
CRUACHAN CRUIN
Glen Falloch
BEN GLAS
Inveraran
CARN LIATH
GARABAL HILL
Ardlui
SITHEAN A CHATA
GLEN GYLE
BRANNIE BURN
GLEN SHIRA
Glen Fyne
Loch Sloy
COIRE NA BAINTIGHEARNA
A83
Loch Fyne
A815
Glen Kinglas
Ben Ime
Loch Arklet
INVERSNAID
Hell's Glen B839
Glen Mor B828
A83
Ben Arthur
Glen Croe
TARBET
A82
Loch Lomond
ARROCHAR
Loch Long
A82
N
0 Km 5
0 Miles 3
15
25
30
35
Lochgoilhead
25
20
15
10
05

Figure 9.2.

(a) Fractured and partially serpentinized olivine phenocryst surrounded by a reaction rim of orthopyroxene; kentallenite, Cruachan Cruinn. XN x 13.

(b) Zoned phenocryst of clinopyroxene in a groundmass of plagioclase and biotite; pyroxene - mica diorite, main Arrochar intrusion. XN x 10.

(c) Large hornblende crystal with a brown core (darker) and green rim (lighter), poikilitically enclosing olivine, clinopyroxene (Cpx) and plagioclase (P) in the core; peridotite, main Arrochar intrusion. PPL x 10.

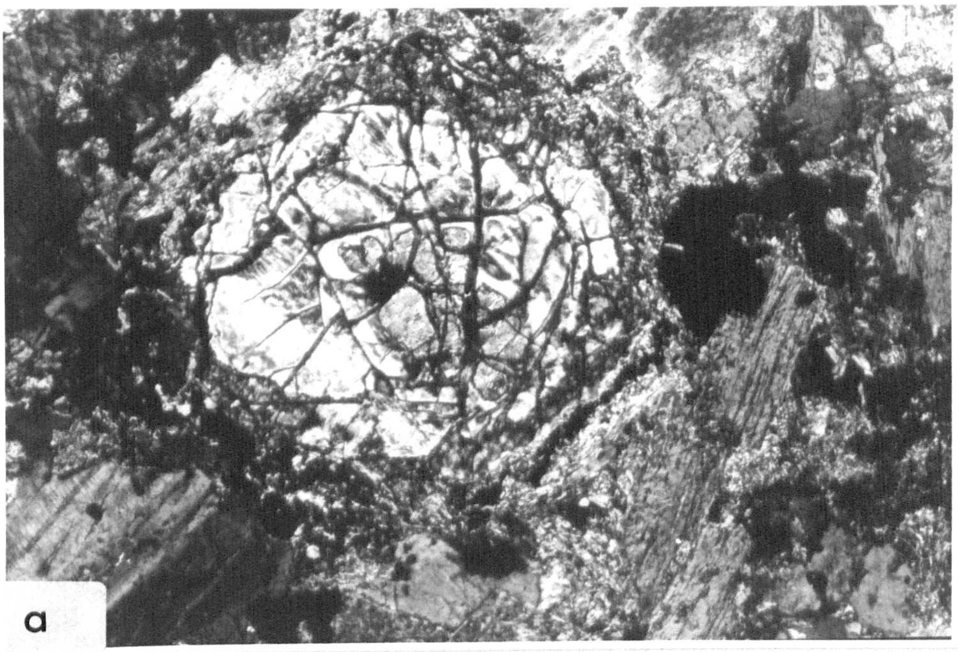
a

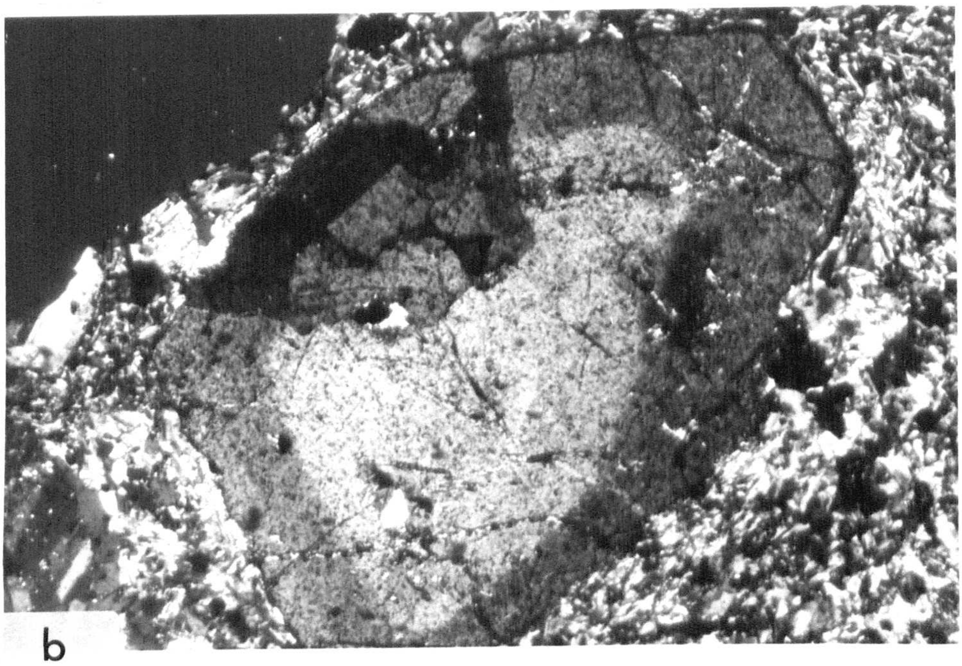
b

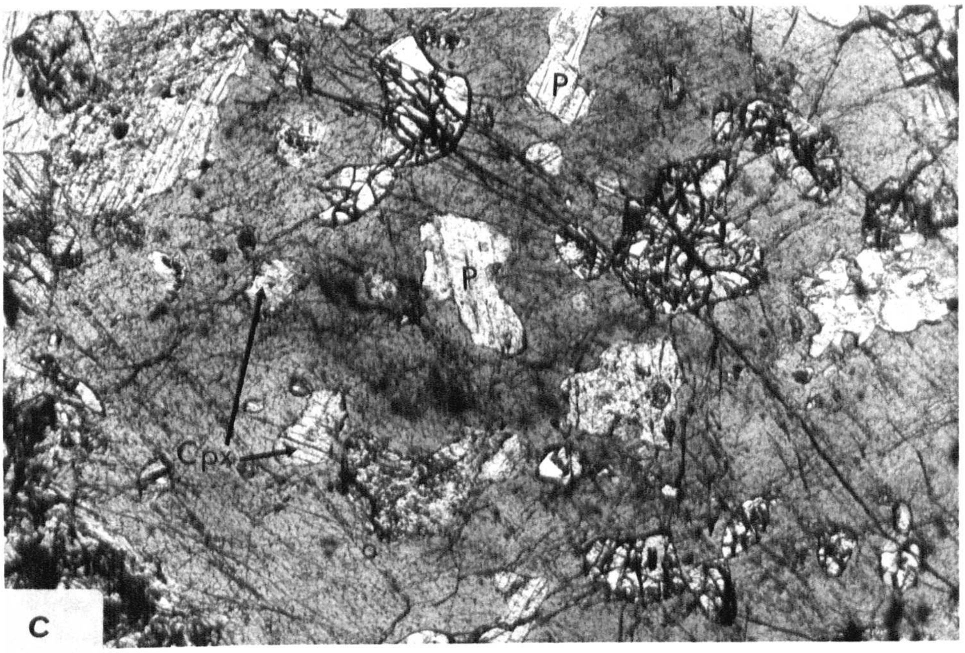
P
P
Cpx
c

Figure 9.3.

(a) Hornblende crystal with a clinopyroxene core, and grains of primary magnetite; appinite west of Creag Tharsuinn, main Arrochar mass. PPL x 13.

(b) Idiomorphic hornblende crystal with an overgrowth of actinolite (A); appinite, Clachan Hill pipe, Glen Shira. XN x 40.

(c) Phenocryst of clinopyroxene containing small olivine grains and with margins indicating corrosion by amphibole; pyroxene-mica diorite, main Arrochar intrusion. PPL x 40.

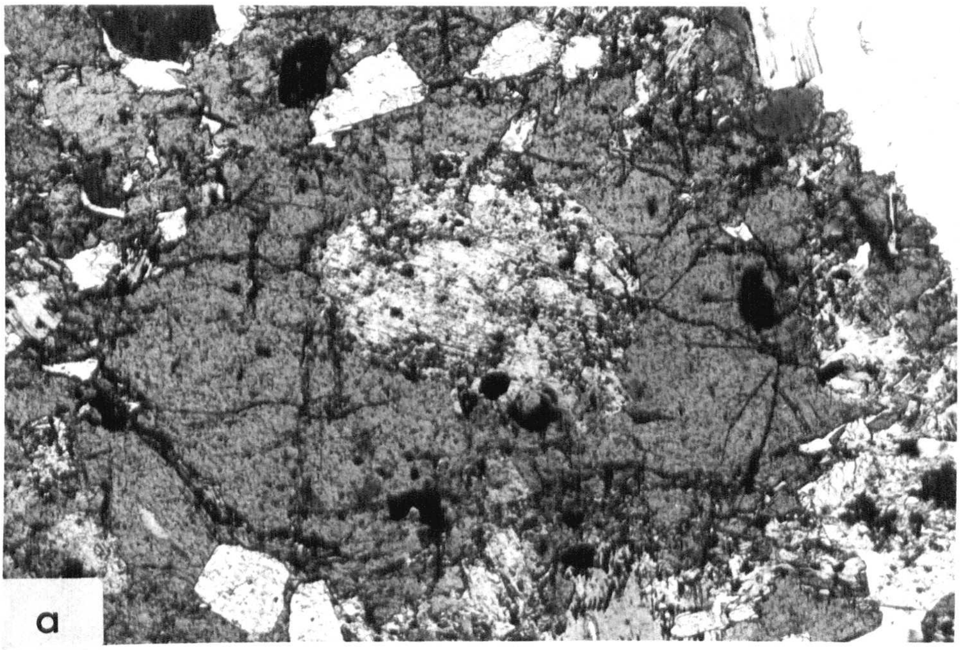
a

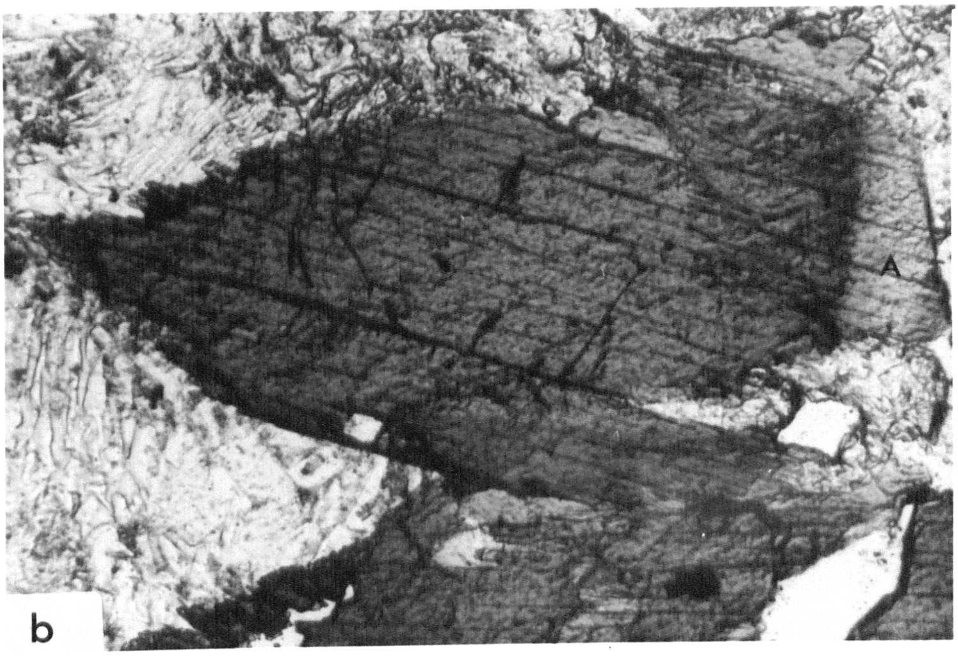
A
b

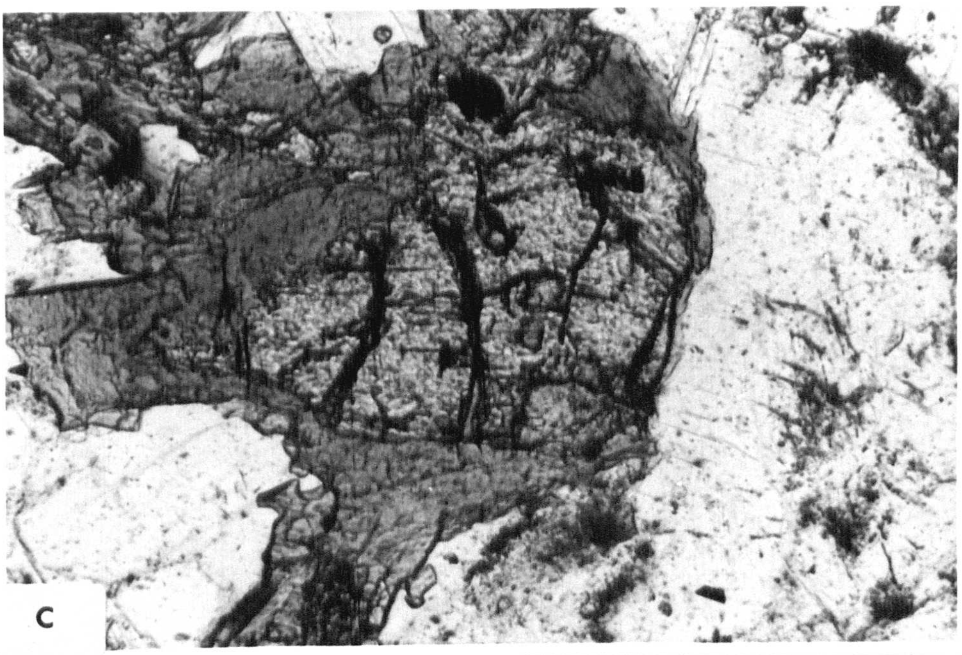
c

Figure 9.4. Zoned plagioclase phenocryst $_{(An_{48-52})}$ with a saussuritized core, in a groundmass of biotite and feldspar; pyroxene - mica diorite, Glen Gyle intrusion. XN x 35.

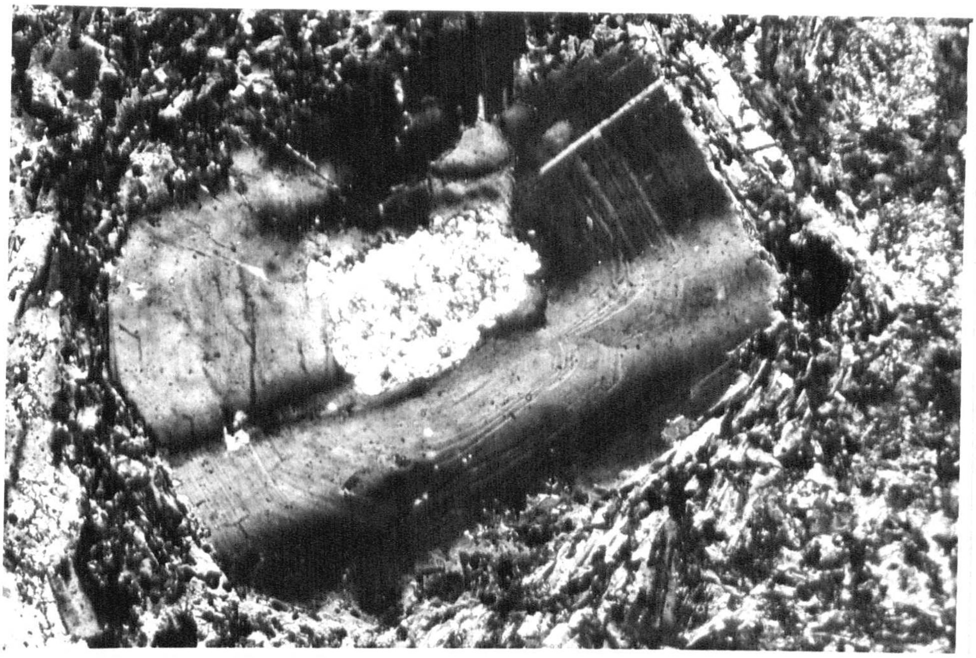

Figure 9.5. Pyroxene compositions from the Loch Lomond appinite suite in the pyroxene quadrilateral (after Hess and Poldervaart 1951).

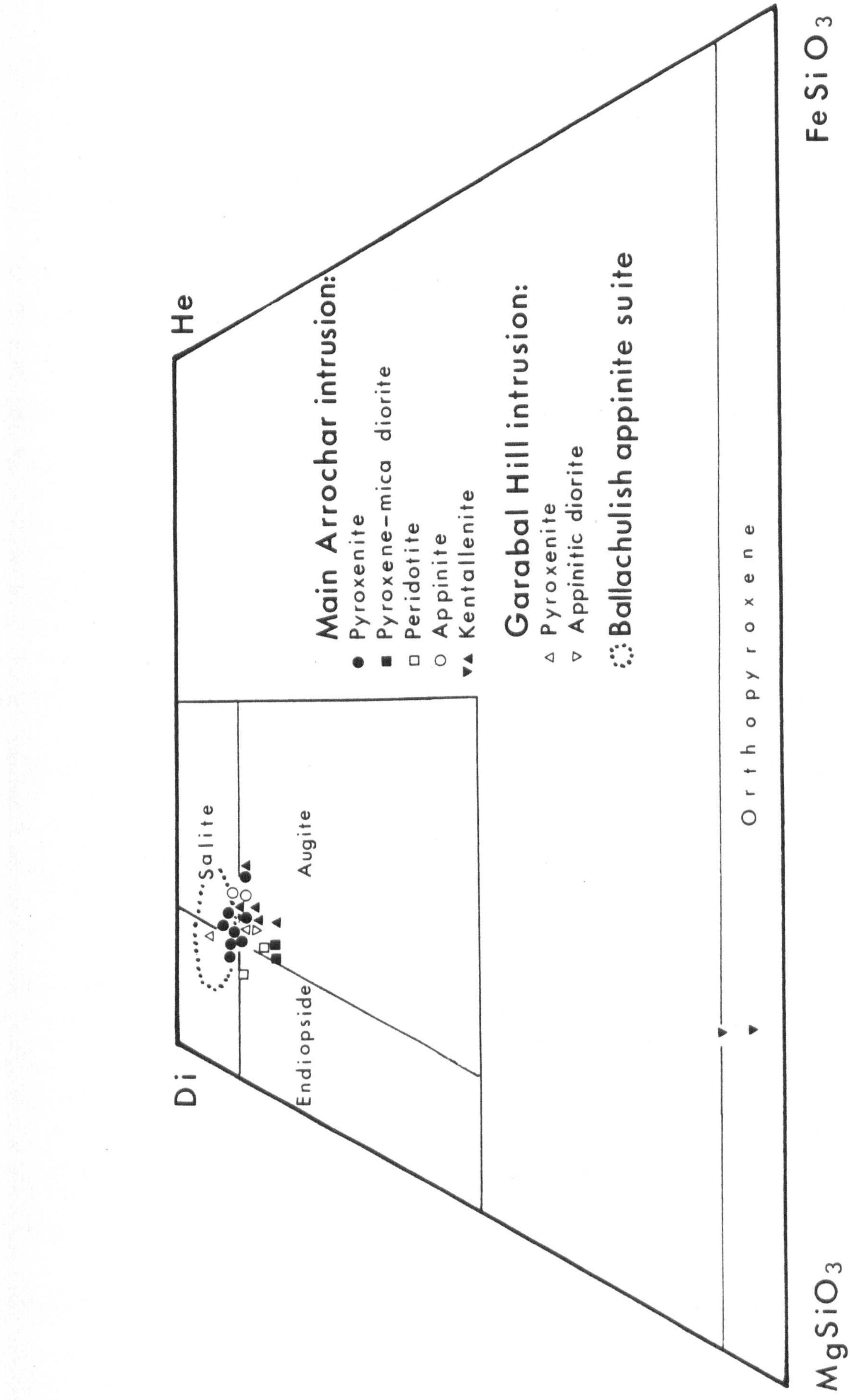
Di
He
MgSiO$_3$
FeSiO$_3$
Salite
Endiopside
Augite
Orthopyroxene
Main Arrochar intrusion:
● Pyroxenite
■ Pyroxene-mica diorite
□ Peridotite
○ Appinite
▼▲ Kentallenite
Garabal Hill intrusion:
△ Pyroxenite
▽ Appinitic diorite
Ballachulish appinite suite

Figure 9.6. Amphibole compositions from the Loch Lomond appinite suite shown in their corresponding fields of calcic amohiboles (after Leake 1978).

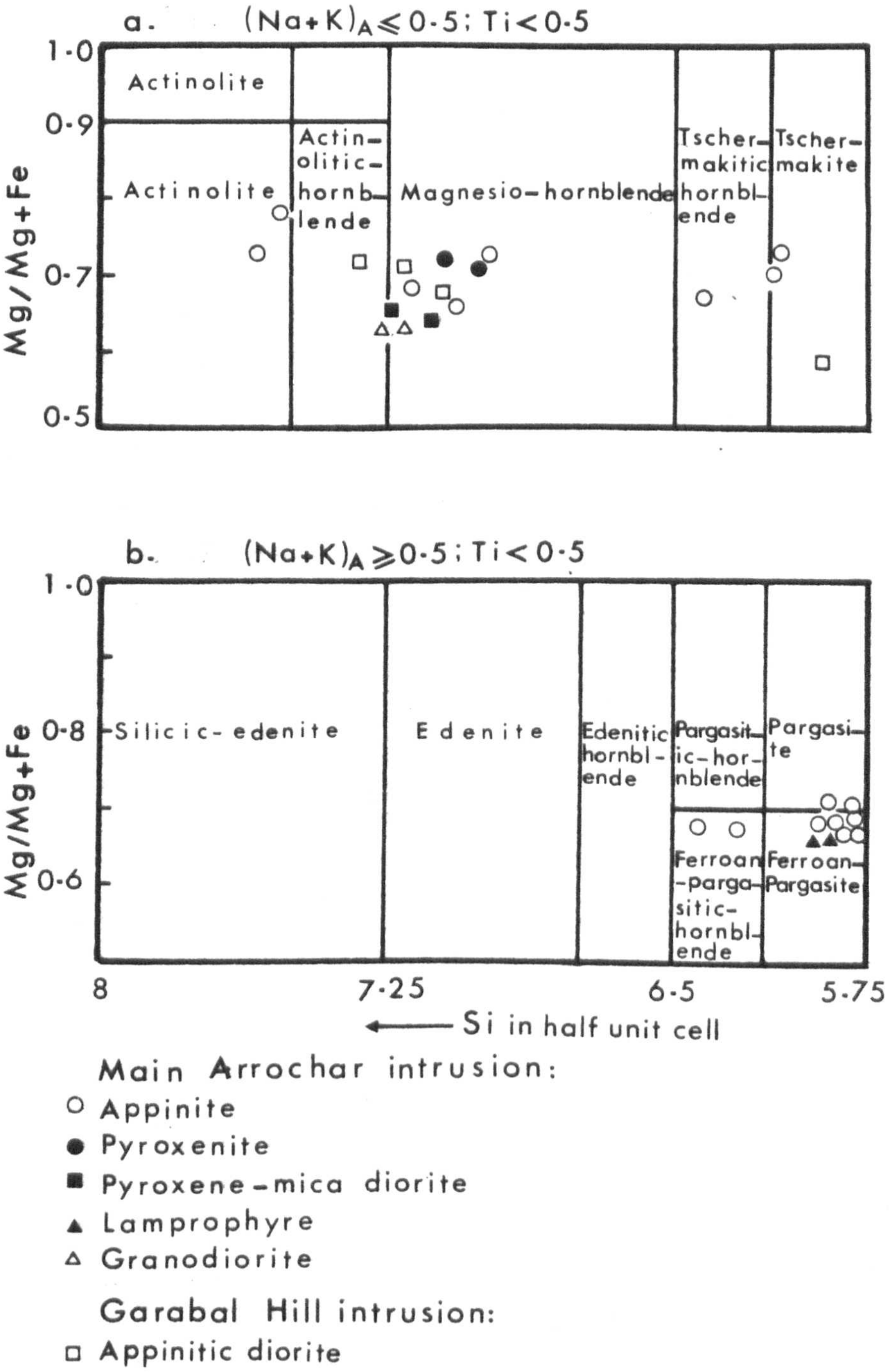

Calcic amphibole: $(Ca+Na)_B \geqslant 1{\cdot}34$; $Na_B < 0{\cdot}67$

Figure 9.7. Mica compositions from the Loch Lomond appinite suite in the main phlogopite - biotite fields (after Deer *et al.* 1966).

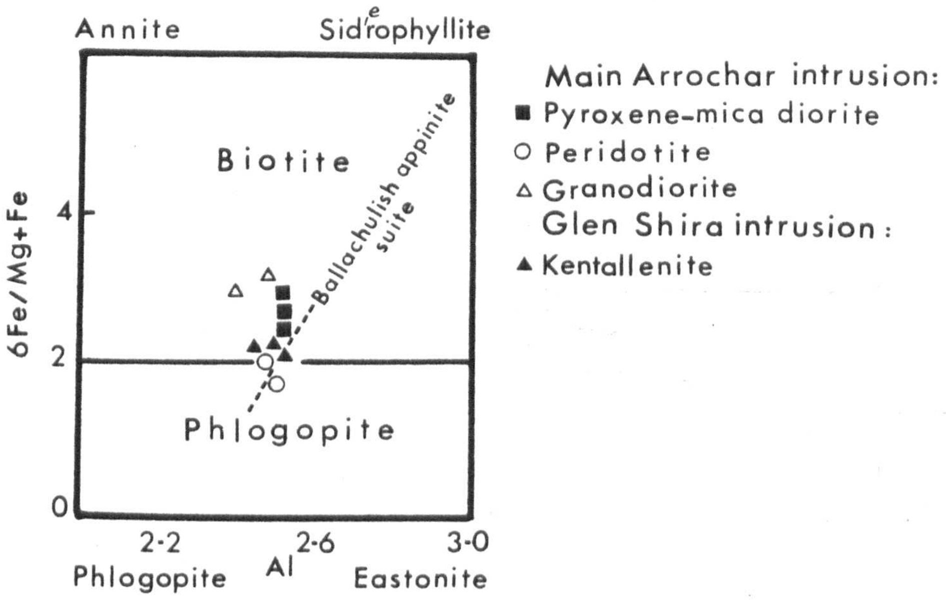
Annite
Sidérophyllite
Biotite
Ballachulish appinite suite
Phlogopite
6Fe/Mg+Fe
4
2
0
2·2
2·6
3·0
Phlogopite
Al
Eastonite
Main Arrochar intrusion:
■ Pyroxene-mica diorite
○ Peridotite
△ Granodiorite
Glen Shira intrusion:
▲ Kentallenite

Table 9.1. Means and standard deviations of the major and trace element analyses and estimated modal compositions of the representative rock types from the Loch Lomond appinite suite.

Coarse-grained rocks

	1		2		3		4*		5*	
	Mean (3 anals)	S.D.	Mean (2 anals)	S.D.	Mean (3 anals)	S.D.	Mean	S.D.	Mean	S.D.
SiO_2	44.98	4.39	46.02	1.20	47.38	1.17	52.41	4.46	54.26	1.38
TiO_2	0.55	0.09	0.57	0.34	0.97	0.44	1.12	0.46	0.69	0.12
Al_2O_3	2.87	0.37	7.86	0.46	13.90	0.52	16.02	2.50	11.63	1.13
Fe_2O_3	4.60	2.30	2.38	0.24	1.95	0.19	3.43	1.03	1.99	0.36
FeO	5.60	0.21	8.38	0.70	7.90	0.52	5.89	1.58	6.16	0.52
MnO	0.16	0.05	0.18	0.02	0.17	0.03	0.15	0.03	0.16	0.03
MgO	21.02	4.29	21.57	1.80	11.65	1.43	6.16	3.02	12.80	2.88
CaO	14.91	3.92	9.16	1.70	9.68	1.91	6.66	1.37	6.77	0.53
Na_2O	0.20	0.15	0.60	0.90	1.94	0.55	2.80	1.05	1.91	0.57
K_2O	0.08	0.07	0.42	0.00	1.44	1.03	1.84	0.72	2.47	1.09
P_2O_5	0.03	0.02	0.03	0.01	0.16	0.11	0.26	0.17	0.24	0.07
H_2O+	4.67	2.53	2.79	1.65	2.26	0.37	2.68	0.98	2.06	0.66
CO_2	0.29	0.03	0.29	0.07	0.24	0.48	0.87	0.54	0.24	0.04
Total	99.96		99.87		99.64		99.89		101.48	
Trace elements (p.p.m.)										
Cr	1271	1208	1900	424	-	-	151	140	850	176
Co	46	33	69	1	-	-	37	12	50	9
Ni	281	284	462	230	-	-	67	110	435	174
Ba	342	5.60	35	7	-	-	480	687	774	212
Ce	19	18	9	0	-	-	24	22	36	12
Cl	185	13	190	78	-	-	165	36	402	171
Cu	20	15	74	6	-	-	63	60	51	14
Ga	10	5	10	1	-	-	21	3	16	3
La	12	4	<10	-	-	-	<10	-	18	16
Nb	11	15	6	4	-	-	14	16	7	2

Pb	19	10	8	5	-	-	16	2	16	4
Rb	52	51	9	4	-	-	50	33	84	11
S	131	44	105	7	-	-	288	310	472	353
Sc	36	26	29	15	-	-	26	14	23	4
Sr	252	346	137	39	-	-	474	199	569	122
Th	18	24	4	0	-	-	16	24	11	14
V	139	39	104	26	-	-	269	163	192	27
Y	1	-	1	0	-	-	-	-	-	-
Zn	49	16	89	2	-	-	94	17	84	9
Zr	87	120	37	11	-	-	185	77	-	-

Modal analyses

Olivine	7.0	4.2	20.0	15.5	0.0	-	0.0	0.0	15.0	1.0
Orthopyroxene	Tr	-	4.0	1.4	15.5	-	0.0	0.0	1.0	0.5
Clinopyroxene	83.0	8.5	35.0	2.8	21.4	-	3.0	1.7	20.0	2.0
Amphibole	3.0	4.2	25.0	32.0	0.0	-	50.0	16.6	0.0	0.0
Biotite	2.5	3.5	2.5	3.5	6.4	-	2.0	3.7	6.0	0.5
Plagioclase	0.0	0.0	8.0	8.0	48.6	-	30.0	15.1	40.0	2.5
Anorthoclase	0.0	0.0	0.0	0.0	0.0	-	0.0	0.0	10.0	1.0
K-feldspar	0.0	0.0	0.0	0.0	8.1**	-	2.0	2.7	0.0	0.0
Quartz	0.0	0.0	0.0	0.0	0.0	-	4.0	2.8	0.0	0.0
Calcite (prim.)	0.0	0.0	0.0	0.0	0.0	-	1.0	0.0	0.0	0.0
Opaque ores	1.5	2.1	2.5	0.7	0.0	-	2.5	2.0	5.0	1.0
Apatite (prim.)	0.0	0.0	0.0	0.0	0.0	-	Tr	-	0.0	0.0
Sphene (prim.)	0.0	0.0	0.0	0.0	0.0	-	Tr	-	0.0	0.0
Chlorite (sec.)	0.5	0.7	1.0	1.4	0.0	-	2.5	3.2	0.0	0.0
Epidote (sec.)	0.0	0.0	0.0	0.0	0.0	-	0.5	1.5	0.0	0.0
Serpentine (sec.)	1.0	1.4	2.0	0.0	0.0	-	0.0	0.0	3.0	0.5
Uralite (sec.)	0.0	0.0	0.0	0.0	0.0	-	0.5	1.1	0.0	0.0
Sericite (sec.)	1.5	2.1	0.0	0.0	0.0	-	2.0	3.7	0.0	0.0
Total	100		100		100		100		100	

Table 9.1. (Contd.)

	Coarse-grained rocks					Medium-grained rocks			
	6*		7	8*		9		10	
	Mean	S.D.		Mean	S.D.	Mean (2 anals)	S.D.	Mean (2 anals)	S.D.
SiO_2	55.36	5.12	55.40	66.78	1.02	56.23	2.18	66.80	0.88
TiO_2	0.92	0.26	0.99	0.43	0.08	1.00	0.15	0.49	0.05
Al_2O_3	15.75	2.14	14.85	15.56	0.65	15.71	1.24	15.33	0.80
Fe_2O_3	1.77	0.57	2.23	1.19	0.79	2.20	0.62	1.00	0.17
FeO	5.48	1.60	6.17	2.30	0.12	5.10	0.67	2.62	0.20
MnO	0.15	0.03	0.18	0.11	0.04	0.14	0.02	0.08	0.02
MgO	5.87	2.69	5.52	1.85	0.26	4.90	1.54	1.86	0.01
CaO	7.15	2.08	7.88	2.48	1.29	6.28	0.96	2.19	1.64
Na_2O	2.81	0.54	2.56	3.87	0.24	3.11	0.38	3.46	0.20
K_2O	2.25	0.97	1.47	3.38	0.71	2.25	0.76	3.38	0.37
P_2O_5	0.21	0.11	0.15	0.16	0.03	0.22	0.07	0.18	0.02
H_2O+	1.72	0.80	2.61	1.51	0.95	2.00	1.16	2.00	1.41
CO_2	0.57	0.61	0.41	0.34	0.31	1.00	1.53	0.31	0.10
Total	100.01		100.42	99.96		100.14		99.70	
			Trace elements (p.p.m.)						
Cr	229	186	167	58	18	142	46	43	15
Co	31	12	39	9	6	28	9	14	4
Ni	71	46	57	35	27	46	39	20	12
Ba	529	238	420	695	150	621	190	550	42
Ce	29	29	25	34	29	22	16	14	8
Cl	241	64	159	176	50	181	52	168	27
Cu	71	36	105	15	10	47	29	17	10
Ga	20	4	19	19	5	22	5	16	2
La	18	15	9	26	17	11	8	18	9
Nb	8	4	10	14	5	12	3	15	1

Pb	16	6	20	20	7	14	2	21	1
Rb	64	35	33	98	30	67	31	113	32
S	222	149	245	867	1456	565	687	200	64
Sc	22	10	24	5	0.05	22	6	7	1
Sr	433	116	340	495	136	482	167	317	18
Th	16	14	12	18	25	23	28	29	36
V	200	63	238	76	17	214	53	82	11
Y	-	-	-	-	-	-	-	13	4
Zn	75	16	93	40	19	80	11	52	9
Zr	173	40	160	215	15	210	42	200	21

Modal analyses

Olivine	0.0	0.0	0.0	0.0	0.0	0.0	-	0.0	0.0
Orthopyroxene	3.0	2.0	2.0	0.0	0.0	0.0	-	0.0	0.0
Clinopyroxene	25.0	15.0	50.0	0.0	0.0	5.0	-	2.0	1.5
Amphibole	3.0	5.0	0.0	10.0	14.0	64.0	-	2.0	0.0
Biotite	15.0	3.2	1.0	10.0	2.8	0.0	-	10.0	2.8
Plagioclase	45.0	10.0	40.0	60.0	1.5	[30]	-	80.0	2.8
Anorthoclase	0.0	0.0	0.0	0.0	0.0		-	0.0	0.0
K-feldspar	1.0	1.5	2.0	5.0	7.0		-	2.0	0.0
Quartz	2.0	1.3	4.0	12.0	3.5	0.0	-	2.0	0.5
Calcite (prim.)	0.0	0.0	1.0	0.0	0.0	0.0	-	0.0	0.0
Opaque ores	4.0	3.5	0.0	1.5	0.7	Tr	-	1.0	0.5
Apatite (prim.)	Tr	-	0.0	Tr	-	0.0	-	0.0	0.0
Sphene (prim.)	Tr	-	0.0	Tr	-	0.0	-	0.0	-
Chlorite (sec.)	2.0	2.4	Tr	1.5	1.0	2.0	-	1.0	0.5
Epidote (sec.)	Tr	-	Tr	0.0	0.0	0.0	-	0.0	0.0
Serpentine (sec.)	0.0	0.0	0.0	0.0	0.0	Tr	-	0.0	0.0
Uralite (sec.)	0.0	0.0	0.0	0.0	0.0	0.0	-	0.0	0.0
Sericite (sec.)	0.0	0.0	0.0	0.0	0.0	0.0	-	0.0	0.0
Total	100		100	100		100		100	

Table 9.1. (Contd.)

1 Pyroxenite.

2 Peridotite.

3 Gabbro (Nockolds 1941).

4 Appinite.

5 Kentallenite.

6 Pyroxene - mica diorite.

7 Pyroxene diorite.

8 Granodiorite.

9 Lamprophyre.

10 Felsite or porphyritic microgranodiorite.

* Major and trace element analyses from Bowes and Wright (1979).

** Value including other accessories.

Table 9.2. Mean chemical analyses and standard deviations of pyroxenes in rocks from the appinite suite of the Loch Lomond district.

	1		2		3		4		5		6		7	
	Mean (8 anals)	S.D.	Mean (3 anals)	S.D.	Mean (2 anals)	S.D.	Mean (2 anals)	S.D.	Mean (2 anals)	S.D.	Mean (5 anals)	S.D.	Mean (2 anals)	S.D.
SiO_2	51.99	0.73	50.05	0.88	52.23	0.27	51.44	0.70	51.50	0.56	49.61	1.03	52.76	0.40
TiO_2	0.49	0.12	0.81	0.14	0.31	0.06	0.39	0.03	0.41	0.03	0.83	0.21	0.25	0.13
Al_2O_3	2.45	0.33	3.65	0.21	1.87	0.43	2.79	0.07	2.43	0.15	3.21	0.87	1.45	0.01
FeO	6.84	0.85	6.73	0.69	5.46	1.33	6.65	0.17	8.23	0.08	8.11	0.16	14.94	0.68
MnO	0.14	0.12	0.12	0.11	0.07	0.10	0.20	0.01	0.21	0.02	0.18	0.15	0.44	0.02
MgO	15.51	0.59	15.48	0.28	17.20	0.23	17.27	0.49	14.93	0.42	15.20	0.44	25.92	1.68
CaO	22.17	0.35	22.15	0.74	21.49	0.49	20.44	0.43	22.13	0.23	20.83	0.32	1.76	0.40
Na_2O	0.45	0.32	0.40	0.34	0.65	0.29	0.22	0.00	0.00	0.00	0.33	0.26	0.00	0.00
Cr_2O_3	0.00	0.00	0.55	0.12	0.60	0.48	0.00	0.00	0.00	0.00	0.09	0.09	0.00	0.00
Total	100.04		99.94		99.88		99.40		99.84		98.39		97.52	
Formulae on the basis of 6 oxygens														
Si	1.92	0.08	1.87	0.03	1.92	0.02	1.91	0.00	1.92	0.00	1.88	0.03	1.95	0.03
Ti	0.01	0.00	0.02	0.00	0.01	0.00	0.01	0.00	0.00	0.00	0.02	0.01	0.01	0.01
Al	0.11	0.01	0.15	0.01	0.08	0.01	0.12	0.01	0.10	0.01	0.14	0.04	0.06	0.01
Fe	0.21	0.03	0.19	0.01	0.17	0.04	0.20	0.01	0.26	0.00	0.25	0.00	0.46	0.07
Mn	0.01	0.00	0.01	0.00	0.00	0.00	0.01	0.00	0.01	0.00	0.01	0.00	0.01	0.00
Mg	0.85	0.03	0.85	0.01	0.94	0.01	0.94	0.00	0.83	0.01	0.85	0.01	1.43	0.07
Ca	0.88	0.01	0.88	0.04	0.85	0.01	0.81	0.01	0.88	0.02	0.85	0.01	0.07	0.01
Na	0.03	0.02	0.03	0.02	0.01	0.02	0.01	0.02	0.00	0.00	0.23	0.02	0.00	0.00
Cr	0.00	0.00	0.02	0.01	0.02	0.01	0.00	0.00	0.00	0.00	0.01	0.01	0.00	0.00
Al_4	0.08	0.00	0.13	0.04	0.08	0.02	0.09	0.00	0.08	0.00	0.12	0.01	0.05	0.03
Al_6	0.03	0.00	0.02	0.02	0.00	0.00	0.03	0.00	0.02	0.01	0.02	0.01	0.01	0.03

Table 9.2. (Contd)

1 Clinopyroxene crystals, pyroxenite, main Arrochar mass (Appendix B.3 – 8).

2 Clinopyroxene phenocrysts, appinitic diorite, Garabal Hill (Appendix B.3 – 67).

3 Clinopyroxene crystals in peridotite, Coire nan Each, southeast of the main Arrochar mass (Appendix B.3 –4).

4 Calcic - augite phenocrysts in pyroxene - mica diorite, Creag Tharsuinn, southeast of the main Arrochar mass (Appendix B.3 – 11).

5 Calcic - augite crystals in appinite, northwest of Ben Narnain, main Arrochar mass.

6 Calcic - augite phenocrysts in kentallenite, Brannie Burn mass, Glen Shira (Appendix B.3 – 49).

7 Orthopyroxene reaction rim surrounding olivine from the same specimen as in 6.

FeO = total iron.

Table 9.3. Mean chemical analyses and standard deviations of olivine in rocks from the appinite suite of the Loch Lomond district.

	1		2		3	
	Mean (2 anals)	S.D.	Mean (3 anals)	S.D.	Mean (2 anals)	S.D.
SiO_2	39.09	0.08	37.85	0.42	37.84	0.01
Al_2O_3	0.00	0.00	0.03	0.08	0.00	0.00
FeO	8.98	1.42	20.46	1.13	23.75	0.36
MnO	0.76	0.13	0.27	0.04	0.29	0.06
MgO	50.05	1.15	41.11	0.87	38.58	0.12
CaO	0.00	0.00	0.03	0.10	0.07	0.16
Cr_2O_3	0.00	0.00	0.05	0.10	0.00	0.00
Total	98.88		99.80		100.53	
	Formulae on the basis of 4 oxygens					
Si	0.99	0.005	0.98	0.003	0.98	0.00
Al	0.00	0.00	0.01	0.003	0.00	0.00
Fe	0.19	0.03	0.44	0.02	0.51	0.01
Mn	0.00	0.00	0.01	0.00	0.01	0.00
Mg	1.84	0.04	1.59	0.02	1.50	0.01
Ca	0.00	0.00	0.01	0.003	0.00	0.00
Cr	0.00	0.00	0.01	0.003	0.00	0.00
Fo-content	90.84	1.50	79.09	1.25	74.16	0.36

1 Forsteritic core of a zoned olivine phenocryst in kentallenite, Brannie Burn mass, Glen Shira (Appendix B.3 – 49).

2 Chrysolitic rim of olivine phenocryst in 1.

3 Chrysolite in pyroxene - mica diorite, Creag Tharsuinn, south-east of the main Arrochar mass (Appendix B.3 – 11).

FeO = total iron.

Table 9.4. Mean chemical analyses and standard deviations of amphiboles in rocks from the appinite suite of the Loch Lomond district.

	1		2	3		4		5	6		7	
	Mean (2 anals)	S.D.		Mean (2 anals)	S.D.	Mean (2 anals)	S.D.		Mean (3 anals)	S.D.	Mean (2 anals)	S.D.
SiO_2	42.75	0.37	40.39	40.55	0.30	41.24	0.33	40.94	41.94	1.34	48.16	3.02
TiO_2	2.84	0.38	2.52	2.44	0.17	3.14	0.13	4.45	2.60	0.01	0.53	0.20
Al_2O_3	12.05	0.30	12.35	12.16	0.56	12.82	0.15	11.92	11.32	0.90	8.46	2.53
FeO	10.97	0.46	11.55	11.55	0.15	11.68	0.27	15.05	12.12	0.32	11.25	0.67
MnO	0.18	0.01	0.00	0.00	0.00	0.00	0.00	0.00	0.05	0.01	0.13	0.12
MgO	15.10	0.59	14.55	14.21	0.28	13.91	0.13	11.17	14.18	0.42	15.24	0.95
CaO	11.60	0.10	12.00	11.85	0.08	11.56	0.31	11.11	11.25	0.15	11.62	0.27
Na_2O	2.14	0.28	1.59	1.93	0.31	2.35	0.00	1.67	1.62	0.54	1.28	0.02
K_2O	0.58	0.02	1.32	1.22	0.02	0.83	0.05	1.12	0.7	0.53	0.40	0.00
Cr_2O_3	0.00	0.00	0.00	0.12	0.17	0.00	0.00	0.00	0.11	0.19	0.00	0.00
Total	98.21		96.27	96.03		97.53		97.43	95.89		95.65	

Formulae on the basis of 23 oxygens

Si	6.23	0.01	6.07	6.11	0.01	6.12	0.01	6.15	6.29	0.20	6.87	0.33
Ti	0.31	0.04	0.28	0.27	0.02	0.35	0.01	0.50	0.29	0.01	0.06	0.02
Al	2.07	0.07	2.19	2.16	0.08	2.23	0.01	2.11	2.00	0.16	1.56	0.47
Fe	1.34	0.07	1.45	1.45	0.01	1.44	0.05	1.89	1.49	0.04	1.38	0.06
Mn	0.02	0.00	0.00	0.00	0.00	0.00	0.00	0.00	0.01	0.01	0.02	0.01
Mg	3.28	0.10	3.26	3.19	0.91	3.06	0.01	2.50	1.59	1.73	3.34	0.14
Ca	1.81	0.00	1.93	1.91	0.03	1.83	0.04	1.79	1.85	0.06	1.83	0.07
Na	0.6	0.07	0.46	0.56	0.08	0.67	0.01	0.49	0.47	0.15	0.36	0.18
K	0.11	0.00	0.25	0.23	0.01	0.15	0.01	0.21	0.30	0.20	0.07	0.01
Cr	0.00	0.00	0.00	0.01	0.00	0.00	0.00	0.00	0.10	0.02	0.00	0.00
Al_4	1.77	0.007	1.93	1.89	0.01	1.88	0.01	1.85	1.71	0.06	1.13	0.33
Al_6	0.30	0.08	0.26	0.27	0.07	0.35	0.01	0.26	0.29	0.04	0.43	0.14

	8	9		10		11		12		13	14	15
		Mean (2 anals)	S.D.	Mean (2 anals)	S.D.	Mean (2 anals)	S.D.	Mean (2 anals)	S.D.			
SiO_2	46.44	48.16	0.87	49.46	0.38	49.65	0.70	49.29	0.28	50.61	52.42	53.66
TiO_2	0.74	0.79	0.04	0.82	0.23	0.45	0.40	0.80	0.30	0.48	0.00	0.00
Al_2O_3	6.62	6.31	0.06	5.96	0.30	5.73	0.03	5.36	0.51	4.99	3.93	3.64
FeO	11.60	13.17	0.51	12.53	0.81	14.73	0.23	15.12	0.43	12.11	9.15	11.26
MnO	0.15	0.18	0.02	0.30	0.03	0.28	0.14	0.78	0.06	0.25	0.23	0.34
MgO	15.92	14.83	0.35	15.37	0.75	14.58	0.01	13.74	0.15	16.93	18.44	16.68
CaO	10.83	11.46	0.45	11.93	0.17	11.42	0.31	11.53	0.40	11.00	11.98	12.55
Na_2O	1.41	1.27	0.22	1.26	0.27	1.28	0.24	0.73	0.13	0.66	0.00	0.62
K_2O	0.23	0.25	0.03	0.45	0.035	0.53	0.03	0.28	0.05	0.32	0.00	0.12
Cr_2O_3	0.16	0.00	0.00	0.43	0.61	0.00	0.00	0.00	0.00	0.00	0.00	0.17
Total	94.10	96.42		98.51		98.65		97.63		97.35	96.15	99.04
					Formulae on the basis of 23 oxygens							
Si	7.00	7.13	0.05	7.15	0.07	7.20	0.07	7.25	0.49	7.32	7.54	7.59
Ti	0.08	0.09	0.00	0.09	0.03	0.05	0.04	0.09	0.00	0.05	0.00	0.00
Al	1.18	1.10	0.02	1.01	0.05	0.98	0.01	0.93	0.08	0.85	0.67	0.61
Fe	1.46	1.63	0.08	1.51	0.09	1.78	0.03	1.86	0.04	1.47	1.10	1.33
Mn	0.02	0.02	0.01	0.03	0.01	0.03	0.02	0.09	0.01	0.03	0.03	0.04
Mg	3.58	3.27	0.04	3.31	0.17	3.20	0.05	3.01	0.01	3.65	3.95	3.51
Ca	1.75	1.77	0.01	1.84	0.02	1.77	0.49	1.82	0.07	1.71	1.85	1.90
Na	0.41	0.36	0.06	0.35	0.08	0.36	0.07	0.21	0.04	0.19	0.00	0.17
K	0.04	0.04	0.01	0.08	0.01	0.1	0.01	0.05	0.01	0.06	0.00	0.02
Cr	0.02	0.00	0.00	0.05	0.01	0.00	0.00	0.00	0.00	0.00	0.00	0.02
Al_4	1.00	0.87	0.05	0.85	0.01	0.80	0.07	0.75	0.49	0.68	0.46	0.41
Al_6	0.18	0.23	0.03	0.16	0.02	0.18	0.06	0.18	0.03	0.17	0.21	0.20

Table 9.4. (Contd.)

1 Pargasite in pegmatitic appinite, Coire nan Each, south of the main Arrochar mass (Appendix B.3 —3).

2 Ferroan pargasite in appinite, northwest of Ben Narnain, main Arrochar mass.

3 Ferroan - pargasite, appinite (Appendix B.3 — 1); locality as in 1.

4 Ferroan - pargasitic - hornblende, pegmatitic appinite (Appendix B.3 — 3); locality as in 1.

5 Tschermakite, appinitic diorite, Garabal Hill (Appendix B.3 — 67).

6 Tschermakitic - hornblende, appinite, locality as in 2.

7 Magnesio - hornblende, pyroxenite, main Arrochar mass (Appendix B.3 — 8).

8 Magnesio - hornblende, appinite, locality as in 2.

9 Magnesio - hornblende, pegmatitic appinite (Appendix B.3 — 3); locality as in 1.

10 Magnesio - hornblende, appinitic diorite (Appendix B.3 — 67); locality as in 5.

11 Magnesio - hornblende in pyroxene - mica diorite, Creag Tharsuinn, southeast of the main Arrochar mass (Appendix B.3 — 11).

12 Magnesio - hornblende, central granodiorite, main Arrochar mass (Appendix B.3 — 17).

13 Actinolitic - hornblende, appinitic diorite (Appendix B.3 — 67); locality as in 5.

14 Actinolite, appinite, locality as in 2.

15 Actinolite, pegmatitic appinite (Appendix B.3 — 3); locality as in 1.

FeO = total iron.

Table 9.5. Mean chemical analyses and standard deviations of micas in rocks of the Loch Lomond appinite suite.

	1		2		3		4	
	Mean (3 anals)	S.D.	Mean (3 anals)	S.D.	Mean (2 anals)	S.D.	Mean (2 anals)	S.D.
SiO_2	35.99	0.30	36.04	0.37	36.54	0.16	37.22	0.49
TiO_2	5.18	1.05	5.80	0.61	4.28	0.12	4.62	1.30
Al_2O_3	14.24	0.12	14.05	0.44	13.70	0.39	14.38	0.27
FeO	18.35	2.19	14.71	0.27	20.18	0.70	13.18	1.01
MnO	0.04	0.06	0.06	0.11	0.41	0.80	0.07	0.10
MgO	12.98	0.92	14.42	0.71	11.60	0.06	17.23	2.23
CaO	0.02	0.03	0.13	0.03	0.00	0.00	0.00	0.00
Na_2O	0.11	0.16	0.15	0.25	0.00	0.00	0.23	0.32
K_2O	9.39	0.27	10.04	0.15	9.98	0.13	9.56	0.09
Cr_2O_3	0.04	0.05	0.08	0.14	0.00	0.00	0.00	0.00
Total	96.34		95.48		96.69		96.49	
Formulae on the basis of 22 oxygens								
Si	5.34	0.07	5.42	0.03	5.56	0.05	5.46	0.01
Ti	0.58	0.12	0.66	0.08	0.49	0.01	0.51	0.15
Al	2.53	0.03	2.49	0.05	2.45	0.06	2.49	0.01
Fe	2.31	0.26	1.85	0.05	2.57	0.08	1.62	0.14
Mn	0.01	0.01	0.01	0.02	0.05	0.01	0.01	0.01
Mg	2.91	0.22	3.23	0.13	2.63	0.02	3.75	0.44
Ca	0.01	0.01	0.02	0.01	0.00	0.00	0.00	0.00
Na	0.03	0.04	0.04	0.07	0.00	0.00	0.65	0.09
K	1.80	0.06	1.93	0.03	1.93	0.35	1.77	0.01
Cr	0.01	0.01	0.01	0.01	0.00	0.00	0.00	0.00
Al_4	2.51	0.01	2.49	0.05	2.44	0.04	2.49	0.01
Al_6	0.02	0.03	0.00	0.00	0.01	0.01	0.00	0.00

1 Biotite in pyroxene - mica diorite, Creag Tharsuinn, main Arrochar mass (Appendix B.3 – 11).

2 Biotite in kentallenite, Brannie Burn mass, Glen Shira (Appendix B.3 – 49).

3 Biotite, central granodiorite, main Arrochar mass (Appendix B.3 – 17).

4 Phlogopite in peridotite, Coire nan Each southeast of the main Arrochar mass (Appendix B.3 – 4).

FeO = total iron.

Table 9.6. Chemical analyses of feldspars in rocks from the appinite suite of the Loch Lomond district.

	1	2	3 Mean (2 anals)	S.D.	4	5	6 (2 anals)	S.D.
SiO_2	62.93	63.94	62.73	0.47	68.18	61.51	60.43	0.38
TiO_2	0.00	0.00	0.69	0.04	0.00	0.00	0.00	0.00
Al_2O_3	18.31	18.18	19.97	0.16	19.58	23.72	24.75	0.01
FeO	0.00	0.58	0.34	0.03	0.28	0.15	0.04	0.10
MnO	0.00	0.00	0.00	0.00	0.15	0.00	0.00	0.00
CaO	0.00	0.00	1.35	0.08	0.17	4.97	5.78	0.2
Na_2O	0.00	3.21	5.68	0.34	11.34	8.59	8.43	0.07
K_2O	16.56	11.40	9.45	0.33		0.60	0.26	0.01
Total	97.80	97.31	100.21		99.70	99.54	99.69	

Formulae on the basis of 8 oxygens

Si	2.98	2.99	2.88	0.01	2.99	2.75	2.69	0.01
Ti	0.00	0.00	0.02	0.01	0.00	0.00	0.00	0.00
Al	1.02	1.00	1.10	0.01	1.01	1.25	1.29	0.01
Fe	0.00	0.02	0.01	0.00	0.01	0.01	0.05	0.01
Mn	0.00	0.00	0.00	0.00	0.01	0.00	0.00	0.00
Ca	0.00	0.00	0.06	0.01	0.01	0.24	0.28	0.00
Na	0.00	0.29	0.42	0.03	0.96	0.74	0.72	0.01
K	1.00	0.68	0.50	0.02	0.00	0.03	0.01	0.01
Al_4	0.02	0.01	0.12	0.01	0.01	0.25	0.31	0.01
Al_6	1.01	0.99	0.98	0.01	1.00	1.00	0.98	0.01

	7	8	9 Mean (3 anals)	S.D.	10 Mean (3 anals)	S.D.	11	12	13
SiO_2	57.32	57.74	60.15	1.20	56.35	1.32	54.01	50.96	53.26
TiO_2	0.00	0.00	0.00	0.00	0.00	0.00	0.00	0.00	0.24
Al_2O_3	25.60	25.98	24.21	1.02	27.22	0.83	28.01	30.55	28.33
FeO	0.16	0.27	0.20	0.04	0.20	0.17	0.46	0.73	0.37
MnO	0.33	0.00	0.00	0.00	0.00	0.00	0.00	0.00	0.00
CaO	7.66	7.78	6.98	0.54	10.04	1.05	10.52	13.63	11.94
Na_2O	6.60	6.91	8.72	0.63	6.06	0.73	5.35	3.95	6.11
K_2O	0.35	0.46	0.21	0.09	0.27	0.06	0.35	0.34	0.21
Total	98.02	99.14	100.47		100.14		98.70	100.16	100.46

Formulae on the basis of 8 oxygens

Si	2.62	2.62	2.71	0.02	2.54	0.45	2.47	2.32	2.43
Ti	0.00	0.00	0.00	0.00	0.00	0.00	0.00	0.00	0.01
Al	1.38	1.49	1.28	0.03	1.45	0.04	1.51	1.64	1.55
Fe	0.01	0.01	0.01	0.00	0.01	0.01	0.02	0.03	0.01
Mn	0.01	0.00	0.00	0.00	0.00	0.00	0.00	0.00	0.00
Ca	0.37	0.40	0.29	0.03	0.48	0.06	0.52	0.66	0.54
Na	0.58	0.65	0.68	0.05	0.52	0.57	0.48	0.35	0.46
K	0.02	0.03	0.01	0.01	0.02	0.00	0.02	0.02	0.01
Al_4	0.38	0.38	0.29	0.02	0.46	0.04	0.53	0.68	0.57
Al_6	1.00	1.11	0.99	0.01	0.99	0.01	0.98	0.96	0.98

Table 9.6. (Contd.)

1 Orthoclase in lamprophyre, Creag Tharsuinn, southeast of the main Arrochar mass.

2 Anorthoclase, lamprophyre; locality as in 1.

3 Anorthoclase in kentallenite, Brannie Burn mass, Glen Shira (Appendix B.3 – 49).

4 Albite in appinite, Coire nan Each, southeast of the main Arrochar mass (Appendix B.3 – 1).

5 Oligoclase, pegmatitic appinite (Appendix B.3 – 3); locality as in 4.

6 Oligoclase, kentallenite (Appendix B.3 – 49); locality as in 3.

7 Andesine, appinite (Appendix B.3 – 1); locality as in 4.

8 Andesine, pyroxene - mica diorite (Appendix B.3 - 11); locality as in 1.

9 Andesine, appinitic diorite, Garabal Hill (Appendix B.3 – 67).

10 Andesine, central granodiorite, main Arrochar mass (Appendix B.3 – 17).

11 Labradorite, pyroxene - mica diorite (Appendix B.3 – 11); locality as in 1.

12 Labradorite, peridotite, main Arrochar mass (Appendix B.3 – 4).

13 Labradorite, kentallenite (Appendix B.3 – 49); locality as in 3.

FeO = total iron.

CHAPTER 10 PETROCHEMISTRY

Using 92 representative specimens of the appinite suite from the main Arrochar intrusion (18), Inversnaid intrusion (5), Glen Gyle intrusions (11), Ben Glas intrusions (5), Cruachan Cruinn intrusions (7), Glen Shira intrusions (12) and Garabal Hill - Glen Fyne intrusion (34; including 20 major element analyses from Nockolds 1941), it can be shown that the overall variation from ultramafic to mafic and, less frequently to feldspathic types ranges from 34 to 68 wt. % SiO_2 (Appendix B.3; also see Fig. 10.1). On an alkali *vs.* SiO_2 diagram most of the compositions follow a continuous differentiation trend and lie in an elongate field which largely corresponds with the field of the high alumina basalt series but with representatives in the field of the tholeiitic series and others in the field of the mildly alkaline rock series (Fig. 10.1). This indicates greater affiliation with the calcalkaline characters than that shown by the Ballachulish appinite suite. On an AFM plot, there is considerable spread, however, basic, intermediate and acidic types define a trend which generally corresponds with that for calcalkaline rock series (Fig. 10.2). This is particularly the case for the intermediate and acidic compositions as was the case for the appinite suite of the Ballachulish district. However, for the majority of the ultramafic rocks the overall trend of the composition is generally parallel to that at the basic part of the field of alkali olivine basalt series with evidence of high iron enrichment. On the basis of these features the Loch Lomond appinite suite is considered to be part of a normal calcalkaline series.

10.1 Major element variations

The continuous variation in the major element chemistry of the suite is shown by plots of S.I. *vs.* various oxides. These also serve to indicate the close affinity of the Ballachulish and Loch Lomond suites. The continuous curvilinear trends shown by plots of both MgO and Al_2O_3 *vs*. S.I. reflect fractionation and the progressive development from ultramafic to acidic compositions (Figs. 10.3a, b). The greater scatter of Al_2O_3 at values of S.I. < 35 reflects the crystallisation of Ca-rich plagioclase in appinites and pyroxene - mica diorites (Chapter 9). The Na_2O *vs*. S.I. plot shows a corresponding pattern.

The general trend shown by FeO *vs*. S.I. plots also points to the same fractionation process with the greater spread above S.I. values of 30 reflecting the crystallisation of the opaque ores in some of the appinites (Fig. 10.3c). It also shows the replacement of the dominant olivine and clinopyroxene fractionation in some ultramafic rocks (lower FeO) by the dominant amphibole fractionation in appinites (higher FeO). Variations in TiO_2 also indicate the same features as shown by FeO.

The considerable scatter of CaO above S.I. values of 60 indicates the dominant olivine fractionation in dunite (< 1 wt. % CaO), olivine and clinopyroxene fractionation in peridotites (and certain pyroxenites) (8-12 wt. % CaO) and the dominant clinopyroxene fractionation in pyroxenite (19 wt. % CaO) (Fig. 10.3d). The flat pattern shown for the 60 - 35 range of S.I. indicates the similar proportions of Ca-rich (clinopyroxene, plagioclase and amphibole) and Ca-poor (olivine and mica) phases in these rocks. The decreasing CaO below S.I. value of 30 indicates the progressive domination of the plagioclase fractionation in the intermediate and acidic rocks.

The petrogenetic information obtained from oxide *vs*. S.I. plots is consistent with crystallisation differentiation that produced rocks ranging in composition from ultramafic to acidic types from a common parent magma. The pronounced differentiation of olivine and clinopyroxene, particularly in the early stages shown by the occurrence of monomineralitic rocks such as dunite and pyroxenite in the larger masses of Garabal Hill and Arrochar resulted in a wider range of compositional variation than that shown for the Ballachulish appinite suite. In addition, the lower MgO/S.I. and higher Al_2O_3/S.I. ratios compared to those of the Ballachulish cluster, are indicative of the relatively lower MgO and higher Al_2O_3 in the parent magma (Figs. 10.3a, b).

10.2 Fractional crystallisation on the basis of CMAS model

Assessment of plots in the CMAS tetrahedron model of Cox *et al.* (1979) provides the following information concerning the successive appearance of different phases on the liquidus under varying physical conditions during the various stages of fractional crystallisation:

1. The affinity of the position of dunite to that of olivine in the projections from Qtz into the En-Ky-Wol plane and from Ky into the En-Wol-Fo plane show that olivine fractionation dominated the early stages of crystallisation (Figs. 10.4a, b).
2. On the evidence that peridotites and pyroxenites lie on a trend that defines olivine - clinopyroxene fractionation in a projection from Ky into the En-Wol-Fo plane, the olivine fractionation was followed and replaced by clinopyroxene fractionation (Fig. 10.4b).
3. Compositional plots of hornblendites and appinites follow a trend that defines clinopyroxene - amphibole - biotite fractionation in the above projection (Fig. 10.4b). This indicates that clinopyroxene fractionation was successively followed by amphibole and biotite fractionation.
4. The affinity of compositional plots of the feldspathic pyroxene - mica diorites, hornblende diorites and granodiorites to the position of feldspar in both the projections from Qtz into the En-Ky-Wol plane and from Ky into the En-Plag-Qtz plane and the gap and bend shown in both projections (Fig. 10.4a, c) indicate that plagioclase fractionation dominated in the latter stages of crystallisation.

10.2A Discussion and comparison based on CMAS model

The successive fractionation of olivine, clinopyroxene, amphibole, biotite and plagioclase that indicates variation in P_{Gas} (Chapter 9; also see Chapters 3-6), resulted in the progressive development of ultramafic, mafic, intermediate and feldspathic rock types (*cf.* Fig. 10.4a). Apart from certain ultramafic rocks the majority of the analyses plot in the fields shown for the Ballachulish appinite suite in all the above projections (Figs. 10.4a - c). This indicates a general correspondence between the petrogenetic histories of the Ballachulish and Loch Lomond clusters.

10.3 Trace element chemistry

The general variation trends shown by Ni, Cr and Co *vs.* MgO plots also reflect differentiation and the progressive evolution of ultramafic, mafic, intermediate and acidic rock types (Fig. 10.5a - c). In addition, there is a general correspondence with the fields established for the Ballachulish appinite suite. This indicates that fractionation processes similar to those determined for the Ballachulish cluster (Chapter 7), were operative in the development of the rock types of the Loch Lomond cluster. This is consistent with the interpretation based on the major element chemistry. The extremely high Cr contents of certain pyroxenites and peridotites (> 1600 p.p.m.) reflects the high degree of clinopyroxene fractionation in these rocks. The scatter in Cr *vs.* MgO plots for 16 - 8 wt. % MgO is probably related to the variable proportions of clinopyroxene, amphibole and plagioclase in appinites, pyroxene - mica diorites and kentallenites (Fig. 10.5b).

The spread shown by V *vs.* Fe_2O_3 with the possible separation into two trends, one being flatly disposed and the high V contents (> 400 p.p.m.) of some of the rocks (Fig. 10.5d) are interpreted as resulting from the crystallisation of opaque ores, particularly titan - magnetite, in certain appinites which are markedly rich in TiO_2 (Appendix B.3 – 1, 3, 5, 24, 40).

The relatively limited compositional range indicated by Rb *vs.* K_2O plots and the lower average K/Rb ratio (300) for the Loch Lomond cluster as compared to the Ballachulish cluster probably reflect the lower K_2O content in the parent liquid of the former suite (Figs. 10.5e, f). The exceptionally high K/Rb ratios in certain rock types (700 - 2000) can be attributed to the contamination or re-equilibration of these rocks during the intrusion of the Newer granites.

On the basis of a Zr/Y *vs.* Zr plot and comparison with the compositional fields of basalts in different geotectonic environments, many of the rocks lie in or close to the field of "within plate basalts" (Fig. 10.6). This indicates a continental tectonic setting.

10.4 The nature of the parent magma

The nature of the parent magma for the appinite suite particularly in the Loch Lomond region, has been the subject of controversy ever since Nockolds (1941) considered it to be represented by the pyroxene - mica diorite of the Garabal Hill - Glen Fyne complex. Later workers have thought the parental magma to be somewhat more basic (Money 1964; McArthur 1971). The present investigation supports the latter view for the following reasons:

1. The average pyroxene - mica diorite composition (P) lies closer to the acidic than the basic end of the series on oxide *vs.* S.I. diagrams (Figs. 10.3a - d) and in a projection from Qtz into the En-Ky-Wol plane (Fig. 10.4a). Thus it seems unlikely for it to have given the cumulates dunite, peridotite and pyroxenite.
2. If the pyroxene - mica diorite does represent the parent liquid, then all the rock types that plot towards its basic side in the above mentioned variation diagrams, may represent its cumulates, and their minerals should be expected to show similar compositions to those in pyroxene - mica diorite. However, the clinopyroxenes from pyroxenite and peridotite and micas from peridotite and kentallenite

correspond with a more basic rock composition than that of the pyroxene - mica diorite (*cf.* Figs. 9.5, 9.7). This shows that the latter type was itself derived from a more basic magma.

There is a general correspondence between the Loch Lomond and Ballachulish clusters on the basis of most of the major and trace element plots and on the basis of plots into CMAS model. As the parent magma of the former is interpreted to contain relatively lower MgO and higher Al_2O_3 than for the latter (Section 10.1), a composition for the parent magma of the Loch Lomond cluster is considered to be approximately midway between that of the pyroxene - mica diorite of Nockolds (1941) and the mean kentallenite composition at Ballachulish (Table 2.1 – 6). This is consistent with the closer affinity of the Loch Lomond suite to the high alumina basalt series and the greater affinity of the Ballachulish suite to the more alkaline series (see Figs. 10.1, 7.1).

10.5 Conclusions

1. The major and trace element chemistry of the Loch Lomond appinite suite is consistent with crystallisation differentiation of a normal calcalkaline magma that evolved in continental tectonic environment.
2. A parent liquid of composition intermediate between the average pyroxene - mica diorite of Nockolds (1941) and the mean kentallenite of the Ballachulish region is suggested as the starting point for fractionation in the Loch Lomond region.
3. The successive fractionation of olivine, clinopyroxene, amphibole, biotite and plagioclase indicates variation in P_{Gas}.
4. There is a general similarity in compositions and petrogenesis between the appinite suites of the Loch Lomond and Ballachulish districts.

Figure 10.1. Alkali *vs.* SiO_2 diagram for the Loch Lomond appinite suite with division into various fields for basaltic series after Schwarzer and Rogers (1974).

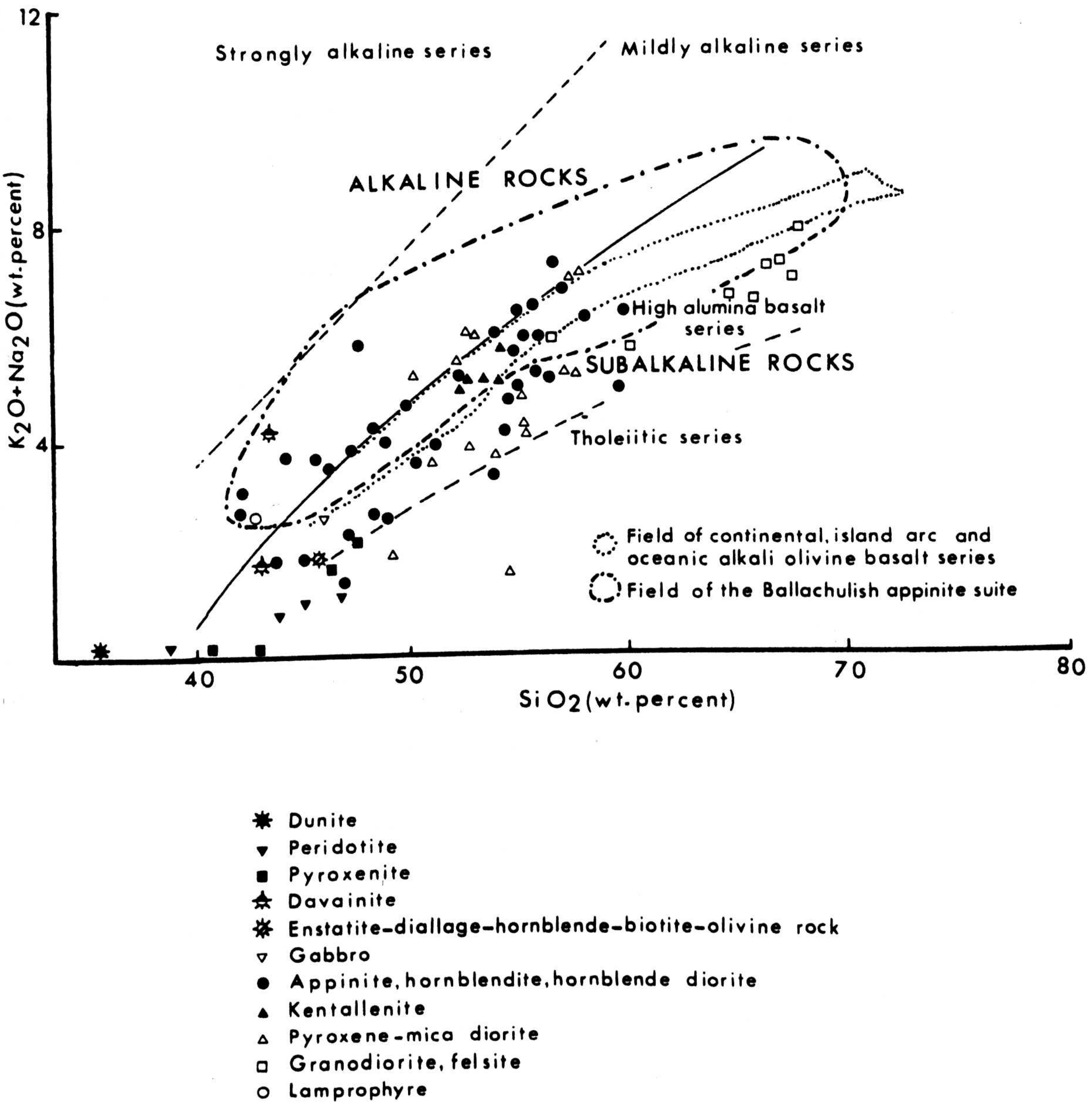
Strongly alkaline series
Mildly alkaline series
ALKALINE ROCKS
High alumina basalt series
SUBALKALINE ROCKS
Tholeiitic series
Field of continental, island arc and oceanic alkali olivine basalt series
Field of the Ballachulish appinite suite
K2O+Na2O (wt.percent)
12
8
4
SiO2 (wt.percent)
40
50
60
70
80
✱ Dunite
▼ Peridotite
■ Pyroxenite
☆ Davainite
✱ Enstatite-diallage-hornblende-biotite-olivine rock
▽ Gabbro
● Appinite, hornblendite, hornblende diorite
▲ Kentallenite
△ Pyroxene-mica diorite
□ Granodiorite, felsite
○ Lamprophyre

Figure 10.2. AFM diagram for the Loch Lomond appinite suite with division into various fields for basaltic series after Schwarzer and Rogers (1974).

Figure 10·2

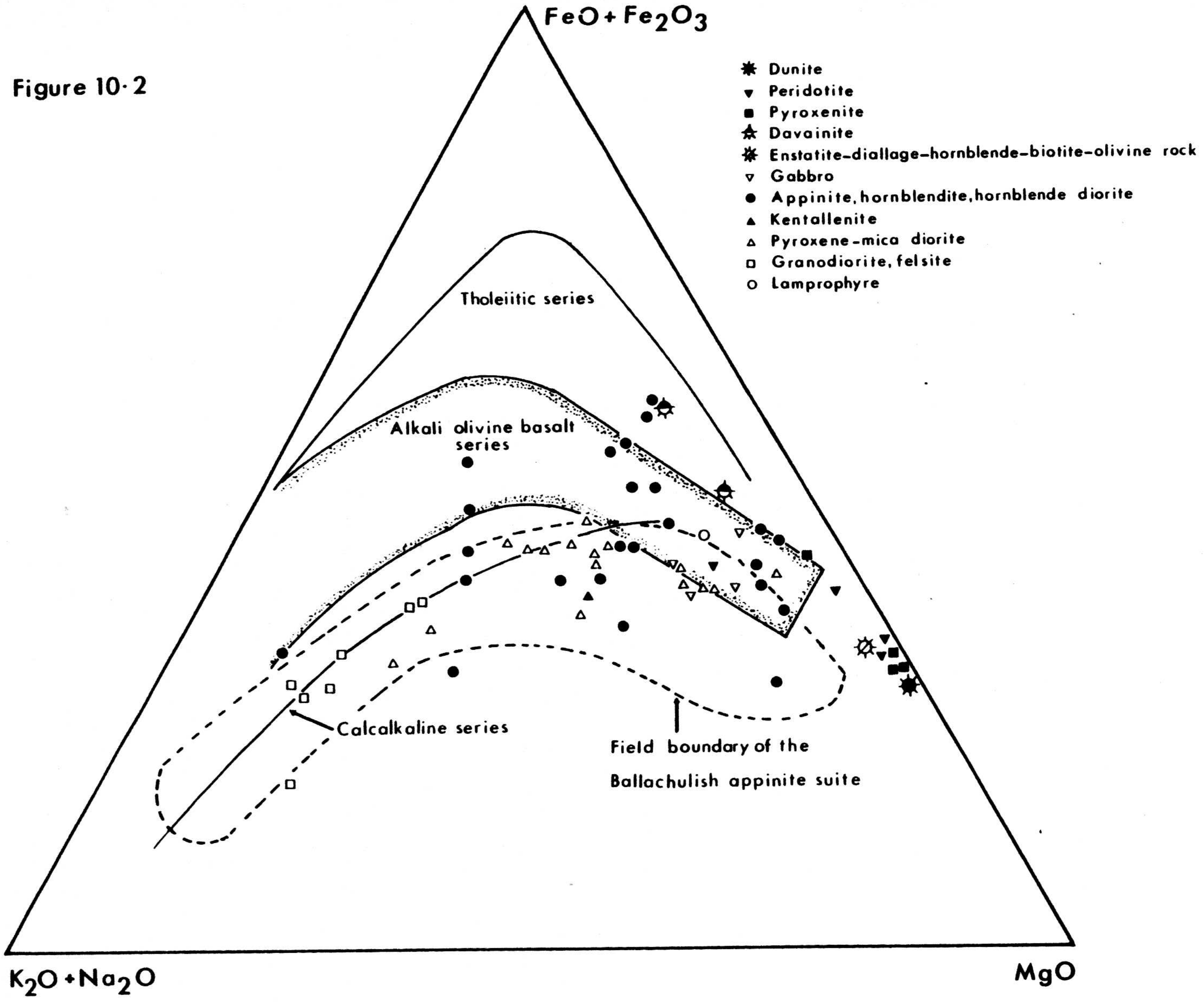
FeO + Fe_2O_3
K_2O + Na_2O
MgO
✱ Dunite
▼ Peridotite
■ Pyroxenite
☆ Davainite
✱ Enstatite–diallage–hornblende–biotite–olivine rock
▽ Gabbro
● Appinite, hornblendite, hornblende diorite
▲ Kentallenite
△ Pyroxene–mica diorite
□ Granodiorite, felsite
○ Lamprophyre
Tholeiitic series
Alkali olivine basalt series
Calcalkaline series
Field boundary of the Ballachulish appinite suite

Figure 10.3 (a - d). Plots of MgO, Al_2O_3, FeO and CaO against S.I., respectively (symbols as in Fig. 10.2).

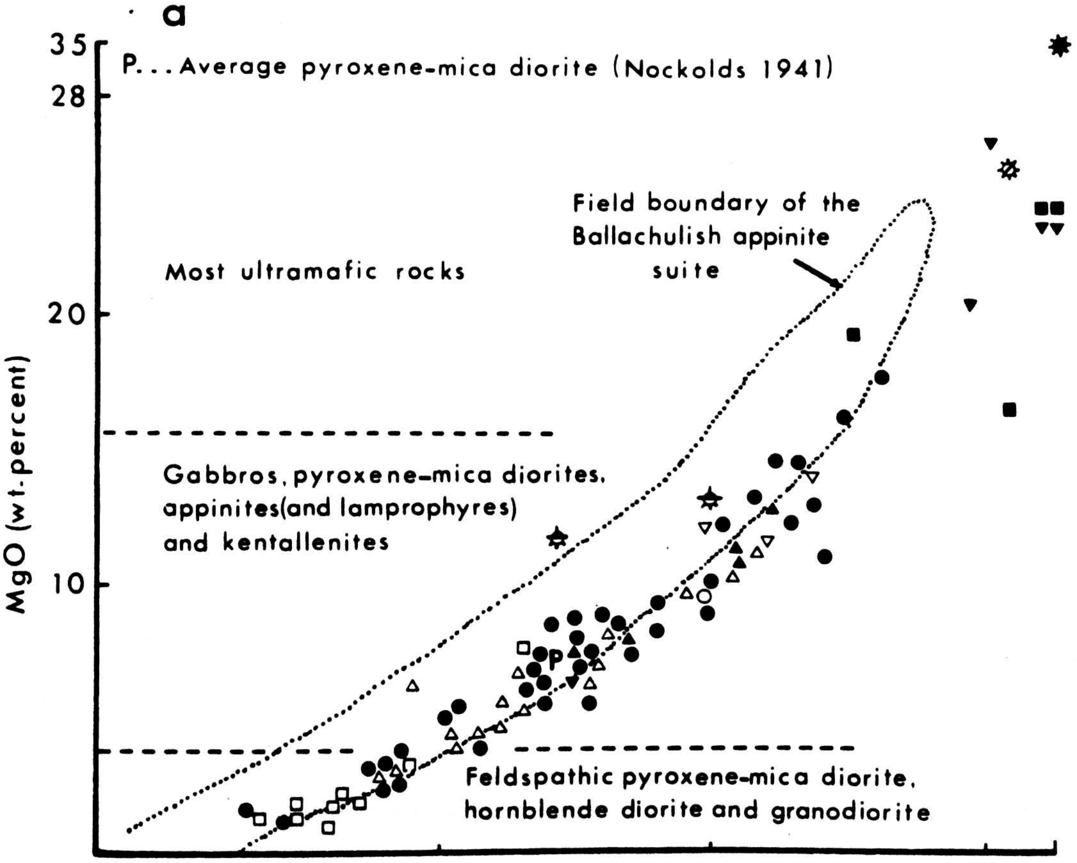
a
35
28
20
10
MgO (wt.percent)
P...Average pyroxene-mica diorite (Nockolds 1941)
Most ultramafic rocks
Field boundary of the Ballachulish appinite suite
Gabbros, pyroxene-mica diorites, appinites(and lamprophyres) and kentallenites
Feldspathic pyroxene-mica diorite, hornblende diorite and granodiorite
P

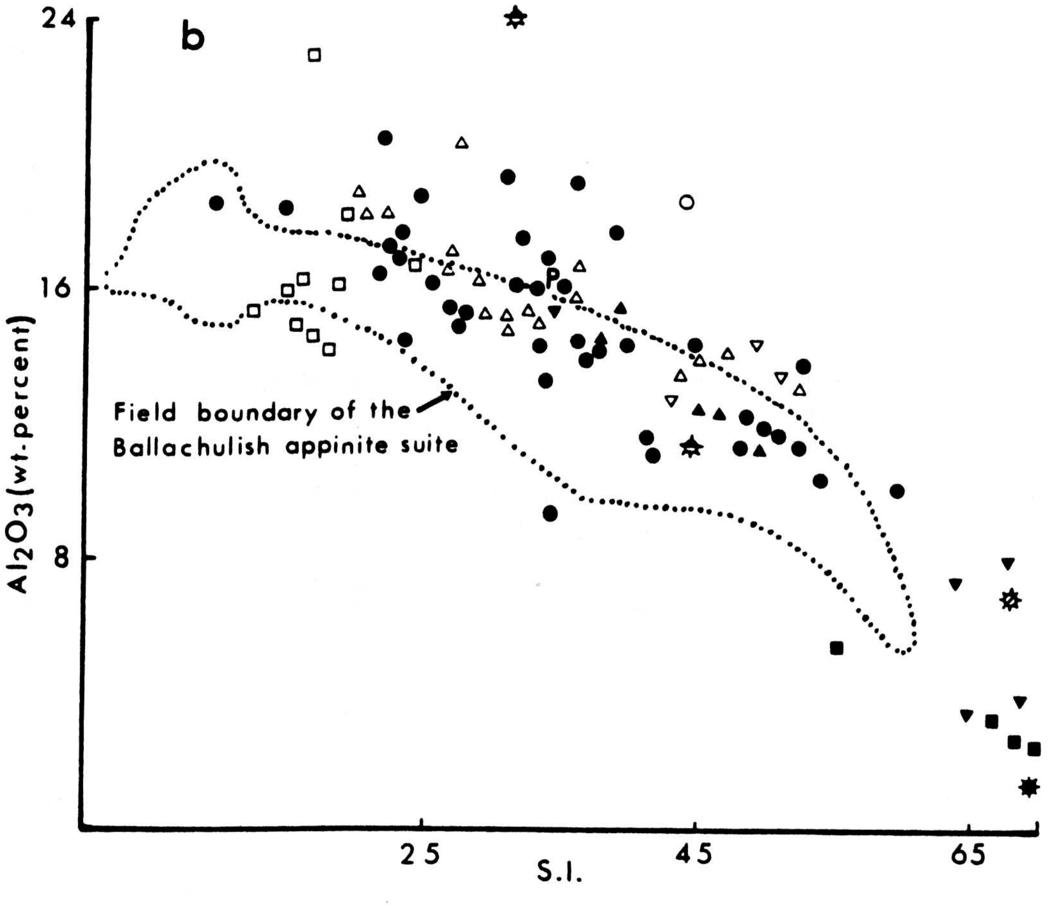
b
24
16
8
Al2O3 (wt.percent)
Field boundary of the Ballachulish appinite suite
P
25
45
65
S.I.

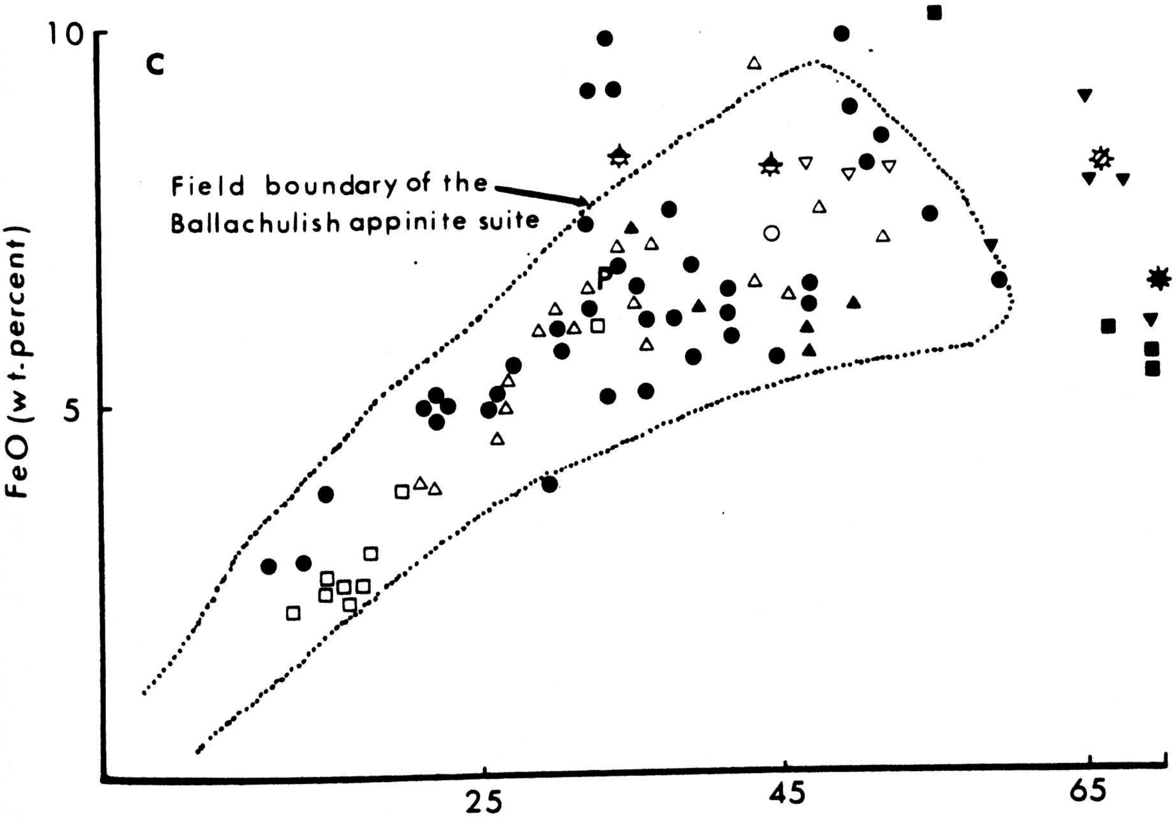
c
Field boundary of the Ballachulish appinite suite
P
FeO (wt.percent)
10
5
25
45
65

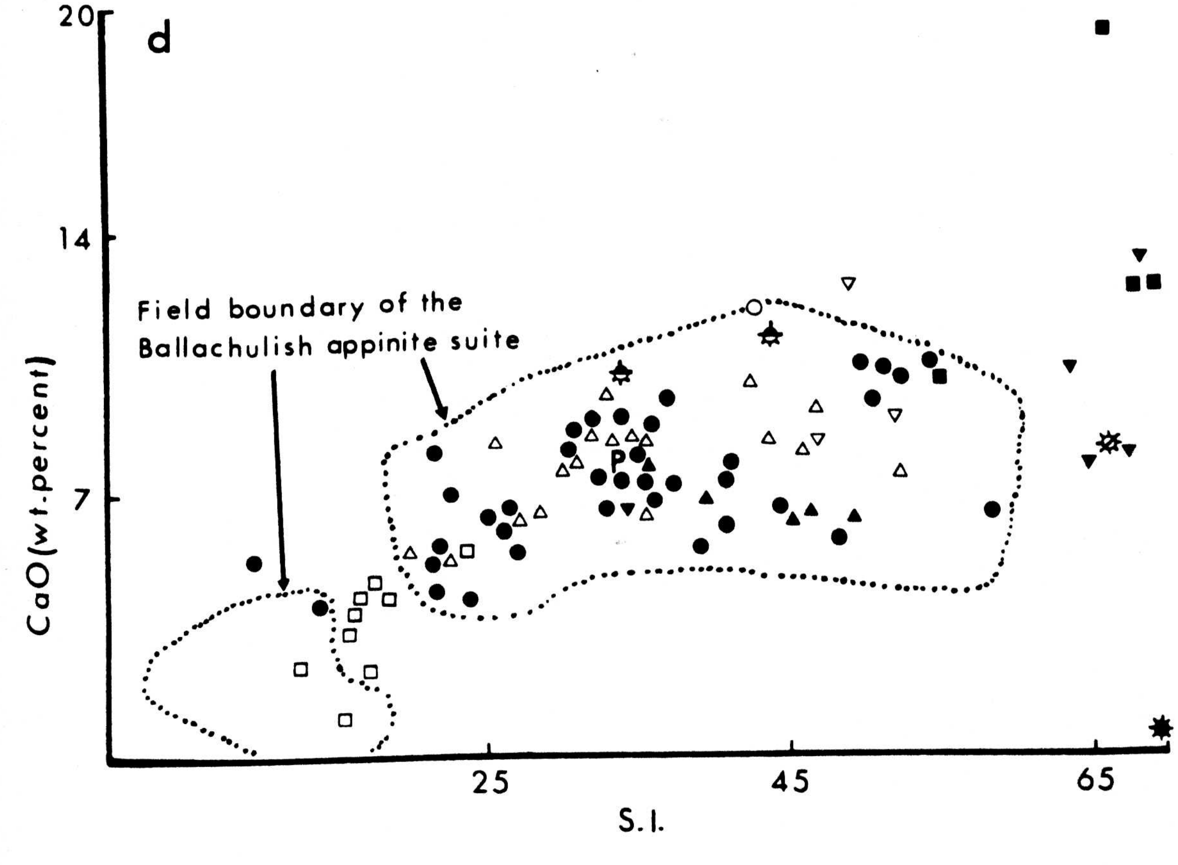
d
Field boundary of the Ballachulish appinite suite
P
CaO (wt.percent)
20
14
7
25
45
65
S.I.

Figure 10.4 (a - c). Variation of the Loch Lomond appinite suite, and its comparison with the Ballachulish appinite suite, in the CMAS fractionation model shown by projections into various planes from particular points.

Figure 10·4a

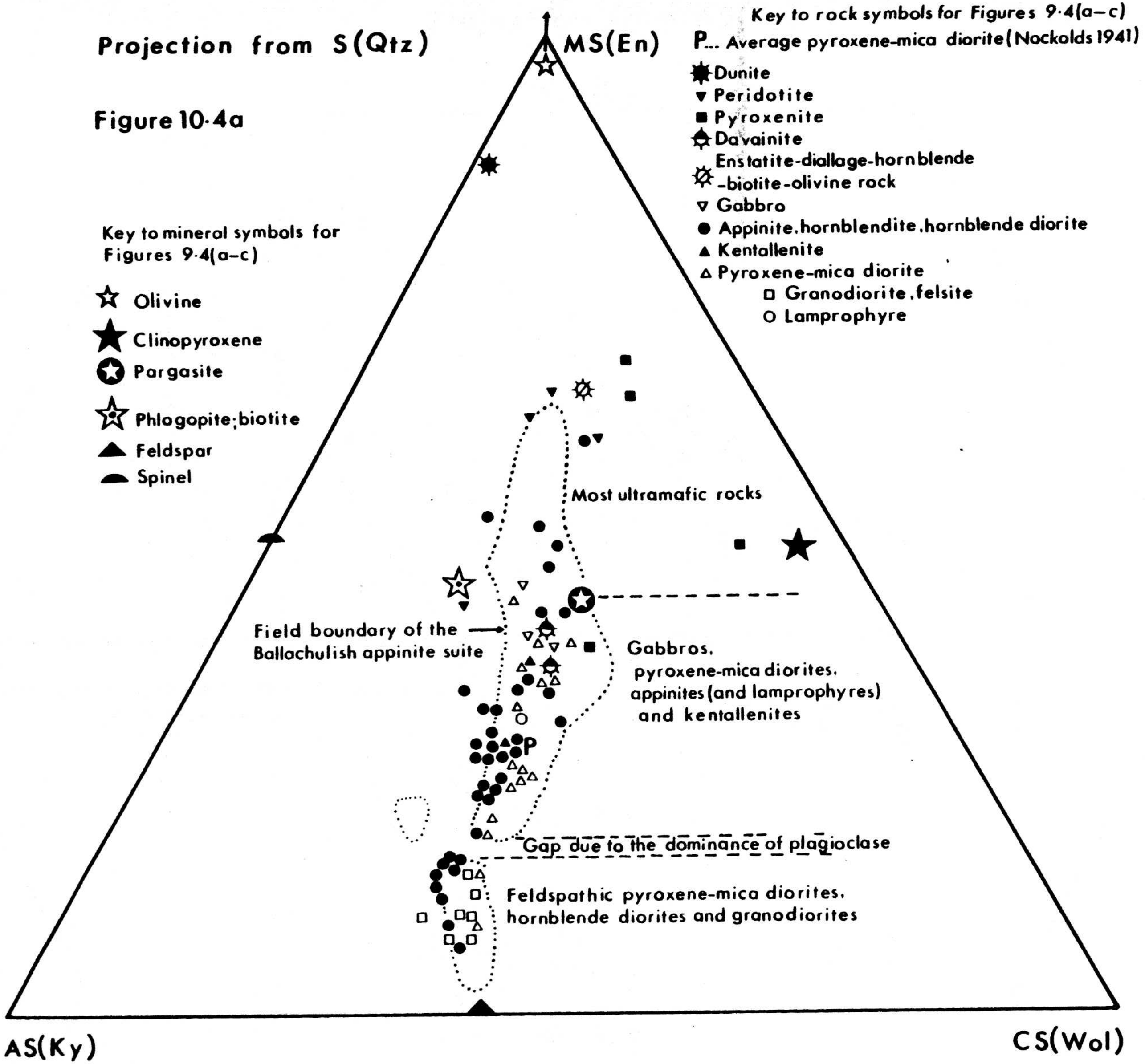
Projection from S(Qtz)
MS(En)
AS(Ky)
CS(Wol)
Key to mineral symbols for Figures 9·4(a–c)
☆ Olivine
★ Clinopyroxene
Pargasite
Phlogopite; biotite
▲ Feldspar
Spinel
Key to rock symbols for Figures 9·4(a–c)
P... Average pyroxene-mica diorite (Nockolds 1941)
Dunite
▼ Peridotite
■ Pyroxenite
Davainite
Enstatite-diallage-hornblende-biotite-olivine rock
▽ Gabbro
● Appinite, hornblendite, hornblende diorite
▲ Kentallenite
△ Pyroxene-mica diorite
□ Granodiorite, felsite
○ Lamprophyre
Most ultramafic rocks
Field boundary of the Ballachulish appinite suite
Gabbros, pyroxene-mica diorites, appinites (and lamprophyres) and kentallenites
P
Gap due to the dominance of plagioclase
Feldspathic pyroxene-mica diorites, hornblende diorites and granodiorites

Fig. 10·4b

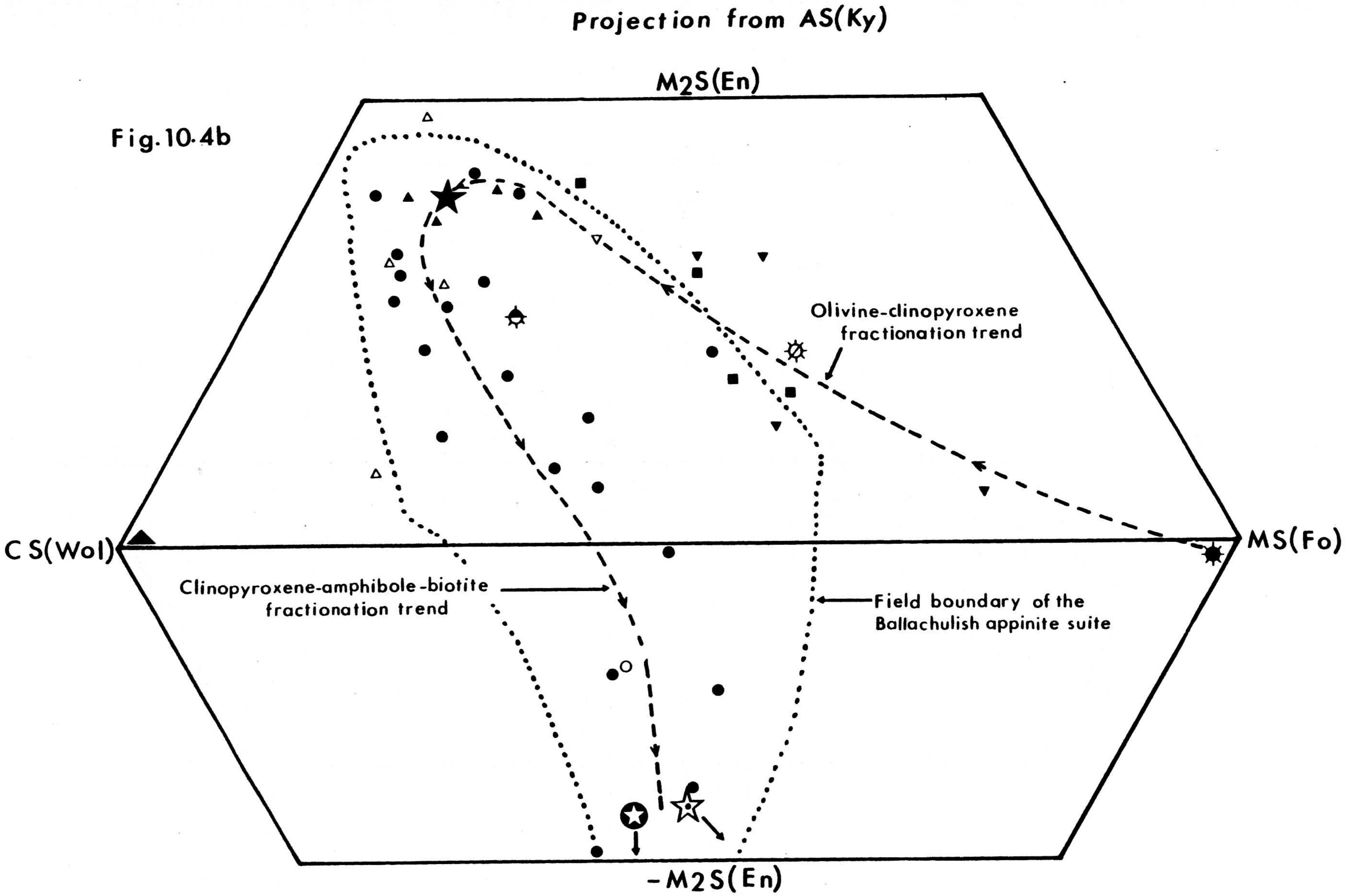

Projection from AS(Ky)

Fig.10.4c

Projection from AS(Ky)

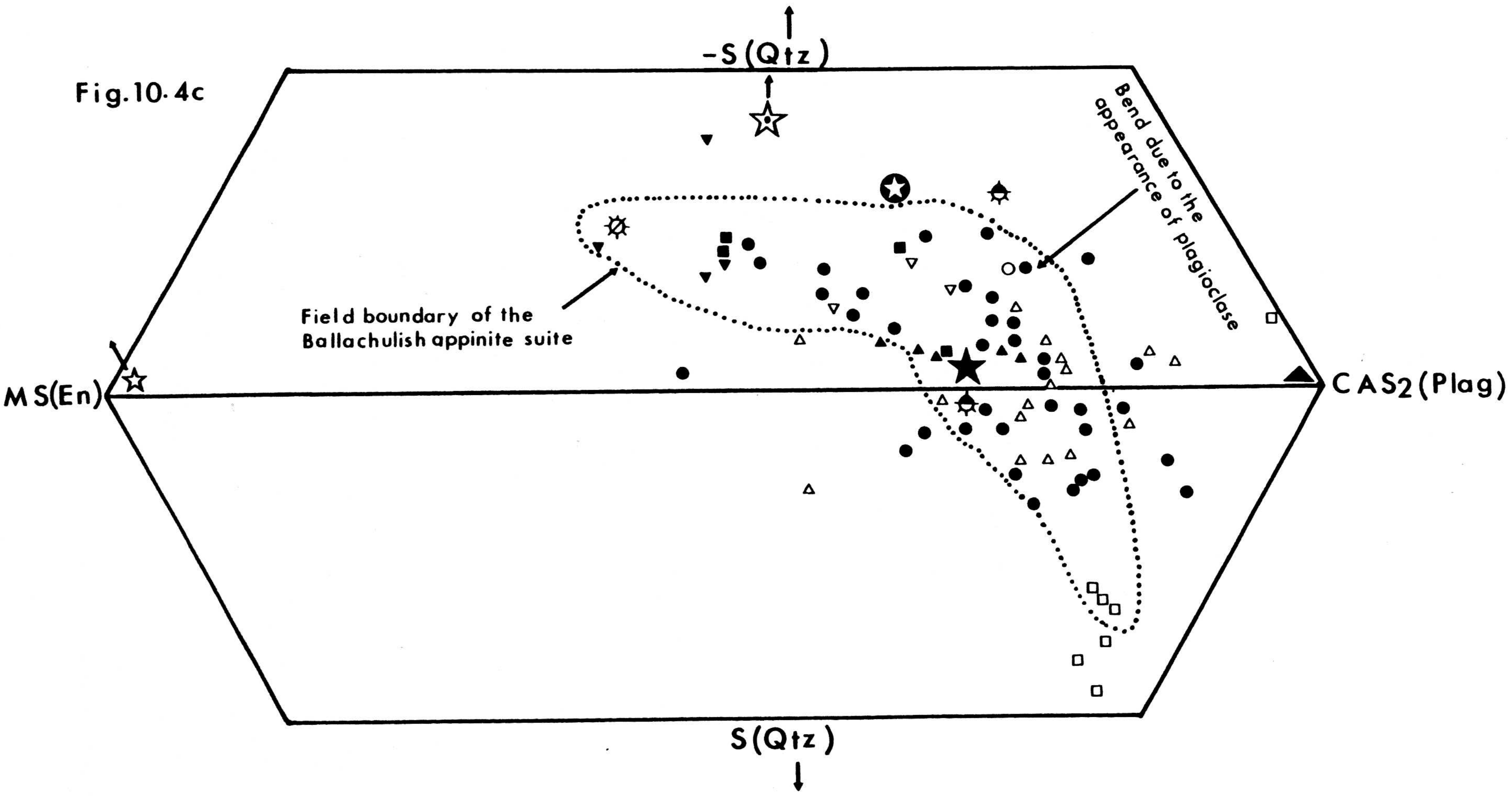

Figure 10.5 (a - f). Plots of Ni, Cr and Co *vs.* MgO, V *vs.* Fe_2O_3, Rb *vs.* K_2O and K/Rb *vs.* K_2O, respectively.

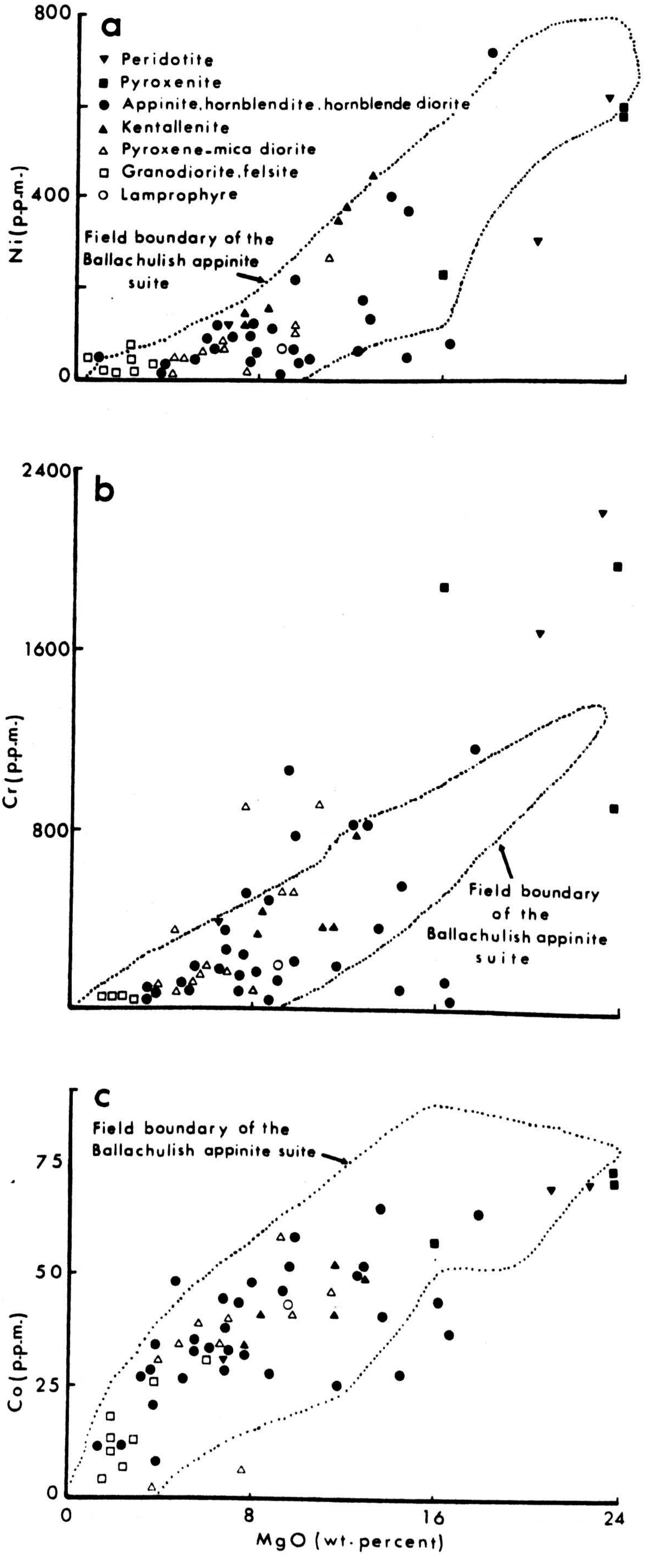
a
▼ Peridotite
■ Pyroxenite
● Appinite, hornblendite, hornblende diorite
▲ Kentallenite
△ Pyroxene-mica diorite
□ Granodiorite, felsite
○ Lamprophyre
Field boundary of the Ballachulish appinite suite
Ni (p.p.m.)
800
400
0
b
Cr (p.p.m.)
2400
1600
800
Field boundary of the Ballachulish appinite suite
c
Field boundary of the Ballachulish appinite suite
Co (p.p.m.)
75
50
25
0
0
8
16
24
MgO (wt. percent)

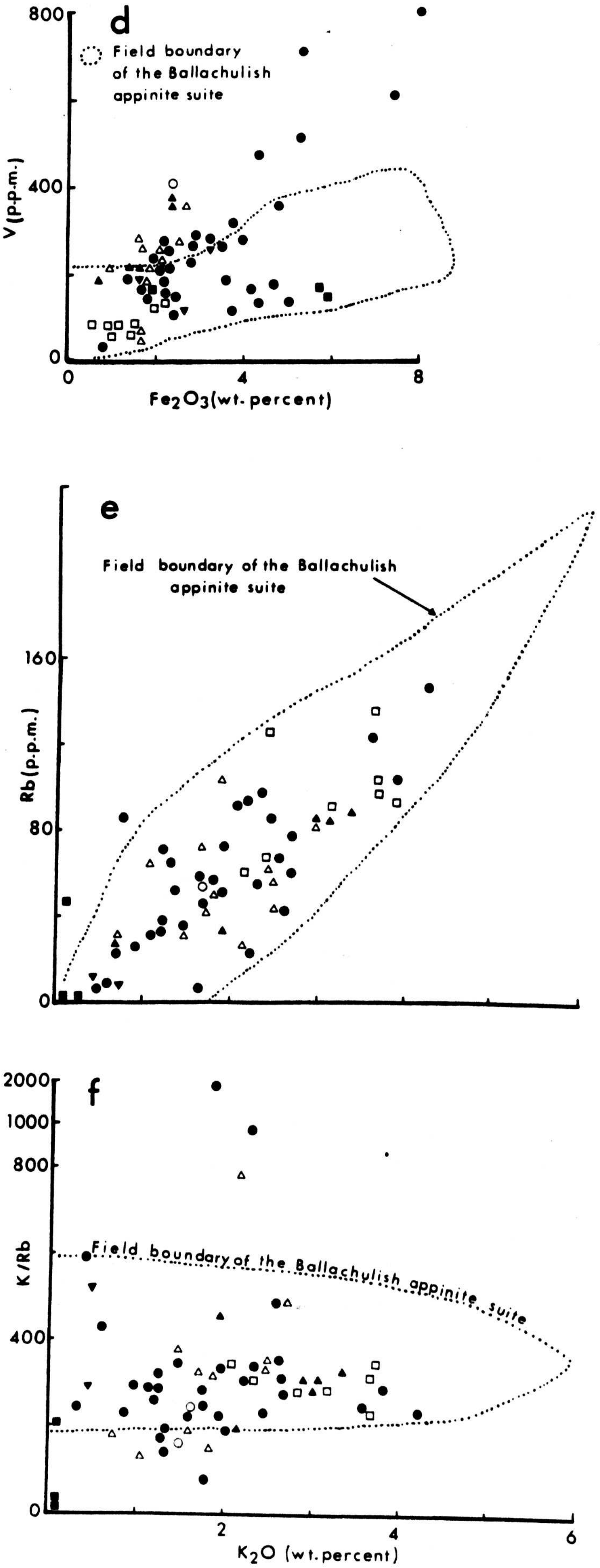
d
Field boundary of the Ballachulish appinite suite
V(p.p.m.)
800
400
0
0
4
8
Fe2O3(wt. percent)
e
Field boundary of the Ballachulish appinite suite
Rb(p.p.m.)
160
80
0
f
2000
1000
800
400
0
K/Rb
Field boundary of the Ballachulish appinite suite
2
4
6
K2O (wt.percent)

Figure 10.6. Plots of Zr/Y *vs*. Zr and comparison with compositional fields of basalts in different geotectonic environments (after Pearce and Norry 1979).

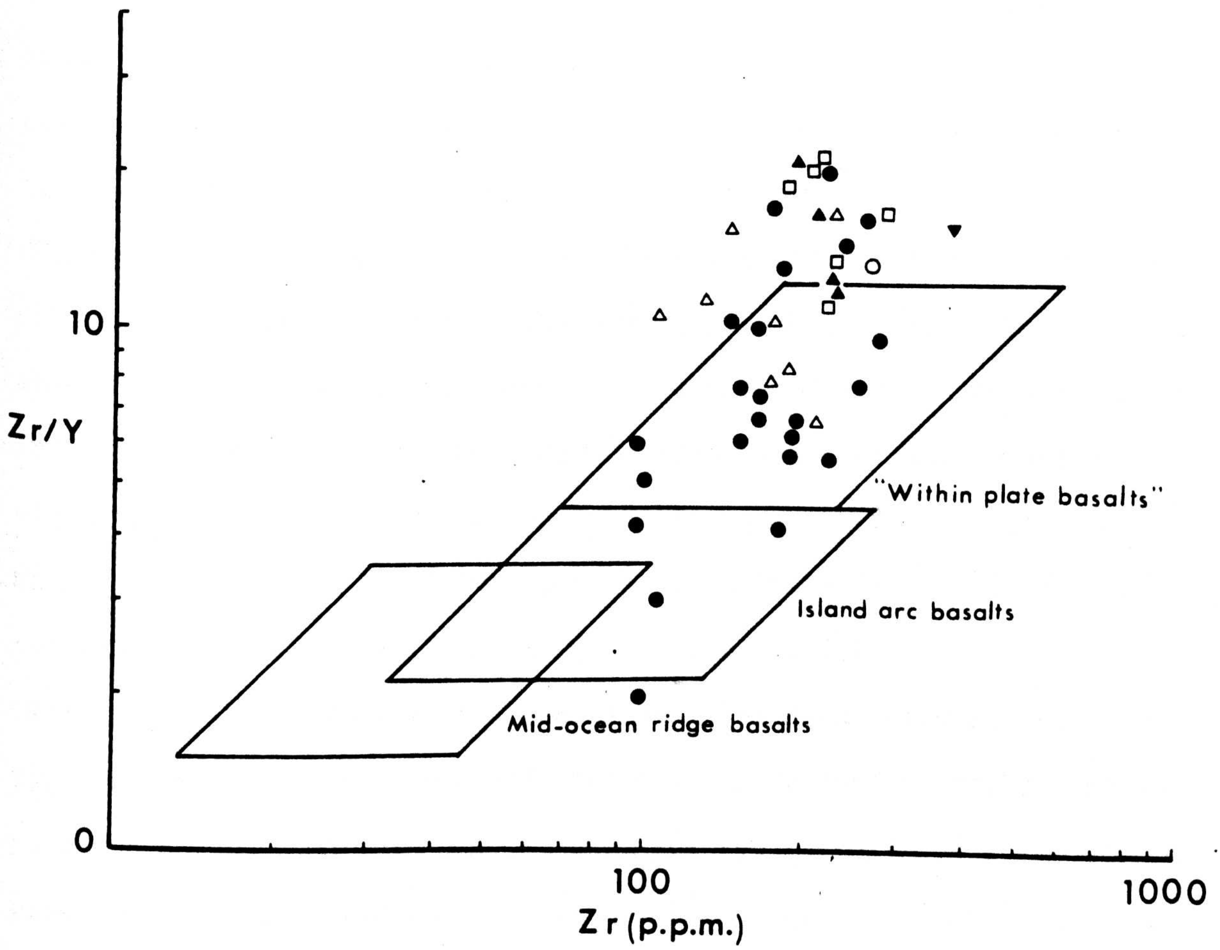
Zr/Y
10
0
Zr (p.p.m.)
100
1000
"Within plate basalts"
Island arc basalts
Mid-ocean ridge basalts

CHAPTER 11 PETROGENESIS

There are clear parallels between the Loch Lomond and Ballachulish appinite suites. The differences that do exist can be accounted for in terms of differences in the "primary" magma (these are related to overall geotectonic position -- see Chapter 13) and in the gas pressure reached in the various pipes before the explosive activity took place.

The regular patterns of the major and trace element plots, the successive fractionation of olivine, clinopyroxene, amphibole, mica and plagioclase shown by the CMAS plots and the coincidence or parallism of the trends from different intrusions and with those at Ballachulish, indicate both the cognate nature of the suite and the dominant control of fractional crystallisation (Section 10.1, 10.2, 10.3). The considerable petrographic variation seen can be accounted for by crystallisation under variable P_{Gas}, from an original magma of normal calc-alkaline characters with a composition intermediate between the average pyroxene-mica diorite of Nockolds (1941) and the mean kentallenite of the Ballachulish region (Section 9.2, 9.4; also see Chapter 10). Olivine$_{(Fo_{91-74})}$ from both the kentallenite of Glen Shira and the pyroxene-mica diorite of the main Arrochar intrusion generally corresponds in composition with olivine from the kentallenite of the Kentallen pipe and from the lamprophyric marginal facies of the Ardsheal Hill pipe, at Ballachulish; this indicates the appearance of olivine on the liquidus at c. 1800°C with a pressure c.25 kb and at a depth of 70-80 km (c.f. Sections 9.2; also see Chapters 3, 8). Apart from slight differences, the pyroxenes, amphiboles, micas and plagioclases from various rock types in the various pipes of the Loch Lomond cluster also show a general correspondence in composition to those from the Ballachulish cluster; crystallisation at P_{H_2O} of c. 1-4 kb is indicated (c.f. Table 11.1; Sections 9.2 - 9.5). This, and the association of explosion-breccia with the igneous rocks and the type of deformation shown by the country rocks, all indicate that emplacement occurred at high crustal levels, as at Ballachulish (c.f. Section 8.1; McArthur 1971).

11.1 Crystallisation history in relation to emplacement and explosive activity

11.1A Main Arrochar intrusion

The occurrence of a finer-grained diorite and kentallenite as a marginal facies to the diorite which makes up the major part of the intrusion and the presence of olivine in these rocks (Section 9.2) indicates the emplacement of magma from depth. The reaction rim of orthopyroxene surrounding olivine in the marginal kentallenite indicates a temperature range of 1550° - 1500°C and a P_{H_2O} of <1 kb for this stage of crystallisation (c.f. Section 8.1A). This indicates the emplacement of high temperature magma high up into the crust with retention of temperature sufficiently elevated for orthopyroxene crystallisation. The relatively large grain size of the main mass of diorite is related to the volume of the intruding magma. With decreasing temperature clinopyroxene appeared on the liquidus probably at a temperature of c. 1125°C (c.f. Section 8.1A). The presence of biotite and the reaction rim of amphibole surrounding clinopyroxene, indicating increased P_{H_2O} (c. 2 - 4 kb) in magma and a temperature of 900° - 770°C, is related to the release of gas phase due to the clinopyroxene crystallisation and to the restriction of gas uprise presumably by a structural trap (c.f. Sections 5.2, 5.3, 8.1, 9.2). The finer grain size of the groundmass which crystallised at a P_{H_2O} of <1 kb (and at a temperature of <770°C) points to a pressure decrease in the magma following the development of the reaction rims of amphibole on clinopyroxene phenocrysts. The occurrence of explosion-breccia seen in the marginal parts of the intrusion (McArthur 1971, map 4) indicates that this pressure decrease is related to the first phase of explosive activity which may have occurred at a P_{H_2O} of 4 kb and at a temperature of 770°C (Table 11.1).

On the basis of CMAS plots, and of a primary magma that was relatively less basic than that at Ballachulish (c.f. Sections 10.2, 10.4), the ultramafic rocks and some of the appinites represent cumulates while all of the diorites represent liquid compositions. The highly fractured and deformed nature of hornblende crystals in the appinite and peridotite west of Creag Tharsuinn and northwest of Ben Narnain is consistent with the emplacement of disrupted cumulates as crystal mushes while the presence of lamprophyric margins points to the emplacement of residual liquid. The emplacement of large "blocks" of disrupted cumulates together with crystal mushes and residual liquid is shown in these intrusions by the association of pyroxenite ("block(s)" of cumulates) with peridotite (crystal mush derived as disrupted cumulate) and appinite (crystals of disrupted cumulate in residual liquid).

The successive fractionation of clinopyroxene, amphibole and mica now present in the ultramafic rocks, appinite and hornblende-rich coarse-grained diorite (Sections 9.2, 10.2) indicates crystallisation conditions of decreasing temperature (c. 1125° - 770°C) but increasing P_{H_2O} (< 1 - 4 kb) which must correspond to the period of crystal accumulation. In both the appinite and the hornblende-rich diorite the medium-grained feldspathic groundmass represents the composition of residual liquid which crystallised under decreased P_{H_2O} (< 1 kb) and temperature (< 770°C). This points to a second phase of explosive activity in the main Arrochar intrusion corresponding to that deduced for some of the intrusions at Ballachulish (P_{H_2O} of c. 4 kb and T of 770°C; Table 11.1; also see Sections 8.1A, C, D).

On the basis of chemical features, the central granodiorite (McArthur 1971, map 4) is consistent with being a complementary feldspathic differentiate of the other rock types of the complex (Sections 10.1 - 10.3). Evidence related to the transfusion of breccia blocks by appinitic magma, like those seen in the Gleann Chàrnan and Rudha Mòr pipes of the Ballachulish region (c.f. Sections 8.1C-E), is lacking at Arrochar. Thus the development of granodiorite can be related to the emplacement of an uncontaminated residual liquid that was probably trapped at relatively deeper level during explosive activity. The dominant fractionation of plagioclase shown by CMAS plots (Section 10.2) points to crystallisation conditions corresponding to those for the matrix of diorites (c.f. Table 11.1).

11.1B Other intrusions of the Loch Lomond suite

The petrogenesis of the other masses of the Loch Lomond cluster can be accounted for in the same manner as for the Arrochar mass and for various masses at Ballachulish. The variations in the proportions of peridotite, pyroxenite, appinite, diorite etc. relate to the relative proportions of cumulate and residual liquid development. The magmatic temperature range throughout is similar to that established for the Ballachulish suite but in the Loch Lomond suite the P_{Gas} reached before explosive breaching of the traps is generally not as high as at Ballachulish; this is presumed to be related to the relative strengths of the structural traps. Accordingly the major proportions of the Loch Lomond masses are dominated by residual liquid compositions rather than by cumulates (or disrupted cumulates).

Table 11.1 Pressure-temperature conditions for igneous and explosive activity in the main Arrochar intrusion

Rock type	Diorite with marginal kentallenitic facies	Explosive activity	Ultramafic rocks	Appinite and coarse-grained diorite	Explosive activity	Granodiorite
Temperature $^{\circ}C$	$1550^{\circ}-<770^{\circ}$	770°	$1125^{\circ}-770^{\circ}$	$1125^{\circ}-\ 770^{\circ}$	770°	$<770^{\circ}$
P_{H_2O} in kb	$<1-4$	4	$<1-4$	$<1-4$	4 kb	<1 kb?

PART 4

COMPARATIVE STUDIES

CHAPTER 12 COMPARATIVE STUDIES

Rocks from the appinite suite of Ardara, Donegal and Colonsay, Western Scotland, the scyelite - pyroxenite - appinitic type rock association of Sutherland and lavas of the Old Red Sandstone age of Western Scotland are compared with the appinite suites of the Ballachulish and Loch Lomond districts to establish (a) which products of the late Caledonian magmatic activity were comagmatic and (b) whether magma genesis, emplacement and crystallisation conditions described for the appinite suite of the type area (Chapter 8) were widespread in Caledonides.

12.1 Ardara appinite suite

The appinitic intrusions of Ardara were emplaced into subvolcanic pipes which cut the Dalradian metasediments around the Ardara pluton in Donegal, Ireland (Fig. 1.1; also see Pitcher and Berger 1972, fig. 7.3). Rock types are peridotite, pyroxenite, pyroxene - mica diorite, hornblendite, appinite and hornblende diorite with associated breccia, with the hornblendic types known as the appinitic series (French 1966, 1977; Hall 1967). These contain phenocrysts of clinopyroxene, and some phlogopite as well as amphibole in a groundmass of plagioclase. Quartz and K-feldspar interstitially occur in the groundmass of hornblende diorite (Table 12.1 – 2-7).

The amphiboles are zoned and vary in composition from edenitic - hornblende at their cores to magnesio - hornblende at margins. Overgrowths of actinolite and actinolitic - hornblende compositions are occasionally seen (Table 12.2, Fig. 12.1). Highly corroded grains of clinopyroxene commonly occur in their cores. Phenocrysts of clinopyroxene surrounded by amphibole are also common.

The high Si content of the amphibole phenocrysts (6.38 - 7.15 in half unit cell, Table 12.2) as compared to those from the appinites of

Western Scotland (mostly <6.25 in half unit cell, *cf.* Figs. 5.1, 9.6) indicates that amphibole in the Ardara appinite suite is mainly a product of clinopyroxene - liquid reaction rather than of a direct igneous crystallisation.

12.1A Petrochemistry

Eight major and trace element analyses carried out in the present investigation (Table 12.1 — 1-8) and 17 major element analyses from Hall (1967) are used for comparison. The overall variation from ultramafic to mafic rocks ranges from 44 to 57 wt. % SiO_2. On an alkali *vs.* SiO_2 diagram the majority of the compositions are distributed in the subfields of the subalkaline rocks and show a greater correspondence with the tholeiitic series than is shown by the Ballachulish and Loch Lomond clusters (Fig. 12.2a).

A continuous differentiation trend is shown on an AFM plot (Fig. 12.3a). It is generally parallel to that of the field of the alkali - olivine basalt series with evidence of some mild iron-enrichment. Certain compositions lie below the basic end of the trend shown for the calcalkaline rock series. In addition the majority of the plots lie in the field shown for the Ballachulish and Loch Lomond clusters, particularly in the part of the fields for the more basic members of these clusters. On the basis of these data it is concluded that the Ardara appinite suite was derived from a parent magma transitional in character between calcalkaline and tholeiitic.

Major element variation

Continuous variation trends reflecting differentiation and a close correspondence with the trends for both the Ballachulish and Loch Lomond clusters are shown by MgO and Al_2O_3 *vs.* S.I. plots (Figs. 12.4a, 12.5a).

The spread shown by FeO *vs.* S.I. plots (Fig. 12.6a) is due to the replacement of the dominant olivine and clinopyroxene fractionation in peridotites and pyroxenites (S.I. > 55; lower FeO) by the dominant amphibole fractionation in hornblendites and appinites (S.I. *c*. 55-30; higher FeO) as well as due to the crystallisation of the opaque ores in some of the latter types (see Chapters 7, 10). This interpretation is consistent with the presence of a high modal percentage of amphibole (>80%) and of a certain amount of the opaque ores in rocks with FeO > 8.0 wt. % (see Hall 1967, table 1 – 12-10) . The compositional plots for these rocks lie above the fields shown for the Ballachulish and Loch Lomond clusters which indicate that amphibole fractionation was more pronounced and probably the high gas pressure conditions existed for a longer duration in certain pipes of the Ardara cluster than in those of the former two clusters. However, the position of all the plots above the average trend lines shown for the Ballachulish and Loch Lomond clusters on a CaO *vs*. S.I. diagram (Fig. 12.7a), reflects a more prominant role of clinopyroxene fractionation in the development of the overall magmatic trend of the Ardara appinite suite than in that of the other two suites.

Fractionation trends in CMAS model

Plots of the Ardara appinite suite in the CMAS tetrahedron model provide evidence about the successive appearance of different phases on the liquidus during the various stages of fractional crystallisation.

The majority of the compositions plot above and below the pargasite position on a trend parallel to the pargasite - feldspar join while certain compositional plots show affinities to the positions of olivine (En apex) and clinopyroxene in a projection from Qtz into the En - Ky - Wol plane (Fig. 12.8a). This indicates olivine fractionation followed and replaced by the successive fractionation of clinopyroxene, amphibole and mica. The proximity of certain compositions to the position of olivine (En apex) and the convergence of the general variation trend towards the middle of the clinopyroxene - pargasite join in a projection from Ky into the Plag - En - Qtz plane (Fig. 12.9a) also indicate the same fractionation process.

Certain compositions lie closer to the position of clinopyroxene than to that of pargasite and do not occur in the fields shown for the Ballachulish and Loch Lomond clusters in either the projection from Qtz into the En - Ky - Wol plane or the projection from Ky into the Plag - En - Fo plane (Figs. 10.8a, 10.10a). This reflects the more pronounced role of the clinopyroxene fractionation in the Ardara rocks as predicted from CaO *vs*. S.I. plots (Fig. 12.7a).

The successive fractionation of olivine, clinopyroxene, amphibole and mica indicate crystallisation differentiation under a variable P_{Gas} such as described for the similar fractionation histories of the Ballachulish and Loch Lomond clusters (Chapters 8, 11).

Trace element chemistry

The variation trends shown by Ni, Cr and Co *vs*. MgO plots also reflect differentiation and magmatic characters (Figs. 12.11a, 12.12a, 12.13a). The lower Ni/MgO ratios shown by the Ardara rocks than by the Ballachulish and Loch Lomond rocks (Fig 12.11a) indicate affinities of the Ardara appinite suite to the tholeiitic series (*cf*. Figs. 12.2a, 7.7b; also see Gill 1979). However, there is a close correspondence between the Ardara and Ballachulish clusters on the bases of Cr and Co *vs*. MgO plots (Figs. 12.12a, 12.13a).

The average K/Rb ratio of 220 obtained for the Ardara rocks is lower than that for either the Ballachulish or the Loch Lomond cluster (400 and 300, respectively; *cf*. Fig. 12.14a). The possible reasons for this variation are discussed in Chapter 13.

The available data for Zr and Y do not permit equivocal conclusions to be drawn. The data are meagre and show considerable scatter when plotted on a Zr/Y *vs*. Zr discrimination diagram (Fig. 12.15). Whether the occurrence of certain plots in the field of island arc basalts is due to closer affiliation of the Ardara appinite suite with the island arc or orogenic environment than applies to the Ballachulish and Loch Lomond clusters is something that requires additional evidence.

12.1B Discussion

The comparison of the Ardara cluster with those at Ballachulish and Loch Lomond indicates that not only does the former cluster represent many petrographic and chemical features characteristic of the other two clusters but also represents corresponding environments and genesis described for the other two, *i.e.* crystallisation differentiation from a gas-rich basaltic magma in pipe-like intrusions under a variable P_{Gas} (see Chapters 8, 11). The closer affinity of the Ardara cluster to the tholeiitic series than that shown by the other two clusters indicates variation in composition of the parent magma for the appinite suite on a regional basis. The possibility that the Ardara cluster was derived from a basaltic magma in a tectonic setting closer to the island arc or orogenic environments than the other two clusters is something that needs to be borne in mind. However, any such difference in geotectonic environment in no way precludes the rocks of the Ardara cluster from being referred to as an "appinite suite".

The replacement of clinopyroxene by amphibole on the liquidus occurs at >10 kb, 8-9 kb and ~ 5 kb (in a temperature range of 1100-1000°C) in tholeiitic, calcalkaline and alkaline liquids, respectively, and clinopyroxene can crystallise at higher P_{H_2O} in tholeiitic liquids than in calcalkaline and alkaline liquids (Yoder and Tilley 1962, figs. 27-29). Therefore, the marked role of the clinopyroxene fractionation in the Ardara cluster does not necessarily mean that the major part of crystallisation at Ardara occurred under a generally lower gas pressure as compared to that at Ballachulish and Loch Lomond; it can be related to the affinity of the parent magma at Ardara being closer to the tholeiitic series than those of the other two clusters. This further shows that a higher P_{H_2O} was maintained to stabilise amphibole at Ardara than that at the other two localities. Such an interpretation is supported by the evidence of considerable transport of breccia being indicative of elevated gas pressure, in pipes of the Ardara appinite suite (see French 1966).

12.2 Colonsay appinite suite

Members of the appinite suite with associated breccia also intrude into Torridonian sediments in the island of Colonsay at Balnahard, Kiloran Bay and Scalasaig (Geological Survey of Scotland 1" = 1 mile Sheet 35). The major rock types at these localities are kentallenite, hornblende syenite and appinite, respectively. A small appinite mass has also been found intruded into Torridonian rocks in Ross of Mull, north of Colonsay (Sheet 35, also see Fig. 1.1). The field relationships and detailed petrography of these rocks have been described by Ghaly (1964) who noted a considerable resemblance in the mode of occurrence and petrography of these rocks with those of Ballachulish.

12.2A Petrochemistry

The five analysed representative specimens of ultramafic and mafic types show a SiO_2 range of 43-50 wt. % (Table 12.1 – 9-13). On an alkali *vs.* SiO_2 diagram these compositions follow a general trend along the boundary between the fields of the alkaline and subalkaline rocks (Fig. 12.2a). On an AFM plot they lie parallel to and below the MgO-rich end of the field shown for the alkali olivine basalt series (Fig. 12.3a). Also on both of these plots the analyses fall within the fields shown for the Ballachulish and Loch Lomond clusters. These features point to the Colonsay rocks having been derived from a magma of high-potassium calcalkaline characters as was the Ballachulish appinite suite (Chapter 7).

The Colonsay rocks also follow the continuous differentiation trends shown for the Ballachulish and Loch Lomond clusters on the bases of MgO and Al_2O_3 *vs*. S.I. plots (Figs. 12.4a, 12.5a). The majority of the compositions also occur in the fields shown for the above major clusters on the bases of FeO and CaO *vs*. S.I. plots (Figs. 12.6a, 12.7a). This indicates that fractionation processes similar to those described for the ultramafic and mafic rocks of the Ballachulish and Loch Lomond clusters, were responsible for the evolution of the Colonsay rocks. This is supported by their compositional plots shown in various projections of the CMAS model (Figs. 12.8a, 12.9a, 12.10a). They fall in the fields of the above major clusters and indicate the successive fractionation of olivine, clinopyroxene, amphibole and mica which, in turn, reflect variation in P_{Gas} (see Chapters 8, 11).

The trace element chemistry of these rocks also confirms crystallisation differentiation, the trends having considerable resemblance to those of the Ballachulish and Loch Lomond clusters. These features can be seen from their Ni, Cr and Co *vs*. MgO plots which also follow the trends shown for the above major clusters (Figs. 12.11a, 12.12a, 12.13a). However, on a Cr *vs*. MgO plot the Colonsay rocks follow the average variation trend of the Ballachulish suite but not that of the Loch Lomond suite (Fig. 12.12a). This indicates a greater similarity of these rocks with those of the former cluster as shown by the correspondence in compositions of their parent magmas. This is also supported by the average K/Rb ratio (370) for the Colonsay rocks which is closer to that for the former cluster (400) than to that for the latter (300) (*cf*. Fig. 12.14a).

The considerable resemblance between the Colonsay and Ballachulish clusters on the bases of their mode of occurrence, petrography, magmatic characters and crystallisation history and their location in the same district, Argyll (see Chapter 1, Fig. 1.1), indicates that the Colonsay cluster can be treated as being part of the Ballachulish cluster.

12.3 Scyelite - pyroxenite - appinitic type rock association of Sutherland

Small igneous masses of these rock types known as hybrids of Ach'uain type (Read 1925, 1926) are scattered throughout central and southern Sutherland (Geological Survey of Scotland 1" = 1 mile Sheets 102, 103, 108, 109). They have been interpreted as having been formed by the mixture of granite and ultrabasic magmas and on this basis formation of the appinite suite as the product of contamination or hybridisation has been proposed (Deer 1935; Holgate 1950; Joplin 1959; Read 1961; Mercy 1965). The present investigation does not support such a viewpoint for the genesis of the appinite suite of the type area at Ballachulish or for those at either Loch Lomond or Ardara. Rather it points to them as being the products of crystallisation differentiation of a basaltic magma (Chapters 2 - 11; Sections 12.1, 12.2). In order to investigate the possible genetic history of the Sutherland rocks, they are compared with the appinite suite of the Ballachulish and Loch Lomond regions, particularly on the basis of major and trace element chemistry.

Members of the scyelite - pyroxenite - appinitic type rock association, intruding the siliceous and semipelitic granulites of Moine assemblage on the northeastern shore of Loch Shin near to as well as WNW of Overscaig Hotel and on Cnoc a'Ghriama (Sheet 108), have been sampled and analysed. The rock types are scyelite, pyroxenite and hornblende diorite which has amphibole-rich varieties designated as appinitic type rocks (Table 12.1 — 14-33).

Petrographic information is given by Read (1931). Scyelites contain large crystals of olivine, clinopyroxene, amphibole and phlogopite. Olivine is partially serpentinised while clinopyroxene is surrounded and replaced by tremolitic amphibole. Pyroxenites are highly altered. In relatively fresh samples equant grains of clinopyroxene, partially altered to fibrous amphibole, contain small grains of olivine in the core (Table 12.1 – 33).

The appinite-like rocks generally contain large idiomorphic hornblende crystals in a groundmass of clinopyroxene, biotite, plagioclase$_{(An_{7-15})}$, orthoclase, microcline and quartz. The hornblende is both acicular and stumpy. It varies in colour from light green to pale green. Overgrowths of actinolite occur commonly. There is clinopyroxene in some of these hornblende crystals. Equant grains of highly zoned clinopyroxene are also abundant in certain appinitic type rocks. Primary biotite is common while secondary biotite grown on the hornblende crystals is noticed rarely. Primary sphene, apatite and magnetite are accessories. The mineralogical and textural features of these rocks closely correspond with the appinites from the Back Settlement pipe of the type area, Ballachulish.

12.3A Petrochemistry

Using analytical data for 20 representative specimens it can be shown that the overall variation from ultramafic to mafic rocks ranges from 38 to 56 wt. % SiO_2 (Table 12.1 – 14-33). Two major groups of rocks are distinguished on the basis of their SiO_2 contents, (a) scyelites and SiO_2-poor appinitic type rocks, with $SiO_2 < 50$ wt. % and (b) pyroxenites and SiO_2-rich appinitic type rocks with $SiO_2 > 50$ wt. %. On an alkali *vs.* SiO_2 diagram the compositional plots for the majority of rocks from the former group follow a general trend close to the boundary between the fields of alkaline and subalkaline rock series and also occur in the fields shown for the Ballachulish and Loch Lomond clusters. On the other hand, the compositional plots for the rocks of the latter group lie in the field defining tholeiitic rock series and do not occur in the fields shown for the Ballachulish and Loch Lomond clusters. There is a gap between the two major groups. In addition pyroxenites can be discriminated from the SiO_2-rich appinitic type rocks on the basis of the lower alkali contents in the former than in the latter (Fig. 12.2a).

On an AFM plot the scyelites are more MgO-rich than any of the rocks of the other suites investigated. The plots for pyroxenites lie with those of the MgO-poor scyelites and the overall trend of scyelites and pyroxenites is generally parallel to the MgO-rich end of the field shown for alkali olivine basalt series. All the appinitic type rocks plot with the Colonsay rocks just below the MgO-rich end of the field of the alkali olivine basalt, and within the fields shown for the Ballachulish and Loch Lomond clusters (Fig. 12.3a).

Major element variation

On an MgO *vs*. S.I. plot the scyelites follow a regular trend that represents a continuation of the trends for the Ballachulish and Loch Lomond clusters (Fig. 12.4a). This indicates a very high degree of olivine fractionation from a basaltic magma. The plots of SiO_2-poor appinitic type rocks are also consistent with being genetically related to the appinite suites of Ballachulish and Loch Lomond as well as with scyelites. However, both the pyroxenites and SiO_2-rich appinitic type rocks have lower MgO and higher S.I. values than expected if they were the result of normal fractionation.

The discrimination into two groups of rocks can also be seen on Al_2O_3, FeO and CaO *vs*. S.I. variation diagrams. Plots for scyelites and SiO_2-poor appinitic type rocks fall parallel to or in the "patterns" - "fields" of the appinite suite on the basis of Al_2O_3 and FeO *vs*. S.I. plots (Figs. 12.5a, 12.6a). Similarly scyelites fall on a regular negative trend that points towards the plots shown for SiO_2-poor appinitic type rocks occurring in the fields of the appinite suite on the basis of CaO *vs*. S.I. plot (Fig. 12.7a). On the other hand, pyroxenites and SiO_2-rich appinitic type rocks do not fit to the patterns of scyelites and SiO_2-rich appinitic type rocks or to those of the appinite suite and have characters well away from a normal differentiation series, particularly on a CaO *vs*. S.I. plot.

Comparison on the basis of CMAS fractionation model

The crystallisation sequence shown by the compositional plots of scyelites and SiO_2-poor appinitic type rocks in a projection from Qtz into the En - Ky - Wol plane (Fig. 12.8a) indicate a dominant olivine fractionation followed by clinopyroxene, amphibole and mica fractionation in the former and a dominant amphibole fractionation in the latter and thus show a close correspondence with the ultramafic and mafic rocks of the appinite suite. On the other hand, compositional plots of pyroxenites and SiO_2-rich appinitic type rocks do not follow such a pattern and lie farther from the fields of the appinite suite towards the En - Wol join which points to the high proportion of clinopyroxene in these rocks. This corresponds with their different patterns shown on alkali *vs.* SiO_2 and MgO and CaO *vs.* S.I. plots (Figs. 10.2a, 10.4a, 10.7a). Similar conclusions can be drawn from the interpretation of plots in projections from Ky into the Plag - En - Qtz plane and from Ky into the Plag - En - Fo plane (Figs. 12.9a, 12.10a).

Trace element chemistry

The two groups of rocks can also be partially discriminated on the basis of Ni, Cr and Co *vs.* MgO plots (Figs. 12.11a, 12.12a, 12.13a). Scyelites and SiO_2-poor appinitic type rocks have generally parallel trends to those shown for the Ballachulish and Loch Lomond clusters but plots for pyroxenites and SiO_2-rich appinitic type rocks are scattered and do not follow these patterns completely, particularly on a Co *vs.* MgO plot (Fig. 12.13a).

Discussion

The information obtained from the major and trace element variations and the CMAS plots of the Sutherland rocks indicates that scyelites and SiO_2-poor appinitic type rocks are the products of a normal crystallisation differentiation in a basaltic magma. Fractionation processes similar to those described for the ultramafic and mafic rocks of the Ballachulish and Loch Lomond clusters were responsible for their development. Scyelites can be related to the dunite from the Garabal Hill complex of the latter cluster in the nature and degree of fractionation (see Chapters 9, 10). The SiO_2-poor appinitic type rocks are not only similar to the appinites from the two major clusters in chemical features but the former also show mineralogical and textural features which are the characteristics of the appinite from the Back Settlement pipe of the type area, Ballachulish, *e.g.* the presence of idiomorphic hornblende crystals with clinopyroxene cores and with rhythmic overgrowths of actinolite (see Chapter 2; Figs. 2.5; 2.7). This correspondence in mineralogical as well as textural features in turn reflects correspondence in environments and genesis. Therefore, both the scyelites and the SiO_2-poor appinitic type rocks can be referred to as the members of a true appinite suite with the latter types corresponding to the original definition of appinite.

The different patterns shown by pyroxenites and SiO_2-rich appinitic type rocks indicate that these rocks are not the direct products of crystallisation differentiation. Rather certain chemical characteristics point to hybridisation (or contamination) being involved in their production. For example, all the pyroxenites closely correspond with scyelites on the basis of alkalis, Al_2O_3, FeO and S.I. values while the majority of the SiO_2-rich appinitic type rocks correspond with SiO_2-poor ones on the basis of alkalis and S.I. values but pyroxenites and SiO_2-rich appinitic type rocks have much higher SiO_2 and CaO contents when compared with scyelites and SiO_2-poor appinitic type rocks (Figs. 12.2a, 12.4a, 12.6a, 12.7a). This suggests that the latter types are the products of interaction of basic material with foreign material rich in SiO_2 and CaO. This interpretation is consistent with the occurrence of plots shown for pyroxenites with those of scyelites and of the SiO_2-rich appinitic type rocks with those of the

SiO_2-poor ones, on an AFM plot (Fig. 12.3a). The composition of the interacting material was probably granodioritic and the resultant mixed products represent the hybrids of Ach'uain type as referred to by Read (1925, 1926).

12.4 Lavas

Lavas of Old Red Sandstone age representing a basalt - andesite - rhyolite association of the orogenic regions (Turner and Verhoogen 1960; Green and Ringwood 1968) are exposed on the Lorne Plateau, in Glen Coe and on Ben Nevis (Fig. 1.1; Geological Survey of Scotland 1" = 1 mile Sheets 45, 53; Roberts 1966, 1974; Haslam 1968; Groome and Hall 1974). These lavas show a close spatial and temporal relationship to the widely distributed plutonic and hypabyssal suites of rocks including the appinite suite, early lamprophyres and latter porphyrites, in the region, all of which were produced at the later stages of Caledonian orogeney (Chapter 1; also see Bowes *et al.* 1965; Bowes and McArthur 1976). In view of a possible genetic relationship of lavas with various plutonic and hypabyssal rocks of the region, Groome and Hall (1974) carried out a petrogenetic and comparative study for the Lorne lavas on the basis of chemical data. They concluded that only the basalts and andesites were developed from basic magmas produced from the melting of a mantle source while the rhyolites and ignimbrites represent a small amount of acidic magma locally produced in the crust due to the uprise of basic magmas.

Considerable similarities have been noticed between the Lorne and Glen Coe lavas on the basis of their petrographic features, stratigraphic sequences and age (Bailey 1925; Bailey and Maufe 1960; Roberts 1966; Brown 1972) which indicate that the above conclusions could equally apply to the Glen Coe lavas, although there the proportion of basic rocks is very small while the proportion of acidic rocks is considerable. However, very limited work has been done to compare the Glen Coe lavas with those at Lorne and with the appinite suite on the basis of chemistry. In addition, the analytical data from the appinite suite used by Groome and Hall (1974) for comparison with Lorne lavas was limited and mostly related to the cumulative rock types (*cf.* Chapters 7, 8). The purpose of the present comparative study is to ascertain whether there is a genetic relationship between the basalts and andesites from the Lorne Plateau and Glen Coe lavas.

12.4A Petrochemistry

Unfortunately only one major element analysis was available from the Glen Coe basalts, given by Bailey and Maufe (1960). Using this together with 10 analyses from the Glen Coe andesites (Table 12.3) and 22 analyses from the basaltic and andesitic lavas of Lorne (Groome and Hall 1974, tables 1, 2), it can be shown that the overall variation from basaltic to andesitic compositions ranges from 48 to 63% SiO_2 (*cf.* Fig. 12.2b). On an alkali *vs.* SiO_2 diagram the compositional plots of the Glen Coe lavas generally correspond with those from the Lorne lavas, all lying across the boundary between the fields shown for the alkaline and subalkaline rock series. The majority of the basaltic compositions ($SiO_2 < 52$ wt. %) have their plots lying in the field of the mildly alkaline rock series while the majority of the andesitic compositions ($SiO_2 > 52$ wt. %) have their plots occurring in the field of alkali olivine basalt series (Fig. 12.2b). Both the lavas also correspond with each other on an AFM plot but their general variation follows the trend shown for the calcalkaline rock series (Fig. 12.3b). In addition, the majority of the plots occur in the fields of the Ballachulish and Loch Lomond appinite clusters but show closer affinities to the former cluster than to the latter on both alkali *vs.* SiO_2 and AFM plots. These features suggest that both the Glen Coe and Lorne lavas are likely to have been derived from the same parent magma which was transitional in character between alkaline and subalkaline, *i.e.* high-potassium calcalkaline, similar to that suggested for the Ballachulish appinite suite (see Chapter 7; also see Groome and Hall 1974).

Major element variation

Both the Lorne and Glen Coe lavas also show a close correspondence with each other as well as with the appinite suite on the basis of many of the oxide *vs*. S.I. plots, and occur in a range of 32 - 15 S.I. values. The overall continuous variation trend of lavas, reflecting differentiation, closely follows the trends shown for the Ballachulish and Loch Lomond appinite clusters on the basis of MgO *vs*. S.I. plots (Fig. 12.4b). The compositional plots for both of these groups of lavas also lie together, above and below the trends shown for the two major clusters of the appinite suite, and show an overall general negative trend but with a greater spread on Al_2O_3 *vs*. S.I. plots (Fig. 12.5b). The general negative trend reflects the dominant fractionation of plagioclase while the spread indicates the variable proportions of olivine, clinopyroxene and plagioclase.

The correspondence between the Lorne and Glen Coe lavas and the appinite suite is not very strong on the basis of FeO *vs*. S.I. plots (Fig. 12.6b). The orientation of the general trend shown by compositions from the Lorne lavas towards the olivine-rich rocks of the appinite suite indicates that olivine fractionation took place in the early stages. The relatively lower FeO in these rocks as compared to the appinite suite shows that amphibole and magnetite did not become the dominant fractionating phases. However, in the majority of the compositions from the Glen Coe lavas the varying FeO at constant S.I. values of 20 reflects the varying proportions of the opaque ores (Table 12.3).

A general correspondence between the Lorne and Glen Coe lavas and the appinite suite is also indicated by CaO *vs*. S.I. plots (Fig. 12.7b). The overall positive trend shown by the majority of compositional plots of the lavas indicates clinopyroxene and plagioclase fractionation. The spread shown by the Lorne lavas in a range of 25 to 15 S.I. values is probably due to the high accumulation of plagioclase, apatite and olivine (and some hypersthene) in certain rock types. This interpretation is consistent with the relatively high proportions of normative anorthite, apatite and calcite in the Ca-rich types and of normative hypersthene in the Ca-poor ones (see Groome and Hall 1974, table 1 – 8, table 2 – 7 ,10).

Fractionation trends in the CMAS model

The olivine, clinopyroxene and plagioclase fractionation indicated by oxide *vs*. S.I. plots are also shown in the various projections of the CMAS model. The olivine fractionation in the early stages can be predicted from plots lying on a trend parallel to the olivine (En apex) - feldspar join in a projection from Qtz into the En - Ky - Wol plane (Fig. 12.8b). The clinopyroxene and plagioclase fractionation is shown by the variation of plots lying on a continuous trend approximately normal to the clinopyroxene - feldspar join in a projection from Ky into the Plag - En - Qtz plane (Fig. 12.9b).

The occurrence of the compositional plots closer to the positions of clinopyroxene and plagioclase than to that of olivine in the above projections as well as in a projection from Ky into the Plag - En - Fo plane (Fig. 12.10b) indicates that clinopyroxene and plagioclase fractionation was dominant over olivine fractionation.

A complete correspondence is shown by the Lorne and Glen Coe lavas, with each other, on the basis of their CMAS plots but their fractionation history differs somewhat from the appinite suite. The amphibole and biotite fractionation which occurred in the appinite suite is not indicated by the lavas. However, these plots provide evidence of relationship between the two suites. A majority of the lava compositions fall in those parts of the fields of the Ballachulish and Loch Lomond clusters which may indicate a dominant clinopyroxene - plagioclase fractionation in all the above projections.

Trace element chemistry

A considerable resemblance is also shown between the Lorne and Glen Coe lavas on the basis of their trace element chemistry. However, due to the different crystallisation history of the lavas than that of the appinite suite, the variation trends of the former markedly differ from the latter. For example, the general variation trend shown by the Ni *vs.* MgO plots of the lavas indicates a much steeper slope than that shown by the common variation trend of the Ballachulish and Loch Lomond clusters (Fig. 12.11b). This reflects the dominant role of the olivine and clinopyroxene fractionation relative to that of the amphibole and mica fractionation in the lavas as compared to the appinite suite. The scatter in the plots indicates the variable proportions of olivine, clinopyroxene and plagioclase in the lavas. Similar features are also shown by the Cr and Co *vs.* MgO plots (Figs. 12.12b, 12.13b). However, a prominent gap can be noticed in the variation trend of the Lorne lavas on the basis of their Cr contents (*c.* 250 - 150 p.p.m.), with the Glen Coe lavas (all andesites) having their plots with those shown for the Cr-poor rock types from Lorne (Fig. 12.12b). The gap can possibly be due to the dominant fractionation of clinopyroxene in the Cr-rich group and of plagioclase in the Cr-poor from both the Lorne and Glen Coe lavas, reflecting crystallisation under highly variable P_{Gas}, with higher P_{Gas} in the former case than in the latter (see Roberts 1974; also see Chapters 7 - 11).

The K/Rb ratios of lavas are much higher in the basic compositions as compared to the appinite suite and generally show decrease with fractionation (*cf.* Fig. 12.14b). Groome and Hall (1974) have suggested hornblende crystallisation as one of the possible explanations. Hornblende occurs as phenocryst or in the groundmass in variable proportions in the majority of the basalts and andesites (see Bailey and Maufe 1960; Groome and Hall 1974) and it strongly discriminates against Rb relative to K

(Beswick 1976). Thus the findings of Beswick support the view of Groome and Hall.

The occurrence of the compositions from the Glen Coe lavas in or close to the "within plate basalt" field on the basis of their Zr/Y *vs.* Zr plots (Fig. 12.15) is consistent with evolution in continental tectonic environment.

Discussion

In addition to correspondence in petrography, stratigraphical sequences and age between the Lorne and the Glen Coe lavas, mentioned earlier, there is also correspondence on the basis of their major and trace element chemistry. This indicates them to be one cognate suite of rocks derived from a common parent magma. The similarities between the lavas and the appinite suite on the bases of magmatic affinity, tectonic setting and many of the major element variations and the CMAS plots indicate that in addition to their spatial and temporal relationship they are genetically related. Further evidence of this is provided in Chapter 13.

The differences between the lavas and the appinite suite in major and trace element chemistry are due to their crystallisation under different physical environments while the narrower compositional range of the lavas follows from the lower degree of fractionation. The dominant fractionation of plagioclase points to the low pressure conditions in lavas expected from crystallisation under volcanic environment.

12.5 Conclusions

1. The Ardara appinite suite was derived from a parent magma of transitional character between calcalkaline and tholeiitic. Due to closer affinity to the tholeiitic series than to the alkaline series, clinopyroxene fractionation was dominant and the replacement of clinopyroxene and amphibole took place at higher P_{H_2O} (> 5 kb) than that in the Ballachulish and Loch Lomond clusters (< 5 kb).

2. The Colonsay appinite suite represents transitional character between alkaline and calcalkaline types and closely corresponds to the Ballachulish appinite suite on the bases of magmatic affinity and crystallisation history. The former suite seems to be part of the latter.
3. The scyelite - pyroxenite - appinitic type rock association of Sutherland does not represent a cognate, petrogenetic suite of rocks. Scyelites and SiO_2-poor appinitic type rocks are the products of crystallisation differentiation from a basaltic magma of transitional character between alkaline and calcalkaline and are genetically related to the appinite suite. Pyroxenites and SiO_2-rich appinitic type rocks represent the hybrids of Ach'uain type and were probably formed by the interaction of a granodioritic liquid with scyelites and SiO_2-poor appinitic type rocks, respectively.
4. The Lorne and Glen Coe lavas are one cognate suite of rocks derived from a common parent magma of high-potassium calcalkaline character. They are also genetically related to the appinite suite of Western Scotland. The differences between the lavas and the appinite suite on the bases of certain major and trace element variations are due to the crystallisation of the two suites under different physical environments.
5. The comparative study indicates that magma genesis, emplacement and crystallisation conditions, described for the appinite suite of the type area were widespread in Caledonides.

Figure 12.1. Compositional fields for amphibole from the appinite suite of Ardara, Donegal (after Leake 1978).

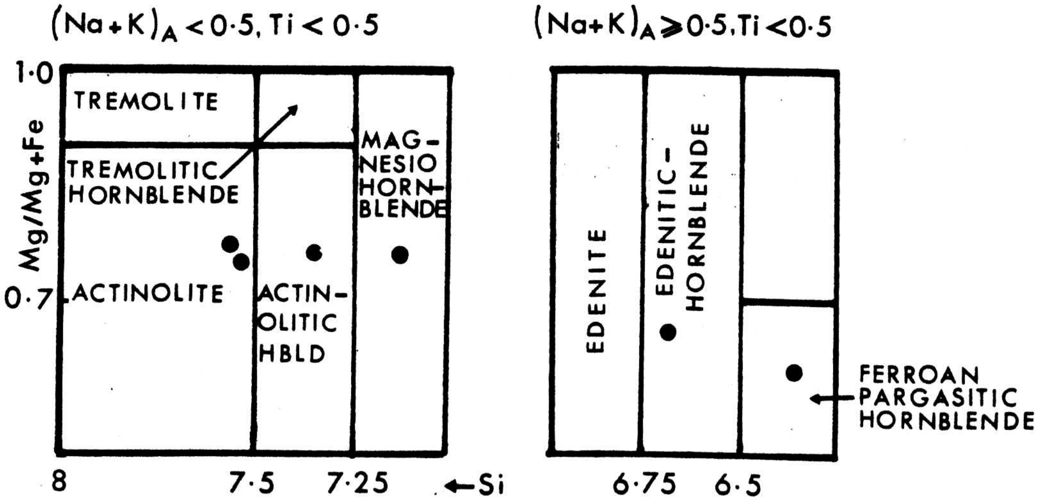
$(Na+K)_A < 0.5, Ti < 0.5$
$(Na+K)_A \geq 0.5, Ti < 0.5$
1·0
0·7
Mg/Mg+Fe
TREMOLITE
TREMOLITIC HORNBLENDE
MAG-NESIO HORN-BLENDE
ACTINOLITE
ACTIN-OLITIC HBLD
8
7·5
7·25
← Si
EDENITE
EDENITIC-HORNBLENDE
FERROAN PARGASITIC HORNBLENDE
6·75
6·5

Figure 12.2 (a - b). Alkali *vs.* SiO_2 diagram for the various igneous rock suites of Old Red Sandstone age from Scotland and Ireland.

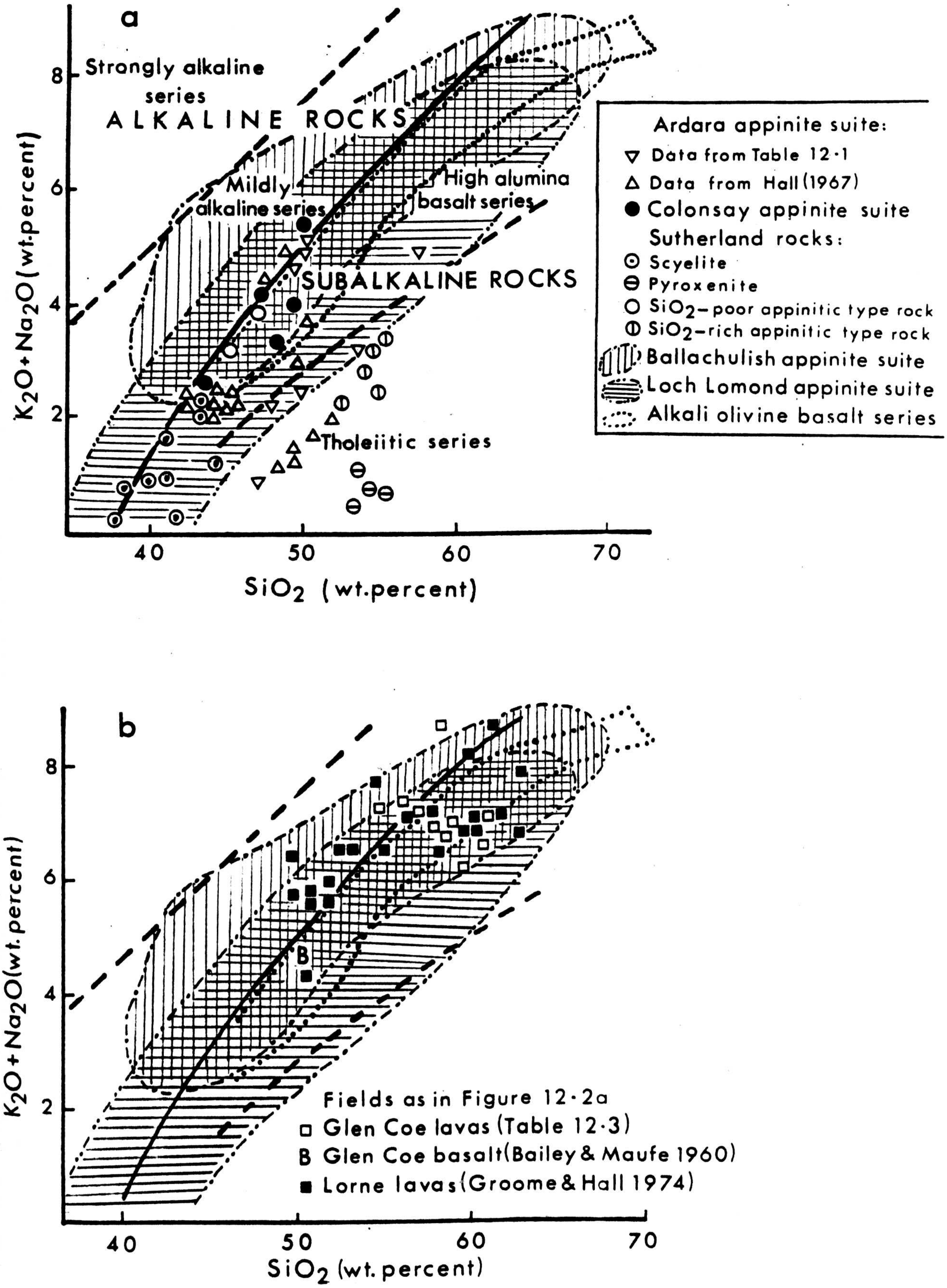
a
Strongly alkaline series
ALKALINE ROCKS
Mildly alkaline series
High alumina basalt series
SUBALKALINE ROCKS
Tholeiitic series
K₂O+Na₂O (wt.percent)
SiO₂ (wt.percent)
2
4
6
8
40
50
60
70
Ardara appinite suite:
▽ Data from Table 12·1
△ Data from Hall (1967)
● Colonsay appinite suite
Sutherland rocks:
⊙ Scyelite
⊖ Pyroxenite
○ SiO₂–poor appinitic type rock
⦶ SiO₂–rich appinitic type rock
Ballachulish appinite suite
Loch Lomond appinite suite
Alkali olivine basalt series
b
B
Fields as in Figure 12·2a
□ Glen Coe lavas (Table 12·3)
B Glen Coe basalt (Bailey & Maufe 1960)
■ Lorne lavas (Groome & Hall 1974)
K₂O+Na₂O (wt. percent)
SiO₂ (wt. percent)
2
4
6
8
40
50
60
70

Figure 12.3 (a - b). Comparison on the basis of AFM plots.

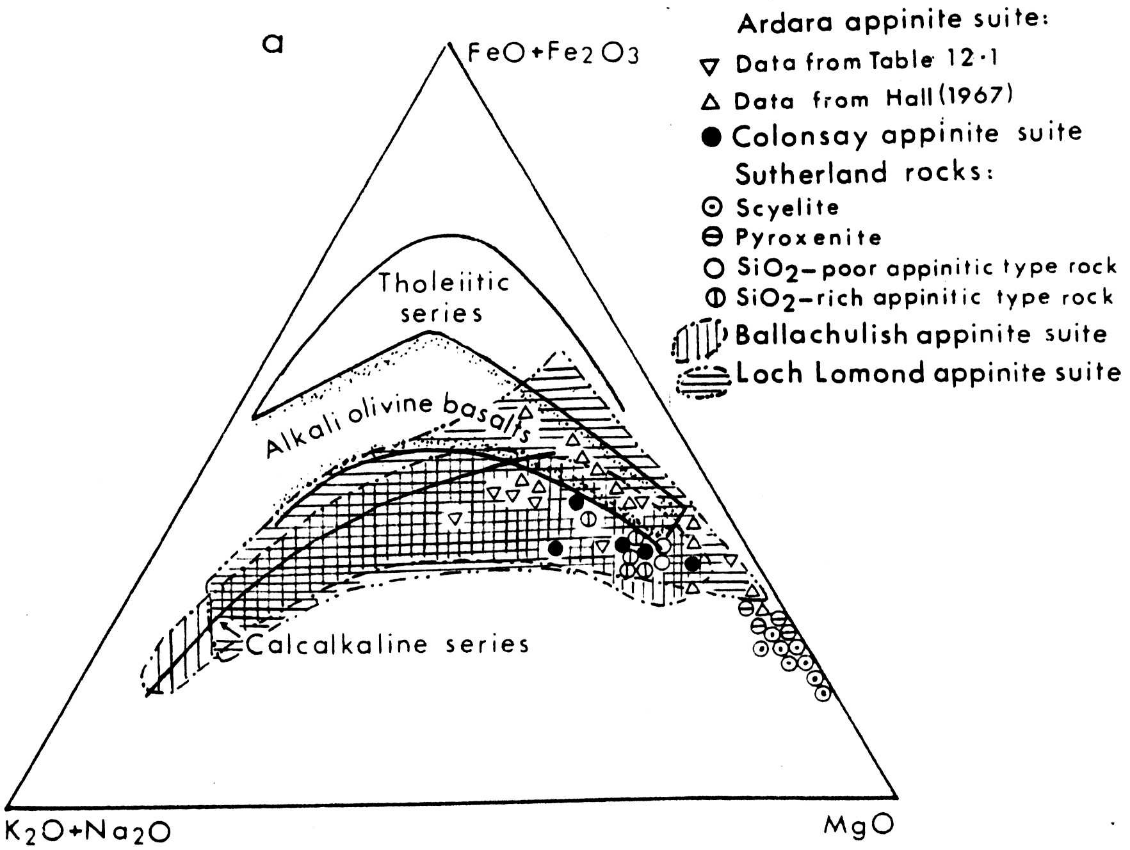
a
FeO+Fe$_2$O$_3$
Ardara appinite suite:
▽ Data from Table 12·1
△ Data from Hall (1967)
● Colonsay appinite suite
Sutherland rocks:
⊙ Scyelite
⊖ Pyroxenite
○ SiO$_2$-poor appinitic type rock
⦶ SiO$_2$-rich appinitic type rock
Ballachulish appinite suite
Loch Lomond appinite suite
Tholeiitic series
Alkali olivine basalts
Calcalkaline series
K$_2$O+Na$_2$O
MgO

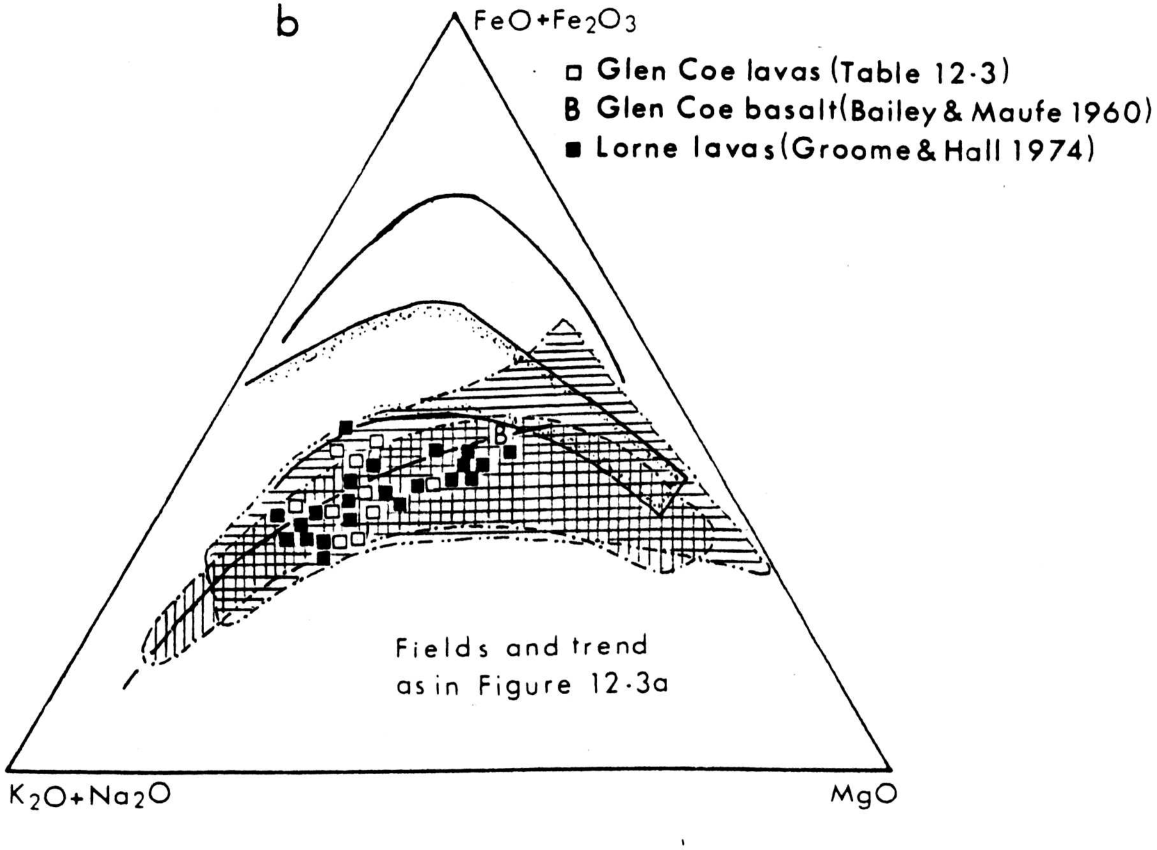
b
FeO+Fe$_2$O$_3$
□ Glen Coe lavas (Table 12·3)
B Glen Coe basalt (Bailey & Maufe 1960)
■ Lorne lavas (Groome & Hall 1974)
B
Fields and trend as in Figure 12·3a
K$_2$O+Na$_2$O
MgO

Figures 12.4 (a,b) - 12.7 (a - b). Comparison on the basis of MgO, Al_2O_3, FeO and CaO *vs*. S.I. variations.

Fig 12·4

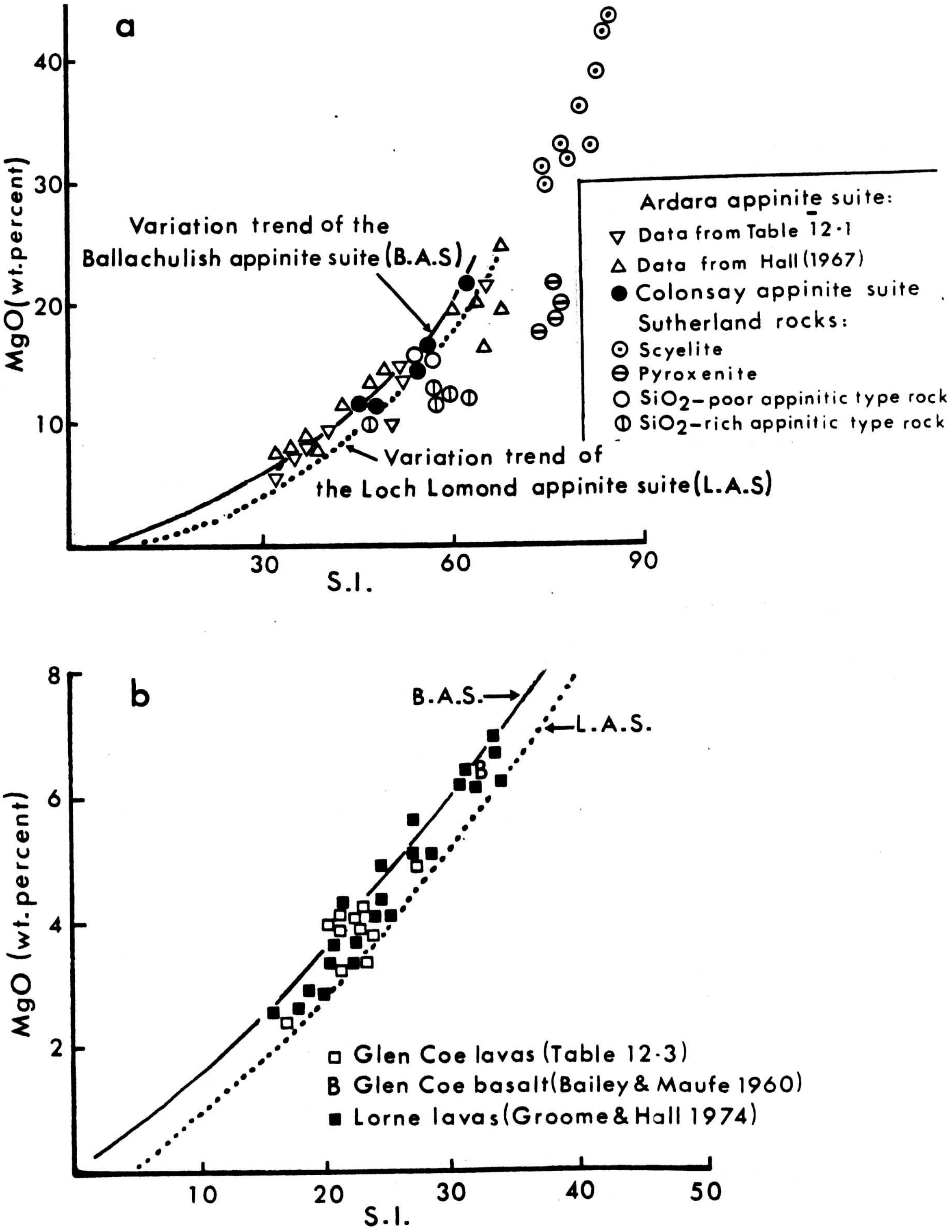
a
40
30
20
10
MgO(wt.percent)
30
60
90
S.I.
Variation trend of the Ballachulish appinite suite (B.A.S)
Variation trend of the Loch Lomond appinite suite(L.A.S)
Ardara appinite suite:
▽ Data from Table 12·1
△ Data from Hall (1967)
● Colonsay appinite suite
Sutherland rocks:
⊙ Scyelite
⊖ Pyroxenite
○ SiO_2-poor appinitic type rock
⦶ SiO_2-rich appinitic type rock
b
8
6
4
2
MgO (wt.percent)
10
20
30
40
50
S.I.
B.A.S.
L.A.S.
B
□ Glen Coe lavas (Table 12·3)
B Glen Coe basalt(Bailey & Maufe 1960)
■ Lorne lavas(Groome & Hall 1974)

Fig.12·5

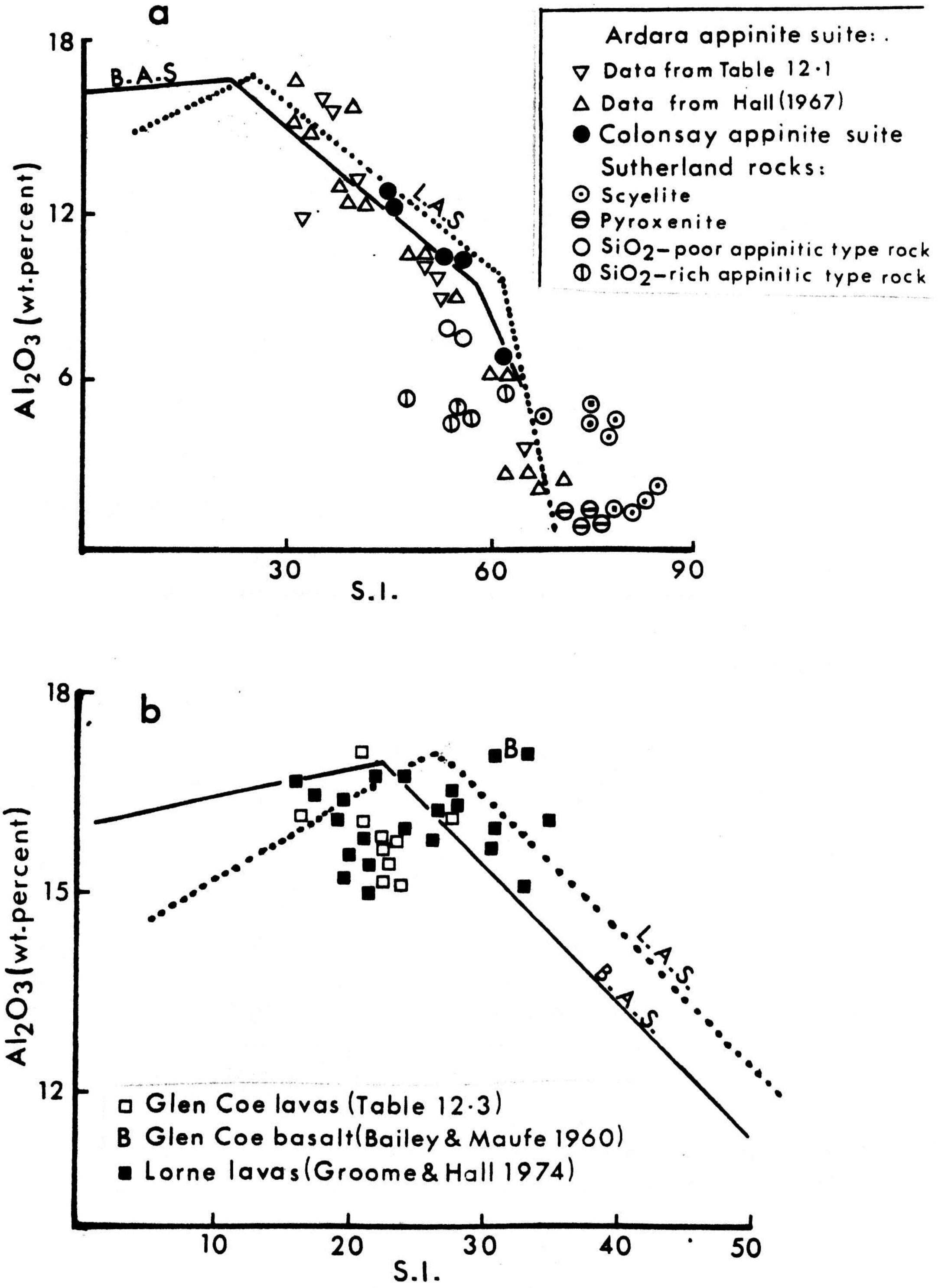
a
18
12
6
Al$_2$O$_3$ (wt.percent)
30
60
90
S.I.
B.A.S
L.A.S
Ardara appinite suite:
▽ Data from Table 12·1
△ Data from Hall (1967)
● Colonsay appinite suite
Sutherland rocks:
⊙ Scyelite
⊖ Pyroxenite
○ SiO$_2$-poor appinitic type rock
⦶ SiO$_2$-rich appinitic type rock
b
18
15
12
Al$_2$O$_3$ (wt.percent)
10
20
30
40
50
S.I.
B
L.A.S.
B.A.S.
□ Glen Coe lavas (Table 12·3)
B Glen Coe basalt (Bailey & Maufe 1960)
■ Lorne lavas (Groome & Hall 1974)

Fig.12·6

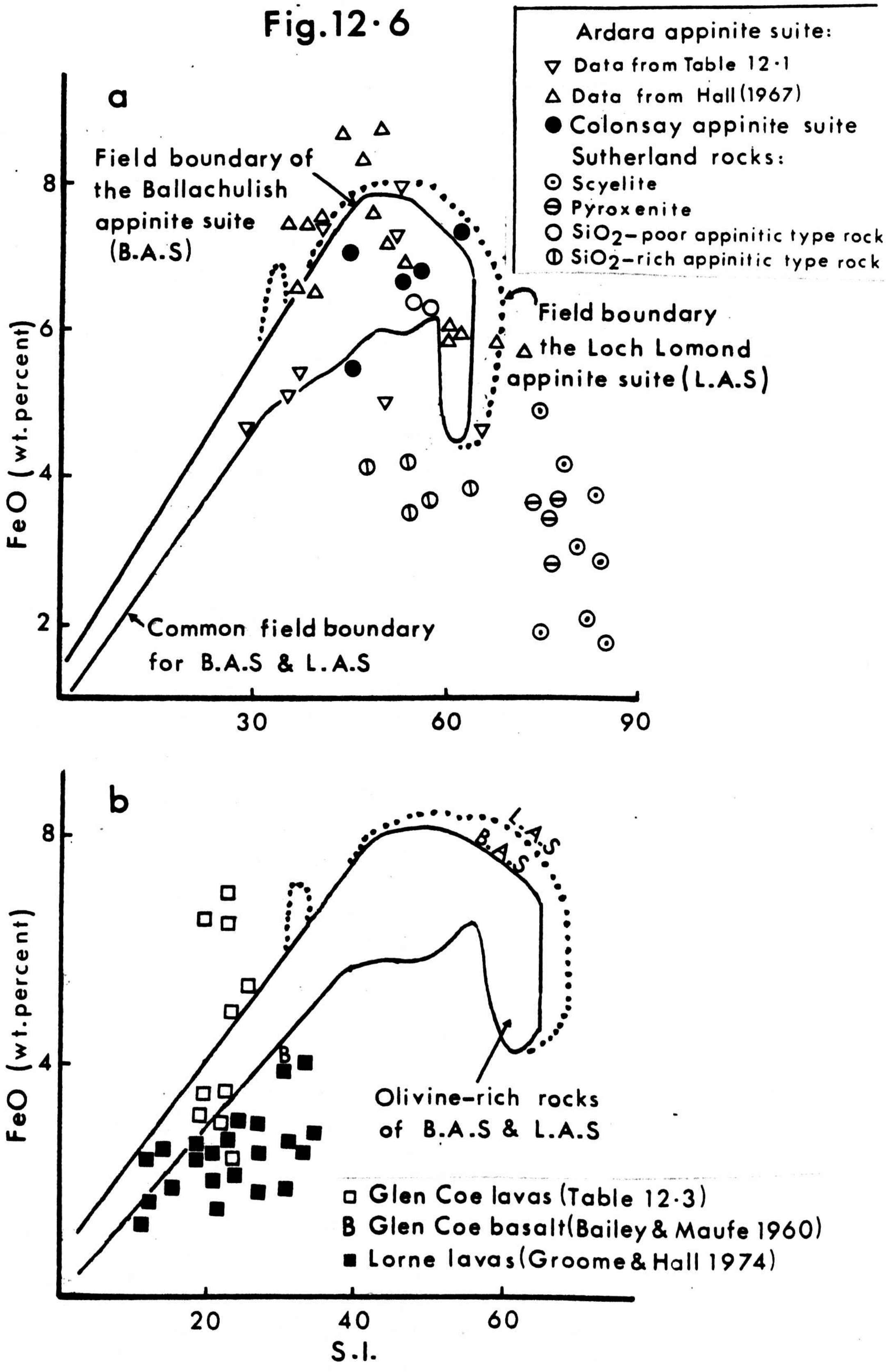
Ardara appinite suite:
▽ Data from Table 12·1
△ Data from Hall (1967)
● Colonsay appinite suite
Sutherland rocks:
⊙ Scyelite
⊖ Pyroxenite
○ SiO2-poor appinitic type rock
⦶ SiO2-rich appinitic type rock
a
Field boundary of the Ballachulish appinite suite (B.A.S)
Field boundary the Loch Lomond appinite suite (L.A.S)
Common field boundary for B.A.S & L.A.S
FeO (wt. percent)
2
4
6
8
30
60
90
b
L.A.S
B.A.S
Olivine-rich rocks of B.A.S & L.A.S
B
□ Glen Coe lavas (Table 12·3)
B Glen Coe basalt (Bailey & Maufe 1960)
■ Lorne lavas (Groome & Hall 1974)
FeO (wt.percent)
4
8
20
40
60
S.I.

Fig.12·7

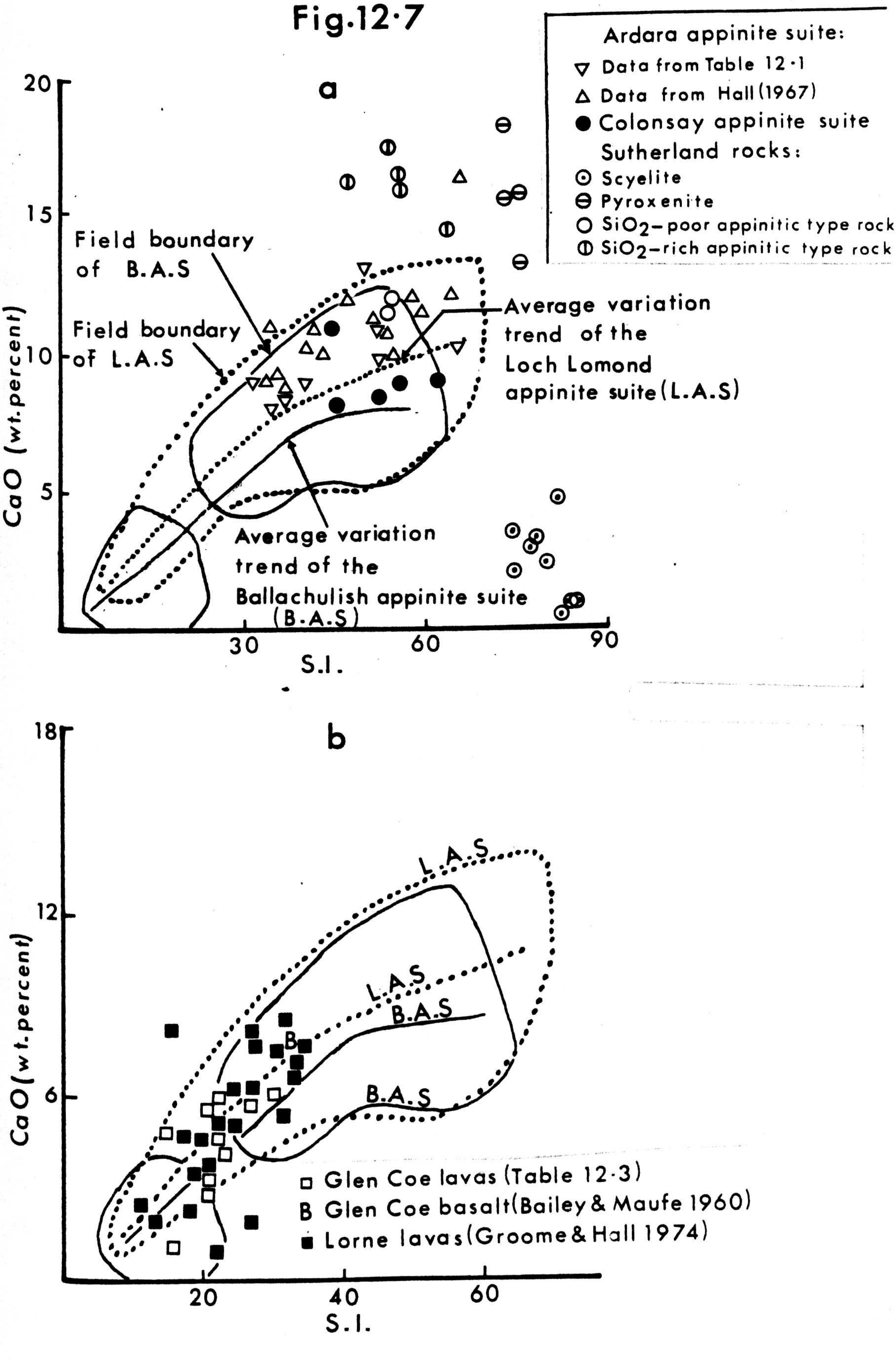
Ardara appinite suite:
▽ Data from Table 12·1
△ Data from Hall (1967)
● Colonsay appinite suite
Sutherland rocks:
⊙ Scyelite
⊖ Pyroxenite
○ SiO2–poor appinitic type rock
⦶ SiO2–rich appinitic type rock
a
20
15
10
5
CaO (wt. percent)
30
60
90
S.I.
Field boundary of B.A.S
Field boundary of L.A.S
Average variation trend of the Loch Lomond appinite suite (L.A.S)
Average variation trend of the Ballachulish appinite suite (B.A.S)
b
18
12
6
CaO (wt. percent)
20
40
60
S.I.
L.A.S
L.A.S
B.A.S
B.A.S
B
□ Glen Coe lavas (Table 12·3)
B Glen Coe basalt (Bailey & Maufe 1960)
■ Lorne lavas (Groome & Hall 1974)

Fig.12·8

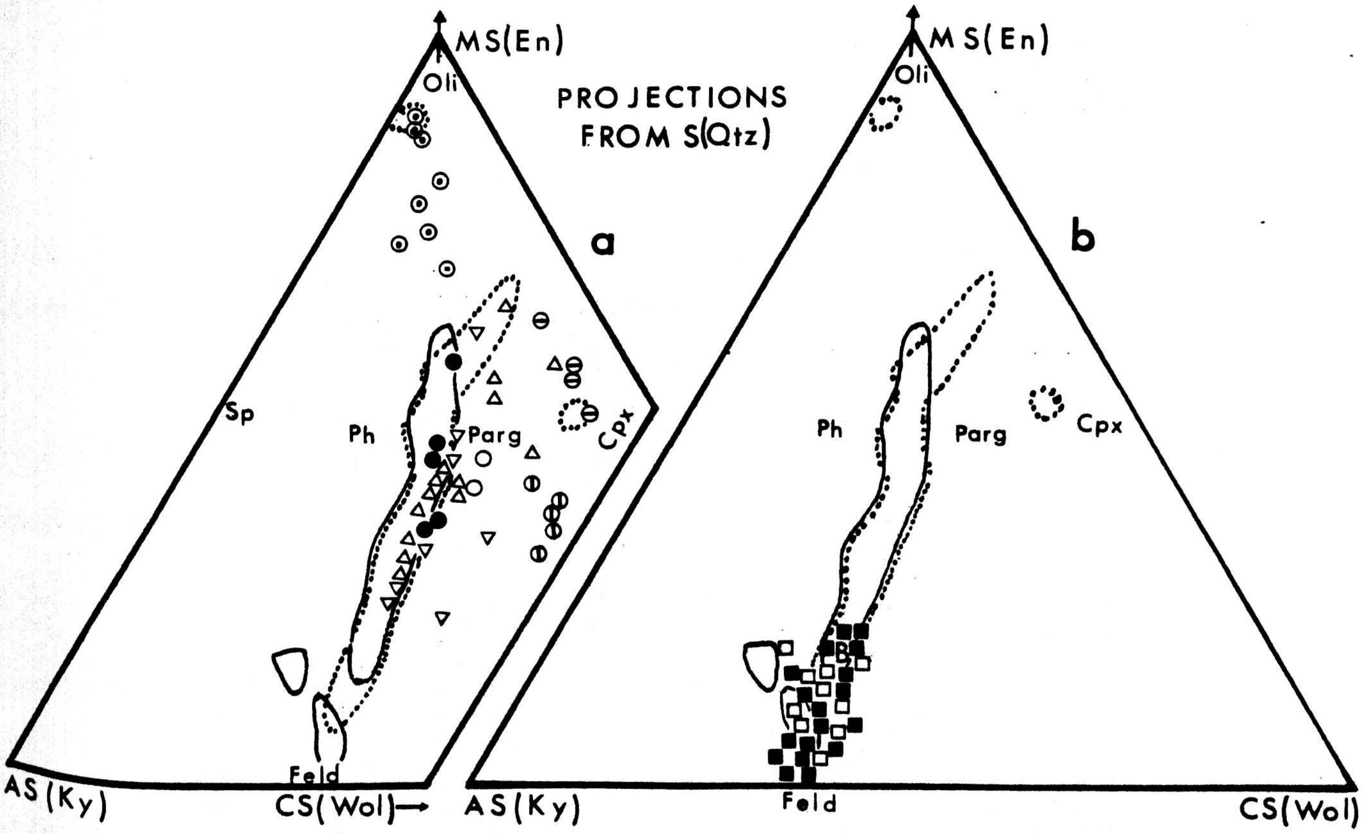

Fig.12·9

PROJECTIONS FROM AS(Ky)

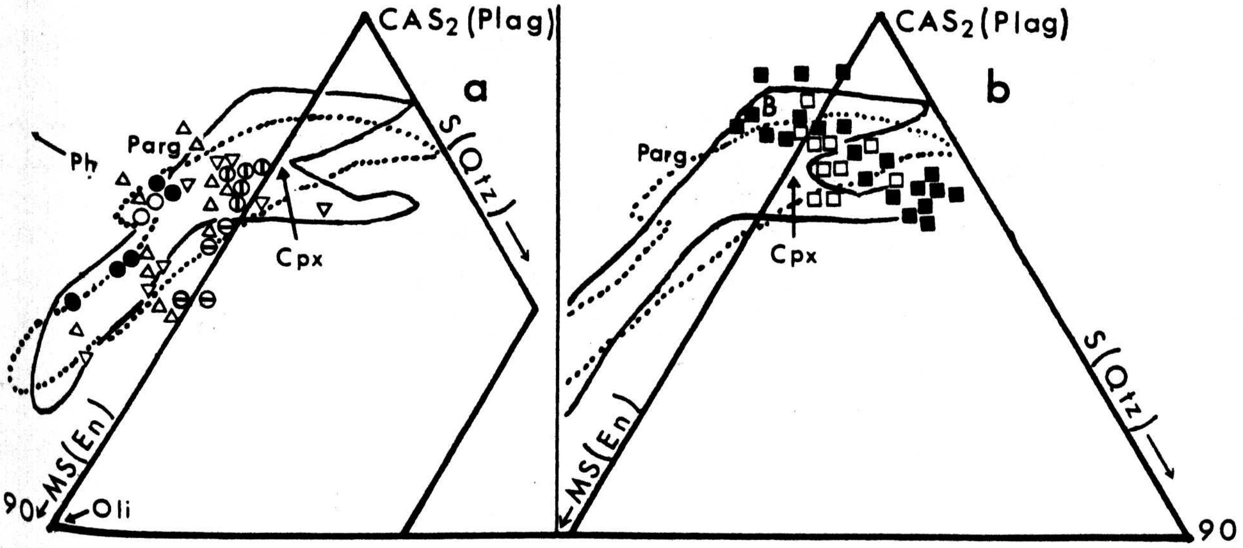

Fig 12·10

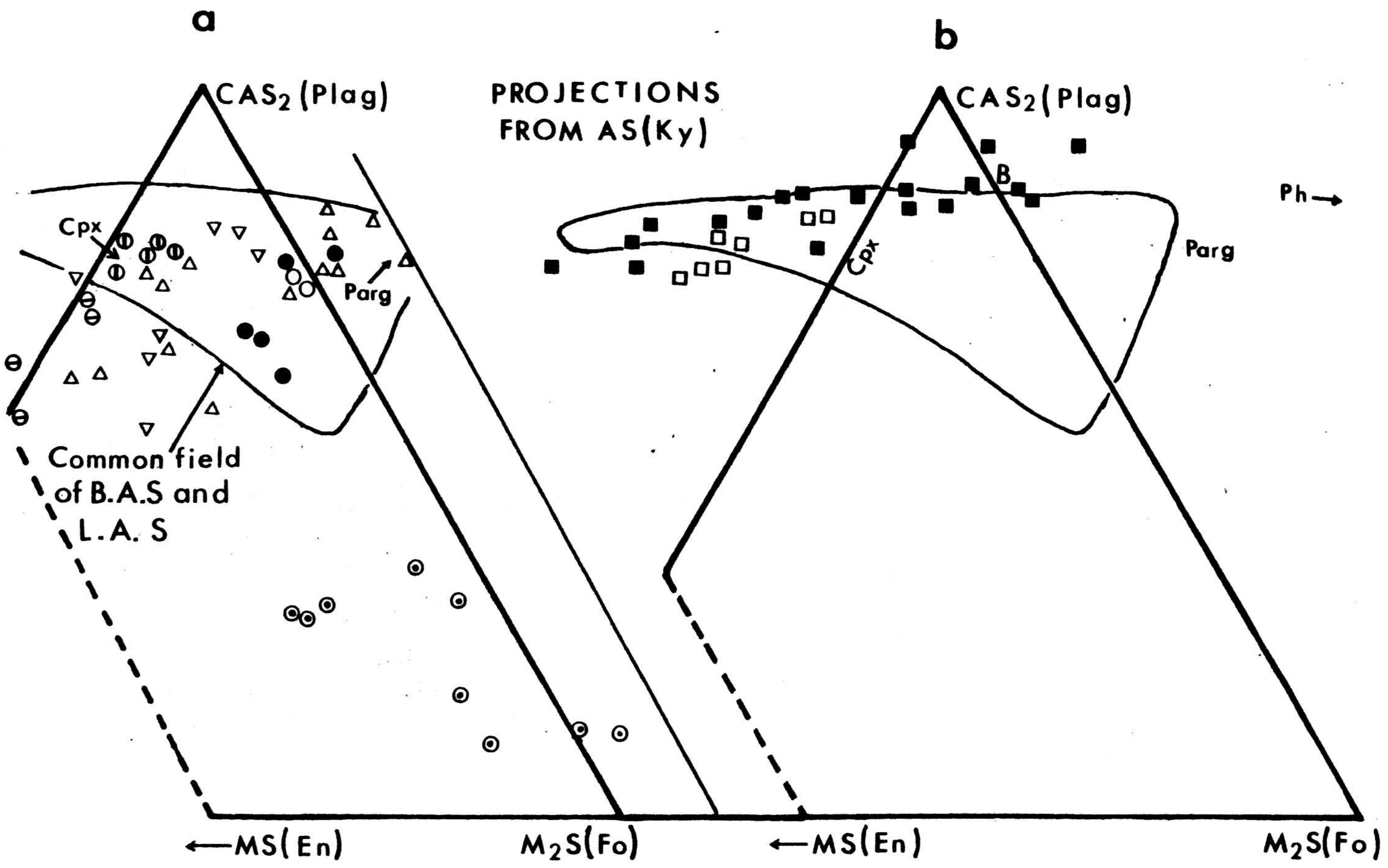
a
b
PROJECTIONS FROM AS(Ky)
CAS$_2$ (Plag)
Cpx
Parg
Common field of B.A.S and L.A. S
←MS(En)
M$_2$S(Fo)
CAS$_2$(Plag)
B
Ph→
Parg
Cpx
←MS(En)
M$_2$S(Fo)

Fold out sheet

Key to symbols in Figures
12·8a, 12·9a and 12·10a
Ardara appinite suite:
▽ Data from Table 12·1
△ Data from Hall (1967)
● Colonsay appinite suite
Sutherland rocks:
⊙ Scyelite
⊖ Pyroxenite
○ SiO_2-poor appinitic type rock
⦶ SiO_2-rich appinitic type rock

Key to symbols in Figures
12·8b 12·9b and 12·10b
□ Glen Coe lavas (Table 10·3)
B Glen Coe basalt (Bailey & Maufe 1960)
■ Lorne lavas (Groome & Hall 1974)

Abbreviations in Figures 12·8 (a,b)—12·10(a,b)
Oli = Olivine; Cpx = Clinopyroxene;
Parg = Pargasite; Ph = Phlogopite, biotite;
Sp = Spinel; Feld = Feldspar;
⬭ B.A.S = Ballachulish appinite suite
◌ L.A.S = Loch Lomond appinite suite

Figures 12.11 (a,b) - 12.14 (a,b). Comparison on the basis of Ni, Cr and Co *vs*. MgO and K/Rb *vs*. K_2O variations. Except for the Lorne lavas the rest of the data belong to the present investigation (Tables 12.1, 12.3). Key to symbols and abbreviations is given on the fold out sheet following Figure 12.14a,b.

Fig. 12·11

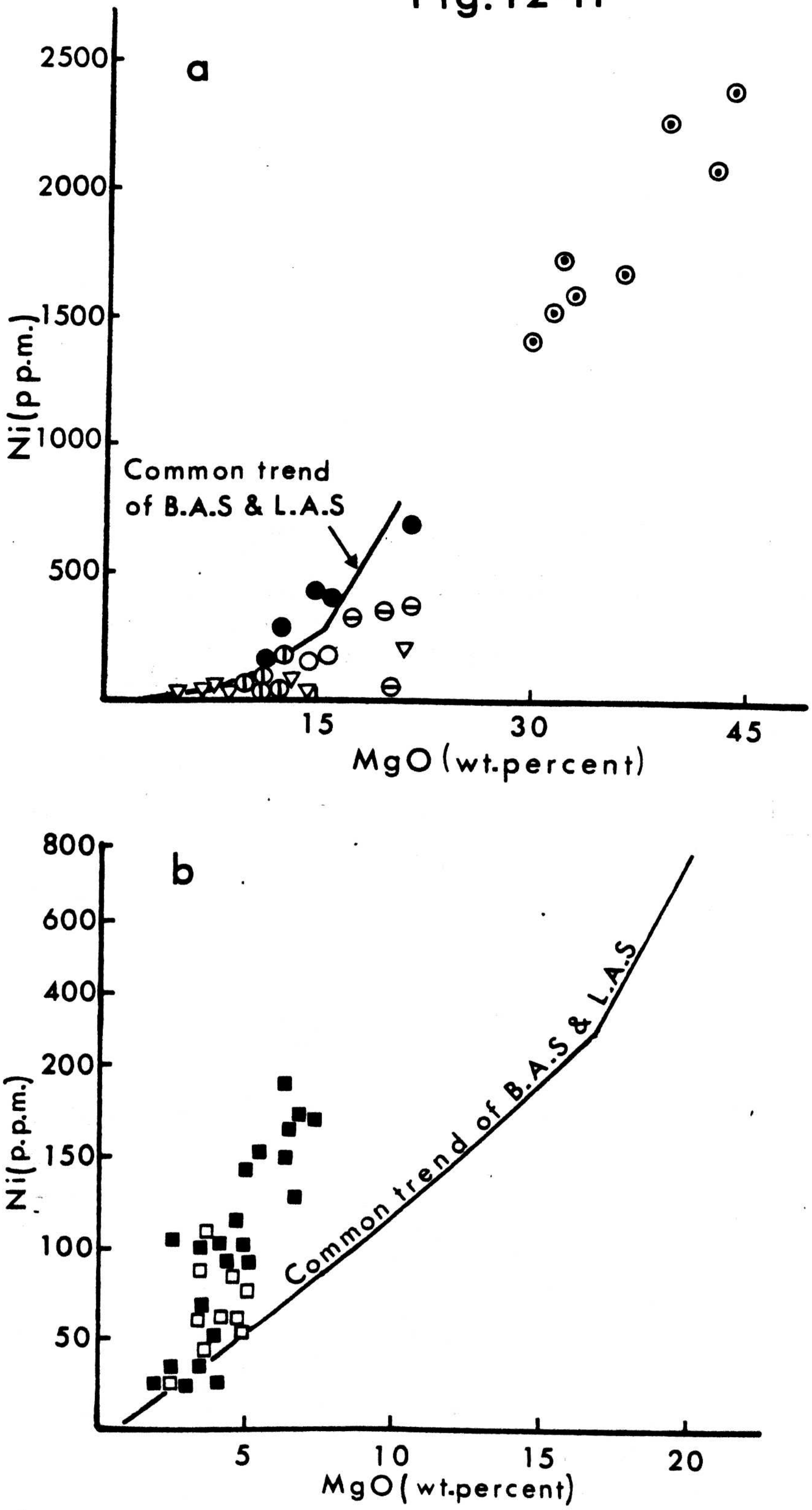
a
Ni(p.p.m.)
2500
2000
1500
1000
500
Common trend of B.A.S & L.A.S
15
30
45
MgO (wt.percent)
b
Ni(p.p.m.)
800
600
400
200
150
100
50
Common trend of B.A.S & L.A.S
5
10
15
20
MgO (wt.percent)

Fig. 12·12

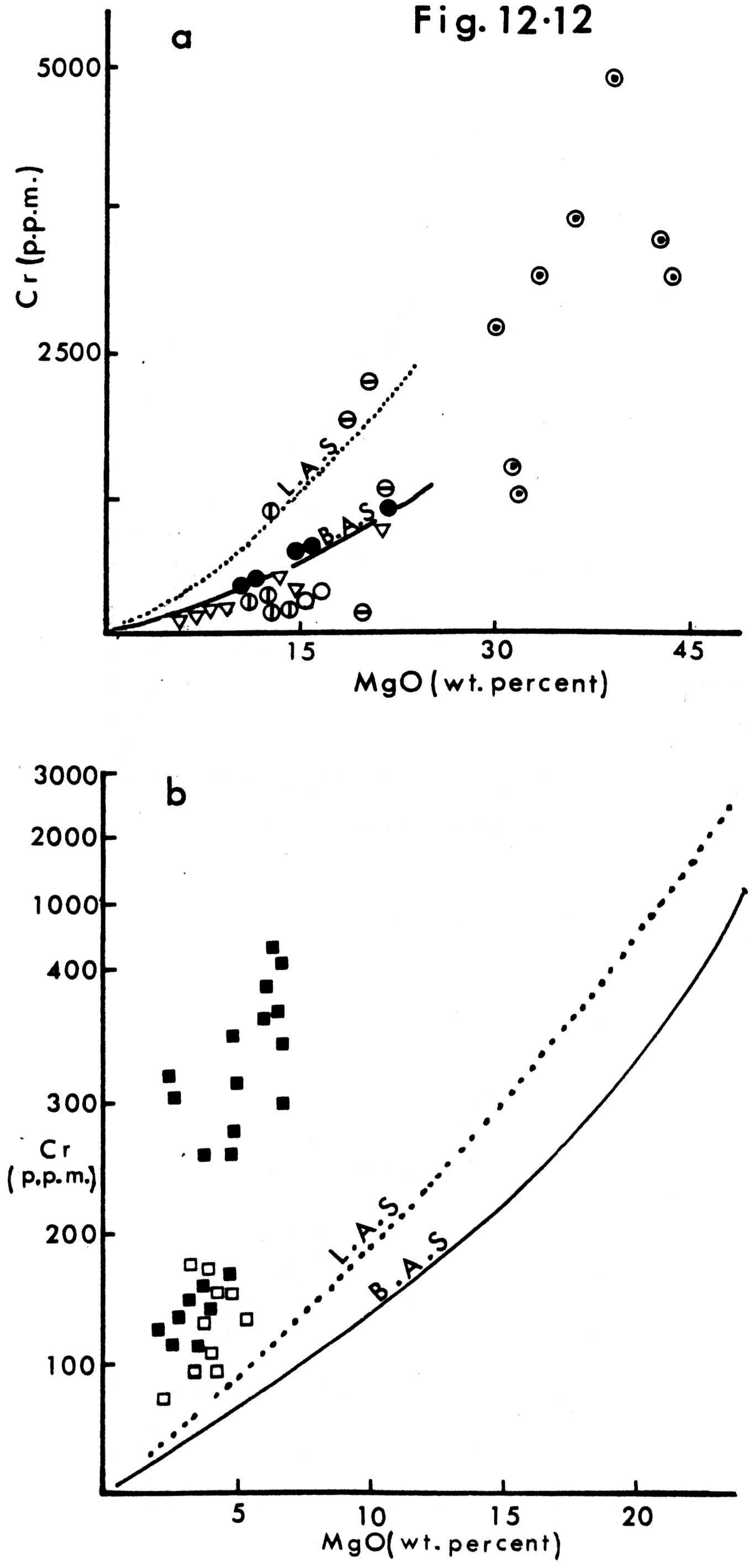
a
5000
2500
Cr (p.p.m.)
L.A.S.
B.A.S.
15
30
45
MgO (wt. percent)
b
3000
2000
1000
400
300
200
100
Cr
(p.p.m.)
L.A.S.
B.A.S.
5
10
15
20
MgO (wt. percent)

Fig. 12·13

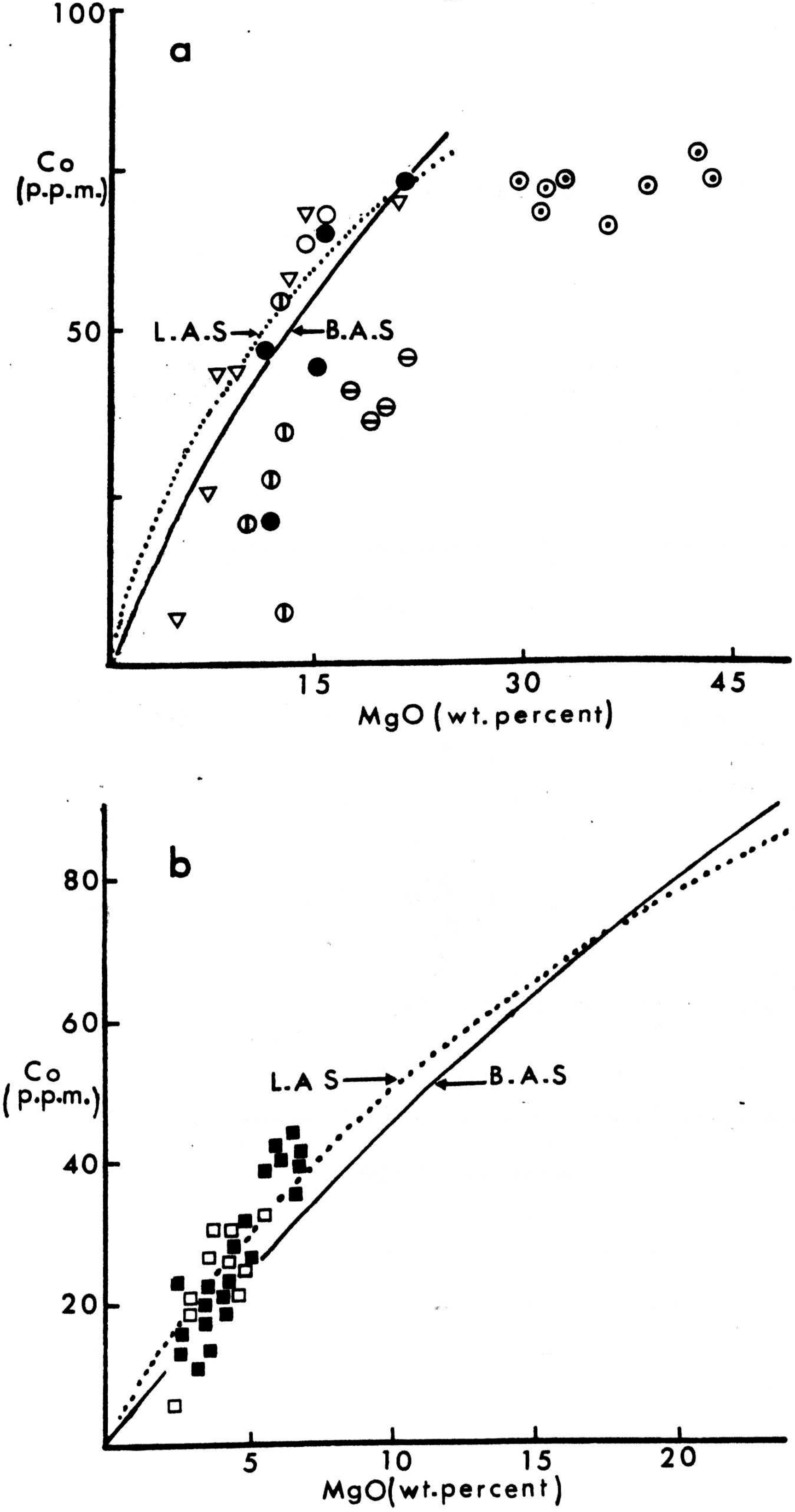
a
100
50
Co
(p.p.m.)
L.A.S
B.A.S
15
30
45
MgO (wt. percent)
b
80
60
40
20
Co
(p.p.m.)
L.A S
B.A.S
5
10
15
20
MgO(wt.percent)

Fig. 12·14

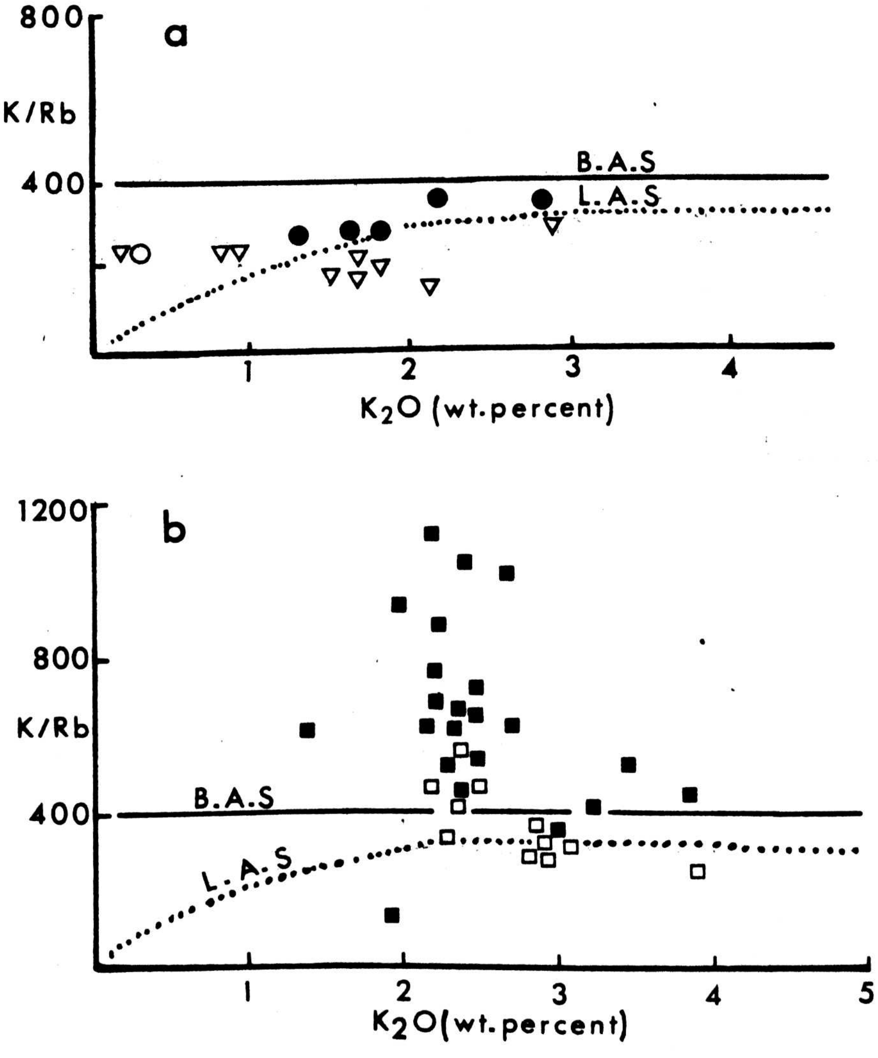
a
800
K/Rb
400
B.A.S
L.A.S
1
2
3
4
K₂O (wt.percent)
b
1200
800
K/Rb
400
B.A.S
L.A.S
1
2
3
4
5
K₂O(wt.percent)

Fold out sheet

Key to symbols in Figures
12·11a, 12·12 a, 12·13a and 12·14a
▽ Ardara appinite suite (Table 12·1)
● Colonsay appinite suite
Sutherland rocks:
⊙ Scyelite
⊖ Pyroxenite
○ SiO_2-poor appinitic type rock
⦶ SiO_2-rich appinitic type rock

Key to symbols in Figures
12·11b, 12·12b, 12·13b and 12·14b
□ Glen Coe lavas (Table 12·3)
■ Lorne lavas (Groome & Hall 1974)

Abbreviations in Figures 12·11(a,b)—12·14(a,b)
⬭ B.A.S = Ballachulish appinite suite
◌ L.A.S = Loch Lomond appinite suite

Figure 12.15. Comparison on the basis of Zr/Y *vs*. Zr discrimination diagram of Pearce and Norry (1979); data plotted include only analyses carried out in the present investigation; *cf*. Tables 12.1, 12.3.

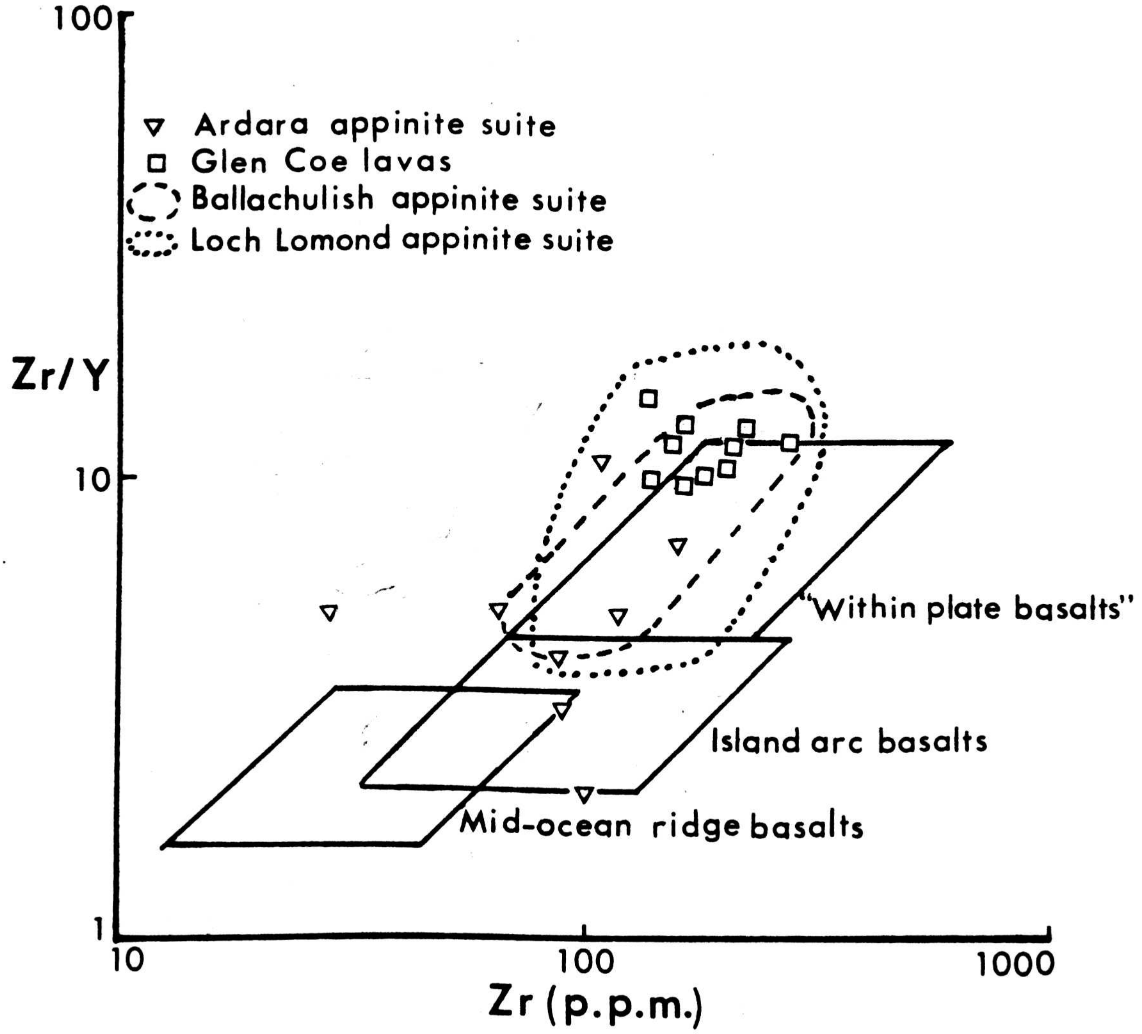
100
10
1
Zr/Y
▽ Ardara appinite suite
□ Glen Coe lavas
Ballachulish appinite suite
Loch Lomond appinite suite
"Within plate basalts"
Island arc basalts
Mid-ocean ridge basalts
10
100
1000
Zr (p.p.m.)

Table 12.1. Major and trace element analyses with estimated modal compositions from the appinite suites of Ardara and Colonsay and from the scyelite - pyroxenite - appinitic type rock association of Sutherland.

	1	2	3	4	5	6	7	8	9	10	11	12	13
SiO_2	47.07	47.88	49.41	49.69	50.01	50.33	53.65	57.43	43.84	47.29	48.21	49.33	49.84
TiO_2	0.46	1.10	1.24	0.71	1.17	0.92	0.45	0.55	0.91	1.00	0.86	0.50	0.60
Al_2O_3	3.50	9.71	13.15	8.80	15.99	15.57	10.08	11.72	6.79	12.72	10.30	10.44	12.20
Fe_2O_3	5.86	2.77	1.67	2.72	3.27	3.29	1.59	1.55	3.46	2.99	2.25	2.65	2.94
FeO	4.61	7.22	7.32	7.90	5.07	5.38	4.98	4.53	7.33	7.04	6.80	6.62	5.46
MnO	0.17	0.18	0.14	0.18	0.11	0.15	0.12	0.13	0.20	0.17	0.20	0.19	0.15
MgO	21.32	13.20	9.30	14.33	7.14	7.92	9.93	5.20	21.62	11.54	15.63	14.84	11.42
CaO	10.16	10.80	8.92	9.84	7.98	8.32	13.20	8.99	9.09	10.90	8.98	8.49	8.12
Na_2O	0.74	1.27	2.96	1.62	2.86	3.20	1.71	2.06	0.74	2.22	1.72	1.81	2.54
K_2O	0.11	0.93	1.68	0.82	2.16	1.68	1.50	2.87	1.86	1.96	1.63	2.17	2.84
P_2O_5	0.02	0.05	0.17	0.05	0.21	0.18	0.07	0.27	0.09	0.43	0.19	0.29	0.33
H_2O	4.83	3.38	3.02	3.38	3.11	2.75	1.33	2.01	3.49	1.22	1.87	1.92	2.97
CO_2	0.57	0.15	0.50	0.15	0.25	0.42	0.37	1.92	0.56	0.05	0.48	0.15	0.24
Total	99.42	98.64	99.48	100.19	99.33	100.01	98.98	99.23	99.98	99.53	99.12	99.40	99.68
Trace elements (p.p.m.)													
Cr	873	482	217	318	155	200	142	52	1099	474	740	714	541
Co	70	59	44	68	26	44	36	7	73	22	66	45	48
Ni	179	57	2	7	25	44	10	9	690	138	415	407	288
Ba	52	191	224	148	528	375	339	407	675	406	527	530	609
Ce	23	37	63	51	48	34	39	46	23	28	23	28	40
Cu	23	61	33	21	47	32	25	8	35	48	51	33	33
Ga	6	17	18	24	26	19	12	17	11	16	10	12	14
La	0	9	18	11	18	11	13	20	0	2	3	8	17
Nb	4	6	7	3	12	8	4	8	2	0	3	3	0
Pb	0	10	17	10	21	16	10	19	1	3	6	6	10

Rb	4	33	85	29	125	65	70	84	56	20	48	50	66
Sr	48	213	334	122	559	585	310	368	240	4	346	515	686
Th	3	11	11	6	12	3	6	10	4	36	4	1	4
Y	6	23	43	25	24	13	10	20	12	1	12	12	12
Zn	51	65	76	80	84	68	56	66	83	15	80	77	64
Zr	28	89	100	89	119	63	106	149	7	58	32	5	63

Modal analyses

Olivine	5	0	0	0	-	0	0	0	-	-	-	-	-
Clinopyroxene	10	0	15	0	-	20	25	25	-	-	-	-	-
Amphibole	5	85	33	85	-	45	35	5	-	-	-	-	-
Phlogopite	0	10	5	0	-	Tr	Tr	10	-	-	-	-	-
Plagioclase	25	5	30	15	-	25	30	40	-	-	-	-	-
Orthoclase	0	0	0	Tr	-	5	5	5	-	-	-	-	-
Microcline	0	0	0	0	-	Tr	Tr	5	-	-	-	-	-
Quartz	0	0	0	Tr	-	5	5	10	-	-	-	-	-
Calcite (prim.)	0	0	0	0	-	Tr	Tr	Tr	-	-	-	-	-
Opaque ores	0	0	1	Tr	-	0	0	0	-	-	-	-	-
Apatite (prim.)	0	0	0	0	-	0	0	Tr	-	-	-	-	-
Sphene (prim.)	0	0	1	0	-	Tr	Tr	Tr	-	-	-	-	-
Chlorite (sec.)	0	Tr	0	0	-	0	0	Tr	-	-	-	-	-
Epidote (sec.)	0	Tr	0	0	-	0	0	Tr	-	-	-	-	-
Sericite	0	0	10	0	-	0	0	0	-	-	-	-	-
Fine grained mixt.	50	0	0	0	-	0	0	0	-	-	-	-	-
Total	100	100	100	100		100	100	100	-	-	-	-	-

Table 12.1. (Contd.)

	14	15	16	17	18	19	20	21	22	23	24
SiO_2	37.70	38.31	39.85	41.05	41.15	41.82	43.27	43.45	44.38	46.32	47.87
TiO_2	0.06	0.10	0.10	0.11	0.22	0.09	0.27	0.25	0.21	0.93	0.45
Al_2O_3	1.24	1.83	1.84	2.27	4.11	3.58	4.43	5.05	4.58	7.48	7.39
Fe_2O_3	5.71	4.68	3.68	5.16	4.62	5.10	3.86	5.96	3.57	2.18	2.68
FeO	3.05	2.84	3.73	1.76	3.67	2.08	4.89	1.88	4.18	6.21	6.39
MnO	0.14	0.10	0.11	0.12	0.14	0.12	0.12	0.13	0.13	0.13	0.16
MgO	36.15	42.41	39.08	43.57	33.05	33.03	31.21	29.86	31.81	14.33	15.66
CaO	2.49	0.99	0.50	0.97	3.04	4.90	3.58	2.16	3.27	11.58	12.00
Na_2O	0.20	0.17	0.18	0.26	0.77	0.18	0.58	0.32	0.64	1.18	1.08
K_2O	0.00	0.60	0.72	0.65	0.85	0.07	1.16	1.91	0.56	2.17	2.89
P_2O_5	0.03	0.06	0.03	0.06	0.12	0.07	0.12	0.11	0.20	0.04	0.05
H_2O	11.19	7.06	9.81	3.25	6.26	6.49	4.14	7.66	6.18	3.85	2.35
CO_2	0.00	0.16	0.45	0.15	1.46	0.36	1.15	1.15	0.50	1.03	0.02
Total	97.96	99.31	100.08	99.38	99.46	99.47	99.07	99.89	100.21	97.96	99.47
Trace elements (p.p.m.)											
Cr	3639	3465	4914	3151	-	3148	1439	2705	1195	150	125
Co	66	77	72	73	-	73	68	73	72	61	67
Ni	1676	2064	2266	2388	-	1583	1527	1418	1330	130	125
Ba	43	223	186	14	-	49	364	315	156	700	675
Ce	8	24	3	12	-	20	27	36	46	25	30
Cu	9	3	31	6	-	3	4	21	6	160	155
Ga	1	2	2	3	-	2	5	6	7	10	11
La	2	2	0	4	-	5	9	8	14	2	2
Nb	1	8	5	4	-	4	5	3	6	10	9
Pb	2	1	0	5	-	5	5	0	1	10	12

Rb	4	18	20	21	-	4	27	60	14	75	73
Sr	107	140	19	17	-	71	402	72	248	207	211
Th	2	1	3	2	-	5	5	4	7	1	1
Y	0	5	0	2	-	0	8	6	6	7	7
Zn	52	52	43	42	-	39	60	53	68	50	52
Zr	16	80	2	33	-	29	49	30	87	0	0

Modal analyses

Olivine	-	-	-	-	30	20	20	-	25	0	0
Clinopyroxene	-	-	-	-	15	20	25	-	Tr	10	15
Amphibole	-	-	-	-	33	10	40	-	35	70	65
Phlog.-biot.	-	-	-	-	15	10	10	-	35	5	10
Plagioclase	-	-	-	-	0	0	0	-	Tr	5	5
Orthoclase	-	-	-	-	0	0	0	-	0	3	2
Microcline	-	-	-	-	0	0	0	-	0	5	0
Quartz	-	-	-	-	0	0	0	-	0	2	3
Opaque ores	-	-	-	-	5	Tr	2	-	3	0	Tr
Apatite (prim.)	-	-	-	-	0	0	0	-	0	0	0
Sphene (prim.)	-	-	-	-	0	0	0	-	0	0	Tr
Calcite (sec.)	-	-	-	-	1	Tr	1	-	0	0	Tr
Chlorite (sec.)	-	-	-	-	1	0	2	-	2	0	0
Serpentine (sec.)	-	-	-	-	0	40	0	-	0	0	0
Sericite	-	-	-	-	0	0	0	-	0	0	0
Total	-	-	-	-	100	100	100		100	100	100

Table 12.1. (Contd.)

	25	26	27	28	29	30	31	32	33
SiO_2	52.59	53.29	53.66	54.07	54.13	54.72	55.06	55.22	55.53
TiO_2	0.45	0.13	0.13	0.38	0.23	0.13	0.30	0.44	0.13
Al_2O_3	5.61	1.15	1.71	4.63	4.52	1.15	4.63	5.64	1.23
Fe_2O_3	2.83	3.10	1.66	2.95	3.01	1.63	2.76	3.64	2.38
FeO	3.88	3.42	3.66	3.68	3.54	3.57	4.49	4.17	2.80
MnO	0.16	0.21	0.17	0.17	0.18	0.15	0.21	0.21	0.17
MgO	12.47	21.67	17.40	12.58	11.59	19.78	12.73	9.96	18.98
CaO	14.67	13.35	18.36	16.96	17.60	16.04	17.06	16.22	16.34
Na_2O	1.67	0.41	0.95	2.65	3.20	0.66	2.25	2.99	0.63
K_2O	0.59	0.04	0.10	0.14	0.04	0.06	0.22	0.42	0.05
P_2O_5	0.08	0.02	0.02	0.06	0.93	0.02	0.06	0.17	0.03
H_2O	3.85	1.51	0.74	0.06	0.29	1.88	0.00	0.00	1.01
CO_2	1.03	0.62	0.70	0.11	0.12	0.13	0.00	0.12	0.10
Total	99.85	98.92	99.24	99.44	99.38	99.92	99.77	99.20	99.38
				Trace elements (p.p.m.)					
Cr	1081	1265	1854	178	250	2298	300	117	25
Co	55	46	41	8	28	39	35	21	17
Ni	170	350	311	36	81	342	70	52	37
Ba	263	36	22	159	441	23	118	859	384
Ce	44	18	32	20	59	18	33	35	25
Cu	5	2	0	0	0	0	0	7	21
Ga	4	3	8	3	10	2	6	11	0
La	9	0	9	1	11	2	5	5	2
Nb	1	3	4	0	7	3	8	8	2
Pb	9	4	3	3	13	2	14	12	9
Rb	17	2	4	4	3	2	5	8	3
Sr	348	127	178	379	710	129	606	898	130
Th	4	2	1	2	7	0	2	2	0
Y	3	5	11	1	11	2	8	10	5
Zn	57	37	37	28	45	33	69	47	36
Zr	55	20	31	33	39	22	59	13	24

Modal analyses

Olivine	0	-	-	-	0	-	0	0	Tr
Clinopyroxene	50	-	-	-	20	-	25	0	80
Amphibole	30	-	-	-	40	-	65	60	20*
Phlog.-biot.	5	-	-	-	0	-	0	0	0
Plagioclase	5	-	-	-	40	-	10	40	0
Orthoclase	0	-	-	-	0	-	0	0	0
Microcline	Tr	-	-	-	0	-	0	0	0
Quartz	0	-	-	-	0	-	0	Tr	0
Opaque ores	Tr	-	-	-	0	-	0	0	0
Apatite (prim.)	Tr	-	-	-	0	-	0	0	0
Sphene (prim.)	0	-	-	-	0	-	Tr	Tr	0
Calcite (sec.)	0	-	-	-	0	-	0	0	0
Chlorite (sec.)	0	-	-	-	0	-	0	0	0
Serpentine (sec.)	0	-	-	-	0	-	0	0	0
Sericite	10	-	-	-	0	-	0	0	0
Total	100	-	-	-	100	-	100	100	100

Ardara
1 Altered peridotite.
2 - 7 Appinite and hornblende diorite.
8 Pyroxene - mica diorite.

Colonsay and Ross of Mull
9 Kentallenite, Balnahard intrusion, Colonsay.
10 Appinite, Scalasaig intrusion, Colonsay.
11 Hornblendite, Loch Kerry, Gruinard, Ross of Mull.
12 Altered appinite, locality as in 10.
13 Hornblende syenite, north shore of Port Easdale, Kiloran Bay, Colonsay.

Cnoc á Ghriama, Sutherland
14 - 17 Altered scyelite.
18 - 22 Scyelite.
23 - 24 SiO_2-poor appinitic type rock.
25 SiO_2-rich appinitic type rock.
26 - 27 Pyroxenite.
28 - 29 SiO_2-rich appinitic type rock.
30 Pyroxenite.
31 - 32 SiO_2-rich appinitic type rock.
33 Pyroxenite.

* Amphibole mostly secondary after clinopyroxene.

Table 12.2. Amphibole compositions from the appinite of Ardara (Table 12.1 –2).

	1	2	3	4	5	6
SiO_2	45.64	53.55	53.54	43.37	50.55	51.82
TiO_2	0.83	0.00	0.17	0.91	0.39	0.22
Al_2O_3	10.05	3.80	3.26	12.17	7.28	4.87
FeO	12.20	9.29	9.07	13.80	9.64	9.93
MnO	0.26	0.19	0.00	0.00	0.17	0.24
MgO	13.60	17.94	18.28	12.83	17.05	17.17
CaO	12.70	13.38	12.92	12.50	12.33	13.08
Na_2O	1.47	0.57	0.71	1.91	1.29	0.87
K_2O	0.63	0.12	0.18	0.80	0.14	0.22
Total	97.38	98.84	98.13	98.29	98.84	98.42
Trace elements (p.p.m.)						
Cr	b.d.	b.d.	b.d.	1987	b.d.	1873
Co	4276	b.d.	b.d.	1636	2409	b.d.
Ni	3031	b.d.	b.d.	b.d.	b.d.	b.d.
Formula on the basis of 23 oxygens						
Si	6.71	7.53	7.57	6.38	7.15	7.36
Ti	0.09	0.00	0.02	0.10	0.04	0.02
Al	1.74	0.63	0.54	2.11	1.21	0.81
Fe	1.50	1.09	1.07	1.70	1.14	1.18
Mn	0.03	0.02	0.00	0.00	0.02	0.03
Mg	2.98	3.76	3.85	2.81	3.59	3.63
Ca	2.00	2.01	1.96	1.97	1.87	1.99
Na	0.42	0.15	0.19	0.54	0.35	0.24
K	0.12	0.02	0.03	0.15	0.02	0.04
Al_4	1.29	0.47	0.43	1.62	0.85	0.64
Al_6	0.45	0.16	0.11	0.49	0.36	0.54

1 Edenitic hornblende crystal.

2 - 3 Actinolitic overgrowths on edenitic hornblende in 1.

4 - 6 Zoned hornblende crystal with a core of ferroan - pargasitic - hornblende composition (4), a rim of magnesio - hornblende composition (5) and an overgrowth of actinolitic hornblende composition (6).

b.d. = below detection limit (see Appendix A.2).

FeO = total iron.

Table 12.3. Major and trace element analyses and estimated modal compositions of andesites from the Glen Coe lavas.

	1	2	3	4	5	6	7	8	9	10
SiO_2	54.10	56.09	56.42	57.44	58.32	58.78	58.89	59.12	60.17	60.97
TiO_2	1.24	1.07	1.36	1.06	0.81	0.78	1.09	0.17	1.04	0.77
Al_2O_3	15.71	15.51	17.13	16.55	15.81	15.19	16.10	15.31	16.45	15.85
Fe_2O_3	3.55	2.34	2.48	2.86	0.00	0.00	2.21	0.00	1.89	2.52
FeO	3.43	4.00	4.85	3.54	7.04	5.46	3.99	6.80	3.20	2.89
MnO	0.13	0.09	0.15	0.11	0.11	0.11	0.12	0.12	0.13	0.12
MgO	4.13	4.12	4.13	5.05	3.65	3.98	3.85	3.44	2.32	3.76
CaO	4.79	4.94	5.95	6.15	3.90	3.70	4.47	5.57	4.97	4.84
Na_2O	4.54	4.17	4.84	3.68	3.90	3.90	4.85	3.97	3.85	4.84
K_2O	2.93	3.05	2.32	2.23	2.95	2.99	2.81	2.30	3.92	2.25
P_2O_5	0.35	0.34	0.39	0.37	0.27	0.29	0.37	0.24	0.47	0.25
H_2O	3.01	2.52	0.00	0.81	1.83	2.59	0.00	1.61	0.00	0.54
CO_2	1.81	1.03	0.00	0.03	1.11	1.19	1.06	0.43	1.16	0.00
Total	99.72	99.27	100.02	99.88	99.70	98.96	99.81	99.08	99.57	99.60
				Trace elements (p.p.m.)						
Cr	89	145	147	132	109	132	93	175	63	168
Co	24	25	28	34	21	17	26	18	5	31
Ni	51	53	83	79	61	65	50	109	27	89
Ba	756	2002	714	767	995	943	955	897	523	1014
Ce	59	62	61	68	54	49	87	58	88	48
Cu	7	54	13	36	64	70	0	55	24	1
Ga	41	27	59	15	16	9	22	10	16	35
La	30	32	31	33	12	26	33	23	50	20

Nb	14	17	17	13	11	12	15	11	16	9
Pb	14	20	18	17	14	17	17	22	27	18
Rb	64	78	38	59	94	84	78	46	125	40
Sr	788	707	934	979	956	984	379	1171	274	970
Th	8	7	8	5	11	10	12	6	8	8
Y	15	15	16	15	12	15	16	13	21	8
Zn	0	107	81	81	67	64	87	67	148	84
Zr	191	99	207	171	174	158	216	136	284	135

Modal analyses

Olivine	0	0	-	5	0	0	0	5	-	-
Clinopyroxene	0	0	-	5	0	0	0	15	-	-
Amphibole	Tr	0	-	0	0	0	0	10	-	-
Biotite	0	0	-	10	10	0	0	1	-	-
Plagioclase	65	75	-	75	70	80	75	65	-	-
Orthoclase	0	0	-	0	10	0	0	-	-	-
Quartz	0	0	-	0	5	0	0	-	-	-
Opaque ores	20	5	-	5	4	5	5	3	-	-
Apatite (prim.)	0	0	-	0	1	0	0	Tr	-	-
Chlorite (sec.)	15	20	-	0	0	15	20	1	-	-
Total	100	100		100	100	100	100	100	-	-

PART 5

TECTONIC SETTING, SOURCE OF MAGMA AND CONCLUSIONS

CHAPTER 13 TECTONIC SETTING AND SOURCE OF MAGMA

13.1 Tectonic setting

The variation of magma type from high potassium calc-alkaline at Ballachulish to normal calc-alkaline at Loch Lomond and to transitional between calc-alkaline and tholeiitic at Ardara, Donegal corresponds with variations observed in modern day calc-alkaline volcanic suites associated with subduction (c.f. Dickinson 1975). Accordingly the derivation of the magma from which the appinite suite crystallised is interpreted as being related to subduction in the British Caledonides. Such subduction is generally thought to have ceased by late Silurian or early Devonian times (Williams 1972; Lambert & McKerrow 1976; McKerrow & Cocks 1976) while the time of emplacement of the appinite suite must have been during the latter part of Silurian times; it predates granites such as Ballachulish granite that were emplaced at about the Silurian - Devonian boundary (c. 410 m.y.). As yet radiometric methods have not produced an age of crystallisation and emplacement for the appinite suites investigated. The 413-415 m.y., K-Ar mineral ages (Brown 1972) must represent minimum ages and probably represent time of uplift associated with granite emplacement. Possibly the nearest estimation at present is that of 430 ± 4 m.y. for the Loch Borolan alkaline igneous complex (van Breemen et al. 1979) with its marginal appinite-like ledmorite suite, with pyroxenite (Parsons & McKirdy 1983, fig. 1), a suite that would appear to be related to the Sutherland appinitic-type rocks described in Chapter 12.

Some workers (e.g. Stillman & Francis 1979) consider that the late Caledonian calc-alkaline lavas and Newer granites emplaced about the Silurian - Devonian boundary, were formed subsequent to the closure of Iapetus ocean and so post-date subduction. However, several workers have regarded this magmatism as a result of an active subduction and thus comparable to other calc-alkaline magmatisms of the world (Groome & Hall 1974; Mitchell & McKerrow 1975; Phillips et al. 1976; French et al. 1979; Johnstone et al. 1979). Both northward- and southward-dipping subduction zones have been inferred by different workers on the basis of stratigraphic and structural and chemical data (Fitton & Hughes 1970; Church & Gayer 1973; Leggett et al. 1979; Stillman & Williams 1979) but generally the suture zone (Iapetus) is considered to be ENE-trending and located, at present erosion level, between the Lake District and Southern Uplands (see Thirlwall 1981, p.139).

The systematic northwestwards increase in the concentration of several large ion lithophile elements and light REE in the ORS lavas north of the Southern Uplands fault is interpreted by Thirlwall (1981, 1982) as being related to a subduction zone that changed its strike from ENE in Ireland to NNE in North Sea (Fig. 13.1). If the appinite suite is consanguineous with the ORS lavas, as suggested in Chapter 12, then it should show petrochemical changes related to distance from the former site of subduction, comparable to those shown by the ORS lavas.

13.1A Spatial chemical variation

On the basis of a northwesterly relative plate motion, the respective positions of the Ballachulish, Loch Lomond and Ardara clusters are in decreasing order of distance from the proposed location of the subduction zone (Fig. 13.1). When compared with the Loch Lomond cluster the Ballachulish cluster has (1) higher K_2O, Ba, Sr and Ce but lower Th and (2) higher La/Y and K/Rb ratios (Figs 13.2, 13.3). These features correspond with those reported by Thirlwall (1981, 1982) for the ORS lavas and are likewise consistent with subduction related genesis.

The increase in K_2O, Ba, Sr and Ce contents and in La/Y ratios with distance from the proposed subduction zone towards a continental environment shown by the appinite suite and lavas in Scotland correspond with spatial chemical variations observed in most calc-alkaline rock series found across the destructive plate margins, but the increase in K/Rb ratio and a decrease in Th content are in contrast to this (see Jakeš & White 1972; Wood et al. 1979). Moreover, the variation shown by the Ardara cluster on the basis of K_2O, Ba and Sr contents and La/Y and K/Rb ratios is consistent with that shown by the other two clusters but the mean Ce and Th contents in Ardara cluster are comparable to those of the Ballachulish cluster and are thus not in accord with other observed chemical variations (Figs 13.2a-c, 13.3; also see Section 12.1). This apparent discrepancy could be attributed to either insufficient and unrepresentative sampling of Ardara cluster or to mantle heterogeneity. However, Th contents and K/Rb ratios in the Ballachulish cluster and Loch Lomond masses indicate that the geotectonic positions may not simply have been that of a northwestward-dipping subduction zone.

The following are factors that need consideration:

1. Longman et al. (1979) have suggested that in addition to the Iapetus subduction zone, subduction also took place in Arenig times further northwards with a northwesterly-dipping subduction zone represented by the Highland boundary fault zone. This was associated with the closure of a marginal basin related to the northwesterly movement of the Ordovician Ballantrae island arc.
2. Wright and Bowes (1979) have suggested that the Great Glen fault, which is close to the Ballachulish cluster and whose development controlled the formation of the pipe-shaped structures used during the uprise of the appinite suite there (Bowes & Wright 1967), may have acted as a favoured channelway for the uprise of volatiles from the mantle. Any such activity could complicate any geochemical pattern resulting from subduction related magmatism.
3. van Breemen and Bluck (1981) and Thirlwall (1981, p.38) have

pointed out that incorporation of lower crustal material may have occurred into the region where basic magmas are being generated.

While these and possibly other features may add complications, the geochemical features are best interpreted as indicating that the generation of the magma from which the appinite suite crystallised was subduction-related phenomenon associated with the overall geotectonic evolution of the British Caledonides.

13.2 Source of magma

The high levels of Ni and Cr in olivine and clinopyroxene from the Ballachulish and Loch Lomond clusters (Chapters 3, 4, 9) and in the majority of the rock types from all the major clusters (Chapters 7, 10, 12), indicate crystallisation from a primitive melt. In the ultramafic and many of the mafic rocks representing cumulate compositions, the extremely high Ni and Cr contents can be related to enrichment in cumulate crystals compared to residual liquid (c.f. Chapter 8). However, the Ni (c. 100 - 400 p.p.m.) and Cr (c. 200 - 600 p.p.m.) contents of the mafic and intermediate rocks interpreted as representing residual liquid compositions (i.e. residual liquid dominating cumulate crystals) correspond to those of mantle-derived, mid-ocean-ridge basalts (c.f. Sun et al. 1979). In addition, the average K/Rb ratios of the Ballachulish and Loch Lomond clusters fall in range of that shown by a mantle of chondritic composition while Ardara cluster has a lower average K/Rb ratio. The average K/Rb ratios for all these clusters are within the ranges of those shown for ultramafic rocks and calc-alkaline and alkaline basalts of a mantle origin (Fig. 13.13). All this evidence indicates magma generation in the mantle, something that has also been shown by Thirlwall (1982) for the ORS lavas on the basis of Nd and Sr isotopes as well as major and trace element compositions. Moreover, a mantle source is indicated by the crystallisation temperatures (c. 1800° - 1700°C; see Chapters 3, 8, 11) of olivine in the appinite suites of the Ballachulish and Loch Lomond regions. Based on the Phanerozoic geothermal gradient of Tarling (1980), a minimum depth of about 200 km is inferred.

The high levels of volatiles in rocks of the appinite suite can be attributed to the melting of a hydrous mantle, i.e. of phlogopite-amphibole-peridotite composition (see Kushiro 1974; Mysen *et al*. 1974; Wyllie 1973) although it must be borne in mind that (1) the tectonic position of crystallisation with structural traps impeding uprise probably meant that a higher volatile proportion than normal may have been retained in the magma chambers and (2) the Great Glen fault and related transcurrent faults must be very deep structures and may have concentrated into localised regions volatiles escaping from the mantle.

13.3 Conclusions

1. Many features of the spatial chemical variation in the appinite suite are consistent with a genetic relation of magma generation with a northwesterly-dipping subduction zone.
2. Magmas for the appinite suite were generated as a result of melting of a hydrous mantle, probably at a depth of 200 km.

Figure 13.1 Suggested position of the surface trace of the late Silurian subduction zone in British Caledonides (after Thirlwall 1981). While many authors place northern Scotland further to the northeast (i.e. a different sense of movement on the Great Glen Fault), this does not affect the argument concerning the positions of the Ballachulish, Loch Lomond and Ardara clusters in relation to the Iapetus suture.

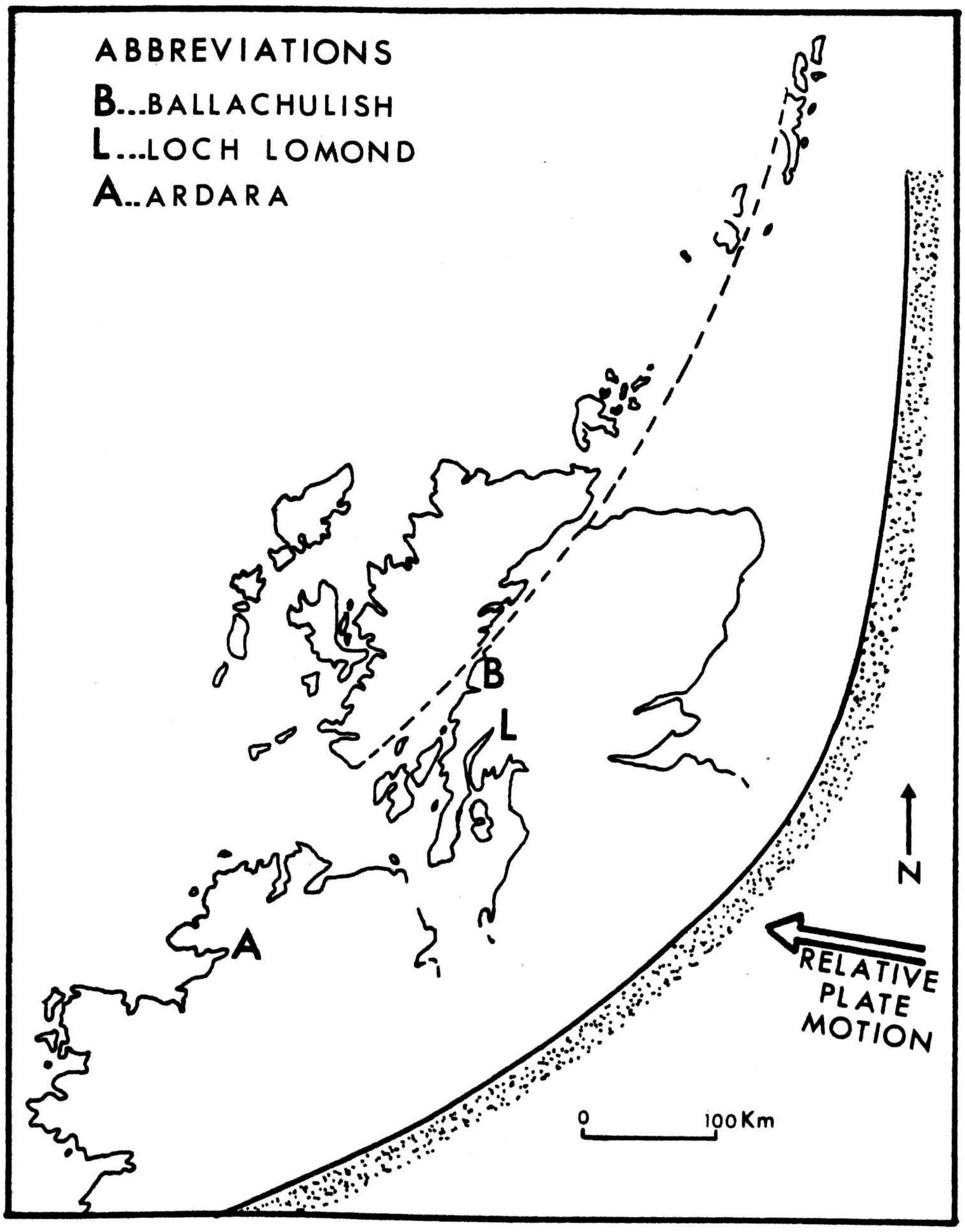
ABBREVIATIONS
B...BALLACHULISH
L...LOCH LOMOND
A..ARDARA
B
L
A
N
RELATIVE PLATE MOTION
0
100Km

Figure 13.2 (a-c) Mean concentrations of Ba, Sr, Ce and Th and mean La/Y ratios in various rock types from Ballachulish, Loch Lomond and Ardara appinite suites.

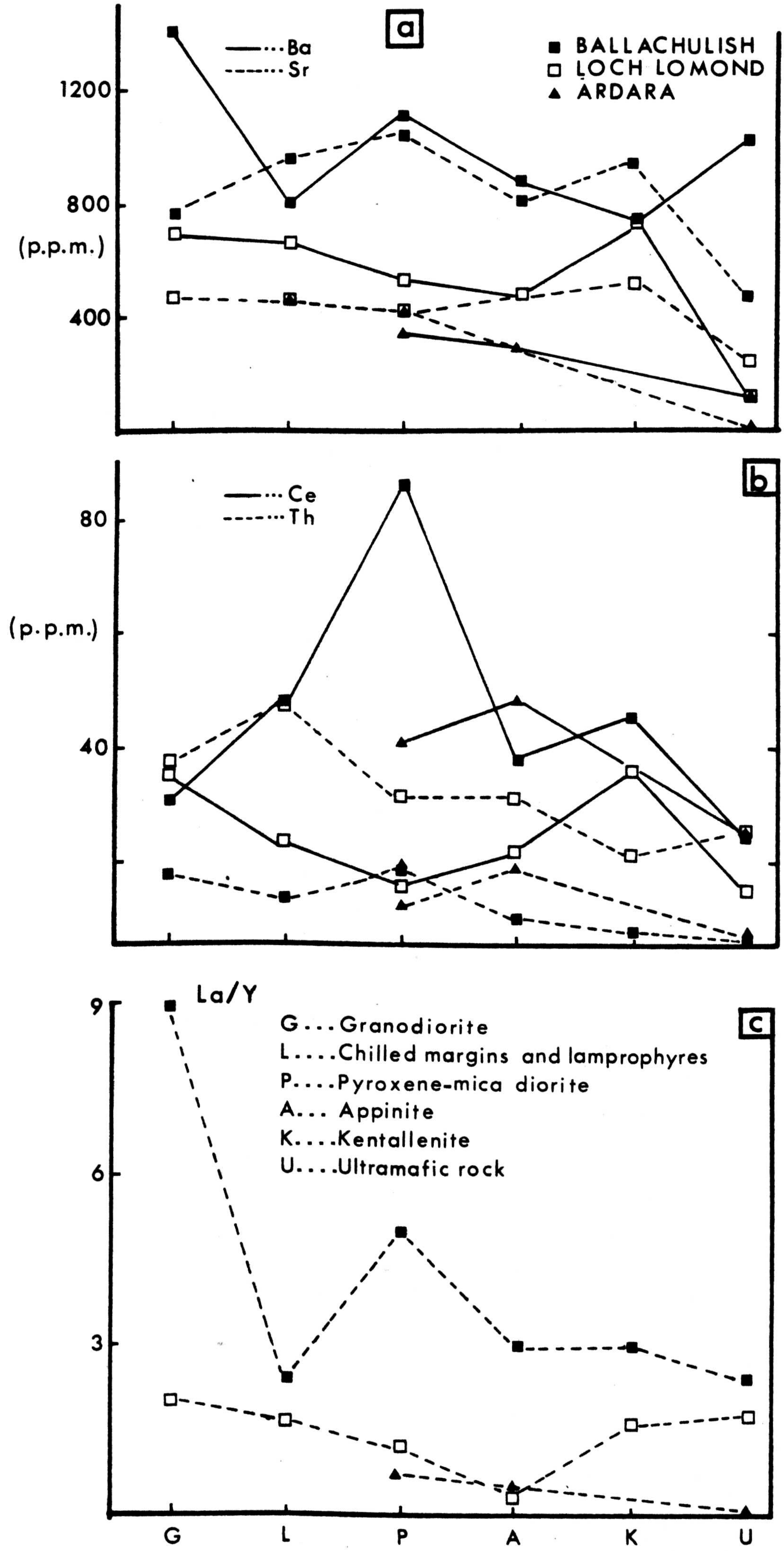
a
——··· Ba
------··· Sr
■ BALLACHULISH
□ LOCH LOMOND
▲ ARDARA
1200
800
(p.p.m.)
400
b
——··· Ce
------··· Th
80
(p.p.m.)
40
c
La/Y
9
6
3
G ... Granodiorite
L .... Chilled margins and lamprophyres
P .... Pyroxene-mica diorite
A ... Appinite
K .... Kentallenite
U .... Ultramafic rock
G
L
P
A
K
U

Figure 13.3 Comparison of the appinite suites with various mantle and mantle-derived compositions on the basis of K/Rb vs K_2O variations (mainly after Beswick 1976).

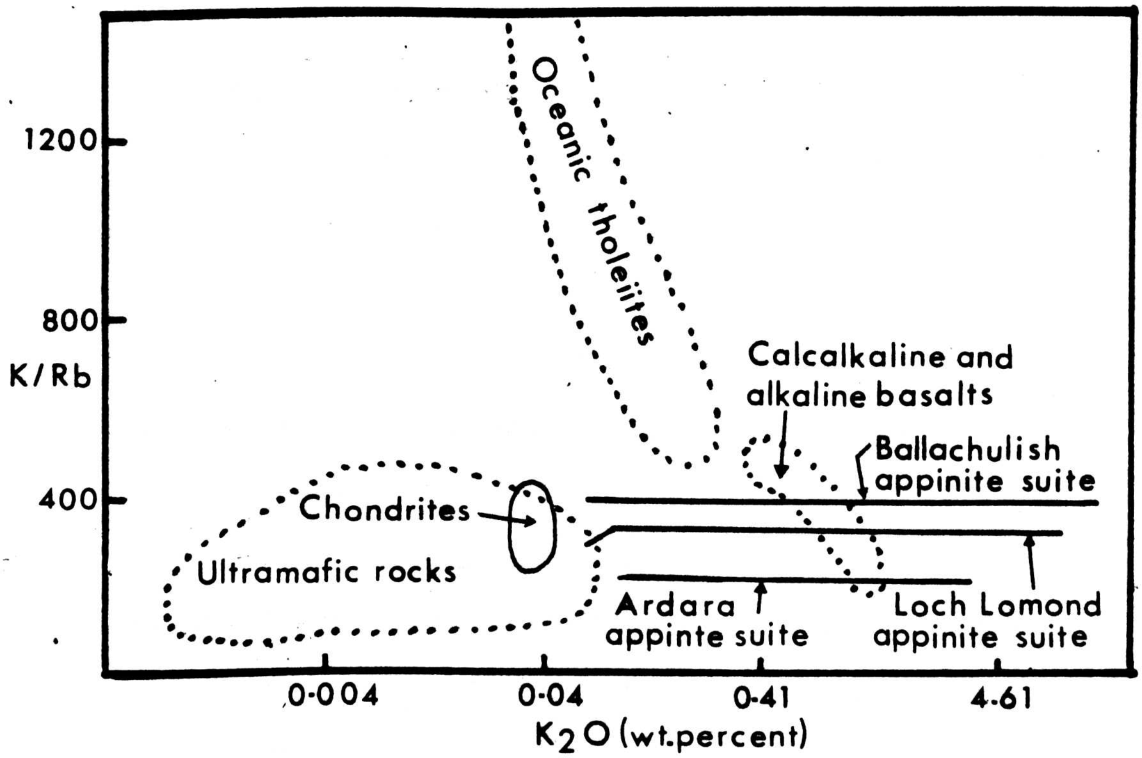
1200
800
K/Rb
400
Oceanic tholeiites
Calcalkaline and alkaline basalts
Ballachulish appinite suite
Chondrites
Ultramafic rocks
Ardara appinte suite
Loch Lomond appinite suite
0·004
0·04
0·41
4·61
K2O (wt.percent)

CHAPTER 14 CONCLUSIONS

The following are the major conclusions derived from the present investigation.

1. The appinite suite of western Scotland and northwestern Ireland was developed from volatile-rich basaltic magma.
    - (a) For the Ballachulish suite and the Colonsay masses the magma was of high-potassium calc-alkaline type (Chapter 7).
    - (b) For the Loch Lomond suite the magma was of normal calc-alkaline type (Chapter 10).
    - (c) For the Ardara suite the magma was transitional between tholeiitic and calc-alkaline (Chapter 12).
2. In the Ballachulish appinite suite:
    - a. Olivine was the first mineral on the liquidus and it crystallised at a temperature of c. 1800° C, pressure of c. 25 kb and at a depth of c. 70-80 km, before the magma entered into pipes (Chapters 3, 8).
    - b. Following the crystallisation of olivine, emplacement to high level in the crust occurred and magma uprise was impeded by structural traps (Chapters 2, 8).
    - c. Crystallisation occurred under highly variable P_{Gas} due to explosive activity in the pipes and the successive fractionation of clinopyroxene, amphibole, mica and plagioclase (in the later stages) led to the progressive development of ultramafic rocks, kentallenites, appinites (and lamprophyre) and leucocratic diorite or granodiorite, some representing cumulates, others representing crystallisation of residual liquids and still some representing mixtures resulting from explosive emplacement (see conclusion 2h, below).

d. Clinopyroxene crystallised in a temperature range of c. 1125° - 1000° C under increasing P_{H_2O} (c. <1 - 1.5 kb) (Chapters 4, 8).

e. The large idiomorphic pargosite crystals in both appinite and hornblendite, and amphibole rims on clinopyroxene in many of the diorites developed in a temperature range of c. 960° - 770° C and at a P_{H_2O} of c. 2 - 4 kb. The actinolite overgrowths on pargasite crystals in appinite and hornblendite developed in a temperature range of c. 790° - 750° C at or above 5 kb (Chapter 5).

f. In kentallenites phlogopite crystallised at a temperature of about 1000° C and at a P_{H_2O} of about 1 kb while in appinites and diorites phlogopite and/or biotite appeared on the liquidus at a temperature of c. 825° - 770° C above 1 kb (Chapters 5, 6).

g. Explosive activity associated with the emplacement of ultramafic rocks, appinite and most of the diorites occurred at a P_{H_2O} of c. 4 - 5 kb and at a temperature of c. 770° - 750° C while that associated with the emplacement of kentallenites occurred at a P_{H_2O} of c. 1 kb and at a temperature of c. 1000° C (Chapter 8).

h. Accumulation of mafic phases occurred before explosive activity in the pipes and the marginal ultramafic rocks, appinites and some kentallenites represent explosively-disrupted cumulates emplaced as "blocks" of cumulates, crystal mushes and individual crystals associated with variable proportions of the residual liquid that crystallised after the explosive activity (Chapter 8).

j. The late leucocratic rocks in some of the intrusions (e.g. Rudha Mòr and Ardsheal Hill - Lagnaha) crystallised at a P_{H_2O} of <1 kb and at a temperature of $<770^{\circ}$ C, from the residual melt which probably also contained a small component of hybrid secondary liquid produced by solution of silica from quartzite at high P - T (Chapter 8).

k. Post-crystallisation gas-streaming (carbonation and hydration) occurred in the pipes and it altered many of the rock types. The small pipes at Rudha Mòr and Back Settlement were the loci of such phenomenon (Chapters 2, 8).

3. On the basis of petrogenetic processes the Loch Lomond appinite suite shows a general correspondence to the Ballachulish appinite suite with variations in the nature and proportions of products representing variations in crystallisation conditions. P_{Gas} (maximum 4 kb) reached before explosive breaching of the traps was generally not as high as at Ballachulish (maximum 5 kb). This is presumed to be related to the relative strength of the structural traps. It resulted in the Loch Lomond masses being dominated by residual liquid compositions rather than cumulate compositions (Chapters 9, 10, 11).

4. Except for the small difference in the parent magma composition, the petrogenetic processes involved in the development of Ardara cluster were comparable to those of the Ballachulish and Loch Lomond clusters (Chapter 12).

5. The lamprophyres and lavas of the Old Red Sandstone magmatism (late Silurian) are genetically related to the appinite suite (Chapters 2, 7 -12).

6. The scyelite-pyroxenite-appinitic type rock association of Sutherland does not represent a cognate petrogenetic suite of rocks. Scyelites and SiO_2 - poor appinitic type rocks

represent the hybrids -- Ach'uain hybrids (Chapter 12).

7. The magmas from which the appinite suite crystallised were mantle-derived at depths of c. 200 km and associated with a northwestward-dipping subduction zone active in late Silurian times, i.e. in the latter stages of Caledonian orogeny (Chapter 13).

References

Albini, A., Cristofolini, Ř., Di Girolamo, P. & Stanzione, D. 1980. Rare-earth and other trace-element distributions in the calc-alkaline volcanic rocks from deep boreholes in the Phlegrean Fields, Campania (South Italy). Chem. Geol. 28, 123-33.

Anderson, J. G. C. 1935. The Arrochar intrusive complex. Geol. Mag. 72, 263-83.

Anderson, J. G. C. 1937. Intrusions of the Glen Follach area. Geol. Mag. 74, 458-68.

Arculus, R. J. & Curran, E. G. 1972. The genesis of the calcalkaline rock suite. Earth Planet. Sci. Lett. 15, 255-62.

Bailey, E. B. 1925. The pre-Tertiary geology of Mull, Loch Aline and Oban.(Expl. Sheet 44). Mem. Geol. Surv. Scotland.

Bailey, E. B. & Maufe, H. B. 1916. The geology of Ben Nevis and Glen Coe and the surrounding country. (Expl. Sheet 53). Mem. Geol. Surv. Scotland.

Bailey, E. B. & Maufe, H. B. 1960. The geology of Ben Nevis and Glen Coe and the surrounding country. (Expl. Sheet 53; 2nd ed.). Mem. Geol. Surv. Scotland.

Barberi F., Bizouard, H. & Varet, J. 1971. Nature of the clinopyroxene and iron enrichment in alkalic and transitional basaltic magmas. Contrib. Mineral. Petrol. 33, 93-107.

Bell, K. 1968. Age relations and provenance of the Dalradian Series of Scotland. Bull. Geol. Soc. Am. 79, 1167-94.

Beswick, A. E. 1976. K and Rb relations in basalts and other mantle derived material. Is phlogopite the key? Geochim. Cosmochim. Acta. 40, 1167-83.

Binns, R. A. 1965a. The mineralogy of basic rocks from the Willyama complex, Broken Hill District, New South Wales. Mineralog. Mag. 35, 306-326.

Binns, R. A. 1965b. Hornblendes from some basic hornfelses in New England region, New South Wales. Mineralog. Mag. 34, 52-65.

Bluck, B. J. 1980. Age and origin of Ballantrae ophiolite and significance to the Caledonian orogeny and Ordovician time scale. Geology 8, 492-5.

Bowen, N. L. & Schairer, J. F. 1935. The system MgO-FeO-SiO_2. Am. J. Sci. 29, 151-217.

Bowes, D. R. 1962. Kentallenite-lamprophyre-granite age relations at Kentallen, Argyll. Geol. Mag. 99, 119-22.

Bowes, D. R., Ghaly, T. S. & Wright, A. E. 1965. Appinites in Caledonides. Geol. Mag. 102, 180-81.

Bowes, D. R., Kinloch, E. D. & Wright, A. E. 1964. Rhythmic amphibole overgrowths in appinites associated with explosion-breccias in Argyll. Mineralog. Mag. 33, 963-73.

Bowes, D. R. & McArthur, A. C. 1976. Nature and genesis of the appinite suite. Krystalinikum 12, 31-46.

Bowes, D. R., MacDonald, A. S., Matheson, G. D. & Wright, A. E. 1963. An explosion-breccia-appinite complex at Gleann Chàrnan, Argyll. Trans. Geol. Soc. Glasgow 25, 19-30.

Bowes, D. R. & Wright, A. E. 1961. An explosion-breccia complex at Back Settlement, near Kentallen, Argyll. Trans. Geol. Soc. Edinburgh 18, 293-314.

Bowes, D. R. & Wright, A. E. 1967. The explosion-breccia pipes near Kentallen, Scotland, and their geological setting. Trans. R. Soc. Edinburgh 67, 109-42.

Boyd, F. R., England, J. L. & Davis, B. T. C. 1964. Effects of pressure on the melting and polymorphism of enstatite, Mg SiO_3. J. Geophys. Res. 69, 2101-9.

Briden, J. C. 1970. Palaeomagnetic results from the Arrochar and Garabal Hill - Glen Fyne igneous complex, Scotland. Geophys. J. R. Astron. Soc. London 21, 457-70.

Brown, E. H. 1977. The crossite content of Ca-amphibole as a guide to pressure of metamorphism. J. Petrol. 18, 53-72.

Brown, J. F. 1972. Rb-Sr studies and related geochemistry on the Caledonian calcalkaline igneous rocks of N.W. Argyllshire. Thesis, Ph.D. University College, Oxford (Unpub.).

Church, W. R. & Gayer, R. A. 1973. The Ballantrae Ophiolite. Geol. Mag. 110, 497-510.

Clough, C. T. 1905. The Geology of mid-Argyll. (Expl. Sheet 37). Mem. Geol. Surv. Scotland.

Cox, K. G., Bell, J. D. & Pankhurst, R. J. 1979. The interpretation of igneous rocks. George Allen & Unwin, London.

Czamanske, G. K. & Wones, D. R. 1973. Oxidation during magmatic differentiation, Finnmarka Complex, Oslo area, Norway: part 2, The mafic silicates. J. Petrol. 14, 349-80.

Dakyns, J. R. & Teall, J. J. H. 1892. On the plutonic rocks of Garabal Hill and Meal Breac. Q. J. Geol. Soc. London 48, 104-21.

Deer, W. A. 1935. The Cairnsmore of Carphain igneous complex. Q. J. Geol. Soc. London 91, 47-76.

Deer, W. A., Howie, R. A. & Zussman, J. 1962. Rock forming minerals. Vol. 3: Sheet silicates. Longman, London.

Deer, W. A., Howie, R. A. & Zussman, J. 1963. Rock forming minerals. Vol. 3: Chain silicates. Longman, London.

Deer, W. A., Howie, R. A. & Zussman, J. 1966. An introduction to the rock-forming minerals. Longman, London.

Deer, W. A., Howie, R. A. & Zussman, J. 1977. Rock forming minerals. Vol. 2A (2nd ed.): Single-chain silicates. Longman, London.

Dickinson, W. R. 1975. Potash-depth (K-h) relations in continental margin and intra-oceanic magmatic arcs. Geology, 3, 53-6.

Edgar, A. D., Green, D. H. & Hibberson, W. O. 1976. Experimental petrology of a highly potassic magma. J. Petrol. 17, 339-56.

Elders, S. 1935. Comparison of three Scottish magmas. Geol. Mag. 72, 80-5.

Fitton, J. G. & Hughes, D. J. 1970. Volcanism and plate tectonics in the British Ordovician. Earth Planet. Sci. Lett. 8, 223-8.

French, W. J. 1966. Appinitic intrusions clustered around the Ardara pluton, County Donegal. Proc. R. Ir. Acad. 64(B), 303-22.

French, W. J. 1977. Breccia-pipes associated with the Ardara pluton, County Donegal. Proc. R. Ir. Acad. 77(B), 101-17.

French, W. J. & Cameron, E. P. 1981. Calculation of the temperature of crystallisation of silicates from basaltic melts. Mineralog. Mag. 44, 19-26.

French, W. J., Hassan, M. D. & Westcott, J. 1979. The petrogenesis of Old Red Sandstone volcanic rocks of the western Ochils, Stirlingshire. In: Harris, A. L., Holland, C. H. & Leake, B. E. (eds) The Caledonides of British Isles - reviewed. Spec. Publ. Geol. Soc. London 8, 635-42.

Gandy, M. K. 1973. Melting relations of some calcalkaline lavas from the Eastern Sidlaw Hills, Perthshire. Earth Planet. Sci. Lett. 19, 230-4.

Gandy, M. K. 1975. The petrology of the Lower Old Red Sandstone lavas of the Eastern Sidlaw Hills, Perthshire, Scotland. J. Petrol. 16, 189-211.

Ghaly, T. S. 1964. The nature and genesis of some ultramafic and associated rocks in the Scottish Highlands. Thesis, Ph.D., University of Glasgow (unpubl.).

Gibb, F. G. F. 1973. The zoned clinopyroxenes of the Shiant Isles sill, Scotland. J. Petrol. 14, 203-30.

Giles, M. R. 1980. The petrology of the Galway Granite. Thesis, Ph.D., University of Glasgow (unpubl.).

Gill, J. B. 1978. Role of trace element partition coefficients in in models of andesite genesis. Geochim. Cosmochim. Acta. 42, 709-24.

Green, T. H. & Ringwood, A. E. 1968. Genesis of the calcalkaline igneous rock suite. Contrib. Mineral. Petrol. 18, 105-62.

Groome, D. R. & Hall, A. 1974. The geochemistry of the Devonian lavas of the northern Lorne Plateau, Scotland. Mineralog. Mag. 39, 621-40.

Hall, A. 1966. A petrogenetic study of the Rosses granite complex, Donegal. J. Petrol. 7, 202-20.

Hall, A. 1967. The chemistry of appinitic rocks associated with the Ardara pluton, Donegal, Ireland. Contrib. Mineral. Petrol. 16, 156-71.

Hall, A. 1972. New data on the composition of Caledonian granites. Mineralog. Mag. 38, 847-62.

Haslam, H. W. 1968. The crystallisation of intermediate and acid magmas at Ben Nevis, Scotland. J. Petrol. 9, 84-104.

Helz, R. T. 1973. Phase relations of basalts in their melting range at P_{H_2O} = 5 kb as a function of oxygen fugacity. Part I. Mafic phases. J. Petrol. 14, 249-302.

Hess, H. H. & Poldervaart, A. 1951. Pyroxenes in crystallisation of basaltic magmas. J. Geol. 59, 472-82.

Hill, J. B. 1905. The geology of Mid-Argyll. (Expl. Sheet 37). Mem. Geol. Surv. Scotland.

Hill, J. B. & Kynaston, H. 1900. On kentallenite and its relations to other igneous rocks in Argyllshire. Q. J. Geol. Soc. London, 56, 531-58.

Holgate, N. 1950. The Glen Benvie igneous complex of Perthshire. Q. J. Geol. Soc. London 106, 433-60.

Irvine, T. N. & Findlay, T. C. 1972. Alpine-type peridotite with particular reference to the Bay of Islands complex. In: The ancient oceanic lithosphere. Symposium, Dep. Energy, Mines & Resources, Ottawa, Canada 42, 97-128.

Jakeš, P. & Smith, I. E. 1970. High potassium calcalkaline rocks from Cape Nelson, Eastern Papua. *Contrib. Mineral. Petrol*. **28**, 259-71.

Jakeš, P. & White, A. J. R. 1972. Major and trace element abundances in volcanic rocks of orogenic areas. *Bull. Geol. Soc. Am*. **83**, 29-40.

Johannsen, A. 1931. *A descriptive petrography of the igneous rocks*. Vol. **1**, University of Chicago Press, Chicago.

Johnstone, G. S., Plant, J. & Watson, J. V. 1979. Caledonian granites in relation to regional geochemistry in northern Scotland. *In*: Harris, A. L., Holland, C. H. & Leake, B. E. (eds). *The Caledonides of the British Isles - reviewed*. Spec. Publ. Geol. Soc. London **8**, 663-7.

Joplin, G. A. 1959. On the origin and occurrence of basic bodies associated with discordant batholiths. *Geol. Mag*. **96**, 361-73.

Kerr, P. F. 1959. *Optical Mineralogy*. McGraw-Hill, London.

Kushiro, I. 1960. Si-Al relation in clinopyroxenes from igneous rocks. *Am. J. Sci*. **258**, 548-54.

Kushiro, I. 1965. The liquidus relations in the system forsterite-$CaAl_2SiO_6$-silica and forsterite-nepheline-silica at high pressures. *Yearb. Carnegie Inst. Washington* **64**, 82-9.

Kushiro, I. 1974. Melting of hydrous upper mantle and possible generation of andesitic magma: An approach from synthetic systems. *Earth Planet. Sci. Lett*. **22**, 294-9.

Lambert, R. St. J. & McKerrow, W. S. 1976. The Grampian Orogeny. *Scott. J. Geol*. **12**, 271-92.

Lamoen, H. V. 1980. Ti-zoning in corona hornblende of iron ore-bearing gabbros. Susimaki, Finland. *Neues Jahrb. Mineral. Monatshefte*. **2**, 88-96.

Leake, B. E. 1965a. The relationship between compositions of calciferous amphibole and grade of metamorphism. *In*: Pitcher,

W. S. & Flinn, G. W. (eds) Controls of metamorphism. Geol. J. Spec. Issue 1, 299-318.

Leake, B. E. 1965b. The relationship between tetrahedral aluminum and the maximum possible octahedral aluminum in natural calciferous and subcalciferous amphiboles. Am. Mineral. 50, 843-851.

Leake, B. E. 1971. On aluminous and edenitic hornblendes. Mineralog. Mag. 38, 389-407.

Leake, B. E. 1978. Nomenclature of amphiboles. Mineralog. Mag. 42, 533-63.

Le Bas, M. J. 1962. The role of aluminum in igneous clinopyroxenes with relation to their parentage. Am. J. Sci. 260, 267-88.

Leggett, J. K., McKerrow, W. S. & Eales, M. H. 1979. The Southern Uplands of Scotland: A Lower Palaeozoic accretionary prism. J. Geol. Soc. London, 136, 755-70.

Longhi, J., Walker, D. & Hays, J. F. 1978. The distribution of Fe and Mg between olivine and lunar basaltic liquids. Geochim. Cosmochim. Acta. 42, 1545-58.

Longman, C. D., Bluck, B. J. & van Breeman, O. 1979. Ordovician conglomerates and the evolution of the Midland Valley. Nature, London 280, 578-81.

MacDonald, G. A. & Katsura, T. 1964. Chemical composition of Hawaiian lavas. J. Petrol. 5, 82-133.

McArthur, A. C. 1971. On the structural control of Caledonian igneous masses in the south-west Highlands of Scotland. Thesis, Ph.D., University of Glasgow (unpubl.).

McKerrow, W. S. & Cocks, L. R. M. 1976. Progressive faunal migration across the Iapetus Ocean. Nature, London 263, 304-6.

Mercy, E. P. L. 1965. Caledonian igneous activity. In: Craig, G. Y. (ed.) The geology of Scotland, 229-67. Oliver & Boyd, Edinburgh.

Mitchell, A. H. G. & McKerrow, W. S. 1975. Analogous evolution of the Burma orogen and the Scottish Caledonides. Bull. Geol. Soc. Am. 86, 305-15.

Miyashiro, A. 1973. Metamorphism and metamorphic belts. George Allen & Unwin, London.

Money, M. S. 1964. The dioritic intrusion and associated breccias clustered around the Glen Fyne granite. Thesis, Ph.D., University of London (unpubl.).

Mysen, B. O., Kushiro, I., Nicholls, I. A. & Ringwood, A. E. 1974. A possible mantle origin for andesitic magmas: Discussion of a paper by Nicholls and Ringwood. Earth Planet. Sci. Lett. 21, 221-9.

Nicholls, J., Carmichael, I. S. E. & Stormer, J. C. Jr. 1971. Silica activity and P_{total} in igneous rocks. Contrib. Mineral. Petrol. 33, 1-20.

Nockolds, S. R. 1941. The Garabal Hill - Glen Fyne igneous complex. Q. J. Geol. Soc. London 96, 451-511.

O'Hara, M. J. 1976. Data reduction and projection schemes for complex composition. In: Progress in Experimental Petrology. N.E.R.C. Publ. Ser. D, 6, 103-26.

O'Hara, M. J. & Stewart, F. H. 1966. Olivine - liquid reaction and the depth of crystallisation of the East Aberdeenshire gabbros. Nature, London 210, 830-1.

Olesch, M. 1979. Ca-bearing phlogopite: synthesis and solid solubility at high temperatures and pressure of 5 and 10 kilobars. Bull. Mineral. 102, 14-20.

Parsons, I. & McKirdy, A. P. 1983. Inter-relationship of igneous activity and thrusting in Assynt: excavation at Loch Borrolan. Scott. J. Geol. 19, 59-66.

Pearce, J. A. & Norry, M. J. 1979. Petrogenetic implications of Ti, Zr, Y and Nb variations in volcanic rocks. Contrib. Mineral. Petrol. 69, 33-47.

Phillips, W. E. A., Stillman, C. J. & Murphy, T. 1976. A Caledonian plate tectonic model. J. Geol. Soc. London 132, 579-609.

Pitcher, W. S. & Berger, A. R. 1972. The geology of Donegal: a study of granite emplacement and unroofing. Wiley - Interscience, London.

Platten, I. M. 1966. The petrology of some Caledonian minor intrusions in Appin, Argyllshire. Thesis, Ph.D., University of London (unpubl.).

Platten, I. M. 1982. Partial melting of feldspathic quartzite around late Caledonian minor intrusions in Appin, Scotland. Geol. Mag. 119, 413-9.

Raase, P. 1974. Al and Ti contents of hornblende. Indicators of pressure and temperature of metamorphism. Contrib. Mineral. Petrol. 45, 231-6.

Read, H. H. 1925. The geology of the country around Golspie, Sutherlandshire. (Expl. Sheet 103). Mem. Geol. Surv. Scotland.

Read, H. H. 1926. The geology of Strath Oykell and Lower Loch Shin. (Expl. Sheet 102). Mem. Geol. Surv. Scotland.

Read, H. H. 1931. The geology of Central Sutherland and southwestern Caithness. (Expl. Sheets 108 & 109). Mem. Geol. Surv. Scotland.

Read, H. H. 1961. Aspects of Caledonian magmatism in Britain. Liverpool Manchester Geol. J. 2, 653-83.

Reyerson, F. J. & Hess, P. C. 1980. The role of P_2O_5 in silicate melt. Geochim. Cosmochim. Acta. 44, 611-24.

Ringwood, A. E. 1974. The petrological evolution of island-arc systems. J. Geol. Soc. London 130, 183-204.

Roberts, J.-L. 1966. Ignimbrite eruptions in the volcanic history of the Glen Coe Cauldron Subsidence. Geol. J. 5, 173-84.

Roberts, J.-L. 1974. The evolution of the Glen Coe Cauldron. Scott. J. Geol. 10, 269-82.

Roberts, J.-L. 1976. Titanium solubility in synthetic phlogopite solid solutions. Chem. Geol. 17, 213-27.

Roeder, P. L. & Emslie, R. F. 1970. Olivine-liquid equilibrium. Contrib. Mineral. Petrol. 29, 275-89.

Sato, H. 1977. Nickel content of basaltic magmas: identification of primary magmas and a measure of the degree of olivine fractionation. Lithos 10, 113-20.

Schwarzer, R. R. & Rogers, J. J.W. 1974. A worldwide comparison of alkali olivine basalts and their differentiation trends. Earth Planet. Sci. Lett. 23, 286-96.

Smith, J. V., Delaney, J. S., Hervig, R. L. & Dawson, J. B. 1981. Storage of F and Cl in the upper mantle: geochemical implications. Lithos 14, 133-47.

Streckeisen, A. 1979. Classification and nomenclature of volcanic rocks, lamprophyres, carbonatites and melilitic rocks: recommendations and suggestions of the IUGS subcommission on the systematics of igneous rocks. Geology,7, 331-5.

Stillman, C. J. & Francis, E. H. 1979. Caledonide volcanism in Britain and Ireland. In: Harris, A. L., Holland, C. H. & Leake, B. E. (eds) The Caledonides of the British Isles - reviewed. Spec. Publ. Geol. Soc. London 8, 557-77.

Stillman, C. J. & Williams, C. T. 1979. Geochemistry and tectonic setting of some Upper Ordovician volcanic rocks in east and southeast Ireland. Earth Planet. Sci. Lett. 42, 288-310.

Sun, S.-S., Nesbitt, R. W. & Sharaskin, A. Y. 1979. Geochemical characteristics of mid-ocean ridge basalts. Earth Planet. Sci. Lett. 44, 119-38.

Takahashi, E. 1978. Partitioning of Ni^{2+}, Co^{2+}, Fe^{2+}, Mn^{2+} and Mg^{2+} between olivine and silicate melts: compositional dependence of partition coefficient. Geochim. Cosmochim. Acta. 42, 1829-44.

Tarling, D. H. 1980. Lithosphere evolution and changing tectonic regimes. J. Geol. Soc. London 137, 459-67.

·Teall, J. J. H. 1888. British petrography. Dulau & Co., London.

Thirlwall, M. F. 1981. Caledonian plate tectonic model from chemical data. J. Geol. Soc. London 138, 123-138.

Thirlwall, M. F. 1982. Systematic variation in chemistry and Nd-Sr isotopes across a Caledonian calcalkaline volcanic arc: implications for source materials. Earth Planet. Sci. Lett. 58, 27-50.

Turner, F. J. & Verhoogen, J. 1960. Igneous and metamorphic petrology. (2nd ed.), McGraw-Hill, New York.

van Breemen, O., Aftalion, M. & Johnson, M. R. W. 1979. Age of the Loch Borrolan complex, Assynt, and late movement along the Moine Thrust zone. J. Geol. Soc. London 136, 489-95.

van Breemen, O. & Bluck, B. J. 1981. Episodic granite plutonism in the Scottish Caledonides. Nature, London 291, 113-7.

Walker, F. 1927. The igneous geology of Ardsheal Hill, Argyllshire. Trans. R. Soc. Edinburgh 55, 147-57.

Watson, E. B. 1979. Calcium content of forsterite coexisting with silicate liquid in the system Na_2O-CaO-MgO-Al_2O_3-SiO_2. Am. Mineral. 64, 824-9.

Wells, A. K. & Bishop, A. C. 1955. An appinitic facies associated with certain granites in Jersey, Channel Island. Q. J. Geol. Soc. London 111, 143-66.

Williams, A. 1972. Distribution of brachiopod assemblages in relation to Ordovician palaeography. In: Hughes, N. F. (ed.) Organisms and contents through time. Spec. Paper Palaeontology, 12, 241-69.

Wood, D. A., Joron, J.-L. & Treuil, M. 1979. A re-appraisal of the use of trace elements to classify and discriminate between magma series erupted in different tectonic settings. Earth Planet. Sci. Lett. 45, 326-36.

Wright, A. E. & Bowes, D. R. 1979. Geochemistry of the appinite suite. In: Harris, A. L., Holland, C. H. & Leake, B. E. (eds) The Caledonides of the British Isles - reviewed. Spec. Publ. Geol. Soc. London, 8, 699-704.

Wyllie, B. K. N. & Scott, A. 1913. The plutonic rocks of Garabal Hill. Geol. Mag. 10, 499-508 & 536-45.

Wyllie, P. J. 1971. The Dynamic Earth: Textbook in Geosciences. John Wiley & Sons, Inc., London.

Wyllie, P. J. 1973. Experimental petrology and global tectonics -- a preview. Tectonophysics 17, 189-209.

Yoder, H. S. 1965. Diopside-anorthite-water at 5 and 10 kilobars and its bearing on explosive volcanism. Yearb. Carnegie Instn. Wash. 64, 82-9.

Yoder, H. S. 1979. The evolution of igneous rocks. Princeton University Press, Princeton, New Jersey.

Yoder, H. S., Stewart, D. B. & Smith, J. R. 1957. Ternary feldspars. Yearb. Carnegie Inst. Washington 56, 206-14.

Yoder, H. S. & Tilley, C. E. 1962. Origin of basalt magmas: an experimental study of natural and synthetic rock systems. J. Petrol. 3, 342-532.

APPENDIX A

A.1 Analytical methods used in rock analyses

1.1 Wet chemical methods (Appendix B·3 — 59-72, majors only)

Powder ground to 100 mesh was (1) fused with NaOH before determination of SiO_2 by a spectrophotometric method and (2) digested with HF and $HClO_4$ before determination of TiO_2, Al_2O_3, total Fe (as Fe_2O_3) and P_2O_5 by spectrophotometry, MnO, MgO and CaO by atomic absorption methods and Na_2O and K_2O by flame photometry. FeO was determined volumetrically following digestion of powder by HF and H_2SO_4.Fe_2O_3 was then calculated from total Fe determined by spectrophotometry. H_2O and CO_2 were determined gravimetrically using the method of Riley (1958).

Methods of analyses followed the laboratory manual of the Department of Geology, University of Glasgow.

1.2 X-ray fluorescence methods (All except mentioned in Appendix A·1·1, above)

Major element analyses were carried out on fusion beads (Harvey *et al.* 1973) and trace element analyses on pressed pellets (Leake *et al.* 1969) using a Phillips PW 1450 sequential automatic X-ray fluorescence spectrometer, which is driven by a Phillips P/852 M minicomputer. Detection limits (p.p.m.) for trace elements were Cr 1, Co 10, Ni 4, Ba 7, Ce 2, Cu 4, Ga 1, La 1, Nb 1, Pb 1, Rb 1, Sr 3, Th 2, Y 1, Zn 20, Zr 2.

1.3 Data processing

All the XRF data were obtained on punched paper tape. They were processed by Data General Nova 2 minicomputer using a program provided by C. M. Farrow of the Department of Geology, University of Glasgow.

A.2 Analytical methods used in mineral analyses

Mineral analyses were performed on a Cambridge Instrument Microscan 5 X-Ray microanalyser, using an Energy Dispersive System with accelerating potential = 20 kV, probe current = 3 nA and count time = 50 - 200 sec (automatically corrected for dead time). The count time for most of the analyses was 100 seconds. The processing was carried out using the techniques of Sweatman and Long (1969) and Sathan (1976). Detection limits for various elements in different minerals are shown as element % below:

	Olivine	Clinopyroxene	Amphibole	Mica	Feldspar
Si	0.15	0.18	0.17	0.15	0.20
Ti	0.05	0.06	0.07	0.07	0.06
Al_2	0.05	0.09	0.12	0.12	0.15
Fe	0.20	0.16	0.18	0.20	0.07
Mn	0.20	0.06	0.06	0.06	0.06
Mg	0.20	0.15	0.15	0.16	0.08
Ca	0.05	0.18	0.14	0.05	0.06
Na	0.18	0.15	0.20	0.19	0.20
K_2	0.05	0.05	0.07	0.12	0.10
Cr	0.06	0.06	0.06	0.05	0.05
Co	0.08	0.08	0.08	0.08	0.07
Ni	0.08	0.08	0.08	0.08	0.08

REFERENCES

1. Harvey, P. K., Taylor, D. M., Hendry, R. and Bancroft, F. 1972. An accurate fusion method for the analyses of rocks and chemically related minerals by X-ray fluorescence spectrometry. *X-ray Spectrometry*, 2, 33-44.
2. Leake, B. E., Hendry, G. L., Kemp, A., Plant, A. G., Harvey, P. K., Wilson, J. R., Coats, J. S., Aucott, J. W., Lunel, T. and Howart, R. J. 1969. The chemical analyses of rock powders by automatic X-ray fluorescence. *Chem. Geol.*, 5, 7-86.
3. Riley, J. P. 1958. The rapid analysis of silicate rocks and minerals. *Analytica Chemica Acta*, 19, 413-428.
4. Stathan, P. J. 1976. A comparative study of techniques for quantitative analyses of the X-ray spectra obtained with a Si(Li) detector. *X-ray Spectrometry*, 5, 16-28.
5. Sweatman, T. R. and Long, J. V. P. 1969. Quantitative electron-probe microanalyses of rock-forming minerals. *J. Petrol.*, 10, 332-379.

Appendix B.1. Amphibole compositions from the Ballachulish appinite suite.

	1	2	3	4	5	6	7*	8*	9*	10*	11*	12*	13*	14*
SiO_2	40.52	39.78	40.85	40.75	40.96	40.97	52.74	53.23	54.09	52.90	54.18	54.28	53.42	52.56
TiO_2	1.44	1.48	2.14	2.04	2.16	2.06	0.27	0.22	0.27	0.00	0.00	0.44	0.00	0.00
Al_2O_3	13.53	13.33	12.75	12.51	12.57	12.93	3.45	3.50	3.09	2.78	2.53	2.54	1.61	1.51
FeO	15.63	14.66	12.33	11.03	10.91	11.47	9.65	9.35	6.42	13.13	11.46	12.16	14.66	17.26
MnO	0.23	0.32	0.00	0.00	0.00	0.28	0.00	0.20	0.00	0.30	0.28	0.44	0.37	0.50
MgO	11.38	11.57	13.26	14.35	13.93	13.62	17.56	17.76	18.95	15.02	16.39	15.86	15.17	12.57
CaO	12.34	12.37	12.13	12.04	11.95	12.18	12.38	12.85	13.00	12.88	12.88	13.17	12.67	12.52
Na_2O	1.98	2.16	1.92	2.15	1.93	1.96	0.82	0.75	0.00	0.43	0.00	0.32	0.00	0.48
K_2O	1.90	1.69	1.53	1.42	1.29	1.52	0.27	0.31	0.00	0.16	0.18	0.16	0.87	0.09
Total	98.95	97.38	96.90	96.28	95.70	96.99	97.13	98.15	96.04	97.59	97.89	99.36	97.99	97.48
Trace elements (p.p.m.)														
Cr	942	b.d.	b.d.	b.d.	1588	b.d.	b.d.	b.d.	1251	b.d.	b.d.	b.d.	b.d.	b.d.
Co	4080	b.d.	1870	2579	b.d.	2598	2735	1423	2467	b.d.	1442	b.d.	1235	1250
Formulae on the basis of 23 oxygens														
Si	6.06	6.04	6.13	6.12	6.16	6.12	7.56	7.55	7.68	7.67	7.74	7.69	7.75	7.78
Ti	0.24	0.23	0.24	0.23	0.24	0.23	0.03	0.02	0.03	0.00	0.00	0.05	0.00	0.00
Al	2.38	2.38	2.25	2.21	2.23	2.28	0.58	0.58	0.52	0.47	0.43	0.42	0.27	0.26
Fe	1.95	1.86	1.55	1.38	1.37	1.43	1.16	1.10	0.76	1.59	1.37	1.44	1.78	2.14
Mn	0.03	0.04	0.00	0.00	0.00	0.03	0.00	0.02	0.00	0.04	0.03	0.05	0.04	0.06
Mg	2.54	2.62	2.96	3.21	3.12	3.03	3.75	3.75	4.01	3.24	3.49	3.35	3.28	2.77
Ca	1.98	2.01	1.95	1.94	1.92	1.95	1.90	1.95	1.98	2.00	1.97	2.00	1.97	1.99
Na	0.57	0.64	0.56	0.63	0.56	0.57	0.23	0.21	0.00	0.12	0.00	0.09	0.00	0.14
K	0.36	0.33	0.29	0.27	0.23	0.29	0.05	0.06	0.04	0.03	0.03	0.03	0.02	0.02
Al_4	1.94	1.96	1.87	1.88	1.84	1.88	0.44	0.45	0.32	0.33	0.26	0.31	0.25	0.22
Al_6	0.44	0.42	0.38	0.33	0.38	0.40	0.14	0.14	0.20	0.14	0.17	0.11	0.03	0.05

	15*	16*	17	18	19	20	21	22	23*	24*	25*	26	27*	28*
SiO_2	53.34	53.37	40.44	41.33	41.35	41.18	40.77	41.08	53.05	54.46	54.64	40.12	53.41	54.03
TiO_2	0.00	0.23	1.68	2.22	2.08	1.35	2.30	2.46	0.24	0.36	0.00	1.60	0.00	0.21
Al_2O_3	1.97	4.42	13.75	13.78	12.96	12.95	13.32	13.13	4.66	2.65	2.02	13.22	1.94	1.94
FeO	18.36	8.34	13.23	10.55	10.82	10.87	11.19	11.56	8.75	11.39	13.74	14.05	12.55	15.66
MnO	0.50	0.19	0.00	0.18	0.18	0.17	0.00	0.00	0.00	0.17	0.28	0.19	0.36	0.50
MgO	11.98	18.14	13.35	14.42	14.78	15.65	14.50	14.65	17.02	16.51	15.76	12.12	15.45	14.05
CaO	12.37	12.74	12.15	11.69	11.60	12.00	12.00	12.01	12.70	12.24	12.95	11.98	12.20	11.91
Na_2O	0.55	1.14	2.25	2.00	2.18	2.40	2.36	2.54	0.68	0.73	0.00	2.08	0.00	0.55
K_2O	0.13	0.23	1.69	1.36	1.19	1.24	1.33	1.46	0.00	0.23	0.13	1.67	0.00	0.00
Total	99.19	98.80	98.54	97.15	97.14	97.81	97.69	98.89	97.35	98.74	99.52	97.03	95.91	98.85
Trace elements (p.p.m.)														
Cr	b.d.	b.d.	b.d.	b.d.	b.d.	b.d.	b.d.	b.d.	b.d.	b.d.	b.d.	b.d.	b.d.	b.d.
Co	3314	b.d.	1606	1392	2247	b.d.	b.d.	2036	b.d.	2692	1580	b.d.	b.d.	b.d.
Formulae on the basis of 23 oxygens														
Si	7.78	7.49	6.00	6.12	6.12	6.08	6.02	6.02	7.56	7.71	7.76	6.07	7.82	7.79
Ti	0.00	0.02	0.19	0.25	0.23	0.15	0.26	0.27	0.03	0.04	0.00	0.18	0.00	0.02
Al	0.34	0.73	2.41	2.32	2.26	2.25	2.32	2.27	0.78	0.44	0.34	2.36	0.33	0.33
Fe	2.24	0.98	1.64	1.31	1.34	1.34	1.38	1.42	1.04	1.35	1.63	1.78	1.54	1.89
Mn	0.06	0.02	0.00	0.02	0.02	0.02	0.00	0.00	0.00	0.02	0.03	0.02	0.04	0.06
Mg	2.60	3.79	2.95	3.20	3.26	3.44	3.19	3.20	3.60	3.48	3.33	2.73	3.37	3.02
Ca	1.93	1.91	1.93	1.85	1.84	1.90	1.90	1.89	1.93	1.86	1.97	1.94	1.91	1.84
Na	0.16	0.31	0.65	0.57	0.63	0.69	0.65	0.72	0.18	0.20	0.00	0.61	0.00	0.15
K	0.02	0.04	0.32	0.26	0.22	0.23	0.25	0.27	0.00	0.04	0.02	0.32	0.00	0.00
Al_4	0.22	0.51	2.00	1.88	1.87	1.92	1.98	1.98	0.44	0.29	0.24	1.92	0.18	0.21
Al_6	0.12	0.22	0.41	0.43	0.39	0.33	0.34	0.29	0.34	0.16	0.09	0.43	0.15	0.12

Appendix B.1. (Contd.)

	29*	30*	31	32	33*	34*	35*	36*	37	38	39	40	41	42
SiO_2	49.98	54.51	42.36	49.73	54.13	52.16	51.70	52.74	40.97	40.45	41.64	41.19	39.35	39.09
TiO_2	0.26	0.00	1.35	0.75	0.00	0.00	0.28	0.31	1.61	1.30	2.31	2.23	2.43	2.25
Al_2O_3	5.87	2.60	12.91	6.91	1.21	3.18	4.76	4.41	13.43	13.71	12.99	13.08	13.56	13.67
FeO	18.51	7.62	11.90	11.71	15.79	18.51	10.94	10.31	13.71	14.08	10.63	11.09	11.35	11.48
MnO	0.51	0.37	0.22	0.34	0.66	0.57	0.00	0.32	0.26	0.00	0.00	0.00	0.20	0.14
MgO	11.20	19.99	14.37	15.81	13.67	11.76	16.82	17.52	12.80	12.14	14.80	14.56	14.43	13.67
CaO	12.44	12.74	11.75	11.14	12.17	11.94	12.47	12.32	11.88	11.92	11.94	12.00	11.69	11.72
Na_2O	0.56	0.84	2.45	1.88	0.00	0.90	1.49	1.60	2.05	2.46	2.56	2.52	2.45	1.91
K_2O	0.35	0.21	1.93	0.61	0.18	0.00	0.39	0.32	1.72	1.82	1.46	1.31	1.40	1.35
Total	99.67	98.89	99.23	99.87	97.81	99.01	98.84	99.84	98.42	97.87	98.32	97.98	96.85	95.27
							Trace elements (p.p.m.)							
Cr	b.d.	b.d.	b.d.	b.d.	b.d.	b.d.	b.d.	b.d.	b.d.	b.d.	b.d.	b.d.	b.d.	b.d.
Co	b.d.	b.d.	b.d.	b.d.	2427	2121	1621	b.d.	b.d.	2763	b.d.	b.d.	2414	2347
							Formulae on the basis of 23 oxygens							
Si	7.30	7.61	6.19	7.07	7.89	7.64	7.36	7.41	6.09	6.07	6.10	6.07	5.90	5.95
Ti	0.03	0.00	0.15	0.08	0.00	0.00	0.03	0.03	0.18	0.15	0.25	0.25	0.27	0.26
Al	1.01	0.43	2.22	1.16	0.21	0.55	0.80	0.73	2.35	2.42	2.24	2.27	2.40	2.45
Fe	2.26	0.89	1.45	1.39	1.93	2.27	1.30	1.21	1.70	1.77	1.30	1.37	1.42	1.46
Mn	0.06	0.04	0.03	0.04	0.08	0.07	0.00	0.04	0.03	0.00	0.00	0.00	0.02	0.02
Mg	2.44	6.16	3.13	3.35	2.97	2.57	3.57	3.67	2.84	2.71	3.23	3.20	3.23	3.10
Ca	1.95	1.91	1.84	1.85	1.90	1.87	1.90	1.85	1.89	1.92	1.88	1.90	1.88	1.91
Na	0.16	0.23	0.69	0.52	0.00	0.26	0.41	0.42	0.59	0.72	0.73	0.72	0.71	0.56
K	0.06	0.04	0.36	0.11	0.03	0.00	0.07	0.06	0.33	0.35	0.27	0.25	0.27	0.26
Al_4	0.70	0.39	1.81	0.92	0.10	0.36	0.64	0.59	1.91	1.93	1.90	1.93	2.10	2.05
Al_6	0.31	0.04	0.42	0.23	0.10	0.18	0.16	0.14	0.45	0.49	0.35	0.35	0.30	0.40

	43*	44*	45	46*	47*	48	49	50	51	52	53	54	55	56	57
SiO_2	50.90	47.64	41.54	53.60	49.34	43.48	41.17	41.50	42.07	41.99	41.94	46.98	52.20	47.25	43.19
TiO_2	0.65	0.18	2.80	0.26	0.85	1.54	1.77	2.11	2.23	2.03	1.90	1.04	0.00	1.40	1.87
Al_2O_3	3.86	5.06	12.18	4.10	6.40	10.37	10.18	12.15	12.64	12.37	11.37	7.16	2.90	7.03	11.30
FeO	12.73	22.80	12.23	11.55	12.87	13.85	17.16	12.18	11.92	11.50	13.25	14.16	18.57	14.09	13.89
MnO	0.38	0.00	0.21	0.00	0.00	0.21	0.27	0.00	0.00	0.00	0.00	0.00	0.91	0.23	0.24
MgO	15.24	9.83	13.11	17.07	15.12	13.24	13.07	14.60	14.27	14.42	13.45	14.17	11.77	14.23	13.67
CaO	11.38	11.23	11.40	12.29	11.27	11.46	10.98	11.68	11.62	11.48	11.16	11.30	12.30	11.65	11.69
Na_2O	1.42	0.76	2.69	1.24	1.59	2.63	2.32	2.37	2.54	2.27	2.41	1.84	0.67	1.89	2.56
K_2O	0.20	0.30	1.19	0.13	0.57	1.10	1.09	1.33	1.33	1.40	1.24	0.76	0.12	0.87	1.39
Total	96.75	97.79	97.34	99.63	98.01	97.87	98.01	97.92	98.61	97.45	96.71	97.41	99.43	98.63	99.79
Trace elements (p.p.m.)															
Cr	b.d.	b.d.	2579	b.d.	b.d.	b.d.	b.d.	b.d.	1021	b.d.	b.d.	b.d.	b.d.	b.d.	b.d.
Co	b.d.	b.d.	1667	b.d.	1934	2661	b.d.	b.d.	b.d.	2315	b.d.	b.d.	b.d.	b.d.	b.d.
Formulae on the basis of 23 oxygens															
Si	7.46	7.24	6.17	7.47	7.16	6.48	6.24	6.15	6.16	6.21	6.30	6.45	7.63	6.94	6.31
Ti	0.07	0.02	0.31	0.03	0.09	0.17	0.20	0.23	0.25	0.23	0.21	0.12	0.00	0.14	0.21
Al	0.67	0.91	2.13	0.68	1.09	1.82	1.82	2.12	2.18	2.16	2.01	2.25	0.50	1.23	1.95
Fe	1.56	2.90	1.52	1.36	1.56	1.72	2.17	1.51	1.46	1.42	1.66	1.75	2.27	1.73	1.70
Mn	0.05	0.00	0.03	0.00	0.00	0.03	0.03	0.00	0.00	0.00	0.00	0.00	0.11	0.03	0.03
Mg	3.33	2.23	2.90	3.58	3.27	2.93	2.95	3.22	3.11	3.18	3.01	3.12	2.56	3.11	2.98
Ca	1.79	1.83	1.81	1.86	1.75	1.83	1.78	1.85	1.82	1.82	1.80	1.79	1.93	1.83	1.83
Na	0.40	0.22	0.77	0.34	0.45	0.76	0.68	0.68	0.72	0.65	0.70	0.53	0.19	0.54	0.73
K	0.04	0.06	0.23	0.02	0.10	0.21	0.21	0.25	0.25	0.26	0.24	0.14	0.02	0.16	0.26
Al_4	0.54	0.75	1.83	0.53	0.84	1.52	1.76	1.85	1.84	1.79	1.70	1.05	0.37	1.06	1.68
Al_6	0.12	0.16	0.30	0.15	0.25	0.30	0.06	0.27	0.34	0.37	0.31	0.20	0.13	0.16	0.26

Appendix B.1. (Contd.)

	58	59	60	61	62	63	64	65
SiO_2	40.72	41.32	41.88	41.55	41.13	40.87	42.80	42.10
TiO_2	3.25	2.72	0.86	1.18	1.25	1.65	1.74	1.45
Al_2O_3	11.38	11.46	11.50	12.19	11.86	12.05	12.11	12.74
FeO	10.75	11.28	11.17	11.09	10.84	10.40	10.68	11.97
MnO	0.21	0.18	0.00	0.23	0.00	0.15	0.16	0.00
MgO	15.07	14.88	14.24	14.70	14.33	14.26	14.62	14.76
CaO	11.43	11.27	11.59	11.57	11.65	11.68	12.10	12.16
Na_2O	2.93	2.71	1.86	1.95	2.06	1.88	1.69	1.55
K_2O	0.78	0.70	1.00	1.15	1.12	1.19	1.18	1.22
Total	96.51	96.51	94.09	95.60	94.22	94.13	97.10	97.50
Trace elements (p.p.m.)								
Cr	1367	1118	1362	b.d.	b.d.	b.d.	b.d.	b.d.
Co	1328	1685	2740	2472	2857	3767	2468	3852
Formulae on the basis of 23 oxygens								
Si	6.09	6.17	6.38	6.25	6.28	6.24	6.32	6.21
Ti	0.36	0.30	0.10	0.13	0.14	0.19	0.19	0.16
Al	2.00	2.02	2.06	2.16	2.13	2.17	2.10	2.22
Fe	1.34	1.41	1.42	1.40	1.38	1.33	1.32	1.42
Mn	0.03	0.02	0.00	0.03	0.00	0.02	0.02	0.00
Mg	3.36	3.31	3.23	3.30	3.26	3.24	3.21	3.25
Ca	1.83	1.80	1.89	1.87	1.90	1.91	1.91	1.92
Na	0.85	0.78	0.55	0.57	0.61	0.56	0.48	0.44
K	0.15	0.13	0.19	0.22	0.22	0.23	0.22	0.23
Al_4	1.91	1.83	1.62	1.74	1.73	1.76	1.68	1.79
Al_6	0.09	0.18	0.44	0.42	0.41	0.41	0.42	0.43

1 - 14 Zoned pargasite with overgrowths, appinite, large pipe, Back Settlement (Table 7.1 — 9).

15 - 40 Zoned pargasite crystals with overgrowths, appinite, Back Settlement pipe; about 4 m from 1 - 14.

41 - 42 Pargasite crystal, small pipe, Back Settlement.

43 - 45 Pargasite crystal with overgrowths, pyroxene - mica diorite, Rudha Mòr pipe (Table 7.1 — 39).

46 - 57 Zoned pargasite with overgrowths, marginal biotite - pyroxene - hornblende feldspar rock, Rudha Mòr pipe (Table 7.1 — 29).

58 - 59 Pargasite crystal, appinite, Ardsheal Hill pipe (Table 7.1 — 12).

60 - 65 Zoned pargasite crystal appinite, Garbh Allt pipe, Glen Creran (Appendix B.2 — 20).

FeO = total iron; numbers with asterisks indicate overgrowths; b.d. = below detection limit (see Appendix A.2); Ni is below detection limit for all analyses.

Appendix B.2. Major and trace element analyses and estimated modal compositions of rocks from the small pipes on Kentallen - Ardsheal peninsula, Gleann Chârnan pipe and Glen Creran pipes; Ballachulish region.

	North Cuil pipes		Above Duror Inn		Inshaig pipe	Gleann Chârnan pipe				
	1	2	3	4	5	6	7	8	9	10
SiO_2	50.76	68.88	58.37	60.17	59.86	45.40	45.53	50.98	53.69	57.01
TiO_2	0.79	0.37	0.83	0.59	0.63	1.28	1.13	0.77	0.88	0.70
Al_2O_3	15.47	15.93	17.08	19.00	13.08	12.60	12.17	11.76	14.17	16.41
Fe_2O_3	2.38	0.86	2.77	1.63	1.63	3.50	3.43	3.36	2.05	2.14
FeO	6.06	1.49	3.24	3.54	1.20	8.07	8.67	6.25	5.94	4.27
MnO	0.12	0.02	0.08	0.08	0.03	0.17	0.20	0.14	0.11	0.10
MgO	8.79	1.50	3.17	2.10	7.80	14.86	14.53	11.29	9.24	5.46
CaO	8.22	1.10	4.16	1.62	5.62	5.19	8.40	8.82	6.39	4.51
Na_2O	3.14	4.47	3.59	4.20	2.50	2.14	1.47	2.62	3.20	3.96
K_2O	2.52	3.24	4.41	3.45	5.94	1.68	1.42	1.81	3.37	3.40
P_2O_5	0.16	0.14	0.29	0.30	0.05	0.28	0.27	0.22	0.22	0.25
H_2O	1.07	1.91	1.72	3.45	1.18	2.43	2.76	2.29	1.97	1.50
CO_2	0.12	0.25	0.13	0.32	0.05	0.18	0.16	0.15	0.06	0.13
Total	99.60	100.16	99.84	100.45	99.57	97.78	100.13	100.46	101.29	99.84
					Trace elements (p.p.m.)					
Cr	289	30	41	11	53	575	735	521	396	192
Co	72	0	2	0	0	54	45	35	32	25
Ni	77	25	17	3	24	157	157	143	151	83
Ba	1040	2540	1100	1240	1120	470	600	1130	840	980
Ce	35	25	80	70	140	60	35	35	40	65
Cl	451	127	523	154	220	617	591	409	325	267
Cu	73	57	118	155	19	198	29	177	50	32
Ga	15	13	13	13	10	14	11	12	11	15
La	15	45	85	115	75	0	0	0	0	40
Li	7	10	3	14	3	9	15	5	15	23

Nb	0	0	0	10	18	5	6	6	7	7
Pb	28	24	20	25	11	25	24	25	21	28
Rb	61	55	115	196	191	26	31	39	43	114
S	107	847	695	1738	2229	634	64	428	764	114
Sc	31	3	11	1	4	45	48	36	23	16
Sr	1289	1022	962	945	396	672	606	769	988	1173
Th	9	3	8	7	10	5	4	6	8	8
V	433	50	158	87	70	301	232	220	189	162
Y	12	5	12	10	20	19	15	19	24	13
Zn	70	28	62	75	33	131	163	114	95	95
Zr	106	123	129	206	263	75	61	96	194	168

Modal analyses

Olivine	-	-	-	-	-	← 0 →		0	0	0
Orthopyroxene	-	-	-	-	-	← 3 →		0	0	0
Clinopyroxene	-	-	-	-	-	← 66 →		60	40	0
Amphibole	-	-	-	-	-	← 10 →		2	1	20
Phlog.-biot.	-	-	-	-	-	← 15 →		30	45	0
Plagioclase	-	-	-	-	-	← 0 →		2	0	40
Anorthoclase	-	-	-	-	-	← 0 →		0	1	0
Orthoclase	-	-	-	-	-	← 0 →		0	0	30
Perthite	-	-	-	-	-	← 0 →		3	10	0
Quartz	-	-	-	-	-	← 0 →		0	0	0
Calcite (prim.)	-	-	-	-	-	← 2 →		1	0	0
Opaque ore	-	-	-	-	-	← 0 →		0	0	3
Apatite (prim.)	-	-	-	-	-	← 0 →		1	1	0
Sphene (prim.)	-	-	-	-	-	← 2 →		1	1	Tr
Chlorite (sec.)	-	-	-	-	-	← 2 →		Tr	Tr	0
Epidote (sec.)	-	-	-	-	-	← 0 →		0	1	1
Serpentine (sec.)	-	-	-	-	-	← 0 →		0	0	2
Uralite (sec.)	-	-	-	-	-	← 0 →		0	Tr	4
Sericite (sec.)	-	-	-	-	-	← 0 →		0	0	0
Total						← 100 →		100	100	100

Appendix B.2. (Contd.)

	Glen Creran area									
	Màm na Stainge pipe		Clatch Fear Ardsheal pipe	Salachail pipe				Barnamuc pipe		Garbh Allt pipe
	11	12	13	14	15	16	17	18	19	20
SiO_2	49.44	58.50	56.35	50.56	51.88	55.19	56.35	49.21	53.82	4~~9~~9.87
TiO_2	1.21	1.35	0.58	0.75	0.66	0.63	0.56	0.56	0.63	0.83
Al_2O_3	10.89	10.70	15.99	13.66	14.44	14.41	15.95	11.79	16.46	13.58
Fe_2O_3	2.97	3.14	3.03	2.17	3.33	2.26	2.68	2.79	2.59	2.49
FeO	6.18	3.35	3.99	6.40	5.07	5.12	4.59	5.76	4.48	6.33
MnO	0.20	0.18	0.14	0.14	0.15	0.13	0.14	0.17	0.15	0.16
MgO	12.93	8.59	5.76	8.22	7.81	6.68	6.05	14.09	5.50	9.38
CaO	11.51	7.45	6.10	9.02	6.80	7.14	6.38	6.64	7.05	9.06
Na_2O	2.52	2.52	3.81	3.50	3.07	3.19	3.30	2.31	4.07	2.88
K_2O	1.30	3.25	3.58	3.29	2.94	3.28	3.24	2.52	2.51	1.88
P_2O_5	0.35	0.25	0.28	0.35	0.31	0.25	0.30	0.26	0.21	0.55
H_2O	0.00	0.86	0.10	1.49	2.48	1.54	0.00	3.16	1.74	2.52
CO_2	0.00	0.29	0.82	0.02	0.30	0.06	0.00	0.26	0.17	0.32
Total	99.50	100.43	100.53	99.57	99.24	99.88	99.54	99.52	99.38	99.87
	Trace elements (p.p.m.)									
Cr	411	380	166	270	231	285	181	611	158	467
Co	52	29	30	45	35	35	26	43	32	41
Ni	135	17	96	84	137	70	95	462	32	206
Ba	579	948	771	939	591	667	737	483	507	458
Ce	75	74	40	38	32	40	50	41	17	52
Cl	-	-	-	-	-	-	-	-	-	-
Cu	93	19	58	108	50	201	19	38	148	6
Ga	15	18	20	23	21	19	18	14	27	54
La	29	39	12	11	19	13	17	13	12	17
Li	-	-	-	-	-	-	-	-	-	-

Nb	12	14	10	8	10	11	12	7	9	8
Pb	11	31	18	1	15	15	15	18	29	5
Rb	25	58	102	82	95	90	83	63	64	32
S	-	-	-	-	-	-	-	-	-	-
Sc	-	-	-	-	-	-	-	-	-	-
Sr	994	632	1004	957	790	676	1008	755	994	830
Th	4	12	6	5	6	4	8	7	3	4
V	-	-	-	-	-	-	-	-	-	-
Y	22	17	13	14	15	15	16	15	13	28
Zn	104	77	65	66	91	75	64	61	92	66
Zr	98	122	96	65	155	86	98	72	81	89

Modal analyses

Olivine	3	-	0	←	0		→	15	5	-
Orthopyroxene	2	-	0	←	0		→	0	0	-
Clinopyroxene	0	-	10	←	10		→	25	30	-
Amphibole	50	-	10	←	20		→	0	0	-
Phlog.-biot.	5	-	20	←	10		→	10	15	-
Plagioclase	35	-	50	←	45		→	33	40	-
Anorthoclase	0	-	0	←	0		→	15	10	-
Orthoclase	0	-	4	←	4		→	0	0	-
Perthite	0	-	0	←	0		→	0	0	-
Quartz	0	-	5	←	10		→	0	0	-
Calcite (prim.)	0	-	0	←	0		→	0	0	-
Opaque ore	Tr	-	1	←	1		→	1	Tr	-
Apatite (prim.)	Tr	-	Tr	←	0		→	1	Tr	-
Sphene (prim.)	Tr	-	0	←	0		→	0	0	-
Chlorite (sec.)	0	-	0	←	0		→	0	0	-
Epidote (sec.)	0	-	0	←	0		→	0	0	-
Serpentine (sec.)	0	-	0	←	0		→	0	0	-
Uralite (sec.)	0	-	0	←	0		→	0	0	-
Sericite (sec.)	5	-	0	←	0		→	0	0	-
Total	100		100	←	100		→	100	100	

Appendix B.2. (Contd.)

Glen Creran area

Glen Ure pipe

	21	22	23
SiO_2	49.20	57.15	64.58
TiO_2	1.36	0.46	0.61
Al_2O_3	15.10	15.51	15.43
Fe_2O_3	1.39	2.75	1.86
FeO	5.87	4.05	2.00
MnO	0.15	0.13	0.06
MgO	8.25	4.82	2.02
CaO	6.85	6.11	3.09
Na_2O	4.17	3.66	4.44
K_2O	2.17	2.53	3.70
P_2O_5	0.40	0.23	0.19
H_2O	3.57	1.69	0.00
CO_2	0.12	0.16	1.73
Total	98.60	99.25	99.71

Trace elements (p.p.m.)

	21	22	23
Cr	343	243	88
Co	49	23	20
Ni	182	57	9
Ba	783	844	1285
Ce	75	33	59
Cl	-	-	-
Cu	35	60	10
Ga	28	22	27
La	30	14	27
Li	-	-	-

North Cuil pipe

1 Microkentallenite.

2 Leucodiorite.

Above Duror Inn

3 Microdiorite.

4 Diorite.

Inshaig pipe

5 Felsite with chalcopyrite.

Gleann Chàrnan pipe

6-7 Lamprophyric marginal appinite.

8 Feldspathic porphyritic marginal appinite.

Nb	17	11	12
Pb	33	23	32
Rb	71	73	29
S	-	-	-
Sc	-	-	-
Sr	1094	1013	994
Th	9	6	6
V	-	-	-
Y	17	12	3
Zn	83	52	13
Zr	162	52	92

Modal analyses

Olivine	0	0	0
Orthopyroxene	0	15	0
Clinopyroxene	0	35	0
Amphibole	40	0	10
Phlog.-biot.	0	15	20
Plagioclase	55	25	65
Anorthoclase	0	0	0
Orthoclase	0	Tr	2
Perthite	0	0	0
Quartz	0	Tr	2
Calcite (prim.)	0	0	0
Opaque ore	5	0	1
Apatite (prim.)	0	0	0
Sphene (prim.)	0	0	0
Chlorite (sec.)	0	10	0
Epidote (sec.)	0	0	Tr
Serpentine (sec.)	0	0	0
Uralite (sec.)	0	0	0
Sericite (sec.)	0	0	0
Total	100	100	100

9	Bladed appinite
10	Main mass of appinite.

<u>Glen Creran pipes</u>

11	Cortlandic appinite.
12	Hornblende diorite.
13-17	Appinite
18-19	Kentallenite.
20-21	Appinite
22	Pyroxene - mica diorite.
23	Leucocratic diorite.

Appendix B.3. Major and trace element analyses and estimated modal compositions of rocks from the appinite suite of Loch Lomond district.

Main Arrochar intrusion

	1	2	3	4	5	6	7	8	9	10	11	12
SiO_2	42.29	42.93	44.29	45.17	46.14	46.87	47.37	49.79	51.05	52.79	54.05	54.60
TiO_2	2.62	1.40	2.25	0.33	1.61	0.81	0.92	0.44	0.68	0.92	0.81	0.92
Al_2O_3	14.18	18.48	17.42	8.20	16.08	7.53	13.40	3.25	19.20	13.35	14.40	13.74
Fe_2O_3	7.97	2.33	5.28	2.55	4.27	2.21	2.23	1.94	2.08	1.58	1.64	2.00
FeO	9.63	7.17	7.56	7.79	8.85	8.88	7.85	5.85	5.07	7.47	6.64	6.19
MnO	0.17	0.15	0.12	0.17	0.20	0.20	0.20	0.23	0.12	0.18	0.17	0.15
MgO	9.75	9.17	7.67	22.84	7.54	20.30	12.43	16.06	6.00	9.60	9.42	8.35
CaO	7.88	11.95	8.87	7.96	8.85	10.36	9.50	19.44	8.95	9.72	8.58	6.00
Na_2O	2.06	1.00	1.77	0.54	2.29	0.67	1.07	0.37	1.83	2.06	2.06	2.76
K_2O	0.72	1.65	1.94	0.42	1.21	0.42	1.27	0.13	2.18	1.65	1.58	1.27
P_2O_5	0.04	0.01	0.03	0.03	0.07	0.02	0.04	0.00	0.08	0.19	0.11	0.16
H_2O+	2.19	3.05	2.27	3.96	2.73	1.62	3.21	1.75	2.03	0.81	1.08	2.98
CO_2	0.12	0.30	0.56	0.24	0.12	0.34	0.04	0.25	0.87	0.05	0.08	0.62
Total	99.62	99.59	100.20	100.20	99.96	100.23	99.53	99.50	100.14	100.37	100.62	99.74

Trace elements (p.p.m.)

Cr	775	196	49	2200	134	1600	800	1850	188	500	500	475
Co	58	43	46	70	43	69	50	58	33	40	43	40
Ni	39	63	35	625	92	300	175	225	72	113	118	118
Ba	160	200	400	40	190	30	80	19	410	330	470	380
Ce	10	<10	<10	<10	50	<10	15	<10	15	35	<10	60
Cl	113	118	127	247	201	135	36	127	207	314	297	304
Cu	318	88	134	79	182	70	40	33	58	125	117	53
Ga	19	17	22	11	18	10	15	9	19	20	20	19
La	<10	<10	<10	<10	<10	<10	<10	<10	45	<10	15	35
Nb	12	3	9	2	2	7	2	2	2	7	7	9

Pb	11	12	17	5	13	12	12	16	22	13	13	13
Rb	10	57	50	12	39	7	66	46	92	43	74	55
S	690	2090	680	110	611	100	65	95	465	120	240	455
Sc	61	37	52	18	33	40	32	60	19	36	31	30
Sr	260	420	440	165	355	110	330	80	360	445	290	400
Th	<5	<5	45	<5	<5	<5	57	46	26	<5	25	47
V	807	402	706	123	476	186	262	169	239	261	218	221
Y	19	<2	36	<2	<2	<2	<2	<2	<2	<2	9	222
Zn	120	66	73	88	116	91	87	53	71	81	74	91
Zr	100	95	105	30	90	45	75	15	130	150	140	165

Modal analyses

Olivine	0	0	0	30	0	10	0	5	0	15	0	0
Orthopyroxene	0	0	0	3	0	5	0	0	0	5	5	0
Clinopyroxene	1	5	0	35	5	30	5	80	5	20	35	5
Amphibole	70	65	55	0	55	45	50	5	20	0	0	20
Biotite	0	0	1	5	0	0	0	5	8	10	15	10
Plagioclase	20	5	10	20	10	5	5	0	45	40	35	50
Anorthoclase	0	4	0	0	0	0	0	0	0	0	0	0
K-feldspar	0	0	1	0	0	0	3	0	5	2	3	3
Quartz	4	0	2	0	0	0	2	0	5	3	3	4
Calcite (prim.)	0	0	10*	0	0	0	0	0	10*	0	0	6*
Opaque ore	5	Tr	5	3	2	2	2	3	Tr	3	3	1
Apatite (prim.)	0	0	0	0	Tr	0	Tr	0	1	1	0	1
Sphene (prim.)	0	0	1	0	Tr	0	Tr	0	Tr	1	Tr	Tr
Chlorite (sec.)	0	1	Tr	2	8	0	0	1	0	0	0	Tr
Epidote (sec.)	0	0	5	0	0	0	0	0	1	0	1	Tr
Serpentine	0	0	0	0	0	3	0	1	0	0	0	0
Sericite	0	20	10	2	20	0	33	0	0	0	0	0
Total	100	100	100	100	100	100	100	100	100	100	100	100

Appendix B.3. (Contd.)

	Main Arrochar intrusion						Inversnaid intrusion				
	13	14	15	16	17	18	19	20	21	22	23
SiO_2	54.71	55.36	55.40	55.98	65.83	67.42	54.04	54.95	55.51	57.20	57.58
TiO_2	0.81	0.97	0.99	0.89	0.36	0.46	0.97	1.08	1.18	1.02	1.04
Al_2O_3	12.91	16.44	14.85	14.20	16.21	14.77	11.66	16.47	16.81	16.99	16.05
Fe_2O_3	1.51	0.82	2.23	1.49	1.00	1.12	3.61	3.61	3.93	2.37	1.69
FeO	6.75	6.78	6.17	6.01	2.22	2.77	6.45	4.68	4.94	5.07	5.70
MnO	0.17	0.15	0.18	0.15	0.01	0.10	0.18	0.19	0.17	0.14	0.14
MgO	10.91	6.42	5.52	6.93	1.85	1.85	8.85	3.28	3.75	4.49	4.82
CaO	7.66	8.69	7.88	7.15	4.17	3.35	7.24	5.38	4.18	6.87	6.87
Na_2O	1.04	3.03	2.56	2.46	3.99	3.32	2.00	3.19	3.36	3.02	2.85
K_2O	0.62	1.01	1.47	2.32	2.32	3.12	1.22	1.75	1.65	2.15	2.35
P_2O_5	0.14	0.14	0.15	0.20	0.14	0.15	0.09	0.17	0.17	0.17	0.18
H_2O+	2.39	0.56	2.61	1.16	1.30	1.13	2.50	2.47	2.20	0.86	1.09
CO_2	0.10	0.14	0.41	0.61	0.11	0.24	1.37	1.89	1.45	0.10	0.01
Total	99.72	100.50	100.42	99.55	99.51	99.80	100.18	99.12	99.30	100.45	100.37

Trace elements (p.p.m.)

	13	14	15	16	17	18	19	20	21	22	23
Cr	850	164	167	374	47	33	350	16	22	82	117
Co	46	34	39	38	10	12	48	24	27	34	34
Ni	275	68	57	100	15	12	46	7	9	35	38
Ba	530	290	420	530	570	520	380	500	420	500	678
Ce	55	<10	25	100	30	<10	<10	40	<10	10	<10
Cl	221	301	159	318	150	187	147	133	147	194	231
Cu	56	58	105	4	4	10	69	14	18	45	46
Ga	15	21	19	18	17	18	17	24	23	29	29
La	30	<10	<10	50	<10	<10	<10	<10	<10	<10	20
Nb	5	2	10	9	10	16	14	19	20	9	10

Pb	11	14	20	22	30	20	14	14	16	14	16
Rb	94	65	33	97	64	90	23	7	32	60	66
S	264	90	245	180	75	155	145	60	60	65	85
Sc	27	23	24	25	5	8	46	33	33	27	25
Sr	440	300	340	255	595	330	210	440	250	390	38
Th	13	21	12	28	<5	<50	<5	<5	<5	<5	<5
V	218	211	238	198	54	90	354	275	323	199	199
Y	2	12	16	17	10	10	10	32	29	23	20
Zn	96	71	93	78	55	46	88	92	104	71	72
Zr	130	130	160	165	200	185	105	185	180	185	180
					Modal analyses						
Olivine	1	0	0	0	0	0	0	0	-	0	-
Orthopyroxene	0	0	5	0	0	0	0	0	-	2	-
Clinopyroxene	10	40	45	5	0	10	1	0	-	5	-
Amphibole	5	0	0	20	0	5	40	5	-	10	-
Biotite	5	10	3	5	10	10	0	5	-	15	-
Plagioclase	25	45	40	45	60	30	40	45	-	50	-
Anorthoclase	0	0	0	0	0	0	0	0	-	0	-
K-feldspar	0	2	2	3	10	10	3	5	-	1	-
Quartz	1	2	4	5	15	15	3	5	-	3	-
Calcite (prim.)	0	0	1	10*	0	0	5	5	-	Tr	-
Opaque ore	0	1	0	Tr	1	1	4	5	-	5	-
Apatite (prim.)	0	0	0	Tr	1	0	Tr	Tr	-	Tr	-
Sphene (prim.)	0	0	Tr	1	1	Tr	Tr	Tr	-	Tr	-
Chlorite (sec.)	50	Tr	Tr	0	0	10	4	15	-	5	-
Epidote (sec.)	0	0	0	1	0	1	Tr	Tr	-	0	-
Serpentine	0	0	0	0	0	0	0	0	-	0	-
Sericite	3	0	0	5	2	8	0	10	-	5	-
Total	100	100	100	100	100	100	100	100	-	100	-

Appendix B.3. (Contd.)

	Glen Gyle intrusions										
	24	25	26	27	28	29	30	31	32	33	34
SiO_2	42.24	50.08	52.23	52.88	54.76	54.76	54.96	55.87	56.59	57.01	66.96
TiO_2	2.53	1.31	1.14	1.05	0.90	1.21	1.05	0.84	1.02	0.54	0.38
Al_2O_3	14.60	19.90	15.01	15.43	17.40	16.90	16.26	16.23	16.52	18.86	15.40
Fe_2O_3	7.21	2.00	2.50	2.67	1.69	2.78	3.50	2.15	1.92	0.71	1.18
FeO	8.78	4.45	6.64	6.12	5.06	4.91	4.80	4.97	5.05	2.89	2.25
MnO	0.18	0.13	0.17	0.17	0.13	0.13	0.14	0.15	0.13	0.08	0.13
MgO	9.08	3.91	6.70	6.17	3.56	3.35	4.82	5.50	4.24	1.05	1.52
CaO	9.50	8.28	8.64	7.62	7.07	5.78	6.47	6.87	6.42	5.16	2.33
Na_2O	1.90	3.37	2.98	2.88	3.98	3.43	3.23	2.65	3.64	4.16	3.61
K_2O	1.16	1.85	2.42	2.98	1.68	1.18	2.56	1.62	1.48	2.45	3.68
P_2O_5	0.01	0.17	0.33	0.31	0.23	0.17	0.31	0.19	0.21	0.29	0.14
H_2O+	2.24	2.54	0.74	1.90	2.76	3.05	1.23	2.43	1.54	2.88	1.19
CO_2	0.17	1.00	0.17	0.31	0.79	1.86	0.19	0.32	0.80	3.51	0.77
Total	99.60	98.99	99.67	100.49	100.01	99.51	99.52	99.79	99.57	99.59	99.57
	Trace elements (p.p.m.)										
Cr	134	59	161	184	93	19	130	184	-	<15	46
Co	46	30	38	34	27	26	26	34	-	11	4
Ni	57	26	75	89	29	9	50	97	-	6	25
Ba	210	330	740	780	360	410	623	420	-	460	740
Ce	<10	<10	40	<10	<10	<10	30	60	-	<10	75
Cl	139	184	355	224	215	123	190	183	-	164	153
Cu	93	71	19	109	51	14	80	45	-	30	12
Ga	17	26	23	26	20	21	26	23	-	14	17
La	<10	<10	20	<10	10	<10	20	15	-	15	45
Nb	5	7	7	11	14	13	10	10	-	16	10

Pb	5	15	17	12	17	16	14	11	-	16	13
Rb	33	50	57	83	58	34	44	43	-	85	58
S	165	105	105	185	100	1290	155	120	-	95	100
Sc	91	17	35	25	15	21	22	20	-	3	5
Sr	300	630	425	480	460	355	615	455	-	455	505
Th	8	5	19	24	5	5	18	5	-	5	8
V	613	207	275	235	144	290	193	219	-	48	95
Y	52	24	27	13	14	29	29	10	-	13	10
Zn	100	70	88	96	76	96	74	82	-	50	27
Zr	99	170	180	210	140	185	275	170	-	170	210

Modal analyses

Olivine	0	-	0	-	0	0	0	-	-	-	-
Orthopyroxene	0	-	3	-	0	0	0	-	-	-	-
Clinopyroxene	4	-	15	-	20	0	5	-	-	-	-
Amphibole	70	-	0	-	10	5	25	-	-	-	-
Biotite	0	-	10	-	2	5	1	-	-	-	-
Plagioclase	5	-	60	-	45	55	45	-	-	-	-
Anorthoclase	0	-	0	-	0	0	0	-	-	-	-
K-feldspar	0	-	0	-	5	0	5	-	-	-	-
Quartz	2	-	0	-	10	0	10	-	-	-	-
Calcite (prim.)	0	-	0	-	0	5	0	-	-	-	-
Opaque ore	5	-	10	-	3	5	3	-	-	-	-
Apatite	0	-	Tr	-	0	Tr	1	-	-	-	-
Sphene (prim.)	0	-	0	-	0	Tr	0	-	-	-	-
Chlorite (sec.)	1	-	2	-	5	15	5	-	-	-	-
Epidote (sec.)	0	-	0	-	0	Tr	0	-	-	-	-
Serpentine	0	-	0	-	0	0	0	-	-	-	-
Sericite	10	-	0	-	0	10	0	-	-	-	-
Uralite	3	-	0	-	0	0	0	-	-	-	-
Total	100	-	100	-	100	100	100	-	-	-	-

Appendix B.3. (Contd.)

	Ben Glas intrusions					Cruachan Cruinn intrusions						
	35	36	37	38	39	40	41	42	43	44	45	46
SiO_2	47.10	52.46	53.17	56.74	60.63	45.40	47.06	48.61	48.84	53.91	56.32	66.18
TiO_2	1.19	1.33	0.27	0.77	0.82	2.05	1.52	0.65	1.11	0.97	0.89	0.53
Al_2O_3	11.21	15.56	16.91	18.36	16.34	14.36	16.05	9.87	10.88	14.16	14.16	15.90
Fe_2O_3	3.63	1.45	2.32	2.30	1.85	5.14	4.61	2.30	2.76	0.57	1.50	0.88
FeO	9.78	6.20	5.74	2.86	3.68	7.35	6.67	6.41	6.74	7.29	5.52	2.48
MnO	0.22	0.15	0.14	0.13	0.12	0.14	0.12	0.18	0.17	0.15	0.14	0.07
MgO	13.39	8.10	6.50	1.95	2.47	9.27	7.52	17.82	12.86	7.49	7.49	1.87
CaO	5.85	6.84	7.49	4.03	4.18	7.62	8.07	6.62	10.00	7.67	5.67	1.03
Na_2O	0.87	3.16	3.57	3.33	3.53	2.13	2.07	1.63	1.83	2.68	2.78	3.61
K_2O	0.56	1.85	1.72	4.19	2.35	1.58	1.85	2.36	0.68	2.94	2.32	3.64
P_2O_5	0.05	0.24	0.41	0.51	0.22	0.12	0.47	0.22	0.10	0.32	0.15	0.20
H_2O+	4.64	2.25	1.10	2.32	2.58	3.18	2.72	3.05	2.25	1.14	2.24	2.88
CO_2	1.34	0.60	0.21	2.32	0.83	2.13	1.00	0.28	1.87	0.30	0.32	0.38
Total	99.83	100.19	99.55	99.81	99.59	100.47	100.13	100.03	100.09	99.59	99.50	99.65
						Trace elements (p.p.m.)						
Cr	350	450	240	<15	58	190	155	1150	800	325	500	54
Co	65	40	32	10	11	52	48	64	51	33	43	17
Ni	400	150	122	7	14	40	50	725	137	131	125	29
Ba	300	330	270	1010	470	390	380	570	190	620	630	580
Ce	40	25	<10	45	25	30	30	40	25	<10	50	20
Cl	134	214	248	171	189	170	173	339	200	278	117	149
Cu	21	40	22	21	9	8	200	57	12	35	51	24
Ga	18	13	14	22	18	17	23	13	16	18	14	15
La	<10	15	<10	35	25	25	<10	<10	25	20	15	30
Nb	12	14	25	10	17	13	5	4	7	10	14	14

Pb	14	15	11	4	10	14	16	17	10	14	14	22
Rb	11	34	50	148	125	58	73	66	23	85	57	136
S	640	120	90	485	1690	70	235	205	95	110	1430	245
Sc	13	21	9	5	12	39	28	21	43	30	20	6
Sr	150	450	831	535	826	320	420	440	220	605	530	305
Th	<5	<5	61	23	86	<5	<5	<5	<5	56	49	55
V	115	214	144	101	125	521	356	148	270	190	208	75
Y	<2	18	40	24	26	43	26	<2	16	18	11	16
Zn	129	86	92	53	80	81	79	87	79	85	93	59
Zr	95	180	220	165	270	175	150	145	95	220	215	215

Modal analyses

Olivine	0	0	0	0	0	0	-	35	-	-	-	-
Orthopyroxene	0	0	1	0	0	0	-	0	-	-	-	-
Clinopyroxene	0	25	3	3	0	2	-	20	-	-	-	-
Amphibole	35	5	20	30	0	40	-	10	-	-	-	-
Biotite	5	10	10	10	10	2	-	5	-	-	-	-
Plagioclase	10	50	40	40	75	35	-	20	-	-	-	-
Anorthoclase	0	0	0	0	0	0	-		-	-	-	-
K-feldspar	0	2	5	5	4	0	-	0	-	-	-	-
Quartz	5	1	5	5	5	2	-	0	-	-	-	-
Calcite (prim.)	5	Tr	3	5	0	4	-	0	-	-	-	-
Opaque ores	0	5	5	2	3	5	-	1	-	-	-	-
Apatite (prim.)	0	Tr	0	0	0	Tr	-	Tr	-	-	-	-
Sphene (prim.)	0	Tr	Tr	0	1	Tr	-	Tr	-	-	-	-
Chlorite (sec.)	30	2	3	0	2	5	-	5	-	-	-	-
Epidote (sec.)	0	Tr	Tr	0	0	5	-	0	-	-	-	-
Serpentine	0	Tr	Tr	0	0	0	-	3	-	-	-	-
Sericite	10	0	5	0	0	0	-	1	-	-	-	-
Total	100	100	100	100	100	100		100	-	-	-	-

Appendix B.3. (Contd.)

Glen Shira intrusions

	47	48	49	50	51	52	53	54	55	56	57	58
SiO_2	49.94	52.92	53.06	53.60	54.30	54.34	55.01	55.90	58.27	60.17	64.72	68.15
TiO_2	1.15	0.71	0.74	1.08	0.78	1.08	0.78	0.94	0.71	0.76	0.57	0.46
Al_2O_3	20.52	11.31	12.04	15.49	12.04	15.52	13.99	13.87	18.74	16.86	14.79	14.72
Fe_2O_3	4.09	1.71	2.28	3.16	2.17	3.18	1.87	2.07	2.02	2.12	1.45	0.54
FeO	5.15	6.32	5.92	5.41	5.38	5.52	6.08	6.11	3.64	3.70	2.99	2.55
MnO	0.14	0.16	0.15	0.12	0.14	0.15	0.16	0.18	0.12	0.11	0.10	0.05
MgO	3.68	12.60	11.50	6.68	11.17	5.15	6.82	7.67	3.51	3.43	2.35	2.17
CaO	8.08	6.62	6.73	6.31	6.22	6.10	7.40	7.15	4.17	5.43	4.40	2.38
Na_2O	3.28	2.16	2.25	2.39	2.46	2.56	2.50	2.39	3.76	3.68	3.03	4.07
K_2O	1.45	3.09	2.96	2.03	3.30	3.51	3.88	2.61	2.54	2.08	3.68	3.86
P_2O_5	0.45	0.27	0.31	0.34	0.28	0.52	0.34	0.32	0.21	0.20	0.23	0.14
H_2O+	1.84	1.77	1.71	1.99	1.39	1.39	1.06	1.77	1.60	1.02	1.47	0.67
CO_2	0.63	0.24	0.23	0.54	0.29	0.53	0.10	0.31	0.23	0.15	0.59	0.09
Total	100.40	100.88	99.88	99.14	99.92	99.55	99.99	101.29	99.52	99.71	100.37	99.85
Trace elements (p.p.m.)												
Cr	25	775	775	375	700	77	207	223	58	59	59	84
Co	34	49	52	30	41	33	29	32	20	25	12	6
Ni	8	450	375	135	350	48	93	97	28	28	21	71
Ba	440	880	1010	1010	880	720	1030	1050	660	580	870	890
Ce	20	30	25	35	30	80	45	<10	60	20	105	10
Cl	184	397	684	157	370	168	267	149	231	148	217	250
Cu	9	56	58	35	26	129	83	62	9	65	56	23
Ga	25	16	21	22	15	23	20	21	24	20	15	26
La	<10	<10	<10	35	10	<10	<10	<10	50	<10	40	25
Nb	8	8	9	12	7	18	10	10	14	16	10	20

Pb	16	23	16	17	14	17	15	18	18	21	27	20
Rb	35	83	93	92	84	121	112	79	60	50	111	92
S	120	570	270	1005	1050	135	105	200	240	190	120	3050
Sc	23	20	21	25	19	19	32	27	13	12	9	5
Sr	675	635	705	625	625	630	555	750	695	510	645	625
Th	<5	<5	34	<5	<5	64	23	16	16	<5	<5	5
V	170	193	193	246	209	265	186	214	156	131	95	78
Y	23	9	20	24	13	32	16	23	16	21	18	9
Zn	120	73	86	96	77	99	91	91	78	80	57	21
Zr	95	195	230	370	210	250	235	175	260	220	285	230

Modal analyses

Olivine	0	15	15	5	-	0	0	0	0	0	0	0
Orthopyroxene	0	0	1	0	-	0	0	0	0	0	0	0
Clinopyroxene	0	20	20	10	-	2	20	0	1	0	0	1
Amphibole	20	0	0	25	-	25	15	30	30	20	5	2
Biotite	0	5	5	10	-	5	0	5	5	5	10	10
Plagioclase	60	[50]	[50]	45	-	40	55	50	45	60	66	70
Anorthoclase	0			0	-	0	0	0	0	0	0	0
K-feldspar	0	0	0	3	-	3	0	5	5	0	10	10
Quartz	1	0	0	2	-	6	2	5	5	10	5	3
Calcite (prim.)	2	0	0	0	-	0	0	0	0	1	0	0
Opaque ores	4	5	5	Tr	-	3	8	5	3	2	1	1
Apatite (prim.)	0	0	0	0	-	Tr	Tr	0	1	Tr	0	0
Sphene (prim.)	0	0	0	0	-	Tr	0	0	1	0	1	1
Chlorite (sec.)	4	0	0	0	-	1	0	0	1	1	1	1
Epidote (sec.)	0	0	0	0	-	Tr	0	0	0	0	0	0
Serpentine	2	5	5	0	-	0	0	0	0	1	0	0
Sericite	7	0	0	0	-	15	0	0	2	0	1	1
Total	100	100	100	100	-	100	100	100	100	100	100	100

Appendix B.3. (Contd.)

Garabal-Hill intrusion

	59	60	61	62	63	64	65	66	67	68	69	70	71	72
SiO_2	41.18	43.40	43.97	45.16	48.14	48.15	50.32	52.99	54.36	55.94	57.30	60.31	65.47	65.65
TiO_2	0.60	1.34	0.61	0.37	1.35	1.57	1.30	0.60	0.84	0.32	0.86	0.68	0.60	0.64
Al_2O_3	2.92	11.33	2.50	11.53	9.55	10.07	13.56	15.05	11.57	18.60	17.66	14.95	16.06	14.89
Fe_2O_3	5.99	4.61	5.87	4.17	2.19	3.07	4.96	1.34	2.26	1.93	1.56	0.92	1.38	0.72
FeO	5.48	8.68	5.48	8.68	8.78	7.00	6.32	6.59	5.74	3.62	3.97	3.67	1.98	2.06
MnO	0.13	0.21	0.13	8.21	0.94	0.20	0.13	0.35	0.75	0.01	0.11	0.20	0.15	0.06
MgO	23.50	14.30	23.50	14.30	15.85	15.10	12.20	7.50	9.25	3.40	3.50	4.10	2.35	1.60
CaO	12.65	10.45	12.65	10.40	8.42	10.10	6.05	6.25	7.50	5.20	5.20	5.22	3.45	2.75
Na_2O	0.15	0.90	0.07	0.90	1.21	1.62	2.37	4.25	3.35	4.45	4.30	3.84	4.44	4.35
K_2O	0.10	0.76	0.00	0.76	0.70	0.96	1.27	1.82	2.24	3.65	2.60	2.81	4.00	4.08
P_2O_5	0.03	0.06	0.05	0.04	0.14	0.07	0.74	0.45	0.40	0.17	0.27	1.74	0.20	0.15
H_2O+	6.13	3.43	6.13	3.43	2.94	1.54	2.13	3.35	2.75	1.64	1.53	2.20	1.15	1.68
CO_2	0.31	0.21	0.31	0.21	0.25	0.18	0.37	0.17	0.13	0.15	0.44	0.33	0.11	0.25
Total	99.17	99.68	101.27	100.16	100.46	99.63	101.72	100.71	101.14	98.58	99.30	100.97	101.14	98.87

Trace elements (p.p.m.)

	59	60	61	62	63	64	65	66	67	68	69	70	71	72
Cr	1880	70	84	525	570	133	211	880	1050	-	80	-	500	52
Co	72	27	9	65	53	37	26	72	57	-	2	-	43	9
Ni	590	42	29	370	220	70	67	590	230	-	22	-	153	18
Ba	19	600	990	130	250	210	650	19	170	-	260	-	460	880
Ce	<10	25	40	15	25	40	50	<10	30	-	35	-	30	30
Cl	283	182	144	100	128	137	135	283	112	-	188	-	190	156
Cu	27	166	4	605	44	308	40	27	132	-	11	-	19	4
Ga	6	21	16	13	15	14	17	6	10	-	18	-	22	19
La	<10	30	15	<10	15	<10	40	<10	<10	-	35	-	25	<10
Nb	2	12	28	4	4	5	13	2	3	-	10	-	10	19

Pb	10	28	30	9	12	10	27	10	15	-	25	-	19	23
Rb	4	87	106	27	34	27	72	4	21	-	44	-	60	75
S	180	220	120	2325	100	310	65	180	85	-	1070	-	65	135
Sc	39	12	8	42	33	15	12	39	40	-	1	-	22	3
Sr	25	630	650	240	670	1030	570	35	385	-	715	-	401	700
Th	<6	13	<5	120	<5	104	<5	<5	<5	-	31	-	<5	<5
V	153	179	94	138	234	273	143	153	223	-	40	-	222	71
Zn	63	64	31	78	72	84	59	63	86	-	8	-	19	36
Zr	20	185	225	60	135	130	210	20	100	-	190	-	215	220

Modal analyses

Olivine	10	0	10	0	0	0	5	0	0	-	0	0	-	0
Orthopyroxene	0	0	0	0	0	0	0	0	0	-	0	0	-	0
Clinopyroxene	90**	3	90**	3	0	5	30	10	6	-	3	0	-	1
Amphibole	0	90	0	90	0	45	0	0	30	-	2	15	-	3
Biotite	0	1	0	1	0	0	5	Tr	Tr	-	15	5	-	15
Plagioclase	0	2	0	2	50	50	40	80	50	-	75	75	-	75
Anorthoclase	0	0	0	0	0	0	0	0	0	-	0	0	-	0
K-feldspar	0	0	0	0	0	0	1	0	1	-	2	2	-	2
Quartz	0	0	0	0	0	0	1	0	2	-	2	3	-	3
Calcite (prim.)	0	0	0	0	0	0	0	0	0	-	0	0	-	0
Opaque ore	Tr	2	Tr	2	2	Tr	2	2	1	-	1	Tr	-	1
Apatite (prim.)	0	2	0	2	0	0	15	1	0	-	0	0	-	0
Sphene (prim.)	0	Tr	0	Tr	1	0	0	0	0	-	Tr	Tr	-	0
Chlorite (sec.)	0	0	0	0	2	0	1	5	10	-	0	0	-	0
Epidote (sec.)	0	Tr	0	Tr	0	0	0	0	0	-	0	0	-	0
Serpentine	0	0	0	0	0	0	0	0	0	-	0	0	-	0
Sericite	0	0	0	0	0	0	0	2	0	-	0	0	-	0
Fine-grained mixt.	0	0	0	0	45	0	0	0	0	-	-	-	-	-
Total	100	100	100	100	100	100	100	100	100	-	100	100	-	100

Appendix B.3. (Contd.)

Main Arrochar intrusion and its surrounding masses

1	Appinite, small mass, Coire nan Each.
2	Lamprophyric marginal appinite, north of Ben Narnain.
3	Pegmatitic appinite, locality as in 1.
4	Peridotite, locality as in 1.
5	Appinite, north of Coire Fuar.
6	Peridotite, adjacent to 2.
7	Appinite, northwest of Ben Narnain.
8	Pyroxenite adjacent to 7.
9	Hornblende diorite, small mass at Creag Tharsuinn.
10	Pyroxene - mica diorite, locality as in 1.
11	Pyroxene - mica diorite, locality as in 9.
12	Hornblende diorite, small mass, Allt à Balachain.
13	Pyroxene - mica diorite, Allt Coiregrogain.
14	Pyroxene - mica diorite, southwest of Ben Narnain.
15	Pyroxene - mica diorite, headwaters of Glen Loin.
16	Hornblende diorite, locality as in 9.
17	Granodiorite, main Arrochar mass (central).
18	Felsite, small mass, southeast of Ben Vane.

Inversnaid intrusion

19-21	Hornblende diorite, northwestern margin of the main intrusion.
22	Marginal porphyritic pyroxene - mica diorite.
23	Pyroxene - mica diorite, main mass..

Glen Gyle intrusions

24	Appinite, Stob nan Eighrach.
25	Pyroxene - mica diorite, Allt nan Cat, main mass.
26-27	Pyroxene - mica diorite, Lochan Dubh, main mass.
28	Hornblende diorite, small mass exposed north of the main Allt nan Cat mass.
29	Lamprophyre exposed at the eastern margin of the main Allt nan Cat mass.
30	Hornblende diorite, locality as in 24.
31	Hornblende diorite, small mass exposed north of the large mass at Stob nan Eighrach.
32	Porphyritic pyroxene - mica diorite, locality as in 25.
33	Hornblende diorite, locality as in 28.
34	Granodiorite, locality as in 26.

Ben Glas intrusions

35	Appinite exposed at the northwestern extremity of the main Ben Glas intrusion.
36	Pyroxene - mica diorite, western margin of the main Ben Glas intrusion.
37	Hornblende diorite, main mass.
38	Hornblende diorite adjacent to 37.
39	Diorite, Meall Mòr nan Eag mass.

Cruachan Cruinn intrusion

40-41	Appinite, north of Allt Foinn Glen (north of the horizon of Loch Tay Limestone).
42	Kentallenite, north of Sput Ban.
43	Appinite, locality as in 40.

Cruachan Cruinn intrusion (contd.)

44	Pyroxene - mica diorite adjacent to 42.
45	Hornblende diorite, about 500 m to the west of 40.
46	Felsite, west of Eas Eonan.

Glen Shira intrusion

47	Hornblende diorite, middle mass, Elrigbeag.
48-49	Kentallenite, Brannie Burn.
50	Appinite, Clachan Hill.
51	Kentallenite, locality as in 48.
52	Hornblende diorite, locality as in 50.
53	Hornblende diorite, Ben Chas.
54	Hornblende diorite adjacent to 52.
55	Hornblende diorite, southern mass, Elrigbeag.
56	Quartz diorite, locality as in 55.
57	Granodiorite, locality as in 50.
58	Granodiorite, locality as in 48.

Garabal Hill intrusion

59	Olivine pyroxenite.
60	Pyroxene hornblendite.
61	Olivine pyroxenite.
62	Pyroxene hornblendite.
63	Altered diorite.
64	Appinite.
65	Coarse-grained appinite.
66	Pyroxene diorite.
67	Appinitic diorite.
68	Pyroxene - mica diorite.
69	Pyroxene - mica diorite.
70	Hornblende diorite (appinitic diorite).
71	Hornblende diorite (appinitic diorite).
72	Biotite diorite.

*	Values including secondary calcite.
**	Mostly altered clinopyroxene.